DOCTOR OF PHILOSOPHY

Synthesis and Applications of Proline Derived Guanidine Catalysts in Asymmetric Michael Addition Reactions

Mehdar, Yassin

Award date:
2017

Awarding institution:
Bangor University

Synthesis and Applications of Proline Derived Guanidine Catalysts in Asymmetric Michael Addition Reactions

PhD in Chemistry

In the

School of Chemistry

By

Yassin Taleb Mehdar

500320097

Prifysgol Bangor • Bangor University

Table of Contents

Acknowledgements

In this work I would like to thank Dr. Patrick J. Murphy of Bangor University for his supervision of my work for his help in the processing of the necessary equipment and samples and for his explanations of their use.

Abbreviations

General

c	Concentration (gram/ml)
d	Day(s)
HPLC	High-performance liquid chromatography
h	Hour(s)
IR	Infrared spectroscopy
L	Cell path length (in dm)
min	Minute(s)
mo	Month(s)
MS	Mass spectrometry
M.wt	Molecular weight
NA	Not applicable
nm	Nanometer(s)
NMR	Nuclear magnetic resonance
n.p	Not provided
rt	Room temprature
T	Temperature (degree centigrade)
TLC	Thin layer chromatography
wk	Week(s)
$[\alpha]_{\lambda}^{t}$	Specific rotation,
$[\alpha]_{obs}$	Observed rotation
Λ	Wavelength of incident light (in nm)

Reagents

DCC	*N*,*N*-Dicyclohexylcarbodiimide
CDI	Carbonyldiimidazole
Dipp	2,6-Diisopropylphenyl
DMAP	4-(Dimethylamino)pyridine

Functional groups

Ac	Acetyl
Bn	Benzyl
Boc	t-Butoxycarbonyl
Cbz	Carbobenzyloxy
Cy	Cyclohexyl
Et	Ethyl
iPr	isopropyl
Me	Methyl
Ph	Phenyl

Solvents

DCM	Dichloromethane
DMF	Dimethylformamide
DE	Diethyl ether
EA	Ethyl acetate
MeOH	Methanol
PE	Petroleum ether (40-60)
THF	Tetrahydrofuran

Abstract

This thesis reports the preparation of a range of guandine and guanidinium species used as catalysts for asymmetric Michael additions. The most successful of these were based on the generalized structure **I** (R = Me, iPr, Bn, Cy; R^1, R^2 = H, Me, Ph, 1,2-phenyl, R^3 = Me, Bz, Cbz, Ph) and were effective catalysts of the reaction between of 2-nitrostyrene **52** and **93** leading to yields 35-99 % and up to 44 % enantiomeric excess for the product **94**. Similar reactions using diethyl malonate or 2,4-pentanedione were also catalysed however these were less successful and generally led to low enantiomeric excesses and the formation of unidentifiable polymeric by-products.

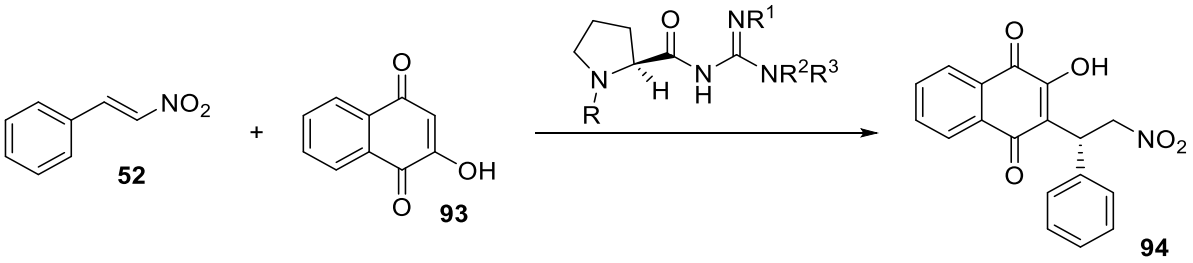

X-ray crystallographic structures were determined for several of these compounds and the hydrogen bonding patterns observed were used to speculate on the mechanism of the reaction and the magnitude of the asymmetric induction.

Introduction

Asymmetric Synthesis: Theory

Asymmetric synthesis as defined by Mosher et al[1] is a reaction where an achiral unit is converted by a reactant into a chiral unit, so that the stereo isomeric products that are formed are in unequal amounts. The term enantiomeric excess was coined in 1971 by Mosher et al in the publication *Asymmetric Organic Reactions*.[2] To understand asymmetric synthesis, optical rotation will first be explained. Normally the enantiomers are denoted by the experimentally determined optical rotation pattern of plane polarized light and are designated as either (+) or (-) x^0.[3,4] The x^0 denotes the angle of rotation of plane polarized light when they are passed through the enantiomeric mixture.[3-5] The enantiomers are specified by their specific rotation as per the formula below:

$$[\alpha]_{\lambda}^{t} = [\alpha]_{obs} / L*C$$

From the above equation it indicates that the experimental value of the enantiomers varies considerably with temperature, concentration and solvent media under which it is estimated and thus provides very little reliable evidence of enantiomeric purity.[3-5]

Absolute Configuration

Furthermore it also does not give any evidence of the absolute configuration of a stereogenic centre. The absolute configuration of a stereogenic centre is generally determined by the Cahn-Ingold-Prelog rules which are used to determine the *R* **2**/**4** and the *S* **1**/**3** isoforms as shown below.[3,4] (Figure 1)

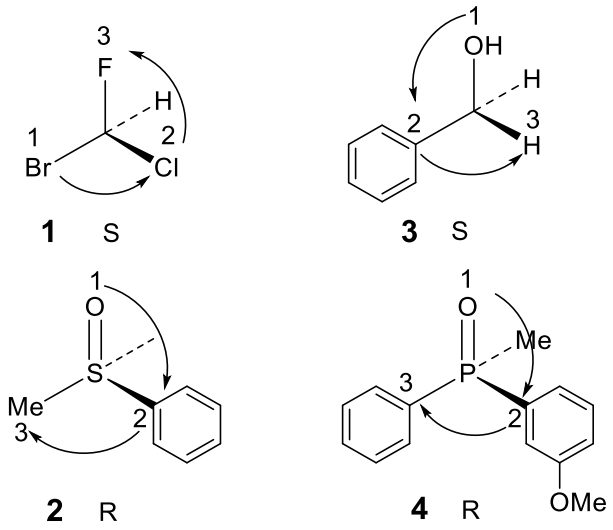

Figure 1: Showing Cahn-Ingold-Prelog rules for specifying the absolute configuration of a stereogenic centre which are used to determine the *R* and the *S* isoforms.

Enantioselective Reactions (Re and Si) and Topicity (Face selectivity)

In a particular enantioselective reaction, the trigonal centre that generates a new asymmetric carbon can be used to define the face being reacted by using the same Cahn-Ingold-Prelog rules used to define absolute configuration. These faces are referred to as 'enantiotopic'. However as the trigonal centre is not itself chiral, but rather forms a potential chiral centre, the term prochiral is sometimes tagged instead of 'enantiotopic'.[3-5]

Thus in this case when the molecule is viewed from the side of the newly formed bond, such that the groups in decreasing priority are arranged clockwise it is called the Re face, while if the groups in decreasing priority are arranged anticlockwise it is called the Si face. The concept can be illustrated by the reaction of hydride on ketone as shown below.[3-5] (Figure 2)

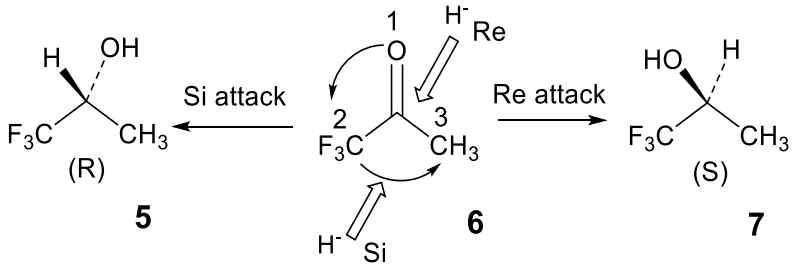

Figure 2: Re and Si concepts**5** and **7**.

In this figure it must be realized that there is no connection between the Re and Si concept with *R* and *S*. However if in this example the hydride attack is replaced by EtMgBr the Re attack will form the *R* isomer **9** and the Si attack will form the *S* isomer **8** as shown below.[3-5] (Figure 3)

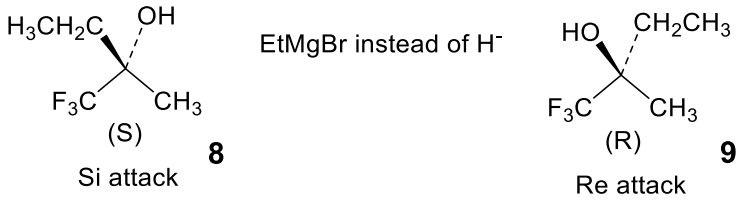

Figure 3: Formation of Ri and Si by EtMgBr replacement

Defining the Enantiotopic Atoms and Groups

Often the term prochiral is used to describe a tetrahedral group that has two enantiotopic atoms or groups like CX_2WY. To distinguish the two X groups, one of the X groups can be replaced with a dummy group of higher priority. When dummy group gives (*S*) configuration then the atom X is considered to be pro-*S*. However if dummy group gives (*R*) configuration then the atom X is considered to be pro-R. The following example as X=H will provide the explanation as plotted below:[3-5] (Figure 4)

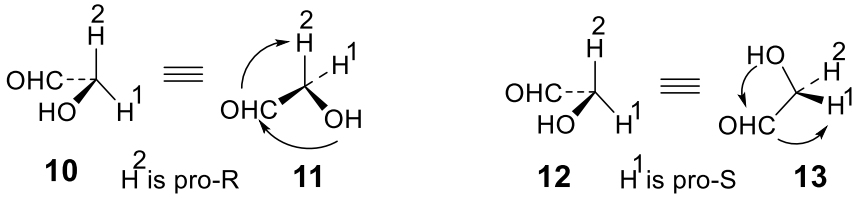

Figure 4: The pro-R and pro-S

As explained in the above figure there is no correlation between the pro-R, pro-S and the actual stereochemistry of the product. For example, replacing the pro-*R* methoxy- in the acetal with hydrogen will give the (*S)*-isomer **14** while if the methoxy-group in the acetal is replaced by chlorine atom it will form the (*R)*-isomer **15**.[3-5] (Figure 5)

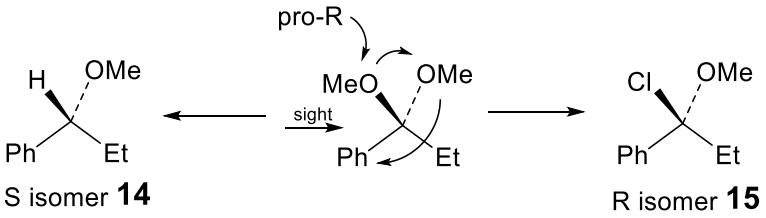

Figure 5: Replacing pro-R methoxy- and (*S)*- and (*R)*-isomers

Significance of Asymmetric Synthesis

Enantioselective synthesis is a key process in modern chemistry, particularly in the field of pharmaceuticals as it is well known that the different enantiomers or diastereomers of a molecule often have hugely different biological activity.[6] As such the study of asymmetric methods for the synthesis of natural and unnatural molecules for use as pharmaceuticals is an area of immense importance.

Enantiomeric Excess and Separation Techniques Enantiomers

Enantiomeric excess (ee) is a measure of the purity for the formed chiral substances. It indicates the degree to which a sample contains a specific enantiomer in greater amounts with respect to the other. A racemic mixture (composing equal amounts of enantiomer) has an ee of 0% while a single completely pure enantiomer has an ee of 100%. Thus if the sample has 70% of one enantiomer and 30% of the other enantiomer then the ee of the mixture is 40.[7]

From a functional point of view the enantiomeric excess is defined as the absolute difference between the mole fractions (F) of each enantiomer (F- and F+), where the sum of F- and F+ is 1.[8] In practice this can be determined from the observed optical rotation ($[\alpha]_{obs}$) if the optical rotation of one pure enantiomer ($[\alpha]_{max}$) is known. (Equation 1) Enantiomeric excess can e determined in another way if the amount of each enantiomer produced is known for example by chromatographic analysis.[8] (Equation 2). In this equation the sum of the enantiomers R and S is 1.

$$ee = ([\alpha]_{obs}/[\alpha]_{max}) \times 100 \qquad \text{(Equation 1)}$$

$$ee = ((R\text{-}S)/(R+S)) \times 100 \qquad \text{(Equation 2)}$$

Enantiomeric excess is used as one of the indicators of estimating the success of an asymmetric synthesis. Considering the reaction event for mixtures of diastereomers, the analogous definitions like diastereomeric excess and percent diastereomeric excess are also in common use.[8,9] As stated above a mixture having a sample 70 % of R isomer and 30% of S isomer will have an enantiomeric excess of 40%. Thus the mixture might be considered as 40% pure R with 60% of a racemic mixture that contributes 30% R and 30% S to the overall composition.[8]

When enantiomeric excess (ee) of a mixture is given then the fraction of the major isomer, for example R may be determined using $R = +ee/2 + 50$ % and the minor isomer by using $S = -ee/2 + 50$ %. It should be noted that non-racemic mixture of two enantiomers will have a net optical rotation. Hence it is possible to determine the specific rotation of the mixture and from the knowledge of the specific rotation of the pure enantiomer; the optical purity can be estimated.[8] (Equation 3)

$$\text{Optical purity (\%)} = [\alpha]_{obs} / [\alpha]_{max} \times 100 \qquad \text{(Equation 3)}$$

Normally the contribution of each component of the mixture to the total optical rotation is directly proportional to its mole fraction hence the numerical value of the optical purity will be identical to the enantiomeric excess.[10]

This property has led to informal use of the two terms (purely excess) interchangeable, because optical purity was the traditional way of measuring enantiomeric excess. However, methods like chiral column chromatography and NMR spectroscopy can be used to measure the amount of each enantiomer individually. In some cases the equivalence term enantiomeric excess and optical purity might not always hold true. For example specific rotation of certain compounds vary as a function of their concentration,[11] similarly, non-linear effects are also known in the different molar concentrations of R/S mixtures[12] and there is the possibility of enhanced or diminished specific rotation by the addition of achiral impurites.[9]

Experimental techniques for separating enantiomers (Role of HPLC)

Determination of the enantiomeric excess of the racemic mixtures can be achieved by a variety of techniques, the most useful methods for the determination of enantiomeric excess of racemic mixtures (homochiral systems) include:[13]

i. Analytical HPLC using a chiral column.
ii. By using chiral shift agent to form such complex that would be able to discriminate and separate the enantiomer. This can be determined by the proton splitting proton NMR signals.
iii. By forming a derivative with a homochiral reagent so as to turn the enantiomeric excess into a diastereoisomeric excess that can be measured by simple gas chromatography, HPLC or NMR spectroscopy.

If GC is employed, the two enantiomers that are to be analyzed undergo rapid and reversible diastereomeric interactions with the chiral groups present on the stationary phase. Thus these diastereomeric will have very short stability and for the separation to be possible the compounds must be volatile (as in gas chromatography) and must be thermally stable. This stability is not an issue with HPLC in which a similar set of interactions occur. When estimating the ee using analytical HPLC the racemic sample should first be analysed using a predetermined HPLC system. After any enantiomeric synthesis, the enriched molecule can then be determined by comparison of its HPLC data with the racemic mixture. For the formation of diastereomeric mixtures two prerequisites are needed, firstly a site for derivation must be present, such as an alcohol or an amine. Secondly the NMR spectra of the two diasterisomers must be sufficiently different (in chemical shift) to allow for a discrimination between the two.[13]

HPLC offers the simplest method for determination of ee and an example is the analysis of the natural product (5*R*,6*Z*)-dendrolasin-5-acetate **16**.[14] (Figure 6)

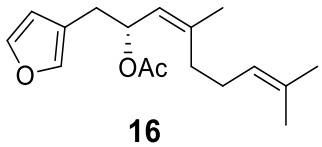

16

Figure 6: (5*R*,6*Z*)-dendrolasin-5-acetate.

Compound **16** was thought to be the (5R,6Z) isomer and in order to confirm this both the racemic acetate and both enantiomers of the acetate were prepared. HPLC analysis was performed under identical conditions using 5% isopropanol in *n*-hexane and the results in (figure 6) were obtained.[14]

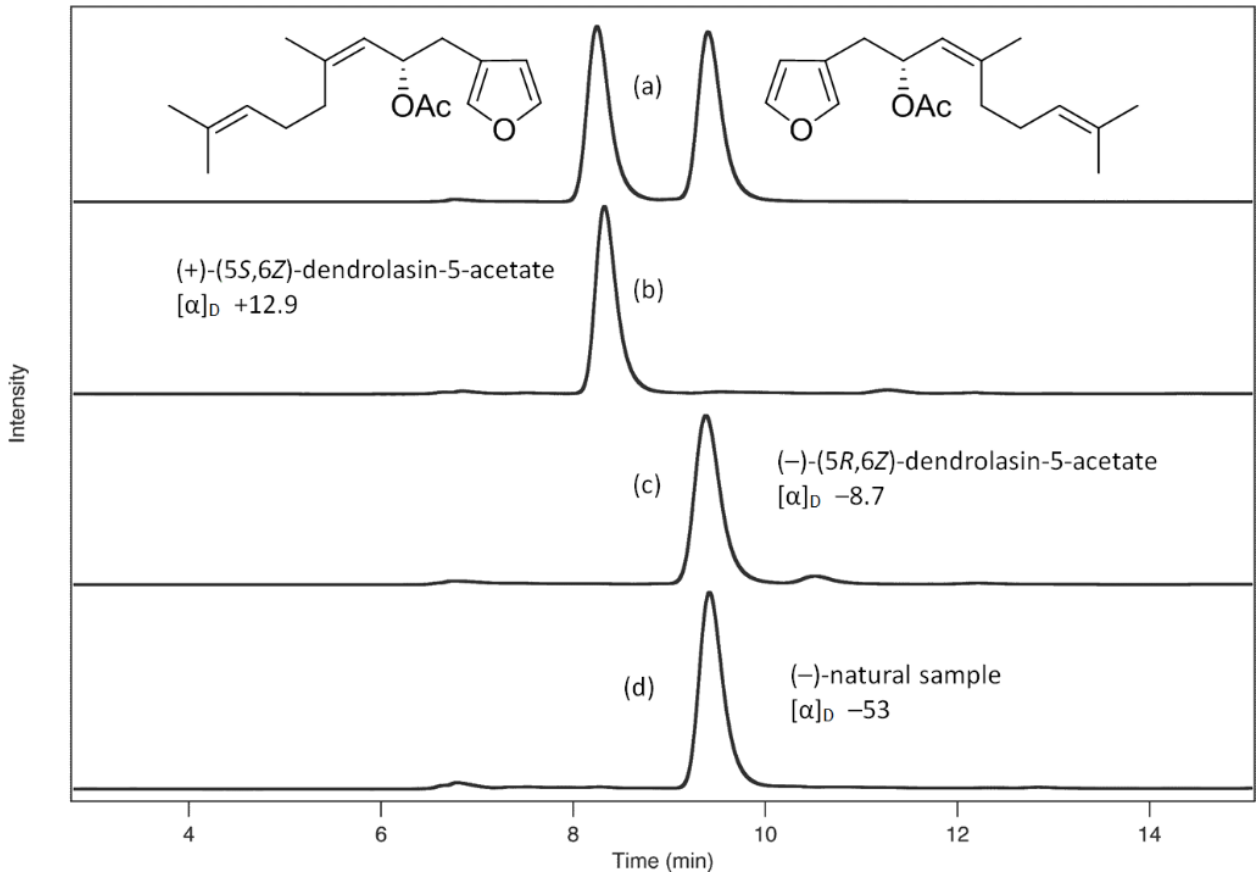

Figure 7: Enantioselective HPLC profiles (5% isopropanol in n-hexane) of 1: (a) synthetic racemic mixture; (b) synthetic (+)-enantiomer; (c) synthetic (−)-enantiomer; (d) natural sample from *H. jacksoni.*

As can be seen the racemic sample separates into two distinct bands and the (+)-enantiomer elutes before the (−)-enantiomer at retention times 8.3 and 9.5 minutes respectively (trace a). Traces (b) and (c) are the ones corresponding separate (+)-enantiomer and (−)-enantiomers and finally trace (d) illustrates that the natural (−)-enantiomer is shown to correspond exactly to the synthetic material (figure 7). This work also highlights the problems associated with optical rotation data as there are large discrepancies in the magnitude of the rotations of the various samples leading to unreliable data analysis using this method.[14]

.

Organocatalysis

The history of organocatalytic reactions

The early work on asymmetric organocatalysis demonstrated that the reactions were inefficient and limited in scope. On the other hand, organometallic catalysts have provided a vast array of methods for a wide variety of reactions and has received major emphasis. In recent years however, organic catalysis is becoming an increasingly important segment of organic chemistry, which offers a number of advantages over the metal-based and bioorganic methods. The simplicity of operation and ready availability of these inexpensive bench-stable catalysts (which are more potent than enzymes or other bioorganic catalysts) makes organocatalysis an attractive option for the synthesis of complex structures.[15-17]

The history of organocatalytic reactions has a rich past, where ample evidence specified that such catalysis played a determinant role in the formation of prebiotic building blocks like the sugars. Hence these reactions have led to the introduction and increased use of homochirality in the biological world. Some enantiomerically enriched amino acids such as *L*-alanine and *L*-isovaline, might have been present in up to an 15% enantiomeric excess (ee) in carbonaceous meteorites, which may have been able to catalyze the aldol-type dimerization of glycolaldehyde, as well as the reaction between glycolaldehyde and formaldehyde to produce sugar derivatives.[14-16] For example, Pizzarello and co-workers were able to show[18] that *L*-isovaline, which was found in the Murchison meteorite, promoted the self-aldol reaction of glycolaldehyde in water, to generates aldol products such as *L*-threose and *D*-erythrose. Proline, the most effective natural amino acid catalyst in aldol-type condensations was found to be scarcely present in meteorites.

Evidence indicates that asymmetric photolysis in interstellar clouds might produce optically active proline, however, there is a possibility that proline may also have been transported to Earth. The formation of sugars under the prebiotic conditions was amplified in a number of unique de-novo constructions of complex differentiated carbohydrates. Hence it is possible that these aldol products were the precursors of complex molecules like the RNA and DNA. [15-17]

Prebiotic RNA generally played a pivotal role in combining a number of major biochemical transformations needed for life, where sugars served as chiral templates. For examples, it is speculated that amino acid homochirality in proteins was found during asymmetric aminoacylation, which is in fact the first step in protein synthesis and hence it was critical for the transition from the putative RNA world to the translation of proteins. Hence from this concept, the selectivity (*L*- or *D*-) of amino acids was done in large part by the pre-established homochirality pattern of RNA.[15-17]

Organic molecules were used as catalysts from the very early age of synthetic chemistry. In fact the discovery of the first organocatalytic reaction was attributed to J. Von Liebig,[19] who accidentally discovered that dicyanide **17** transformed into oxamide **20** in the presence of an aqueous solution of acetaldehyde. From this observation this efficient reaction found industrial application by forming the basis of the Degussa oxamide synthesis.[19] (Scheme 1)

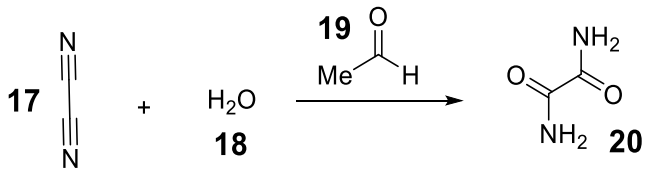

Scheme 1: Preparation of oxamide **20**.

The discovery of enzymes and enzymes functions had a deep impact on the development of the asymmetric catalytic reactions.[15-17] The first asymmetric reaction was a decarboxylative kinetic resolution which was noted by Pasteur.[20] He observed that the organism *Penicillium glauca* destroyed more rapidly one of the enantiomers from a racemic solution of ammonium tartrate.

The symmetric decarboxylation reactions were further examined in non-enzymatic conditions by George Breding[21] in the early 1900s. He had a notable interdisciplinary interest and was motivated to find the chemical origin of enzyme activity observed in living organisms. From his early experiments he demonstrated enantiomeric enrichment in the thermal decarboxylation of optically active camphor carboxylic acids in *D*- and *L*-limonenes. From an extension of this work he further noted this decarboxylation reaction in the presence of chiral alkaloids such as nicotine or quinidine, and explained the basic kinetic equation of this kinetic resolution. In fact, the first asymmetric carbon–carbon bond forming reaction was attributed to his name.[21]

In addition, Rosenthaler[22] was able to prepare mandelonitrile **25** by the addition of HCN to benzaldehyde **21** in the presence of an isolated enzyme, emulsion. Breding performed this same reaction in the presence of alkaloids as catalysts, like the *pseudo*-enantiomeric quinine **23** and quinidine **24**. Furthermore it was noted that nitrogen-containing natural products like alkaloids (strychnine, brucine and cinchona alkaloids) and amino acids like short oligopeptides were amongst the first organic catalysts to be tested.[23] (Scheme 2)

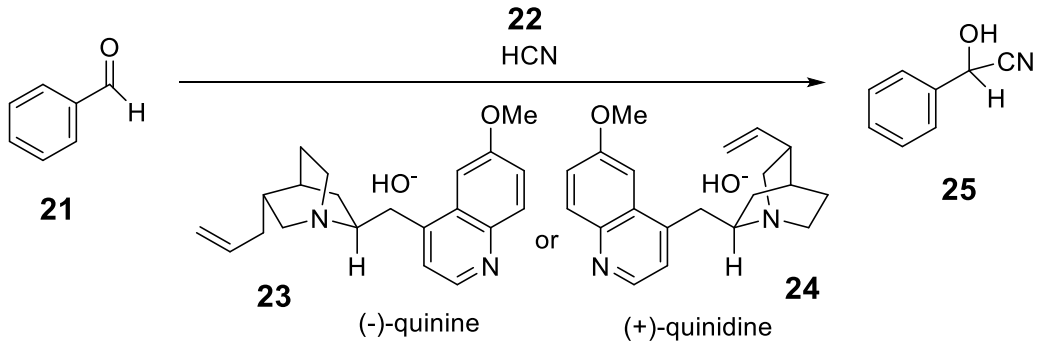

Scheme 2: Enantioselctive synthesis of mandelonitrile

Further acylative kinetic resolutions of racemic secondary alcohols were started in the late 1920s by Vavon[24] in France and independently by Wegler[25] in Germany. These scientists established that brucine and strychnine were able to induce an enantiomeric enrichment either in the esterification of *meso*-dicarboxylic acids or in the kinetic resolution of secondary alcohols with low enantiomeric excess. Wolfgang Langenbeck's contribution was also important because he developed reactions which were promoted by simple amino acids, or by small oligopeptides.[24, 25]

Most of these studies involved processes which displayed enzyme-like reactions of simple amino acids or small peptides. However enamine-type reactions were amongst the first to be discovered. This finding was studied by Dakin[26] who, in 1909, found that in a Knoevenagel-type condensation between aldehydes and carboxylic acids or esters with active methylene groups, the amine catalysts were able to be mediated by amino acids. The reaction was further extended to aldol and related transformations, from the early 1930s onwards with remarkable success, mainly with the non-asymmetric systems.[26]

After the reinvestigation of Breding's asymmetric cyanohydrins synthesis done by Prelog[27] in the mid-1950s confirmed the concept of asymmetric synthesis, and gave the way for more efficient reactions.

The discovery of synthetically potent levels of enantioselectivity can be traced to the late 1950s, when Parcejus[28] demonstrated that methy-1-phenyl-1-ketene **26** could be converted to a pheny-1-methy-1-propionate **29** in 74% ee by using O-acetylquinine **28** as a catalyst.This impressive finding inspired further studies on the cinchona catalyst system.[28] (Scheme 3)

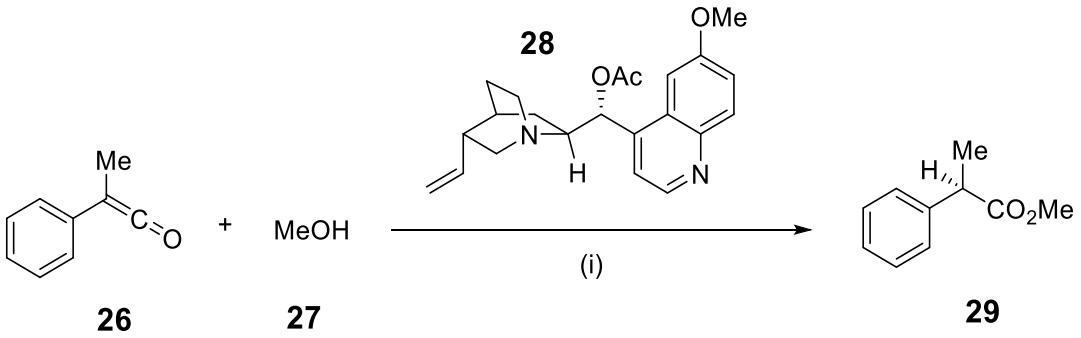

Scheme 3: Parcejus reaction. (i) Toluene -111 ^{o}C.

Bergson[29] reported the first Michael addition of β-keto esters to acrolein by incorporating 2-(hydroxymethy1)-quinuclidine as the catalyst. He never determined the enantiomeric excess, but amply noted the optical activity of their products. Wynberg,[30] reviewed the exhaustive studies of the use of cinchona alkaloids as chiral Lewis-base/nucleophilic catalysts, and demonstrated this class of alkaloid to be a versatile catalyst, promoting a variety of 1,2- and 1,4-additions for a wide range of nucleophiles to carbonyl compounds. Proline derived amides were also shown to be catalysts in this process, for example in the synthesis of **35** from **30** and **33** using catalyst **31**, which was mediated via the intermediate enamine **32**[31] **(**scheme 6). Notably in these early studies it was observed that natural cinchona alkaloids were far superior, in terms of catalytic activity and selectivity, to modified cinchona alkaloids which were generally derived by modification of the C-9 hydroxyl group.[31] To substantiate this finding, Wynberg proposed that the natural cinchona alkaloids acted as bifunctional catalysts which utilized both the tertiary amine and hydroxyl group to activate and orient the nucleophile and electrophile respectively. This arrangement was necessary to produce optimum asymmetric catalysis. The potential of organocatalytic reactions was further established by the discovery of the *L*-proline-mediated asymmetric Robinson annulation reactions in the early 1970s.[31] The Hajos-Parrish-Eder-Sauer-Wiechert reaction (which is an intramolecular aldol reaction) provided access to some of the key intermediates for the synthesis of natural products. It also offered a practical and enantioselective route for the Wieland-Miescher ketone **39**.[32,33] (Scheme 4)

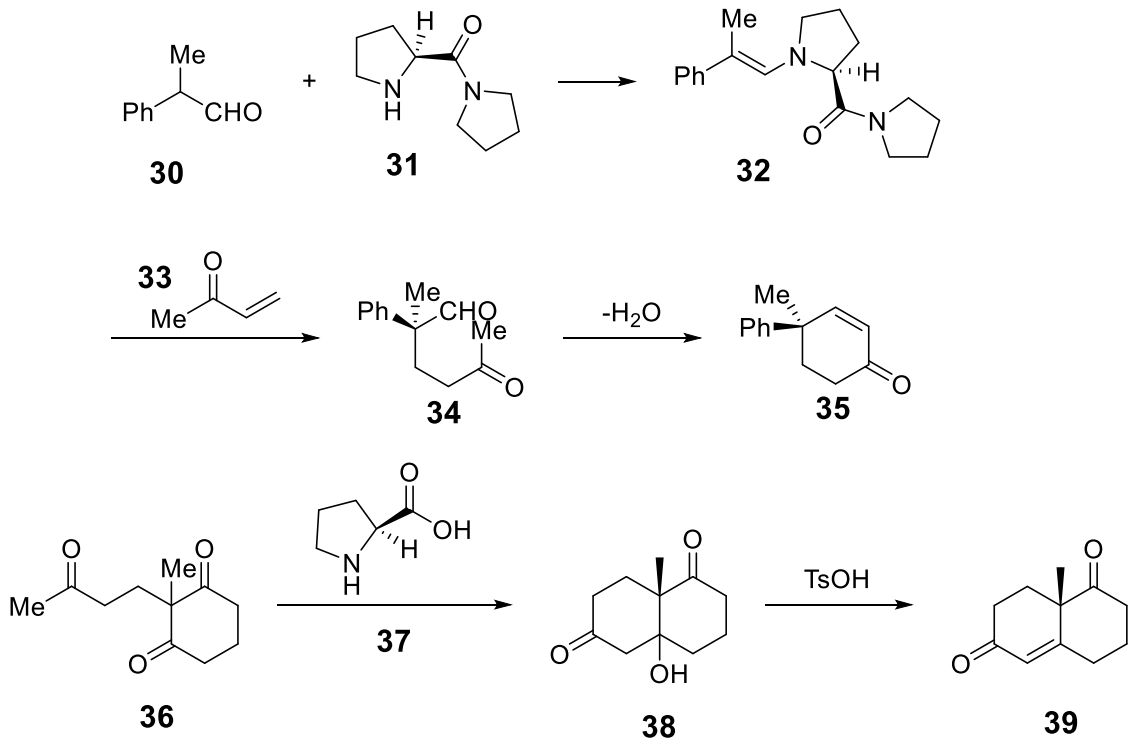

Scheme 4: Some early organocatalytic reactions.

In the late 1970's and early 1980's there was an advent of not only more general efficient asymmetric organocatalysts but also of various organocatalytic reactions that created the major turning point. [34,35] For example chiral diketopiperazines, such as **40**, were developed as chiral Bronsted acids by for the asymmetric hydrocyanation reactions. This reaction paved the way for many processes including the efficient hydrocyanation reactions of aldimines **41** which was developed by Lipton and Jacobsen.[34,35] (Scheme 5)

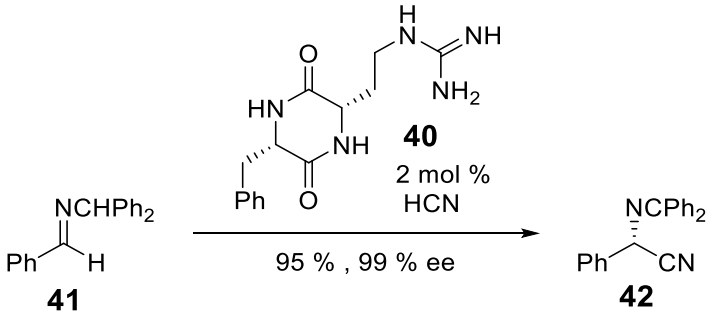

Scheme 5: Hydrocyanation reaction

The discovery of efficient phase-transfer reactions is traced back the mid-1980s, when researchers at Merck group reported the synthesis of (+)-indacrinone **45** from the phase transfer methylation of the 2-phenyl-1-indanone systems **43**.[36] This compound was methylated in 95% yield with an ee of 94%) in the presence of a catalytic amount of the *N*-trifluoromethylbenzylcinchoninium bromide **44** in a 2 phase mixture of 50% aqueous NaOH and toluene.[36] The authors speculated on an π-stacking ion pair mechanism between the indanone enolate and the benzyl cinchonium cation mediated by hydrogen bonding between the hydroxyl group and the enolate oxyanion.[36] (Scheme 6)

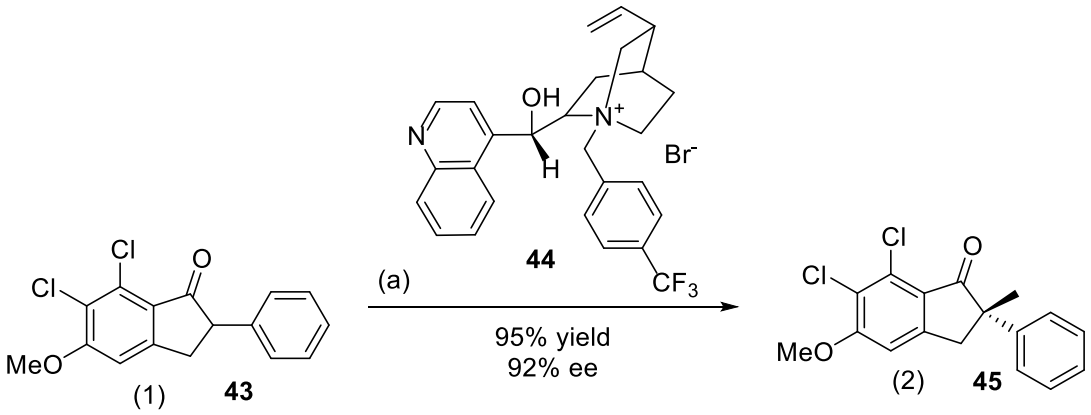

Scheme 6: (a) NaOH (50% aq.), toluene CH_3Cl, rt. 20 h.

The investigation the Hajos-Parrish-Eder-Sauer-Wiechert reaction by List and Barbas[37] in the late 1990s indicated an avenue for a number of related transformations including the enantioselective intermolecular cross-aldol reactions as well as the Mannich, Michael and Diels-Alder-type transformations. Furthermore the catalysts that were initially identified were naturally occurring molecules which had a rigid backbone and these organocatalytic reactions mainly evolved actually from the ligand chemistry of organometallic reactions. Currently many of the large array of ligands developed for metal-mediated reactions feature as the design elements found in the best performing organocatalysts.[37]

The main utility of synthetic molecules compared to their natural counterparts is their readily availability as both enantiomers. This allows for two complementary strategies in catalyst development. Firstly the targeted variation of the structure of an already efficient catalyst family or secondly the generation and testing a large number of catalysts, possibly in a library of structures, and then selecting of those having the best kinetic/selectivity profile.[17]

Types of Organocatalysts

Proline **37**, the only natural occurring secondary amino acid, exhibits useful activity in many organocatalytic processes. This is possibly because the nitrogen atom is more basic that that of the other naturally occurring amino acids.[38] Proline also has an enhanced nucleophilicity when compared to the other amino acids and it is able to act as a nucleophile with both carbonyl compounds and Michael acceptors and to form both iminium ion and enamine intermediates.[38] Under these reaction conditions it is also interesting that the carboxylic function of the amino acid is acting as Bronsted acid which is the basis of proline acting as bifunctional organo- or biocatalyst.[38] (Figure 8)

(S)-proline (R)-proline

Figure 8: R and S enantiomers of proline **37**.

Since proline mediated reactions have exceptional enantioselectivity, the reactions might be rationalised by the capacity of proline to orchestrate highly organized transition states through extensive hydrogen bonding network. In the reactions catalyzed by proline, proton transfer from amine or the carboxylic acid group of proline are essential for charge stabilization and to facilitate the carbon- carbon bond formation in transition state.[38]

The cinchona alkaloids are found in the *pseudo*-enantiomeric pairs of quinine/quinidine **45/46** and cinchonine/cinchonidine **47/48** and these and their derivatives are amongst the most efficient organocatalysts available. The main feature that is responsible for their synthetic utility is due to the presence of their tertiary quinuclidine nitrogen, which complements the proximal polar hydroxyl function of the natural compound. Furthermore the presence of these Lewis acidic (H-bonding) and Lewis basic (quinuclidine nitrogen) sites provides a bifunctionally catalytic nature to the compounds.[23] (Figure 9)

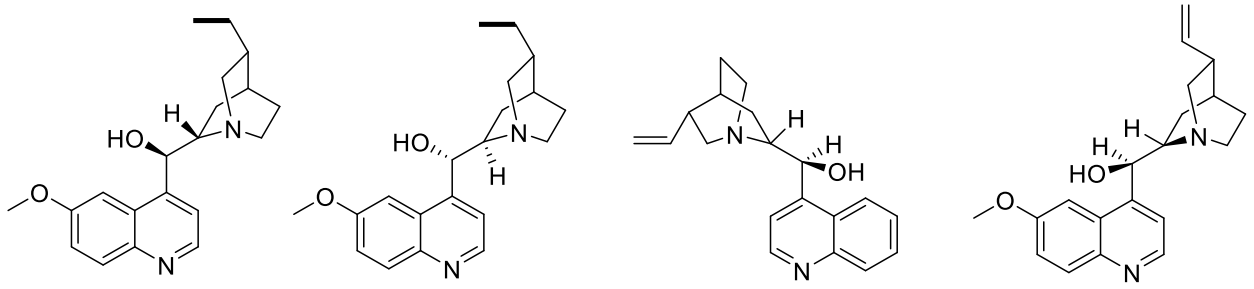

Figure 9: Pseudoenantiomeric catalyst pairs.

The range of the reactions over which the cinchona alkaloids impart high enantioselectivity is spectacular. It was observed that modification of the cinchona backbone causes a decrease or even complete loss of selectivity, and hence these modifications were disregarded in catalyst modifications. The main event that caused modified cinchonas to be of interest was the development of dimeric cinchona alkaloid ligands, used for the asymmetric dihydroxylation of simple olefins. It was also found that a very large number and variety of derivatives offered very high levels of selectivity a wide variety of reactions.[23]

TADDOL **49** which is one of the oldest and very versatile, chiral auxiliaries is another organocatalyst. The initial design of TADDOL **49** was governed by certain practical considerations, since it was derived from tartaric acid which was the least-expensive chiral starting material that had a twofold symmetry available from the natural sources. The two hydroxyl functions of the genuine molecule could function as a double hydrogen-bond donor that allowed the formation of bidentate complexes. In fact these functions could be easily substituted that liked to formation of variety of derivatives.[39] (Figure 10)

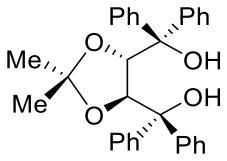

49

Figure 10: TADDOL catalyst.

Similarly the enantiomeric atropoisomers of 1,1’-binaphthyl-2,2’-diol (BINOL) **50** and 2,2'-Bis(diphenylphosphino)-1,1'-binaphthyl (BINAP) **50** were developed. These compounds have axial

dissymmetry induced by the restricted rotation about the biaryl bond and are widely used as ligands for both stoichiometric and catalytic asymmetric reactions having many analogues and derivatives that were very recently developed.[39] (Figure 11)

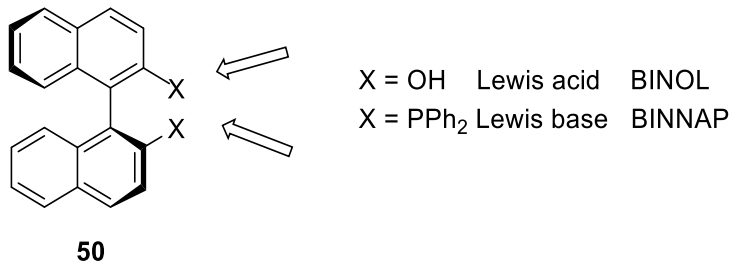

50

Figure 11: 1,1'-Binaphthyl-2,2'-diol (BINOL) and *bis*-diphenyphosphine (BINAP).

Organocatalysis using thioureas

Thiourea derivatives **51** have been intensively investigated because they are able to coordinate to substrate molecules via strong hydrogen bonding interactions as shown in (figure 12). A considerable number of reports have appeared in which the thiourea motif is central to the activity of bifunctional organocatalysts.[40-42]

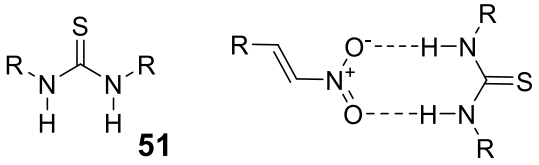

Figure 12: Hydrogen bonding interactions in thiourea organocatalysts.

Okino, et al[43] reported the use of the thioureaderivative **51** as a bifunctional organocatalysts inthe Michael addition of 1,3-dicarbonyl compounds to β-nitrostyrene **52**. For example diethyl malonate **53** gave the adduct **55** in 86 % yield and 93% ee on stirring with **54** in toluene at room temperature for 24 hours.[43] (Scheme 7)

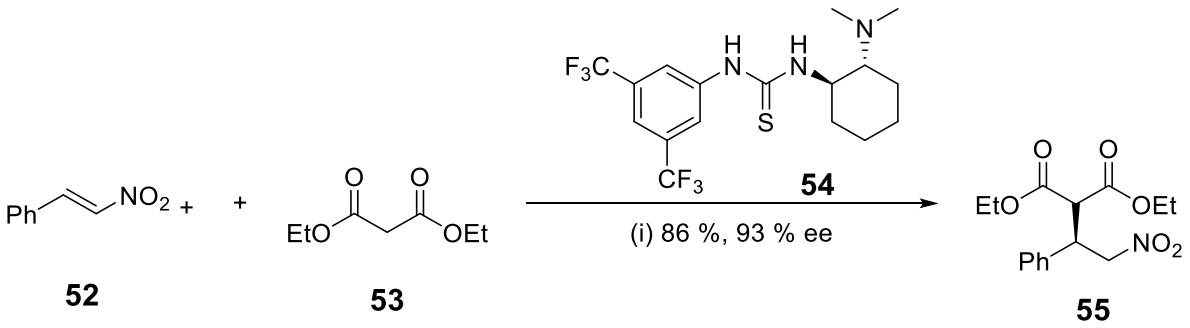

Scheme 7: Enantioselective Michael reaction by catalyst **55**. (i) Toluene, rt, 24 hrs.

Similarly, the research groups of Connon[44] and Dixon[45] reported the use of the cinchona derived thiourea **57** as a catalyst in Michael reactions. For example Dixon reported the addition of dimethyl malonate to β-nitrostyrene in dichloromethane as solvent in 95 % yield and 94 % ee.[44,45] (Scheme 8)

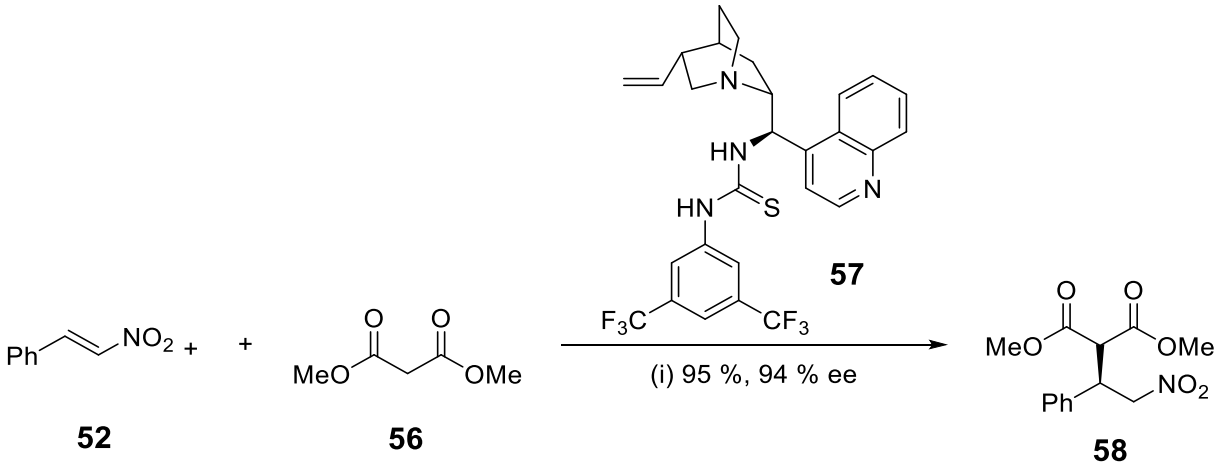

Scheme 8: Enantioselective Michael reaction using catalyst **57**. (i) CH_2Cl_2, -20 ^oC, 30 hrs.

Guanidines and guanidinium salts as bifunctional organocatalysts

Guanidines **59** offer an interesting aspect to organocatalysis as they are able to act as both a base (Bronsted) and once protonated to give a guanidinium ion **60** as an acid (Bronsted). The guanidinium species is ubiquitous in nature as it is found in the amino acid arginine and as such is a common motif at the active site of many enzymes, when it acts as a hydrogen bond donor for phosphates and carboxylates.[46] (Figure 13)

59 **60**

Figure 13: Generalized guanidine structure **59** and the corresponding guanidinium ion **60**.

A good example of the capability of guanidine to act as organocatalysts is shown in the work of Yu et al.[46] who demonstrated that the guanidine **62** was an efficient catalyst for the Michael reaction of the β-ketoesters **61** with 2-nitrostyrene **52**. This reaction was very efficient both in terms of yields 98% and of enantioselctivity 95%.[46] (Scheme 9)

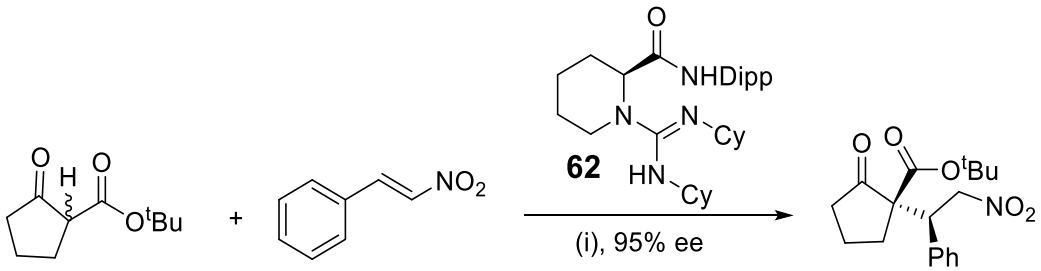

Scheme 9: Guanidine organocatalyst **62**. Dipp = 2,6-Diisopropylphenyl. (i) Ethyl acetate, -15 ^{o}C.

The mechanism of this reaction illustrates the nature of the guanidine in that it acts as a base to deprotonate the β-ketoesters **61**, leading to an enolate which then co-ordinates with the guanidinium species and this in turn hydrogen bonds to the nitro group of **52** and creates a rigid and highly organizedtransition state **65**. The design of these catalysts **64** was such that all these criteria were met to enable this successful transformation and wide range of similar Michael addition of malonates with nitrostyrene using **62** have been reported.[46] (Figure 14)

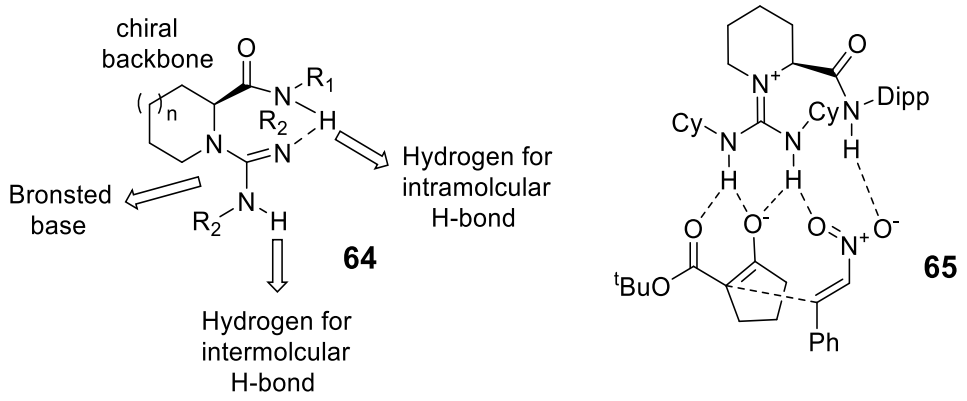

Figure 14: Designation of the bifunctional catalyst **64** and the transition state intermediate **65**. R^1 = Dipp, R^2 = Cy, n = 1.

Recently Terada, et al.[47] successfully developed a series of novel axially chiral guanidines as highly efficient Brønsted base catalysts to promote Michael reactions. For examples the addition of diphenyl phosphite **66** to β-nitrostyrene **52** was catalyzed by 5 mol % of **67** in t-BuOMe as a solvent at -40 °C and gave a 98% yield of adduct **68** in an 92% ee.[47] (Scheme 10)

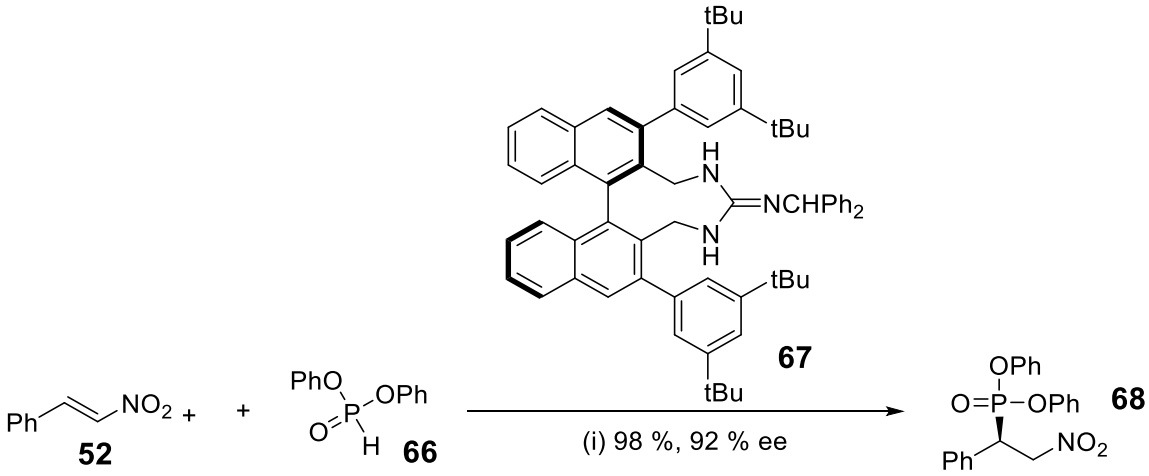

Scheme 10: Michael additions catalyzed by **67**. (i) tBuOMe, -40 °C, 10 min.

Similarly, catalyst **69** gave a high enantioselectivity in the addition of the malonate to nitrostyrene **52** (Scheme 11).[48] In a similar fashion to the example shown above, it is thought that the catalyst activates the reaction through hydrogen bond interactions producing a well-defined

orientation for the transition state involved in the process. Yields as high as 99 % with enantioselectivities of 79 % ee were reported in the presence of toluene as a solvent.[48]

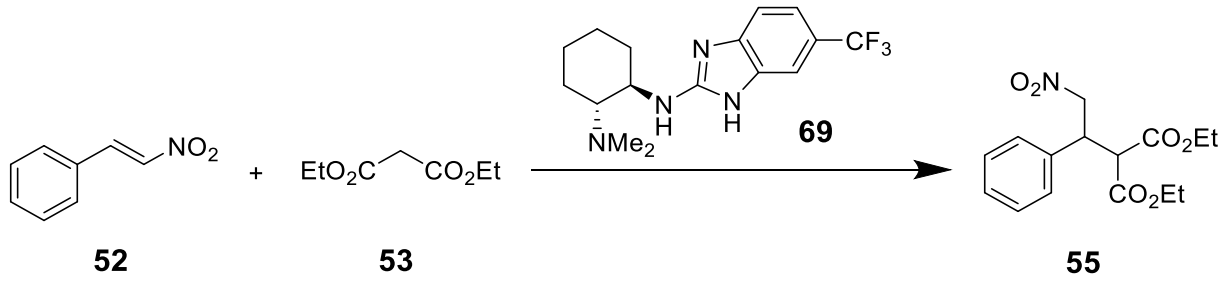

Scheme 11: The addition of the malonate **53** to β-nitrostyrene **52.**

An interesting compound containing both guanidine and thiourea moieties **71** was reported by Shubina.[49] He reported the Michael additions of acetyl acetone **70** to trans-β-nitrostyrene **52** catalyzed by **71** at 20 mol % in toluene at rt which resulted in the formation of the corresponding adduct **72** in yields 54% but gave a low 25% ee. The poor ee reported for this process was thought to arise from a high conformational activity of the guanidine-thiourea complex formed with the enolised acetylacetone, which leads to several different transition states which are all of very similar energy.[49] (Scheme 12)

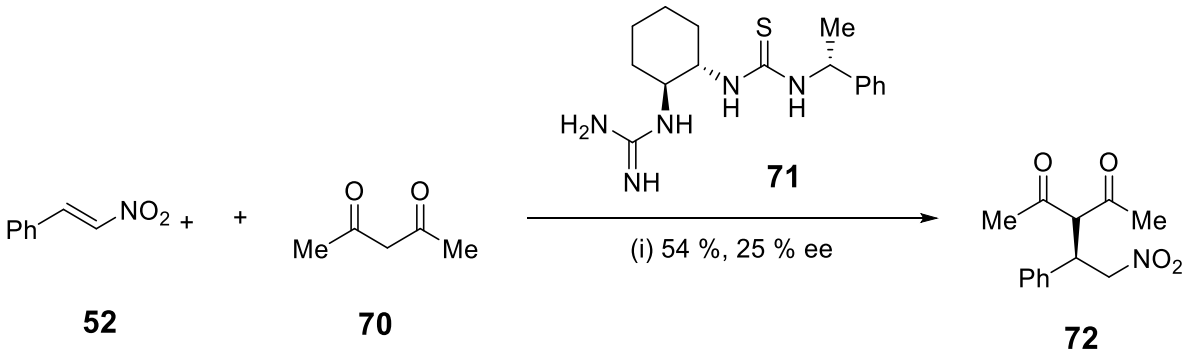

Scheme 12: Michael additions catalyzed by **71**. Toluene, rt, 120 h.

Bronsted acid-base guanidium catalysts.

Some chiral guanidine derivatives, for example **73** and **74**, have been recently been reported to act as organocatalysts and have the benefit of dual hydrogen-bonding during their catalytic cycles.[50] (Figure 15)

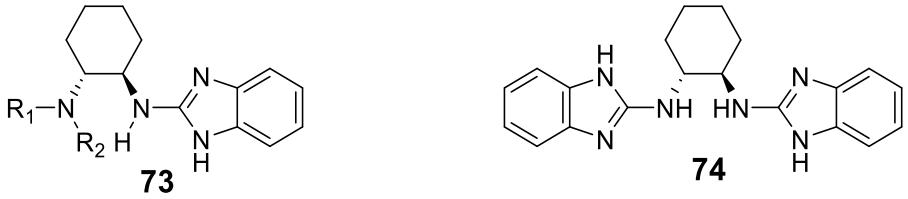

Figure 15: Hydrogen bond donor catalysts **73** and **74**.
R^1, R^2 = H, Me, Et, 2,5-dimethylpyrrol-1-yl or piperidin-1-yl.

These organocatalysts have a high activity and they are general catalyst for the enantioselective addition of malonates, β-ketoesters, and 1,3-diketones to nitroalkenes such as β-nitrostyrene **52**.[50] For example, Gómez-Torres et al.[50] reported the addition of acetylacetone **70** to maleimide **75** catalysed by the guanidine/guanidinium catalyst **76**. This reaction gave a 81 % isolated yield of the adduct **77** with an enantiomeric excess of 99 %. (Scheme 13)

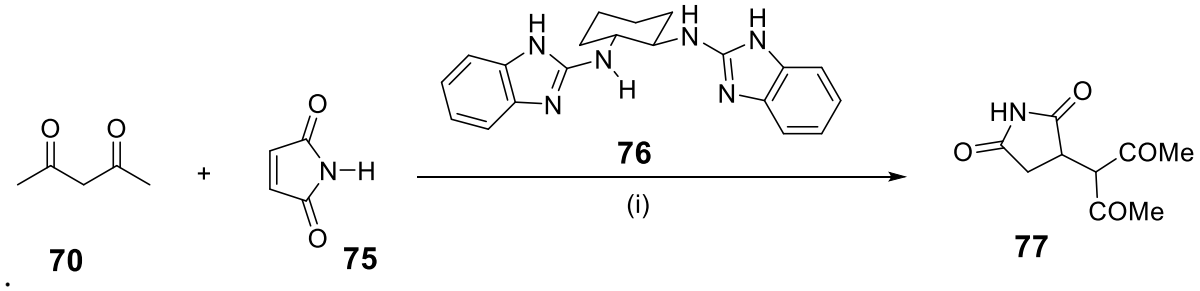

Scheme 13: The addition of acetylacetone **70** to maleimide **75** catalysed by **76**; (i) **76** (0.1 eqv.), TFA (0.1 eqv). 30 °C, 24 h, 81 %, 99 % ee.

The guanidine acts as a base deprotonating the acetylacetone whilst the guanidinium group acts as a coordination site for the maliemide. The nucleophilic enolate can now coordinate in a bidentate manner to the newly formed guanidinium ion and performs a Si face attack to the now activated malonate. This occurs via a single hydrogen bonding interaction with the carbonyl group.[51] (Figure 16)

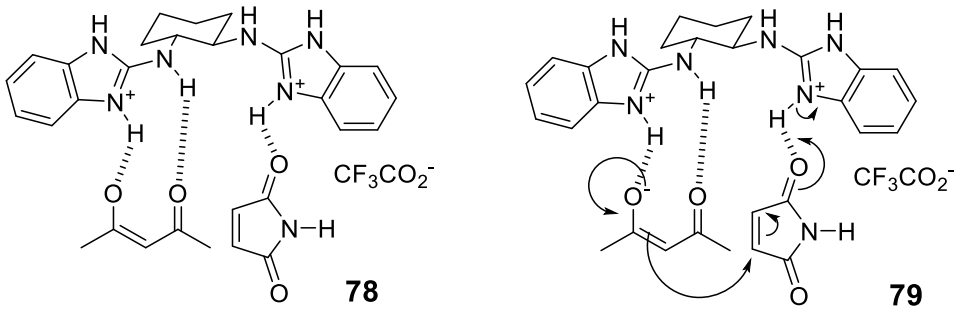

Figure 16: Transition state and mechanism for the conjugate addition of **67** to **72**.

Conclusion

As can be seen by the examples discussed above there is considerable interest in organocatalysis, driven by the efficiency of the processes and their ability to effect transformations in the absence of transition metals. However many of these catalysts are complex structures which require multistep syntheses and as such are highly expensive and would not be applicable to large scale synthesis which would limit their use in practical applications for example in the pharmaceutical industry. The guanidine motif is interesting in so much as it can act as both a base to remove a proton and then once deprotonated as an acid site for coordination of the anionic species formed. In addition the basicity of the guanidine can be lowered by the addition of acyl containing substituents which will lead to a similar behavior (acidic) to that observed in thioureas. Within this project we hope to prepare a range of homochiral substituted guanidines which are simplistic in nature and are thus easily prepared and investigate their application to enantioselective transformations.

Background, aims and objectives

Previous work within the group has focused on the application of c2-symmetric guanidinium salts **80a-e** as catalysts for various asymmetric transformations.[51,52] (Figure 17)

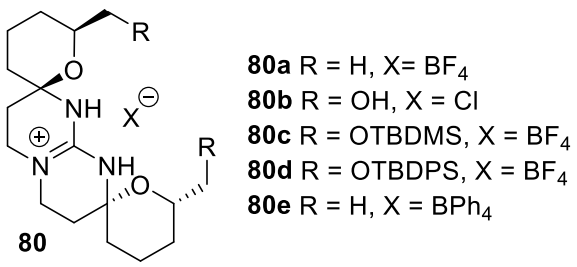

Figure 17: Guanidinium salts **80a-d**.

Early studies[51,52] included the application of **80a-d** to asymmetric phase transfer catalysis and it was found that guanidinium salt **80a** transformed effectively nearly complete conversion of **81** to the desired product, which was obtained as the (*R)*-enantiomer in 86% ee. The catalyst **80b** gave the worst results with very low conversion and low ee, which can be attributed to its poor solubility in the organic phase of the reaction. The silyl protected catalysts **80c** and **80d** gave a lower percentage conversion but, still gave the alkylated products as the (*R)*-enantiomer in good ee, 65% and 74%, respectively.[51,52] (Scheme 14, Table 1).

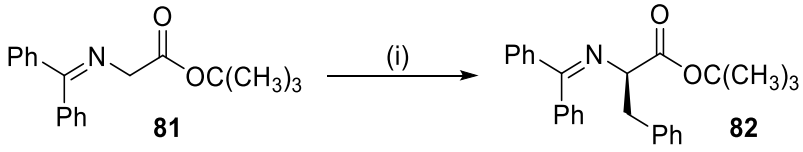

Scheme 14: (i) Catalyst **80**, (0.1 eqv), NaOH (2M), BnBr (2 eqv), CH_2Cl_2, 16 h, 0 °C.

Table 1: phase transfer benzylation of **81**.

Entry	Catalyst **7**	% conv.	% ee
1	**80a**	>97%	86% (R)
2	**80b**	15%	21% (R)
3	**80c**	70%	65% (R)
4	**80d**	80%	74% (R)

The catalyst **80a** was also successfully applied to the phase transfer epoxidation of chalcones **10** leading to the chalcone epoxides **84** in 51-99% yield and in excellent ees of 85-94%.[51,52] (Scheme 15)

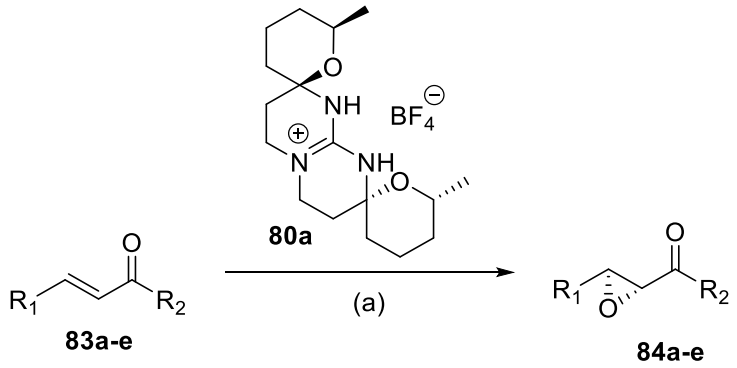

Scheme 15: (a) **80a** (0.1-0.025 eqv), NaOCl, LiOCl or KOCl (aq), Toluene, 16-72 h °C-rt. R_1 = Ph, 4-ClPh, C_6H_{13}, R_2 = Ph, 4-ClPh.

Application of the free guanidine form **80a** was less successful as a catalyst when applied to the nitro-aldol (Henry reaction) or nitro-Michael reactions. It was found that using the free base **80** in the reaction of isovaleraldehyde **85** with nitromethane gave **86** in 52% yield and in disappointing 20% ee. Similarly **80** catalysed the Michael addition of 2-nitropropane to chalcone **87** to yield **88** in 70% yield and a poor 23% ee. (Scheme 16) [51,52]

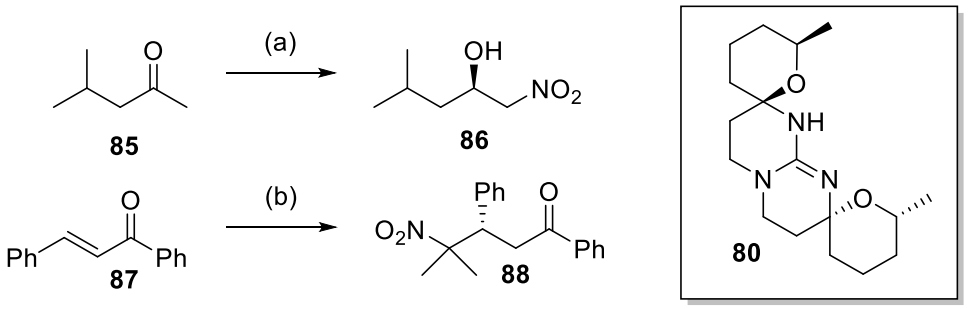

Scheme 16: (a) **80a**, CCl_4, rt, 16 h; (b) **80a**, THF, rt, 24 h.

Interestingly the guanidinium salts **80a-e** were found to be good catalysts for the conjugate addition of pyrrolidine **52** to unsaturated lactone **51**.[51,52] It was observed that there was an increase in rate of reaction for all the guanidine salts **80a-e** over the uncatalysed reaction. It was found that catalyst **80a** gave a 4.3-fold increase in reaction rate, whilst the TBDMS-catalyst **80c** gave a 9.6-fold increase. A further improvement was found when catalyst **80e** was employed, in which the BF_4^- counter-ion was exchanged for the more bulky BPh_4^-, which led to a 16.3-fold increase in reaction rate over the uncatalysed process. The effect of the BPh_4^- counter-ion in this process is that it is less coordinating and has a decreased hydrogen bonding interaction with the guanidine, thus allowing an easier formation of the proposed intermediate **92**. Interesting the TBDPS-catalyst **80d** gave very little increase in rate possibly showing that there is an inter-play between steric bulk and lipophilicity. Disappointingly no asymmetric induction was observed in this reaction which was attributed to the site of addition being too far removed from any possible point of asymmetric induction within the intermediate **92**.[51,52] (Scheme 17)

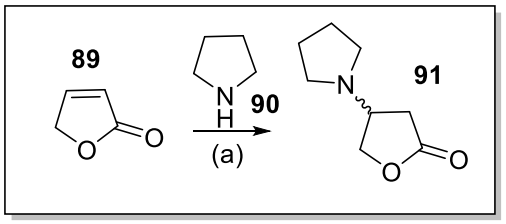

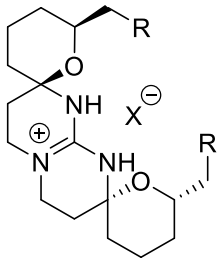

No catalyst $T_{1/2}$ = 115 min

80a	$T_{1/2}$ = 27 min(4.3 x)
80b	$T_{1/2}$ = 43 min(2.7 x)
80c	$T_{1/2}$ = 12 min(9.6 x)
80d	$T_{1/2}$ = 108 min(1.1 x)
80e	$T_{1/2}$ = 7 min(16.3 x)

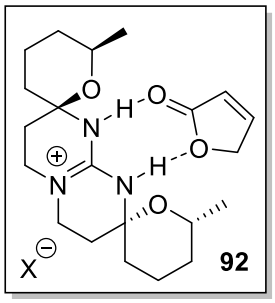

Scheme 17: (a) **80a-e** (0.1 eqv), 0.3 M in $CDCl_3$ rt.

A similar effect was observed with the Michael addition of 2-hydroxy-1,4-napthoquinone **93** to β-nitrostyrene **52**,which was catalysed by the tetracyclic guanidine salts **80e**, but only in the presence of an acid such as *L*-proline **37**.[51,52] It was observed that the two substrate molecules **93** and **52** which were unreactive on combination in THF were slowly converted to the product **94** in the presence of catalyst **80e** with a $T_{1/2}$ of 465 h. The reaction was also catalyzed slowly in the presence of *L*-proline with a $T_{1/2}$ of 579 h in THF. However if the two catalysts **80e** and *L*-proline were used in combination the reaction proceeded with a $T_{1/2}$ of 80 h. Unfortunately no appreciable enantioselectivity was observed in any of the catalysed reactions which again, can be attributed to the site of reaction being too far removed from the point of asymmetric induction within the proposed intermediate **95**.[51,52] (Scheme 18)

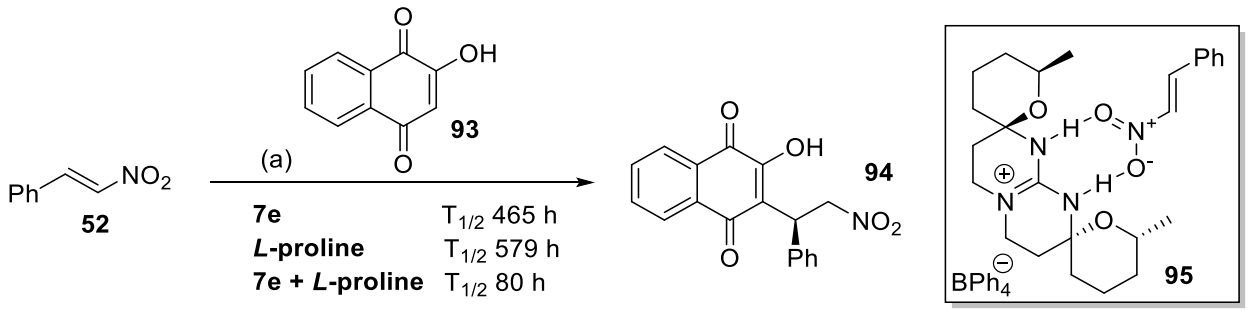

Scheme 18: (a) THF, catalysts (0.05 eqv)

As was apparent from our work in this area and the work of other groups, there is potential for the application of guanidine or guanidinium catalysts in asymmetric catalysis. The nature of many organocatalysts hinges on the formation of highly organised transition states which are held together by effective hydrogen-bonding networks. In these catalysts the presence of these Lewis acidic (H-bonding) and Lewis basic sites leads to the concept of a bifunctional catalytic mode being favoured. Guanidine derivatives are interesting in so much as they are able to act as both powerful bases which are orders of magnitude more basic than simple amines, but once protonated are effective H-bonding sires with potential for interaction with negatively charged functional groups, for example carboxylates, enolates, carbonyls, enols, phosphates and nitro-groups. It might also be possible to apply the primary amine of guanidine to organocatalysis with a synchronous dual activation (simultaneous Lewis acidic and Lewis basic interactions).[51,52]

With this concept in mind the key aim of this work was the investigation of the Michael reaction in the presence of novel guanidine or guanidinium catalysts which it was hoped would lead to the formation of a high enantioselective adduct and thus enable a stereospecific reaction to be achieved. We hoped to model our catalysts on a proline scaffold as this appears to be one that is successfully applied to a range of other successful catalytic processes. Initial aims were to prepare a range of guanidine catalysts **96** which were able to be modified at the nitrogen of the proline R-group, which might act as a control over the steric factors in any potential reactions. These prolines are then covalently bonded to a guanidine moiety via the amide and could be "tuned" by the nature of the R^1 groups on the non-amide nitrogens, leading to some measure of electronic and hydrogen bonding control which might occur for example with a nitro function **99** (figure 18). Protonation of the catalysts, during deprotonation, might result in a range of possible structures in which one might imagine protonation at the proline nitrogen **97** or at the guanidine **98** and this might lead to a range of intramolecular hydrogen bonding patterns. We might also be able to investigate catalysis of guanidinium salts **100** as the hydrogen bonding motif in these could potentially lead to a catalytic species in itself. (Figure 18)

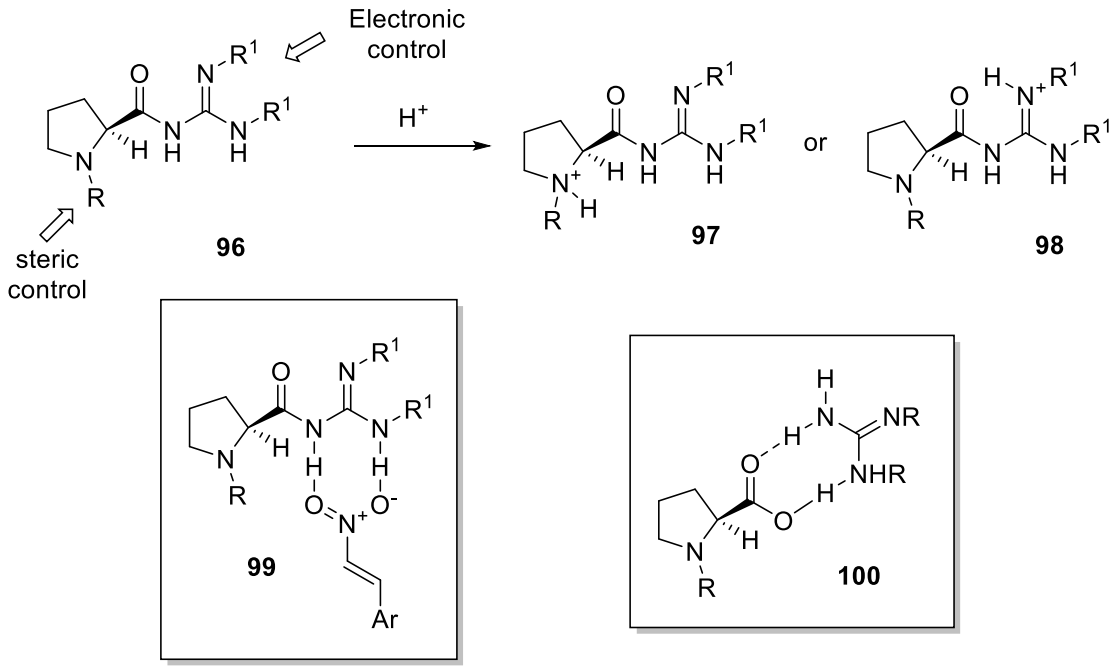

Figure 18: Guanidines and guanidiume salts.

Thus our initial aim is to prepare a range of guanidine catalysts and the next chapter deals with the successes and problems encountered in this investigation.

DISCUSSION

Investigation into the catalytic activity of guanidine salts on Michael additions

Preparation of catalysts

This chapter of the thesis covers the preparation of the various proline catalysts and a brief discussion of the motivation behind their synthesis. It is not a chronological discussion of the work but is organized in such a way to cover all the areas investigated. Data analysis is given where appropriate and mention of other data discussed later, including X-ray structures.

N-substituted prolines

We intended to study a range of *N*-substituted prolines and we set about the synthesis of these compounds beginning with *N*-methyl-*L*-proline **101** which was prepared using a literature method.[53] This involved the use of formaldehyde under hydrogenation conditions with Pd on carbon in methanol. In our hands this reaction proceeded in 68-94 % yield over 7 attempts, to give the desired compound **101** as a crystalline solid which had spectroscopic and optical rotation data in agreement with the literature.[53] (Scheme 19)

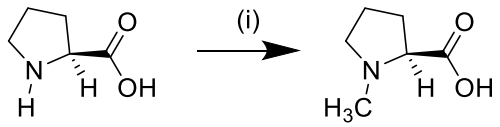

Scheme 19: Preparation of *N*-methyl-*L*-proline **101**
(i) CH_2O, H_2, Pd/C, MeOH, 16-48 h.

N-benzyl-*L*-proline **102** was synthesized in a different manner, by the dropwise addition of BnCl **103** to a solution of **37** and KOH in *i*PrOH at 40 °C over 3 h. After stirring for a further 6 h the reaction was then neutralized with HCl to pH 5-6 then stirred overnight. The product was filtered from the solution, washed with $CHCl_3$ to give **102** in 46% yield which had spectroscopic and optical rotation data in agreement with the literature[54]. (Scheme 20)

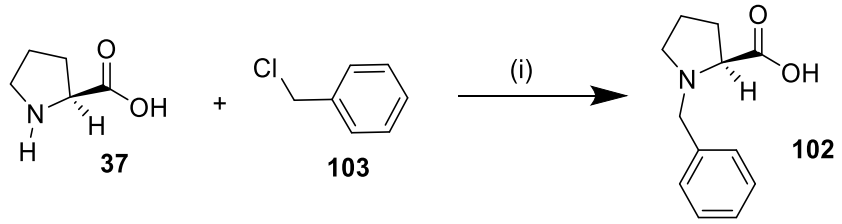

Scheme 20: Preparation of *N*-benzyl *L*-proline **102**
(i) KOH, *i*PrOH, HCl, 40 °C, 20 h.

N-Isopropyl-*L*-proline **104** was prepared by a reaction reaction between *L*- proline **37** with acetone **105** under hydrogenation conditions over Pd/C. After stirring for two days, work up gave **104** as a crystalline yellow solid in 95% yield, which had spectroscopic and optical rotation data in agreement with the literature.[55] (Scheme 21)

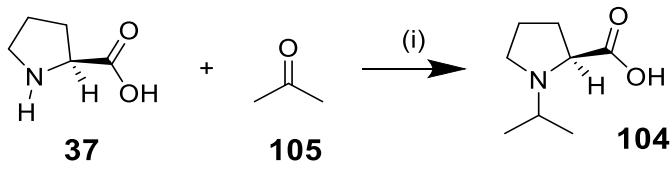

Scheme 21: Preparation of isopropyl-*L*-proline **104**
(i) H_2, Pd/C, rt, 24 h.

Where salts were used in any reaction the general method for their preparation was to dissolve both the desired guanidine and *N*-methyl-*L*-proline **101** in the required solvent or a solvent in which both dissolve, typically dry methanol, and then evaporate the mixture to dryness. This mixture was then re-dissolved in the required solvent when used in further reaction (*vide infra*). (Scheme 22)

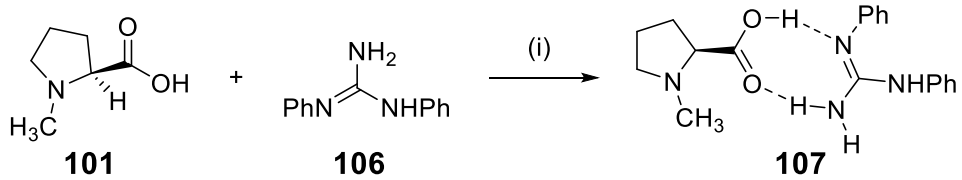

Scheme 22: Preparation of **107**, (i) dry MeOH

Proline *N*-Cbz-Guanidine derivatives

Initially we were interested in preparing acyl protected guanidines to use as coupling agents for our *N*-alkylated prolines. We intended to study the simple benzoyl guanidine **109**, which was prepared by dissolving guanidine hydrochloride in NaOMe solution, and after 3 h ethyl benzoate **108** was added and the mixture stirred at rt for 18 h and at reflux for 5 h. On work up and recrystallization a poor yield of 2% of **109** was obtained. The reaction was repeated using guanidine carbonate and sodium ethoxide in ethyl alcohol followed by filtration under an inert atmosphere which gave a solution of guanidine free from inorganic salts, which were thought to be a problem in the previous preparation. After evaporation of this solution neat ethyl benzoate **108** was added and the mixture stirred for 20 h. After recrystallization from hot dioxane **109** was obtained in an acceptable 32 % yield; spectroscopic data was in agreement with the literature.[56] (Scheme 23)

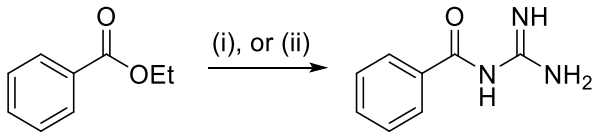

108 **109**

Scheme 23: Preparation of **109**: (i) Guanidine hydrochloride, NaOMe, MeOH. (ii) Guanidine carbonate, NaOEt, EtOH.

Benzoyl guanidine **109** was coupled with *N*-methyl-*L*-proline **101** by stirring the proline derivative with the activating agent CDI in dry DMF for 16 h followed by the addition of guanidine **109**. After 3 d, an extractive work up and column chromatography gave **110** as a crude oil. On initial inspection the reaction appeared to be successful, however on standing at room temperature, particularly if dissolved in a solvent the compound underwent a rapid decomposition to give a poorly soluble solid which was analysed by NMR and proved to be the starting material **109**. (Scheme 24)

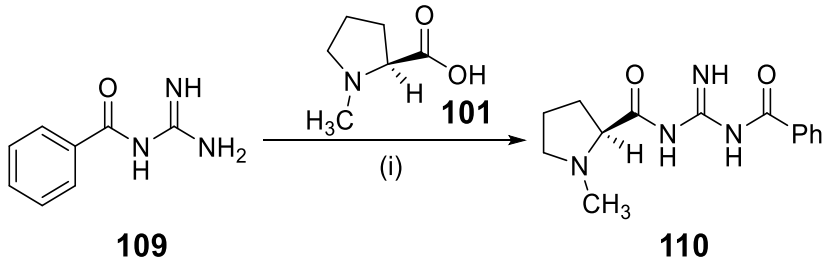

Scheme 24: Preparation of **85**: (i) CDI, DMF, rt, 3 d.

This decomposition suggested that **110** was might be acting as an acyl transfer reagent, such as is found in peptide coupling and that the benzoyl guanidine is a good leaving group. This observation has implications for the work as it is apparent that a fine balance must be drawn between leaving group ability and activation. This also suggests that we were serendipitous to some extent, as in tandem with this work we were engaged in the preparation of Cbz-protected guanidine derivatives which were found to be more stable to the conditions of purification and handling which we have employed so far.

The derivatives of the *N*-substituted prolines were prepared from the protected *N*-Cbz-Guanidine **113** which was prepared by the addition of a solution of benzoyl chloride **111** dissolved in dioxane to a solution of guanidine hydrochloride **112** dissolved in water. After stirring for 15 h, an extractive work up and recrystallization gave guanidine **113** as a white solid in 82% which had spectroscopic data in agreement with the literature.[57] (Scheme 25)

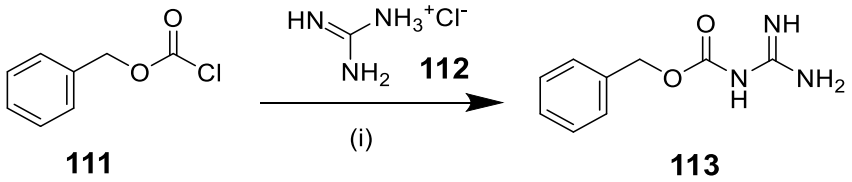

Scheme 25: Preparation of *N*-Cbz-guanidine **113**: (i) NaOH, Doxane, water, 22 h.

We initially tried to prepare compound **114** by adapting a coupling method found in the literature[53] used on similar proline derivatives. We thus dissolved *N*-methyl-*L*-proline **101** and *N*-Cbz-Guanidine **113** in dry DMF in the presence of DMAP. The coupling reagent DCC was then added at 0°C and the mixture stirred overnight and after worked up we obtained a complex mixture of products. The method proved problematic as initially the reagents did not appear to dissolve fully

and NMR analysis did not give any signals indicative of the proline ring expected in the target compound. We thus repeated the reaction again using CDI as the coupling agent which was added to the proline **101** and on stirring for 3 h this dissolved at which point the guanidine **113** was added and the reaction stirred for 24 h. We initially worked up this reaction by the addition of methanol, evaporation of the DMF in a freeze dryer and chromatography. However, this process resulted in the formation of the by-product **115** (from **113**, CDI and MeOH) which proved difficult to remove from the desired product even on repeated chromatography. We modified the work up by adding water to hydrolyze the unreacted CDI and after column chromatography we obtained **114** in 68 and 68-73 % yield over 2 attempts. Interestingly examination of the X-ray structure of **115** (figure 20) revealed a distinctive hydrogen bonding pattern (figure 21) in which the NH_2 of the guanidine was H-bonded to each of the carbonyls, possibly explaining the activation of the benzoyl substituted proline guanidine to hydrolysis. (Scheme 26)

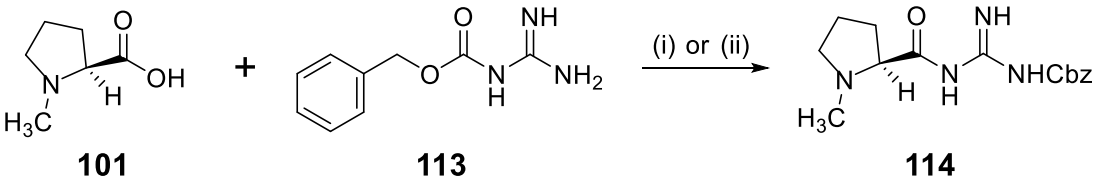

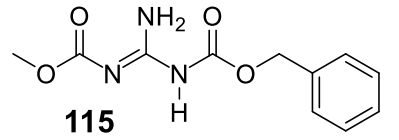

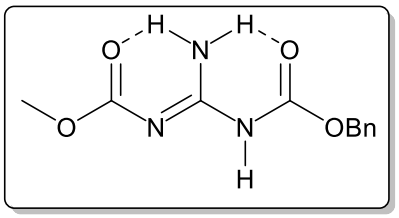

figure 21

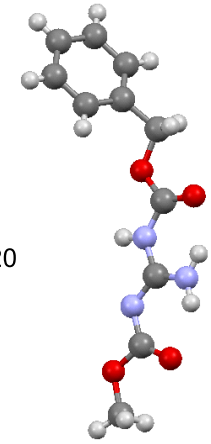

figure 20

Scheme 26: Preparation of **114**. (i) DCC, DMAP, DMF, 0°C, 16 h. (ii) CDI, DMF, rt, 20-48 h.

The analytical data obtained for **114** confirmed its structure. The compound gave a negative optical rotation value of $[\alpha]_D^{21}$ -64.8 whilst the proton NMR spectrum gave a signal at δ_H 8.88 (3H, br. s, 3 x NH) ppm for the guanidine NH protons and signals at δ_H 7.25 (1H, s, CH), 7.22-7.11 (4H, m, CH) ppm for the aromatic ring. The benzyl methylene was observed at δ_H 5.00 (2H, s, CH_2) ppm, whilst the methyne proton for the proline was observed as a double doublet at δ_H 2.86 (1H, dd, J = 10.4, 4.9 Hz, CH) ppm. The methyl signal was observed at δ_H, 2.23 (3H, s, Me) ppm, whilst the

remaining signals for the proline ring were at δ_H 2.99-2.84 (1H, m, CH), 2.27-2.13 (1H, m, CH), 2.14-2.04 (1H, m, CH), 1.78-1.71 (1H, m, CH) and 1.67-1.56 (2H, m, CH_2) ppm. The carbon spectrum exhibited the required 13 non-equivalent signals with the methyne carbon in the proline ring at δ_C 69.0 ppm. Finally analysis by mass spectrometry gave an ion 305.2 (100%) for $M+H^+$, which on accurate mass measurement gave a mass of 305.1610 Daltons which corresponded well to the required mass of 305.1608 Daltons for $C_{15}H_{21}N_4O_3^+$ ($[M+H^+]$).

The benzyl substituted compound **116** was prepared in a similar manner to **114** by reacting *N*-benzyl-*L*-proline **102** with CDI in dry DMF for 3 h, followed by the addition of Cbz-guanidine **113** at 0°C. After stirring for two days, the reaction diluted with water and extracted with ethyl acetate and after chromatography an 89% yield of **116** was obtained as a white solid. (Scheme 27)

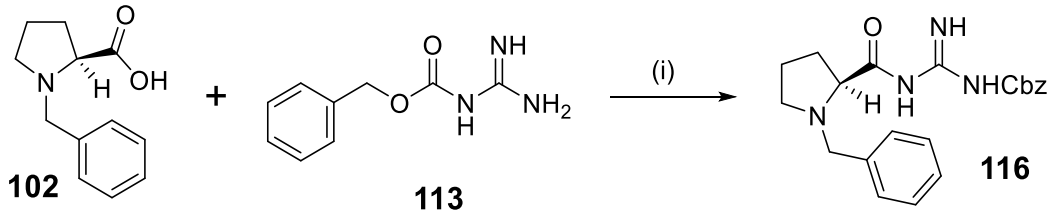

Scheme 27: Preparation of **116**. (i) CDI, DMF, rt, 2 d.

The analytical data obtained for **116** confirmed its structure. The compound gave a negative optical rotation value of $[\alpha]_D^{22}$ -67.1 whilst the proton NMR spectrum gave two signals at δ_H 9.75 (1H, br s, NH) and 8.76 (2H, s, NH) ppm for the guanidine NH protons and signals at δ_H 7.43-7.36 (2H, m, 2 x CH), 7.36-7.30 (3H, m, 3 x CH) and 7.31-7.16 (5H, m, Ph) ppm for the two benzene rings. The benzyl methylene for the Cbz group was observed as two doublets at δ_H 5.15 (1H, d, *J* 12.5 Hz, CH) and 5.10 (1H, d, *J* 12.5 Hz, CH) ppm whilst the *N*-benzyl methylene was observed as a singlet at δ_H 3.69 (2H, s, CH_2) ppm. The distinctive methyne proton for the proline was observed as a double doublet at δ_H 3.24 (1H, dd, *J* 10.3, 4.4 Hz, CH_2) ppm, whilst the remaining signals for the proline ring were at δ_H 3.69 (2H, s, CH_2), 3.03-3.13 (1H, m, CH), 2.36-2.51 (1H, m, CH), 2.13-2.28 (1H, m, CH), 1.81-1.91 (1H, m, CH) and 1.64-1.81 (2H, m, CH_2) ppm. The carbon spectrum gave the required 17 non-equivalent signals with the methyne carbon in the proline ring appearing at δ_C 66.9 ppm. Finally analysis by mass spectrometry gave an ion at 381.2 Daltons for $M+H^+$,

which on accurate mass measurement gave a mass of 381.1919 Daltons which corresponded well to the required mass of 381.1921 Daltons for $C_{21}H_{25}N_4O_3^+$ ([M+H$^+$]).

The *N*-isopropyl compound **117** was similarly prepared by reacting *N*-isopropyl-*L*-proline **104** with CDI in dry DMF over 3-4 h at rt, followed by the addition of **113** at 0°C. After stirring for two days, the reaction was diluted with water and extracted with ethyl acetate. After co-evaporation heptane, chromatography gave a 99% of **117** was obtained as a yellow oil. (Scheme 28)

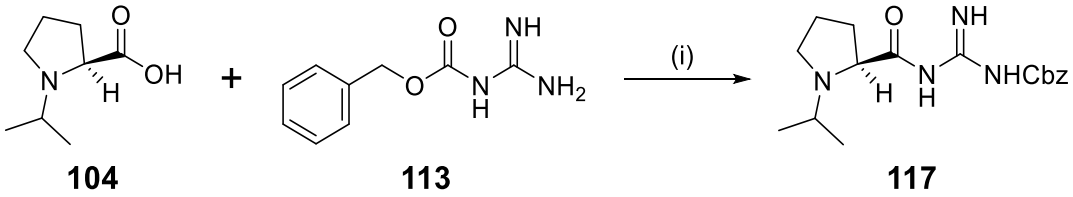

104 **113** **117**

Scheme 28: Preparation of **117**. (i) CDI, DMF, rt, 2 d.

The analytical data obtained for **117** confirmed its structure. The compound gave a negative optical rotation value of $[\alpha]_D^{20}$ -31.1 whilst the proton NMR spectrum gave three signals at δ_H 9.93 (1H, br s, NH), 9.05 (1H, br s, NH) and 8.86 (1H, br s, NH) ppm for the guanidine NH protons and signals at δ_H 7.39-7.43 (2H, m, 2 x CH) and 7.28-7.37 (3H, m, 3 x CH) ppm for the benzene protons. The benzyl methylene was observed as two doublets at δ_H 5.16 (1H, d, *J* 12.5 Hz, CH) and 5.12 (1H, d, *J* 12.5 Hz, CH) ppm, whilst the two methyne protons for the proline and isopropyl were observed as a double doublet at δ_H 3.34 (1H, dd, *J* 10.6, 2.4 Hz, CH) and 3.05-3.16 (1H, m, CH) ppm respectively. The remaining signals for the proline ring were at δ_H 2.72-2.83 (1H, m, CH), 2.48-2.58 (1H, m, CH), 2.07-2.20 (1H, m, CH), 1.89-1.98 (1H, m, CH), 1.74-1.84 (1H, m, CH) and 1.62-1.74 (1H, m, CH) ppm, whilst the two isopropyl methyl signals were observed at δ_H 1.06 (3H, d, *J* 7.0 Hz, Me) and 1.04 (3H, d, *J* 7.0 Hz, Me) ppm. The carbon spectrum gave the required 15 non-equivalent signals with the methyne carbon in the proline ring appearing at δ_C 65.7 ppm. Finally analysis by mass spectrometry gave an ion 333.2 Daltons for M+H$^+$, which on accurate mass measurement gave a mass of 333.1920 Daltons which corresponded well to the required mass of 333.1921 Daltons for $C_{17}H_{25}N_4O_3^+$ ([M+H$^+$]).

The *N*-cyclohexyl compound **119** was similarly prepared by reacting *N*-cyclohexyl-*L*-proline **118** with CDI in dry DMF to give instant dissolution and an orange solution which was stirred for 4 h at rt, following which Cbz-Guanidine **113** was added at 0^{o}C. After 18 h, the reaction

was diluted with water and extracted with ethyl acetate which on evaporation gave crude **119**, which was dissolved in a minimum amount of MeOH and diethyl ether added to the cloud point and on cooling overnight gave **119** in 93% yield as a pale yellow solid. (Scheme 29)

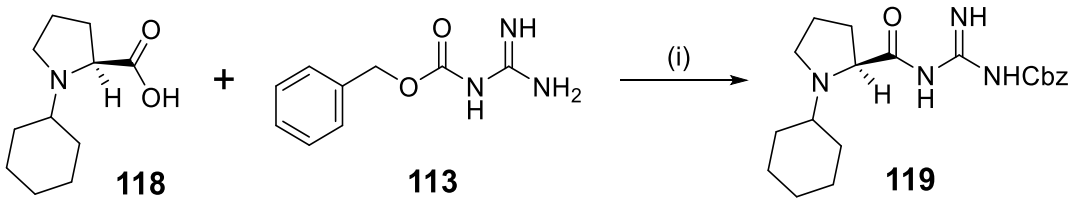

Scheme 29: Preparation of **119**. (i) CDI, DMF, rt, 18 h

The analytical data obtained for **119** confirmed its structure. The compound gave a negative optical rotation value of $[\alpha]_D^{16}$ -63.5 whilst the proton NMR spectrum gave three signals at δ_H 9.92 (1H, s, NH), 9.08 (1H, s, NH) and 8.87 (1H, s, NH) ppm for the guanidine NH protons and signals at δ_H 7.38-7.49 (2H, m, 2 x CH) and 7.27-7.37 (3H, m, 3 x CH) ppm for the aromatic protons. The benzyl methylene was observed as a pair of doublets at δ_H 5.16 (1H, d, *J* 12.3 Hz, CH) and 5.12 (1H, d, *J* 12.3 Hz, CH) ppm, whilst the two methyne protons for the proline and Cy were observed as a double doublet at δ_H 3.38 (1H, dd, *J* 2.9, 10.7 Hz, CH) ppm and 3.11-3.21 (1H, m, CH) ppm respectively. The remaining signals for the proline and aliphatic Cy rings were at δ_H 2.52-2.62 (1H, m, CH), 2.32-2.42 (1H, m, CH), 2.04-2.18 (1H, m, CH), 1.55-1.98 (8H, m, 8 x CH) and 1.05-1.27 (5H, m, 5 x CH). The carbon spectrum gave the required 18 non-equivalent signals with the methyne carbon in the proline ring appearing at δ_C 67.2 ppm. Finally analysis by mass spectrometry gave an ion 373.2 Daltons for $M+H^+$, which on accurate mass measurement gave a mass of 373.2233 Daltons which corresponded well to the required mass of 373.2234 Daltons for $C_{20}H_{29}N_4O_3^+$ ($[M+H^+]$).

The yields for the Cbz- protected proline derivatives was found to very high in all four compounds investigated and we next proceeded to prepare some analogues with aryl substituted guanidines.

Proline diphenylguanidine derivatives

With the desired range of Cbz-substituted compounds successfully prepared we proceeded to make a range of guanidine substituted compounds. The first of these compounds **120** was prepared by reacting *N*-methyl-*L*-proline **101** with CDI in dry DMF over 24 h, the reaction was then cooled to 0°C and commercially available diphenyl guanidine **106** was added and the mixture stirred overnight at rt. After the addition of water, the reaction was extracted with ethyl acetate, dried, evaporated then co-evaporated with heptane to remove traces of DMF. Purification by column chromatograpy gave **120** in 28% yield as a pale yellow solid. (Scheme 30)

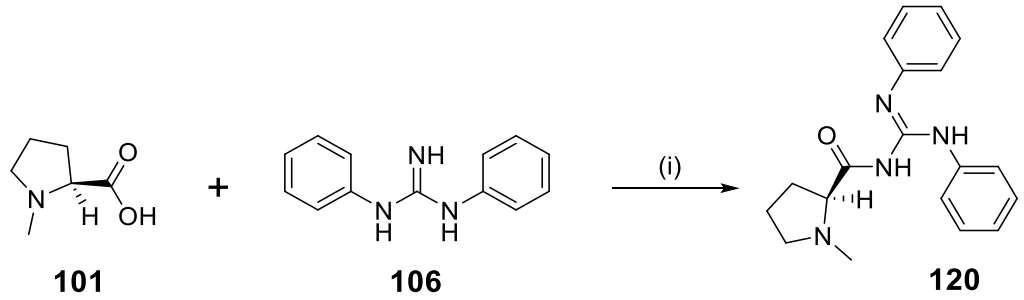

101 **106** **120**

Scheme 30: Preparation of **120**. (i) CDI, DMF, rt, 40 h.

The analytical data obtained for **120** confirmed its structure. The compound gave a positive optical rotation value of $[\alpha]_D^{20}$ +38.1 whilst the proton NMR spectrum gave two signals at δ_H 9.92 (1H, br. s, NH) and 9.78 (1H, s, NH) ppm for the guanidine NH protons and signals at δ_H 7.70 (2H, d, *J* 7.9 Hz, 2 x CH), 7.27-7.36 (4H, m, 4 x CH), 6.98-7.07 (2H, m, 2 x CH) and 6.90 (2H, d, *J* 7.7 Hz, 2 x CH) ppm for the aromatic ring protons. The methyne proton for the proline was observed as a double doublet at δ_H 2.93 (1H, dd, *J* 10.5, 4.2 Hz, CH) ppm, whilst the remaining signals for the proline ring were at δ_H 2.62-2.69 (1H, m Hz, CH), 2.20 (1H, ddd, *J* 5.9, 8.9, 10.8 Hz, CH), 2.01-2.14 (1H, m, CH), 1.60-1.78 (2H, m, 2 x CH) and 1.35-1.51 (1H, m, CH) ppm. The *N*-methyl signal was observed as a singlet at δ_H 2.10 (3H, s, Me). The carbon spectrum gave the required 15 non-equivalent signals with the methyne carbon of the proline ring appearing at δ_C 55.7 ppm. Finally analysis by mass spectrometry gave an ion 323.2 for $M+H^+$, which on accurate mass measurement gave a mass of 323.1861 Daltons which corresponded well to the required mass of 323.1866 Daltons for $C_{19}H_{23}N_4O^+$ ($[M+H^+]$).

The corresponding *N*-benzyl compound **121** was prepared in a similar manner, by reaction *N*-benzyl-*L*-proline **102** with CDI in dry DMF for 5 h at rt, whereupon the reaction was cooled to

0°C and 1,3-diphenylguanidine **106** was added and the mixture stirred overnight. After an extractive work up, purification by column chromatography gave **121** in 33 % yield as a pale yellow solid. (Scheme 31)

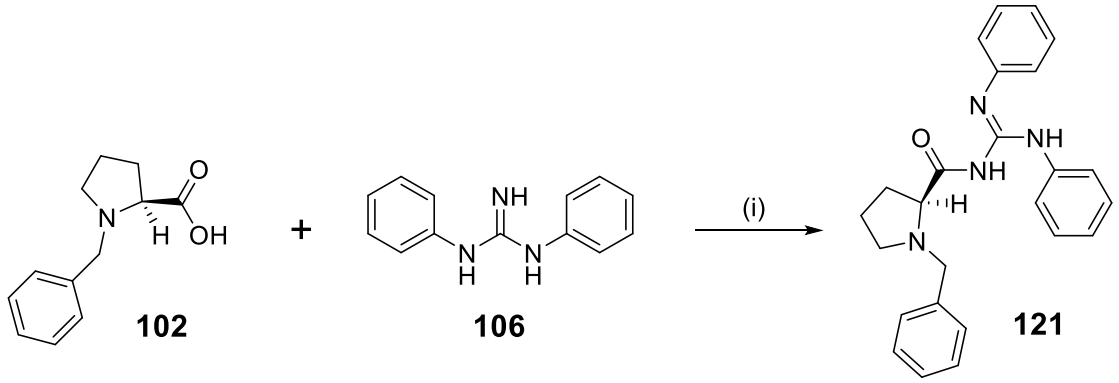

Scheme 31: Preparation of **121**. (i) CDI, DMF, rt, 20 h.

The analytical data obtained for **121** confirmed its structure. The compound gave a positive optical rotation value of $[\alpha]_D^{21}$ +22.3 whilst the proton NMR spectrum gave two signals at δ_H 9.93 9.97 (1H, s, NH) and 9.89 (1H, s, NH) ppm for the guanidine NH protons and signals at δ_H 7.67 (2H, d, *J* 8.0 Hz, 2 x CH), 7.38 (2H, t, *J* 7.7 Hz, 2 x CH), 7.30 (2H, t, *J* 7.7 Hz, 2 x CH).7.17-7.23 (3H, m, 3 x CH), 7.10 (1H, t, *J* 7.4 Hz, CH) 6.95-7.04 (3H, m, 3 x CH) and 6.69-6.75 (2H, m, 2 x CH)ppm for the aromatic ring protons. The benzyl methylene was observed as two doublets at δ_H 3.66 (1H, d, *J* 13.0 Hz, CH) and 3.37 (1H, d, *J* 13.0 Hz, CH) ppm, whilst the methyne proton for the proline was observed as a double doublet at δ_H 3.26 (1H, dd, *J* 10.3, 3.6 Hz, CH) ppm. The remaining signals for the proline ring were at δ_H 2.59-2.66 (1H, m, CH), 2.09-2.28 (2H, m, 2 x CH), 1.82-1.92 (1H, m, CH), 1.70-1.77 (1H, m, CH), 1.50-1.64 (1H, m, CH) ppm. The carbon spectrum gave 19 non-equivalent signals with the methyne carbon in the proline ring appearing at δ_C 58.7 ppm. Finally analysis by mass spectrometry gave an ion at 399.2 Daltons for $M+H^+$, which on accurate mass measurement gave a mass of 399.2179 Daltons which corresponded well to the required mass of 399.2177 Daltons for $C_{25}H_{27}N_4O^+$ ($[M+H^+]$).

Similarly, the *N*-isopropyl substituted compound **122** was prepared by reacting isopropyl-*L*-proline **104** with CDI in dry DMF for 5 h at rt, followed by cooling to 0°C, whereupon 1,3-diphenylguanidine **106** was added and the mixture stirred overnight. After an aqueous work up and extraction with ethyl acetate, column chromatography gave **122** in 84% yield as a white solid. (Scheme 32)

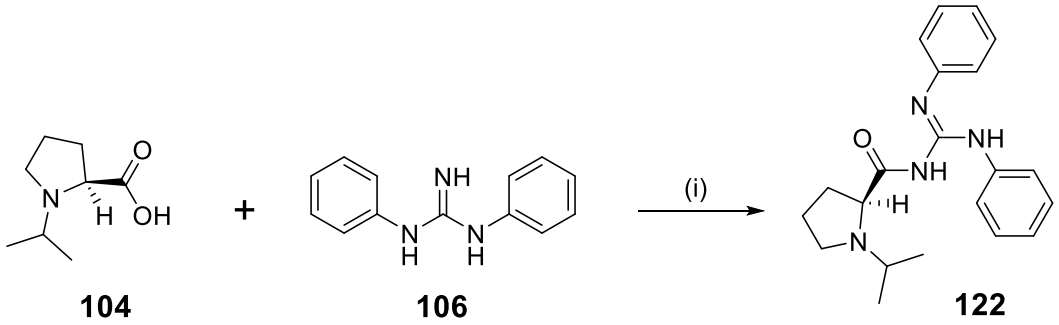

104 **106** **122**

Scheme 32: Preparation of **122**. (i) CDI, DMF, rt, 52 h.

The analytical data obtained for **122** confirmed its structure. The compound gave a positive optical rotation value of $[\alpha]_D^{16}$ +52.1, whilst the proton NMR spectrum gave two signals at δ_H 10.23 (1H, s, NH) and 9.99 (1H, s, NH) ppm for the guanidine NH protons and signals at δ_H 7.73 (2H, d, *J* 8.0 Hz, 2 x CH), 7.28-7.37 (4H, m, 4 x CH), 6.99-7.08 (2H, m, 2 x CH) and 6.91-6.96 (2H, m, 2 x CH) ppm for the aromatic ring protons. The methyne protons for the proline and isopropyl were observed as a double doublet at δ_H 3.25 (1H, dd, *J* 9.7, 2.9 Hz, CH) ppm and at 2.65-2.72 (1H, m, CH) ppm respectively. The remaining signals for the proline ring were observed at δ_H 2.45-2.57 (1H, m, CH), 2.33 (1H, ddd, *J* 5.6, 8.9, 11.4 Hz, CH), 1.91-2.08 (2H, m, 2 x CH), 1.68-1.77 (1H, m, CH) and 1.42-1.57 (1H, m, CH). The two isopropyl methyl signals were observed at δ_H 0.74 (3H, d, J = 6.4, Me) and 0.73 (3H, d, J = 6.4, Me) ppm. The carbon spectrum gave 17 non-equivalent signals with the methyne carbon in the proline ring appearing at δ_C 52.9 ppm. Finally analysis by mass spectrometry gave an ion at 351.2 Daltons for $M+H^+$, which on accurate mass measurement gave a mass of 351.2183 Daltons which corresponded well to the required mass of 351.2179 Daltons for $C_{21}H_{27}N_4O^+$ ($[M+H^+]$).

The *N*-cyclohexyl-substituted compound **123** was prepared by reacting *N*-cyclohexyl-*L*-proline **118** with CDI in dry DMF over 4 h at rt, followed by cooling to 0°C, whereupon 1,3-diphenylguanidine **106** was added and the mixture stirred for 2 d. After an aqueous work up and extraction with ethyl acetate, column chromatography gave **123** in 84% yield as an off white solid. (Scheme 33)

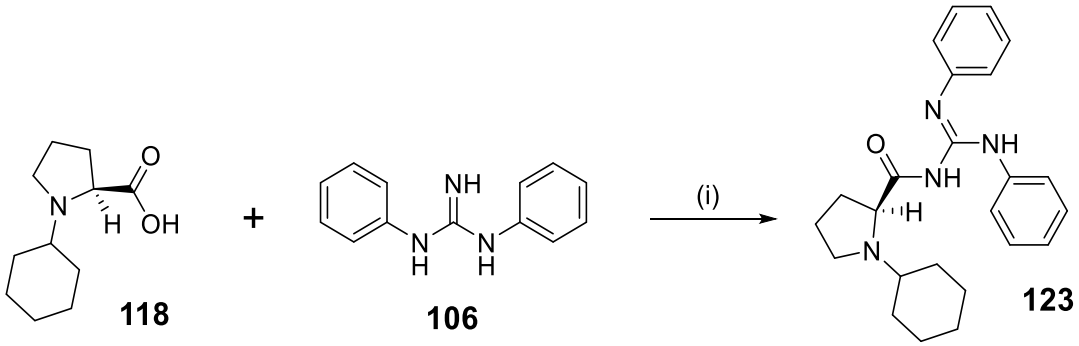

Scheme 33: Preparation of **123**. (i) CDI, DMF, rt, 48 h.

The analytical data obtained for **123** confirmed its structure. The compound gave a positive optical rotation value of $[\alpha]_D^{15}$ +6.5 whilst the proton NMR spectrum gave two signals at δ_H 10.21 (1H, s, NH) and 9.98 (1H, s, NH) ppm for the guanidine NH protons and signals at δ_H 7.72 (2H, d, *J* 7.5 Hz, 2 x CH), 7.25-7.30 (4H, m, 4 x CH), 6.97-7.10 (2H, m, 2 x CH) and 6.93 (2H, d, *J* 7.3 Hz, CH) ppm for the aromatic ring protons. The two methyne protons for the proline and cyclohexyl group were observed as a double doublet at δ_H 3.28 (1H, dd, *J* 3.0, 9.4 Hz, CH) and 2.71 (1H, t, *J* 7.5 Hz, CH) ppm respectively. The remaining signals for the proline and cyclohexyl rings were observed at 2.33 (1H, ddd, *J* 5.6, 8.5, 11.4, CH), 2.04-2.14 (1H, m, CH), 1.91-2.03 (1H, m, CH), 1.41-1.75 (7H, m, 7 x CH), 1.36 (1H, d, *J* 12.3 Hz, CH), 0.90-1.05 (3H, m, 3 x CH), 0.75-0.87 (1H, m, CH) and 0.60-0.74 (1H, m, CH) ppm. The carbon spectrum gave 20 non-equivalent signals with the methyne carbon in the proline ring appearing at δ_C 50.6 ppm. Finally analysis by mass spectrometry gave an ion at 391.2 Daltons for $M+H^+$, which on accurate mass measurement gave a mass of 391.2482 Daltons which corresponded well to the required mass of 391.2492 Daltons for $C_{24}H_{31}N_4O^+$ ($[M+H^+]$).

In general the yields for the synthesis of the diphenyl-substituted proline guanidines were found to be better for the more non-polar (lipophilic) *N*-substituted prolines. The reason for this is unclear but it might be due to ease of work up as these are far more soluble in the ethyl acetate which was used for extraction. We next went on to investigate the preparation of some mono-phenyl substituted guanidine derivatives.

Proline monophenylguanidine derivatives

We wished to prepare mono-phenyl substituted guanidines and as this guanidine or its salts are not cheaply available we needed to prepare it. A literature preparation from aniline **124** was found[57] which involved the addition of an aqueous nitric acid solution cautiously to a cooled (0°C) solution of aniline in ethanol which generated aniline nitrate salt. Following this an aqueous solution of cyanamide was added and the mixture heated at reflux overnight. After cooling, the addition of diethyl ether, precipitated phenylguanidinium nitrate **126** in 86% yield as a gray solid. Data and melting point was in agreement with the literature.[58] (Scheme 34)

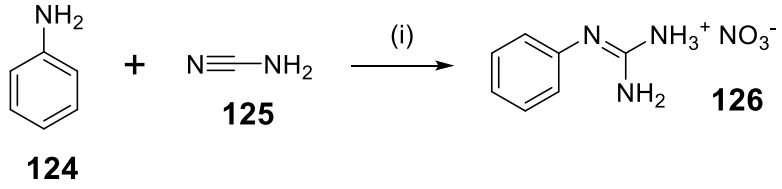

Scheme 34: Preparation of **126**. (i) HNO_3, EtOH, 0°C, 18 h.

The phenylguanidinium nitrate **126** was then reacted *N*-Methyl-*L*-proline, which was suspended in dry DMF, following which CDI was added and the mixture stirred for 2-3 h. In a separate flask phenylguanidinium nitrate **126** was treated with sodium methoxide in methanol then evaporated to dryness and the solution of activated proline was then added to this via cannula and the mixture stirred for 5 days. Water was added and the mixture extracted with ethyl acetate and the combined extracts washed with water, dried ($MgSO_4$) and evaporated under reduced pressure and purification by column chromatography to give the compound **127** in 40% yield as a pale yellow solid. (Scheme 35)

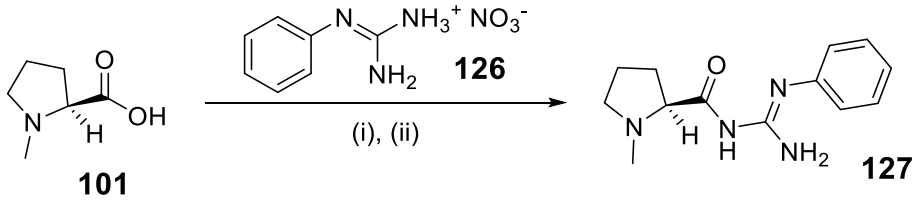

Scheme 35: (i) CDI, DMF, 3 h. (ii) Na, 3h; then rt, 5 d.

The analytical data obtained for **127** confirmed its structure. The compound gave a negative optical rotation value of $[\alpha]_D^{16}$ -80.1 whilst the proton NMR spectrum gave signals at δ_H 7.33 (2H,

t, *J* 8.0, 2 x CH), 7.06 (1H, t, *J* 7.5 H, CH), 6.95-7.00, (2H, m, 2 x CH) ppm for the aromatic ring protons, and a signal at δ_H 5.00-6.89 (3H, br s, 3 x NH) ppm for the guanidine NH protons. The methyne proton for the proline was observed as a double doublet at δ_H 3.02 (1H, dd, *J* 10.4, 4.8 Hz, CH) ppm whilst the *N*-methyl signal was observed at δ_H 2.44 (3H, s, Me) ppm. The remaining signals for the proline ring were at δ_H 3.10-3.24 (1H, m, CH), 2.38-2.46 (1H, m, CH), 2.20-2.32 (1H, m, CH), 1.91-2.00 (1H, m, CH) and 1.75-1.87 (2H, m, 2 x CH) ppm. The carbon spectrum gave the required 11 non-equivalent signals with the methyne carbon of the proline ring appearing at δ_C 56.5 ppm. Finally analysis by mass spectrometry gave an ion 247.2 for $M+H^+$, which on accurate mass measurement gave a mass of 247.1552 Daltons which corresponded well to the required mass of 247.1553 Daltons for $C_{13}H_{19}N_4O^+$ ($[M+H^+]$).

Similarly *N*-benzyl-*L*-proline **128** was dissolved in dry DMF and CDI was then added and the mixture stirred for 16 h. In a separate flask phenylguanidinium nitrate **126** was treated with sodium methoxide in methanol then evaporated to dryness and the solution of activated proline was then added to this via cannula and the mixture stirred for 5 days. Water was added and the mixture extracted with ethyl acetate and the combined extracts washed with water, dried ($MgSO_4$) and evaporated under reduced pressure and purification by column chromatography gave the compound **128** in 52% yield as a yellow oil.(Scheme 36)

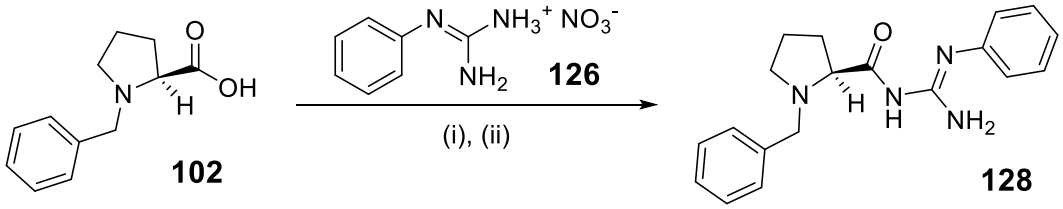

Scheme 36: (i) CDI, DMF, 16 h. (ii) Na, 3h; then rt, 5 d.

The analytical data obtained for **128** confirmed its structure. The compound gave a negative optical rotation value of $[\alpha]_D^{16}$ -47.6 whilst the proton NMR spectrum gave signals at δ_H 7.20-7.45 (7H, m, 7 x CH), 7.04 (1H, t, *J* 7.4 Hz, CH) and 6.96-7.01 (2H, m, 2 x CH) ppm for the aromatic ring protons. A broad signal at δ_H 5.50-7.20 (3H, br s, 3 x NH) ppm corresponded to the three guanidine NH protons. The benzyl methylene was observed as two doublets at δ_H 3.80 (1H, d, *J* 12.5 Hz, CH) and 3.68 (1H, d, *J* 12.5 Hz, CH) ppm, whilst the methyne proton of the proline was

observed as a double doublet at δ_H 3.27 (1H, dd, *J* 4.4, 10.4 Hz, CH) ppm. The remaining signals for the proline ring were observed at δ_H 3.00-3.17 (1H, m, CH), 2.40-2.53 (1H, m, CH), 2.17-2.33 (1H, m, CH), 1.92-2.03 (1H, m, CH) and 1.70-1.87 (2H, m, 2 x CH) ppm. The carbon spectrum gave 15 non-equivalent signals with the methyne carbon in the proline ring appearing at δ_C 67.3 ppm. Finally analysis by mass spectrometry gave an ion 323.2 Daltons for $M+H^+$, which on accurate mass measurement gave a mass of 323.1864 Daltons which corresponded well to the required mass of 323.1866 Daltons for $C_{19}H_{23}N_4O^+$ ($[M+H^+]$).

We next attempted to prepare the *N*-isopropyl mono-phenyl guanidine substituted compound **129** which was attempted by reacting *N*-isopropyl-*L*-proline **104** with CDI to dry DMF overnight then transferring to a solution of phenylguanidine via cannula and stirring for 2 d. Again, after an aqueous work up and extraction with ethyl acetate, ^{1}H NMR spectroscopy demonstrated that a complex mixture of products had been formed and attempted isolation of the components of this mixture by repeated column chromatography proved imposible. (Scheme 37)

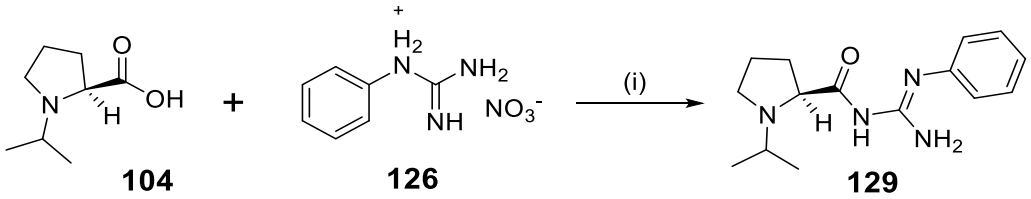

Scheme 37: (i) CDI, DMF, 3 hrs (ii) Add to 126 treated with NaH for 3h, then rt, 2 d.

We did not attempt the preparation of the *N*-cyclohexyl analogue of **119** for reasons which will become apparent in the next chapter and the reasons for the failure to prepare **129** are unclear. We next moved onto the preparation of several 1.1-dimethyl-substituted guanidines.

Proline dimethylguanidine derivatives

As we wished to modify the substitution pattern on the guanidine and wished to prepare an *N*,*N*-disubstituted guanidine compound and intended to utilise commercially available 1,1-dimethylguanidine hemisulfate **130**. We thus reacted *N*-methyl-*L*-proline **101** under our standard conditions by activating it using CDI, followed by the addition of this activated ester to a solution of 1,1-dimethylguanidine generated from its hydrochloride salt by treatment with sodium hydride. After hydrolysis and extractive work up it was found that very little material was recovered and it

was theorized that perhaps the product was highly water soluble. A small sample of the aqueous phase was evaporated and analysis of this gave no indication of the successful formation of **131**. (Scheme 38)

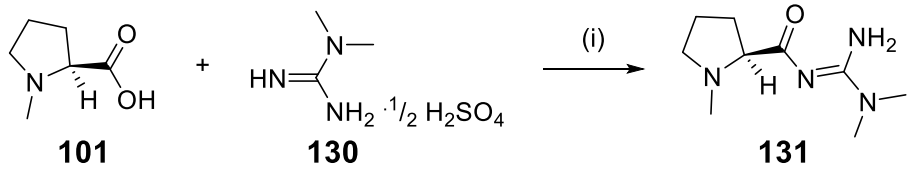

101 **130** **131**

Scheme 38: (i) CDI, DMF, 4 hrs (ii) Add to **130** treated with NaH for 3h, then rt, 2 d.

We were concerned that the polarity of the *N*-methyl substituents was a problem in this reaction and thus investigated the other less polar substituents and also avoided an aqueous work up. The *N*-benzyl substituted derivative **132** was thus prepared in a similar fashion by reacting *N*-benzyl-*L*-proline **102** with CDI in dry DMF over 3-4 h and adding this intermediate via cannula to a solution of 1,1-dimethylguanidine generated by reacting **130** with a slight excess of NaH in DMF for 1 h. After stirring for 42 h the reaction was diluted with 1-2 mL of water then freeze dried and purified by column chromatography to give a crude product which did seem to contain **132** on inspection of the ^{1}H NMR spectrum. Attempted chromatography of the crude product was difficult as the compound co-eluted with imidazole which is a by-product of the CDI Coupling reaction. We attempted to purify the fractions containing the product after chromatography by extracting with water, however the product was water soluble and the majority of it was lost in the aqueous phase. We attempted similar reactions with *N*-isopropyl-*L*-proline **104** in an attempt to prepare **133** and *N*-cyclohexyl-*L*-proline **118** to prepare **134** and met with similar results in that the products were inseparable from the byproducts by chromatography and were very soluble in water. In the case of **134** only crude recovered starting material was obtained. (Scheme 39)

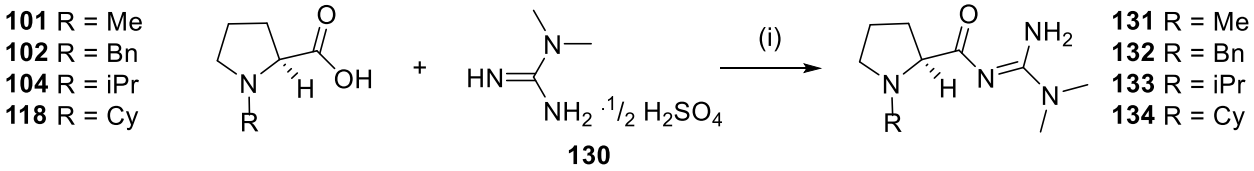

Scheme 39: Attempted preparation of **131-134**. (i) CDI, DMF, 24-72 h (ii) Add to **130** treated with NaH for 3 h, then rt, 2 d.

The dimethyl-substituted prolines proved impossible to purify and were apparently very polar materials due to their solubility in water and the observation that they required methanolic solvent mixtures during column chromatography purification. The high solubility of these compounds in water might be due to the increased basicity of the guanidine which has two electron donating group attached to it, as opposed to the previously prepared compounds which all have two or three electron with drawing substituents. With the disappointing results from these compounds we moved back to a system which had only electron withdrawing substituents.

We wished to prepare a guanidine with a more restricted substitution pattern and were inspired by the work involving 2-aminobenzimidazoles as compounds in Michael additions[50] and also by the report[59] of the benzimidazole-proline derivative **136** which has been used as a compound in the Hajos-Parrish-Eder-Sauer-Wiechert reaction leading to **137** in high yields and ee in this and other aldol type reactions.[59] (Scheme 40)

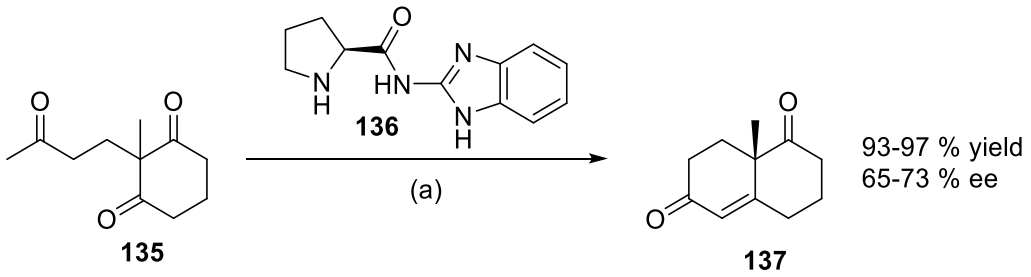

Scheme 40: a) **136** (0.05 mmol), TFA (0.05 mmol), THF, DMSO, MeOH or H_2O, rt. 24 h.

Proline 2-aminobenzimidazole derivatives

The first 2-aminobenzimidazole compound, **139** was prepared by reacting *N*-methyl-*L*-proline **101** with CDI in dry DMF over 4 h at rt, followed by the addition of commercially available 2-aminobenzimidazole **138**. After stirring for 42 h, an aqueous work up followed by extraction with ethyl acetate and chromatography gave **139** in 55% yield as a white solid. (Scheme 41)

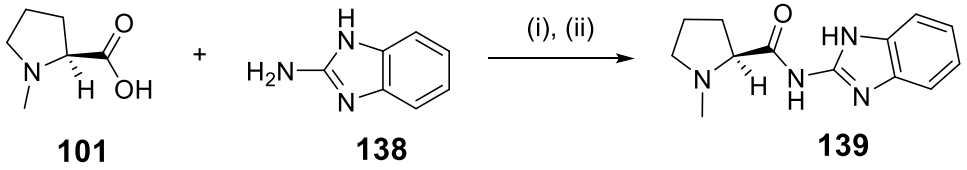

Scheme 41: Preparation of **139**. (i) CDI, DMF, 4 h. (ii) **138**, rt, 42 h.

The analytical data obtained for **139** confirmed its structure. The compound gave a negative optical rotation value of $[\alpha]_D^{16}$ -116.9 whilst the proton NMR spectrum gave a broad signal at δ_H 9.50-12.0 (2H, br s, 2 x NH) ppm for the guanidine NH protons and signals at δ_H 7.42-7.55 (2H, m, 2 x CH) and 7.17-7.25 (2H, m, 2 x CH) ppm for the aromatic ring protons. The methyne proton of the proline ring was observed as a doublet of doublets at δ_H 3.16 (1H, dd, *J* 4.6, 10.6, CH) ppm, whilst the *N*-methyl signal was observed as a singlet at δ_H 2.47 (3H, s, Me). The remaining signals for the proline ring were at δ_H 3.16-3.24 (1H, m, CH), 2.42-2.52 (1H, m, CH) 2.25-2.38 (1H, m, CH), 1.94-2.04 (1H, m, CH) and 1.77-1.90 (2H, m, 2 x CH) ppm. The carbon spectrum gave the 10 non-equivalent signals with the methyne carbon in the proline ring at δ_C 56.8 ppm. Finally analysis by mass spectrometry gave an ion 245.1 for $M+H^+$, which on accurate mass measurement gave a mass of 245.1399 Daltons which corresponded well to the required mass of 245.1397 Daltons for $C_{13}H_{17}N_4O^+$ ($[M+H^+]$).

Similarly the *N*-benzyl compound **140** was prepared by reacting *N*-benzyl-*L*-proline **102** with CDI in dry DMF for 4 h at rt then 2-aminobenzimidazole **138** was added. After 48 h, aqueous workup extracting with ethyl acetate followed by column chromatography gave **140** in 96% yield as a white solid. (Scheme 42)

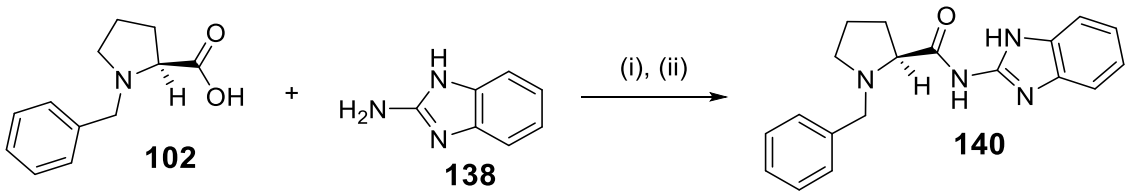

Scheme 42: Preparation of **140**. (i) CDI, DMF, 4 h. (ii) **138**, rt, 48 h.

The analytical data obtained for **140** confirmed its structure. The compound gave a negative optical rotation value of $[\alpha]_D^{16}$ -106.8 whilst the proton NMR spectrum gave two signals at δ_H 10.84

(1H, s, NH) and 10.30 (1H, br s, NH) ppm for the guanidine NH protons and signals at δ_H 7.45-7.65 (1H, m, CH) and 7.05-7.38 (8H, m, 8 x CH) ppm for the aromatic ring protons. The benzyl methylene was observed as two doublets at δ_H 3.79 (1H, d, *J* 12.7 Hz, CH) and 3.64 (1H, d, *J* 12.7 Hz, CH) ppm, whilst the methyne appeared as a double doublet at δ_H 3.37 (1H, dd, *J* 10.6, 4.2 Hz, CH). The remaining signals for the proline ring were observed at δ_H 3.02-3.12 (1H, m, CH), 2.41-2.51 (1H, m, CH), 2.16-2.31 (1H, m, CH), 1.89-2.00 (1H, m, CH) and 1.65-1.84 (2H, m, CH_2) ppm. The carbon spectrum gave the required 15 non-equivalent signals with the methyne carbon of the proline ring appearing at δ_C 66.7 ppm. Finally analysis by mass spectrometry gave an ion 321.2 for $M+H^+$, which on accurate mass measurement gave a mass of 321.1710 Daltons which corresponded exactly to the required mass of 321.1710 Daltons for $C_{19}H_{21}N_4O^+$ ([$M+H^+$]).

The *N*-isopropyl compound **141** was similarly prepared by reacting isopropyl-*L*-proline **104** with CDI in dry DMF for 3 h at rt, followed by the addition of 2-aminobenzimidazole **138**. After 44 h, an aqueous workup extracting with ethyl acetate followed by column chromatography gave 1**41** in 86% as a white solid adduct. (Scheme 43)

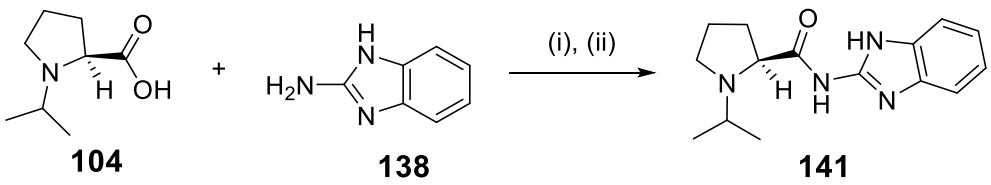

Scheme 43: Preparation of **141**. (i) CDI, DMF, 4 h. (ii) **138**, rt, 44 h.

The analytical data obtained for **141** confirmed its structure. The compound gave a negative optical rotation value of $[\alpha]_D^{16}$ -110.5 whilst the proton NMR spectrum gave two signals at δ_H 11.00 (1H, s, NH) and 10.60 (1H, s, NH) ppm for the guanidine NH protons and signals at δ_H 7.30-7.65 (2H, m, 2 x CH) and 7.16-7.24 (2H, m, 2 x CH) ppm for the aromatic ring protons. The methyne proton signals for the the proline and the isopropyl group were observed as a double doublet at δ_H 3.47 (1H, dd, *J* 10.5, 2.8 Hz, CH) and a multiplet at 3.14-3.21 (1H, m, CH) ppm respectively. The remaining signals for the proline ring were observed at δ_H 2.78-2.91 (1H, m, CH), 2.59 (1H, ddd, *J* 5.8, 9.1, 10.9, CH), 2.09-2.23 (1H, m, CH), 1.98-2.08 (1H, m, CH) and 1.65-1.88 (2H, m, CH_2) ppm, whilst the two methyl signals were observed as doublets at δ_H 1.11 (3H, d, *J* 6.5 Hz, Me) and 1.10 (3H, d, *J* 6.5 Hz, Me). The carbon spectrum gave 12 non-equivalent signals with the

methyne carbon of the proline ring occurring at δ_C 51.0 ppm. Finally analysis by mass spectrometry gave an ion 273.2 for $M+H^+$, which on accurate mass measurement gave a mass of 273.1710 Daltons which corresponded exactly to the required mass of 273.1710 Daltons for $C_{15}H_{21}N_4O^+$ ($[M+H^+]$).

Similarly the *N*-cyclohexyl compound **142** was prepared by reacting *N*-cyclohexyl-*L*-proline **118** with CDI in dry DMF for 4 h at rt after which, 2-aminobenzimidazole **138** was added. After 48 h, aqueous workup extracting with ethyl acetate followed by column chromatography gave **142** in 84% yield as a pale yellow solid. (Scheme 44)

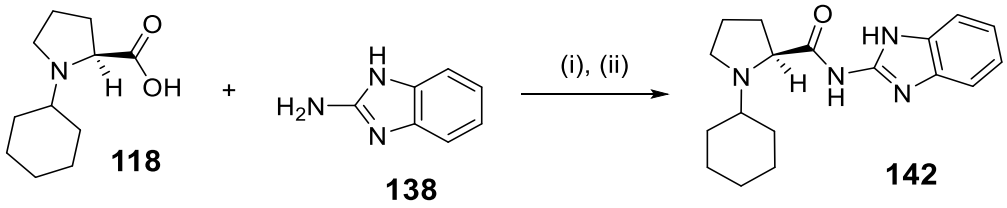

Scheme 44: Preparation of **142**. (i) CDI, DMF, rt, 4 h. (ii) **138**, rt, 48 h.

The analytical data obtained for **142** confirmed its structure. The compound gave a negative optical rotation value of $[\alpha]_D^{15}$ -105.1 whilst the proton NMR spectrum gave three signals at δ_H 12.10 (1H, s, NH) and 10.72 (1H, s, NH) ppm for the guanidine NH protons and signals at δ_H 7.36-7.52 (2H, m, 2 x CH) and 7.04-7.14 (2H, m, 2 x CH) ppm for the aromatic ring protons. The two methyne protons for the proline and cyclohexyl groups were observed as a double doublet at δ_H 3.55 (1H, dd, *J* 10.1, 3.0 Hz, CH) and a multiplet at 3.12-3.20 (1H, m, CH) ppm respectively. The remaining signals for the proline and cyclohexyl rings were observed at δ_H 2.56-2.66 (1H, m, CH), 2.40-2.50 (1H, m, CH), 2.03-2.17 (1H, m, CH), 1.81-1.95 (2H, m, 2 x CH), 1.63-1.81 (5H, m, 5 x CH), 1.49-1.59 (1H, m, CH) and 1.02-1.28 (5H, m, 5 x CH) ppm. The carbon spectrum gave 15 non-equivalent signals with the methyne of the proline ring at δ_C 313.2 ppm. Finally analysis by mass spectrometry gave an ion 333.2 for $M+H^+$, which on accurate mass measurement gave a mass of 313.2016 Daltons which corresponded well to the required mass of 313.2023 Daltons for $C_{18}H_{25}N_4O^+$ ($[M+H^+]$).

The 2-aminobenzimidazole compounds were very easily prepared with good yields for all four compounds and were easily purified by chromatography, which was in contrast to many of the previous compounds prepared.

Miscellaneous Preparations

The guanidine salt TBD.HBPh$_4$ **144** was required for part of the work and was prepared by adding a solution of NaBPh$_4$ in H$_2$O to the guanidine TBD **143** dissolved in dilute hydrochloric acid (10 %), and the mixture stirred for 48 h. The precipitated product was filtered, washed off with water and methanol then triturated with methanol to give **144** in 84% yield which had data in agreement with the literature.[60] (Scheme 45)

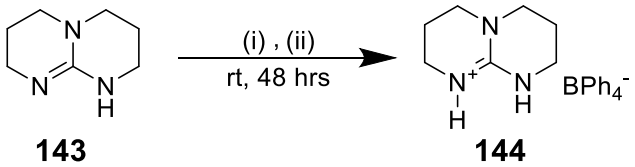

143 **144**

Scheme 45: Preparation of **144**: (i) HCl (aq. 10%). (ii) NaBPh$_4$

We also utilised diphenylguanidine **106**, Cbz-guanidine **113** and N,N'-Bis-Boc-guanidine **145**, phenylbiguanine hydrochloride **146** and the guanidine salts **147-151** as catalysts in our studies. Cbz-guanidine **113** was prepared as reported previously and other guanidines were commercially available. The salts **147-151** were prepared from these compounds by either combining the corresponding guanidine and carboxylic acid in the reaction solvent, or by premixing the components in methanol and evaporating this mixture to dryness before dissolving in the required reaction solvent. (Figure 22)

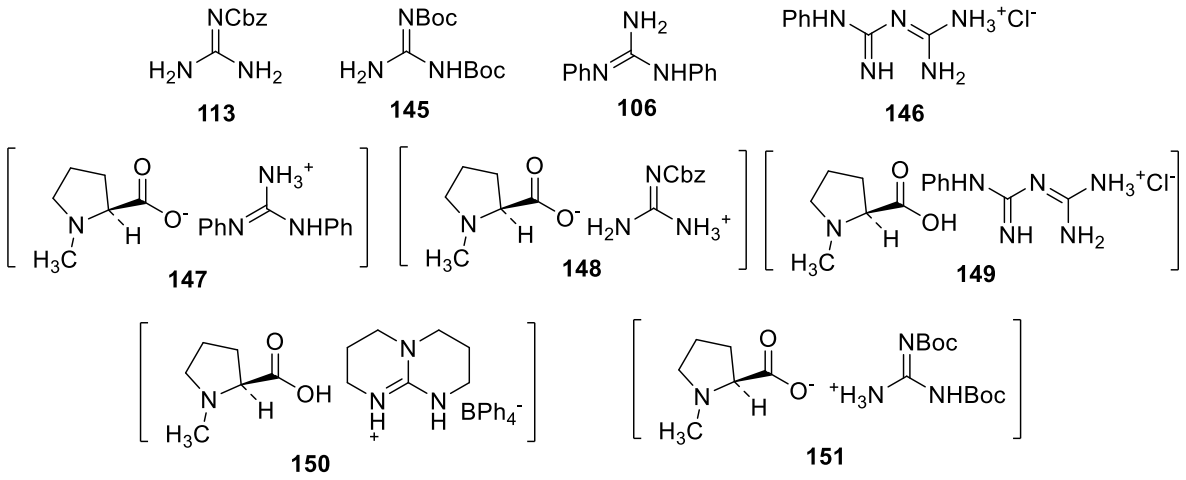

Figure 22: Guanidines and guanidinium salts used in the studies

Investigations into the guanidinium salt mediated asymmetric Michael addition reaction

We initially studied the Michael addition of diethyl malonate **53** with β-nitrostyrene **52** which has been shown to be a reaction catalyzed by a wide range of organocatalysts.[43,48] (Scheme 46)

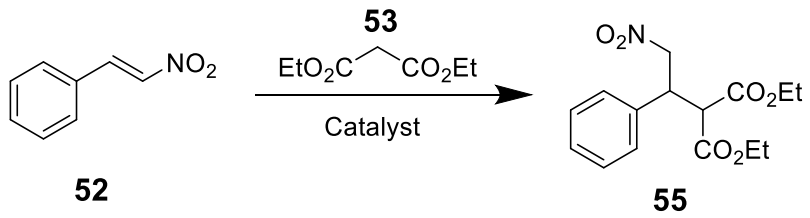

Scheme 46: Michael addition reaction and catalysts studies.

Our initial investigations involved the study of the reaction catalysed by the simple base triethylamine **150**, which was performed to obtain a racemic sample of the adduct **55**. We thus took a sample of 2-nitrostyrene **52** and diethyl malonate **53** in the presence of a catalytic amount (0.1 eqv.) of triethylamine **150** in toluene and followed the reaction by NMR. (Table 2, entry 1) On investigation of this reaction it was found that after 2 days the conversion of the starting material **52** and **53** to the adduct **55** was 28%. This was calculated by integrating the CH vinylic proton at δ 8.02 (1H, d J = 13.7 Hz) of the starting material **52** and the CH proton at δ 3.82 (1H, d, J = 9.3 Hz) in the adduct **55** and comparing the relative intensities. Purification of the product by column chromatography gave **55** in 25% yield.

We repeated the reaction with diphenyl guanidine **106** and on analysis of the NMR after 2 days it was apparent that the reaction had gone to completion entry 2. This is not surprising as the basicity of guanidines (pK$_a$ = 13-14) is much higher than that of simple amines (pK$_a$ = 10-11). We wished to see if this guanidine **106** could catalyze the reaction in the presence of the homochiral acid *N*-methyl-*L*-proline **101** and combined them in toluene and reacted them under the standard conditions (entry 3). Analysis by proton NMR indicated a complete reaction after 1 day and on purification we obtained a disappointing 27 % yield of the adduct **55**. This yield is surprising as the NMR spectrum of the reaction is clean and there did not appear to be any other by-product in the reaction. However in this and later reactions the precipitation of an insoluble solid was observed suggesting a base catalysed polymerisation might be occurring under the reaction conditions. We were unable to get clean NMR data on this precipitated solid and the nature and mode of this decomposition is still unclear. Analysis of the product **55** by chiral HPLC gave a 7% enantiomeric

excess so this reaction was proceeding in essentially a racemic manner. The rapid conversion and low yield might suggest that either the guanidine salt might be in equilibrium with its free base which is deprotonating the malonate or that the *N*-methyl-*L*-proline **101** is acting as a catalyst independently of the guanidine. We attempted to catalyze the reaction using *N*-methyl-*L*-proline **101** alone and found that no reaction occurred possibly because it was insoluble in dichloromethane. (Table 2, entry 4)

We repeated this reaction in dichloromethane and in this case had to pre-form the salt in methanol before dissolution in the reaction solvent. These three reaction varied by the amount of the malonate **53** present and in the first case (Table 2, entry 4) the use of a large excess of reagent led to a complete conversion after 3 d and a high isolated yield of 80%. The use of a lower equivalence of 1.1 equivalents gave again a rapid conversion over 2 d but a much lower isolated yield of 18 %; again no other major impurities were apparent in the NMR spectra. Using 2 equivalents of malonate gave a complete reaction in 28 hours and this reaction was monitored more closely using regular NMR sampling. After 1 h of reaction it had reached a 13% completion and after 2 h it had reached 33% conversion which suggests a reasonably rapid conversion rate. The isolated yield for the adduct **55** was again low at 35 % which is hard to explain. Analysis of the products of these three reactions by chiral HPLC again gave a low enantiomeric excess (3 - 7%), so they were proceeding in essentially a racemic manner. (Table 2)

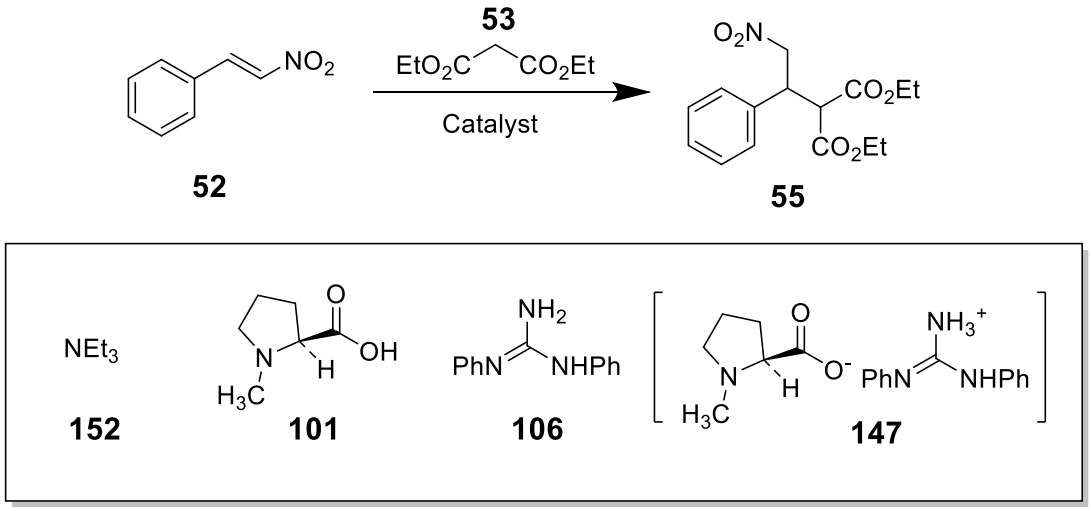

Scheme 47: Michael addition reaction and catalysts **101**, **106**, **147** and **152**.

Table 2: Entries 1-6.

Entry	Catalyst (0.1 eqv.)	Malonate (eqv.)	Solvent	Time	Conversion (NMR)	Yield/%	ee %
1	**152**	1.0	Toluene	3 d	28 %	25	NA
2	**106**	1.1	Toluene	2 d	100 %	ND	NA
3	**101**	1.1	Toluene	1 d	100 %	27	7 (R)
4	**147**	10.7	CH_2Cl_2	3 d	100 %	80	4 (R)
5	**147**	1.1	CH_2Cl_2	2 d	100 %	18	7 (R)
6	**147**	2.0	CH_2Cl_2	28 h	100 %	35	3 (R)

We next investigated the reaction of the biguanine salt **153** which we hoped might be less reactive as a catalyst as it is protonated. We attempted to use it as a catalyst on its own and found that it was insoluble in dichloromethane (Table 3, entry 1) and other non-protic solvents, and in fact it was only sparingly soluble in methanol. We thus combined **153** with *N*-methyl-*L*-proline **101** in methanol and attempted to use this combination as a catalyst. Unfortunately, this mixture was again largely insoluble in THF and no reaction occurred. (Table 3, entry 2) We next attempted the more polar solvent DMF (Table 3, entry 3) in which the reaction did appear to proceed to 26% conversion after 8 days and eventually 58% conversion after 35 days, however the isolated reaction yield was very poor at 14 %. The ee of this reaction (entry 3) was determined as 3 % but this was not of

significant interest. It is possible in this case that the DMF may have been acting as a catalyst. (Table 3)

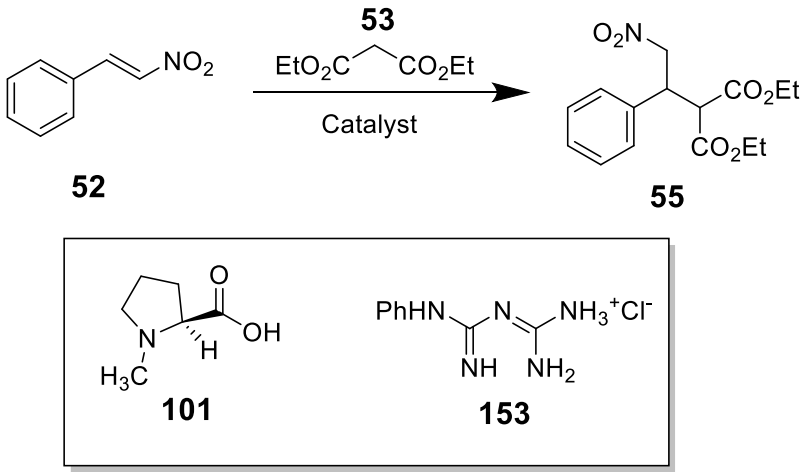

Scheme 48: Michael addition reaction and catalysts studies.

Table 3: Entries 1-3.

Entry	Catalyst (0.12 eqv.)	Malonate (eqv.)	Solvent	Time	Conversion	Yield/%	ee %
1	**153**(i)	1.5	CH_2Cl_2	1 d	No reaction	NA	NA
2	**153/101**	1.5	THF	4 d	No reaction	NA	NA
3	**153/101**	1.5	DMF	35 d	58 %	14	3.4 (R)

(i) Catalyst **153** (0.1 eqv.)

The final series of reactions we performed were on the less basic acyl deactivated guanidine **82** and **145**, which have one Cbz- and two Boc-groups attached to them respectively. The reaction catalyzed by **82** gave a very slow rate of conversion with only 10 % product being observed after 1 d, 15 % after 2 d, 64 % after 15 d and finally 91 % being observed after 38 d. (Table 4, entry 1) The double deactivated catalyst **145** gave only a 5 % conversion after 37 d (Table 4, entry 2) and this was also observed to have a small and roughly equal amount (by NMR) of an unidentified impurity. The slow rate of reaction for these two substrates is encouraging for our studies as it should enable the study of the *N*-methyl-*L*-proline **101** in combination with guanidine of this nature to be studied. Thus a combination of the chiral acid **101** with the base **113** were used and we observed the rapid conversion of **53** to the adduct **55** in 66% conversion over 1 d. Unusually on continued monitoring

of this reaction it was apparent that the reaction ratio of the starting material **53** and the product **55** was actually decreasing over time which suggests that **55** is being consumed in a side reaction (table 4 entry 3). In order to prevent this the reaction was performed at a lower temperature (4-5 °C) and it was observed that the conversion was 25% after 1 d, 31 % after 2 d, 37 % after 3 d, and 82 % after 6 d. On purification a 71% yield of the adduct **55** was obtained with an ee of 1 % (Table 4, entry 4). The reaction of the doubly deactivated guanidine **145** with *N*-methyl-*L*-proline **101** as catalysts (Table 4, entry 5) gave no reaction under a variety of conditions. Inspired by a report[48] on the acceleration of the proline mediated reactions using salt **143** we investigated the reaction of **101** with **143** as co-catalysts in dry DCM. On standing for 7 d there was no catalytic effect and no reaction was observed. (Table 4, entry 6)

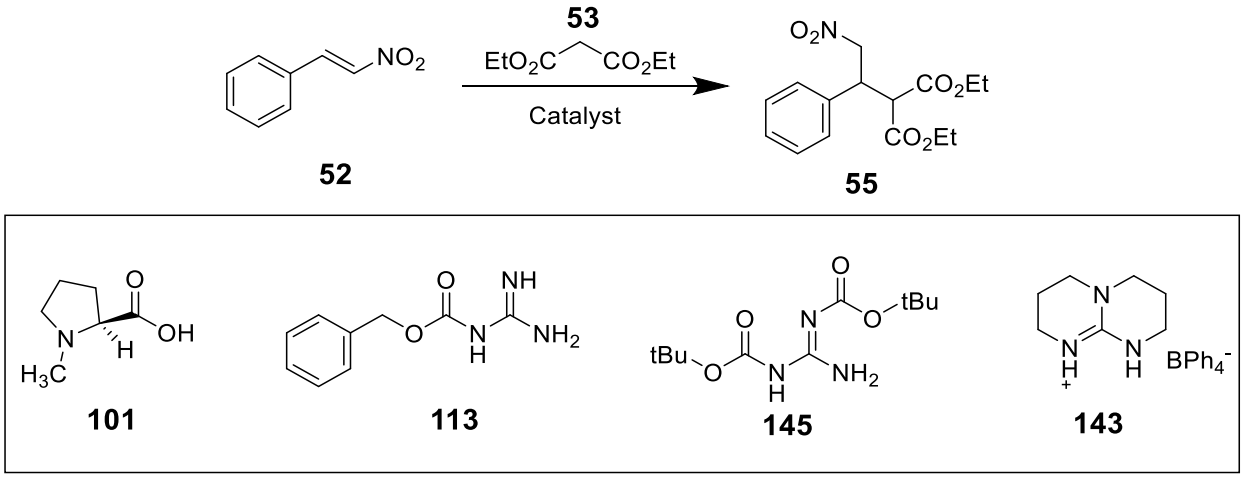

Scheme 49: Michael addition reaction and catalysts **101**, **113**, **143** and **145**.

Table 4: Entries 1-6.

Entry	Catalyst (0.1 eqv.)	Malonate (eqv.)	Solvent	Time	Conversion	Yield/%	ee %
1	**113**	14.5	CH_2Cl_2	38 d	91%	61	NA
2	**143**	1.5	CH_2Cl_2	37 d	5 %	ND	NA
3	**113**/**101**	1.5	CH_2Cl_2	1 d	66 %	28	3 (R)
4[(i)]	**113**/**101**	3.0	CH_2Cl_2	6 d	82 %	71	1 (R)
5	**145**/**101**	3.0	CH_2Cl_2	6 d	No reaction	NA	NA
6	**143**/**101**	3.0	CH_2Cl_2	7 d	No reaction	NA	NA

(i) Reaction performed at 4-5 ^oC.

The final phase of this investigation was to use the covalently bound catalysts **110** and **114**. Unfortunately as we were unable to prepare the catalyst **110** only preliminary experiments using **114** were attempted. The reactions (Table 5, entries 1-3) were performed in a variety of solvents and were disappointed to observe that the reaction did not occur in the relatively non-polar solvents dichloromethane and THF and only proceeded to 23% conversion after 2 d in DMF, with an isolated yield of 29 % and its ee was again very poor at 4 %. Again the DMF solvent might have been acting as a catalyst in the final case. (Table 5)

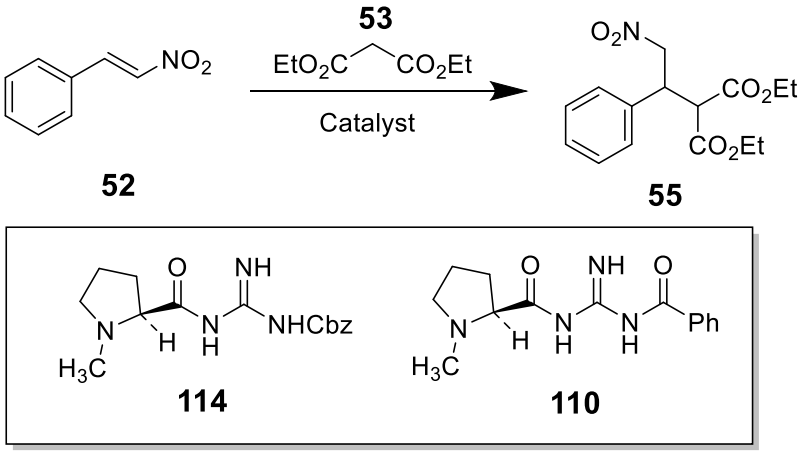

Scheme 50: Michael addition reaction and catalysts **110** and **114**.

Table 5: Entries 1-3.

Entry	Catalyst	Malonate	Solvent	Time	Conversion	Yield/%	ee %

	(0.1 eqv.)	(eqv.)					
1	**114**	1.5	DMF	2 d	23 %	29 %	4
2	**114**	1.5	CH_2Cl_2	5 d	No reaction	NA	NA
3	**114**	1.5	THF	8 d	No reaction	NA	NA

The conclusion from this initial study is that it is possible to effect the Michael addition of diethylmalonate **53** with nitrostyrene **52** using guanidines and guanidinium salts however using *N*-methyl-*L*-proline **101** as the chiral acid in this reaction is not successful. There also appears to be a problem associated with the use of malonate as in some cases as unidentifiable by-products are generated in these reactions and these were leading to diminished yields. We were disappointed with these results but encouraged that the acyl deactivated guanidines were acting as catalysts and this led us to look at the design of a different range of catalysts in which the *N*-alkylated proline moiety was covalently bonded via an amide bond to a guanidine.

As previously stated, the generalized structure **154** was initially envisaged which has a guanidine to act as a H-bonding site (complex **155**) and has the ability to have a position of steric control (R) at the proline. The substituents (R^1) on the guanidine should offer the ability to "tune" the nature of the H-bonding by variation in the electron donating and withdrawing effects. (Figure 23)

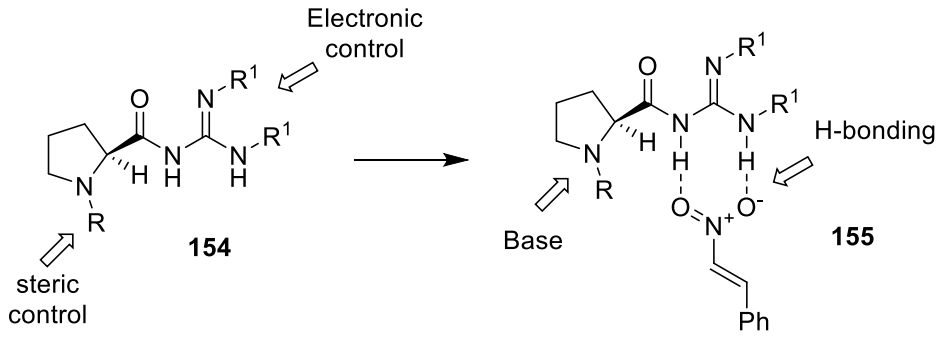

Figure 23: Generalised catalyst structure **154**

The Michael addition reaction of 2-Hydroxy-1,4-napthoquinone 1 to β-Nitrostyrene 2

A study within the Murphy group[51,52] investigated the Michael addition of 2-hydroxy-1,4-napthoquinone **93** to β-nitrostyrene **52** catalyzed by the tetracyclic guandinium salts **80a-d**. The ee's

reported in this process were unfortunately low however the reported improved catalysis of the process by the salt **80a** in conjunction with *L*-proline **37** were of interest. (Scheme 51)

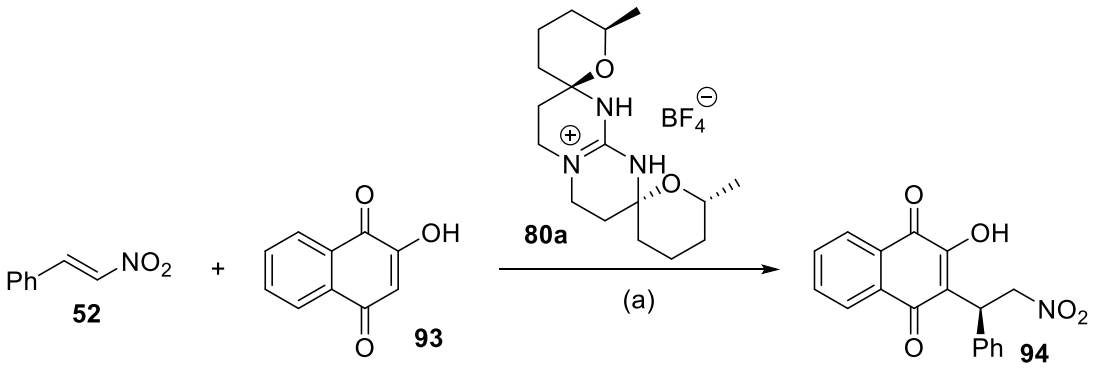

Scheme 51: Michael reaction catalyzed by guanidine salts **80**a (a) THF, *L*-Proline **37**.

We decided to apply the catalysts prepared in the previous section of this work to this reaction as it seemed to be a good candidate for catalysis. It might also not suffer the problems of by-product formation and low yields as in previous investigation as it had been demonstrated to be a robust system in our hands.

We initially investigated the Cbz-protected *N*-alkyl-*L*-proline catalysts **114**, **116**, **117** and **119** in this reaction and the results are shown in. (Table 6) (Scheme 51)

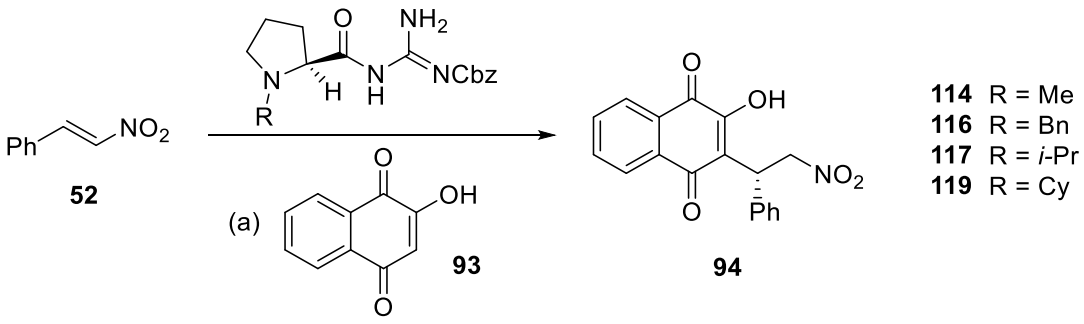

Scheme 51, Catalysts **114**, **116**, **117** and **119** 0.1 eqv, at 0°C 7-8 h then rt, see (Table 6)

Table 6: Entries and results.

Entry	Catalyst (0.1 eqv.)	Acetonitrile	DCM	THF	Toluene	EtOAc
1	**114**[(i)]	Time: 21 h Yield: 87%	Time: 72 h Yield: 94%	Time: 48 h Yield: 95%	Time: 21 h Yield: 86%	Time: 25 h Yield: 92%

		5% ee (R)	29% ee (R)	16% ee (R)	26% ee (R)	25% ee (R)
2	**114**	Time: 88 h Yield: 93% 34% ee (R)	Time: >88 h Yield: 99% 37% ee (R)	Time: >100 h Yield: 50% 18% ee (R)	Time: >100 Yield: 75% 44% ee (R)	Time: >100 Yield: 76% 31% ee (R)
3	**116**	Time: 5 h Yield: 93% 7% ee (R)	Time: 47 h Yield: 90% 8% ee (R)	Time: >100 h Yield: 94% 15% ee (R)	Time: >100 h Yield: 86% 13% (R)	Time: >100 h Yield: 92% 5% (R)
4	**117**	Time: <10 h Yield: 89% 15% ee (R)	Time: <20 h Yield: 90% 5% (R)	Time: <20 h Yield: 89% 1% ee (R)	Time: 32 h Yield: 90% 5% (R)	Time: <20 h Yield: 90% 4% (R)
5	**119**	Time: 39 h Yield: 99% 1% ee (R)	Time: 39 h Yield: 89% 4% ee (R)			

(i) Contained impurity **115** (ca. 12 %).

(ii) Precipitate formation during reaction.

Catalyst **114** was investigated firstly and we chose a range of solvents as show in entry 1 of (Table 6). Pleasingly in 4 of the 5 solvents we were able to see a significant ee in the product of 15 - 29% ee of the R enantiomer of the product as determined by HPLC and by optical rotation. The best ee of 29% was observed when using dichloromethane as solvent and the worst was acetonitrile. The reaction time for the processes was quite variable and we monitored the reactions by NMR sampling until a high conversion was apparent. As the project progresses it became apparent that our sample of the catalyst **114** was contaminated by the work up byproduct 12 % so it was decided to repeat the reactions with pure **114** (Table 6 entry 2). These repeat reactions gave a marked improvement in ee for all of the solvents except THF with respectable ee's of 34%, 37%, 44% and 31% for acetonitrile, dichloromethane, toluene and ethyl acetate respectively and the much improved ee for acetonitrile might suggest that the impurity was accelerating or catalyzing the reaction in this solvent, however this theory was not tested.

With this success we next moved to the more bulky *N*-substituents benzyl (**116**, entry 3), isopropyl (**117**, entry 4) and cyclohexyl (**119**, entry 5). In the case of the benzyl substituents the ees were generally lower (5 - 15 %) for this catalyst when compared to the corresponding examples with **114**. Further reductions were observed across the range of solvents for **117** (1 - 5 % ee) and for

119 (1 - 4 % ee). Interestingly reactions in acetonitrile are generally quicker than those in dichloromethane and the reactions in THF, toluene and ethyl acetate can be very slow (>100 h) and there is no clear correlation between rate of reaction and ee. One conclusion that is apparent however is that the bulky groups are not increasing the ee of this reaction.

We next investigated the *N,N'*-diphenyl substituted *N*-alkyl-*L*-proline catalysts **120** - **123** which again differ by the bulkiness of the nitrogen substituent and the electron withdrawing nature of the phenyl rings. (Scheme 52, Table 7)

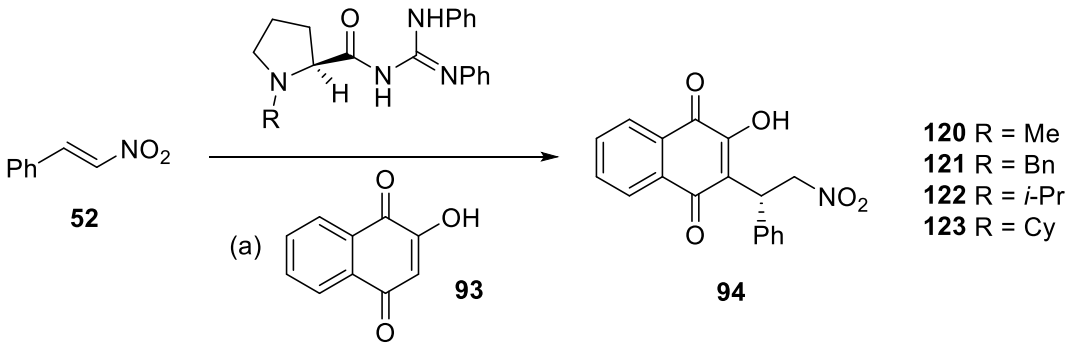

Scheme 52, Catalysts **120**-**123** 0.1 eqv, at 0°C for 7-8 h then rt, see (Table 7)

Table 7: Entries and results.

Entry	Catalyst (0.06 eqv.)	Acetonitrile	DCM	THF	Toluene	EtOAc
1	**120**[(i)]	Time: 42 h Yield: 90% 4% ee (R)	Time: <72 h Yield: 93% 1% ee (R)	Time: >100 h Yield: 41% 3% ee (R)	Time: >100 h Yield: 38% 3% ee (R)	Time: >100 h Yield: 40% 4% ee (R)
2	**121**	Time: 38 h Yield: 72% 6% ee (R)	Time: 38 h Yield: 76% 3% ee (R)	Time: >72 h Yield: 51% 1% (R)	Time: >72 h Yield: 35% 1% ee (R)	Time: >72 h Yield: 79% 3% ee (R)
3	**122**	Time: 22 h Yield: 95% 3% ee (R)	Time: 22 h Yield: 68% 5% ee (R)			
4	**123**	Time: 58 h Yield: 81% 1% ee (R)	Time: 58 h Yield: 90% 1% ee (S)			

(i) Using with 0.04 eqv. of catalyst **120**.

Owing to a lower amount of catalyst **120** only 0.04 equivalent were used in these reaction and it was apparent (entry 1, table 7) that the catalyst gave a very low ee (1 - 4 % ee) in all 5 solvents tested. Again acetonitrile and dichloromethane give the fastest reaction and highest yield with yields being much lower in the other three solvents. Similar results were observed for the more bulky *N*-substituents benzyl (**121**, entry 2), isopropyl (**122**, entry 3), cyclohexyl (**123**, entry 4) which gave very poor ees (1- 6% ee) across all 5 solvents, with yields being best in acetonitrile and dichloromethane. The reasons for this low reactivity and selectivity will be discussed in the next chapter.

We next investigated the mono-phenyl substituted *N*-alkyl-*L*-proline catalysts **127** and **128** which due problems in the synthesis of the *N*-isopropyl substituted analogue were the only ones available. (Scheme 53) (Table 8)

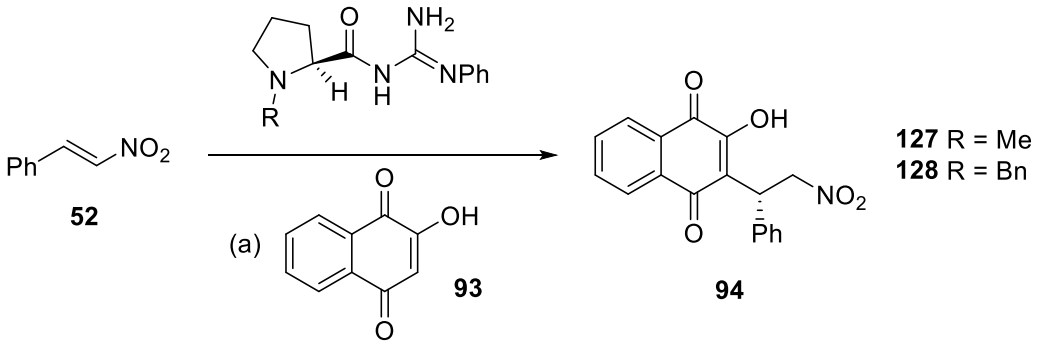

Scheme 53, Catalysts **127** and **128** 0.1 eqv, entries 1-3 at 0°C, see Table 8.

Table 8: Entries and results.

Entry	Catalyst (0.1 eqv.)	Acetonitrile	DCM	THF	Toluene	EtOAc
1	**127**	Time: <21 h Yield: 93 % 16% ee (R)	Time: 4 h Yield: 91 % 21% ee (R)	Time: 96 h Yield: 85 % 16% ee (R)	No reaction[(i)]	Time: 96 h Yield: 87 % 22% ee (R)
2[(ii)]	**127**		Time: 54 h Yield: 92 % 25% ee (R)			
3	**128**	Time: 48 h Yield: 91 % 1% ee (S)	Time: 48 h Yield: 93 % 1% ee (S)	Time: 48 h Yield: 36 % 2% ee (S)	Time: 48 h Yield: 90 % 2% ee (S)	Time: 68 h Yield: 82 % 4% ee (S)

(i) Catalyst **127** was insoluble in toluene.
(ii) Performed at -20°C.

On reverting back to a di-substituted guanidine **127**, the ees (16 - 22 %) of the product in the range of solvents was seen to increase to levels close to those of the CBz-protected substrate **127**. This was an interesting observation as was the improved ee observed in ethyl acetate and the very rapid reaction observed dichloromethane. We repeated the dichloromethane reaction at a lower temperature and obtained a slight but not significant increase in ee to 25 %. Toluene proved to be an unsuitable solvent for this reaction as the catalyst had a very low solubility. The benzyl substituted catalyst **128** gave consistently poor ees (1 - 4 % ee) across the range of solvents with a generally slower reaction rate being observed when compared to **127**.

We next investigated the 2-aminobenzimidazole *N*-alkyl-*L*-proline catalysts **139-142** in which we were able to prepare the complete range of catalysts with all four of the substituents studied so far. (Table 9) (Scheme 54)

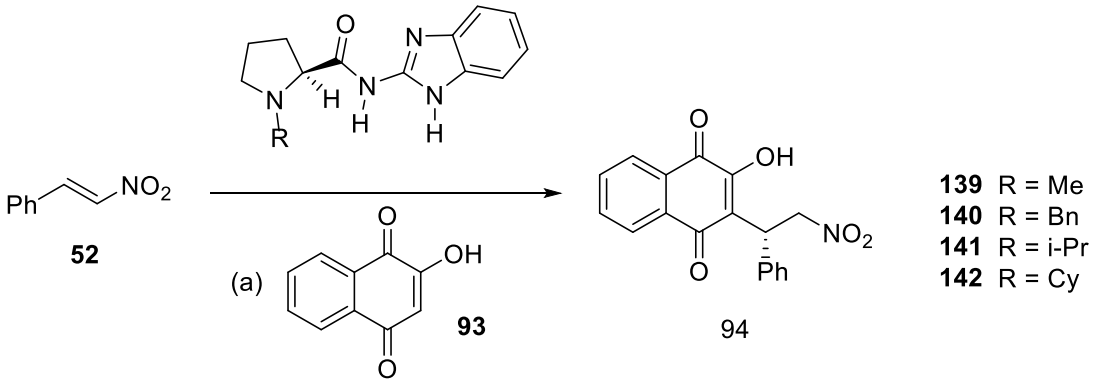

Scheme 54, Catalysts **139 - 142** 0.1 eqv, at 0°C for 7-8 h then rt, see Table 9.

Table 9: Entries and results.

Entry	Catalyst (0.1 eqv.)	Acetonitrile	DCM	Toluene
1	**139**	Time: 39 h Yield: 90 % 7 (R)	Time: 39 h Yield: 88 % 27 (R)	Time: >100 h Yield: 87 % 32 (R)
2	**140**	Time: 58 h Yield: 89 % 3 (R)	Time: 58 h Yield: 92 % 12 (R)	
3	**141**	Time: 88 h Yield: 81 % 2 (R)	Time: <100 h Yield: 90 % 9 (R)	
4	**142**	Time: 58 h Yield: 91 % 2 (R)	Time: 58 h Yield: 96 % 9 (R)	

The results using **139 - 142** were in line with previous observations, in that the methyl substituted proline base **139** gave the best ees in any of the reactions attempted. The ees were also best in the less polar solvents dichloromethane (27% ee) and toluene (32% ee) as opposed to the

more polar solvent acetonitrile (7% ee). (entry 1) The more bulky benzyl (**140**), isopropyl (**141**) and cyclohexyl (**142**) substituents led to a lowering of ee (2 -3% ee in acetonitrile and 9 - 12% ee in dichloromethane) in all cases and a trend towards increasing reaction time in some cases (Table 9, entries 2-4).

The conclusion from these studies is that the catalysts **114**, **127** and **139** gave appreciable ees with the solvents of choice tending to be dichloromethane and acetonitrile. The need for a methyl substituents on the proline was apparent as more bulky substituents gave much lower ees by comparison. The di-substituted guanidine catalysts **114** and **127** gave the best ees but the effectively tri-substituted 2-aminobenzimidazole catalyst **139** gave reasonable ees across all 5 solvents tested. (Figure 24)

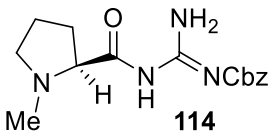

114

CH_2Cl_2 (37% ee, 99% yield, 88 h)
CH_3CN (34% ee, 93% yield, 88 h)
THF (18% ee, 50% yield, > 100 h)
Toluene (44% ee, 75% yield, > 100 h)
EtOAc (31% ee, 76% yield, > 100 h)

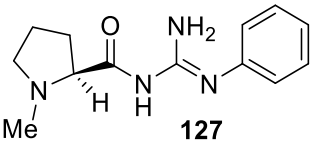

127

CH_2Cl_2 (21% ee, 91% yield, 4 h)
CH_2Cl_2 (25% ee, 92% yield, 54 h) at -20 C
CH_3CN (16% ee, 93% yield, 21 h)
THF (16% ee, 85% yield, 96 h)
EtOAc (22% ee, 87% yield, 96 h)

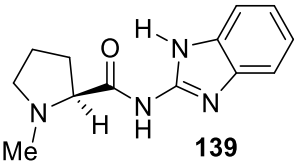

139

CH_2Cl_2 (27% ee, 88% yield, 39 h)
CH_3CN (7% ee, 90% yield, 39 h)
Toluene (32% ee, 87% yield, > 100 h)

Figure 24: Catalysts **114**, **127** and **139.**

These ees whilst not spectacular do show a trend in this process and we were intrigued to investigate the process further and attempted to elucidate the structures of these catalysts by X-ray crystallography in the hope that this might offer some insight to the processes occurring in these reactions.

X-ray analysis of the guanidine catalysts 3 and 4

We were keen to postulate a mechanistic rationale for this reaction and to attempt to rationalize the differences in the reactivity and ees of the different catalyst series employed. We attempted to grow crystals of the solid catalysts and submit these for X-ray crystallography at the EPSRC service in Southampton. We were able to grow good crystals of the 8 catalysts **114**, **120**, **122**, **123**, **127**, **139**, **140** and **141** (blue). (Figure 25)

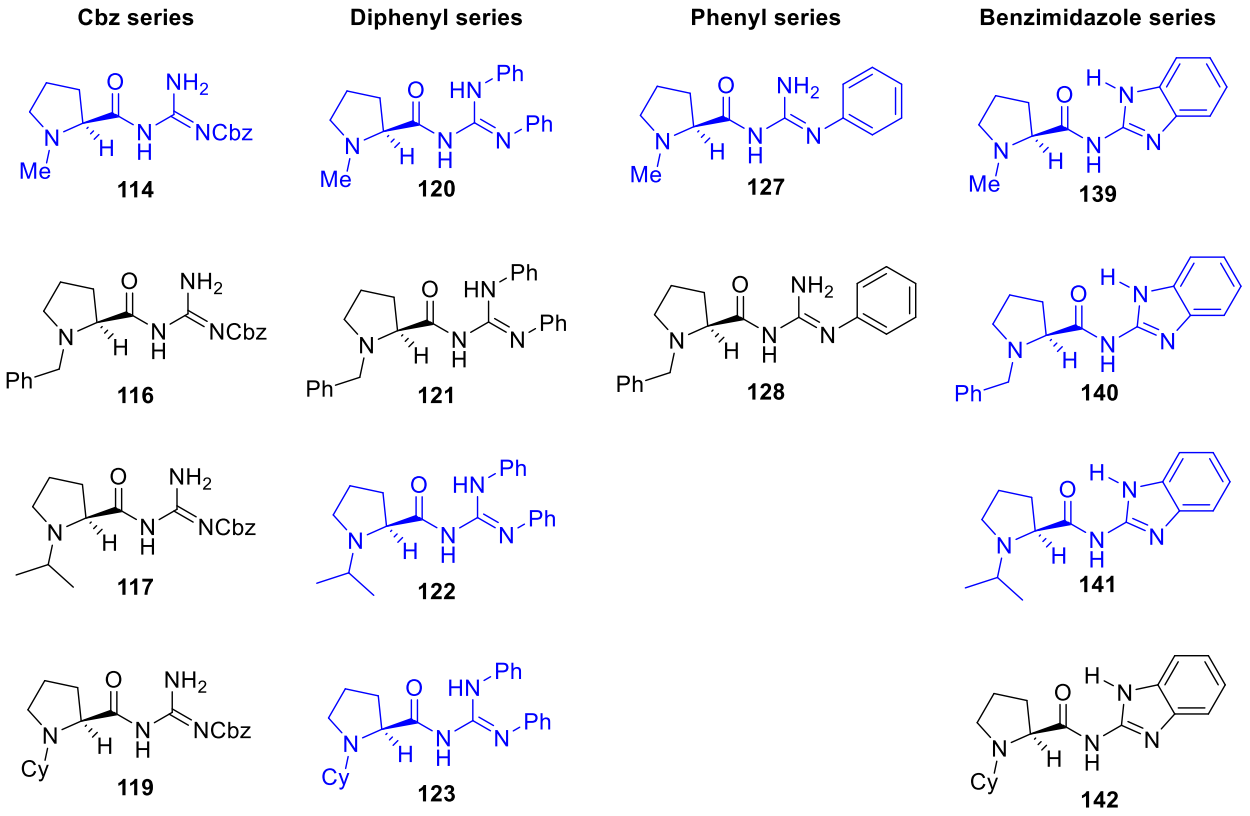

Figure 25: Catalysts studied by X-ray crystallography (blue).

Inspection of the X-ray structure of the Cbz-substituted catalyst **114** (figure 26) indicates a very interesting set of hydrogen-bonds, which are depicted in (Figure 27). There are two independent molecules in the unit cell which differ largely at the conformation of the benzyl group and have three strong hydrogen bonds between the proline nitrogen and the amide N-H (bond (a) N---H-N distance = 2.261/2.267 Å) and two NH---O bonds (bond (b) distance = 2.025/1.871 Å and bond (c) distance = 1.830/2.004 Å). These bonds seem to be holding the proline amide and guanidine in a planar and rigid conformation. The also appears to be a C-H---O bond between the benzyl

methylene and the benzyl carbonyl (bond (d) distance = 2.332/2.363 Å), however this is not as strong as the other interactions. The methyl group on the proline is pointing away from the proximal guanidine nitrogen and is in an anti-configuration to the amide carbonyl. (Figure 26).

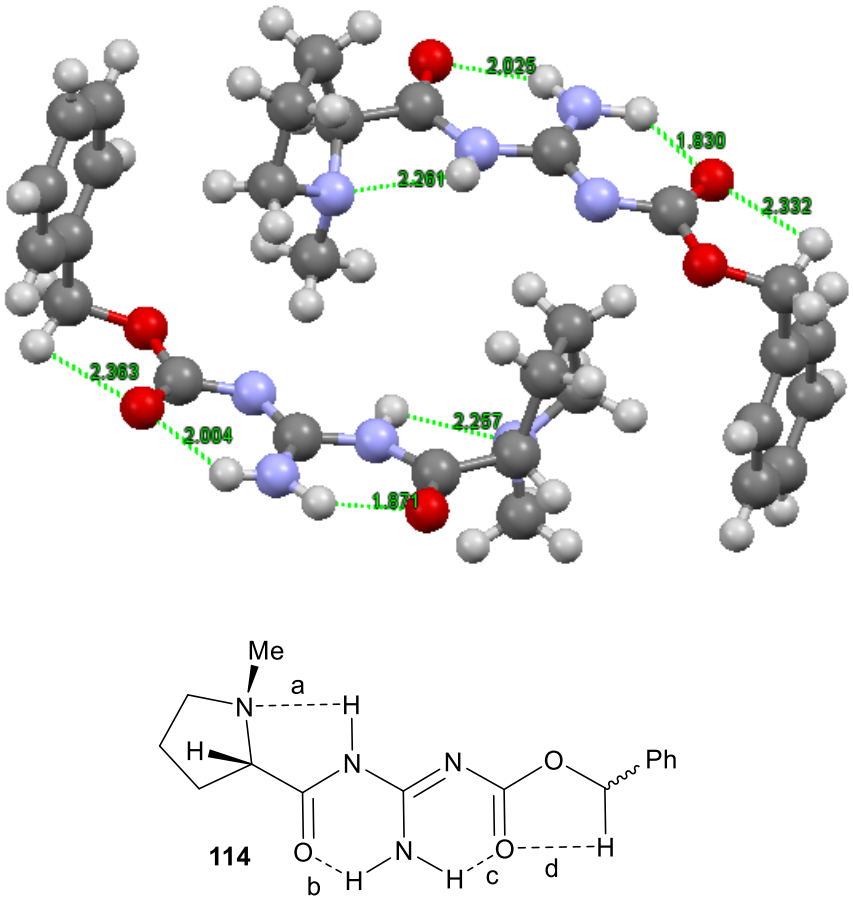

Figure 26: X-ray structure and H-bonding in **114**.

If this structure were present in a solution phase then protonation of the *N*-methyl of the proline might lead to a disruption of the hydrogen-bonding. This might lead to the conclusion that protonation of the guanidine leading to **157** rather than **158** might be a more favourable process as it would minimise disruption. The H-bond between the proline amine and guanidine might explain the slow rate of reaction of this and other catalysts as the deactivated guanidine is not likely to be a strong base. (Scheme 55)

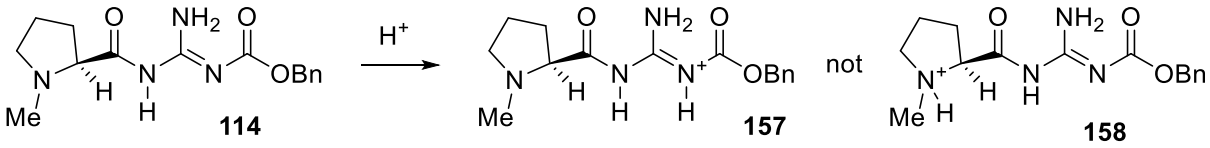

Scheme 55: Protonation of **114**.

We were also able to obtain X-ray structures for three of the diphenyl catalysts **120**, **122** and **123** which all show similar hydrogen bonding patterns in their X-ray structure. (Figures 27, 28 and 29)

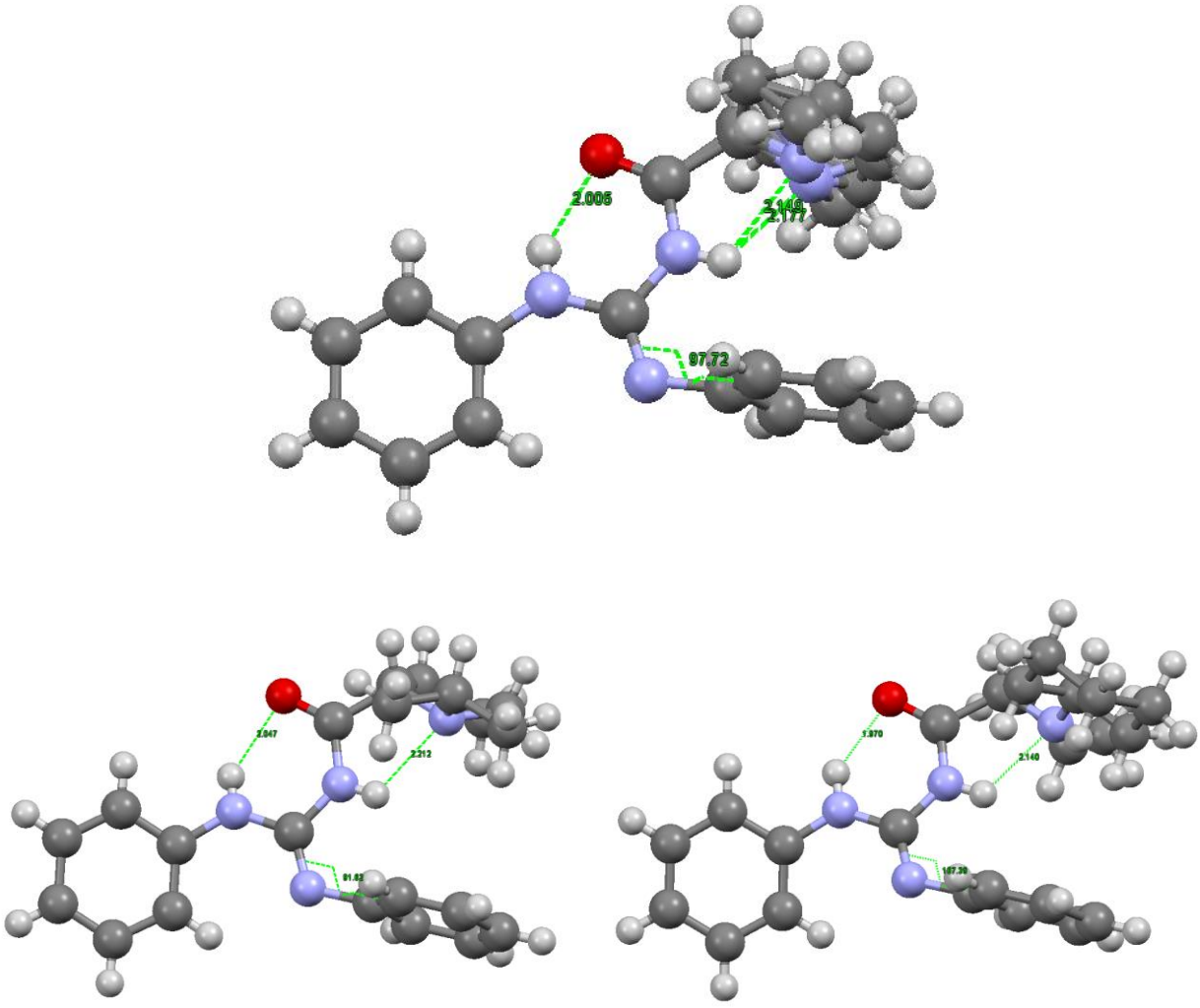

Figures 27, **28** and **29**: X-ray structures of **120**, **122** and **123**.

From these structures it is apparent that there is a H-bond between the proline nitrogen and the guanidine N-H (bond (a) NH---N bond distance, **120 =** 2.177/2.149 Å, **122 =** 2.212 Å and **123** = 2.140 Å) and also a strong hydrogen bond between the amide carbonyl oxygen and the other guanidine N-H (bond (b) NH---O bond distance **120** = 2.006 Å, **122** = 2.047 Å and **123** = 1.970 Å).

A very interesting feature of these compounds is orientation of the phenyl groups in the X-ray structure as it is apparent that the imine phenyl ring (C=N-Ph) is twisted out of conjugation with then imine with a dihedral (C-N-C-C) angle of 97.72º, 91.62º and 107.39º being observed for **120**, **122** and **123** respectively. All three of the R-groups are again pointing away from the proximal guanidine nitrogen and are in an anti-configuration to the amide carbonyl, however there is considerable disorder in the structure of the N-methyl substituted catalyst **120**. (Figures 30, 31 and **32**).

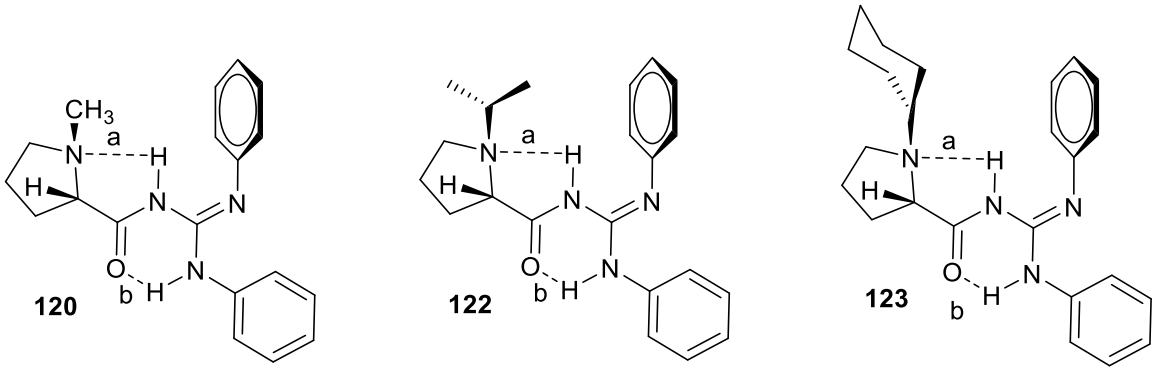

Figures 30, **31** and **32**: Hydrogen bonding in **120, 122** and **123**.

These observations open up several interesting possibilities, firstly the rotation of the phenyl groups out of plane will block access to the proline nitrogen lone pair if it is acting as a base for deprotonation of an incoming enolate. Secondly if this blockage is occurring, then protonation might be preferred at the imine nitrogen leading to structure **159**, where protonation is remote from the chiral centre as opposed to protonation at the proline nitrogen (**160**). Thirdly if disruption of the proline-guanidine N---HN bond does occur this might be an energetically unfavourable process and prevent the proline being involved in any catalytic process. (Scheme 56)

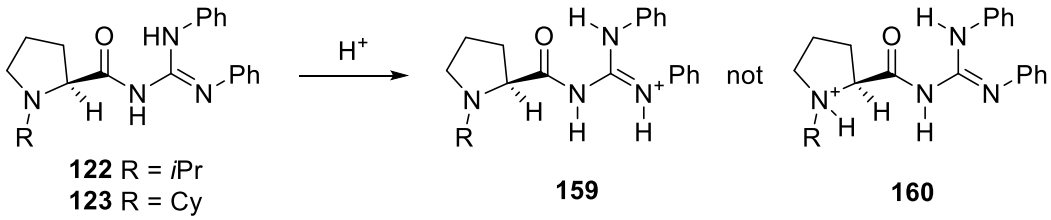

Scheme 56: protonation of **122** and **123**.

Some evidence is available from NMR to support the different conformations of the phenyl rings in solution as even in polar NMR solvents (DMSO, MeOH) it is apparent that different signals are observed for each of the phenyl rings suggesting that on the NMR timescale these phenyls are not rapidly interconverting. It is also interesting to observe that for all the cyclohexyl and isopropyl catalysts, distinct signals are observed for each methylene and methyl group again suggesting discrimination on diastereotopic grounds in these groups.

We obtained an X-ray structure for the mono-phenyl substituted catalyst **127** which interestingly displayed completely dissimilar hydrogen bonding to that observed for the Cbz catalyst **114** and the diphenyl catalysts. (figure 33)

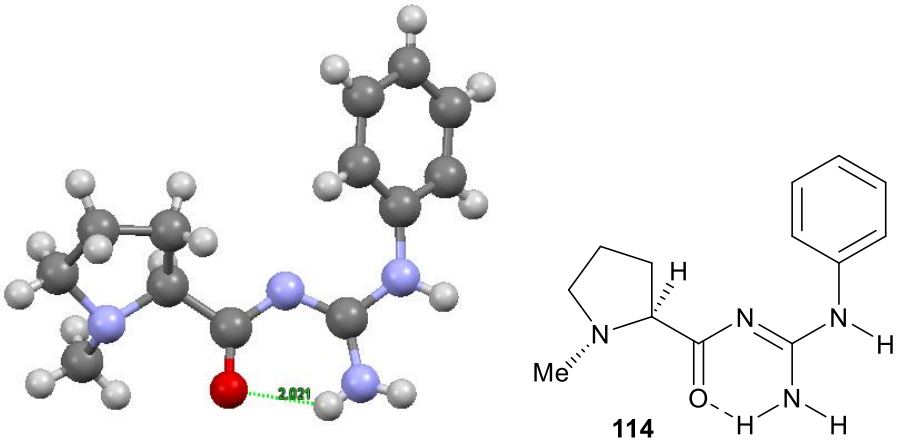

Figure 33: X-ray structure and H-bonding in **114**.

Interestingly the hydrogen bonding pattern in this molecule is different in that there is no H-bond between the proline nitrogen and the amide as there is no N-H present on the amide as it has formed imine-type structure with the guanidine. It is worthy of note that this is unique in the series of X-rays obtained and it is interesting that this catalyst give the shortest reaction time for completion of the Michael addition reaction studied of 4 h at room temperature in dichloromethane. This might suggest that the hydrogen bond between the amide N-H and the proline nitrogen is the major factor in impeding the reaction rate and the enantioselectivity.

Finally, we were able to obtain crystallographic data for three of the 2-aminobenzimidazole catalysts **139**, **140** and **141** and again these display similar hydrogen bonding patterns in their X-ray structure (Figures 34, 35 and 36).

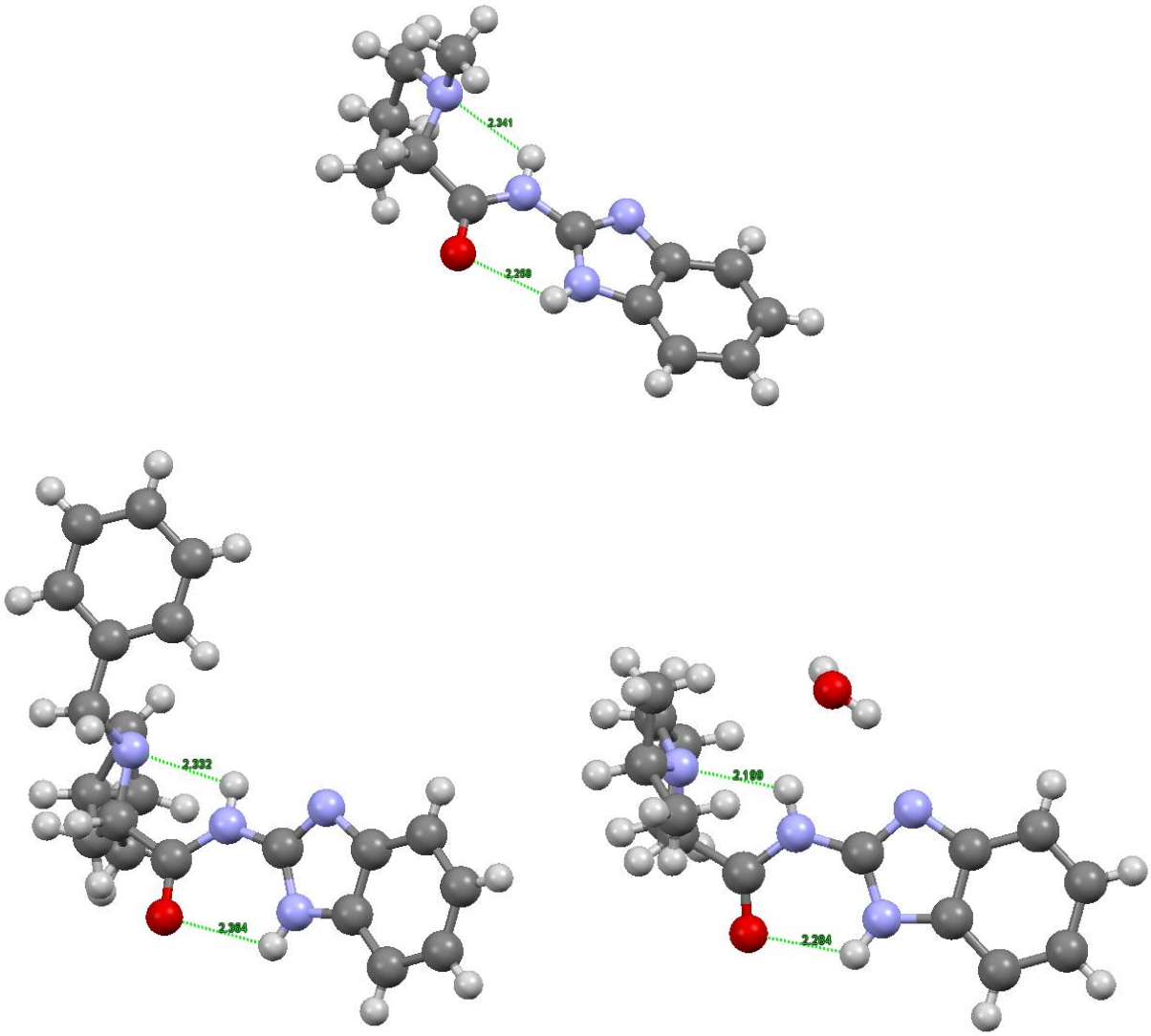

Figure 34, **35** and **36**: X-ray structure of **139**, **140** and **141**.

From these structures it is apparent that again there is a strong H-bond between the proline nitrogen and the guanidine N-H (bond (a); NH---N bond distance for **139** = 2.341 Å, **140** = 2.332 Å and **141** = 2.199 Å) and also a strong hydrogen bond between the amide carbonyl oxygen and the other guanidine N-H (bond (b); NH---O a bond distance for **139** = 2.268 Å, **140** 2.364 Å and for **141** 2.284 Å). This bond is present in **141**, even though it has co-crystallised with a molecule of water, which in itself might demonstrate that the possibility for protonation is possible at the proline nitrogen. Both of the R-groups are again found pointing away from the proximal guanidine nitrogen and are in an anti-configuration to the amide carbonyl. (Figures 37, 38 and 39).

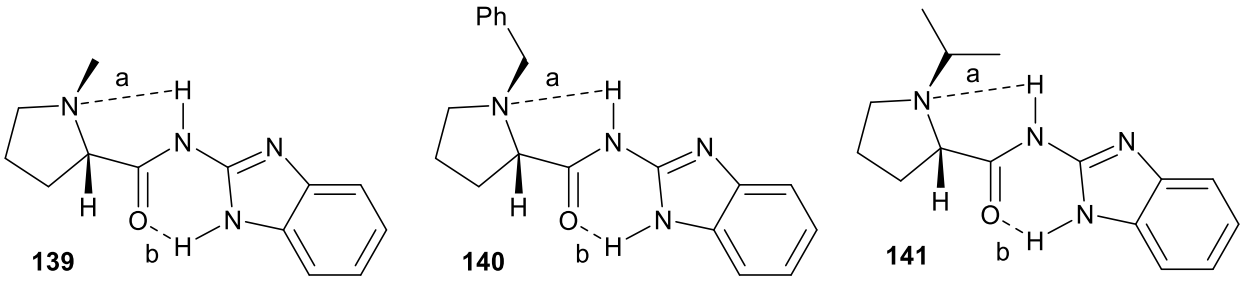

Figures 37, 38 and **39**: Hydrogen bonding in **139**, **140** and **141**

Again there appears to be two sites for protonation and if the hydrogen bonding and any steric factors prevent protonation at the proline nitrogen leading to **162**, then protonation might be preferred at the benzimidazole imine nitrogen leading to structure **161**, where again protonation is remote from the proline chiral centre. (Scheme 57)

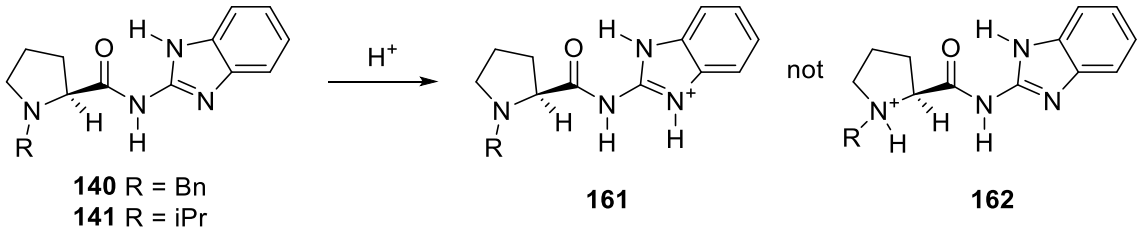

Scheme 57: protonation of **140** and **141**

It is apparent that a similar H-bonding pattern is occurring across three of the systems we have data for. Strong hydrogen bonds between the proline nitrogen and N-H of the amide nitrogen are present (bonds (a)) for three of the structural types, however catalyst **127** displayed a distinctly different pattern of H-bonding with an imine type structure and this characteristic H-bond absent. Strong hydrogen bonds between the amide oxygen and the amine nitrogen of the guanidine (bonds (b)) were observed in all cases. (Figure 40)

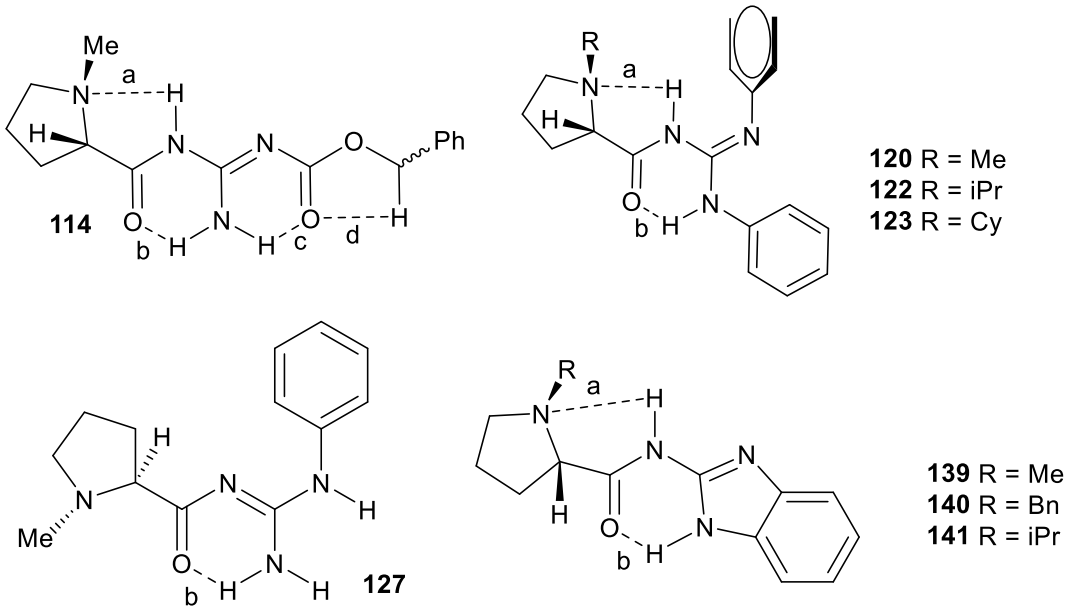

Figure 40: Hydrogen bonding patterns observed in catalysts **114**, **120**, **122**, **123**, **127**, **139**, **140** and **141**.

The additional hydrogen bonding found in catalyst **114** is similar to that reported in other dicarbonyl-derived guanidines for example the synthetic intermediate **21** reported by Moody at al.[61] in their synthesis of the natural product distomadine B.[61] This intermediate shows identical hydrogen bonding patterns to our catalyst **114**. (Figure 41)

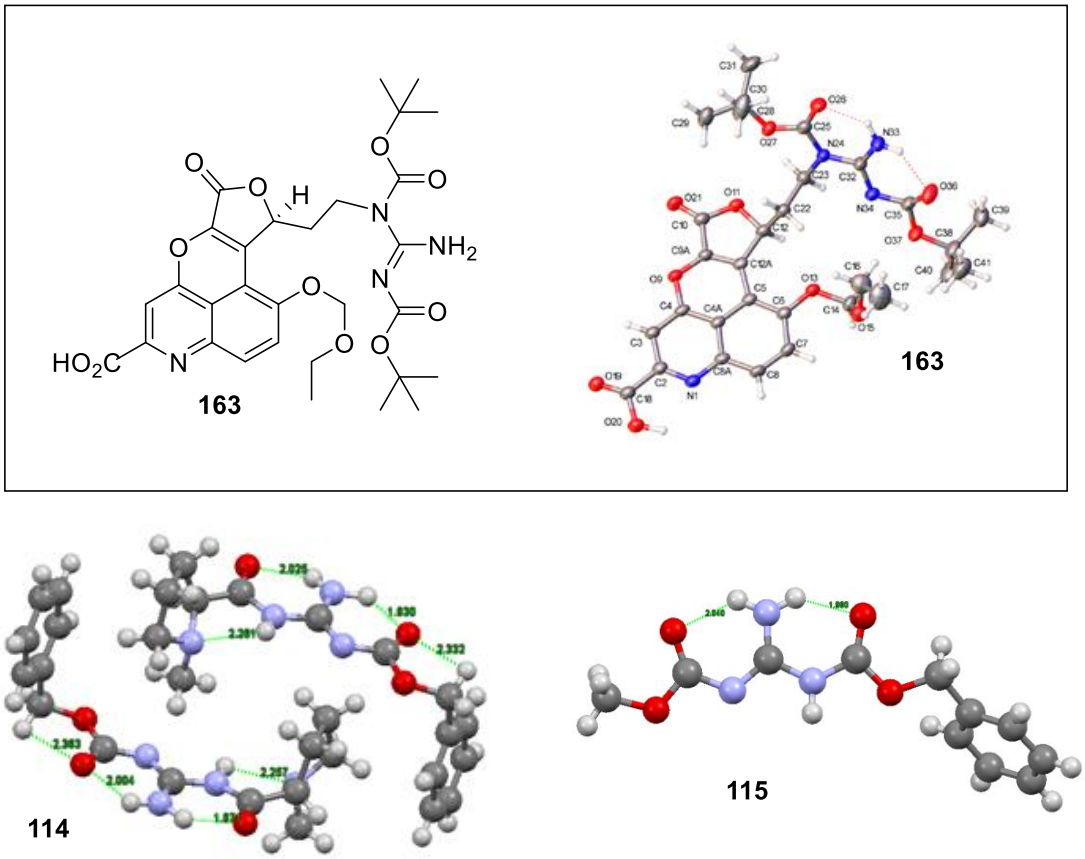

Figure 41: X-ray structure of **163** compared to **114** and **115**.[60]

In trying to relate the yields observed in the catalytic reactions to the structure it is very apparent that three most successful catalyst systems are those in which the proline substituent is a methyl group (compounds **114**, **127** and **139**) and it is apparent that when you move away from this substituent the ee of the reaction diminishes appreciably. We might thus conclude that the increase of steric bulk around this part of the molecule has a detrimental effect on the stereoselectivity of the reaction. A similar effect was observed with the diphenyl substituted catalyst **120** where there was a complete loss of stereoselectivity. From the X-ray structure this might be explained by the position of the imine phenyl ring which appears to block the proline nitrogen and the guanidine function from approach by any reactants. The three catalysts that give good selectivity appear to have a rigid hydrogen bonded structure and access to the proline nitrogen for protonation seems to be unhindered by any substituents. This might explain their ability to catalyse the reaction with some selectivity and might point the way to future developments of catalysts (this will be discussed in the concluding chapter). (Figure 42)

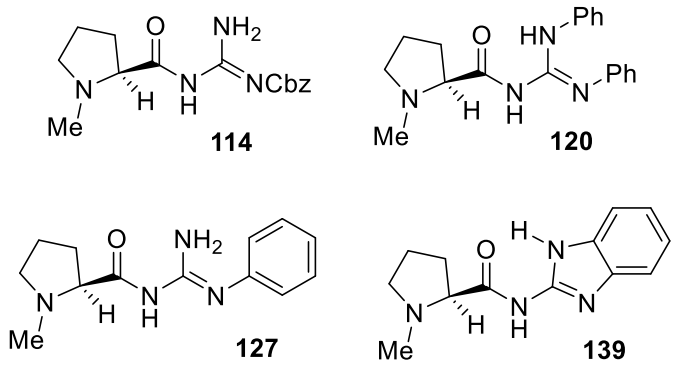

Figure 42: Methyl substituted catalysts.

One factor which has not been considered is the conformation of the proline nitrogen once protonated. Nitrogen is not considered to be a chiral atom as the interconversion of the two tetrahedral forms of tri-substituted amines is generally rapid. However consideration of the possible protonated forms of our catalysts **164** leads to the formation of two different cations **165** and **166** which are diastereomers and might not rapidly interconvert. This might lead us to suppose that the selectivity in the reaction might also be dependent on the amount of each of these intermediates formed in solution (if formed at all) and the relative catalytic activity of each of these species. (Scheme 58)

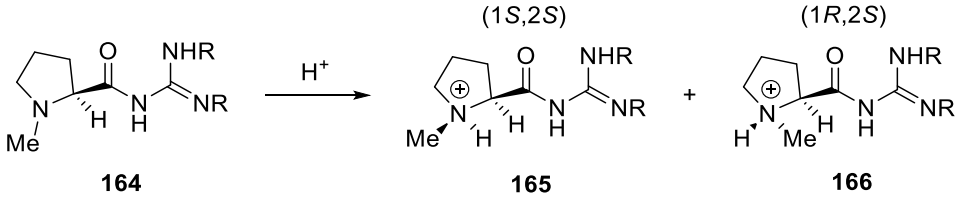

Scheme 58: Diastereomers formed by the protonation of 164

We can conclude from the X-ray structures that, with the exception of **127**, there is a similarity in hydrogen bonding patterns across the various catalysts and that steric factors play a role in the selectivity of their activity. Through this discussion we have ignored intermolecular hydrogen bonding and this of course plays a major role in the formation of crystals. It is difficult to relate solid phase structural motifs to those found in solution and most of the conclusions in this chapter are speculative. We have not performed molecular modelling studies on our catalysts and

this might be prudent before further work is performed. We are currently involved in a collaboration with Dr O'Donoghue (Durham University) to determine the pKa values for our catalysts to see if a trend can be determined from this information. Full details of the X-ray data are available in appendices 2-10 and show details of much of the intermolecular hydrogen bonding in these compounds.

Conclusion and further work

In this work the preparation of a range of proline-guanidine based catalysts has been achieved and their application to the Michael addition of diethyl malonate **53**, acetoacetate **70** and **93** to nitrostyrene **52**. Of these catalysts the most successful were the *N*-methyl proline catalysts **114**, **127** and **139** which gave ees of 7-44 %. (Figure 43)

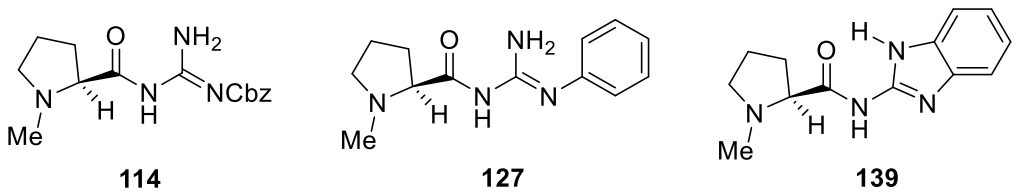

Figure 43: most successful catalysts

A mechanistic rationale for this reaction is difficult to determine and even with X-ray crystallographic data we can only speculate as to the nature of any intermediates present in the reaction. It is apparent from the preference of the (*R)*-stereochemistry in the product the reaction must be occurring as shown below with the enol adding to the top face of the as depicted below. (Scheme 59)

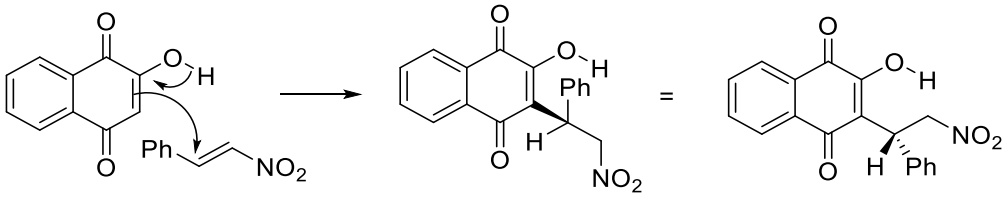

Scheme 59: Mechanism of reaction.

Our goal was to have an associative mechanism where potentially the enol/enolate was bound to the molecule via a hydrogen bonding interaction with the proline motif. Several structures can be visualized where there hydrogen bonding at the proline nitrogen, for example **167**. This in turn might lead to a disruption in any existing bonding and a structural change in the catalyst leading to other tautomeric forms for example structure **168**. There are obviously other hydrogen bonding

models possible in which the enolate hydrogen bonds via a single (structure **169**) or dual hydrogen bonding motif (structure **170**). (Scheme 60)

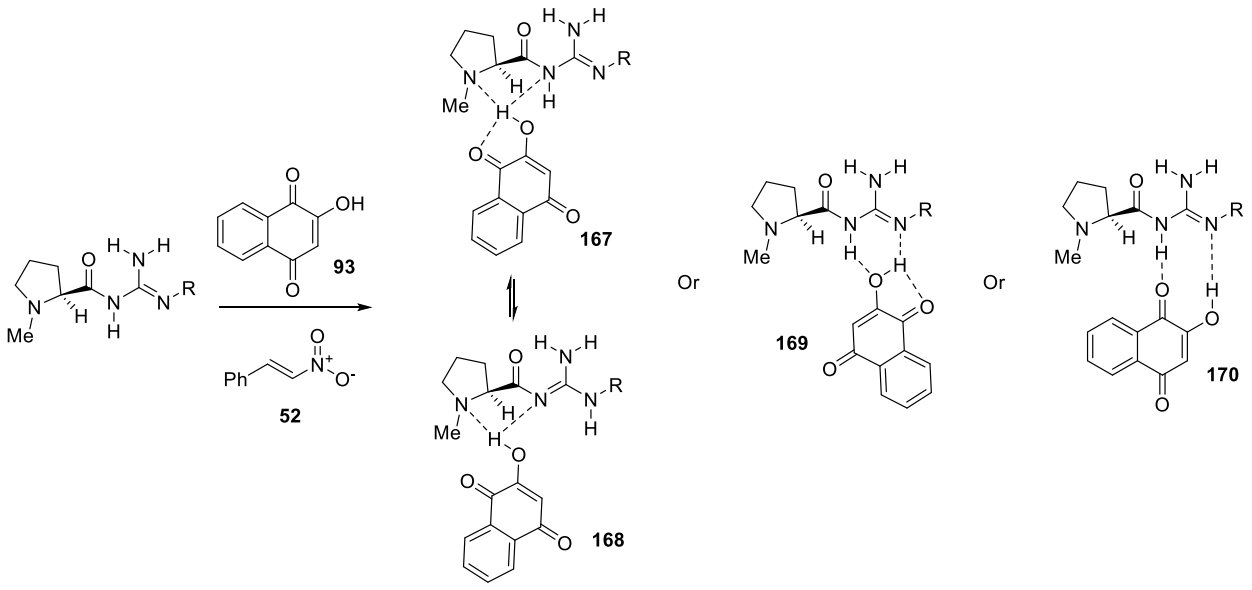

Scheme 60: Possible hydrogen bonding modes of the catalysts

If the association of the enolate is the first process occurring in this reaction then the mode of approach of nitrostyrene **52** is obviously dependent on the structure of the intermediate. An alternate mode of interaction in which the nitrostyrene **52** first associates with the catalyst is less convincing. This is because the mode of hydrogen bonding of the nitro-group would most likely be a bidentate one **171**, and the structures (from X-ray) of the un-protonated catalysts do not seem to be able to allow this. However on protonation the bidentate mode of this interaction is possible, but the nature of the protonation is not known. One conclusion from this mechanistic consideration is that the presence of an acid catalyst might possibly be a useful modification to the reaction conditions in future studies. (Figure 44)

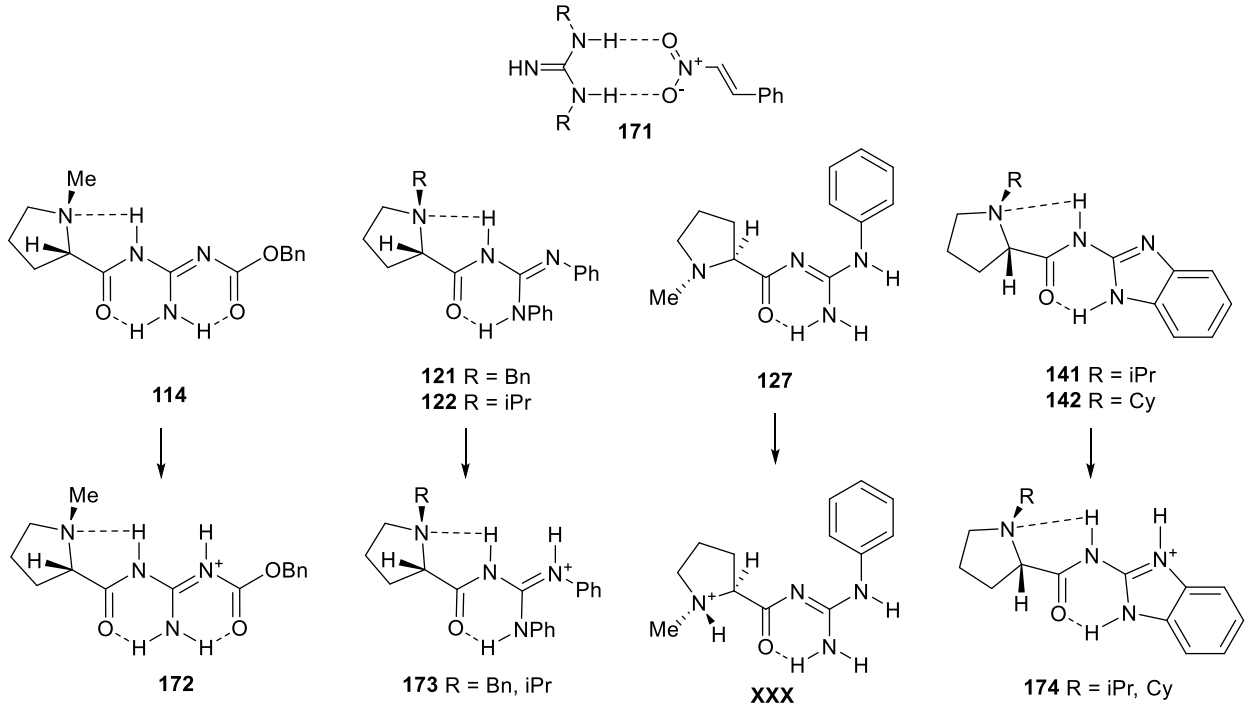

Figure 44: Possible protonated intermediates.

These catalysts were considered to be a first generation catalyst and a further part of the the project undertaken in the lab focused on the preparation of the C_2-symmetric proline catalysts **175-178** which were applied to the reaction of **52** with **93**. (Scheme 61)

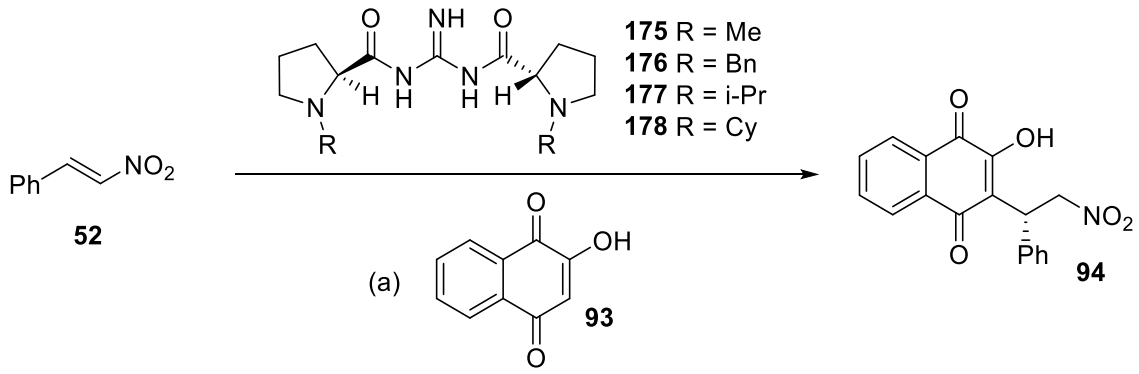

Scheme 61: Reaction catalyzed by **175-178**

Interestingly the dimethylated catalyst **175** was not easily prepared as it was very polar and was not amenable to extractive work up. This was possibly due to high solubility or that decomposition was occurring in water, similarly attempts at non-aqueous work ups proved difficult

as the product was not easily purified by silica gel chromatography. However, the catalysts **176-178** were prepared and did catalyse the reaction in 46-95% yield over 24-48 hours in dichloromethane, however no appreciable ees were observed. Efforts are being still being made to prepare **175** and similar tri-substituted guanidine derivatives.

It is apparent from our work that the guanidine **114** is the most efficient in the reaction we have studied and some possibilities are available for modifications. Several structures can be considered in which modifications are made to the guanidine NH_2 (**179** and **180**) leading to disruption of hydrogen bonding and possibly modifying the mode of action. Modifications to the carbamate protecting group for example changing to a Boc **181** or isopropyl **182** group might add a remote steric control group and this might improve on any selectivity in the reaction. (Figure 45)

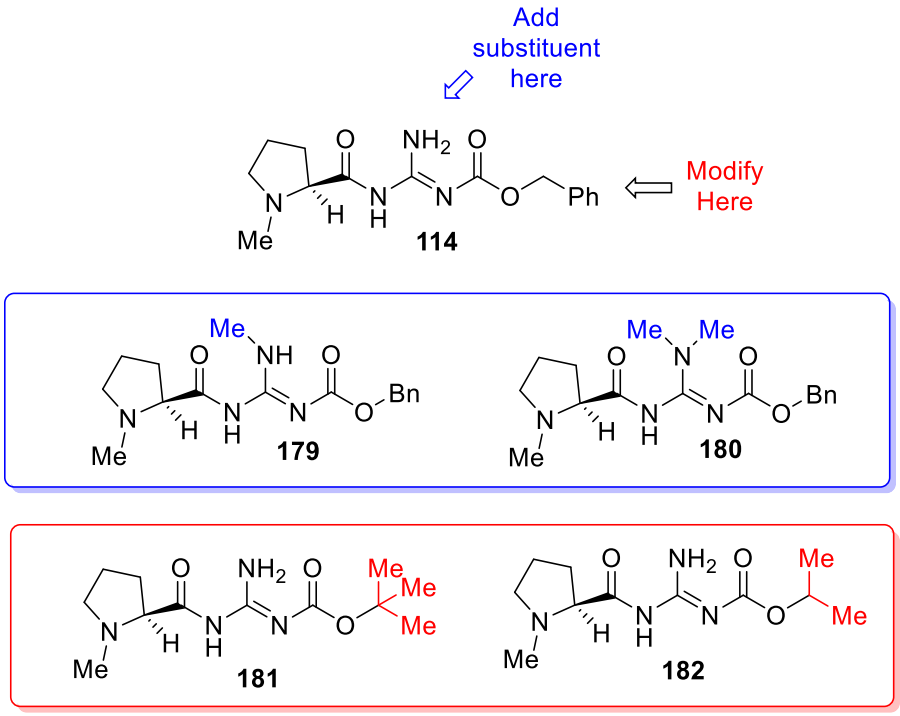

Figure 45: Potential modifications of the structure **114**

The original goal of this project was to create a series of simple and flexible compounds which were easy to prepare and would offer ease of modification to achieve enantioselectivity in range of organocatalytic reactions. A recent report by Bhowmick et al. reported[61] the most structurally simple organocatalyst being the hydrazine derivative of *L*-proline **185**. This was a viable catalyst for the aldol reaction of ketones **183** with aldehydes **184** leading to the aldol products **186** in 32-99% ee. Similarly a low-molecular-weight cyclohexanediamine derived thiourea catalyst **188**

was reported[62] by Dixon et al. for intramolecular Michael additions to α,β-unsaturated esters. They reported the transformation of **187** into **189** in 86% yield and 94% ee. (Scheme 62)

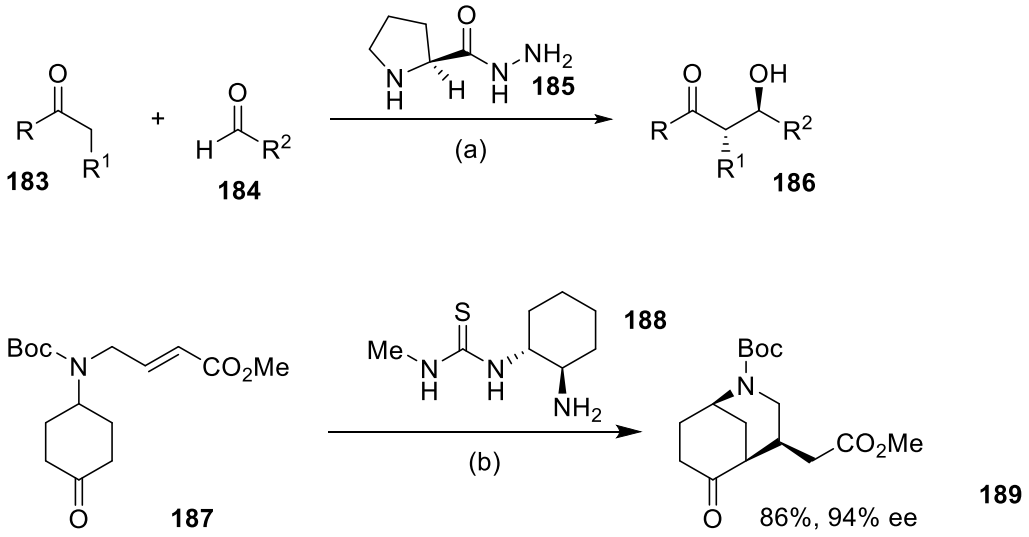

Scheme 62: Newly developed catalysts **185** and **188**. (a) **185** (0.1 eqv), PTSA, (0.05 eqv.) in H_2O; R = alkyl, R^1 = H, alkyl, R^2 = Aryl. (b) **188** (0.05 eqv), $PhCO_2H$ (0.025 eqv), CH_2Cl_2, 50°C, 48 h.

From this work we can speculate that modifications of the hydrazine catalyst **185** by alkylation on the proline **190** or the hydrazine **191**, might enable base mediated reaction to be achievable and the hydrazine might offer hydrogen bonding capability for an incoming Michael acceptor. A more simplistic approach might be desirable as well and the guanidine **192**, thiourea **193** and even the urea **194** derivatives might be catalysts. The thiourea derivative might also be a candidate for deactivation using Boc **195** or Cbz **196** groups. (Figure 46)

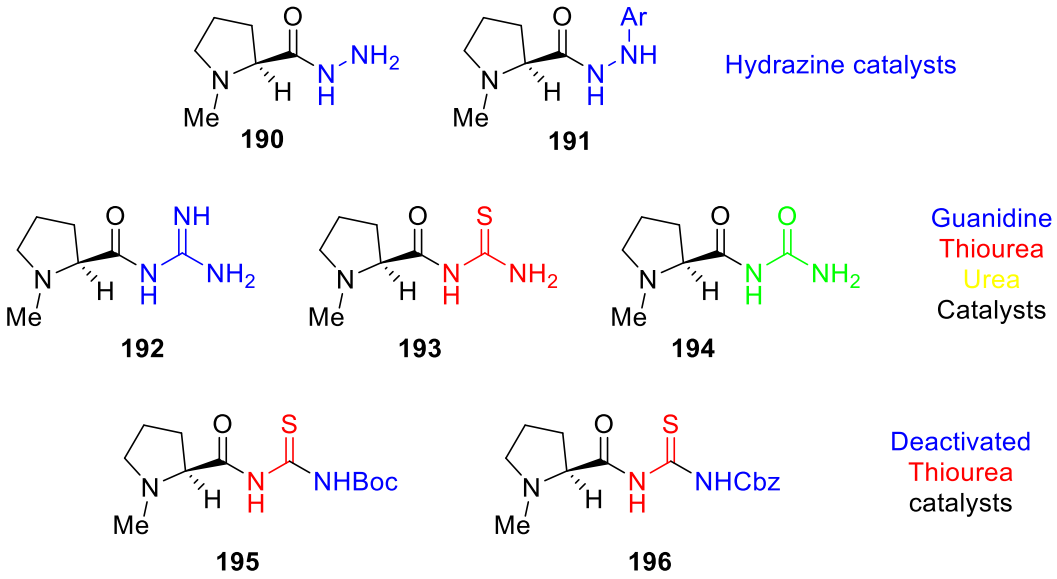

Figure 46: Proposed new catalysts

In conclusion we have developed a range of catalysts which can mediate the enantioselective Michael addition of **93** to 2-nitrostyrene **52**. The ees for this reaction are not high but are predictable based on structural considerations and this work has pointed the way for future developments in this area

Experimental

General Procedures:

Unless otherwise noted, reactions were stirred and monitored by TLC. TLC plates were visualized using iodine, phosphomolybdic acid or under UV light. All anhydrous reactions were conducted under a static argon atmosphere using oven dried glassware that had previously been cooled under a constant stream of nitrogen.

Materials

Reagents and starting materials were purchased from commercial suppliers and used without further purification unless otherwise noted. All anhydrous solvents used in reactions were distilled over either sodium wire and benzophenone (THF/DE) or calcium hydride (DCM), and used either immediately or stored over molecular sieves prior to use. Flash column chromatography was performed on Davisil® silica gel (35-70 microns) with the eluent specified in each case, TLC was conducted on precoated E.Merck silica gel 60 F_{254} glass plates.

Instrumentation

Melting points were determined using a Gallenkamp MF370 instrument and are uncorrected. ^{1}H and ^{13}C NMR spectra were recorded on a Bruker Avance 400 or 500 spectrometer with an internal deuterium lock at ambient temperature at 400 or 500 MHz with internal references of δ_H 7.26 and δ_C 77.016 ppm for $CDCl_3$, δ_H 3.31 and δ_C 49.0 ppm for CD_3OD and δ_H 2.54 ppm and δ_H 39.52 ppm for DMSO. All mass spectra were performed at the EPSRC National Mass Spectrometry Service Centre based in Swansea. Low resolution Chemical Ionisation (CI) and Electrospray Ionisation (ESI) mass spectra were recorded on a Micromass Quattro II spectrometer and high resolution mass spectra were recorded on either a Finnigan MAT 900 XLT or a Finnigan MAT 95 XP. Infrared samples were prepared as thin films or solutions using sodium chloride plates or as KBr discs; spectra were recorded on a Bruker Tensor 37 FT-IR.

Preparation of *N*-alkylated Prolines

***N*-methyl-*L*-proline 101[53]**

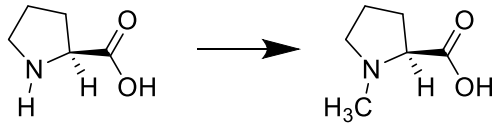

37 **101**

L-proline (2.04 g, 17.72 mmol) was dissolved in methanol (20 mL) together with formaldehyde solution (32% aqueous, 1.5 mL, 10.2 mmol) and the mixture was stirred. The flask was purged with N_2 gas and 10% Pd/C (0.509 g) was added following which the flask was purged with hydrogen gas (balloon) and stirred overnight. The solution was filtered through Celite© and evaporated to dryness and the solid obtained dissolved in a minimum of methanol (ca 10 ml) and diethyl ether was added to the cloud point (ca 1 mL) and the solution was cooled overnight in a freezer to give crystal of **101** which were removed by decanting the mother liquor. After drying under high vacuum the title compound **101** (1.23 g, 9.60 mmol) was obtained as a crystalline white solid in 68-94 % yield.[53]

R_f 0.23 (90% ME/DE); Mp 142-144 °C (lit. Mp 142-145 °C); $[\alpha]_D^{22}$ -84.0 (MeOH, c = 2.0); (lit. $[\alpha]_D^{23}$ -78.0 (MeOH, c = 2.0)); δ_H (D_2O) 3.78 (1H, dd, *J* 9.0, 7.2 Hz, CH), 3.56-3.52 (1H, m, CH), 2.99-2.90 (1H, m, CH), 2.75 (3H, s, Me), 2.35-2.29 (1H, m, CH), 2.00-1.79 (3H, m, CH); δ_C (D_2O) 172.6, 69.7, 55.5, 39.8, 27.9, 21.8; ν_{max} (KBr disk) 2900, 1668, 1611, 1467, 1400, 1353, 1326, 1233, 1182, 1112, 1055, 1024, 807, 774 cm^{-1}; MS (EI) m/z 129.0751 (7 %) $[M^+]$, 128.0717 (100 %) $[M-H]^-$, MS (ESI) m/z 130.0759 $[M+H]^+$, HRMS (ESI) m/z $C_6H_{10}NO_2$ $[M-H]^-$ requires 128.0717, found 128.0717.

Reaction Comments: This reaction was repeated seven times on scales ranging from 17.87 to 52.11 mmol to give a 68-94 % yield of **101**.

Preparation of *N*-benzyl-*L*-proline 102[54]

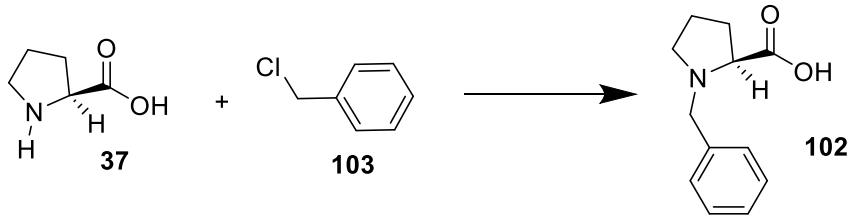

L-Proline (10.00 g, 86.86 mmol) and KOH (14.7 g, 262.06 mmol, 3.02 eqv.) were dissolved in *i*-PrOH (1L) and heated with stirring to 40 °C. As soon as the solution became transparent, benzyl chloride **103** (12.03 g, 10.94 ml, 95.02 mmol, 1.1 eqv.) was added in a dropwise fashion over 3 h. After cooling the reaction was neutralized using concentrated HCl to 5-6 pH and and chloroform (100 mL) was added and the mixture stirred overnight. The reaction was filtered and the residue washed with $CHCl_3$. The chloroform layers were separated, dried ($MgSO_4$) and evaporated to give the crude product which was triturated with acetone (100 mL) and filtered then washed with further acetone. After drying in a vacuum desiccator (P_2O_5) for two days the product **102** (8.20 g, 40.0 mmol) was obtained as a pale yellow solid in 46 % yield.[54]

R_f 0.36 (80% ME/EA); Mp 170-171 °C (lit. Mp 174-175 °C); $[\alpha]_D^{19}$ -22.5 (EtOH, c = 1.0), (lit. $[\alpha]_D^{20}$ -25.8 (EtOH, c = 1.0)) δ_H ($CDCl_3$) 7.51-7.44 (2H, m, 2 x CH), 7.41-7.35 (3H, m, 3 x CH), 5.84 (1H, br s OH), 4.39 (1H, d, *J* 12.9 Hz, CH), 4.31 (1H, d, *J* 12.9 Hz, CH), 3.98-3.85 (1H, m, CH), 3.71-3.60 (1H, m, CH), 3.10-2.93 (1H, m, CH), 2.42-2.21 (2H, m, 2 x CH), 2.10-1.88 (2H, m, 2 xCH); δ_C ($CDCl_3$) 171.4, 131.0, 130.7, 129.7, 129.4, 67.0, 57.9, 53.6, 29.0, 23.1; ν_{max} (KBr disk) 3432, 3036, 2873, 1745, 1634, 1394, 1321, 1203, 1005 cm^{-1}; MS (EI) m/z (%) 205.11 (14) $[M^+]$, 204.10 (100) $[M-H]^-$, MS (ESI) m/z, 206.11 $[M+H]^+$, HRMS (ESI) m/z $C_{12}H_{14}NO_2$ $[M-H]^-$ requires 204.1030, found 204.1030.

Preparation of *N*-isopropyl-*L*-proline 104[55]

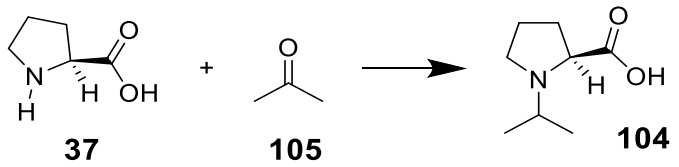

Acetone **105** (16.6 g, 19.0 ml, 260.57 mmol, 5.0 eqv) was added to *L*-proline **37** (6.0 g, 52.11 mmol) and stirred for 1 h then dry MeOH (10 mL) was added and the mixture stirred for a further 1 h. then Pd/C (0.5 g, 4.53 mmol) was cautiously added. Hydrogen gas was introduced (balloons) and the mixture was stirred for 42 h replenishing the hydrogen as needed. The reaction was then filtered through Celite© and evaporated to dryness to give a crude product which was re-dissolved in a minimum amount of methanol and the product precipitated by the addition of diethyl ether to give **104** in 95% yield (7.78 g, 49.5 mmol) as yellow crystals.[55]

R_f 0.21 (50 % ME/DE); Mp 189 °C; $[\alpha]_D^{18}$ -68.1 (MeOH, c 1.28); (lit. $[\alpha]_D^{20}$ -55.0 (MeOH, c = 1.28) δ_H (D_6-DMSO) 3.67 (1H, dd, *J* 4.7, 8.1 Hz, CH), 3.50 (1H, ddd, 2.7, 7.1, 11.0, CH), 3.37 (1H, septet, *J* 6.4 Hz, CH), 2.97 (1H, app dt, *J* 11.0, 6.6, CH), 1.96-2.05 (2H, m, CH_2), 1.79-1.89 (1H, m, CH), 1.52-1.67 (1H, m, CH), 1.19 (3H, d, *J* 6.4 Hz, Me), 1.17 (3H, d, *J* 6.4 Hz, Me); δ_C (D_6-DMSO) 169.9, 65.6, 55.1, 51.3, 29.9, 24.2, 18.4, 18.2; ν_{max} (KBr disk) 3432, 3036, 2873, 1634, 1394, 1321, 1203, 1080, 1005 cm^{-1}; MS (EI) m/z (%) 157.1 (9) $[M^+]$, 156.1 (100) $[M-H]^-$, MS (ESI) m/z 158.1 $[M+H]^+$, HRMS (ESI) m/z $C_8H_{14}NO_2$ $[M-H]^-$ requires 156.1030, found 156.1032.

Preparation of guanidine catalysts

Preparation of *N*-carbamimidoylbenzamide 109.[56]

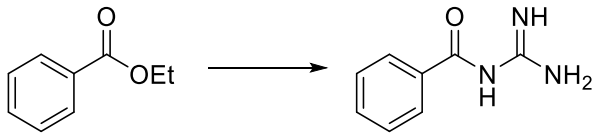

108 **109**

Sodium metal (2.33g, 99.9 mmol) was dissolved in dry ethanol (60 ml) under a constant flow of dry nitrogen gas to produce a solution of sodium ethoxide. Guanidine carbonate (9.0 g, 49.95 mmol, 0.5 eqv) was added and the mixture stirred for 24 h at rt. The reaction was filtered under an inert atmosphere to remove precipitated sodium carbonate, ethyl benzoate **108** (10.5 g, 70.0 mmol, 0.7 eqv) was added and the reaction stirred for a further 24 h. The reaction was evaporated to dryness at 70°C under rotary evaporation following which dioxane (ca 100 mL) was added to the residue and the mixture heated under reflux and then hot filtered. After cooling the filtrate to rt, on standing white crystals of **109** (3.68 g, 22.55 mmol) were obtained in 32 % yield.[56]

R_f 0.28 (10% MeOH/EA); Mp 184-186 °C (lit. 190-195 °C.); δ_H (MeOH), 7.84-7.86 (2H, d, CH), 7.42-7.51 (1H, m, CH), 7.38-7.41 (2H, t, CH), 6.29 (1H, s, NH), 4.72 (1H, s, NH), 0.78 (2H, s, NH_2); δ_C (MeOH) 126.2, 127.0, 133.8, 134.9, 164.4, 168.9; ν_{max} (KBr disc) 3422, 3314, 3204, 1659, 1626, 1589, 1532, 1448, 1366, 1287, 1136 cm^{-1}; MS (ESI) m/z 164.0815 $[M+H]^+$, HRMS (ESI), m/z $C_8H_{10}N_3O^+$ $[M+H]^+$ requires 164.0818 found 164.0815.

Attempted Preparation of (*S*)-*N*-(*N*-benzoylcarbamimidoyl)-1-methylpyrrolidine-2-carboxamide 110

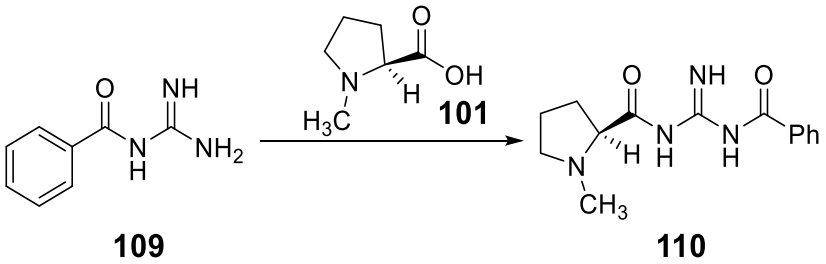

109 **110**

N-Methyl-*L*-proline **101** (0.5 g, 3.87 mmol, 1.0 eqv) and CDI (0.75 g, 4.65 mmol, 1.2 eqv) were dissolved in dry DMF (5 mL) and stirred at rt for 5 h. *N*-carbamimidoylbenzamide **91** (0.63 g, 3.87 mmol, 1.0 eqv) was then added and the mixture stirred for a further 24 h. After freeze drying to remove DMF the mixture was then purified by column chromatography (70% ethyl acetate in petrol) to give **110** (0.06 g, 0.22 mmol) as an oil which decomposed on exposure to air or solvent to give recovered **109**.

Preparation of *N*-Cbz-Guanidine 113[57]

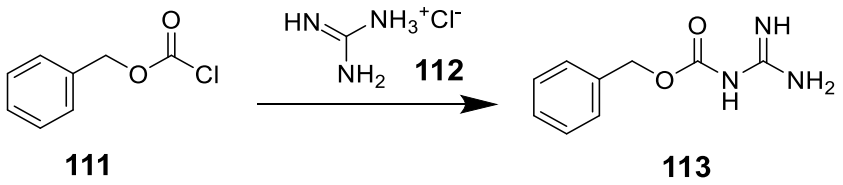

111 **113**

Guanidine hydrochloride (45.7 g, 478.4 mmol, 6.25 eqv) was dissolved in water (100 Ml) and NaOH (20.75 g, 518.8 mmol, 6.25 eqv) was added and the mixture stirred for 30 min and then cooled at 0 ^{o}C. A solution of benzyl chloroformate **112** (10.7 g, 10.7 ml, 62.7 mmol, 1.0 eqv) in dioxane (25 mL) was then added in a drop wise manner over 16 h and stirring continued for 48 h at rt. The mixture was extracted with ethyl acetate (4 x 100 mL) and the combined extracts washed with brine (2 x 50 mL) and dried ($MgSO_4$). After removal of the solvents by evaporation, the crude product was recrystallized from EA/PE to give **113** (9.93 g, 51.4 mmol) as a white solid in 82% yield.[57]

R_f 0.18 (80% EA/PE); Mp 140-141 °C; (lit. 140-142 ^{o}C.); δ_H (DMSO) 7.20-7.35 (5H, m, CH), 6.95 (4H, br. s, 2 x NH, NH_2), 4.95 (2H, s, CH_2); δ_C (DMSO) 163.1, 162.7, 138.0, 128.1, 127.2, 64.4; ν_{max} (KBr disk) 3418, 3307, 3203, 1663, 1629, 1597, 1539, 1452, 1376, 1290, 1132 cm^{-1}; MS (ESI) m/z 194.0923 $[M+H]^+$, HRMS (ESI) m/z $C_9H_{12}N_3O_2^+$ $[M+H]^+$ requires 194.0924, found 194.0923.

Preparation of (*S*)-Benzyl-2-(benzyloxycarbonyl)carbamimidoylcarbamoyl) pyrrolidine-1-carboxylate 114

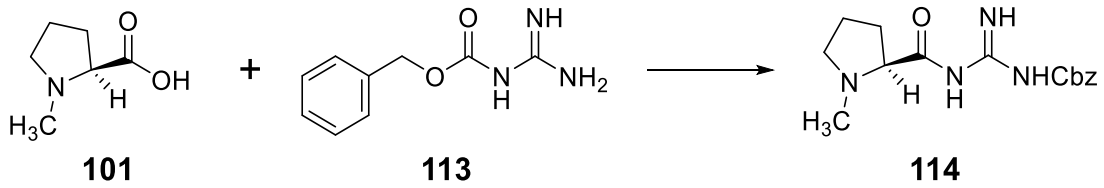

101 **113** **114**

N-Methyl-*L*-proline **101** (0.5 g, 3.87 mmol, 1.0 eqv) was dissolved in DMF (10 mL). After that add CDI (0.75 g, 4.65 mmol, 1.2 eqv) as a coupling agent. After 3 h cooled at (0 °C) and then add *N*-Cbz-Guanidine **113** (0.74 g, 3.87 mmol, 1.0 eqv) then leave it to be stirred for 5 h then stirring continued for 24 h at rt. Purification by column chromatography (0-60% DE in PE) gave **114** (0.86 g, 2.80 mmol) was obtained as a white solid in 68-73% yield.

R_f 0.17 (10% DE/PE); Mp 67-70 °C; $[\alpha]_D^{21}$ -64.8 ($CHCl_3$, c = 1.0); δ_H ($CDCl_3$) 9.66 (1H, br. s, NH), 8.92 (2H, br. s, NH), 7.35-7.30 (2H, m, 2 x CH), 7.28-7.18 (3H, m, CH), 5.05 (2H, s, CH_2), 3.06-3.00 (1H, m, CH), 2.94 (1H, dd, J = 10.4, 4.9 Hz, CH_2), 2.36-2.31 (1H, m, CH_2), 2.30 (3H, s, Me), 2.23-2.12 (1H, m, CH_2), 1.86-1.78 (1H, m, CH_2), 1.76-1.63 (2H, m, CH_2); δ_C ($CDCl_3$) 178.0, 163.9, 158.9, 136.6, 128.5, 128.2, 128.0, 69.0, 67.0, 56.5, 41.7, 31.4, 24.7; ν_{max} (KBr disk) 3395, 3279, 3086, 2945, 1704, 1656, 1611, 1375, 1090 cm^{-1}; MS (EI) m/z (%) 304.2488(3) [M^+], MS (ESI) 305.1610 $[M+H]^+$, HRMS (ESI) m/z $C_{15}H_{21}N_4O_3^+$ $[M+H]^+$ requires 305.1608, found 305.1610.

Reaction Comments: This reaction was repeated three times on scales ranging from 0.774-3.870 mmol to give 68-73 % yields.

Preparation of (*S*)-benzyl-(amino(1-benzylpyrrolidine-2-arboxamido)methylene)carbamate 116

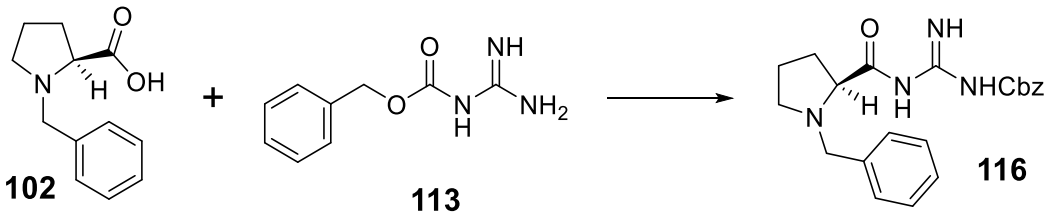

N-Benzyl-*L*-proline **116** (1.0 g, 4.87 mmol, 1.0 eqv) was dissolved in dry DMF (5 mL) and CDI (0.95 g, 5.85 mmol, 1.2 eqv) was added and the mixture stirred for 3 h. The reaction was cooled (0 °C) and Cbz-Guanidine **113** (0.95 g, 4.87 mmol, 1.0 eqv) was added and the mixture stirred overnight. A precipitate formed overnight which was re-dissolved by the addition of further dry DMF (6 mL) and stirring continued for 1 d. The reaction was diluted with water (200 mL) and extracted with EA (2 x 100 mL), the combined extracts dried ($MgSO_4$) and evaporated under reduced pressure. Purification by column chromatography (0-60% EA in PE) gave the **116** (1.63 g, 4.29 mmol) in 89% yield as a white solid yield.

R_f 0.10 (20% EA/PE); Mp 101-103 °C; $[\alpha]_D^{21}$ -67.1 ($CHCl_3$, c = 1.0); δ_H ($CDCl_3$) 9.75 (1H, br s, NH), 8.76 (2H, s, NH), 7.43-7.36 (2H, m, 2 x CH), 7.36-7.30 (3H, m, 3 x CH), 7.31-7.16 (5H, m, Ph), 5.15 (1H, d, *J* 12.5 Hz, CH), 5.10 (1H, d, *J* 12.5 Hz, CH), 3.69 (2H, s, CH_2), 3.24 (1H, dd, *J* 10.3, 4.4 Hz, CH_2), 3.03-3.13 (1H, m, CH), 2.36-2.51 (1H, m, CH), 2.13-2.28 (1H, m, CH), 1.81-1.91 (1H, m, CH), 1.64-1.81 (2H, m, CH_2); δ_C ($CDCl_3$) 177.9, 163.6, 158.5, 136.8, 136.7, 129.5, 128.6, 128.4, 128.1, 128.0, 127.8, 67.0, 66.9, 59.7, 54.2, 31.0, 24.2; ν_{max} (KBr disc) 3381, 3059, 2938, 1703, 1652, 1607, 1553, 1404, 1118, 1028 cm^{-1}; MS (ESI) m/z 381.2 $[M+H]^+$, HRMS (ESI) m/z $C_{21}H_{25}N_4O_3^+$ $[M+H]^+$, requires 381.1921, found 381.1919.

Preparation of (*S*)-Benzyl-(amino(1-isopropylpyrrolidine-2-carboxamido)methylene)carbamate 117

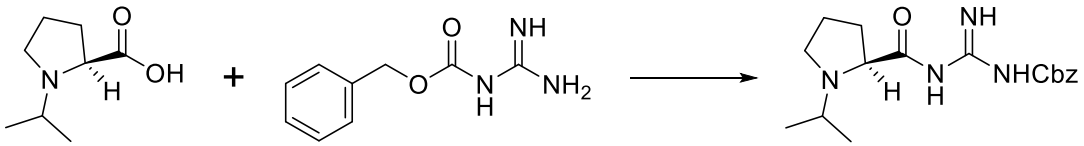

104 **113** **117**

Isopropyl-*L*-proline **117** (1.0 g, 6.36 mmol, 1.0 eqv) was dissolved in dry DMF (10 mL) and CDI (1.24 g, 7.63 mmol, 1.2 eqv) was added and the mixture stirred for 4 h. Cbz-Guanidine **113** (1.23 g, 6.36 mmol, 1.0 eqv) was added to the dark yellow solution and the mixture stirred overnight. The reaction was diluted with water (200 mL) and extracted with EA (2 x 100 mL), the combined extracts dried ($MgSO_4$) and evaporated under reduced pressure. The residue was co-evaporated with heptane (4 x 50 mL) to remove trace amount of DMF followed by purification by column chromatography (0-100% EA in PE) to give **117** (2.09 g, 6.29 mmol) in 99% yield as an oily yellow adduct.

R_f 0.30 (80% EA/PE); $[\alpha]_D^{20}$ -31.1 ($CHCl_3$, c = 1.0); δ_H ($CDCl_3$) 9.93 (1H, br s, NH), 9.05 (1H, br s, NH), 8.86 (1H, br s, NH), 7.39-7.43 (2H, m, 2 x CH), 7.28-7.37 (3H, m, 3 x CH), 5.16 (1H, d, *J* 12.5 Hz, CH), 5.12 (1H, d, *J* 12.5 Hz, CH), 3.34 (1H, dd, *J* 10.6, 2.4 Hz, CH), 3.05-3.16 (1H, m, CH), 2.72-2.83 (1H, m, CH), 2.48-2.58 (1H, m, CH), 2.07-2.20 (1H, m, CH), 1.89-1.98 (1H, m, CH), 1.74-1.84 (1H, m, CH), 1.62-1.74 (1H, m, CH), 1.06 (3H, d, *J* 7.0 Hz, Me), 1.04 (3H, d, *J* 7.0 Hz, Me); δ_C (D_6-DMSO) 178.5, 157.1, 150.7, 137.2, 128.3, 127.6, 127.6, 65.7, 63.8, 51.9, 49.6, 30.9, 24.2, 20.9, 19.3; ν_{max} (KBr disc) 3388, 3080, 2968, 1706, 1651, 1562, 1413, 1275, 1135 cm^{-1}; MS (ESI) m/z 333.2 $[M+H]^+$, HRMS (ESI) m/z $C_{17}H_{25}N_4O_3^+$ $[M+H]^+$ requires 333.1921, found 333.1920.

Preparation of (*S*)-benzyl(amino(1-cyclohexylpyrrolidine-2-

carboxamido)methylene)carbamate 119

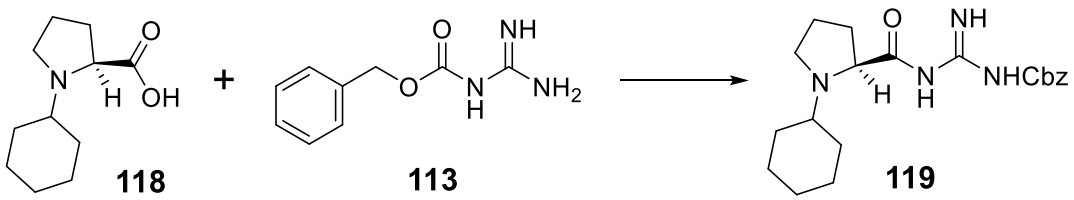

N-Cyclohexyl-*L*-proline **119** (0.4 g, 2.03 mmol, 1.0 eqv) was dissolved in dry DMF (5 mL) and CDI (0.39 g, 2.43 mmol, 1.2 eqv) was added and the mixture stirred for 4 h. Cbz-Guanidine **113** (0.39 g, 2.03 mmol, 1.0 eqv) was then added and stirring continued for 18 h. The reaction was diluted with water (200 mL) and extracted with EA (2 x 100 mL) and the combined extracts dried ($MgSO_4$) and evaporated under reduced pressure. The residue was dissolved in a minimum amount of ME and DE was added to the cloud point which on cooling overnight in a freezer gave **119** (0.70 g, 1.88 mmol) in 93% yield as a pale yellow solid.

R_f 0.19 (80% EA/PE); Mp 167-168 °C; $[\alpha]_D^{16}$ -63.5 ($CHCl_3$, c = 1.0); δ_H ($CDCl_3$) 9.92 (1H, s, NH), 9.08 (1H, s, NH), 8.87 (1H, s, NH), 7.38-7.49 (2H, m, 2 x CH), 7.27-7.37 (3H, m, 3 x CH), 5.16 (1H, d, *J* 12.3 Hz, CH), 5.12 (1H, d, *J* 12.3 Hz, CH), 3.38 (1H, dd, *J* 2.9, 10.7 Hz, CH), 3.11-3.21 (1H, m, CH), 2.52-2.62 (1H, m, CH), 2.32-2.42 (1H, m, CH), 2.04-2.18 (1H, m, CH), 1.55-1.98 (8H, m, 8 x CH), 1.05-1.27 (5H, m, 5 x CH). δ_C ($CDCl_3$) 179.8, 163.8, 158.7, 136.6, 128.4, 128.3, 128.0, 67.0, 64.5, 62.4, 51.1, 31.6, 31.5, 30.8, 25.8, 25.4, 25.4, 24.6; ν_{max} (KBr disk) 3407, 3273, 3058, 2932, 1702, 1650, 1604, 1450, 1374, 1090 cm^{-1}; MS (ESI) m/z 373.2 $[M+H]^+$, HRMS (ESI) m/z $C_{20}H_{29}N_4O_3^+$ $[M+H]^+$ requires 373.2234, found 373.2233.

Preparation of (*S*)-*N*-(*N*,*N*'-diphenylcarbamimidoyl)-1-methylpyrrolidine-2-carboxamide 120

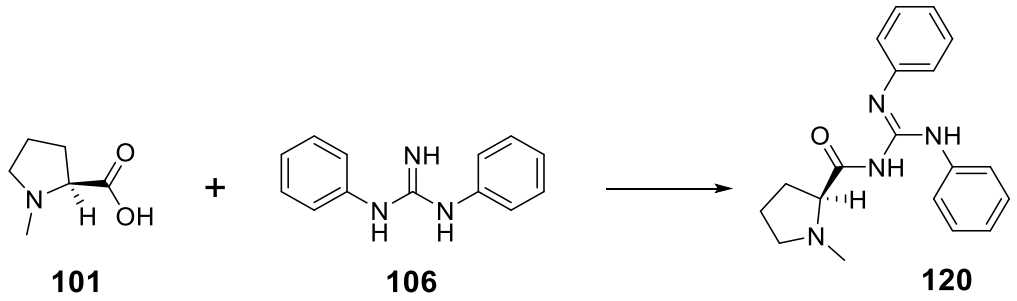

101 **106** **120**

N-Methyl-*L*-proline **101** (2.0 g, 15.48 mmol, 1.0 eqv) was dissolved in dry DMF (8 mL) and CDI (3.01 g, 18.58 mmol, 1.2 eqv) was added and the mixture stirred for 1 d. The mixture was cooled (0 °C) and 1,3-Diphenylguanidine **106** (3.27 g, 15.48 mmol, 1.0 eqv) was added and the mixture stirred for 1 d. The reaction was diluted with water (50 mL) and extracted with EA (3 x 80 mL) and the combined extracts washed with water (3 x 100 mL), dried ($MgSO_4$) and evaporated under reduced pressure. Purification by column chromatography (0-80% EA in PE) gave **120** (1.37 g, 1.2 mmol) in 28% as a yellow solid.

R_f 0.39 (80% EA/PE); Mp 110 °C; $[\alpha]_D^{20}$ +38.1 ($CHCl_3$, c = 1.0); δ_H (D_6-DMSO) 9.92 (1H, br. s, NH), 9.78 (1H, s, NH), 7.70 (2H, d, *J* 7.9 Hz, 2 x CH), 7.27-7.36 (4H, m, 4 x CH), 6.98-7.07 (2H, m, 2 x CH), 6.90 (2H, d, *J* 7.7 Hz, 2 x CH), 2.93 (1H, dd, *J* 10.5, 4.2 Hz, CH), 2.62-2.69 (1H, m Hz, CH), 2.20 (1H, ddd, *J* 5.9, 8.9, 10.8 Hz, CH) 2.01-2.14 (1H, m, CH), 2.10 (3H, s, Me), 1.60-1.78 (2H, m, 2 x CH), 1.35-1.51 (1H, m, CH); δ_C (D_6-DMSO) 174.3, 147.4, 140.8, 139.2, 129.2, 128.7, 122.7, 122.4, 122.2, 119.3, 68.1, 55.7, 40.8, 30.3, 24.2; ν_{max} (KBr disc) 3550, 3057, 2944, 1701, 1604, 1420, 1321, 1208, 1157, 1080 cm^{-1}; MS (ESI) m/z 323.2 $[M+H]^+$, HRMS (ESI) m/z $C_{19}H_{23}N_4O^+$ $[M+H]^+$ requires 323.1866, found 323.1865.

Preparation of (*S*)-1-benzyl-*N*-(*N*,*N*'-diphenylcarbamimidoyl)pyrrolidine-2-carboxamide 121

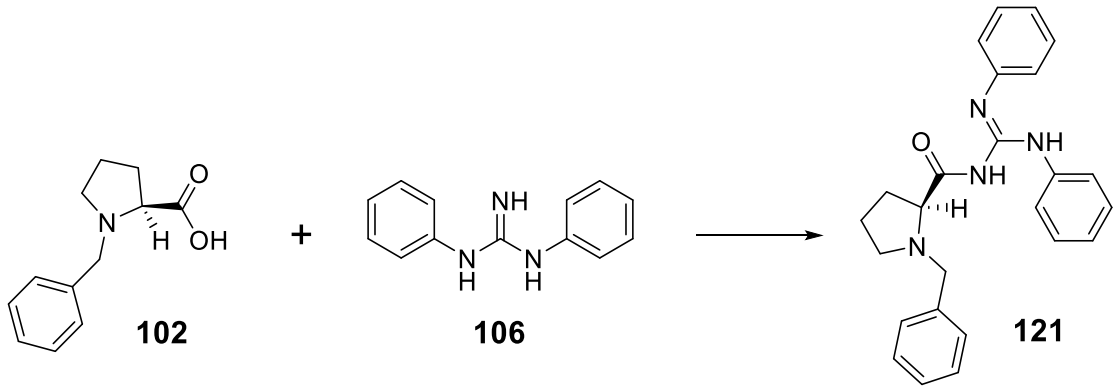

N-Benzyl-*L*-proline **121** (1.0 g, 4.87 mmol, 1.0 eqv) was dissolved in dry DMF (4 mL) CDI (0.95 g, 5.85 mmol, 1.2 eqv) was added and the mixture stirred for 5 h. 1,3-Diphenylguanidine **106** (1.03 g, 4.87 mmol, 1.0 eqv) was then added and the mixture stirred for 1 d. The reaction was diluted with water (200 mL) and extracted with EA (2 x 100 mL) and the combined extracts dried ($MgSO_4$) and evaporated under reduced pressure. The residue was co-evaporated with toluene to remove trace amount of DMF followed by purification by column chromatography (0-60% EA in PE) to give **121** (0.64 g, 1.60 mmol) in 33% yield as a pale yellow solid.

R_f 0.32 (30% EA/PE); Mp 135-136 °C; $[\alpha]_D^{21}$ +22.3 ($CHCl_3$, c = 1.0); δ_H (D_6-DMSO) 9.97 (1H, s, NH), 9.89 (1H, s, NH), 7.67 (2H, d, *J* 8.0 Hz, 2 x CH), 7.38 (2H, t, *J* 7.7 Hz, 2 x CH), 7.30 (2H, t, *J* 7.7 Hz, 2 x CH).7.17-7.23 (3H, m, 3 x CH), 7.10 (1H, t, *J* 7.4 Hz, CH) 6.95-7.04 (3H, m, 3 x CH), 6.69-6.75 (2H, m, 2 x CH), 3.66 (1H, d, *J* 13.0 Hz, CH), 3.37 (1H, d, *J* 13.0 Hz, CH), 3.26 (1H, dd, *J* 10.3, 3.6 Hz, CH), 2.59-2.66 (1H, m, CH), 2.09-2.28 (2H, m, 2 x CH), 1.82-1.92 (1H, m, CH), 1.70-1.77 (1H, m, CH), 1.50-1.64 (1H, m, CH); δ_C (D_6-DMSO) 174.8, 147.0, 140.3, 139.0, 137.7, 129.4, 128.7, 128.4, 128.3, 127.0, 122.9, 122.4, 122.3, 119.3, 66.7, 58.7, 53.3, 30.2, 24.0; ν_{max} (KBr disc) 3550, 3054, 2924, 1698, 1651, 1588, 1321, 1205, 1077, 1028 cm^{-1}; MS (ESI) m/z 399.2 $[M+H]^+$, HRMS (ESI) m/z $C_{25}H_{27}N_4O^+$ $[M+H]^+$ requires 399.2179, found 399.2177.

Preparation of (*S*)-*N*-(*N*,*N*'-diphenylcarbamimidoyl)-1-isopropylpyrrolidine-2-carboxamide 122

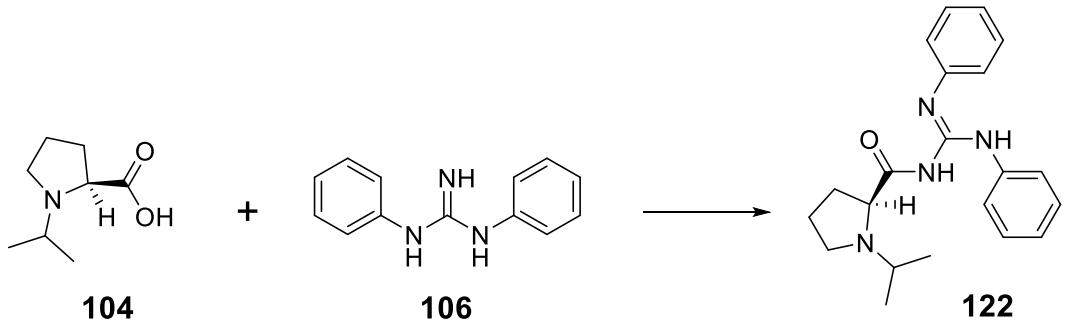

104 **106** **122**

N-Isopropyl-*L*-proline **122** (1.0 g, 6.36 mmol, 1.0 eqv) was dissolved in dry DMF (10 mL) and CDI (1.24 g, 7.63 mmol, 1.2 eqv) was added and the mixture stirred for 5 h. 1,3-Diphenylguanidine **106** (1.30 g, 6.36 mmol, 1.0 eqv) was added and the mixture stirred overnight. The reaction was diluted with water (200 mL) and extracted with EA (2 x 100 mL) and the combined extracts dried ($MgSO_4$) and evaporated under reduced pressure. Purification by column chromatography (0-80% EA in PE) gave **122** (1.87 g, 5.34 mmol) in 84% yield as a pale yellow solid.

R_f 0.32 (20% EA/PE); Mp 136 °C; $[\alpha]_D^{16}$ +52.1 ($CHCl_3$, c = 1.0); δ_H ($CDCl_3$) 10.23 (1H, s, NH), 9.99 (1H, s, NH), 7.73 (2H, d, *J* 8.0 Hz, 2 x CH), 7.28-7.37 (4H, m, 4 x CH), 6.99-7.08 (2H, m, 2 x CH), 6.91-6.96 (2H, m, 2 x CH), 3.25 (1H, dd, *J* 9.7, 2.9 Hz, CH), 2.65-2.72 (1H, m, CH), 2.45-2.57 (1H, m, CH), 2.33 (1H, ddd, *J* 5.6, 8.9, 11.4 Hz, CH), 1.91-2.08 (2H, m, 2 x CH), 1.68-1.77 (1H, m, CH), 1.42-1.57 (1H, m, CH), 0.74 (3H, d, J = 6.4, Me), 0.73 (3H, d, J = 6.4, Me); δ_C ($CDCl_3$) 176.5, 147.9, 141.0, 139.3, 129.6, 128.9, 123.1, 122.7, 122.6, 119.8, 64.8, 52.9, 50.3, 31.5, 24.8, 21.5, 19.7; ν_{max} (KBr disk) 3350, 3261, 3050, 2829, 1791, 1680, 1588, 1301, 1079, 894 cm^{-1}; MS (EI) m/z (%) 349.2 (3) $[M-H]^-$, MS (ESI) m/z 351.2 $[M+H]^+$, HRMS (ESI) m/z $C_{21}H_{27}N_4O^+$ $[M+H]^+$ requires 351.2179, found 351.2183.

Preparation of (*S*)-1-cyclohexyl-*N*-(*N*,*N*'-diphenylcarbamimidoyl)pyrrolidine-2-

Carboxamide 123

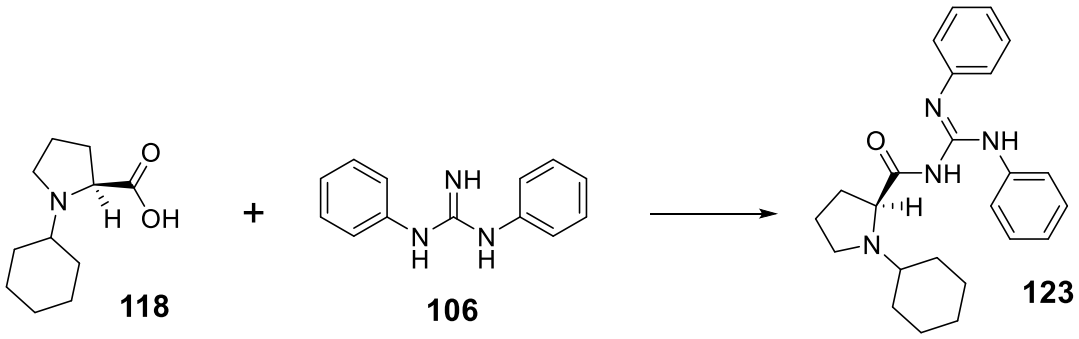

N-Cyclohexyl-*L*-proline **123** (1.01 g, 5.07 mmol, 1.0 eqv) was dissolved in dry DMF (5 mL) following which CDI (0.99 g, 6.08 mmol, 1.2 eqv.) was added and the mixture stirred for 4 h. 1,3-Diphenylguanidine **106** (1.07 g, 5.07 mmol, 1.0 eqv) was then added and the mixture stirred for 18 h. The reaction was diluted with water (200 mL) and extracted with EA (3 x 100 mL) and the combined extracts dried ($MgSO_4$) and evaporated under reduced pressure. The solid product was triturated with DE (2 x 50 ml) to give **123** (1.67 g, 4.28 mmol) in 84% yield as off white solid.

R_f 0.25 (15% EA/PE); Mp 78-79 °C; $[\alpha]_D^{15}$ +6.5 (ME, c = 1.0); δ_H ($CDCl_3$) 10.21 (1H, s, NH), 9.98 (1H, s, NH), 7.72 (2H, d, *J* 7.5 Hz, 2 x CH), 7.25-7.30 (4H, m, 4 x CH), 6.97-7.10 (2H, m, 2 x CH), 6.93 (2H, d, *J* 7.3 Hz, CH), 3.28 (1H, dd, *J* 3.0, 9.4 Hz, CH), 2.71 (1H, t, *J* 7.5 Hz, CH), 2.33 (1H, ddd, *J* 5.6, 8.5, 11.4, CH), 2.04-2.14 (1H, m, CH), 1.91-2.03 (1H, m, CH), 1.41-1.75 (7H, m, 7 x CH), 1.36 (1H, d, *J* 12.3 Hz, CH), 0.90-1.05 (3H, m, 3 x CH), 0.75-0.87 (1H, m, CH), 0.60-0.74 (1H, m, CH); δ_C ($CDCl_3$) 176.6, 147.9, 141.0, 139.3, 129.6, 128.9, 123.0, 122.7, 122.7, 119.8, 64.6, 61.7, 58.6, 32.0, 31.3, 30.2, 25.9, 25.3, 25.2, 24.7; ν_{max} (KBr disk) 3058, 2927, 1691, 1650, 1589, 1316, 1028, 750 cm^{-1}; MS (ESI) m/z 391.2 $[M+H]^+$, HRMS (ESI) m/z $C_{24}H_{31}N_4O^+$ $[M+H]^+$ requires 391.2492, found 391.2482.

Preparation of phenylguanidinium nitrate 126 [58]

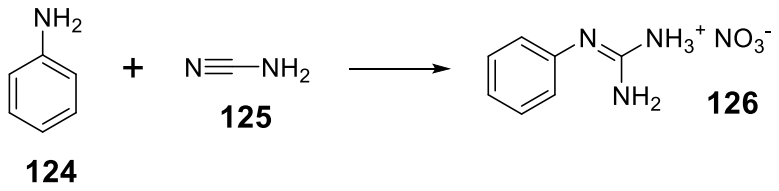

Aniline **124** (9.3 g, 9.12 mL, 99.9 mmol, 1.0 eqv) was dissolved in EtOH (75 mL) and an aqueous solution of HNO_3 (9.0 mL, 131.2 mmol, of a 65% w/w solution prepared from 90 % w/w nitric acid by dilution into water **(CAUTION)**) was then added. An aqueous solution of cyanamide (50% w/w, 12.6 g, 11.5 mL, 148.0 mmol, 1.48 eqv) was then added to the mixture which was heated to reflux for 16 h. The mixture was cooled in ice and diethyl ether (800 mL) was added and the mixture stirred vigorously for 1 h. The grey precipitate was removed by filtration and washed with DE and dried under vacuum to give **126** (11.7 g, 85.9 mmol) as a grey solid in 86% yield.[58]

R_f 0.26 (20% EA/PE); Mp 112-115 °C (lit. Mp 120-122 °C); δ_H (D_6-DMSO) 9.53 (NH, part exchanged), 8.33 (NH, part exchanged), 7.42-7.49 (1H, m, CH), 7.27-7.37 (3H, m, 3 x CH), 7.22-7.27 (1H, m, CH), 5.42 (NH part exchanged); δ_C (DMSO) 155.7, 135.3, 129.7, 126.5, 124.5; ν_{max} (KBr disc) 3347, 3050, 1675, 1629, 1582, 1384, 1112 cm^{-1}; MS (ESI) m/z 136.1 $[M+H]^+$, HRMS (ESI) m/z $C_7H_{10}N_3^+$ $[M+H]^+$ requires 136.0869, found 136.0867.

Preparation of (*S*)-1-methyl-*N*-(*N*'-phenylcarbamimidoyl)pyrrolidine-2-carboxamide 127.

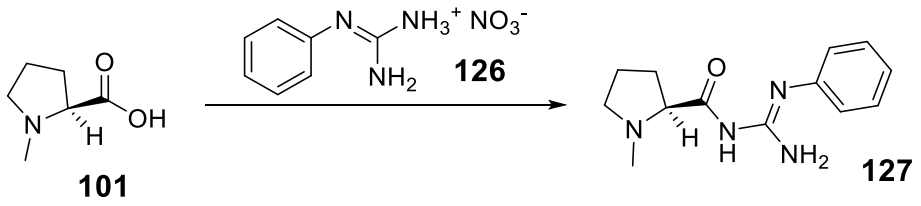

N-Methyl-*L*-proline **101** (0.50 g, 3.87 mmol, 1 eqv.) was suspended in dry DMF (10 ml), CDI (0.75 g, 4.65 mmol, 1.2 eqv.) was added and the mixture stirred for 3 h. In a separate flask, sodium metal (0.09 g, 3.87 mmol, 1 eqv) was added to methanol (4 mL) and after complete reaction, phenylguanidinium nitrate **126** (0.84 g, 4.26 mmol, 1.1 eqv.) was added and the solution stirred for 30 min. This mixture was evaporated under high vacuum to dryness and the activated proline solution was added via cannula and the resultant mixture stirred for 5 days. Water (100 mL) was added and the mixture extracted with EA (3 x 100 ml) and the combined extracts washed with water (3 x 500 mL), dried ($MgSO_4$) and evaporated under reduced pressure. Purification of the residue by column chromatography (0-50% EA in PE) gave **127** (0.38 g, 1.53 mmol) in 40% yield as a pale yellow solid.

R_f 0.28 (50% EA/ PE); Mp 133 °C; $[\alpha]_D^{16}$ -80.1 ($CHCl_3$, c = 1.0); δ_H ($CDCl_3$) 7.33 (2H, t, *J* 8.0, 2 x CH), 7.06 (1H, t, *J* 7.5 H, CH), 6.95-7.00, (2H, m, 2 x CH),5.00-6.89 (3H, br s, 3 x NH), 3.10-3.24 (1H, m, CH), 3.02 (1H, dd, *J* 10.4, 4.8 Hz, CH), 2.44 (3H, s, Me), 2.38-2.46 (1H, m, CH), 2.20-2.32 (1H, m, CH), 1.91-2.00 (1H, m, CH), 1.75-1.87 (2H, m, 2 x CH); δ_C ($CDCl_3$) 176.7, 148.2, 146.1, 129.7, 123.6, 122.9, 69.2, 56.5, 41.7, 31.1, 24.5; ν_{max} (KBr disc) 3314, 3085, 2903, 1631, 1590, 1515, 1391, 1286, 1183, 1039 cm^{-1}; MS (ESI) m/z 247.2 $[M+H]^+$, HRMS (ESI) m/z $C_{13}H_{19}N_4O^+$ $[M+H]^+$ requires 247.1553, found 247.1552.

Preparation of (*S*)-1-benzyl-*N*-(*N*'-phenylcarbamimidoyl)pyrrolidine-2-carboxamide 128.

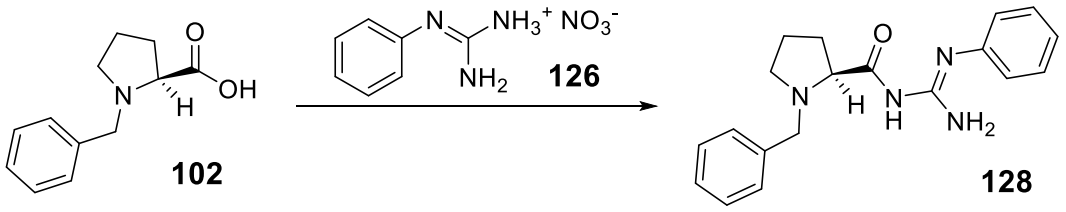

N-benzyl-*L*-proline **102** (2.0 g, 9.74 mmol, 1 eqv.) was dissolved in dry DMF (10 ml), CDI (1.9 g, 11.69 mmol, 1.20 eqv.) was added and the mixture stirred for 16 h. In a separate flask, sodium metal (0.224 g, 9.74 mmol 1.0 eqv.) was added to methanol (8 mL) and after complete reaction, phenylguanidinium nitrate **126** (1.93 g, 9.74 mmol, 1.0 eqv.) was added and the solution stirred for 30 min. This mixture was evaporated under high vacuum to dryness and the activated proline solution was added via cannula and the resultant mixture stirred for 5 days. Water (100 mL) was added and the mixture extracted with EA (3 x 100 ml) and the combined extracts washed with water (3 x 500 mL), dried ($MgSO_4$) and evaporated under reduced pressure. Purification of the residue by column chromatography (0-50% EA in PE) gave **128** (1.63 g, 5.06 mmol) in 52% yield as a yellow oil.

R_f 0.31 (20% EA/PE); $[\alpha]_D^{16}$ -47.6 ($CHCl_3$, c = 1.0); δ_H ($CDCl_3$) 7.20-7.45 (7H, m, 7 x CH), 7.04 (1H, t, *J* 7.4 Hz, CH), 6.96-7.01 (2H, m, 2 x CH), 5.50-7.20 (3H, br s, 3 x NH), 3.80 (1H, d, *J* 12.5 Hz, CH), 3.68 (1H, d, *J* 12.5 Hz, CH), 3.27 (1H, dd, *J* 4.4, 10.4 Hz, CH), 3.00-3.17 (1H, m, CH), 2.40-2.53 (1H, m, CH), 2.17-2.33 (1H, m, CH), 1.92-2.03 (1H, m, CH), 1.70-1.87 (2H, m, 2 x CH); δ_C ($CDCl_3$) 176.4, 149.7, 146.6, 137.4, 129.7, 129.3, 128.7, 127.6, 123.5, 122.9, 67.3, 59.9, 54.2, 30.1, 24.3; ν_{max} (KBr disk) 3413, 3060, 2943, 1659, 1643, 1589, 1305, 1064, 752 cm^{-1}; MS (ESI) m/z 323.2 $[M+H]^+$, HRMS (ESI) m/z $C_{19}H_{23}N_4O^+$ $[M+H]^+$ requires 323.1866, found 323.1864.

Preparation of (*S*)-1-isopropyl-*N*-(*N*'-phenylcarbamimidoyl)pyrrolidine-2-carboxamide 129.

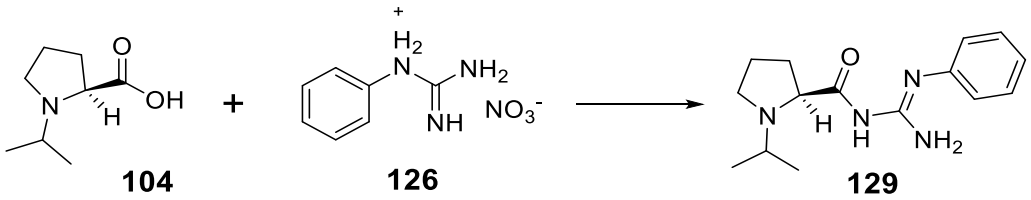

104 **126** **129**

N- isopropyl-*L*-proline **104** (1.5 g, 9.54 mmol, 1 eqv.) was dissolved in dry DMF (10 ml) and CDI (1.86 g, 11.45 mmol, 1.20 eqv.) was added and the mixture stirred for 16 h. In a separate flask, phenylguanidinium nitrate **126** (1.29 g, 9.54 mmol, 1 eqv.) was suspended in dry DMF (10 mL) and NaH (60% dispersion in mineral oil NaH, 0.38 g, 9.54 mmol, 1.0 eqv.) was added and the mixture. The solution of CDI activated proline was then added to this mixture via cannula and the mixture stirred for 2 d. Water (100 mL) was added and the mixture extracted with EA (3 x 100 ml) and the combined extracts washed with water (3 x 500 mL), dried ($MgSO_4$) and evaporated under reduced pressure to give a crude product. Attempted purification by column chromatography was unsuccessful as was attempted recrystallisation

Attempted preparation of the dimethylguanidine catalysts 132a-d

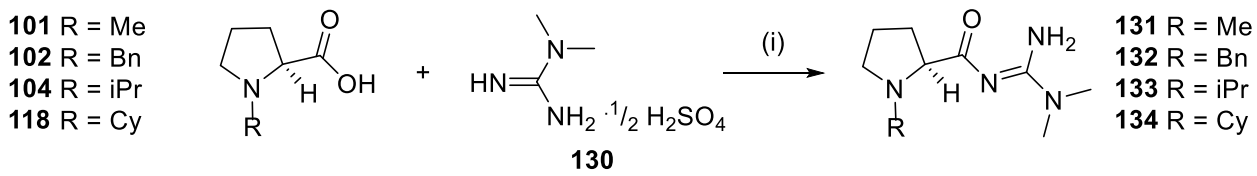

Attempted preparation of 131: *N*-Methyl-*L*-proline **101** (1.0 g, 7.74 mmol, 1.66 eqv) was dissolved in dry DMF (9 mL) and CDI (1.51 g, 9.29 mmol, 2.0 eqv) was added and the mixture stirred for 4 h. In a separate flask NaH (60% dispersion in oil, 0.19 g, 4.65 mmol, 1.00 eqv was suspended in dry DMF (2 mL) and 1,1-dimethylguanidine hemisulfate **130** (0.67 g, 4.95 mmol, 1.06 eqv) was added and the mixture stirred for 30 min. The activated proline solution was then added to this flask via cannula and the mixture stirred for 2 d. Water (100 mL) was added and the mixture extracted with EA (3 x 100 ml) and the combined extracts washed with water (3 x 500 mL). Attempted removal of the imidazole by washing an ethyl acetate solution of this mixture with water led to loss of the majority of the material.

Attempted preparation of 132: *N*-Benzyl-*L*-proline **102** (1.0 g, 4.87 mmol, 1.85 eqv.) was dissolved in dry DMF (5 mL), CDI (0.95 g, 5.85 mmol, 1.2 eqv) was then added and the mixture stirred for 3 h. In a separate flask NaH (60% dispersion in oil, 0.24 g, 6.00 mmol, 1.9 eqv.) was suspended in dry DMF (2 mL) and 1,1-dimethylguanidine hemisulfate **130** (0.43 g, 3.16 mmol, 1.0 eqv) was added and the mixture stirred for 20 min. The activated proline solution was then added to this flask via cannula and the mixture stirred for 18 h. Water (2-3 drops) was added and the mixture co-evaporated to remove the DMF and the residue purified by column chromatography (0-100% EA in PE) to give a crude mixture of **132** and imidazole (1.21 g) as a yellow waxy solid. Attempted removal of the imidazole by washing an ethyl acetate solution of this mixture with water led to loss of the majority of the material.

Partial data from crude mixture: R_f 0.38 (50% EA in PE); ($CDCl_3$) 9.50-12.50 (2H, br s, NH_2), 7.22-7.80 (5H, m, Ph), 4.21 (1H, d, *J* 12.4 Hz, CH), 3.38 (1H, d, *J* 12.4 Hz, CH), 3.25 (1H, t, *J* 8.4 Hz, CH), 2.96-3.08 (1H, m, CH), 3.07 (6H, s, 2 x Me), 2.25-2.40 (1H, m, CH), 2.12-2,25 (1H, m, CH), 1.88-2.00 (1H, m, CH), 1.60-1.83 (2H, m, CH_2); δ_C ($CDCl_3$) 185.0, 161.0, 138.3, 129.7, 128.2, 127.1, 71.3, 59.1, 53.1, 36.7, 30.0, 22.4; MS (ESI) m/z 275.2 $[M+H]^+$, HRMS (ESI) m/z $C_{15}H_{23}N_4O^+$ $[M+H]^+$ requires 275.1866, found 275.1866.

Attempted Preparation of 133: *N*-Isopropyl-*L*-proline **104** (1.0 g, 6.36 mmol, 2.0 eqv.) was dissolved in dry DMF (8 mL) and CDI (1.24 g, 7.63 mmol, 2.4 eqv.) was added and the mixture

stirred for 4 h. In a separate flask NaH (60% dispersion in oil, 0.15 g, 3.75 mmol, 1.2 eqv.) was suspended in dry DMF (2 mL) and 1,1-dimethylguanidine hemisulfate **130** (0.43 g, 3.16 mmol, 1.0 eqv.) was added and the mixture stirred for 30 min. The activated proline ester was then added to this flask via cannula and the mixture stirred for 39 h. Water (2-3 drops) was added and the mixture co-evaporated to remove the DMF and the residue purified by column chromatography (0-100 % ME in EA) to give a crude mixture of **133**, imidazole and the starting material **104** (1.05 g) as an orange solid. Attempted removal of the imidazole by washing an ethyl acetate solution of this mixture with water led to loss of the majority of the material.

Partial data from crude mixture: R_f 0.23 (80% ME in EA); δ_C ($CDCl_3$) 184.1, 160.5, 67.5, 36.4, 30.52, 24.03, 20.14, 18.56; MS (EI) m/z (%) 226.2 (5) $[M^+]$, 225.2 (40) $[M-H]^-$, MS (ESI) m/z 227.2 $[M+H]^+$, HRMS (ESI) m/z $C_{11}H_{23}N_4O^+$ $[M+H]^+$ requires 227.1866, found 227.1866.

Attempted Preparation of 134: *N*-cyclohexyl-*L*-proline **118** (1.0 g, 5.07 mmol, 1.86 eqv) was dissolved in dry DMF (8 mL) and CDI (0.99 g, 6.08 mmol, 2.24 eqv) was added and the mixture stirred for 4 h. In a separate flask NaH (60% dispersion in oil, 0.22 g, 5.5 mmol, 2.0 eqv) was suspended in dry DMF (2 mL) and 1,1-dimethylguanidine hemisulfate **130** (0.37 g, 2.72 mmol, 1.0 eqv) of was added and the mixture stirred for 30 min. The activated proline ester was then added to this flask via cannula and the mixture stirred for 48 h. Water (2-3 drops) was added and the mixture co-evaporated to remove the DMF and the residue purified by column chromatography (0-100 % ME in EA) to give a crude product (0.89 g) as a brown oil. Analysis of this oil by NMR and MS indicated only the presence of imidazole and the starting material **118**.

Preparation of (*S*)-*N*-(1H-benzo[d]imidazol-2-yl)-1-methylpyrrolidine-2-carboxamide 139

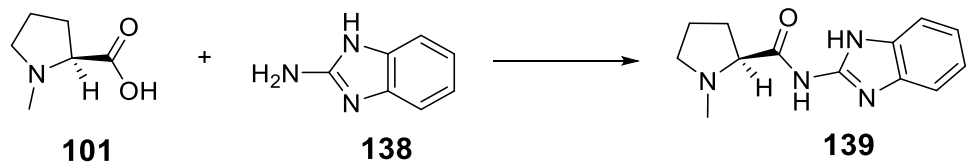

101 **138** **139**

N-Methyl-*L*-proline **101** (1.0 g, 7.74 mmol, 1.0 eqv) was added to dry DMF (9 mL) and CDI (1.51 g, 9.29 mmol, 1.2 eqv) was added and the mixture stirred for 4 h. 2-Aminobenzimidazole **138** (1.05 g, 7.74 mmol, 1.0 eqv) was then added and the mixture stirred for 38 h. Water (100 mL) was added and the mixture extracted with EA (3 x 100 ml), the combined extracts were dried ($MgSO_4$) and evaporated under reduced pressure. Purification by column chromatography (0-50% ME in EA) gave **139** (1.04 g, 4.25 mmol) in 55% as a pale yellow solid.

R_f 0.16 (20% ME/EA); Mp 242-244 °C; $[\alpha]_D^{16}$ -117 ($CDCl_3$, c = 1.0); δ_H ($CDCl_3$) 9.50-12.0 (2H, br s, 2 x NH), 7.42-7.55 (2H, m, 2 x CH), 7.17-7.25 (2H, m, 2 x CH), 3.16-3.24 (1H, m, CH), 3.16 (1H, dd, *J* 4.6, 10.6, CH), 2.47 (3H, s, Me), 2.42-2.52 (1H, m, CH), 2.25-2.38 (1H, m, CH), 1.94-2.04 (1H, m, CH), 1.77-1.90 (2H, m, 2 x CH); δ_C ($CDCl_3$) 175.3, 152.7, 146.3, 122.3, 122.3, 68.7, 56.7, 41.9, 31.4, 24.9**;** ν_{max} (KBr disk) 3350, 3244, 3050, 2946, 1702, 1626, 1589, 1310, 1021, 861 cm^{-1}; MS (ESI) m/z 245.1 $[M+H]^+$, HRMS (ESI) m/z $C_{13}H_{17}N_4O^+$ $[M+H]^+$ requires 245.1397, found 245.1399.

Preparation of (*S*)-*N*-(1H-benzo[d]imidazol-2-yl)-1-benzylpyrrolidine-2-carboxamide 140

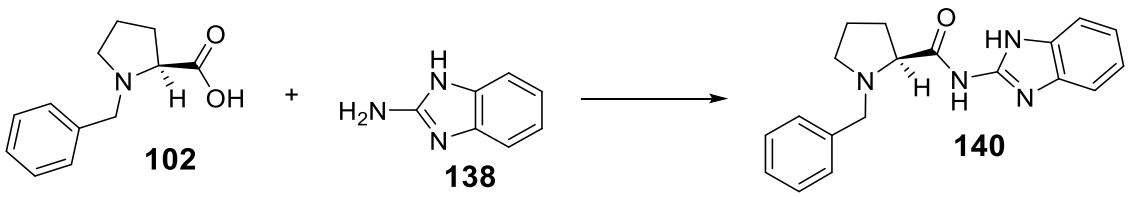

N-Benzyl-*L*-proline **102** (1.0 g, 4.87 mmol, 1.0 eqv) was added to dry DMF (9 mL) and CDI (0.95 g, 5.85 mmol, 1.2 eqv) was added and the mixture stirred for 4 h. 2-Aminobenzimidazole **138** (0.69 g, 4.87 mmol, 1.0 eqv) was then added and the mixture stirred for 48 h. Water (100 mL) was added and the mixture extracted with EA (3 x 100 ml), the combined extracts were dried ($MgSO_4$) and evaporated under reduced pressure. Purification by column chromatography (0-100% EA in PE) gave **140** (1.48 g, 4.64 mmol) in 96% as a pale yellow solid.

R_f 0.47 (20% EA/PE); Mp 228-229 °C; $[\alpha]_D^{16}$ -106.8 ($CDCl_3$, c = 1.0); δ_H ($CDCl_3$) 10.84 (1H, s, NH), 10.30 (1H, br s, NH), 7.45-7.65 (1H, m, CH), 7.05-7.38 (8H, m, 8 x CH), 3.79 (1H, d, *J* 12.7 Hz, CH), 3.64 (1H, d, *J* 12.7 Hz, CH), 3.37 (1H, dd, *J* 10.6, 4.2 Hz, CH), 3.02-3.12 (1H, m, CH), 2.41-2.51 (1H, m, CH), 2.16-2.31 (1H, m, CH), 1.89-2.00 (1H, m, CH), 1.65-1.84 (2H, m, CH_2); δ_C ($CDCl_3$) 175.3, 153.0, 146.1, 137.3, 129.3, 128.8, 127.8, 122.3, 122.3, 66.7, 60.1, 54.3, 31.1, 24.5; ν_{max} (KBr disk) 3350, 3253, 3025, 2942, 1768, 1688, 1624, 1307, 1047, 744 cm^{-1}; MS (ESI) m/z 321.2 $[M+H]^+$, HRMS (ESI) m/z $C_{19}H_{21}N_4O^+$ $[M+H]^+$ requires 321.1710, found 321.1710.

Preparation of (*S*)-*N*-(1H-benzo[d]imidazol-2-yl)-1-isopropylpyrrolidine-2-carboxamide 141

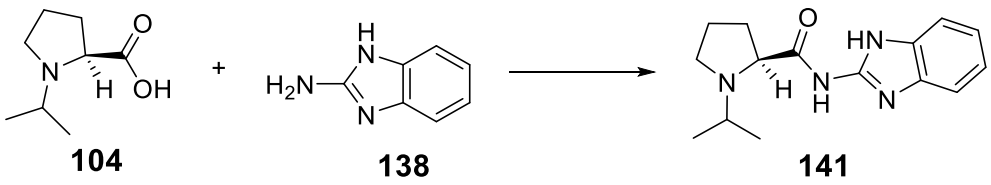

N-isopropyl-*L*-proline **104** (1.0 g, 6.36 mmol, 1.0 eqv) was added to dry DMF (10 mL) and CDI (1.25 g, 7.63 mmol, 1.2 eqv) was added and the mixture stirred for 3 h. 2-Aminobenzimidazole **138** (0.86 g, 6.36 mmol, 1.0 eqv) was then added and the mixture stirred for 40 h. Water (100 mL) was added and the mixture extracted with EA (3 x 100 ml), the combined extracts were dried ($MgSO_4$) and evaporated under reduced pressure. Purification by column chromatography (0-100% EA in PE) gave **141** (1.48 g, 5.45 mmol) in 86% as a pale yellow solid.

R_f 0.25 (20% EA/PE); Mp 112-114 °C; $[\alpha]_D^{16}$ -110.5 ($CDCl_3$, c = 1.0); δ_H ($CDCl_3$) 11.00 (1H, s, NH), 10.60 (1H, s, NH), 7.30-7.65 (2H, m, 2 x CH), 7.16-7.24 (2H, m, 2 x CH), 3.47 (1H, dd, *J* 10.5, 2.8 Hz, CH), 3.14-3.21 (1H, m, CH), 2.78-2.91 (1H, m, CH), 2.59 (1H, ddd, *J* 5.8, 9.1, 10.9, CH), 2.09-2.23 (1H, m, CH), 1.98-2.08 (H, m, CH), 1.65-1.88 (2H, m, CH_2), 1.11 (3H, d, *J* 6.5 Hz, Me), 1.10 (3H, d, *J* 6.5 Hz, Me); δ_C ($CDCl_3$) 176.7, 153.1, 146.1, 122.3, 122.3, 64.2, 53.4, 50.9, 31.7, 24.9, 21.5, 20.1**;** ν_{max} (KBr disk) 3312, 3071, 2927, 1680, 1610, 15536, 1304, 1095, 747 cm^{-1}; MS (ESI) m/z 273.2 $[M+H]^+$, HRMS (ESI) m/z $C_{15}H_{21}N_4O^+$ $[M+H]^+$ requires 273.1710, found 273.1710.

Preparation of (*S*)-*N*-(1H-benzo[d]imidazol-2-yl)-1-cyclohexylpyrrolidine-2-carboxamide 142

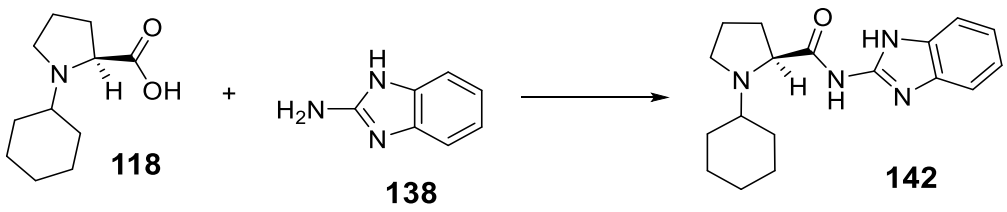

N-cyclohexyl-*L*-proline **118** (1.0 g, 5.07 mmol, 1.0 eqv) was added to dry DMF (10 mL) and CDI (0.99 g, 6.08 mmol, 1.2 eqv) was added and the mixture stirred for 4 h. 2-Aminobenzimidazole **138** (0.71 g, 5.07 mmol, 1.0 eqv) was then added and the mixture stirred for 48 h. Water (100 mL) was added and the mixture extracted with EA (3 x 100 ml), the combined extracts were dried ($MgSO_4$) and evaporated under reduced pressure. Purification by column chromatography (0-60 % EA in PE) gave **142** (1.32 g, 4.23 mmol) in 84% as a pale yellow solid.

R_f 0.37 (20% EA/PE); Mp 129-130 °C; $[\alpha]_D^{15}$ -105.1 (ME, c = 1.0); δ_H (DMSO) 12.10 (1H, s, NH), 10.72 (1H, s, NH), 7.36-7.52 (2H, m, 2 x CH), 7.04-7.14 (2H, m, 2 x CH), 3.55 (1H, dd, *J* 10.1, 3.0 Hz, CH), 3.12-3.20 (1H, m, CH), 2.56-2.66 (1H, m, CH), 2.40-2.50 (1H, m, CH), 2.03-2.17 (1H, m, CH), 1.81-1.95 (2H, m, 2 x CH), 1.63-1.81 (5H, m, 5 x CH), 1.49-1.59 (1H, m, CH), 1.02-1.28 (5H, m, 5 x CH); δ_C (CD_3OD) 175.5, 152.9, 147.1, 123.3, 123.3, 65.4, 63.6, 52.1, 33.1, 32.2, 31.9, 27.0, 26.5, 26.4, 25.5. ν_{max} (KBr disk) 3309, 3230, 3056, 2927, 1686, 1627, 1589, 1308, 1029, 743 cm^{-1}; MS (ESI) m/z 313.2 $[M+H]^+$, HRMS (ESI) m/z $C_{18}H_{25}N_4O^+$ $[M+H]^+$ requires 313.2023, found 313.2016.

Preparation of TBD.HBPh$_4$ 144[60]

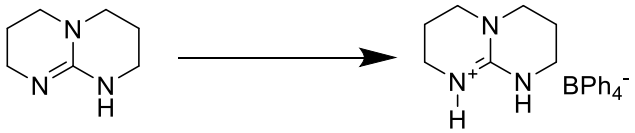

143 **144**

A solution of $NaBPh_4$ (2.05 g, 6.02 mmol, 1.2 eqv) in H_2O (10 ml) was added to a cooled solution of **143** (1.39 g, 5.01 mmol, 1.0 eqv) dissolved in HCl (10%, 10 mL). The resulting precipitate was filtered and washed with water (3 x 10 ml) and MeOH (3 x 5 ml) then triturated with a mixture of chloroform and methanol (4:1, 20 mL) to give **144** (1.93 g, 4.17 mmol) as an off light yellow solid in 84 % yield.[60]

R_f 0.40 (80% EA/PE); Mp 222°C (lit. 223-224°C): δ_H (DMSO) 7.41 (2H, s, NH), 7.16-7.18 (8H, m, CH), 6.92 (8H, t, *J* = 7.4 Hz, CH), 6.78 (4H, t, *J* = 7.2 Hz, CH), 3.26 (4H, t, *J* = 6.0 Hz, CH_2), 3.16 (4H, t, *J* = 4.4 Hz, CH_2), 1.7-1.8 (4H, m, CH_2): ν_{max} (KBr disk) 3415, 3312, 1661, 1623, 1592, 1529, 1451, 1372, 1280, 1130 cm^{-1}; HRMS (ESI), m/z $C_{31}H_{38}BN_4^+$ [M+NH_4^+] requires 477,3190 found 477.3181.

General method for the reaction of β-nitrostyrene 52 and diethyl malonate 53

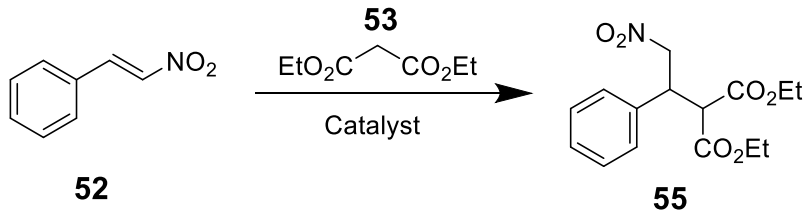

β-nitrostyrene (500.0 mg, 3.37 mmol) was added to a solution of the catalyst (ca. 0.1 eqv) dissolved in the required solvent (5 mL). If required, the catalyst was prepared by combining the required reagents and stirring in the reaction solvent for 10 min, or by firstly dissolving them in dry MeOH and then evaporating the mixture and re-dissolving in the reaction solvent (see Table 2a-2d and discussion). The reaction was then cooled (0 °C) and diethyl malonate (1.2-10 eqv.) was added dropwise. The reaction was stirred to rt and monitored by 1H NMR and on completion the reaction was evaporated onto silica and purified by column chromatography eluting with 5 % ethyl acetate in petrol. For yields and ees see Tables 2-5 and discussion.

Table 2:

Entry	Catalyst	Malonate (eqv.)	Solvent	Time	Conversion (NMR)	Yield/%	ee %
1	**152**	1.0	Toluene	3 d	28 %	25	NA
2	**106**	1.1	Toluene	2 d	100 %	ND	NA
3	**101**	1.1	Toluene	1 d	100 %	27	7 (R)
4	**147**	10.7	CH_2Cl_2	3 d	100 %	80	4 (R)
5	**147**	1.1	CH_2Cl_2	2 d	100 %	18	7 (R)
6	**147**	2.0	CH_2Cl_2	28 h	100 %	35	3 (R)

Entry 1: Catalyst **152** (39.0 mg, 0.37 mmol, 0.1 eqv) in toluene gave **55** (0.263 g, 0.85 mmol) in 25% yield.

Entry 2**:** Catalyst **106** (73.9 mg, 0.34 mmol, 0.1 eqv) in toluene gave crude **55** (1.563 g).

Entry 3**: 101** (48.1 mg, 0.38 mmol, 0.11 eqv) in toluene gave **55** (0.282 g, 0.91 mmol) in 27% yield.

Entry 4**:** Catalyst **106** (70.3 mg, 0.34 mmol, 0.1 eqv) and **101** (48.3 mg, 0.38 mmol, 0.11 eqv) in dichloromethane gave **55** (0.832 g, 2.7 mmol) in 80% yield.

***Entry 5*:** Catalyst **106** (70.9 mg, 0.34 mmol, 0.1 eqv) and **101** (48.9 mg, 0.34 mmol, 0.1 eqv) in dry dichloromethane gave **55** (0.185 g, 0.6 mmol) in 18% yield.

***Entry 6*:** Catalyst **106** (70.8 mg, 0.34 mmol, 0.1 eqv) and **101** (49.8 mg, 3.7 mmol, 0.11 eqv) in dry dichloromethane gave **55** (0.360 g, 1.2 mmol) in 35% yield.

Table 3

Entry	Catalyst	Malonate (eqv.)	Solvent	Time	Conversion	Yield/%	ee %
1	**153**	1.5	CH_2Cl_2	1 d	No reaction	NA	NA
2	**153**/**101**	1.5	THF	4 d	No reaction	NA	NA
3	**153**/**101**	1.5	DMF	35 d	58 %	14	3.4 (R)

Entry 1 Catalyst **153** (71.7 mg, 0.34 mmol, 0.1 eqv) in dry dichloromethane gave no reaction**.**

***Entry 2*:** Catalyst **153** (85.9 mg, 0.41 mmol, 0.12 eqv) and **101** (43.8 mg, 0.34 mmol, 0.1 eqv) in THF gave no reaction

***Entry 3*:** Catalyst **153** (86.1 mg, 0.41 mmol, 0.12 eqv) and **101** (43.6 mg, 0.34 mmol, 0.1 eqv) in dry DMF gave **55** (0.145 g, 0.47 mmol) in 14% yield.

Table 4

Entry	Catalyst	Malonate (eqv.)	Solvent	Time	Conversion	Yield/%	ee %
1	**113**	14.5	CH_2Cl_2	38 d	91%	61	NA
2	**143**	1.5	CH_2Cl_2	37 d	5 %	ND	NA
3	**113**/**101**	1.5	CH_2Cl_2	1 d	66 %	28	3 (R)
4[(i)]	**113**/**101**	3.0	CH_2Cl_2	6 d	82 %	71	1 (R)
5	**145**/**101**	3.0	CH_2Cl_2	6 d	No reaction	NA	NA
6	**143**/**101**	3.0	CH_2Cl_2	7 d	No reaction	NA	NA

***Entry 4*:** Catalyst **113** (65.2 mg, 0.34 mmol, 0.1 eqv) in dry dichloromethane gave **55** (0.63 g, 2.04 mmol) in 61% yield.

***Entry 2*:** Catalyst **145** (86.7 mg, 0.34 mmol, 0.1 eqv) in dry dichloromethane gave 5% conversion to **55** as determined by NMR.

***Entry 3*:** Catalyst **113** (64.5 mg, 0.34 mmol, 0.1 eqv) and **101** (47.4 mg, 0.37 mmol, 0.11 eqv) in dry dichloromethane gave **55** (0.29 g, 0.94 mmol) in 28% yield.

***Entry 4*:** Catalyst **113** (68.0 mg, 0.34 mmol, 0.1 eqv) and **101** (46.9 mg, 0.37 mmol, 0.11 eqv) in dry dichloromethane gave **55** (0.73 g, 2.36 mmol) in 71% yield.

***Entry 5*:** Catalyst **145** (88.0 mg, 0.34 mmol, 0.1 eqv) and **101** (48.5 mg, 0.37 mmol, 0.11 eqv) in dry dichloromethane gave **55** no reaction.

***Entry 6*:** Catalyst **143** (88.0 mg, 0.34 mmol, 0.1 eqv) and **101** (48.5 mg, 0.37 mmol, 0.11 eqv) in dry dichloromethane gave **55** no reaction.

Table 5

Entry	Catalyst	Malonate (eqv.)	Solvent	Time	Conversion	Yield/%	ee %
1	**114**	1.5	DMF	2 d	23 %	29 %	4
2	**114**	1.5	CH_2Cl_2	5 d	No reaction	NA	NA
3	**114**	1.5	THF	8 d	No reaction	NA	NA

***Entry 1*:** Catalyst **114** (102.2 mg, 0.34 mmol, 0.1 eqv) in dry DMF gave **55** (0.3 g, 3.35 mmol) in 29 % yield.

***Entry 2*:** Catalyst **114** (102.3 mg, 0.34 mmol, 0.1 eqv) in dry dichloromethane gave no reaction.

***Entry 3*:** Catalyst **114** (102.0 mg, 0.34 mmol, 0.1 eqv) in dry THF gave no reaction.

General method for reaction of 2-hydroxy-1,4-napthoquinone 93 with β-nitrostyrene 52

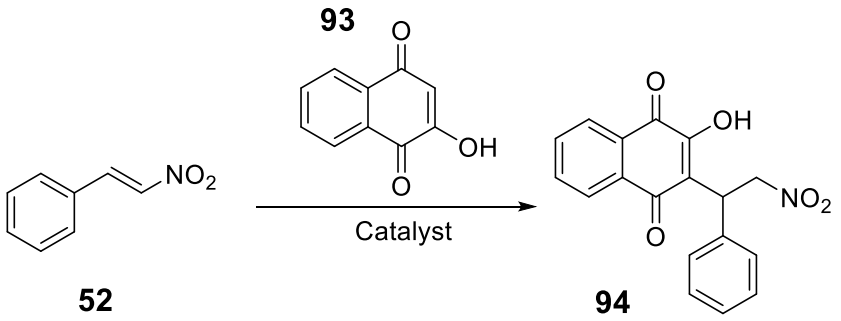

2-Hydroxy-1,4-napthoquinone **93** (100 mg, 0.574 mmol) and the required catalyst (0.04-0.1 eqv, see Tables 4-7) were dissolved in the required dry solvent and cooled to the required temperature (-20 to 0 ^{o}C see tables 3-7). β-Nitrostyrene **52** (128.5 mg, 0.861 mmol, 1.5 eqv) was then added and the mixture stirred for the required time and temperature. In the cases where *L*–proline (0.1 eqv) was added the reaction was stirred for 1 h at rt, before cooling whereupon **93** and **52** were added sequentially as solids. Reaction progress was determined by sampling and determination by H NMR. On completion the solvent was evaporated to give a deep red residue which was purified by column chromatography eluting firstly with 2-4% EA in petrol to remove excess **52** then followed with DCM to give the product **94** as a yellow solid. For sample from (Table 6, Entry 2_d), 44% ee, $[\alpha]_D^{20}$ -16.6 (acetone, c = 1.0), Lit. $[\alpha]_D^{17}$ -44.8 (acetone, c = 1.0),[64], Lit. $[\alpha]_D^{25}$ -34.0 (acetone, c = 1.46).[65] For the determination of enantiomeric excess, samples were analysed either on a Chiralpak IA (250 x 4.6 mm, mobile phase 90 % hexane, 8% ethanol, 2% dichloromethane, 0.1% TFA, 1 mL/min, detecting at 254 nm; R enantiomer 19.5 min, S enantiomer 27.2 min) or on a Chiralcel AS-H IA (250 x 4.6 mm, mobile phase 96 % hexane, 4 % ethanol, 0.1% TFA, 1.5 mL/min at 40 ^{o}C, detecting at 254 nm; R enantiomer 23.5 min, S enantiomer 26.2 min). For yield and ees (see Tables 6-9 and discussion).

Table 6

Entry	Catalyst	Acetonitrile	DCM	THF	Toluene	EtOAc
1	**114**[(i)]	Time: 21 h Yield: 87% 5% ee (R)	Time: 72 h Yield: 94% 29% ee (R)	Time: 48 h Yield: 95% 16% ee (R)	Time: 21 h Yield: 86% 26% ee (R)	Time: 25 h Yield: 92% 25% ee (R)
2	**114**	Time: 88 h Yield: 93% 34% ee (R)	Time: >88 h Yield: 99% 37% ee (R)	Time: >100 h Yield: 50% 18% ee (R)	Time: >100 Yield: 75% 44% ee (R)	Time: >100 Yield: 76% 31% ee (R)
3	**116**	Time: 5 h Yield: 93% 7% ee (R)	Time: 47 h Yield: 90% 8% ee (R)	Time: >100 h Yield: 94% 15% ee (R)	Time: >100 h Yield: 86% 13% (R)	Time: >100 h Yield: 92% 5% (R)
4	**117**	Time: <10 h Yield: 89% 15% ee (R)	Time: <20 h Yield: 90% 5% (R)	Time: <20 h Yield: 89% 1% ee (R)	Time: 32 h Yield: 90% 5% (R)	Time: <20 h Yield: 90% 4% (R)
5	**119**	Time: 39 h Yield: 99% 1% ee (R)	Time: 39 h Yield: 89% 4% ee (R)			

Entry X_R: R = **a**, **b**, **c**, **d** or **e** refer to the solvents acetonitrile, DCM, THF, toluene and EtOAc respectively.

Entry 1_a: Catalyst **114** (17.48 mg, 0.06 mmol, 0.1 eqv) in acetonitrile gave **94** (0.163 g, 0.50 mmol) in 87% yield and 5% ee.

Entry 1_b: Catalyst **114** (17.48 mg, 0.06 mmol, 0.1 eqv) in DCM gave **94** (0.175 g, 0.54 mmol) in 94% yield and 29% ee.

Entry 1_c: Catalyst **114** (17.48 mg, 0.06 mmol, 0.1 eqv) in THF gave **94** (0.176 g, 0.54 mmol) in 95% yield and 16% ee.

Entry 1_d: Catalyst **114** (17.48 mg, 0.06 mmol, 0.1 eqv) in toluene gave **94** (0.160 g, 0.49 mmol) in 86% yield and 27% ee.

Entry 1_e: Catalyst **114** (17.48 mg, 0.06 mmol, 0.1 eqv) in EtOAc gave **94** (0.170 g, 0.53 mmol) in 92% yield and 25% ee.

Entry 2_a: Catalyst **114** (17.48 mg, 0.06 mmol, 0.1 eqv) in acetonitrile gave **94** (0.172 g, 0.53 mmol) in 93% yield and 34% ee.

Entry 2$_b$: Catalyst **114** (17.48 mg, 0.06 mmol, 0.1 eqv) in DCM gave **94** (0.183 g, 0.57 mmol) in 99% yield and 37% ee.

Entry 2$_c$: Catalyst **114** (17.48 mg, 0.06 mmol, 0.1 eqv) in THF gave **94** (0.093 g, 0.29 mmol) in 50% yield and 18% ee.

Entry 2$_d$: Catalyst **114** (17.48 mg, 0.06 mmol, 0.1 eqv) in toluene gave **94** (0.139 g, 0.43 mmol) in 75% yield and 44% ee.

Entry 2$_e$: Catalyst **114** (17.48 mg, 0.06 mmol, 0.1 eqv) in EtOAc gave **94** (0.141 g, 0.44 mmol) in 76% yield and 31% ee.

Entry 3$_a$: Catalyst **116** (21.85 mg, 0.06 mmol, 0.1 eqv) in acetonitrile gave **94** (0.172 g, 0.53 mmol) in 93% yield and 7% ee.

Entry 3$_b$: Catalyst **116** (21.85 mg, 0.06 mmol, 0.1 eqv) in DCM gave **94** (0.168 g, 0.52 mmol) in 90% yield and 8% ee.

Entry 3$_c$: Catalyst **116** (21.85 mg, 0.06 mmol, 0.1 eqv) in THF gave **94** (0.175 g, 0.54 mmol) in 94% yield and 15% ee.

Entry 3$_d$: Catalyst **116** (21.85 mg, 0.06 mmol, 0.1 eqv) in toluene gave **94** (0.160 g, 0.49 mmol) in 86% yield and 13% ee.

Entry 3$_e$: Catalyst **116** (21.85 mg, 0.06 mmol, 0.1 eqv) in EtOAc gave **94** (0.170 g, 0.53 mmol) in 92% yield and 5% ee.

Entry 4$_a$: Catalyst **117** (9.54 mg, 0.03 mmol, 0.1 eqv) in acetonitrile gave **94** (0.083 g, 0.26 mmol) in 89% yield and 3% ee.

Entry 4$_b$: Catalyst **117** (9.54 mg, 0.03 mmol, 0.1 eqv) in DCM gave **94** (0.084 g, 0.26 mmol) in 90% yield and 5% ee.

Entry 4$_c$: Catalyst **117** (9.54 mg, 0.03 mmol, 0.1 eqv) in THF gave **94** (0.083 g, 0.26 mmol) in 89% yield and 1% ee.

Entry 4$_d$: Catalyst **117** (9.54 mg, 0.03 mmol, 0.1 eqv) in toluene gave **94** (0.084 g, 0.26 mmol) in 90% yield and 5% ee.

Entry 4$_e$: Catalyst **117** (9.54 mg, 0.03 mmol, 0.1 eqv) in EtOAc gave **94** (0.084 g, 0.26 mmol) in 90% yield and 4% ee.

Entry 5$_a$: Catalyst **119** (21.39 mg, 0.06 mmol, 0.1 eqv) in acetonitrile gave **94** (0.183 g, 0.57 mmol) in 99% yield and 1% ee.

Entry 5$_b$: Catalyst **119** (21.39 mg, 0.06 mmol, 0.1 eqv) in DCM gave **94** (0.166 g, 0.51 mmol) in 89% yield and 4% ee.

Table 7

Entry	Catalyst	Acetonitrile	DCM	THF	Toluene	EtOAc
1	**120**[(i)]	Time: 42 h Yield: 90% 4% ee (R)	Time: <72 h Yield: 93% 1% ee (R)	Time: >100 h Yield: 41% 3% ee (R)	Time: >100 h Yield: 38% 3% ee (R)	Time: >100 h Yield: 40% 4% ee (R)
2	**121**	Time: 38 h Yield: 72% 6% ee (R)	Time: 38 h Yield: 76% 3% ee (R)	Time: >72 h Yield: 51% 1% (R)	Time: >72 h Yield: 35% 1% ee (R)	Time: >72 h Yield: 79% 3% ee (R)
3	**122**	Time: 22 h Yield: 95% 3% ee (R)	Time: 22 h Yield: 68% 5% ee (R)			
4	**123**	Time: 58 h Yield: 81% 1% ee (R)	Time: 58 h Yield: 90% 1% ee (S)			

Entry 1$_a$: Catalyst **120** (7.4 mg, 0.02 mmol, 0.04 eqv) in acetonitrile gave **94** (0.168 g, 0.52 mmol) in 90% yield and 4% ee.

Entry 1$_b$: Catalyst **120** (7.4 mg, 0.02 mmol, 0.04 eqv) in DCM gave **94** (0.172 g, 0.53 mmol) in 93% yield and 1% ee.

Entry 1$_c$: Catalyst **120** (7.4 mg, 0.02 mmol, 0.04 eqv) in THF gave **94** (0.077 g, 0.24 mmol) in 41% yield and 3% ee.

Entry 1$_d$: Catalyst **120** (7.4 mg, 0.02 mmol, 0.04 eqv) in toluene gave **94** (0.07 g, 0.22 mmol) in 38% yield and 3% ee.

Entry 1$_e$: Catalyst **120** (7.4 mg, 0.02 mmol, 0.04 eqv) in EtOAc gave **94** (0.075 g, 0.23 mmol) in 40% yield and 4% ee.

Entry 2$_a$: Catalyst **121** (22.9 mg, 0.06 mmol, 0.1 eqv) in acetonitrile gave **94** (0.134 g, 0.41 mmol) in 72% yield and 6% ee.

Entry 2$_b$: Catalyst **121** (22.88 mg, 0.06 mmol, 0.1 eqv) in DCM gave **94** (0.141 g, 0.44 mmol) in 76% yield and 3% ee.

Entry 2$_c$: Catalyst **121** (22.88 mg, 0.06 mmol, 0.1 eqv) in THF gave **94** (0.095 g, 0.29 mmol) in 51% yield and 1% ee.

Entry 2$_d$: Catalyst **121** (22.88 mg, 0.06 mmol, 0.1 eqv) in toluene gave **94** (0.065 g, 0.20 mmol) in 35% yield and 1% ee.

Entry 2$_e$: Catalyst **121** (22.88 mg, 0.06 mmol, 0.1 eqv) in EtOAc gave **94** (0.147 g, 0.45 mmol) in 79% yield and 3% ee.

Entry 3$_a$: Catalyst **122** (20.12 mg, 0.06 mmol, 0.1 eqv) in acetonitrile gave **94** (0.176 g, 0.54 mmol) in 95% yield and 3% ee.

Entry 3$_b$: Catalyst **122** (20.12 mg, 0.06 mmol, 0.1 eqv) in DCM gave **94** (0.127 g, 0.39 mmol) in 68% yield and 5% ee.

Entry 4$_a$: Catalyst **123** (22.42 mg, 0.06 mmol, 0.1 eqv) in acetonitrile gave **94** (0.151 g, 0.47 mmol) in 81% yield and 1% ee.

Entry 4$_b$: Catalyst **123** (22.42 mg, 0.06 mmol, 0.1 eqv) in DCM gave **94** (0.168 g, 0.52 mmol) in 90% yield and 1% ee.

Table 8

Entry	Catalyst	Acetonitrile	DCM	THF	Toluene	EtOAc
1	**127**	Time: <21 h Yield: 93 % 16% ee (R)	Time: 4 h Yield: 91 % 21% ee (R)	Time: 96 h Yield: 85 % 16% ee (R)	No reaction[(i)]	Time: 96 h Yield: 87 % 22% ee (R)
2[(ii)]	**127**		Time: 54 h Yield: 92 % 25% ee (R)			
3	**128**	Time: 48 h Yield: 91 % 1% ee (S)	Time: 48 h Yield: 93 % 1% ee (S)	Time: 48 h Yield: 36 % 2% ee (S)	Time: 48 h Yield: 90 % 2% ee (S)	Time: 68 h Yield: 82 % 4% ee (S)

Entry 1$_a$: Catalyst **127** (14.1 mg, 0.06 mmol, 0.1 eqv) in acetonitrile gave **94** (0.172 g, 0.53 mmol) in 93% yield and 16% ee.

Entry 1$_b$: Catalyst **127** (14.14 mg, 0.06 mmol, 0.1 eqv) in DCM gave **94** (0.169 g, 0.52 mmol) in 91% yield and 21% ee.

Entry 1$_c$: Catalyst **127** (14.14 mg, 0.06 mmol, 0.1 eqv) in THF gave **94** (0.158 g, 0.49 mmol) in 85% yield and 16% ee.

Entry 1$_e$: Catalyst **127** (14.14 mg, 0.06 mmol, 0.1 eqv) in EtOAc gave **94** (0.163 g, 0.50 mmol) in 87% yield and 22% ee.

Entry 2$_b$: Catalyst **127** (14.14 mg, 0.06 mmol, 0.1 eqv) in DCM gave **94** (0.170 g, 0.53 mmol) in 92% yield and 25% ee.

Entry 3$_a$: Catalyst **128** (18.51 mg, 0.06 mmol, 0.1 eqv) in acetonitrile gave **94** (0.169 g, 0.52 mmol) in 91% yield and 1% ee.

Entry 3$_b$: Catalyst **128** (18.51 mg, 0.06 mmol, 0.1 eqv) in DCM gave **94** (0.172 g, 0.53 mmol) in 93% yield and 1% ee.

Entry 3$_c$: Catalyst **128** (18.51 mg, 0.06 mmol, 0.1 eqv) in THF gave **94** (0.067 g, 0.21 mmol) in 36% yield and 2% ee.

Entry 3$_d$: Catalyst **128** (18.51 mg, 0.06 mmol, 0.1 eqv) in toluene gave **94** (0.168 g, 0.52 mmol) in 90% yield and 2% ee.

Entry 12$_e$: Catalyst **128** (18.51 mg, 0.06 mmol, 0.1 eqv) in EtOAc gave **94** (0.153 g, 0.47 mmol) in 82% yield and 4% ee.

Table 9

Entry	Catalyst	Acetonitrile	DCM	Toluene
1	**139**	Time: 39 h Yield: 90 % 7 (R)	Time: 39 h Yield: 88 % 27 (R)	Time: >100 h Yield: 87 % 32 (R)
2	**140**	Time: 58 h Yield: 89 % 3 (R)	Time: 58 h Yield: 92 % 12 (R)	
3	**141**	Time: 88 h Yield: 81 % 2 (R)	Time: <100 h Yield: 90 % 9 (R)	
4	**142**	Time: 58 h Yield: 91 % 2 (R)	Time: 58 h Yield: 96 % 9 (R)	

Entry 1$_a$: Catalyst **139** (14.03 mg, 0.06 mmol, 0.1 eqv) in acetonitrile gave **94** (0.167 g, 0.52 mmol) in 90% yield and 7% ee.

Entry 1$_b$: Catalyst **139** (14.03 mg, 0.06 mmol, 0.1 eqv) in DCM gave **94** (0.164 g, 0.51 mmol) in 88% yield and 27% ee.

Entry 1$_d$: Catalyst **139** (14.03 mg, 0.06 mmol, 0.1 eqv) in toluene gave **94** (0.163 g, 0.50 mmol) in 87% yield and 32% ee.

Entry 2$_a$: Catalyst **140** (18.40 mg, 0.06 mmol, 0.1 eqv) in acetonitrile gave **94** (0.166 g, 0.51 mmol) in 89% yield and 3% ee.

Entry 2$_b$: Catalyst **140** (18.40 mg, 0.06 mmol, 0.1 eqv) in DCM gave **94** (0.170 g, 0.53 mmol) in 92% yield and 12% ee.

Entry 3$_a$: Catalyst **141** (15.64 mg, 0.06 mmol, 0.1 eqv) in acetonitrile gave **94** (0.151 g, 0.47 mmol) in 81% yield and 2% ee.

Entry 3$_b$: Catalyst **141** (15.64 mg, 0.06 mmol, 0.1 eqv) in DCM gave **94** (0.167 g, 0.52 mmol) in 90% yield and 9% ee.

Entry 4$_a$: Catalyst **142** (17.94 mg, 0.06 mmol, 0.1 eqv) in acetonitrile gave **94** (0.169 g, 0.52 mmol) in 91% yield and 2% ee.

Entry 4$_b$: Catalyst **142** (17.94 mg, 0.06 mmol, 0.1 eqv) in DCM gave **94** (0.178 g, 0.55 mmol) in 96% yield and 9% ee.

References

1. Mosher, H. S.; Morrison, J. D. *Science* (New York), **1983**, 221, 1013-1019.
2. Morrison, J. D.; Mosher, H, S.: *Asymmetric Organic Reactions*, Prentice-Hall, Englewood Cliff, New Jersey, **1971** (ISBN 0130495514).
3. Blackmond, D. G.; McMillan, C. R.; Ramdeehul, S.; Schorm, A.; Brown, J. M. *J. Am. Chem. Soc*. **2001**, 123, 10103-10104.
4. Girard, C.; Kagan, H. B. *Angew. Chem. Int. Ed*. **1998**, 37, 2922-2959.
5. Blackmond, D. G. *Proc. Nat. Acad*. Sci. **2004**, 101, 5732-5736.
6. Gal, J. "The Discovery of Stereoselectivity at Biological Receptors: Arnaldo Piutti and the Taste of the Asparagine Enantiomers-History and Analysis on the 125th Anniversary", *Chirality*, ***2012***, 24, 959–976.
7. McNaught, A. D.; Wilkinson, A. *IUPAC Compendium of Chem. Terminology (The "Gold Book")*, **2014**, 498-1274.
8. Gawley, R. *J. Org. Chem*., **2006**, 71, 2411–2416.
9. Yamaguchi, S.; Mosher, H. S. *J. Org. Chem*., **1973**, 38, 1870–1877.
10. Vigneron, J. P.; Dhaenens, M.; Horeau, A. *Tetrahedron*, **1973**, 29, 1055-1059
11. Krow, G.; Hill, R. K. *Chem. Commun*. **1968**, 430-431
12. Horeau, A. *Tetrahedron Lett.* **1969**, 10, 3121-3124.
13. Jovanovic, P.; Randelovic, J.; Ivkovik, B.; Suteu, C.; Vujosevic, Z. T.; Savik, V. J, Serb. *Chem. Soc*., **2014**, 79, 767–778.
14. Mudianta I. W.; Challinor V. L.; Winters A. E.; Cheney K. L.; De Voss J. J.; Garson M. J. *J. Org. Chem*., **2013**, 9, 2925-2933.
15. Dalko, P. I.; Moisan, L. *Angew. Chem. Int. Ed., In the golden age of organocatalysis*, **2004**, 43, 5138-5175.
16. Dalko, P. I. T*he McGraw-Hill yearbook, New York*, **2003**, 312-315.
17. Dalko, P. I. *Asymmetric Organocatalysis: A new stream in org. synthesis;* **2007**, 17.
18. Pizzarello, S.; Weber, A. L. *Science*, **2004**, 303, 1151.
19. von Liebig, J. *Justus Liebigs Ann. Chem.*, **1860**, 113, 246-247. doi 10.1002/jlac.18601130213
20. Kagan, H. B.; Jacobsen, E. N.; Pfaltz, A.; Yamamoto, H. *Comprehensive Asymmetric Catal.*, **1999**, 1, 101–118
21. Breding, G.; Balcom, R. W.; *Ber. Deutsch. Chem. Ger*. **1908**, 41, 740–751.
22. Rosentahler, L. Biochem. Z. **1908**, 14, 232.

23. Breding, G.; Fiske, P. S. Biochem. Z. **1912**, 46, 7.
24. Vavon, M. M.; Peignier, P. *Bull Soc. Fr*. **1929**, 45, 293.
25. Wegler, R. Liebigs, *Ann. Chem*. **1932**, 498, 62.
26. Dakin, H. D. *J. Biol. Chem*. **1909**, 7, 49.
27. Prelog, V.; Wilhelm, M. *Helv. Chim. Acta*, **1954**, 37, 1634.
28. Pracejus, H.; *Justus Liebigs* Ann. *Chem*. **1960**, 634, 9–22.
29. Langstrom, B.; Bergson, G. *Acta Chem. Scand*. **1973**, 27, 3118–3119.
30. Wynberg, H. *Top. Stereochem*. **1986**, 16, 87–129.
31. Yamada, S.; Otani, G. *Tetrahedron Lett.* **1969**, 10 4237-4240.
32. Hajos, Z. G.; Parrish, D. R. *J. Org. Chem*. **1974**, 39, 1615–1621.
33. Eder, U.; Sauer, G.; Wiechert, R. *Angew. Chem. Int. Ed. Engl*. **1971**, 10, 496–497.
34. Iyer, M. S.; Gigstad, K. M.; Namdev, N. D.; Lipton, M. *J. Am. Chem. Soc*. **1996**, 118, 4910–4911.
35. Sigman, M. S.; Jacobsen, E. N. *J. Am. Chem. Soc*. **1998**, 120, 4901–4902.
36. Dolling, U. H.; Davis, P.; Grabowski, E. *J. Am. Chem. Soc*. **1984**, 106, 446–447.
37. Yang, J. W.; Hechavarria Fonseca, M. T.; List, B. *J. Am. Chem. Soc*. **2005**, 127, 15036–15037.
38. Makosza, M; Fedorynski, M. *Catal. Rev., Sci. Eng.*, **2003**, 45, 321–367.
39. Seebach, D; Beck, A.K.; Heckel, A. *Angew*. *Chem*. *Int*. *Ed*. *Engl*. **2001**, 40, 92–138.
40. Okino, T.; Hoashi, Y.; Takemoto, Y. *Tetrahedron Lett*. **2003**, 44, 2817-2821.
41. Okino, T.; Nakamura, S.; Furukawa, T.; Takemoto, Y. *Org. Lett*. **2004**, 6, 625-627.
42. Vachal, P.; Jacobsen, E. N. *Org. Lett*. **2000**, 2, 867-870.
43. Okino, T.; Hoashi, Y.; Furukawa, T.; Xu, X.; Takemoto, Y. *J. Am. Chem. Soc*. **2005**, 127, 119–125.
44. Connon, S. *Chem. Commun.,* **2008**, 2499-2510.
45. Ye, J.; Dixon, D. J.; Hynes, P. S. *Chem. Commun*., **2005**, 4481.
46. Yu, Z.; Liu, X.; Zhou, L.; Lin, L.; Feng, X. *Angew. Chem. Int. Ed.*, **2009**, 48, 5195-5198.
47. Terada, M.; Ikehara, T.; Ube, H. *J. Am. Chem. Soc*., **2007**, 129, 14112-14113.
48. Almasi, D.; Alsono, D. A.; Gomez-Bengoa, E.; Najera. C. *J. Org. Chem*., **2009**, 74, 6163-6168.
49. Shubina, T. E.; Freund, M.; Schenker, S.; Clark, T.; Tsogoeva, S. B. *J. Org. Chem*., **2012**, 8, 1485-1498.
50. (a). Gómez-Torres, E.; Alonso, D.A.; Gómez-Bengoa, E.; Nájera, C. *Org. Lett*. **2011**, 13, 6106–6109. (b). Almasi, D.; Alonso, D.A.; Gómez-Bengoa, E.; Nájera, C. *J. Org. Chem*. **2009**,

74, 6163–6168. (c). Lee, M.; Zhang, l.; Yohan, P.; Park, H. C. *J. Tetrahedron*. **2012**, 68, 1452–1459.

51. Murphy, P.J., Allingham, M St., Howard-Jones, A. *J. L. Tetrahedron*, **2003**, 44, 8677–8680.
52. Allingham, M. T.; Bennett, E. L.; Davies, D. H.; Harper, P. M.; Howard-Jones, A.; Mehdar, Y. T. H.; Murphy, P. J.; Thomas, D. A.; Caulkett, P. W. R.; Potter, D.; Lam, C. M.; O'Donoghue, A. C. *Tetrahedron*, **2016**, 72, 496−503.
52. Aurelio, L. Box, J. S.; Brownlee, R.; Hughes, A. B.; Sleebs, M. M. *J. Org. Chem*, **2003**, 68, 2667.
53. Belokon, Y. N.; Tararov, V. I.; Maleev, V. I.; Savel'eva, T. F.; Ryzhov, M. G. *Tetrahedron: Asymmetry*, **1998**, 9, 4249-4252.
54. Fandrick, D. R.; Reeves, J. T.; Bakonyi, J. M.; Nyalapatla, P. R.; Tan, O. Z.; Niemeier, D. Akalay, K. R.; Fandrick, W.; Wohlleben, S.Ollenberger, J. J.; Song, X. Sun,; B. Qu, N.; Haddad, S.; Sanyal, S.; Shen, S.; Ma, D.; Byrne, A. Chitroda, V.; Fuchs, B. A.; Narayanan, N. Grinberg, H.; Lee, N.; Yee, M.; Brenner, C. H. *J. Org. Chem*. **2013**, 78, 3592 – 3615.
55. Kurzer, F. *J. Chem. Soc*., **1956**, 4524-4531.
56. Schmuck, C.; Bickert, V.; Merschky, M.; Geiger, L.; Rupprecht, D.; Dudaczek, J.; Wich, P.; Rehm, T.; Machon, U. *Eur. J. Org. Chem*. **2008**, 2, 324–329.
57. Johns, B. A.; Gudmundsson, K. S.; Turner, E. M.; Allen, S. H.; Samano, V. A.; Ray, J. A.; Freeman, G. A.; Boyd, F. L.; Sexton, C. J.; Selleseth, D. W.; Creech, K. L., Moniri, K. R.. *Bioorg. Med. Chem*., **2005**, 13, 2397–2411
58. Tang, G.; Gün, Ü.; Altenbach, H. *Tetrahedron*, **2012**, 68, 10230 -10235.
59. Sun, X.; Gao, J. P.; Wang, Z. Y. *J. Am. Chem. Soc*., **2008**, 130, 8130–8131.
60. Jolibois, E. R. W.; Lewis, W.; Moody, J. C. *Org. Lett*., **2014**, 16, 1064–1067.
61. Bhowmick, S.; Mondal, A.; Ghosh, A.: Bhowmick. K. C. *Tetrahedron: Asymmetry*, **2015**, 26, 1215–1244.
62. (a). Yamagata, A. D. G.; Datta, S.; Jackson K. E.; Stegbauer, L.; Paton, R. S.; Dixon, D. J. *Angew. Chem. Int. Ed.*, **2015**, 54, 4899-4903. (b). Yamagata, A. D. G.; Dixon, D. J. *Org. Lett.* **2017,** 1894-1897**.**
63**.** Woo, S. B.; Kim, D. Y. *J. Org. Chem*., **2012**, 8, 699-704.
64. Yang, W.; Du, D.-M. *Adv. Synth. Catal.* **2011**, 353, 1241-1246.

Appendix 1: Publication

Tetrahedron 72 (2016) 496–503

Contents lists available at ScienceDirect

Tetrahedron

journal homepage: www.elsevier.com/locate/tet

Synthesis, applications and mechanistic investigations of C_2 symmetric guanidinium salts

Matthew T. Allingham [a], Elliot L. Bennett [a], Deniol H. Davies [a], Philip M. Harper [a], Andrew Howard-Jones [a], Yassin T.H. Mehdar [a], Patrick J. Murphy [a,*], Dafydd A. Thomas [a], Peter W.R. Caulkett [b], David Potter [c], Casey M. Lam [d], AnnMarie C. O'Donoghue [d,*]

[a] School of Chemistry, Bangor University, Bangor, Gwynedd, LL57 2UW, UK
[b] CVGI Department, AstraZeneca Pharmaceuticals, Mereside, Alderley Park, Macclesfield, Cheshire, SK10 4TG, UK
[c] Menai Organics, Menai Technology Enterprise Centre, Deiniol Road, Bangor, Gwynedd, LL57 2UP, UK
[d] Department of Chemistry, Durham University, South Road, Durham, DH1 3LE, UK

ARTICLE INFO

Article history:
Received 18 September 2015
Received in revised form 11 November 2015
Accepted 24 November 2015
Available online 30 November 2015

Keywords:
Guanidine
Guanidinium ions
Phase transfer catalysis
Phase transfer alkylation
Phase transfer epoxidation
Michael addition

ABSTRACT

A range of guanidinium catalysts was prepared in six or seven synthetic steps and applied to the phase transfer alkylation of a glycinate Schiff's base in 21–86% ee as well as the phase transfer epoxidation of some chalcones in 85–94% ee. Using a spectrophotometric method, pK_a values in the range 13.2–13.9 in DMSO have been determined for some of the catalysts highlighting an increase in basicity relative to achiral tetramethylguanidine (pK_a=13.0) and a mechanism involving the protonated guanidinium ion as a phase transfer catalyst is proposed. The use of two of the catalysts for the addition of nucleophiles in Michael addition reactions was investigated and both were found to be effective catalysts. A counterion effect was apparent in these reactions, but no enantioselectivity was observed.

1. Introduction

The guanidine motif is ubiquitous in nature and the protonated guanidinium side chain of the amino acid, arginine, leads to key highly selective hydrogen-bonding and electrostatic interactions with carboxylate and phosphate anionic groups.[1] Many applications of guanidines in synthesis[2] are known and their use as Brønsted base catalysts have been reported.[3] More recently applications of guanidines and protonated guanidines as either bases or hydrogen bond donors in bifunctional organic catalysis have also been reported.[4] We have previously reported the application of C_2 symmetric guanidinium salts in phase transfer catalysis, and in Michael additions, and report our findings in more detail.

2. Preparation of guanidine catalysts 7a–d

Previously[5] we reported the synthesis of the tetracyclic C_2-symmetric guanidines **7a–d** by the conjugate addition of guanidine to the enones **3** and **6**. These enones were prepared from either ethyl *R*-3-hydroxybutyrate **1** or (*S*)-malic acid **4** in five and six steps, respectively. (Scheme 1).

The key reaction in both of these syntheses is the conjugate addition of guanidine to 2 equiv of the enones **3** or **6**, which proceeds in good yield and gives the products **7a** and **7b**, respectively. In the case of the parent catalyst **7a**, the conjugate addition product was easily purified by column chromatography and crystallization from ether/petrol. The hydroxyl substituted catalyst **7b** was found to be very hygroscopic and was thus converted to the silyl-protected catalysts **7c** and **7d** in reasonable overall yield. Catalyst **7e** was prepared by ion exchange of **7a** with $NaBPh_4$.

3. Phase transfer alkylation and epoxidation reactions

With the catalysts **7a–d** in hand, we were interested in the applications of these catalysts to phase transfer catalysis (PTC)[6] and firstly investigated the benzylation of the glycinate Schiff's base **8**[7] leading to the alkylated product **9**. (Scheme 2, Table 1).

* Corresponding authors. Tel.: +44 (0) 1248 382392; fax: +44 (0) 1248 370528 (P.J.M.); e-mail addresses: chs027@bangor.ac.uk (P.J. Murphy), annmarie.odonoghue@durham.ac.uk (A.C. O'Donoghue).

http://dx.doi.org/10.1016/j.tet.2015.11.058
0040-4020/

Appendix 2
X-ray of compound 114

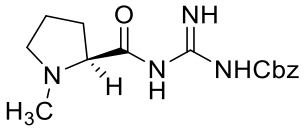

UK National Crystallography Service

Table 1. Crystal data and structure refinement details.

Identification code	**2016ncs0664**	
Empirical formula	$C_{15}H_{20}N_4O_3$	
Formula weight	304.35	
Temperature	100(2) K	
Wavelength	0.71073 Å	
Crystal system	Monoclinic	
Space group	*P*21	
Unit cell dimensions	a = 5.5616(3) Å	α = **90°**
	b = **17.9003(13) Å**	β = **94.111(5)°**
	c = **15.5410(9) Å**	γ = **90°**
Volume	**1543.19(17) Å^3**	
Z	4	
Density (calculated)	1.310 Mg / m^3	
Absorption coefficient	0.094 mm^{-1}	
F(000)	648	
Crystal	Plate; colourless	
Crystal size	0.173 × 0.045 × 0.010 mm^3	
θ range for data collection	2.276 – 30.051°	
Index ranges	$-7 \le h \le 7$, $-24 \le k \le 25$, $-20 \le l \le 21$	
Reflections collected	30287	
Independent reflections	8146 [R_{int} = 0.0855]	
Completeness to θ = 25.242°	99.7 %	
Absorption correction	Semi–empirical from equivalents	
Max. and min. transmission	1.00000 and 0.47050	
Refinement method	Full-matrix least-squares on F^2	
Data / restraints / parameters	8146 / 1 / 423	
Goodness-of-fit on F^2	1.004	
Final *R* indices [$F^2 > 2\sigma(F^2)$]	*R1* = 0.0684, *wR2* = 0.1188	
R indices (all data)	*R1* = 0.1515, *wR2* = 0.1447	
Absolute structure parameter	?	
Extinction coefficient	n/a	
Largest diff. peak and hole	0.262 and –0.220 e Å^{-3}	

Diffractometer: *Rigaku AFC12* goniometer equipped with an enhanced sensitivity (HG) *Saturn724+* detector mounted at the window of an *FR-E+ SuperBright* molybdenum rotating anode generator with HF *Varimax* optics (100µm focus). **Cell determination and Data collection**: CrystalClear-SM Expert 2.0 r7 (Rigaku, 2011). **Data reduction and cell refinement & Absorption correction:** CrysalisPRO 171.38.41 (Rigaku Oxford Diffraction 2015). **Structure solution**: SHELXST (G. M. Sheldrick, Acta Cryst. (2008) A**64** 112–122). S**tructure refinement**: SHELXL97 (G. M. Sheldrick (1997), University of Göttingen, Germany). **Graphics:** Mercury 3.5.1 (CCDC 2014). **Publication material:** WinGX: Farrugia, L. J. (2012). J. Appl. Cryst. 45, 849-854.

Special details:

Table 2. Atomic coordinates [× 10^4], equivalent isotropic displacement parameters [$Å^2$ × 10^3] and site occupancy factors. U_{eq} is defined as one third of the trace of the orthogonalized U^{ij} tensor.

Atom	*x*	*y*	*z*	U_{eq}	*S.o.f.*
O2	3423(5)	5669(2)	–719(2)	31(1)	1
O3	–555(5)	5682(2)	–557(2)	29(1)	1
O6	5896(5)	4228(2)	5571(2)	39(1)	1
O5	1952(5)	4175(2)	5778(2)	39(1)	1
O4	–2627(6)	3408(2)	2807(2)	47(1)	1
N4	1826(6)	6061(2)	560(2)	23(1)	1
N2	3889(7)	6322(2)	1850(2)	30(1)	1
N3	6103(7)	6045(3)	686(3)	31(1)	1
N6	1375(7)	3574(2)	3190(2)	29(1)	1
C8	1765(7)	5803(3)	–266(3)	23(1)	1
O1	7892(6)	6274(3)	2300(2)	68(2)	1
N7	–769(6)	3755(3)	4398(3)	34(1)	1
C7	3969(7)	6140(3)	981(3)	24(1)	1
N8	3494(6)	3853(3)	4458(2)	33(1)	1
C21	–560(8)	3439(3)	2612(3)	31(1)	1
N5	2421(7)	3628(2)	1538(2)	42(1)	1
C20	116(9)	3310(3)	1699(3)	33(1)	1
C27	3843(10)	6486(3)	6705(4)	46(2)	1
C15	1166(9)	4143(3)	–1702(4)	43(2)	1
C25	6049(8)	5377(3)	6401(3)	36(2)	1
C9	–966(8)	5340(3)	–1401(3)	33(1)	1
C23	3567(7)	4090(3)	5295(3)	30(1)	1
C22	1342(7)	3731(3)	4065(3)	27(1)	1
N1	2823(8)	6830(3)	3416(3)	58(1)	1
C10	–729(8)	4511(3)	–1361(3)	29(1)	1
C28	5516(9)	6917(4)	6318(4)	47(2)	1
C12	–2186(9)	3312(4)	–904(3)	44(2)	1
C24	6320(9)	4543(3)	6432(3)	42(2)	1
C13	–327(9)	2949(3)	–1266(3)	37(1)	1
C11	–2397(9)	4078(4)	–950(4)	43(2)	1
C17	3381(10)	3197(4)	861(4)	54(2)	1
C26	4119(9)	5726(4)	6747(3)	43(1)	1
C6	5803(9)	6344(4)	2461(3)	44(2)	1
C19	418(11)	2459(3)	1498(4)	58(2)	1
C30	7718(9)	5821(4)	6030(4)	53(2)	1
C29	7451(10)	6582(4)	5980(4)	61(2)	1
C14	1338(10)	3373(4)	–1655(4)	51(2)	1
C16	2279(14)	4406(3)	1311(4)	78(2)	1
C1	3181(14)	7631(4)	3435(5)	91(3)	1
C5	5041(10)	6426(4)	3374(3)	56(2)	1
C4	4504(11)	5639(4)	3753(3)	70(2)	1
C2	1738(11)	6546(5)	4179(4)	86(3)	1
C3	2113(13)	5703(7)	4099(6)	134(5)	1
C18	2818(12)	2411(4)	1125(5)	79(2)	1

Table 3. Bond lengths [Å] and angles [°].

O2–C8	1.223(5)
O3–C8	1.353(5)
O3–C9	1.451(5)
O6–C23	1.357(5)
O6–C24	1.456(5)
O5–C23	1.221(5)
O4–C21	1.211(6)
N4–C7	1.325(5)
N4–C8	1.363(5)
N2–C6	1.375(6)
N2–C7	1.394(6)
N2–H52	0.90(5)
N3–C7	1.313(6)
N3–H50	0.91(4)
N3–H51	0.97(7)
N6–C21	1.373(5)
N6–C22	1.389(6)
N6–H55	0.88(6)
O1–C6	1.212(6)
N7–C22	1.317(6)
N7–H53	0.90(4)
N7–H54	1.07(7)
N8–C22	1.322(5)
N8–C23	1.367(6)
C21–C20	1.511(7)
N5–C16	1.438(7)
N5–C17	1.438(7)
N5–C20	1.441(6)
C20–C19	1.567(8)
C20–H20	1.0000
C27–C26	1.370(8)
C27–C28	1.379(8)
C27–H27	0.9500
C15–C10	1.380(7)
C15–C14	1.383(8)
C15–H15	0.9500
C25–C30	1.380(8)
C25–C26	1.384(7)
C25–C24	1.501(8)
C9–C10	1.490(8)
C9–H9A	0.9900
C9–H9B	0.9900
N1–C5	1.435(8)
N1–C1	1.448(9)
N1–C2	1.460(7)
C10–C11	1.398(7)
C28–C29	1.369(8)
C28–H28	0.9500
C12–C13	1.376(8)
C12–C11	1.377(8)
C12–H12	0.9500
C24–H24A	0.9900
C24–H24B	0.9900
C13–C14	1.371(7)
C13–H13	0.9500
C11–H11	0.9500
C17–C18	1.504(10)
C17–H17A	0.9900
C17–H17B	0.9900
C26–H26	0.9500
C6–C5	1.516(7)
C19–C18	1.496(8)
C19–H19A	0.9900
C19–H19B	0.9900
C30–C29	1.372(9)
C30–H30	0.9500
C29–H29	0.9500
C14–H14	0.9500
C16–H16A	0.9800
C16–H16B	0.9800
C16–H16C	0.9800
C1–H1A	0.9800
C1–H1B	0.9800
C1–H1C	0.9800
C5–C4	1.565(9)
C5–H5	1.0000
C4–C3	1.474(9)
C4–H4A	0.9900
C4–H4B	0.9900
C2–C3	1.529(13)
C2–H2A	0.9900
C2–H2B	0.9900
C3–H3A	0.9900
C3–H3B	0.9900
C18–H18A	0.9900
C18–H18B	0.9900
C8–O3–C9	116.9(3)
C23–O6–C24	116.6(4)
C7–N4–C8	117.5(4)
C6–N2–C7	126.8(4)
C6–N2–H52	114(3)
C7–N2–H52	118(3)
C7–N3–H50	119(2)
C7–N3–H51	116(4)
H50–N3–H51	126(5)
C21–N6–C22	127.7(4)
C21–N6–H55	116(4)
C22–N6–H55	116(4)
O2–C8–O3	121.1(4)
O2–C8–N4	129.8(4)
O3–C8–N4	109.1(3)
C22–N7–H53	121(3)
C22–N7–H54	114(4)
H53–N7–H54	124(4)
N3–C7–N4	128.1(4)
N3–C7–N2	117.4(4)
N4–C7–N2	114.4(4)
C22–N8–C23	117.1(4)
O4–C21–N6	123.9(5)
O4–C21–C20	122.2(4)
N6–C21–C20	113.9(4)
C16–N5–C17	110.9(5)
C16–N5–C20	113.0(5)
C17–N5–C20	107.2(4)

N5–C20–C21	112.8(4)	C25–C26–H26	119.4
N5–C20–C19	103.9(4)	O1–C6–N2	124.1(5)
C21–C20–C19	111.9(4)	O1–C6–C5	122.6(4)
N5–C20–H20	109.4	N2–C6–C5	113.2(5)
C21–C20–H20	109.4	C18–C19–C20	104.1(5)
C19–C20–H20	109.4	C18–C19–H19A	110.9
C26–C27–C28	119.9(6)	C20–C19–H19A	110.9
C26–C27–H27	120.0	C18–C19–H19B	110.9
C28–C27–H27	120.0	C20–C19–H19B	110.9
C10–C15–C14	120.5(5)	H19A–C19–H19B	109.0
C10–C15–H15	119.8	C29–C30–C25	121.4(6)
C14–C15–H15	119.8	C29–C30–H30	119.3
C30–C25–C26	117.8(6)	C25–C30–H30	119.3
C30–C25–C24	121.1(5)	C28–C29–C30	119.9(6)
C26–C25–C24	121.0(6)	C28–C29–H29	120.0
O3–C9–C10	112.1(4)	C30–C29–H29	120.0
O3–C9–H9A	109.2	C13–C14–C15	121.9(5)
C10–C9–H9A	109.2	C13–C14–H14	119.0
O3–C9–H9B	109.2	C15–C14–H14	119.0
C10–C9–H9B	109.2	N5–C16–H16A	109.5
H9A–C9–H9B	107.9	N5–C16–H16B	109.5
O5–C23–O6	120.8(4)	H16A–C16–H16B	109.5
O5–C23–N8	130.6(4)	N5–C16–H16C	109.5
O6–C23–N8	108.6(4)	H16A–C16–H16C	109.5
N7–C22–N8	128.0(4)	H16B–C16–H16C	109.5
N7–C22–N6	117.8(4)	N1–C1–H1A	109.5
N8–C22–N6	114.2(4)	N1–C1–H1B	109.5
C5–N1–C1	112.4(5)	H1A–C1–H1B	109.5
C5–N1–C2	105.6(5)	N1–C1–H1C	109.5
C1–N1–C2	113.1(6)	H1A–C1–H1C	109.5
C15–C10–C11	117.4(5)	H1B–C1–H1C	109.5
C15–C10–C9	121.8(5)	N1–C5–C6	113.0(4)
C11–C10–C9	120.8(5)	N1–C5–C4	104.4(4)
C29–C28–C27	119.7(7)	C6–C5–C4	109.8(5)
C29–C28–H28	120.1	N1–C5–H5	109.9
C27–C28–H28	120.1	C6–C5–H5	109.9
C13–C12–C11	120.9(6)	C4–C5–H5	109.9
C13–C12–H12	119.6	C3–C4–C5	105.6(6)
C11–C12–H12	119.6	C3–C4–H4A	110.6
O6–C24–C25	110.3(4)	C5–C4–H4A	110.6
O6–C24–H24A	109.6	C3–C4–H4B	110.6
C25–C24–H24A	109.6	C5–C4–H4B	110.6
O6–C24–H24B	109.6	H4A–C4–H4B	108.8
C25–C24–H24B	109.6	N1–C2–C3	102.2(6)
H24A–C24–H24B	108.1	N1–C2–H2A	111.3
C14–C13–C12	118.0(5)	C3–C2–H2A	111.3
C14–C13–H13	121.0	N1–C2–H2B	111.3
C12–C13–H13	121.0	C3–C2–H2B	111.3
C12–C11–C10	121.3(5)	H2A–C2–H2B	109.2
C12–C11–H11	119.4	C4–C3–C2	103.8(7)
C10–C11–H11	119.4	C4–C3–H3A	111.0
N5–C17–C18	102.0(5)	C2–C3–H3A	111.0
N5–C17–H17A	111.4	C4–C3–H3B	111.0
C18–C17–H17A	111.4	C2–C3–H3B	111.0
N5–C17–H17B	111.4	H3A–C3–H3B	109.0
C18–C17–H17B	111.4	C19–C18–C17	105.2(5)
H17A–C17–H17B	109.2	C19–C18–H18A	110.7
C27–C26–C25	121.1(6)	C17–C18–H18A	110.7
C27–C26–H26	119.4	C19–C18–H18B	110.7

C17–C18–H18B	110.7
H18A–C18–H18B	108.8

Symmetry transformations used to generate equivalent atoms:

Table 4. Anisotropic displacement parameters [Å²× 10³]. The anisotropic displacement factor exponent takes the form: $-2\pi^2[h^2a^{*2}U^{11} + \cdots + 2\,h\,k\,a^*\,b^*\,U^{12}]$.

Atom	U^{11}	U^{22}	U^{33}	U^{23}	U^{13}	U^{12}
O2	24(2)	43(2)	26(2)	–8(2)	9(1)	1(2)
O3	20(2)	46(2)	20(2)	–9(2)	–2(1)	7(2)
O6	22(2)	71(3)	23(2)	–16(2)	–1(1)	14(2)
O5	25(2)	68(3)	24(2)	–4(2)	8(1)	7(2)
O4	24(2)	68(3)	48(2)	–20(2)	–3(2)	–3(2)
N4	19(2)	33(2)	16(2)	–3(2)	1(1)	1(2)
N2	28(2)	41(3)	21(2)	–2(2)	1(2)	–8(2)
N3	20(2)	47(3)	25(2)	–1(2)	2(2)	–3(2)
N6	22(2)	43(3)	20(2)	–3(2)	–1(2)	0(2)
C8	22(2)	27(3)	19(2)	2(2)	4(2)	1(2)
O1	25(2)	143(4)	35(2)	9(2)	–3(2)	–28(2)
N7	15(2)	51(3)	36(3)	–7(2)	1(2)	–2(2)
C7	22(2)	28(3)	21(2)	1(2)	2(2)	–2(2)
N8	19(2)	60(3)	20(2)	–4(2)	3(2)	3(2)
C21	27(2)	29(3)	34(3)	–1(2)	–6(2)	1(2)
N5	43(2)	55(3)	25(2)	–1(2)	–4(2)	–20(2)
C20	36(3)	32(3)	30(3)	0(2)	–9(2)	–12(2)
C27	37(3)	57(5)	47(4)	8(3)	16(3)	13(3)
C15	39(3)	45(4)	49(4)	–9(3)	23(3)	–1(3)
C25	23(2)	66(4)	17(3)	–16(2)	–5(2)	13(2)
C9	31(3)	52(4)	16(2)	–4(2)	–2(2)	5(2)
C23	21(2)	49(3)	21(2)	–2(2)	4(2)	10(2)
C22	20(2)	37(3)	25(3)	2(2)	5(2)	1(2)
N1	49(3)	99(4)	26(2)	–10(2)	0(2)	–34(3)
C10	24(2)	44(3)	17(2)	–4(2)	–2(2)	–3(2)
C28	37(3)	61(4)	41(3)	–14(3)	0(3)	–6(3)
C12	36(3)	56(4)	41(3)	–11(3)	12(3)	–17(3)
C24	35(3)	71(4)	19(3)	–20(3)	–7(2)	24(3)
C13	30(3)	39(3)	42(3)	–6(3)	1(2)	–4(3)
C11	24(3)	58(4)	48(3)	–19(3)	11(2)	–5(3)
C17	33(3)	82(5)	45(4)	0(3)	–1(3)	–21(3)
C26	41(3)	58(4)	32(3)	14(3)	19(2)	16(3)
C6	36(3)	67(4)	28(3)	2(3)	–7(2)	–28(3)
C19	94(5)	42(4)	40(3)	–14(2)	23(3)	–35(3)
C30	19(2)	88(5)	53(4)	–36(4)	15(2)	–9(3)
C29	33(3)	88(6)	63(4)	–41(4)	20(3)	–28(3)
C14	44(3)	47(4)	64(4)	–8(3)	26(3)	9(3)
C16	116(6)	53(4)	60(4)	22(3)	–22(4)	–49(4)
C1	107(6)	94(6)	75(5)	–57(4)	26(4)	–57(5)
C5	39(3)	110(6)	17(3)	0(3)	–6(2)	–31(3)
C4	66(4)	116(6)	28(3)	21(3)	2(3)	–17(4)
C2	26(3)	201(11)	30(4)	28(5)	–3(3)	0(5)
C3	47(4)	203(11)	150(8)	143(8)	–2(5)	4(5)
C18	61(4)	84(6)	91(5)	–12(4)	8(4)	21(4)

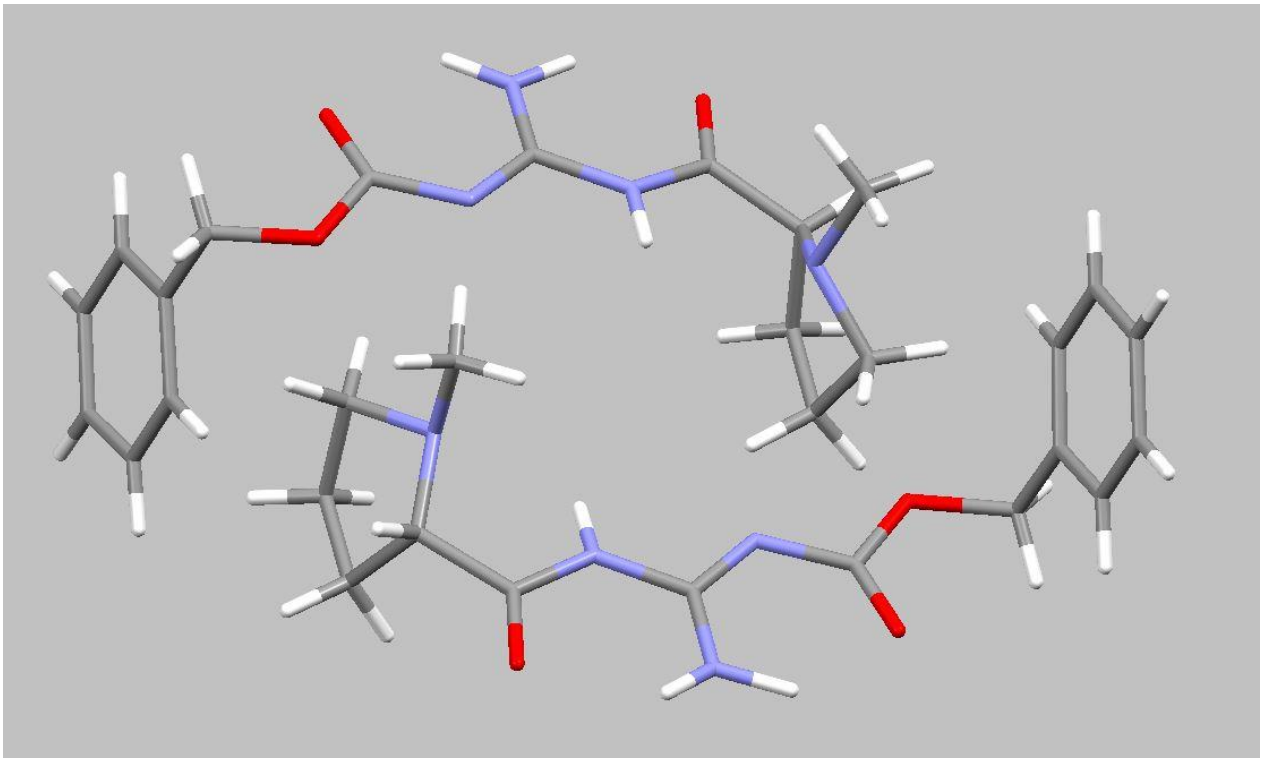

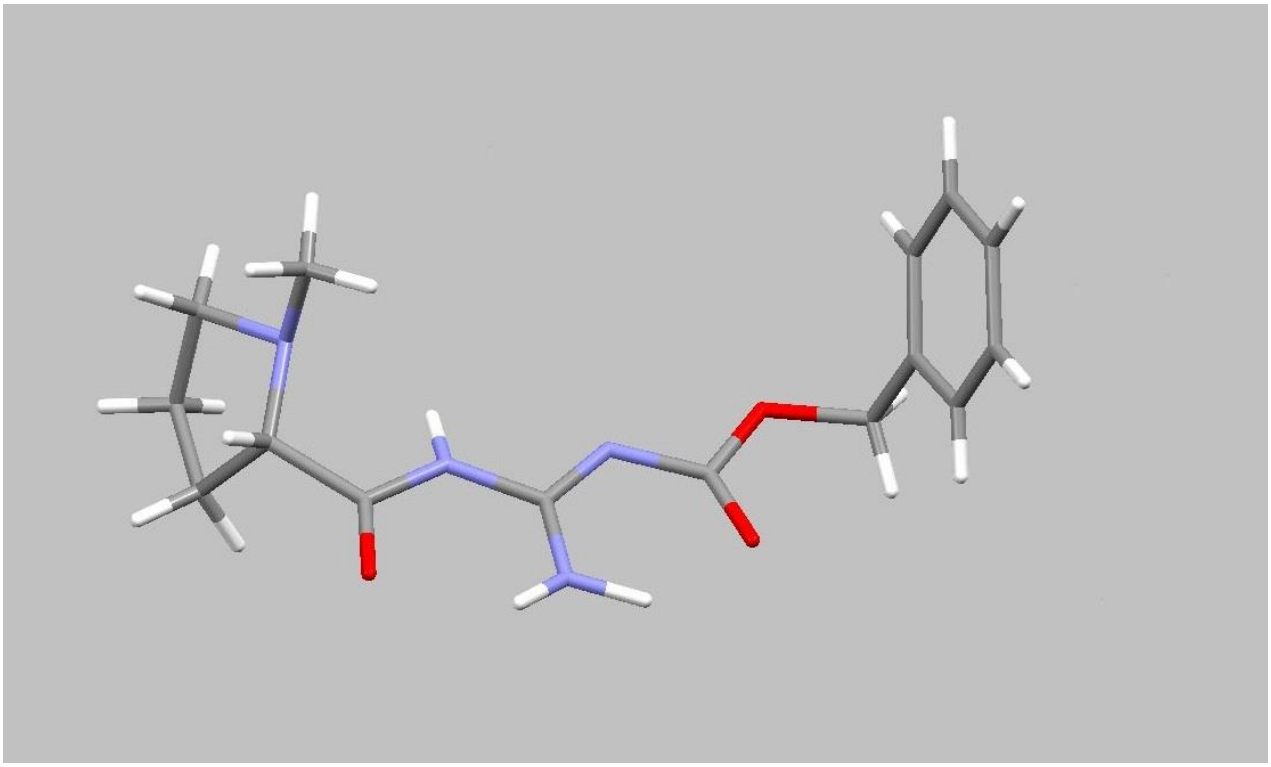

Appendix 3
X-ray of compound 120

UK National Crystallography Service

Table 1. Crystal data and structure refinement details.

Identification code	**2017NCS0158**	
Empirical formula	$C_{19}H_{22}N_4O$	
Formula weight	322.41	
Temperature	30(2) K	
Wavelength	0.6889 Å	
Crystal system	Triclinic	
Space group	*P*–1	
Unit cell dimensions	a = 8.27490(10) Å	α = **82.1070(10)°**
	b = **9.89550(10) Å**	β = **86.6940(10)°**
	c = **21.8743(3) Å**	γ = **85.7750(10)°**
Volume	**1767.32(4) Å^3**	
Z	4	
Density (calculated)	1.212 Mg / m^3	
Absorption coefficient	0.073 mm^{-1}	
F(000)	688	
Crystal	Plate; colourless	
Crystal size	0.100 × 0.100 × 0.030 mm^3	
θ range for data collection	1.824 – 35.874°	
Index ranges	$-14 \le h \le 13$, $-16 \le k \le 16$, $-36 \le l \le 36$	
Reflections collected	30477	
Independent reflections	15842 [R_{int} = 0.0939]	
Completeness to θ = 24.415°	98.5 %	
Absorption correction	Empirical	
Max. and min. transmission	1.0 and 0.994168456942	
Refinement method	Full-matrix least-squares on F^2	
Data / restraints / parameters	15842 / 0 / 551	
Goodness-of-fit on F^2	1.162	
Final *R* indices [$F^2 > 2\sigma(F^2)$]	*R1* = 0.0817, *wR2* = 0.2260	
R indices (all data)	*R1* = 0.0866, *wR2* = 0.2295	
Extinction coefficient	n/a	
Largest diff. peak and hole	0.631 and –0.287 e Å^{-3}	

Diffractometer: Beamline i19, Diamond Light Source Ltd. 3-circle fixed chi goniometer equipped with a PILATUS 2M PIXEL detector, wavelength 0.6998A (100µm focus). **Data collection:** GDA http://www.opengda.org/OpenGDA.html **Cell determination, Data reduction and cell refinement & Absorption correction**: XIA2 0.5.53 Winter, G. (2010) Journal of Applied Crystallography 43, **Structure solution**: SHELXT (G. M. Sheldrick *Acta Cryst.* (2015). A**71**, 3-8). S**tructure refinement**: SHELXL97 (G. M. Sheldrick (1997), University of Göttingen, Germany).

Special details:

Table 2. Atomic coordinates [× 10^4], equivalent isotropic displacement parameters [$Å^2$ × 10^3] and site occupancy factors. U_{eq} is defined as one third of the trace of the orthogonalized U^{ij} tensor.

Atom	*x*	*y*	*z*	U_{eq}	*S.o.f.*
O1	4457(1)	3015(1)	9317(1)	34(1)	1
O2	10115(1)	8038(1)	4375(1)	36(1)	1
N3	7725(2)	2820(1)	9147(1)	26(1)	1
N2	6272(1)	2432(1)	10086(1)	27(1)	1
N7	5365(2)	7298(1)	5137(1)	28(1)	1
N8	6899(2)	8117(1)	4238(1)	29(1)	1
N6	8186(2)	7487(1)	5158(1)	32(1)	1
N4	9134(1)	2327(1)	10065(1)	27(1)	1
C7	7807(2)	2525(1)	9774(1)	25(1)	1
C8	8972(2)	3024(1)	8689(1)	26(1)	1
C26	6714(2)	7627(1)	4852(1)	28(1)	1
C14	8970(2)	2029(1)	10720(1)	26(1)	1
C33	5740(2)	8398(1)	3784(1)	26(1)	1
C6	4753(2)	2661(1)	9863(1)	28(1)	1
C27	5401(2)	6829(1)	5780(1)	27(1)	1
C34	4061(2)	8369(1)	3899(1)	27(1)	1
C12	11723(2)	3389(1)	8301(1)	30(1)	1
C13	10602(2)	3138(1)	8801(1)	27(1)	1
C19	8694(2)	3079(1)	11090(1)	29(1)	1
C9	8493(2)	3148(1)	8075(1)	29(1)	1
C38	6361(2)	8745(1)	3175(1)	29(1)	1
C36	3652(2)	9050(1)	2804(1)	29(1)	1
C11	11245(2)	3526(2)	7693(1)	31(1)	1
C35	3038(2)	8697(1)	3405(1)	29(1)	1
C10	9622(2)	3395(2)	7584(1)	31(1)	1
C18	8539(2)	2772(2)	11732(1)	33(1)	1
C37	5329(2)	9072(1)	2690(1)	30(1)	1
C17	8665(2)	1414(2)	12012(1)	34(1)	1
C15	9119(2)	664(1)	11002(1)	30(1)	1
C25	9731(2)	7665(2)	4922(1)	32(1)	1
C29	5462(2)	4970(1)	6628(1)	31(1)	1
C30	5371(2)	5904(2)	7055(1)	33(1)	1
C28	5473(2)	5424(1)	5994(1)	29(1)	1
C16	8966(2)	364(2)	11645(1)	33(1)	1
C32	5308(2)	7759(2)	6211(1)	38(1)	1
C31	5294(3)	7296(2)	6844(1)	41(1)	1
C5	3480(20)	2440(20)	10379(10)	26(1)	0.587(3)
C24	10926(7)	7329(9)	5425(4)	28(1)	0.714(3)
N5	10156(2)	7331(2)	6068(1)	28(1)	0.587(3)
C20	10141(4)	8654(3)	6291(1)	33(1)	0.587(3)
C21	10928(3)	6189(2)	6475(1)	31(1)	0.587(3)
C22	11062(10)	5054(10)	6063(4)	34(1)	0.587(3)
C23	11611(3)	5814(2)	5427(1)	29(1)	0.587(3)
C1	3832(4)	191(3)	10957(1)	31(1)	0.714(3)
C3	3263(4)	3784(3)	11246(1)	35(1)	0.714(3)
C2	3248(3)	2251(2)	11464(1)	31(1)	0.714(3)
C4	2828(2)	3893(2)	10566(1)	29(1)	0.714(3)
N1	4024(2)	1657(2)	10932(1)	26(1)	0.714(3)
C5A	3330(40)	2480(30)	10355(15)	26(1)	0.413(3)
C24A	11170(20)	7320(20)	5371(11)	28(1)	0.286(3)
C23A	11587(4)	8720(3)	5536(2)	27(1)	0.413(3)
C21A	10996(7)	8697(4)	6216(2)	35(1)	0.413(3)
C22A	11040(5)	7161(4)	6457(2)	32(1)	0.413(3)
N5A	10465(4)	6577(3)	5937(1)	29(1)	0.413(3)
C20A	10852(19)	5096(15)	5963(7)	45(3)	0.413(3)
N1A	3980(6)	2573(4)	10972(2)	30(1)	0.286(3)
C4A	3024(6)	856(5)	10432(2)	31(1)	0.286(3)

C2A	3180(7)	1564(6)	11430(2)	33(1)	0.286(3)
C3A	3318(11)	294(7)	11116(4)	37(1)	0.286(3)
C1A	3692(14)	3987(8)	11099(4)	45(2)	0.286(3)

Table 3. Bond lengths [Å] and angles [°].

O1–C6	1.2314(17)
O2–C25	1.2341(19)
N3–C7	1.3679(16)
N3–C8	1.4022(18)
N3–H3	0.80(2)
N2–C6	1.3664(18)
N2–C7	1.4097(18)
N2–H2	0.83(2)
N7–C26	1.2880(18)
N7–C27	1.4212(17)
N8–C26	1.3679(17)
N8–C33	1.4069(18)
N8–H8	0.77(2)
N6–C25	1.3645(19)
N6–C26	1.4116(18)
N6–H6	0.84(2)
N4–C7	1.2897(17)
N4–C14	1.4251(16)
C8–C13	1.4001(19)
C8–C9	1.4093(18)
C14–C19	1.400(2)
C14–C15	1.4046(18)
C33–C34	1.3994(19)
C33–C38	1.4055(19)
C6–C5	1.50(2)
C6–C5A	1.55(3)
C27–C32	1.400(2)
C27–C28	1.4032(18)
C34–C35	1.3992(19)
C34–H34	0.9500
C12–C11	1.396(2)
C12–C13	1.3991(19)
C12–H12	0.9500
C13–H13	0.9500
C19–C18	1.3968(19)
C19–H19	0.9500
C9–C10	1.389(2)
C9–H9	0.9500
C38–C37	1.3898(19)
C38–H38	0.9500
C36–C35	1.391(2)
C36–C37	1.397(2)
C36–H36	0.9500
C11–C10	1.396(2)
C11–H11	0.9500
C35–H35	0.9500
C10–H10	0.9500
C18–C17	1.397(2)
C18–H18	0.9500
C37–H37	0.9500
C17–C16	1.398(2)
C17–H17	0.9500
C15–C16	1.3986(19)
C15–H15	0.9500
C25–C24	1.509(9)
C25–C24A	1.58(2)
C29–C30	1.396(2)
C29–C28	1.3977(19)
C29–H29	0.9500
C30–C31	1.389(2)
C30–H30	0.9500
C28–H28	0.9500
C16–H16	0.9500
C32–C31	1.396(2)
C32–H32	0.9500
C31–H31	0.9500
C5–N1	1.42(2)
C5–C4	1.60(2)
C5–H5	1.0000
C24–N5	1.509(7)
C24–C23	1.562(9)
C24–H24	1.0000
N5–C20	1.457(3)
N5–C21	1.470(3)
C20–H20A	0.9800
C20–H20B	0.9800
C20–H20C	0.9800
C21–C22	1.527(10)
C21–H21A	0.9900
C21–H21B	0.9900
C22–C23	1.549(9)
C22–H22A	0.9900
C22–H22B	0.9900
C23–H23A	0.9900
C23–H23B	0.9900
C1–N1	1.464(3)
C1–H1A	0.9800
C1–H1B	0.9800
C1–H1C	0.9800
C3–C2	1.527(4)
C3–C4	1.538(4)
C3–H3A	0.9900
C3–H3B	0.9900
C2–N1	1.469(3)
C2–H2A	0.9900
C2–H2B	0.9900
C4–H4A	0.9900
C4–H4B	0.9900
C5A–N1A	1.50(3)
C5A–C4A	1.63(3)
C5A–H5A	1.0000
C24A–N5A	1.46(2)
C24A–C23A	1.55(2)
C24A–H24A	1.0000
C23A–C21A	1.536(5)
C23A–H23C	0.9900
C23A–H23D	0.9900
C21A–C22A	1.537(5)
C21A–H21C	0.9900
C21A–H21D	0.9900
C22A–N5A	1.462(5)
C22A–H22C	0.9900
C22A–H22D	0.9900
N5A–C20A	1.471(15)
C20A–H20D	0.9800

C20A–H20E	0.9800
C20A–H20F	0.9800
N1A–C1A	1.463(9)
N1A–C2A	1.479(7)
C4A–C3A	1.549(9)
C4A–H4A1	0.9900
C4A–H4A2	0.9900
C2A–C3A	1.507(11)
C2A–H2A1	0.9900
C2A–H2A2	0.9900
C3A–H3A1	0.9900
C3A–H3A2	0.9900
C1A–H1A1	0.9800
C1A–H1A2	0.9800
C1A–H1A3	0.9800

C7–N3–C8	129.85(12)
C7–N3–H3	112.0(16)
C8–N3–H3	118.2(16)
C6–N2–C7	130.21(11)
C6–N2–H2	114.1(15)
C7–N2–H2	115.6(15)
C26–N7–C27	117.30(12)
C26–N8–C33	130.08(12)
C26–N8–H8	114.8(16)
C33–N8–H8	115.1(16)
C25–N6–C26	129.70(13)
C25–N6–H6	109.9(17)
C26–N6–H6	120.2(17)
C7–N4–C14	116.47(11)
N4–C7–N3	124.75(12)
N4–C7–N2	121.98(12)
N3–C7–N2	113.27(11)
C13–C8–N3	125.01(12)
C13–C8–C9	119.39(12)
N3–C8–C9	115.59(12)
N7–C26–N8	125.20(12)
N7–C26–N6	121.79(12)
N8–C26–N6	113.00(12)
C19–C14–C15	119.45(12)
C19–C14–N4	120.95(11)
C15–C14–N4	119.59(12)
C34–C33–C38	119.34(12)
C34–C33–N8	124.94(12)
C38–C33–N8	115.72(12)
O1–C6–N2	125.03(13)
O1–C6–C5	124.3(8)
N2–C6–C5	110.7(8)
O1–C6–C5A	119.4(11)
N2–C6–C5A	115.6(11)
C32–C27–C28	118.95(12)
C32–C27–N7	120.67(12)
C28–C27–N7	120.35(12)
C35–C34–C33	119.11(12)
C35–C34–H34	120.4
C33–C34–H34	120.4
C11–C12–C13	121.19(14)
C11–C12–H12	119.4
C13–C12–H12	119.4
C12–C13–C8	119.41(12)
C12–C13–H13	120.3
C8–C13–H13	120.3
C18–C19–C14	120.32(12)
C18–C19–H19	119.8
C14–C19–H19	119.8
C10–C9–C8	120.44(13)
C10–C9–H9	119.8
C8–C9–H9	119.8
C37–C38–C33	120.87(13)
C37–C38–H38	119.6
C33–C38–H38	119.6
C35–C36–C37	119.21(13)
C35–C36–H36	120.4
C37–C36–H36	120.4
C12–C11–C10	119.14(13)
C12–C11–H11	120.4
C10–C11–H11	120.4
C36–C35–C34	121.54(13)
C36–C35–H35	119.2
C34–C35–H35	119.2
C9–C10–C11	120.42(13)
C9–C10–H10	119.8
C11–C10–H10	119.8
C19–C18–C17	120.27(14)
C19–C18–H18	119.9
C17–C18–H18	119.9
C38–C37–C36	119.93(13)
C38–C37–H37	120.0
C36–C37–H37	120.0
C18–C17–C16	119.57(13)
C18–C17–H17	120.2
C16–C17–H17	120.2
C16–C15–C14	119.94(13)
C16–C15–H15	120.0
C14–C15–H15	120.0
O2–C25–N6	125.32(13)
O2–C25–C24	124.1(2)
N6–C25–C24	110.6(2)
O2–C25–C24A	116.1(7)
N6–C25–C24A	118.5(7)
C30–C29–C28	120.60(13)
C30–C29–H29	119.7
C28–C29–H29	119.7
C31–C30–C29	119.36(13)
C31–C30–H30	120.3
C29–C30–H30	120.3
C29–C28–C27	120.09(13)
C29–C28–H28	120.0
C27–C28–H28	120.0
C17–C16–C15	120.44(13)
C17–C16–H16	119.8
C15–C16–H16	119.8
C31–C32–C27	120.55(13)
C31–C32–H32	119.7
C27–C32–H32	119.7
C30–C31–C32	120.45(15)
C30–C31–H31	119.8
C32–C31–H31	119.8

N1–C5–C6	115.2(13)	C5–C4–H4A	111.2
N1–C5–C4	105.7(14)	C3–C4–H4B	111.2
C6–C5–C4	108.6(13)	C5–C4–H4B	111.2
N1–C5–H5	109.1	H4A–C4–H4B	109.1
C6–C5–H5	109.1	C5–N1–C1	113.2(9)
C4–C5–H5	109.1	C5–N1–C2	109.0(9)
C25–C24–N5	113.4(3)	C1–N1–C2	113.75(19)
C25–C24–C23	108.6(6)	N1A–C5A–C6	107.5(18)
N5–C24–C23	103.0(5)	N1A–C5A–C4A	100.3(17)
C25–C24–H24	110.5	C6–C5A–C4A	104.8(18)
N5–C24–H24	110.5	N1A–C5A–H5A	114.3
C23–C24–H24	110.5	C6–C5A–H5A	114.3
C20–N5–C21	114.5(2)	C4A–C5A–H5A	114.3
C20–N5–C24	113.3(4)	N5A–C24A–C23A	106.4(15)
C21–N5–C24	108.3(4)	N5A–C24A–C25	105.5(11)
N5–C20–H20A	109.5	C23A–C24A–C25	104.7(14)
N5–C20–H20B	109.5	N5A–C24A–H24A	113.2
H20A–C20–H20B	109.5	C23A–C24A–H24A	113.2
N5–C20–H20C	109.5	C25–C24A–H24A	113.2
H20A–C20–H20C	109.5	C21A–C23A–C24A	104.3(8)
H20B–C20–H20C	109.5	C21A–C23A–H23C	110.9
N5–C21–C22	101.6(4)	C24A–C23A–H23C	110.9
N5–C21–H21A	111.4	C21A–C23A–H23D	110.9
C22–C21–H21A	111.4	C24A–C23A–H23D	110.9
N5–C21–H21B	111.4	H23C–C23A–H23D	108.9
C22–C21–H21B	111.4	C23A–C21A–C22A	103.0(3)
H21A–C21–H21B	109.3	C23A–C21A–H21C	111.2
C21–C22–C23	102.6(6)	C22A–C21A–H21C	111.2
C21–C22–H22A	111.3	C23A–C21A–H21D	111.2
C23–C22–H22A	111.3	C22A–C21A–H21D	111.2
C21–C22–H22B	111.3	H21C–C21A–H21D	109.1
C23–C22–H22B	111.3	N5A–C22A–C21A	102.6(3)
H22A–C22–H22B	109.2	N5A–C22A–H22C	111.2
C22–C23–C24	105.7(5)	C21A–C22A–H22C	111.2
C22–C23–H23A	110.6	N5A–C22A–H22D	111.2
C24–C23–H23A	110.6	C21A–C22A–H22D	111.2
C22–C23–H23B	110.6	H22C–C22A–H22D	109.2
C24–C23–H23B	110.6	C22A–N5A–C24A	107.2(10)
H23A–C23–H23B	108.7	C22A–N5A–C20A	113.8(6)
N1–C1–H1A	109.5	C24A–N5A–C20A	111.1(11)
N1–C1–H1B	109.5	N5A–C20A–H20D	109.5
H1A–C1–H1B	109.5	N5A–C20A–H20E	109.5
N1–C1–H1C	109.5	H20D–C20A–H20E	109.5
H1A–C1–H1C	109.5	N5A–C20A–H20F	109.5
H1B–C1–H1C	109.5	H20D–C20A–H20F	109.5
C2–C3–C4	102.8(2)	H20E–C20A–H20F	109.5
C2–C3–H3A	111.2	C1A–N1A–C2A	114.1(5)
C4–C3–H3A	111.2	C1A–N1A–C5A	108.3(12)
C2–C3–H3B	111.2	C2A–N1A–C5A	107.4(13)
C4–C3–H3B	111.2	C3A–C4A–C5A	106.2(12)
H3A–C3–H3B	109.1	C3A–C4A–H4A1	110.5
N1–C2–C3	102.30(18)	C5A–C4A–H4A1	110.5
N1–C2–H2A	111.3	C3A–C4A–H4A2	110.5
C3–C2–H2A	111.3	C5A–C4A–H4A2	110.5
N1–C2–H2B	111.3	H4A1–C4A–H4A2	108.7
C3–C2–H2B	111.3	N1A–C2A–C3A	102.9(5)
H2A–C2–H2B	109.2	N1A–C2A–H2A1	111.2
C3–C4–C5	103.0(8)	C3A–C2A–H2A1	111.2
C3–C4–H4A	111.2	N1A–C2A–H2A2	111.2

C3A–C2A–H2A2	111.2
H2A1–C2A–H2A2	109.1
C2A–C3A–C4A	103.3(5)
C2A–C3A–H3A1	111.1
C4A–C3A–H3A1	111.1
C2A–C3A–H3A2	111.1
C4A–C3A–H3A2	111.1
H3A1–C3A–H3A2	109.1
N1A–C1A–H1A1	109.5
N1A–C1A–H1A2	109.5
H1A1–C1A–H1A2	109.5
N1A–C1A–H1A3	109.5
H1A1–C1A–H1A3	109.5
H1A2–C1A–H1A3	109.5

Symmetry transformations used to generate equivalent atoms:

Table 4. Anisotropic displacement parameters [Å²× 10³]. The anisotropic displacement factor exponent takes the form: $-2\pi^2[h^2a^{*2}U^{11} + \cdots + 2\,h\,k\,a^*\,b^*\,U^{12}]$.

Atom	U^{11}	U^{22}	U^{33}	U^{23}	U^{13}	U^{12}
O1	31(1)	42(1)	29(1)	1(1)	–4(1)	–2(1)
O2	30(1)	39(1)	38(1)	9(1)	–3(1)	–7(1)
N3	29(1)	25(1)	25(1)	0(1)	–3(1)	–4(1)
N2	28(1)	28(1)	26(1)	0(1)	–3(1)	–5(1)
N7	30(1)	25(1)	29(1)	2(1)	–4(1)	–7(1)
N8	27(1)	29(1)	30(1)	4(1)	–3(1)	–6(1)
N6	30(1)	32(1)	32(1)	7(1)	–6(1)	–9(1)
N4	29(1)	25(1)	25(1)	0(1)	–3(1)	–4(1)
C7	29(1)	21(1)	26(1)	0(1)	–3(1)	–4(1)
C8	31(1)	21(1)	25(1)	0(1)	–3(1)	–4(1)
C26	29(1)	23(1)	30(1)	2(1)	–4(1)	–5(1)
C14	29(1)	25(1)	25(1)	1(1)	–3(1)	–5(1)
C33	28(1)	21(1)	29(1)	0(1)	–4(1)	–4(1)
C6	30(1)	25(1)	29(1)	–1(1)	–4(1)	–4(1)
C27	29(1)	24(1)	29(1)	0(1)	–3(1)	–6(1)
C34	28(1)	25(1)	29(1)	–2(1)	–2(1)	–3(1)
C12	33(1)	28(1)	28(1)	–1(1)	–2(1)	–6(1)
C13	31(1)	25(1)	26(1)	–1(1)	–3(1)	–4(1)
C19	34(1)	25(1)	28(1)	–1(1)	–2(1)	–4(1)
C9	34(1)	26(1)	26(1)	–1(1)	–5(1)	–5(1)
C38	29(1)	27(1)	30(1)	1(1)	–2(1)	–5(1)
C36	31(1)	28(1)	29(1)	–2(1)	–4(1)	–3(1)
C11	39(1)	28(1)	27(1)	0(1)	0(1)	–8(1)
C35	28(1)	28(1)	31(1)	–4(1)	–3(1)	–1(1)
C10	38(1)	29(1)	26(1)	0(1)	–3(1)	–7(1)
C18	39(1)	31(1)	28(1)	–3(1)	–1(1)	–6(1)
C37	32(1)	28(1)	29(1)	1(1)	–3(1)	–5(1)
C17	42(1)	33(1)	26(1)	0(1)	–1(1)	–11(1)
C15	38(1)	25(1)	27(1)	0(1)	–4(1)	–7(1)
C25	30(1)	27(1)	38(1)	7(1)	–7(1)	–7(1)
C29	37(1)	24(1)	30(1)	1(1)	0(1)	0(1)
C30	41(1)	30(1)	29(1)	–1(1)	–7(1)	–3(1)
C28	34(1)	23(1)	29(1)	–1(1)	1(1)	–2(1)
C16	44(1)	26(1)	28(1)	3(1)	–4(1)	–9(1)
C32	57(1)	24(1)	33(1)	–1(1)	–13(1)	–9(1)
C31	64(1)	28(1)	33(1)	–5(1)	–15(1)	–6(1)
C5	24(3)	25(1)	28(2)	0(1)	–5(2)	–2(2)
C24	23(2)	25(1)	35(2)	0(1)	–4(1)	–3(2)
N5	27(1)	25(1)	29(1)	0(1)	–1(1)	–3(1)
C20	37(1)	27(1)	36(1)	–4(1)	–6(1)	–1(1)
C21	34(1)	26(1)	31(1)	3(1)	–2(1)	–2(1)
C22	37(2)	27(2)	36(3)	1(2)	2(2)	–4(1)
C23	26(1)	28(1)	31(1)	0(1)	–3(1)	–1(1)
C1	38(1)	23(1)	32(1)	–1(1)	–3(1)	–3(1)
C3	50(2)	24(1)	30(1)	–3(1)	–3(1)	–2(1)
C2	41(1)	25(1)	27(1)	–2(1)	–2(1)	–2(1)
C4	33(1)	23(1)	31(1)	1(1)	0(1)	–2(1)
N1	31(1)	22(1)	26(1)	–1(1)	–3(1)	–3(1)
C5A	24(3)	25(1)	28(2)	0(1)	–5(2)	–2(2)
C24A	23(2)	25(1)	35(2)	0(1)	–4(1)	–3(2)
C23A	31(1)	21(1)	29(1)	0(1)	–1(1)	–4(1)
C21A	47(2)	28(2)	30(2)	–3(1)	4(2)	–6(2)
C22A	41(2)	30(2)	26(1)	1(1)	1(1)	–7(1)
N5A	33(1)	26(1)	28(1)	2(1)	–2(1)	–7(1)
C20A	76(8)	23(3)	35(4)	1(2)	–1(3)	–14(4)

N1A	39(2)	21(2)	31(2)	–2(1)	–3(2)	–6(1)
C4A	31(2)	28(2)	34(2)	–3(2)	0(2)	–7(2)
C2A	43(3)	23(2)	33(2)	2(2)	–4(2)	–9(2)
C3A	43(4)	26(2)	41(4)	1(2)	–10(3)	–4(3)
C1A	71(6)	24(3)	39(4)	–6(2)	15(3)	–9(3)

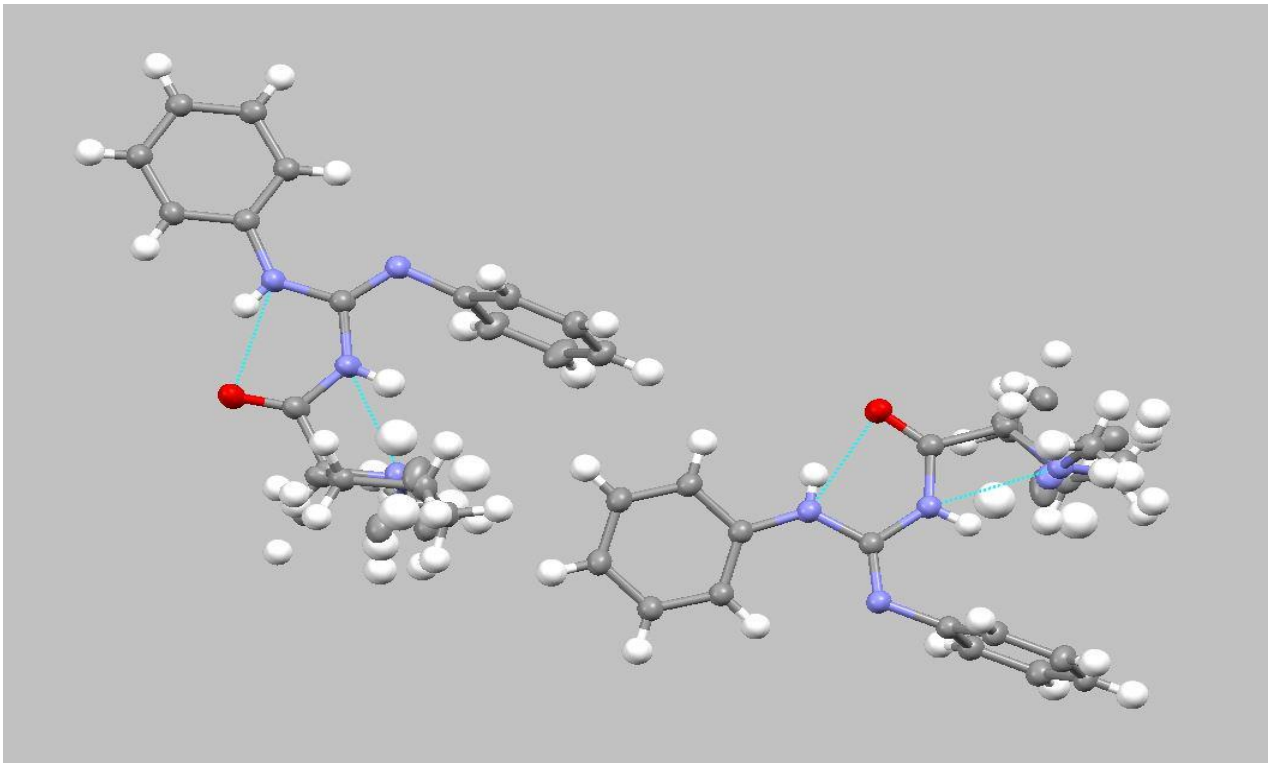

Appendix 4
X-ray of compound 122

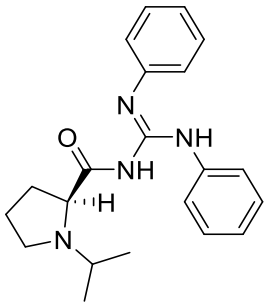

UK National Crystallography Service

Table 1. Crystal data and structure refinement details.

Identification code	**2016ncs0504**	
Empirical formula	$C_{21}H_{26}N_4O$	
Formula weight	350.46	
Temperature	100(2) K	
Wavelength	0.6889 Å	
Crystal system	Monoclinic	
Space group	*P*21	
Unit cell dimensions	a = 8.600(3) Å	α = **90°**
	b = **9.896(4) Å**	β = 10**6.38(2)°**
	c = **11.880(3) Å**	γ = **90°**
Volume	**969.9(6) Å^3**	
Z	2	
Density (calculated)	1.200 Mg / m^3	
Absorption coefficient	0.072 mm^{-1}	
F(000)	376	
Crystal	Plate; colourless	
Crystal size	0.040 × 0.030 × 0.010 mm^3	
θ range for data collection	1.732 – 26.573°	
Index ranges	$-11 \le h \le 11$, $-12 \le k \le 12$, $-15 \le l \le 15$	
Reflections collected	17850	
Independent reflections	4416 [R_{int} = 0.0907]	
Completeness to θ = 24.415°	99.9 %	
Absorption correction	Empirical	
Max. and min. transmission	1.00 and 0.998	
Refinement method	Full-matrix least-squares on F^2	
Data / restraints / parameters	4416 / 1 / 245	
Goodness-of-fit on F^2	1.094	
Final *R* indices [$F^2 > 2\sigma(F^2)$]	*R1* = 0.0491, *wR2* = 0.1291	
R indices (all data)	*R1* = 0.0508, *wR2* = 0.1311	
Absolute structure parameter	0.0(6)	
Extinction coefficient	n/a	
Largest diff. peak and hole	0.314 and –0.239 e Å^{-3}	

Diffractometer: three-circle fixed chi goniometer equipped with a PILATUS2M hybrid pixel detector installed at Diamond Light Source Ltd. Beamline I19. **Data collection:** GDA http://www.opengda.org/OpenGDA.html **Cell determination, Data reduction and cell refinement & Absorption correction**: XIA2 0.4.0.438-g4431aaa, (Winter, G. (2010) J. Appl. Cryst. 43). **Structure**

solution: SHELXT (G. M. Sheldrick, Acta Cryst. (2015). A71, 3-8). S**tructure refinement**: SHELXL97 (G. M. Sheldrick (1997), University of Göttingen, Germany).

Special details:

Table 2. Atomic coordinates [× 10^4], equivalent isotropic displacement parameters [$Å^2$ × 10^3] and site occupancy factors. U_{eq} is defined as one third of the trace of the orthogonalized U^{ij} tensor.

Atom	*x*	*y*	*z*	U_{eq}	*S.o.f.*
O1	652(2)	6239(2)	1922(2)	43(1)	1
N1	2774(2)	4774(2)	2654(2)	27(1)	1
N2	3733(2)	6645(2)	1880(2)	29(1)	1
N3	5528(2)	4905(2)	2716(2)	30(1)	1
N4	831(2)	2800(2)	2996(2)	32(1)	1
C9	4109(2)	5429(2)	2427(2)	26(1)	1
C10	4744(3)	7537(2)	1486(2)	28(1)	1
C8	1187(3)	5168(2)	2388(2)	32(1)	1
C16	5731(2)	3626(2)	3280(2)	29(1)	1
C15	6435(3)	7444(2)	1800(2)	31(1)	1
C21	6148(3)	3559(2)	4504(2)	33(1)	1
C11	3974(3)	8574(2)	735(2)	33(1)	1
C20	6354(3)	2313(3)	5067(2)	38(1)	1
C17	5583(3)	2427(2)	2634(2)	33(1)	1
C19	6173(3)	1129(3)	4420(2)	36(1)	1
C14	7311(3)	8386(2)	1350(2)	37(1)	1
C12	4865(3)	9507(3)	306(2)	38(1)	1
C13	6549(3)	9405(3)	609(2)	39(1)	1
C6	−77(3)	4645(3)	4001(2)	37(1)	1
C18	5800(3)	1187(2)	3206(2)	36(1)	1
C4	477(3)	2276(3)	4063(2)	38(1)	1
C7	116(2)	4170(3)	2797(2)	33(1)	1
C5	640(3)	3500(3)	4847(2)	42(1)	1
C3	275(3)	1892(3)	1977(2)	41(1)	1
C1	702(4)	2457(4)	904(2)	51(1)	1
C2	1041(4)	497(3)	2266(3)	55(1)	1

Table 3. Bond lengths [Å] and angles [°].

O1–C8	1.224(3)
N1–C8	1.368(3)
N1–C9	1.409(3)
N2–C9	1.362(3)
N2–C10	1.409(3)
N3–C9	1.280(3)
N3–C16	1.420(3)
N4–C3	1.475(3)
N4–C4	1.478(3)
N4–C7	1.480(3)
C10–C15	1.399(3)
C10–C11	1.398(3)
C8–C7	1.521(3)
C16–C21	1.398(3)
C16–C17	1.400(3)
C15–C14	1.396(3)
C21–C20	1.390(3)
C11–C12	1.385(3)
C20–C19	1.386(4)
C17–C18	1.389(3)
C19–C18	1.388(4)
C14–C13	1.377(4)
C12–C13	1.393(4)
C6–C5	1.525(4)
C6–C7	1.557(3)
C4–C5	1.510(4)
C3–C2	1.527(4)
C3–C1	1.529(4)

C8–N1–C9	129.7(2)
C9–N2–C10	128.78(18)
C9–N3–C16	117.92(18)
C3–N4–C4	113.12(18)
C3–N4–C7	113.77(19)
C4–N4–C7	106.36(19)
N3–C9–N2	124.45(19)
N3–C9–N1	121.9(2)
N2–C9–N1	113.62(18)
C15–C10–C11	119.2(2)
C15–C10–N2	124.2(2)
C11–C10–N2	116.53(19)
O1–C8–N1	125.1(2)
O1–C8–C7	121.5(2)
N1–C8–C7	113.3(2)
C21–C16–C17	119.2(2)
C21–C16–N3	119.6(2)
C17–C16–N3	121.13(19)
C14–C15–C10	119.1(2)
C20–C21–C16	120.2(2)
C12–C11–C10	120.8(2)
C19–C20–C21	120.3(2)
C18–C17–C16	120.1(2)
C20–C19–C18	119.9(2)
C13–C14–C15	121.5(2)
C11–C12–C13	119.9(2)
C14–C13–C12	119.4(2)
C5–C6–C7	104.7(2)
C19–C18–C17	120.3(2)
N4–C4–C5	104.00(19)
N4–C7–C8	112.60(18)
N4–C7–C6	106.06(19)
C8–C7–C6	109.21(19)
C4–C5–C6	103.8(2)
N4–C3–C2	110.3(2)
N4–C3–C1	111.3(2)
C2–C3–C1	109.2(2)

Symmetry transformations used to generate equivalent atoms:

Table 4. Anisotropic displacement parameters [Å²× 10³]. The anisotropic displacement factor exponent takes the form: $-2\pi^2[h^2a^{*2}U^{11} + \cdots + 2\,h\,k\,a^*\,b^*\,U^{12}]$.

Atom	U^{11}	U^{22}	U^{33}	U^{23}	U^{13}	U^{12}
O1	26(1)	51(1)	51(1)	18(1)	11(1)	7(1)
N1	22(1)	31(1)	30(1)	4(1)	8(1)	–1(1)
N2	22(1)	32(1)	34(1)	4(1)	10(1)	1(1)
N3	23(1)	32(1)	34(1)	3(1)	10(1)	–1(1)
N4	25(1)	37(1)	35(1)	–1(1)	10(1)	–7(1)
C9	22(1)	31(1)	26(1)	–2(1)	8(1)	–3(1)
C10	33(1)	26(1)	27(1)	–2(1)	11(1)	–2(1)
C8	23(1)	42(1)	31(1)	2(1)	7(1)	0(1)
C16	18(1)	34(1)	36(1)	5(1)	10(1)	1(1)
C15	30(1)	29(1)	36(1)	1(1)	11(1)	–1(1)
C21	26(1)	36(1)	37(1)	1(1)	13(1)	2(1)
C11	35(1)	34(1)	32(1)	1(1)	9(1)	–2(1)
C20	31(1)	47(1)	37(1)	11(1)	14(1)	5(1)
C17	26(1)	36(1)	36(1)	2(1)	8(1)	–3(1)
C19	25(1)	36(1)	50(1)	13(1)	16(1)	4(1)
C14	34(1)	36(1)	42(1)	–2(1)	15(1)	–6(1)
C12	46(1)	34(1)	33(1)	5(1)	9(1)	–2(1)
C13	45(1)	38(1)	37(1)	–1(1)	18(1)	–12(1)
C6	27(1)	46(1)	42(1)	–6(1)	16(1)	–6(1)
C18	26(1)	32(1)	49(1)	2(1)	10(1)	0(1)
C4	31(1)	44(1)	41(1)	5(1)	13(1)	–9(1)
C7	20(1)	44(1)	34(1)	0(1)	7(1)	–3(1)
C5	39(1)	56(2)	34(1)	–1(1)	14(1)	–13(1)
C3	28(1)	50(1)	48(1)	–13(1)	13(1)	–11(1)
C1	43(1)	71(2)	38(1)	–17(1)	11(1)	–13(1)
C2	46(2)	47(2)	76(2)	–17(2)	26(2)	–14(1)

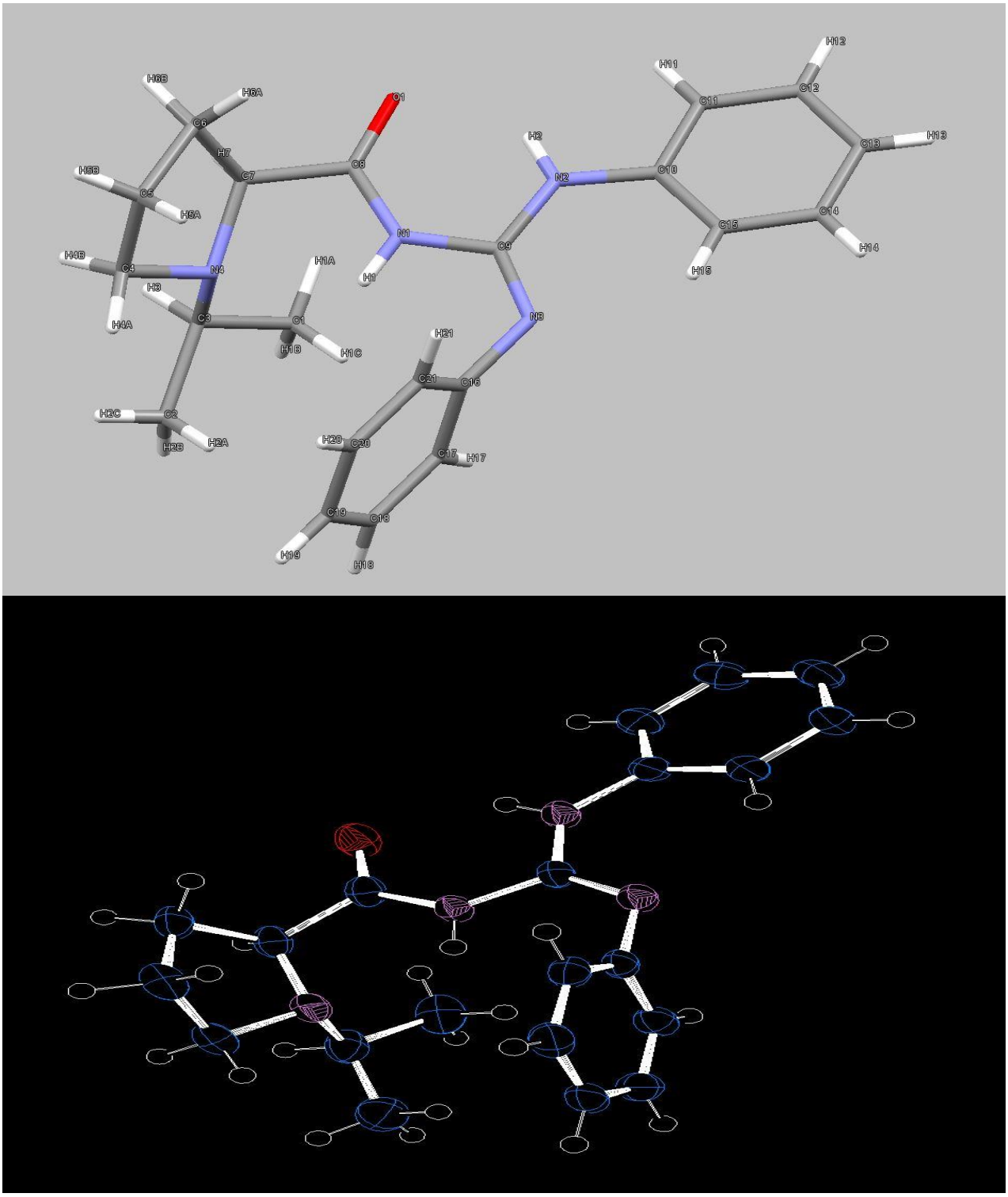
H12
H11
C12
C11
H6B
H6A
O1
C6
H2
H13
C13
H7
C8
N2
C10
H5B
C7
C5
H5A
C14
C15
N1
C9
H14
H16
H4B
H1A
C4
N4
H1
H3
N3
H4A
C3
C1
H21
H1B
H1C
C21
C16
H2C
C2
H20
C20
C17
H17
H2A
H2B
C19
C18
H19
H18

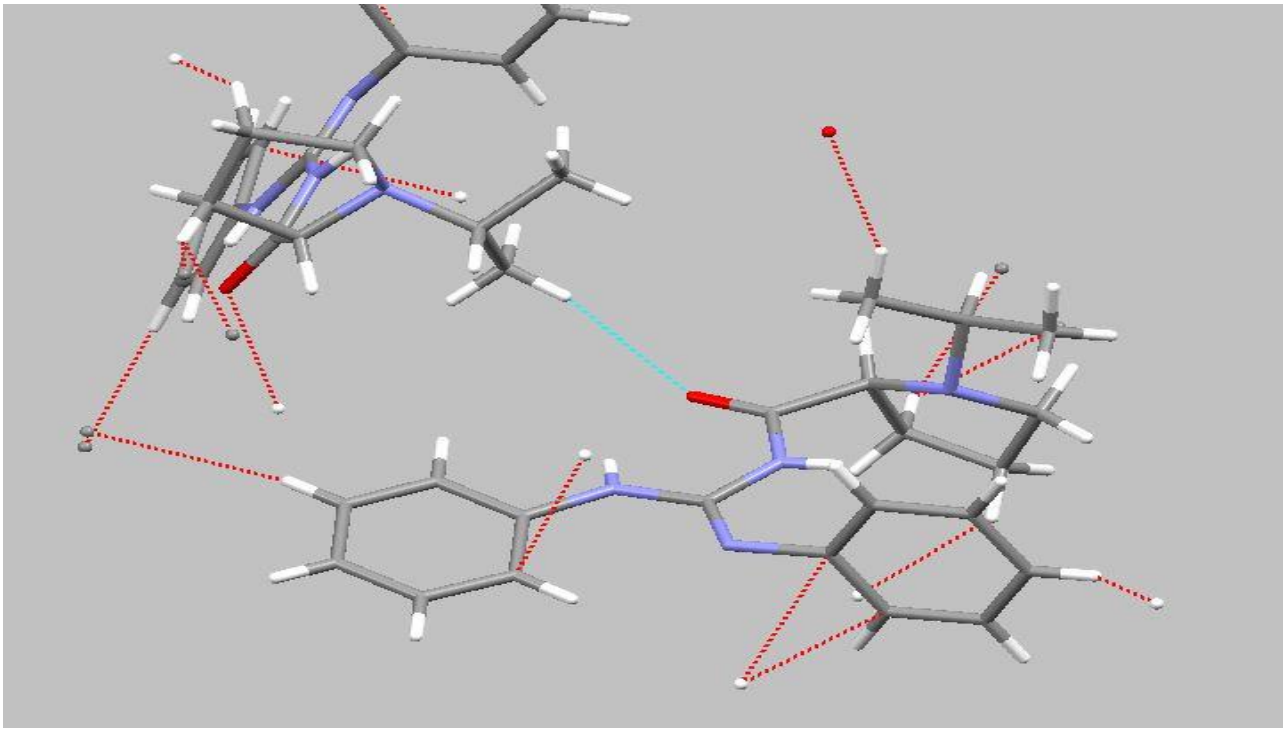

Appendix 5
X-ray of compound 123

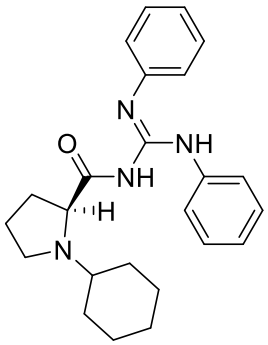

UK National Crystallography Service

Table 1. Crystal data and structure refinement details.

Identification code	**2016ncs0748**	
Empirical formula	$C_{24}H_{30}N_4O$	
Formula weight	390.52	
Temperature	100(2) K	
Wavelength	0.6889 Å	
Crystal system	Monoclinic	
Space group	*P*21	
Unit cell dimensions	a = 9.3748(2) Å	α = **90°**
	b = **9.6012(2) Å**	β = 10**4.848(2)°**
	c = **12.5616(3) Å**	γ = **90°**
Volume	**1092.91(4) Å**^{3}	
Z	2	
Density (calculated)	1.187 Mg / m^3	
Absorption coefficient	0.074 mm^{-1}	
F(000)	420	
Crystal	Plate; colourless	
Crystal size	0.095 × 0.090 × 0.022 mm^3	
θ range for data collection	2.178 – 26.569°	
Index ranges	$-12 \le h \le 12$, $-12 \le k \le 12$, $-16 \le l \le 16$	
Reflections collected	11102	
Independent reflections	4942 [R_{int} = 0.0627]	
Completeness to θ = 24.415°	99.8 %	
Absorption correction	Empirical	
Max. and min. transmission	1.0 and 0.996641639337	
Refinement method	Full-matrix least-squares on F^2	
Data / restraints / parameters	4942 / 1 / 270	
Goodness-of-fit on F^2	1.014	
Final *R* indices [$F^2 > 2\sigma(F^2)$]	*R1* = 0.0519, *wR2* = 0.1233	
R indices (all data)	*R1* = 0.0627, *wR2* = 0.1321	
Absolute structure parameter	?	
Extinction coefficient	n/a	
Largest diff. peak and hole	0.202 and –0.213 e Å^{-3}	

Diffractometer: Beamline i19, Diamond Light Source Ltd. 3-circle fixed chi goniometer equipped with a PILATUS 2M PIXEL detector, wavelength 0.6998A (100μm focus). **Data collection:** GDA http://www.opengda.org/OpenGDA.html **Cell**

determination, Data reduction and cell refinement & Absorption correction: XIA2 0.5.53 Winter, G. (2010) Journal of Applied Crystallography 43, **Structure solution**: SHELXT (G. M. Sheldrick *Acta Cryst.* (2015). A**71**, 3-8). S**tructure refinement**: SHELXL97 (G. M. Sheldrick (1997), University of Göttingen, Germany).

Special details:

Table 2. Atomic coordinates [× 10^4], equivalent isotropic displacement parameters [$Å^2$ × 10^3] and site occupancy factors. U_{eq} is defined as one third of the trace of the orthogonalized U^{ij} tensor.

Atom	*x*	*y*	*z*	U_{eq}	*S.o.f.*
O1	4894(2)	4589(2)	4378(2)	40(1)	1
N2	6204(2)	5760(2)	5909(2)	28(1)	1
N1	4304(2)	5169(2)	7081(2)	27(1)	1
N4	8563(2)	6789(2)	6282(2)	31(1)	1
N3	7413(3)	5957(2)	4528(2)	31(1)	1
C12	7469(3)	6219(3)	5608(2)	27(1)	1
C11	5024(3)	5027(3)	5314(2)	30(1)	1
C10	3803(3)	4830(3)	5900(2)	28(1)	1
C19	8496(3)	6998(3)	7391(2)	29(1)	1
C13	8425(3)	6373(3)	3937(2)	29(1)	1
C18	9318(3)	7547(3)	4198(2)	31(1)	1
C20	7631(3)	8036(3)	7672(2)	34(1)	1
C8	2682(3)	6973(3)	6287(2)	36(1)	1
C9	2523(3)	5855(3)	5404(2)	36(1)	1
C22	8452(3)	7393(3)	9585(2)	35(1)	1
C7	3229(3)	6147(3)	7340(2)	35(1)	1
C23	9331(3)	6368(3)	9309(2)	36(1)	1
C24	9355(3)	6167(3)	8222(2)	34(1)	1
C17	10203(3)	7949(3)	3519(2)	38(1)	1
C6	4643(3)	3954(3)	7819(2)	31(1)	1
C14	8460(4)	5597(3)	3002(2)	38(1)	1
C5	5782(3)	3012(3)	7500(3)	36(1)	1
C21	7610(3)	8225(3)	8762(2)	38(1)	1
C1	5218(4)	4442(3)	9004(2)	40(1)	1
C16	10226(3)	7185(4)	2591(3)	44(1)	1
C15	9372(4)	6001(3)	2349(2)	43(1)	1
C4	6203(4)	1785(3)	8287(3)	46(1)	1
C3	6805(4)	2286(4)	9464(3)	51(1)	1
C2	5684(4)	3215(4)	9804(3)	51(1)	1

Table 3. Bond lengths [Å] and angles [°].

O1–C11	1.226(3)	N1–C10	1.473(3)
N2–C11	1.362(3)	N1–C7	1.473(3)
N2–C12	1.404(3)	N1–C6	1.474(3)
N2–H25	0.84(3)	N4–C12	1.274(3)
		N4–C19	1.424(3)
		N3–C12	1.369(3)
		N3–C13	1.404(3)

N3–H26	0.85(4)
C11–C10	1.522(4)
C10–C9	1.554(4)
C10–H10	1.0000
C19–C20	1.387(4)
C19–C24	1.394(4)
C13–C18	1.392(4)
C13–C14	1.398(4)
C18–C17	1.388(4)
C18–H18	0.9500
C20–C21	1.387(4)
C20–H20	0.9500
C8–C7	1.515(4)
C8–C9	1.524(4)
C8–H8A	0.9900
C8–H8B	0.9900
C9–H9A	0.9900
C9–H9B	0.9900
C22–C21	1.383(4)
C22–C23	1.383(4)
C22–H22	0.9500
C7–H7A	0.9900
C7–H7B	0.9900
C23–C24	1.384(4)
C23–H23	0.9500
C24–H24	0.9500
C17–C16	1.382(5)
C17–H17	0.9500
C6–C1	1.522(4)
C6–C5	1.528(4)
C6–H6	1.0000
C14–C15	1.383(4)
C14–H14	0.9500
C5–C4	1.524(4)
C5–H5A	0.9900
C5–H5B	0.9900
C21–H21	0.9500
C1–C2	1.537(4)
C1–H1A	0.9900
C1–H1B	0.9900
C16–C15	1.379(5)
C16–H16	0.9500
C15–H15	0.9500
C4–C3	1.519(6)
C4–H4A	0.9900
C4–H4B	0.9900
C3–C2	1.520(5)
C3–H3A	0.9900
C3–H3B	0.9900
C2–H2A	0.9900
C2–H2B	0.9900

C11–N2–C12	129.6(2)
C11–N2–H25	113(2)
C12–N2–H25	117(2)
C10–N1–C7	107.7(2)
C10–N1–C6	114.8(2)
C7–N1–C6	114.5(2)
C12–N4–C19	118.7(2)
C12–N3–C13	127.8(2)
C12–N3–H26	118(2)
C13–N3–H26	114(2)
N4–C12–N3	123.9(2)
N4–C12–N2	123.2(2)
N3–C12–N2	112.9(2)
O1–C11–N2	124.8(2)
O1–C11–C10	121.3(2)
N2–C11–C10	113.9(2)
N1–C10–C11	112.0(2)
N1–C10–C9	106.1(2)
C11–C10–C9	109.1(2)
N1–C10–H10	109.9
C11–C10–H10	109.9
C9–C10–H10	109.9
C20–C19–C24	118.9(3)
C20–C19–N4	121.7(2)
C24–C19–N4	119.4(2)
C18–C13–C14	119.2(3)
C18–C13–N3	123.6(3)
C14–C13–N3	117.1(3)
C17–C18–C13	119.9(3)
C17–C18–H18	120.1
C13–C18–H18	120.1
C21–C20–C19	120.2(3)
C21–C20–H20	119.9
C19–C20–H20	119.9
C7–C8–C9	102.4(2)
C7–C8–H8A	111.3
C9–C8–H8A	111.3
C7–C8–H8B	111.3
C9–C8–H8B	111.3
H8A–C8–H8B	109.2
C8–C9–C10	103.5(2)
C8–C9–H9A	111.1
C10–C9–H9A	111.1
C8–C9–H9B	111.1
C10–C9–H9B	111.1
H9A–C9–H9B	109.0
C21–C22–C23	119.1(3)
C21–C22–H22	120.5
C23–C22–H22	120.5
N1–C7–C8	103.8(2)
N1–C7–H7A	111.0
C8–C7–H7A	111.0
N1–C7–H7B	111.0
C8–C7–H7B	111.0
H7A–C7–H7B	109.0
C22–C23–C24	120.5(3)
C22–C23–H23	119.7
C24–C23–H23	119.7
C23–C24–C19	120.4(3)
C23–C24–H24	119.8
C19–C24–H24	119.8
C16–C17–C18	120.8(3)
C16–C17–H17	119.6
C18–C17–H17	119.6
N1–C6–C1	109.7(2)
N1–C6–C5	110.9(2)

C1–C6–C5	110.0(2)
N1–C6–H6	108.7
C1–C6–H6	108.7
C5–C6–H6	108.7
C15–C14–C13	120.0(3)
C15–C14–H14	120.0
C13–C14–H14	120.0
C4–C5–C6	111.7(2)
C4–C5–H5A	109.3
C6–C5–H5A	109.3
C4–C5–H5B	109.3
C6–C5–H5B	109.3
H5A–C5–H5B	107.9
C22–C21–C20	120.8(3)
C22–C21–H21	119.6
C20–C21–H21	119.6
C6–C1–C2	111.9(3)
C6–C1–H1A	109.2
C2–C1–H1A	109.2
C6–C1–H1B	109.2
C2–C1–H1B	109.2
H1A–C1–H1B	107.9
C15–C16–C17	119.3(3)
C15–C16–H16	120.3
C17–C16–H16	120.3
C16–C15–C14	120.8(3)
C16–C15–H15	119.6
C14–C15–H15	119.6
C3–C4–C5	110.9(3)
C3–C4–H4A	109.5
C5–C4–H4A	109.5
C3–C4–H4B	109.5
C5–C4–H4B	109.5
H4A–C4–H4B	108.0
C4–C3–C2	110.4(3)
C4–C3–H3A	109.6
C2–C3–H3A	109.6
C4–C3–H3B	109.6
C2–C3–H3B	109.6
H3A–C3–H3B	108.1
C3–C2–C1	111.5(3)
C3–C2–H2A	109.3
C1–C2–H2A	109.3
C3–C2–H2B	109.3
C1–C2–H2B	109.3
H2A–C2–H2B	108.0

Symmetry transformations used to generate equivalent atoms:

Table 4. Anisotropic displacement parameters [Å²× 10³]. The anisotropic displacement factor exponent takes the form: $-2\pi^2[h^2a^{*2}U^{11} + \cdots + 2\,h\,k\,a^*\,b^*\,U^{12}]$.

Atom	U^{11}	U^{22}	U^{33}	U^{23}	U^{13}	U^{12}
O1	41(1)	45(1)	36(1)	–11(1)	12(1)	–13(1)
N2	28(1)	28(1)	29(1)	–1(1)	9(1)	–3(1)
N1	27(1)	24(1)	32(1)	2(1)	10(1)	2(1)
N4	28(1)	36(1)	28(1)	0(1)	7(1)	–4(1)
N3	33(1)	32(1)	29(1)	–2(1)	10(1)	–6(1)
C12	27(1)	25(1)	30(1)	3(1)	9(1)	0(1)
C11	30(1)	26(1)	33(1)	–1(1)	6(1)	–2(1)
C10	25(1)	23(1)	35(1)	0(1)	7(1)	–1(1)
C19	24(1)	31(1)	30(1)	1(1)	5(1)	–6(1)
C13	30(1)	29(1)	30(1)	7(1)	9(1)	5(1)
C18	29(1)	30(1)	34(1)	5(1)	7(1)	2(1)
C20	38(1)	31(1)	32(1)	4(1)	5(1)	2(1)
C8	33(1)	29(1)	45(2)	–2(1)	9(1)	6(1)
C9	31(1)	32(1)	40(2)	1(1)	2(1)	2(1)
C22	39(1)	39(2)	27(1)	–1(1)	7(1)	–3(1)
C7	32(1)	34(1)	40(2)	–1(1)	13(1)	7(1)
C23	29(1)	46(2)	32(1)	7(1)	3(1)	1(1)
C24	26(1)	41(2)	35(2)	1(1)	6(1)	1(1)
C17	27(1)	46(2)	39(2)	9(1)	6(1)	–5(1)
C6	28(1)	28(1)	38(2)	8(1)	12(1)	1(1)
C14	50(2)	31(1)	36(2)	1(1)	17(1)	1(1)
C5	36(1)	29(1)	46(2)	9(1)	14(1)	6(1)
C21	45(2)	32(1)	36(2)	–3(1)	11(1)	5(1)
C1	40(2)	45(2)	36(2)	6(1)	12(1)	4(1)
C16	36(2)	58(2)	39(2)	14(2)	16(1)	5(2)
C15	56(2)	44(2)	34(2)	4(1)	22(1)	6(2)
C4	40(2)	34(2)	67(2)	22(2)	20(2)	9(1)
C3	38(2)	58(2)	58(2)	31(2)	15(2)	12(2)
C2	48(2)	65(2)	43(2)	19(2)	14(2)	10(2)

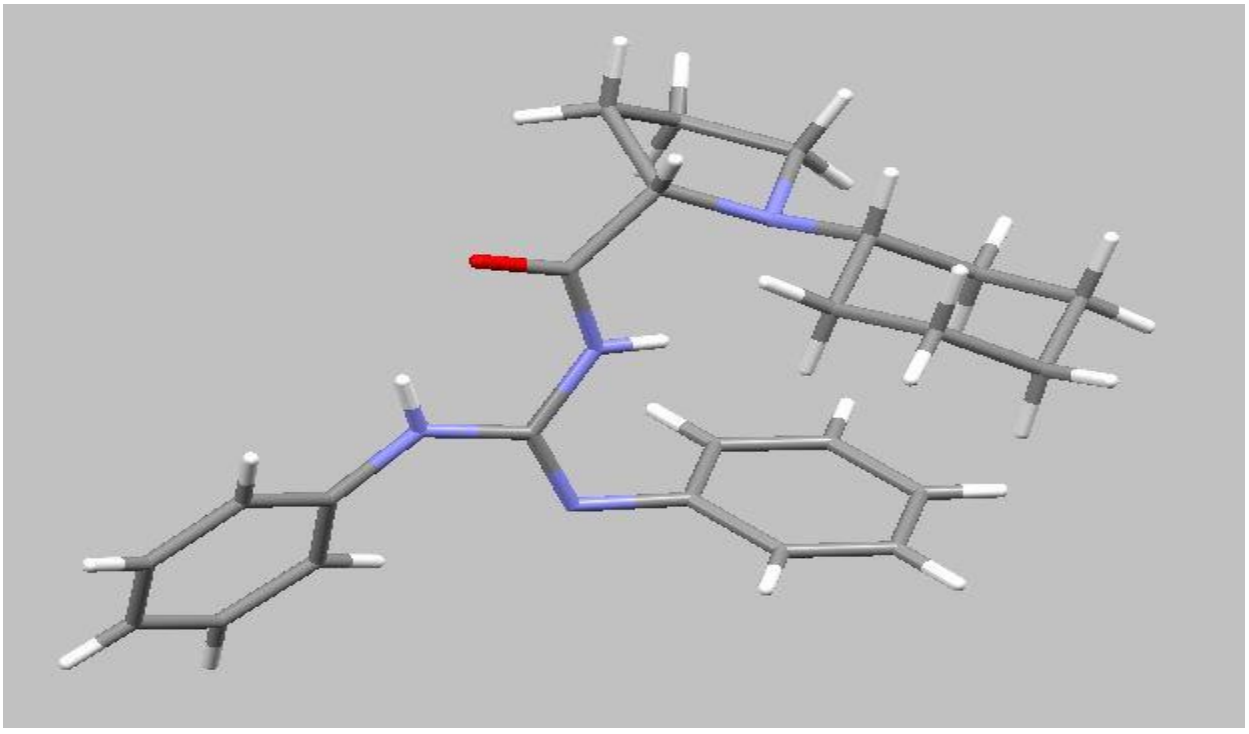

Appendix 6

X-ray of compound 127

UK National Crystallography Service

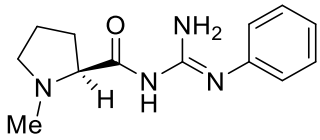

Table 1. Crystal data and structure refinement details.

Identification code	**2017NCS0244**	
Empirical formula	$C_{13}H_{18}N_4O$	
Formula weight	246.31	
Temperature	100(2) K	
Wavelength	0.6889 Å	
Crystal system	Orthorhombic	
Space group	*P*212121	
Unit cell dimensions	a = 7.98857(9) Å	α = **90°**
	b = **11.71525(11) Å**	β = **90°**
	c = **13.99640(13) Å**	γ = **90°**
Volume	**1309.91(2) Å^3**	
Z	4	
Density (calculated)	1.249 Mg / m^3	
Absorption coefficient	0.083 mm^{-1}	
F(000)	528	
Crystal	Plate; colourless	
Crystal size	0.050 × 0.020 × 0.015 mm^3	
θ range for data collection	2.821 – 36.098°	
Index ranges	$-13 \le h \le 13$, $-19 \le k \le 19$, $-22 \le l \le 23$	
Reflections collected	28908	
Independent reflections	6422 [R_{int} = 0.0444]	
Completeness to θ = 24.415°	99.9 %	
Absorption correction	Empirical	
Max. and min. transmission	1.0 and 0.993	
Refinement method	Full-matrix least-squares on F^2	
Data / restraints / parameters	6422 / 0 / 176	
Goodness-of-fit on F^2	1.071	
Final *R* indices [$F^2 > 2\sigma(F^2)$]	*R1* = 0.0474, *wR2* = 0.1203	
R indices (all data)	*R1* = 0.0521, *wR2* = 0.1235	
Absolute structure parameter	0.3(4)	
Extinction coefficient	n/a	
Largest diff. peak and hole	0.528 and –0.237 e Å^{-3}	

Diffractometer: Beamline i19, Diamond Light Source Ltd. 3-circle fixed chi goniometer equipped with a PILATUS 2M PIXEL detector, wavelength 0.6998A (100µm focus). **Data collection:** GDA http://www.opengda.org/OpenGDA.html **Cell determination, Data reduction and cell refinement & Absorption correction**: XIA2 0.5.53 Winter, G. (2010) Journal of Applied Crystallography 43, **Structure solution**: SHELXT (G. M. Sheldrick *Acta Cryst.* (2015). A**71**, 3-8). S**tructure refinement**: SHELXL97 (G. M. Sheldrick (1997), University of Göttingen, Germany).

Special details:

Table 2. Atomic coordinates [× 10^4], equivalent isotropic displacement parameters [$Å^2$ × 10^3] and site occupancy factors. U_{eq} is defined as one third of the trace of the orthogonalized U^{ij} tensor.

Atom	*x*	*y*	*z*	U_{eq}	*S.o.f.*
O1	6111(1)	4260(1)	2164(1)	23(1)	1
N3	4816(1)	2181(1)	2245(1)	22(1)	1
N2	7002(1)	2877(1)	3254(1)	20(1)	1
N4	5770(1)	1112(1)	3490(1)	21(1)	1
N1	8292(1)	5862(1)	2911(1)	23(1)	1
C7	5866(1)	2096(1)	2989(1)	18(1)	1
C6	6995(1)	3921(1)	2847(1)	19(1)	1
C8	6662(1)	843(1)	4333(1)	20(1)	1
C13	7249(2)	–272(1)	4432(1)	23(1)	1
C5	8226(1)	4720(1)	3336(1)	21(1)	1
C12	8039(2)	–609(1)	5273(1)	27(1)	1
C9	6873(2)	1621(1)	5075(1)	23(1)	1
C11	8254(2)	166(1)	6013(1)	28(1)	1
C4	7774(2)	4929(1)	4401(1)	25(1)	1
C2	9032(2)	6585(1)	3662(1)	29(1)	1
C10	7679(2)	1280(1)	5907(1)	26(1)	1
C1	9276(2)	5891(1)	2026(1)	32(1)	1
C3	8110(2)	6212(1)	4560(1)	31(1)	1

Table 3. Bond lengths [Å] and angles [°].

O1–C6	1.2528(12)
N3–C7	1.3403(13)
N3–H1	0.792(19)
N3–H2	0.87(2)
N2–C7	1.3415(13)
N2–C6	1.3482(13)
N4–C7	1.3518(13)
N4–C8	1.4134(13)
N4–H3	0.94(2)
N1–C5	1.4659(13)
N1–C1	1.4672(16)
N1–C2	1.4728(15)
C6–C5	1.5202(15)
C8–C9	1.3916(14)
C8–C13	1.3949(15)
C13–C12	1.3925(16)
C13–H13	0.9500
C5–C4	1.5525(16)
C5–H5	1.0000
C12–C11	1.3885(19)
C12–H12	0.9500
C9–C10	1.3906(15)
C9–H9	0.9500

C11–C10	1.3905(19)
C11–H11	0.9500
C4–C3	1.5424(17)
C4–H4A	0.9900
C4–H4B	0.9900
C2–C3	1.521(2)
C2–H2A	0.9900
C2–H2B	0.9900
C10–H10	0.9500
C1–H1A	0.9800
C1–H1B	0.9800
C1–H1C	0.9800
C3–H3A	0.9900
C3–H3B	0.9900

C7–N3–H1	113.7(13)
C7–N3–H2	117.0(13)
H1–N3–H2	126.0(17)
C7–N2–C6	119.95(9)
C7–N4–C8	126.47(9)
C7–N4–H3	118.0(13)
C8–N4–H3	115.3(13)
C5–N1–C1	112.47(9)
C5–N1–C2	104.44(9)
C1–N1–C2	111.96(10)
N3–C7–N2	125.97(10)
N3–C7–N4	115.53(9)
N2–C7–N4	118.47(9)
O1–C6–N2	127.69(10)
O1–C6–C5	120.87(9)
N2–C6–C5	111.43(9)
C9–C8–C13	119.88(10)
C9–C8–N4	122.53(10)
C13–C8–N4	117.46(9)
C12–C13–C8	120.17(10)
C12–C13–H13	119.9
C8–C13–H13	119.9
N1–C5–C6	113.74(9)
N1–C5–C4	104.67(9)
C6–C5–C4	112.28(9)
N1–C5–H5	108.7
C6–C5–H5	108.7
C4–C5–H5	108.7
C11–C12–C13	120.03(11)
C11–C12–H12	120.0
C13–C12–H12	120.0
C10–C9–C8	119.53(11)
C10–C9–H9	120.2
C8–C9–H9	120.2
C12–C11–C10	119.59(11)
C12–C11–H11	120.2
C10–C11–H11	120.2
C3–C4–C5	104.64(10)
C3–C4–H4A	110.8
C5–C4–H4A	110.8
C3–C4–H4B	110.8
C5–C4–H4B	110.8
H4A–C4–H4B	108.9
N1–C2–C3	103.33(10)

N1–C2–H2A	111.1
C3–C2–H2A	111.1
N1–C2–H2B	111.1
C3–C2–H2B	111.1
H2A–C2–H2B	109.1
C9–C10–C11	120.79(11)
C9–C10–H10	119.6
C11–C10–H10	119.6
N1–C1–H1A	109.5
N1–C1–H1B	109.5
H1A–C1–H1B	109.5
N1–C1–H1C	109.5
H1A–C1–H1C	109.5
H1B–C1–H1C	109.5
C2–C3–C4	104.13(10)
C2–C3–H3A	110.9
C4–C3–H3A	110.9
C2–C3–H3B	110.9
C4–C3–H3B	110.9
H3A–C3–H3B	108.9

Symmetry transformations used to generate equivalent atoms:

Table 4. Anisotropic displacement parameters [Å^2× 10^3]. The anisotropic displacement factor exponent takes the form: $-2\pi^2[h^2a^{*2}U^{11} + \cdots + 2\,h\,k\,a^*\,b^*\,U^{12}]$.

Atom	U^{11}	U^{22}	U^{33}	U^{23}	U^{13}	U^{12}
O1	27(1)	21(1)	22(1)	2(1)	–7(1)	1(1)
N3	24(1)	21(1)	20(1)	–1(1)	–5(1)	0(1)
N2	21(1)	17(1)	20(1)	1(1)	–3(1)	0(1)
N4	26(1)	19(1)	19(1)	0(1)	–5(1)	–2(1)
N1	22(1)	19(1)	27(1)	2(1)	–3(1)	–1(1)
C7	20(1)	18(1)	17(1)	–2(1)	–1(1)	2(1)
C6	19(1)	19(1)	19(1)	0(1)	–1(1)	1(1)
C8	21(1)	20(1)	18(1)	1(1)	–2(1)	–2(1)
C13	24(1)	20(1)	25(1)	1(1)	–2(1)	–1(1)
C5	19(1)	19(1)	24(1)	1(1)	–4(1)	1(1)
C12	25(1)	26(1)	31(1)	6(1)	–5(1)	0(1)
C9	29(1)	22(1)	19(1)	–1(1)	–4(1)	–2(1)
C11	26(1)	33(1)	25(1)	8(1)	–6(1)	–6(1)
C4	28(1)	27(1)	21(1)	–2(1)	–5(1)	–1(1)
C2	28(1)	21(1)	39(1)	–2(1)	–11(1)	–2(1)
C10	29(1)	30(1)	20(1)	1(1)	–5(1)	–6(1)
C1	32(1)	31(1)	34(1)	6(1)	6(1)	–2(1)
C3	37(1)	26(1)	30(1)	–6(1)	–11(1)	4(1)

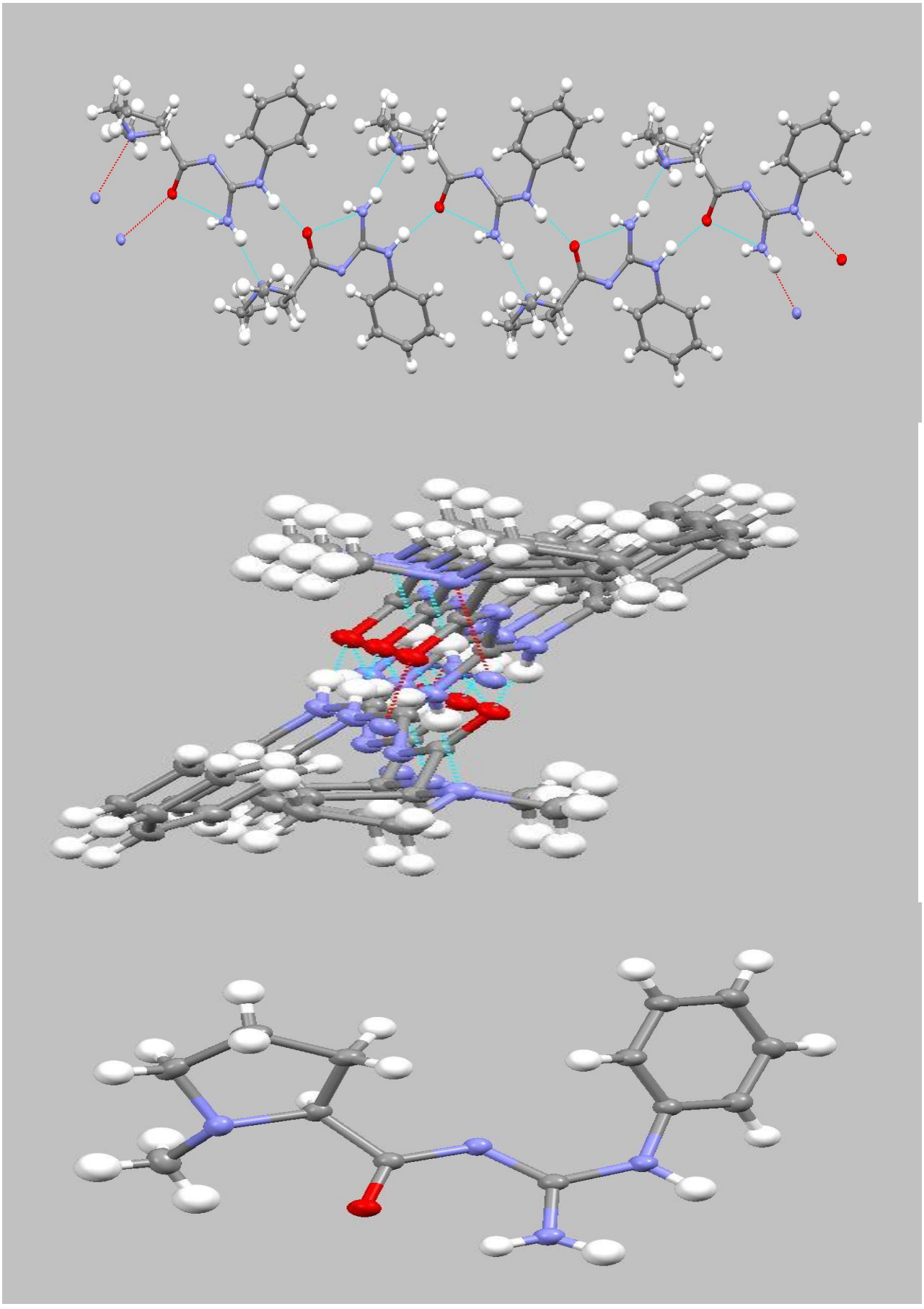

Appendix 7
X-ray of compound 139

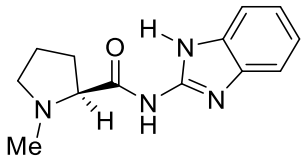

UK National Crystallography Service

Table 1. Crystal data and structure refinement details.

Identification code	**2017ncs0159**	
Empirical formula	$C_{13}H_{16}N_4O$	
Formula weight	244.30	
Temperature	100(2) K	
Wavelength	1.54184 Å	
Crystal system	Monoclinic	
Space group	*P*21	
Unit cell dimensions	a = 9.8292(2) Å	α = **90°**
	b = **12.6358(4) Å**	β = **94.835(2)°**
	c = 10**.1195(2) Å**	γ = **90°**
Volume	**1252.37(5) Å**^{3}	
Z	4	
Density (calculated)	1.296 Mg / m^3	
Absorption coefficient	0.695 mm^{-1}	
F(000)	520	
Crystal	Plate; clear colourless	
Crystal size	0.045 × 0.035 × 0.008 mm^3	
θ range for data collection	4.515 – 70.486°	
Index ranges	$-11 \le h \le 11$, $-14 \le k \le 15$, $-12 \le l \le 12$	
Reflections collected	11865	
Independent reflections	4184 [R_{int} = 0.0523]	
Completeness to θ = 67.684°	98.7 %	
Absorption correction	Semi–empirical from equivalents	
Max. and min. transmission	1.00000 and 0.87199	
Refinement method	Full-matrix least-squares on F^2	
Data / restraints / parameters	4184 / 1 / 343	
Goodness-of-fit on F^2	1.033	
Final *R* indices [$F^2 > 2\sigma(F^2)$]	*R1* = 0.0451, *wR2* = 0.1169	
R indices (all data)	*R1* = 0.0502, *wR2* = 0.1207	
Absolute structure parameter	–0.02(19)	
Extinction coefficient	n/a	
Largest diff. peak and hole	0.353 and –0.217 e Å^{-3}	

Diffractometer: Rigaku AFC11 quarter chi goniometer equipped with a HyPix6000 hybrid pixel detector mounted at the window of 007 HF copper rotating anode generator with Varimax optics. **Cell determination, Data collection, Data reduction and cell refinement & Absorption correction**: CrysAlisPro (Rigaku Oxford Diffraction, 2017) , **Structure solution**: SHELXT (G. M. Sheldrick, Acta Cryst. (1990) A**46** 467–473). **Structure refinement**: SHELXL97 (G. M. Sheldrick (1997), University of Göttingen, Germany).

Special details:

There is disorder in the orientation of the proline 5-membered ring as indicated by the larger thermal parameters. The disorder is not pronounced enough to make a reasonable model of it.**Table 2.** Atomic coordinates [× 10^4], equivalent isotropic displacement parameters [$Å^2$ × 10^3] and site occupancy factors. U_{eq} is defined as one third of the trace of the orthogonalized U^{ij} tensor.

Atom	*x*	*y*	*z*	U_{eq}	*S.o.f.*
O1	5652(2)	4608(2)	7731(2)	40(1)	1
N4	8204(3)	5156(3)	11123(2)	31(1)	1
N6	6396(3)	5714(3)	5132(3)	34(1)	1
N3	8190(3)	5202(3)	8898(3)	31(1)	1
N7	8173(3)	4909(2)	3963(3)	30(1)	1
N8	8231(3)	4735(2)	6171(2)	31(1)	1
N1	4248(3)	3050(3)	10296(3)	37(1)	1
O2	6075(3)	6211(3)	2978(2)	60(1)	1
N2	6404(3)	4267(3)	9886(3)	32(1)	1
C8	9296(3)	5798(3)	9381(3)	30(1)	1
C7	7585(3)	4863(3)	9987(3)	30(1)	1
C13	9296(3)	5765(3)	10772(3)	31(1)	1
C12	10271(4)	6332(3)	11559(3)	37(1)	1
C22	10196(3)	3726(3)	3594(3)	36(1)	1
C6	5473(3)	4218(3)	8800(3)	32(1)	1
C9	10238(3)	6394(3)	8744(3)	35(1)	1
C20	7588(3)	5145(3)	5092(3)	30(1)	1
N5	3866(3)	6326(3)	5599(3)	54(1)	1
C21	9268(3)	4264(3)	4326(3)	31(1)	1
C11	11204(4)	6938(3)	10930(4)	41(1)	1
C10	11180(4)	6965(3)	9542(3)	39(1)	1
C26	9300(3)	4156(3)	5712(3)	30(1)	1
C23	11135(3)	3075(3)	4296(4)	39(1)	1
C5	4149(3)	3660(3)	9051(3)	37(1)	1
C24	11166(4)	2975(3)	5672(4)	39(1)	1
C25	10257(3)	3515(3)	6394(3)	34(1)	1
C1	4723(4)	1977(3)	10141(4)	47(1)	1
C19	5677(4)	6191(4)	4090(3)	40(1)	1
C4	3004(4)	4470(4)	9185(4)	50(1)	1
C18	4398(4)	6753(4)	4426(4)	45(1)	1
C15	3363(6)	7186(5)	6356(5)	70(2)	1
C2	2868(4)	3096(5)	10745(5)	63(1)	1
C17	4717(5)	7950(4)	4828(5)	57(1)	1
C16	4488(5)	8018(5)	6247(5)	68(1)	1
C3	2430(6)	4204(6)	10497(6)	91(2)	1
C14	2834(6)	5506(5)	5311(7)	87(2)	1

Table 3. Bond lengths [Å] and angles [°].

O1–C6	1.215(4)
N4–C7	1.308(4)
N4–C13	1.391(4)
N6–C19	1.359(5)
N6–C20	1.378(4)
N6–H3	0.82(4)
N3–C7	1.364(4)
N3–C8	1.378(5)
N3–H1	0.86(4)
N7–C20	1.355(4)

N7–C21	1.376(4)
N7–H2	0.84(5)
N8–C20	1.321(4)
N8–C26	1.392(4)
N1–C1	1.446(5)
N1–C2	1.468(5)
N1–C5	1.473(5)
O2–C19	1.223(4)
N2–C6	1.371(4)
N2–C7	1.381(5)
N2–H4	0.76(4)
C8–C9	1.393(5)
C8–C13	1.408(4)
C13–C12	1.392(5)
C12–C11	1.389(5)
C12–H12	0.9500
C22–C23	1.388(5)
C22–C21	1.399(5)
C22–H22	0.9500
C6–C5	1.520(5)
C9–C10	1.380(5)
C9–H9	0.9500
N5–C18	1.441(5)
N5–C15	1.441(6)
N5–C14	1.463(7)
C21–C26	1.406(4)
C11–C10	1.403(5)
C11–H11	0.9500
C10–H10	0.9500
C26–C25	1.381(5)
C23–C24	1.396(5)
C23–H23	0.9500
C5–C4	1.537(5)
C5–H5	1.0000
C24–C25	1.382(5)
C24–H24	0.9500
C25–H25	0.9500
C1–H1A	0.9800
C1–H1B	0.9800
C1–H1C	0.9800
C19–C18	1.508(5)
C4–C3	1.524(6)
C4–H4A	0.9900
C4–H4B	0.9900
C18–C17	1.590(7)
C18–H18	1.0000
C15–C16	1.537(8)
C15–H15A	0.9900
C15–H15B	0.9900
C2–C3	1.479(8)
C2–H2A	0.9900
C2–H2B	0.9900
C17–C16	1.475(6)
C17–H17A	0.9900
C17–H17B	0.9900
C16–H16A	0.9900
C16–H16B	0.9900
C3–H3A	0.9900
C3–H3B	0.9900

C14–H14A	0.9800
C14–H14B	0.9800
C14–H14C	0.9800

C7–N4–C13	104.1(3)
C19–N6–C20	126.6(3)
C19–N6–H3	122(3)
C20–N6–H3	110(3)
C7–N3–C8	105.6(3)
C7–N3–H1	129(3)
C8–N3–H1	125(2)
C20–N7–C21	106.4(3)
C20–N7–H2	126(3)
C21–N7–H2	128(3)
C20–N8–C26	104.6(3)
C1–N1–C2	112.7(4)
C1–N1–C5	113.3(3)
C2–N1–C5	104.4(3)
C6–N2–C7	125.8(3)
C6–N2–H4	110(3)
C7–N2–H4	122(3)
N3–C8–C9	131.9(3)
N3–C8–C13	105.8(3)
C9–C8–C13	122.3(3)
N4–C7–N3	114.8(3)
N4–C7–N2	123.1(3)
N3–C7–N2	122.1(3)
N4–C13–C12	130.4(3)
N4–C13–C8	109.6(3)
C12–C13–C8	119.9(3)
C11–C12–C13	118.1(3)
C11–C12–H12	121.0
C13–C12–H12	121.0
C23–C22–C21	116.9(3)
C23–C22–H22	121.6
C21–C22–H22	121.6
O1–C6–N2	123.9(3)
O1–C6–C5	121.9(3)
N2–C6–C5	114.2(3)
C10–C9–C8	116.8(3)
C10–C9–H9	121.6
C8–C9–H9	121.6
N8–C20–N7	113.8(3)
N8–C20–N6	121.9(3)
N7–C20–N6	124.2(3)
C18–N5–C15	108.7(4)
C18–N5–C14	113.2(4)
C15–N5–C14	112.1(4)
N7–C21–C22	132.6(3)
N7–C21–C26	106.0(3)
C22–C21–C26	121.4(3)
C12–C11–C10	121.1(3)
C12–C11–H11	119.5
C10–C11–H11	119.5
C9–C10–C11	121.8(3)
C9–C10–H10	119.1
C11–C10–H10	119.1
C25–C26–N8	130.0(3)
C25–C26–C21	120.8(3)

N8–C26–C21	109.1(3)
C22–C23–C24	121.5(3)
C22–C23–H23	119.3
C24–C23–H23	119.3
N1–C5–C6	113.0(3)
N1–C5–C4	105.6(3)
C6–C5–C4	110.4(3)
N1–C5–H5	109.2
C6–C5–H5	109.2
C4–C5–H5	109.2
C25–C24–C23	121.5(3)
C25–C24–H24	119.3
C23–C24–H24	119.3
C26–C25–C24	118.0(3)
C26–C25–H25	121.0
C24–C25–H25	121.0
N1–C1–H1A	109.5
N1–C1–H1B	109.5
H1A–C1–H1B	109.5
N1–C1–H1C	109.5
H1A–C1–H1C	109.5
H1B–C1–H1C	109.5
O2–C19–N6	122.5(3)
O2–C19–C18	122.4(3)
N6–C19–C18	115.0(3)
C3–C4–C5	104.9(3)
C3–C4–H4A	110.8
C5–C4–H4A	110.8
C3–C4–H4B	110.8
C5–C4–H4B	110.8
H4A–C4–H4B	108.8
N5–C18–C19	112.1(3)
N5–C18–C17	102.9(3)
C19–C18–C17	110.8(3)
N5–C18–H18	110.3
C19–C18–H18	110.3
C17–C18–H18	110.3
N5–C15–C16	101.3(4)
N5–C15–H15A	111.5
C16–C15–H15A	111.5
N5–C15–H15B	111.5
C16–C15–H15B	111.5
H15A–C15–H15B	109.3
N1–C2–C3	104.4(4)
N1–C2–H2A	110.9
C3–C2–H2A	110.9
N1–C2–H2B	110.9
C3–C2–H2B	110.9
H2A–C2–H2B	108.9
C16–C17–C18	105.2(4)
C16–C17–H17A	110.7
C18–C17–H17A	110.7
C16–C17–H17B	110.7
C18–C17–H17B	110.7
H17A–C17–H17B	108.8
C17–C16–C15	101.5(4)
C17–C16–H16A	111.5
C15–C16–H16A	111.5
C17–C16–H16B	111.5

C15–C16–H16B	111.5
H16A–C16–H16B	109.3
C2–C3–C4	103.5(4)
C2–C3–H3A	111.1
C4–C3–H3A	111.1
C2–C3–H3B	111.1
C4–C3–H3B	111.1
H3A–C3–H3B	109.0
N5–C14–H14A	109.5
N5–C14–H14B	109.5
H14A–C14–H14B	109.5
N5–C14–H14C	109.5
H14A–C14–H14C	109.5
H14B–C14–H14C	109.5

Symmetry transformations used to generate equivalent atoms:

Table 4. Anisotropic displacement parameters [Å^2× 10^3]. The anisotropic displacement factor exponent takes the form: $-2\pi^2[h^2a^{*2}U^{11} + \cdots + 2\,h\,k\,a^*\,b^*\,U^{12}]$.

Atom	U^{11}	U^{22}	U^{33}	U^{23}	U^{13}	U^{12}
O1	36(1)	57(2)	27(1)	4(1)	5(1)	–4(1)
N4	31(1)	39(2)	26(1)	–2(1)	6(1)	0(1)
N6	31(1)	46(2)	26(1)	5(1)	10(1)	6(1)
N3	31(1)	40(2)	22(1)	1(1)	7(1)	–2(1)
N7	29(1)	39(2)	23(1)	1(1)	6(1)	0(1)
N8	29(1)	41(2)	25(1)	1(1)	7(1)	1(1)
N1	36(2)	38(2)	39(2)	0(1)	11(1)	0(1)
O2	59(2)	90(2)	31(1)	13(2)	14(1)	28(2)
N2	32(2)	39(2)	26(1)	3(1)	7(1)	–1(1)
C8	27(2)	35(2)	27(2)	–1(1)	6(1)	3(1)
C7	31(2)	34(2)	24(2)	0(1)	8(1)	5(1)
C13	31(2)	35(2)	29(2)	0(1)	7(1)	4(2)
C12	37(2)	46(2)	28(2)	–4(2)	7(1)	–1(2)
C22	33(2)	48(2)	29(2)	–1(2)	9(1)	–2(2)
C6	31(2)	37(2)	29(2)	–2(1)	7(1)	4(1)
C9	32(2)	45(2)	30(2)	5(2)	10(1)	3(2)
C20	31(2)	34(2)	27(2)	0(1)	7(1)	–1(1)
N5	47(2)	67(3)	52(2)	17(2)	20(2)	18(2)
C21	28(2)	40(2)	26(2)	0(1)	7(1)	–4(2)
C11	36(2)	47(2)	39(2)	–5(2)	4(1)	–6(2)
C10	34(2)	46(2)	39(2)	0(2)	12(1)	–6(2)
C26	27(2)	38(2)	27(2)	–2(1)	7(1)	–1(1)
C23	33(2)	44(2)	41(2)	–7(2)	13(1)	1(2)
C5	35(2)	41(2)	35(2)	1(2)	5(1)	–7(2)
C24	36(2)	41(2)	41(2)	6(2)	8(2)	8(2)
C25	32(2)	41(2)	31(2)	1(2)	6(1)	0(2)
C1	51(2)	44(3)	46(2)	2(2)	4(2)	1(2)
C19	38(2)	48(2)	32(2)	5(2)	5(1)	3(2)
C4	32(2)	52(3)	68(3)	9(2)	5(2)	–4(2)
C18	38(2)	62(3)	34(2)	10(2)	7(2)	13(2)
C15	72(3)	90(4)	53(2)	22(2)	30(2)	46(3)
C2	47(2)	86(4)	58(3)	24(3)	28(2)	12(2)
C17	54(3)	50(3)	69(3)	10(2)	16(2)	9(2)
C16	74(3)	66(3)	62(3)	–3(3)	0(2)	22(3)
C3	86(4)	111(5)	82(4)	22(4)	36(3)	55(4)

C14	50(3)	76(4)	135(5)	31(4)	4(3)	–18(3)

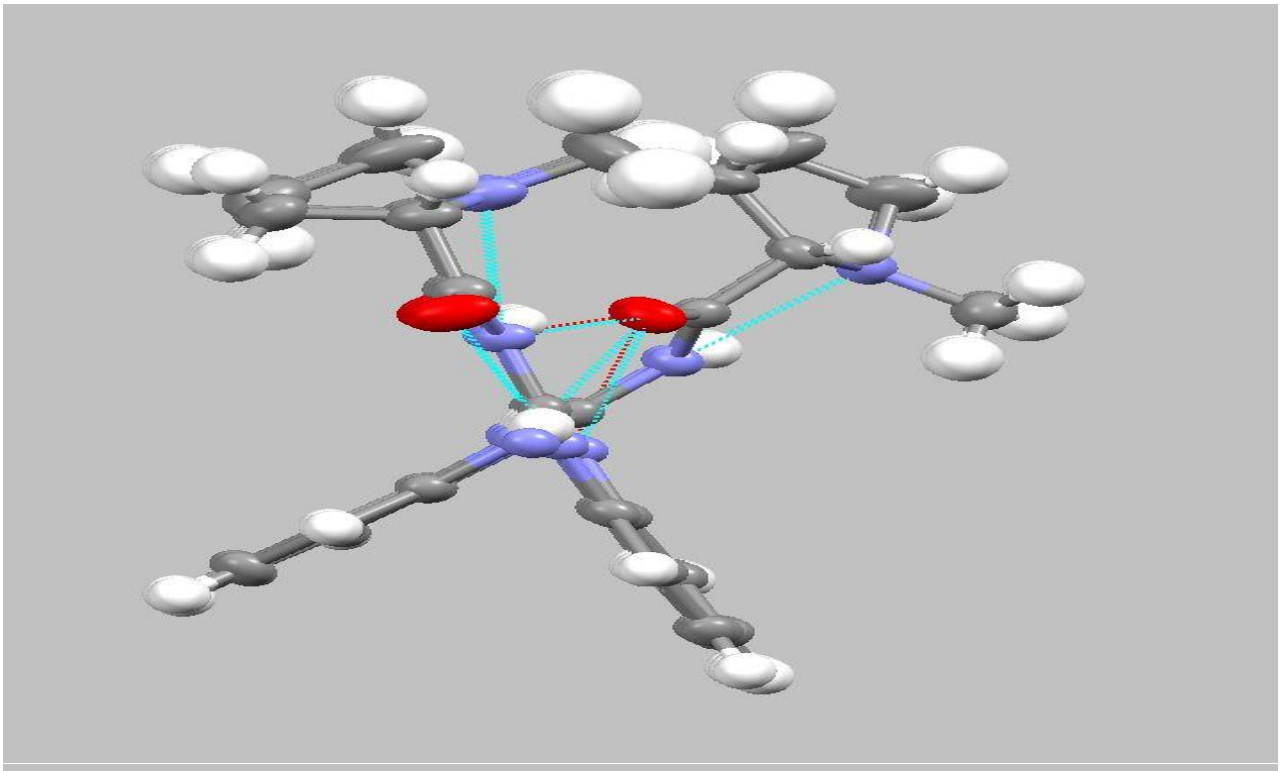

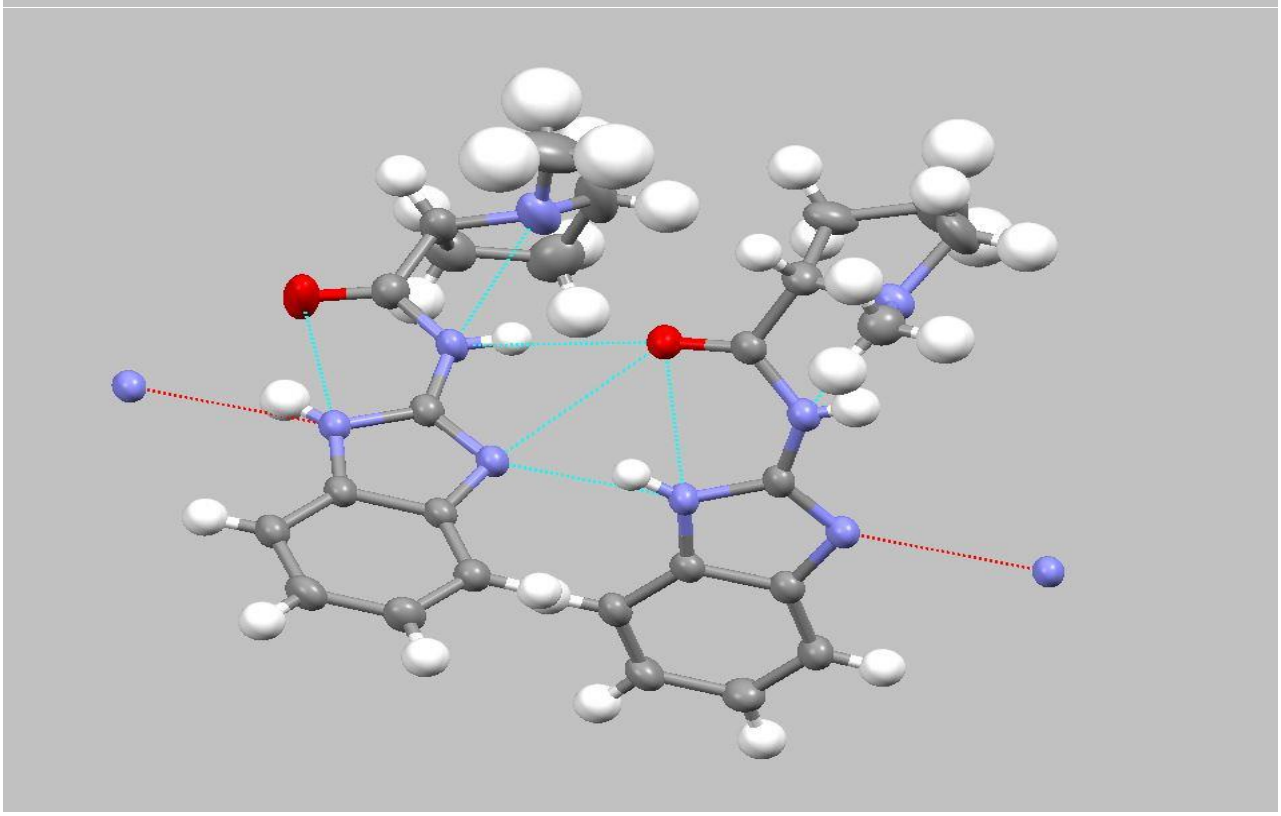

Appendix 8
X-ray of compound 140

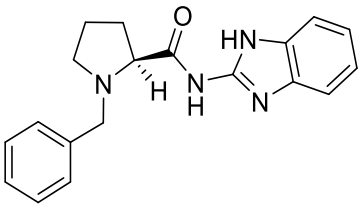

UK National Crystallography Service

Table 1. Crystal data and structure refinement details.

Identification code	**2016ncs0749**	
Empirical formula	$C_{19}H_{20}N_4O$	
Formula weight	320.39	
Temperature	100(2) K	
Wavelength	0.6889 Å	
Crystal system	Hexagonal	
Space group	*P*65	
Unit cell dimensions	a = 9.8466(4) Å	α = **90°**
	b = **9.8466(4) Å**	β = **90°**
	c = **29.7164(12) Å**	γ = **120°**
Volume	**2495.2(2) Å^3**	
Z	6	
Density (calculated)	1.279 Mg / m^3	
Absorption coefficient	0.082 mm^{-1}	
F(000)	1020	
Crystal	Needle; colourless	
Crystal size	0.170 × 0.018 × 0.018 mm^3	
θ range for data collection	2.315 – 26.563°	
Index ranges	$-12 \le h \le 12$, $-12 \le k \le 12$, $-38 \le l \le 38$	
Reflections collected	25029	
Independent reflections	3740 [R_{int} = 0.1031]	
Completeness to θ = 24.415°	99.8 %	
Absorption correction	Empirical	
Max. and min. transmission	1.0 and 0.997	
Refinement method	Full-matrix least-squares on F^2	
Data / restraints / parameters	3740 / 7 / 221	
Goodness-of-fit on F^2	0.948	
Final *R* indices [$F^2 > 2\sigma(F^2)$]	*R1* = 0.0650, *wR2* = 0.1651	
R indices (all data)	*R1* = 0.1011, *wR2* = 0.1916	
Absolute structure parameter	?	
Extinction coefficient	0.014(4)	
Largest diff. peak and hole	0.212 and –0.229 e Å^{-3}	

Diffractometer: Beamline i19, Diamond Light Source Ltd. 3-circle fixed chi goniometer equipped with a PILATUS 2M PIXEL detector, wavelength 0.6998A (100µm focus). **Data collection:** GDA http://www.opengda.org/OpenGDA.html **Cell determination, Data reduction and cell refinement & Absorption correction**: XIA2 0.5.53 Winter, G. (2010) Journal of Applied Crystallography 43, **Structure solution**: SHELXT (G. M. Sheldrick *Acta Cryst.* (2015). A**71**, 3-8). S**tructure refinement**: SHELXL97 (G. M. Sheldrick (1997), University of Göttingen, Germany).

Special details:

Table 2. Atomic coordinates [× 10^4], equivalent isotropic displacement parameters [$Å^2$ × 10^3] and site occupancy factors. U_{eq} is defined as one third of the trace of the orthogonalized U^{ij} tensor.

Atom	*x*	*y*	*z*	U_{eq}	*S.o.f.*
O1	8405(4)	8240(4)	6277(1)	69(1)	1
N4	10036(5)	11145(4)	5158(1)	54(1)	1
N2	8955(5)	8681(5)	5529(1)	56(1)	1
N3	10437(5)	11186(5)	5905(1)	54(1)	1
N1	7032(5)	5681(5)	5303(1)	61(1)	1
C13	9812(5)	10317(6)	5529(2)	54(1)	1
C19	10878(5)	12700(5)	5306(1)	53(1)	1
C18	11397(7)	14092(6)	5068(2)	62(1)	1
C14	11126(5)	12740(5)	5770(1)	52(1)	1
C12	8244(5)	7762(6)	5892(2)	57(1)	1
C16	12423(6)	15512(6)	5766(2)	65(1)	1
C15	11914(5)	14138(5)	6013(2)	58(1)	1
C17	12158(7)	15467(6)	5309(2)	69(1)	1
C3	4703(7)	4818(8)	3726(2)	82(2)	1
C5	3994(7)	3636(7)	4459(2)	79(2)	1
C11	7270(7)	6008(7)	5785(2)	69(1)	1
C4	3746(7)	3570(8)	3991(2)	80(2)	1
C8	7621(7)	4604(7)	5195(2)	77(2)	1
C1	6161(8)	6184(8)	4380(2)	94(2)	1
C7	5403(7)	5091(9)	5160(2)	85(2)	1
C6	5206(7)	4967(8)	4658(2)	76(2)	1
C2	5940(8)	6128(8)	3921(2)	97(2)	1
C10A	8565(15)	5449(13)	5952(4)	60(2)	0.454(7)
C9	8733(11)	4926(12)	5568(3)	68(2)	0.546(7)
C9A	7878(15)	3952(14)	5685(4)	68(2)	0.454(7)
C10	7702(12)	4920(12)	5958(3)	60(2)	0.546(7)

Table 3. Bond lengths [Å] and angles [°].

O1–C12	1.217(5)
N4–C13	1.322(6)
N4–C19	1.398(6)
N2–C12	1.356(6)
N2–C13	1.395(6)
N2–H20	0.88(6)
N3–C13	1.353(6)
N3–C14	1.386(6)
N3–H19	0.88(6)
N1–C11	1.460(6)
N1–C7	1.470(7)
N1–C8	1.477(7)
C19–C18	1.392(6)
C19–C14	1.399(5)
C18–C17	1.377(7)
C18–H18	0.9500
C14–C15	1.396(6)
C12–C11	1.533(8)
C16–C17	1.380(6)
C16–C15	1.393(7)
C16–H16	0.9500
C15–H15	0.9500
C17–H17	0.9500
C3–C4	1.364(9)
C3–C2	1.381(9)
C3–H3	0.9500
C5–C6	1.389(9)
C5–C4	1.406(9)
C5–H5	0.9500
C11–C10	1.430(10)
C11–C10A	1.696(13)
C11–H11	1.0000
C4–H4	0.9500
C8–C9	1.476(10)
C8–C9A	1.663(11)
C8–H8A	0.9900
C8–H8B	0.9900
C1–C6	1.370(9)
C1–C2	1.378(9)
C1–H1	0.9500
C7–C6	1.500(9)
C7–H7A	0.9900
C7–H7B	0.9900
C2–H2	0.9500
C10A–C9A	1.504(14)
C10A–H10A	0.9900
C10A–H10B	0.9900
C9–C10	1.539(12)
C9–H9A	0.9900
C9–H9B	0.9900
C9A–H9A1	0.9900
C9A–H9A2	0.9900
C10–H10C	0.9900
C10–H10D	0.9900
C13–N4–C19	103.9(3)
C12–N2–C13	125.6(4)
C12–N2–H20	125(4)
C13–N2–H20	110(4)
C13–N3–C14	106.1(4)
C13–N3–H19	129(4)
C14–N3–H19	125(4)
C11–N1–C7	113.3(4)
C11–N1–C8	107.1(4)
C7–N1–C8	113.3(4)
N4–C13–N3	114.5(4)
N4–C13–N2	122.0(4)
N3–C13–N2	123.5(4)
C18–C19–N4	130.1(4)
C18–C19–C14	120.0(4)
N4–C19–C14	109.8(4)
C17–C18–C19	117.1(4)
C17–C18–H18	121.5
C19–C18–H18	121.5
N3–C14–C15	131.5(4)
N3–C14–C19	105.7(4)
C15–C14–C19	122.7(4)
O1–C12–N2	124.5(5)
O1–C12–C11	121.2(4)
N2–C12–C11	114.2(4)
C17–C16–C15	121.1(5)
C17–C16–H16	119.4
C15–C16–H16	119.4
C16–C15–C14	116.0(4)
C16–C15–H15	122.0
C14–C15–H15	122.0
C18–C17–C16	123.1(5)
C18–C17–H17	118.5
C16–C17–H17	118.5
C4–C3–C2	119.3(6)
C4–C3–H3	120.3
C2–C3–H3	120.3
C6–C5–C4	120.9(6)
C6–C5–H5	119.6
C4–C5–H5	119.6
C10–C11–N1	105.2(6)
C10–C11–C12	121.1(6)
N1–C11–C12	113.1(4)
N1–C11–C10A	106.3(5)
C12–C11–C10A	99.0(6)
C10–C11–H11	105.4
N1–C11–H11	105.4
C12–C11–H11	105.4
C3–C4–C5	120.1(6)
C3–C4–H4	119.9
C5–C4–H4	119.9
N1–C8–C9	101.4(5)
N1–C8–C9A	106.0(5)
N1–C8–H8A	111.5
C9–C8–H8A	111.5
N1–C8–H8B	111.5
C9–C8–H8B	111.5
H8A–C8–H8B	109.3
C6–C1–C2	122.5(6)
C6–C1–H1	118.7

C2–C1–H1	118.7
N1–C7–C6	113.1(4)
N1–C7–H7A	109.0
C6–C7–H7A	109.0
N1–C7–H7B	109.0
C6–C7–H7B	109.0
H7A–C7–H7B	107.8
C1–C6–C5	117.2(6)
C1–C6–C7	121.7(6)
C5–C6–C7	121.1(5)
C1–C2–C3	119.9(6)
C1–C2–H2	120.0
C3–C2–H2	120.0
C9A–C10A–C11	97.0(8)
C9A–C10A–H10A	112.4
C11–C10A–H10A	112.4
C9A–C10A–H10B	112.4
C11–C10A–H10B	112.4
H10A–C10A–H10B	109.9
C8–C9–C10	98.5(7)
C8–C9–H9A	112.1
C10–C9–H9A	112.1
C8–C9–H9B	112.1
C10–C9–H9B	112.1
H9A–C9–H9B	109.7
C10A–C9A–C8	99.4(8)
C10A–C9A–H9A1	111.9
C8–C9A–H9A1	111.9
C10A–C9A–H9A2	111.9
C8–C9A–H9A2	111.9
H9A1–C9A–H9A2	109.6
C11–C10–C9	99.8(7)
C11–C10–H10C	111.8
C9–C10–H10C	111.8
C11–C10–H10D	111.8
C9–C10–H10D	111.8
H10C–C10–H10D	109.5

Symmetry transformations used to generate equivalent atoms:

Table 4. Anisotropic displacement parameters [Å²× 10³]. The anisotropic displacement factor exponent takes the form: $-2\pi^2[h^2a^{*2}U^{11} + \cdots + 2\,h\,k\,a^*\,b^*\,U^{12}]$.

Atom	U^{11}	U^{22}	U^{33}	U^{23}	U^{13}	U^{12}
O1	79(2)	85(2)	30(2)	–5(2)	6(2)	31(2)
N4	73(2)	66(2)	27(2)	–4(2)	–2(2)	39(2)
N2	82(3)	67(2)	23(2)	–3(2)	2(2)	40(2)
N3	72(2)	72(2)	23(2)	–2(2)	–2(2)	39(2)
N1	73(2)	67(2)	39(2)	–5(2)	10(2)	32(2)
C13	67(3)	74(3)	26(2)	–6(2)	–1(2)	40(2)
C19	64(3)	65(3)	30(2)	–6(2)	–6(2)	33(2)
C18	87(3)	70(3)	34(2)	–1(2)	–9(2)	43(3)
C14	67(3)	69(3)	25(2)	–4(2)	–6(2)	36(2)
C12	69(3)	77(3)	27(2)	0(2)	3(2)	39(2)
C16	86(3)	68(3)	42(3)	–8(2)	–11(2)	39(3)
C15	69(3)	74(3)	31(2)	–8(2)	–8(2)	37(2)
C17	98(4)	70(3)	42(3)	–3(2)	–12(2)	44(3)
C3	88(4)	94(4)	57(4)	–1(3)	–13(3)	42(3)
C5	72(3)	81(4)	79(4)	6(3)	17(3)	35(3)
C11	101(4)	79(3)	35(2)	1(2)	11(2)	51(3)
C4	76(3)	79(4)	78(4)	–8(3)	2(3)	35(3)
C8	90(4)	91(4)	53(3)	–15(3)	9(3)	48(3)
C1	92(4)	86(4)	64(4)	8(3)	–18(3)	15(3)
C7	80(4)	112(5)	65(4)	15(3)	16(3)	49(4)
C6	72(3)	89(4)	61(3)	7(3)	6(3)	35(3)
C2	93(4)	96(5)	59(4)	15(3)	–19(3)	15(3)

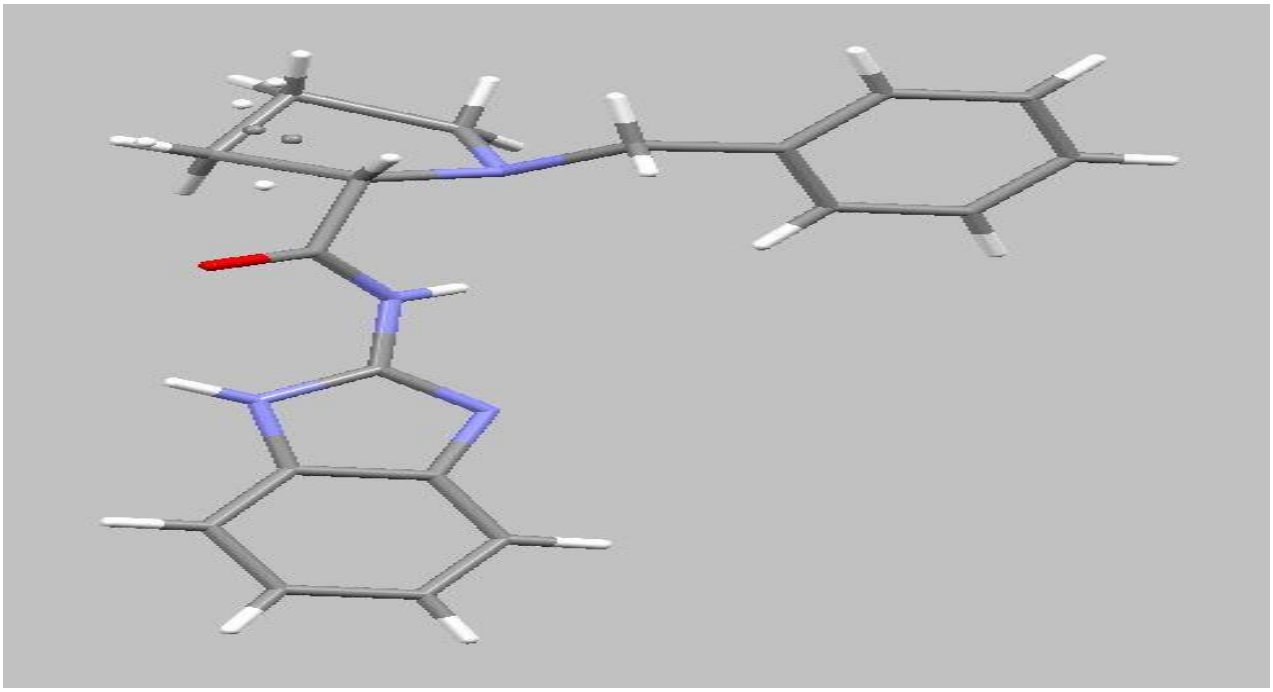

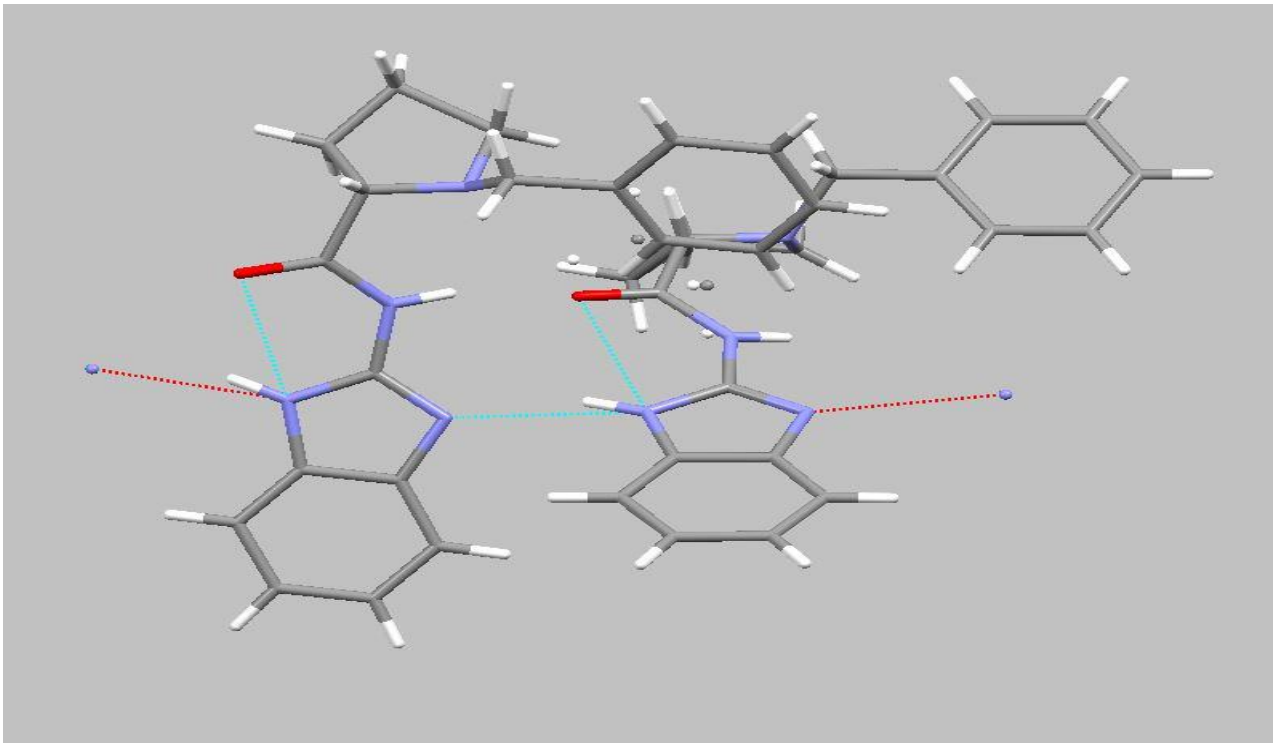

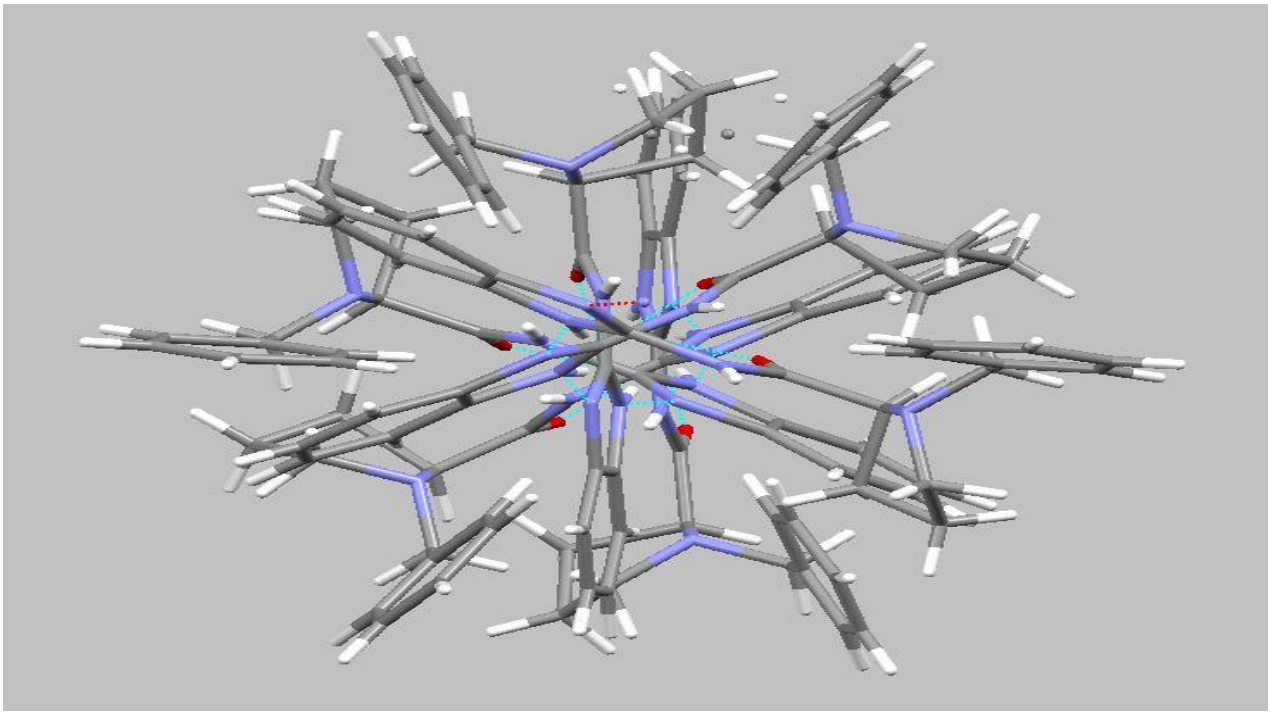

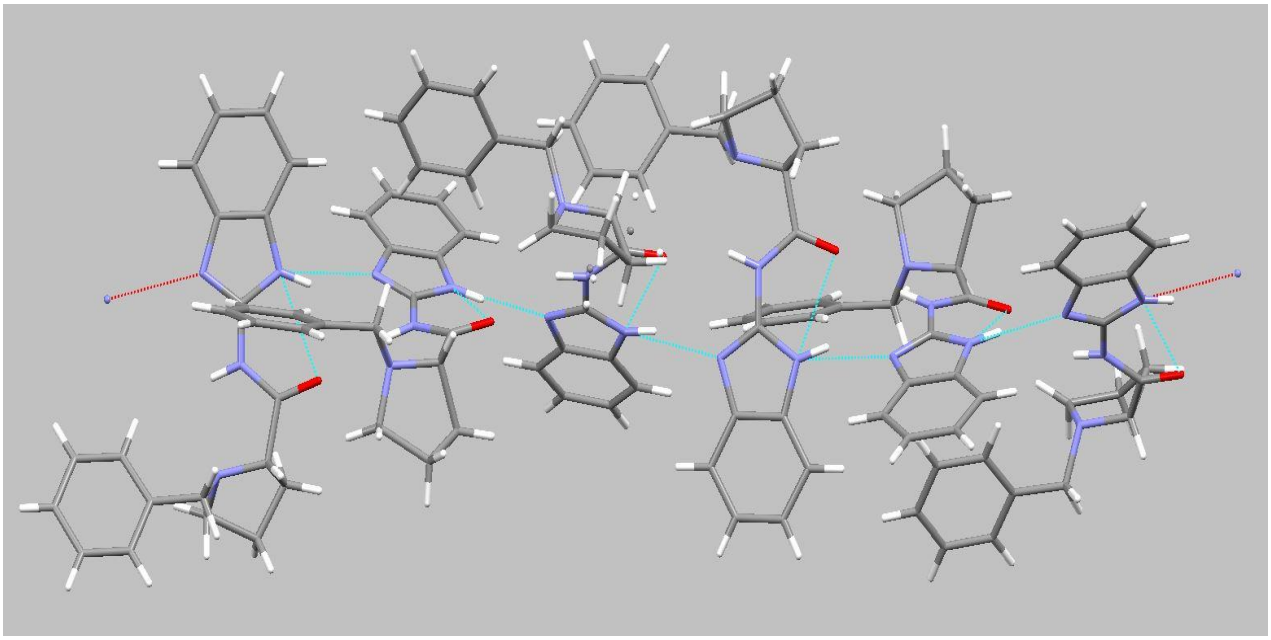

Appendix 9
X-ray of compound 141

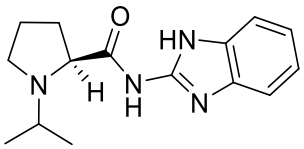

UK National Crystallography Service

Table 1. Crystal data and structure refinement details.

Identification code	**2016ncs0665**	
Empirical formula	$C_{30}H_{42}N_8O_3$	
Formula weight	562.72	
Temperature	100(2) K	
Wavelength	0.71073 Å	
Crystal system	Orthorhombic	
Space group	*P*21212	
Unit cell dimensions	a = 12.0576(2) Å	α = **90°**
	b = **11.3774(2) Å**	β = **90°**
	c = **11.1889(2) Å**	γ = **90°**
Volume	**1534.94(5) Å**^{3}	
Z	2	
Density (calculated)	1.213 Mg / m^3	
Absorption coefficient	0.081 mm^{-1}	
F(000)	604	
Crystal	Plate; colourless	
Crystal size	0.110 × 0.050 × 0.050 mm^3	
θ range for data collection	2.461 – 29.970°	
Index ranges	$-16 \le h \le 16$, $-15 \le k \le 15$, $-15 \le l \le 15$	
Reflections collected	54936	
Independent reflections	4257 [R_{int} = 0.0475]	
Completeness to θ = 25.242°	99.4 %	
Absorption correction	Semi–empirical from equivalents	
Max. and min. transmission	1.00000 and 0.91544	
Refinement method	Full-matrix least-squares on F^2	
Data / restraints / parameters	4257 / 0 / 200	
Goodness-of-fit on F^2	1.066	
Final *R* indices [$F^2 > 2\sigma(F^2)$]	*R1* = 0.0386, *wR2* = 0.0971	
R indices (all data)	*R1* = 0.0433, *wR2* = 0.0998	
Absolute structure parameter	?	
Extinction coefficient	n/a	
Largest diff. peak and hole	0.272 and –0.179 e Å^{-3}	

Diffractometer: *Rigaku AFC12* goniometer equipped with an enhanced sensitivity (HG) *Saturn724+* detector mounted at the window of an *FR-E+ SuperBright* molybdenum rotating anode generator with HF *Varimax* optics (100µm focus). **Cell determination and Data collection**: CrystalClear-SM Expert 2.0 r7 (Rigaku, 2011). **Data reduction and cell refinement & Absorption correction:** CrysalisPRO 171.38.41 (Rigaku Oxford Diffraction 2015). **Structure solution**: SHELXST (G. M. Sheldrick, Acta Cryst. (2008) A**64** 112–122). **Structure refinement**: SHELXL97 (G. M. Sheldrick (1997), University of Göttingen, Germany). **Graphics:** Mercury 3.5.1 (CCDC 2014). **Publication material:** WinGX: Farrugia, L. J. (2012). J. Appl. Cryst. 45, 849-854.

Special details:

Table 2. Atomic coordinates [× 10^4], equivalent isotropic displacement parameters [$Å^2$ × 10^3] and site occupancy factors. U_{eq} is defined as one third of the trace of the orthogonalized U^{ij} tensor.

Atom	*x*	*y*	*z*	U_{eq}	*S.o.f.*
O2	5000	5000	2821(2)	25(1)	1
O1	846(1)	6024(1)	2478(1)	30(1)	1
N2	2597(1)	5300(1)	2694(1)	20(1)	1
N3	1451(1)	3746(1)	1914(1)	19(1)	1
N4	3308(1)	3565(1)	1829(1)	20(1)	1
N1	3323(1)	7155(1)	3884(1)	23(1)	1
C8	1809(1)	6151(2)	2788(2)	22(1)	1
C9	2459(1)	4217(1)	2160(1)	18(1)	1
C15	2819(1)	2573(1)	1328(1)	19(1)	1
C10	1657(1)	2673(1)	1371(1)	18(1)	1
C14	3308(1)	1577(2)	830(2)	22(1)	1
C13	2612(2)	708(1)	393(2)	25(1)	1
C12	1452(2)	821(2)	438(2)	25(1)	1
C11	954(1)	1806(1)	929(2)	23(1)	1
C6	2458(2)	8185(2)	2232(2)	30(1)	1
C7	2249(1)	7313(1)	3275(2)	23(1)	1
C5	3713(2)	8241(2)	2147(2)	35(1)	1
C4	4077(2)	8079(2)	3432(2)	31(1)	1
C3	3264(2)	7056(2)	5186(2)	30(1)	1
C2	2521(2)	6042(2)	5563(2)	40(1)	1
C1	4429(2)	6891(2)	5675(2)	43(1)	1

Table 3. Bond lengths [Å] and angles [°].

O2–H2O	0.82(3)
O1–C8	1.221(2)
N2–C8	1.360(2)
N2–C9	1.3799(19)
N2–H2N	0.88(3)
N3–C9	1.3570(19)
N3–C10	1.387(2)
N3–H3N	0.89(3)
N4–C9	1.317(2)
N4–C15	1.3911(19)
N1–C3	1.464(2)
N1–C7	1.475(2)
N1–C4	1.478(2)
C8–C7	1.525(2)
C15–C14	1.393(2)
C15–C10	1.406(2)
C10–C11	1.391(2)
C14–C13	1.386(2)
C14–H14	0.9500
C13–C12	1.404(3)
C13–H13	0.9500
C12–C11	1.386(2)
C12–H12	0.9500
C11–H11	0.9500
C6–C5	1.517(3)
C6–C7	1.552(3)
C6–H6A	0.9900
C6–H6B	0.9900
C7–H7	1.0000
C5–C4	1.514(3)
C5–H5A	0.9900
C5–H5B	0.9900
C4–H4A	0.9900
C4–H4B	0.9900
C3–C1	1.519(3)
C3–C2	1.521(3)
C3–H3	1.0000
C2–H2A	0.9800
C2–H2B	0.9800
C2–H2C	0.9800
C1–H1A	0.9800
C1–H1B	0.9800
C1–H1C	0.9800
C8–N2–C9	125.81(13)
C8–N2–H2N	118.7(16)
C9–N2–H2N	115.4(16)
C9–N3–C10	106.00(13)
C9–N3–H3N	126.0(16)
C10–N3–H3N	127.9(16)
C9–N4–C15	103.94(13)
C3–N1–C7	115.25(14)
C3–N1–C4	115.16(14)
C7–N1–C4	107.22(14)
O1–C8–N2	123.99(15)
O1–C8–C7	122.28(15)
N2–C8–C7	113.69(13)
N4–C9–N3	114.64(14)
N4–C9–N2	122.14(14)
N3–C9–N2	123.22(14)
N4–C15–C14	129.89(15)
N4–C15–C10	110.06(13)
C14–C15–C10	120.05(14)
N3–C10–C11	132.11(15)
N3–C10–C15	105.36(13)
C11–C10–C15	122.54(14)
C13–C14–C15	117.70(15)
C13–C14–H14	121.1
C15–C14–H14	121.1
C14–C13–C12	121.66(15)
C14–C13–H13	119.2
C12–C13–H13	119.2
C11–C12–C13	121.33(15)
C11–C12–H12	119.3
C13–C12–H12	119.3
C12–C11–C10	116.73(15)
C12–C11–H11	121.6
C10–C11–H11	121.6
C5–C6–C7	103.67(15)
C5–C6–H6A	111.0
C7–C6–H6A	111.0
C5–C6–H6B	111.0
C7–C6–H6B	111.0
H6A–C6–H6B	109.0
N1–C7–C8	111.40(13)
N1–C7–C6	106.36(14)
C8–C7–C6	110.02(14)
N1–C7–H7	109.7
C8–C7–H7	109.7
C6–C7–H7	109.7
C4–C5–C6	102.96(16)
C4–C5–H5A	111.2
C6–C5–H5A	111.2
C4–C5–H5B	111.2
C6–C5–H5B	111.2
H5A–C5–H5B	109.1
N1–C4–C5	103.48(14)
N1–C4–H4A	111.1
C5–C4–H4A	111.1
N1–C4–H4B	111.1
C5–C4–H4B	111.1
H4A–C4–H4B	109.0
N1–C3–C1	108.83(16)
N1–C3–C2	111.28(15)
C1–C3–C2	110.58(19)
N1–C3–H3	108.7
C1–C3–H3	108.7
C2–C3–H3	108.7
C3–C2–H2A	109.5
C3–C2–H2B	109.5
H2A–C2–H2B	109.5
C3–C2–H2C	109.5
H2A–C2–H2C	109.5
H2B–C2–H2C	109.5
C3–C1–H1A	109.5

C3–C1–H1B	109.5
H1A–C1–H1B	109.5
C3–C1–H1C	109.5
H1A–C1–H1C	109.5
H1B–C1–H1C	109.5

Table 4. Anisotropic displacement parameters [Å²× 10³]. The anisotropic displacement factor exponent takes the form: $-2\pi^2[h^2a^{*2}U^{11} + \cdots + 2\,h\,k\,a^*\,b^*\,U^{12}]$.

Atom	U^{11}	U^{22}	U^{33}	U^{23}	U^{13}	U^{12}
O2	15(1)	25(1)	37(1)	0	0	–3(1)
O1	15(1)	25(1)	49(1)	–8(1)	–4(1)	1(1)
N2	14(1)	18(1)	29(1)	–4(1)	–2(1)	–1(1)
N3	13(1)	17(1)	26(1)	–1(1)	0(1)	–2(1)
N4	16(1)	17(1)	25(1)	1(1)	0(1)	1(1)
N1	15(1)	22(1)	31(1)	–7(1)	–2(1)	–2(1)
C8	17(1)	20(1)	29(1)	–3(1)	–1(1)	0(1)
C9	15(1)	17(1)	22(1)	2(1)	–1(1)	–1(1)
C15	18(1)	18(1)	21(1)	2(1)	1(1)	–2(1)
C10	18(1)	16(1)	21(1)	1(1)	1(1)	0(1)
C14	21(1)	20(1)	25(1)	–1(1)	1(1)	2(1)
C13	31(1)	19(1)	26(1)	–3(1)	0(1)	3(1)
C12	29(1)	20(1)	27(1)	–4(1)	–3(1)	–5(1)
C11	20(1)	20(1)	28(1)	–1(1)	–2(1)	–4(1)
C6	30(1)	21(1)	39(1)	1(1)	–6(1)	–3(1)
C7	17(1)	20(1)	32(1)	–6(1)	–2(1)	1(1)
C5	33(1)	27(1)	45(1)	2(1)	5(1)	–5(1)
C4	22(1)	25(1)	47(1)	–5(1)	–2(1)	–5(1)
C3	27(1)	34(1)	30(1)	–12(1)	–4(1)	3(1)
C2	48(1)	44(1)	28(1)	–1(1)	1(1)	–4(1)
C1	35(1)	57(1)	38(1)	–13(1)	–12(1)	10(1)

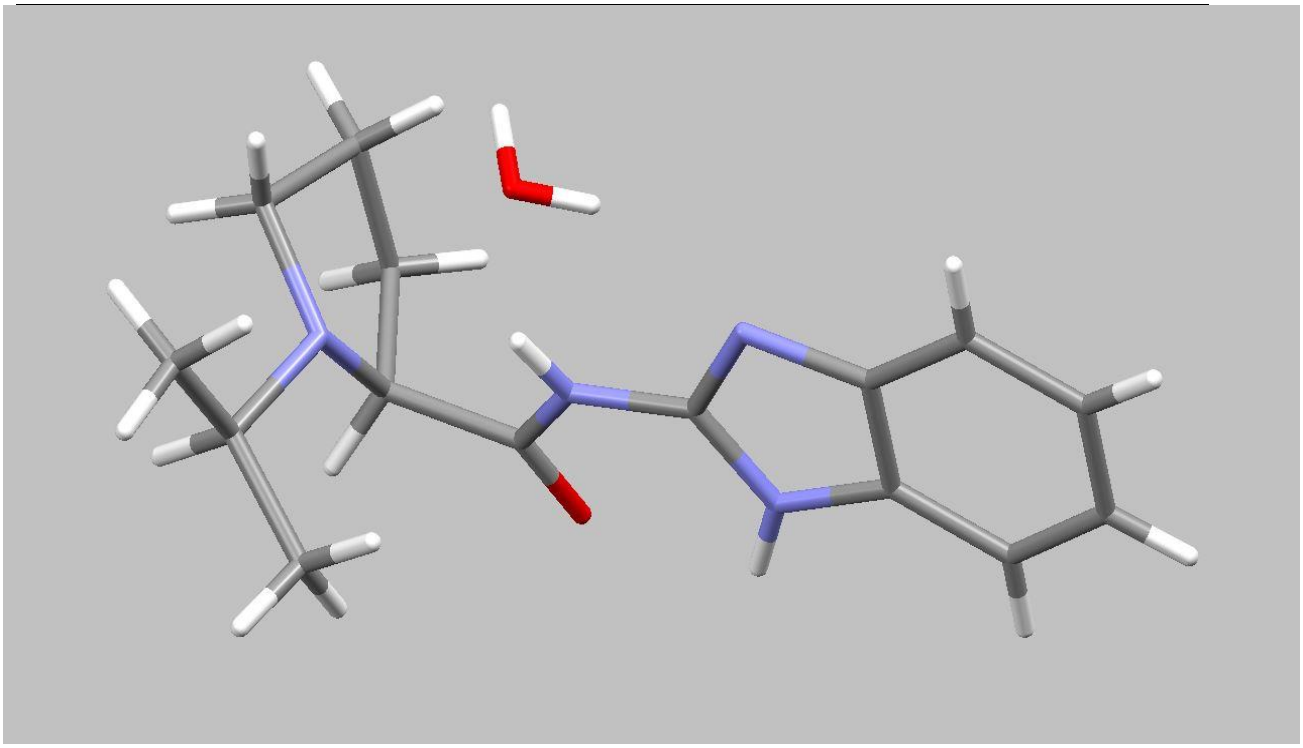

Appendix 10
X-ray of compound 115

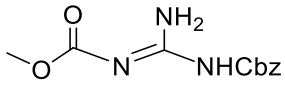

UK National Crystallography Service

Table 1. Crystal data and structure refinement details.

Identification code	**ros1**	
Empirical formula	$C_{11}H_{13}N_3O_4$	
Formula weight	251.24	
Temperature	100(2) K	
Wavelength	0.71073 Å	
Crystal system	Monoclinic	
Space group	*P*21/*c*	
Unit cell dimensions	a = 6.0633(4) Å	α = **90°**
	b = **9.4708(4) Å**	β = **96.386(6)°**
	c = **20.5287(12) Å**	γ = **90°**
Volume	**1171.53(12) Å^3**	
Z	4	
Density (calculated)	1.424 Mg / m^3	
Absorption coefficient	0.110 mm^{-1}	
F(000)	528	
Crystal	Plate; colourless	
Crystal size	0.08 × 0.07 × 0.01 mm^3	
θ range for data collection	2.371 – 29.881°	
Index ranges	$-7 \le h \le 8$, $-13 \le k \le 13$, $-27 \le l \le 26$	
Reflections collected	15643	
Independent reflections	3074 [R_{int} = 0.0828]	
Completeness to θ = 25.242°	99.9 %	
Absorption correction	Semi–empirical from equivalents	
Max. and min. transmission	1.00000 and 0.67595	
Refinement method	Full-matrix least-squares on F^2	
Data / restraints / parameters	3074 / 0 / 176	
Goodness-of-fit on F^2	1.037	
Final *R* indices [$F^2 > 2\sigma(F^2)$]	*R1* = 0.0574, *wR2* = 0.0990	
R indices (all data)	*R1* = 0.1133, *wR2* = 0.1159	
Extinction coefficient	n/a	
Largest diff. peak and hole	0.235 and –0.264 e Å^{-3}	

Diffractometer: *Rigaku AFC12* goniometer equipped with an enhanced sensitivity (HG) *Saturn724+* detector mounted at the window of an *FR-E+ SuperBright* molybdenum rotating anode generator with HF *Varimax* optics (70µm focus). **Cell determination and Data collection**: CrystalClear-SM Expert 2.0 r7 (Rigaku, 2011). **Data reduction and cell refinement & Absorption correction:** CrysalisPRO 171.38.43 (Rigaku Oxford Diffraction 2015). **Structure solution**: SHELXST (G. M. Sheldrick, Acta Cryst. (2008) A**64** 112–122). S**tructure refinement**: SHELXL97 (G. M. Sheldrick (1997), University of Göttingen, Germany). **Graphics:** Mercury 3.5.1 (CCDC 2014). **Publication material:** WinGX: Farrugia, L. J. (2012). J. Appl. Cryst. 45, 849-854.

Special details:

Table 2. Atomic coordinates [× 10^4], equivalent isotropic displacement parameters [Å^2 × 10^3] and site occupancy factors. U_{eq} is defined as one third of the trace of the orthogonalized U^{ij} tensor.

Atom	*x*	*y*	*z*	U_{eq}	*S.o.f.*
O3	11789(2)	2771(1)	8106(1)	20(1)	1
O1	3812(2)	5669(1)	6344(1)	22(1)	1
O2	3974(2)	3360(1)	6643(1)	22(1)	1
O4	13440(2)	4905(1)	8151(1)	21(1)	1
N2	10138(3)	4760(2)	7572(1)	18(1)	1
N3	7944(3)	2698(2)	7317(1)	20(1)	1
N1	6777(3)	4940(2)	6974(1)	19(1)	1
C6	1278(3)	6518(2)	5444(1)	19(1)	1
C9	8348(3)	4065(2)	7306(1)	16(1)	1
C10	11743(3)	4024(2)	7944(1)	16(1)	1
C8	4764(3)	4539(2)	6653(1)	18(1)	1
C1	2866(3)	6713(2)	5012(1)	23(1)	1
C5	–683(3)	7284(2)	5350(1)	23(1)	1
C7	1614(3)	5454(2)	5991(1)	23(1)	1
C4	–1073(4)	8208(2)	4825(1)	27(1)	1
C2	2479(4)	7649(2)	4489(1)	26(1)	1
C3	502(4)	8389(2)	4392(1)	27(1)	1
C11	15210(3)	4310(2)	8596(1)	24(1)	1

Table 3. Bond lengths [Å] and angles [°].

O3–C10	1.233(2)
O1–C8	1.341(2)
O1–C7	1.459(2)
O2–C8	1.214(2)
O4–C10	1.355(2)
O4–C11	1.444(2)
N2–C9	1.333(2)
N2–C10	1.360(2)
N3–C9	1.318(2)
N3–HN1	0.90(2)
N3–HN2	0.91(3)
N1–C8	1.374(3)
N1–C9	1.384(2)
N1–HN3	0.91(2)
C6–C5	1.388(3)
C6–C1	1.392(3)
C6–C7	1.506(3)
C1–C2	1.391(3)
C1–H1	0.9300
C5–C4	1.388(3)
C5–H5	0.9300
C7–H7A	0.9700
C7–H7B	0.9700
C4–C3	1.387(3)
C4–H4	0.9300
C2–C3	1.384(3)
C2–H2	0.9300
C3–H3	0.9300
C11–H11A	0.9600
C11–H11B	0.9600
C11–H11C	0.9600
C8–O1–C7	116.38(14)
C10–O4–C11	116.34(14)
C9–N2–C10	118.47(15)
C9–N3–HN1	115.3(14)
C9–N3–HN2	116.2(15)
HN1–N3–HN2	128(2)
C8–N1–C9	126.62(16)
C8–N1–HN3	117.7(15)
C9–N1–HN3	115.6(15)
C5–C6–C1	119.05(18)
C5–C6–C7	119.70(18)
C1–C6–C7	121.20(18)
N3–C9–N2	128.43(18)
N3–C9–N1	118.54(18)
N2–C9–N1	113.02(15)
O3–C10–O4	120.94(17)
O3–C10–N2	129.64(18)
O4–C10–N2	109.40(15)
O2–C8–O1	125.30(18)
O2–C8–N1	126.13(18)
O1–C8–N1	108.56(15)
C2–C1–C6	120.43(19)
C2–C1–H1	119.8
C6–C1–H1	119.8
C6–C5–C4	120.42(19)
C6–C5–H5	119.8
C4–C5–H5	119.8
O1–C7–C6	108.48(15)
O1–C7–H7A	110.0
C6–C7–H7A	110.0
O1–C7–H7B	110.0
C6–C7–H7B	110.0
H7A–C7–H7B	108.4
C3–C4–C5	120.4(2)
C3–C4–H4	119.8
C5–C4–H4	119.8
C3–C2–C1	120.2(2)
C3–C2–H2	119.9
C1–C2–H2	119.9
C2–C3–C4	119.49(19)
C2–C3–H3	120.3
C4–C3–H3	120.3
O4–C11–H11A	109.5
O4–C11–H11B	109.5
H11A–C11–H11B	109.5
O4–C11–H11C	109.5
H11A–C11–H11C	109.5
H11B–C11–H11C	109.5

Symmetry transformations used to generate equivalent atoms:

Table 4. Anisotropic displacement parameters [Å²× 10³]. The anisotropic displacement factor exponent takes the form: $-2\pi^2[h^2a^{*2}U^{11} + \cdots + 2\,h\,k\,a^*\,b^*\,U^{12}]$.

Atom	U^{11}	U^{22}	U^{33}	U^{23}	U^{13}	U^{12}
O3	26(1)	11(1)	23(1)	1(1)	−3(1)	0(1)
O1	21(1)	14(1)	28(1)	4(1)	−7(1)	−1(1)
O2	23(1)	12(1)	29(1)	1(1)	−2(1)	−3(1)
O4	21(1)	13(1)	29(1)	2(1)	−6(1)	0(1)
N2	19(1)	12(1)	23(1)	1(1)	−1(1)	0(1)
N3	21(1)	12(1)	26(1)	1(1)	−6(1)	−1(1)
N1	19(1)	10(1)	25(1)	2(1)	−2(1)	−1(1)
C6	19(1)	15(1)	22(1)	−2(1)	−2(1)	−1(1)
C9	20(1)	12(1)	17(1)	0(1)	2(1)	−1(1)
C10	20(1)	13(1)	17(1)	−2(1)	3(1)	0(1)
C8	20(1)	16(1)	18(1)	−1(1)	1(1)	2(1)
C1	20(1)	20(1)	30(1)	−2(1)	−1(1)	2(1)
C5	23(1)	22(1)	23(1)	−1(1)	3(1)	2(1)
C7	18(1)	22(1)	27(1)	3(1)	−6(1)	−2(1)
C4	26(1)	24(1)	32(1)	3(1)	−1(1)	7(1)
C2	26(1)	26(1)	26(1)	1(1)	5(1)	−4(1)
C3	31(1)	22(1)	27(1)	5(1)	−3(1)	−1(1)
C11	21(1)	19(1)	29(1)	0(1)	−7(1)	1(1)

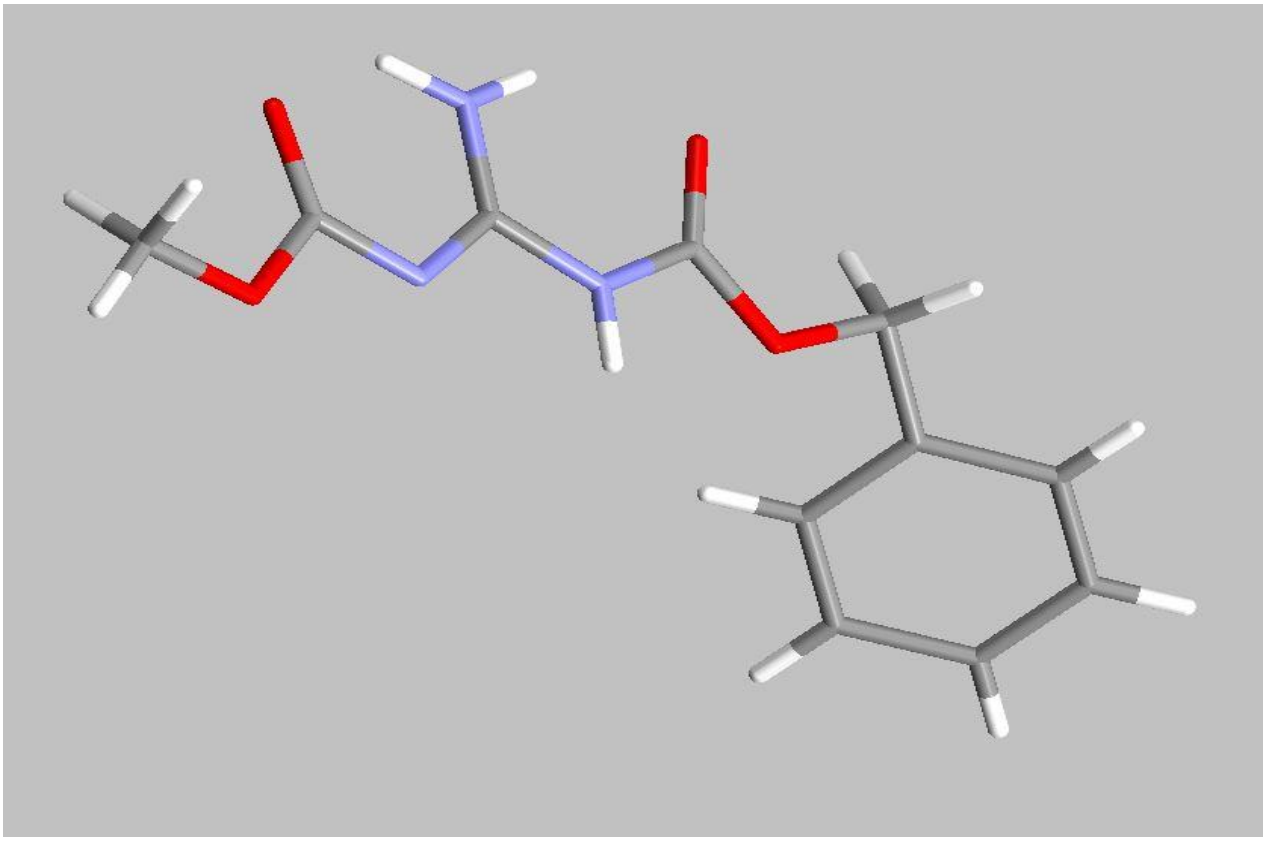

Appendix 11: Supplementary information (NMR, IR, MS and HPLC)

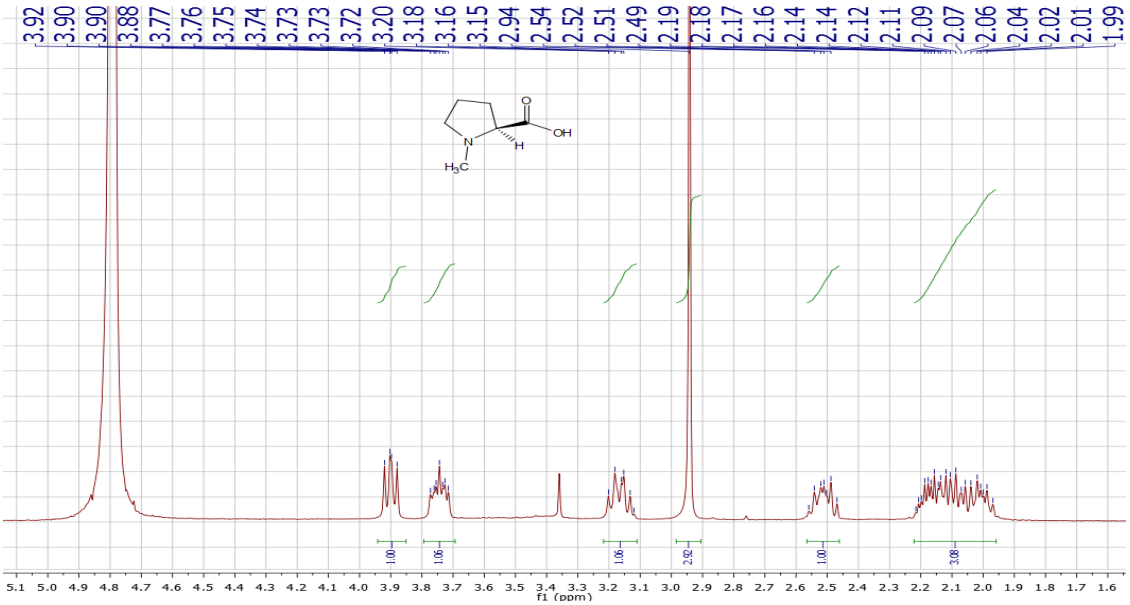

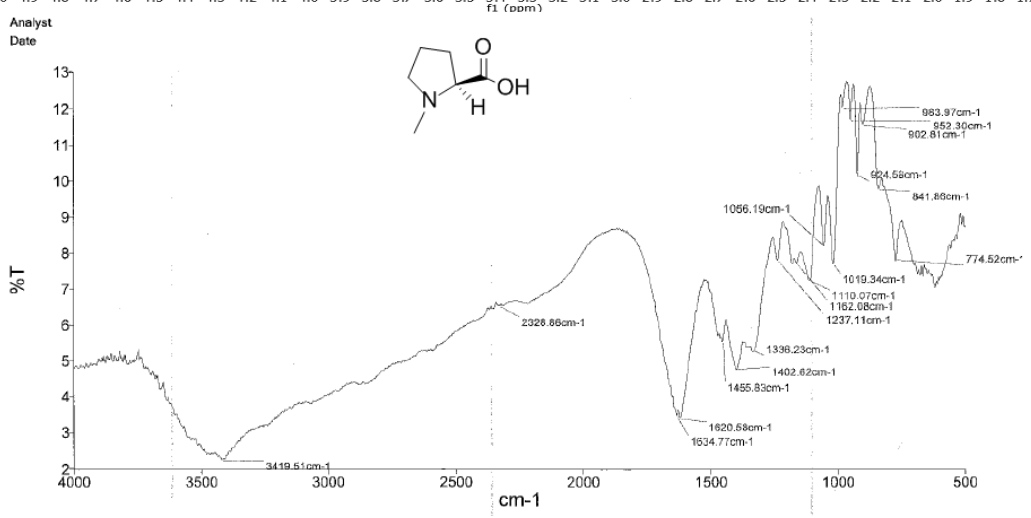

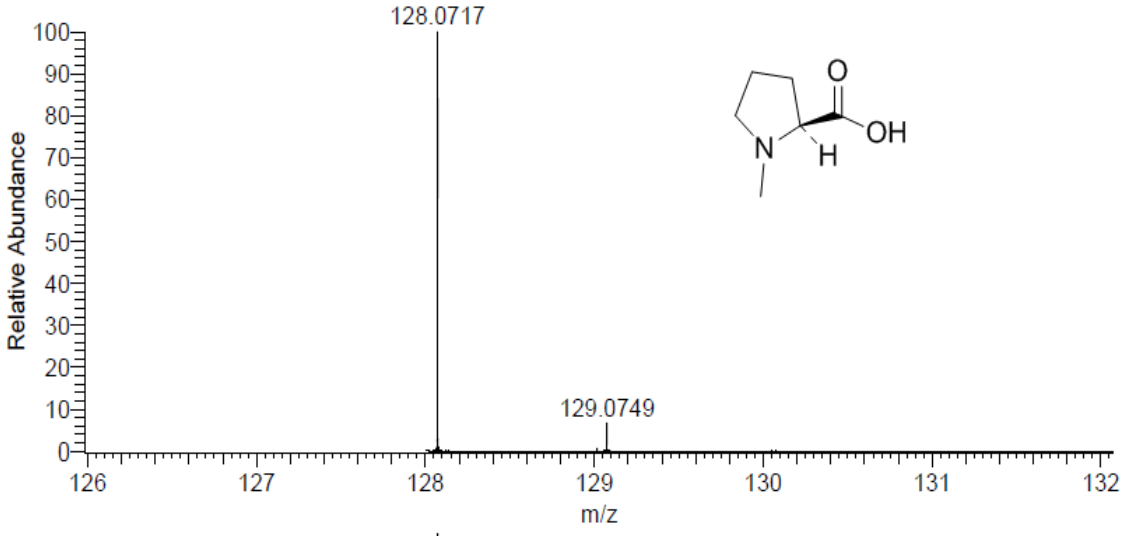

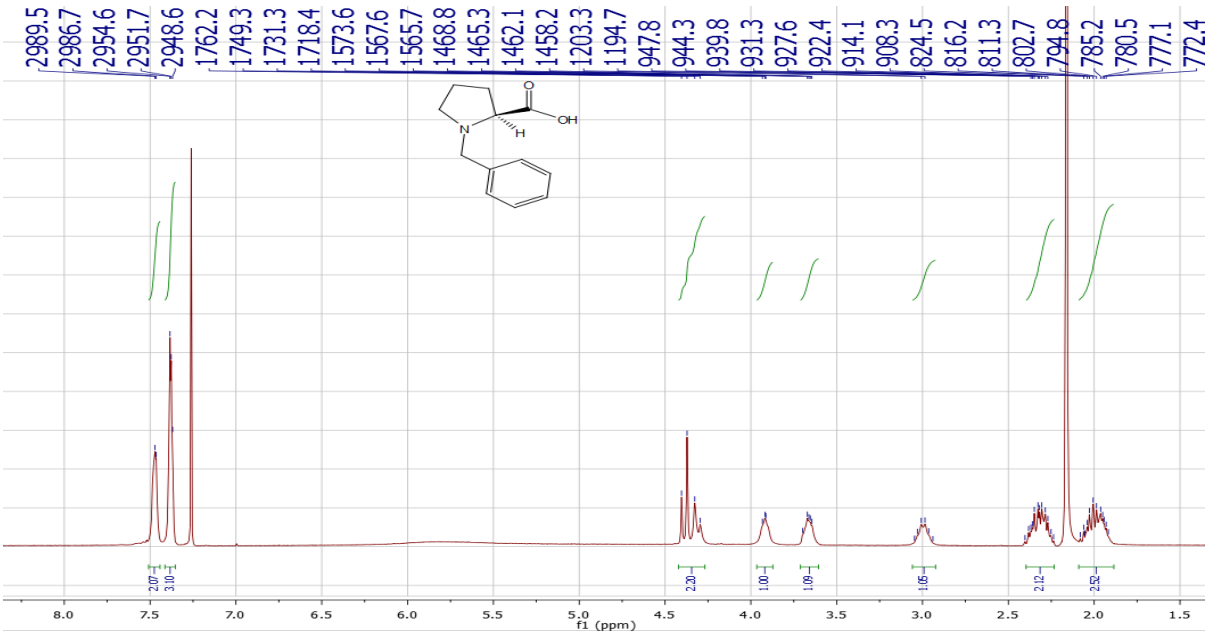
2989.5
2986.7
2954.6
2951.7
2948.6
1762.2
1749.3
1731.3
1718.4
1573.6
1567.6
1565.7
1468.8
1465.3
1462.1
1458.2
1203.3
1194.7
947.8
944.3
939.8
931.3
927.6
922.4
914.1
908.3
824.5
816.2
811.3
802.7
794.8
785.2
780.5
777.1
772.4
O
OH
N
H
2.07
3.10
2.20
1.00
1.09
1.05
2.12
2.52
8.0
7.5
7.0
6.5
6.0
5.5
5.0
4.5
4.0
3.5
3.0
2.5
2.0
1.5
f1 (ppm)

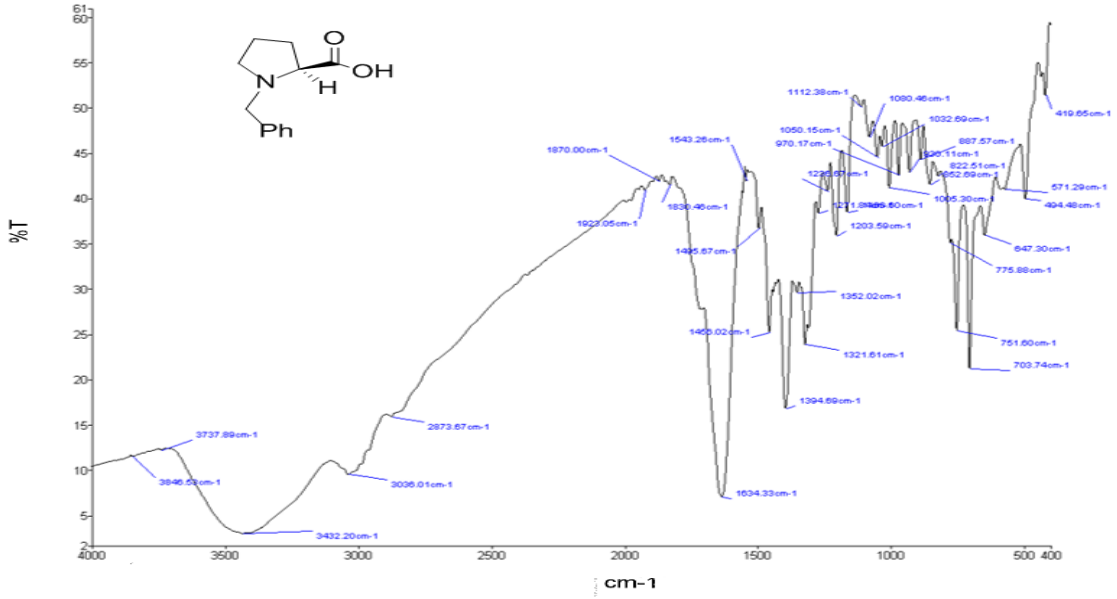
O
OH
N
H
Ph
%T
cm-1
4000
3500
3000
2500
2000
1500
1000
500
400
3737.89cm-1
3846.53cm-1
3432.20cm-1
3036.01cm-1
2873.67cm-1
1870.00cm-1
1923.05cm-1
1839.46cm-1
1543.26cm-1
1495.67cm-1
1634.33cm-1
1112.38cm-1
1080.46cm-1
1050.15cm-1
970.17cm-1
1032.69cm-1
887.57cm-1
822.51cm-1
1203.59cm-1
1352.02cm-1
1460.02cm-1
1321.61cm-1
1394.69cm-1
775.88cm-1
751.60cm-1
703.74cm-1
647.30cm-1
571.29cm-1
494.48cm-1
419.65cm-1

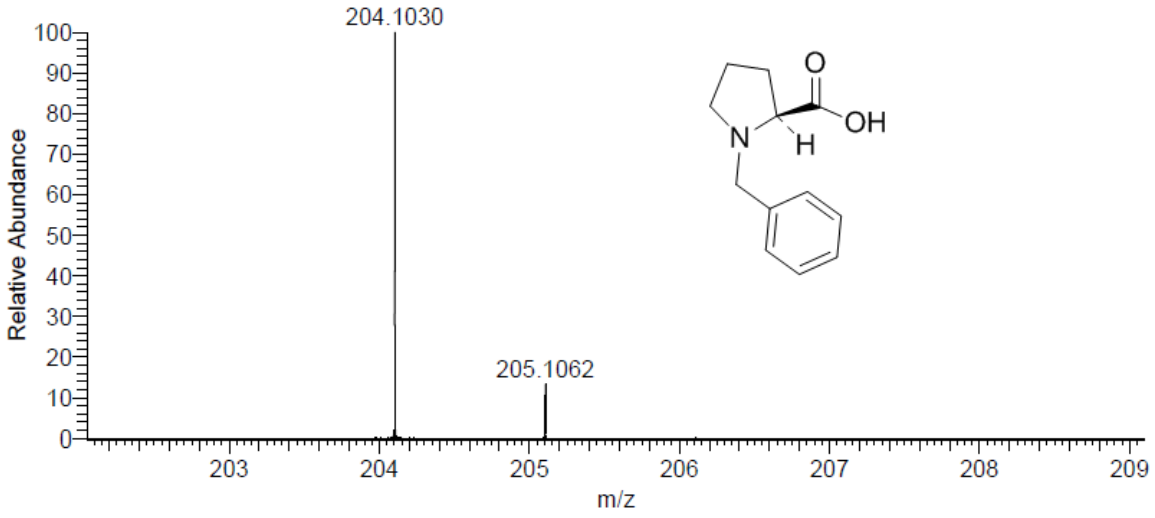
204.1030
205.1062
Relative Abundance
m/z
100
90
80
70
60
50
40
30
20
10
0
203
204
205
206
207
208
209
O
OH
N
H

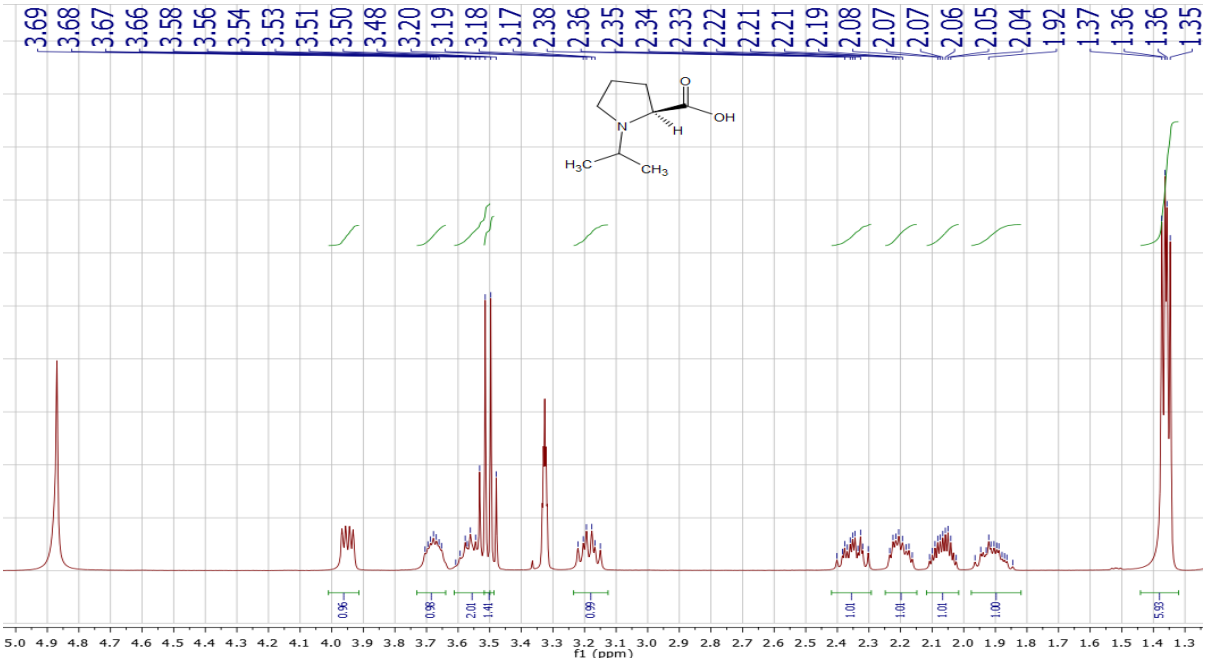
3.69 3.68 3.67 3.66 3.58 3.56 3.54 3.53 3.51 3.50 3.48 3.20 3.19 3.18 3.17 2.38 2.36 2.35 2.34 2.33 2.22 2.21 2.21 2.19 2.08 2.07 2.07 2.06 2.05 2.04 1.92 1.37 1.36 1.36 1.35
O
OH
N
H
H3C
CH3
0.96
0.98
2.01
1.41
0.99
1.01
1.01
1.01
1.00
5.93
f1 (ppm)

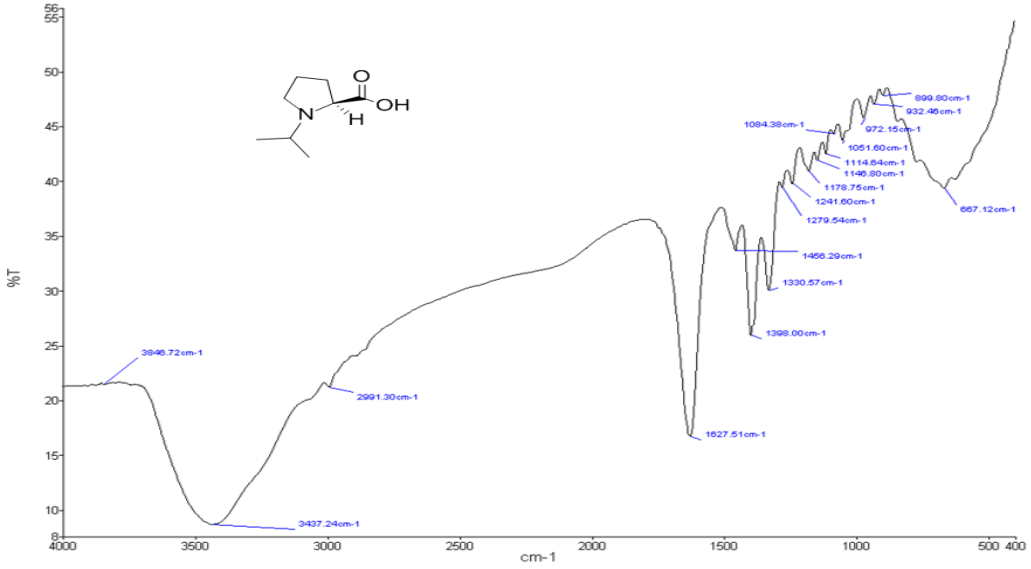
O
OH
N
H
%T
3846.72cm-1
2991.30cm-1
3437.24cm-1
1627.51cm-1
1398.00cm-1
1330.57cm-1
1456.29cm-1
1279.54cm-1
1241.60cm-1
1178.75cm-1
1146.80cm-1
1114.64cm-1
1051.60cm-1
1084.38cm-1
972.15cm-1
932.46cm-1
899.80cm-1
667.12cm-1
cm-1

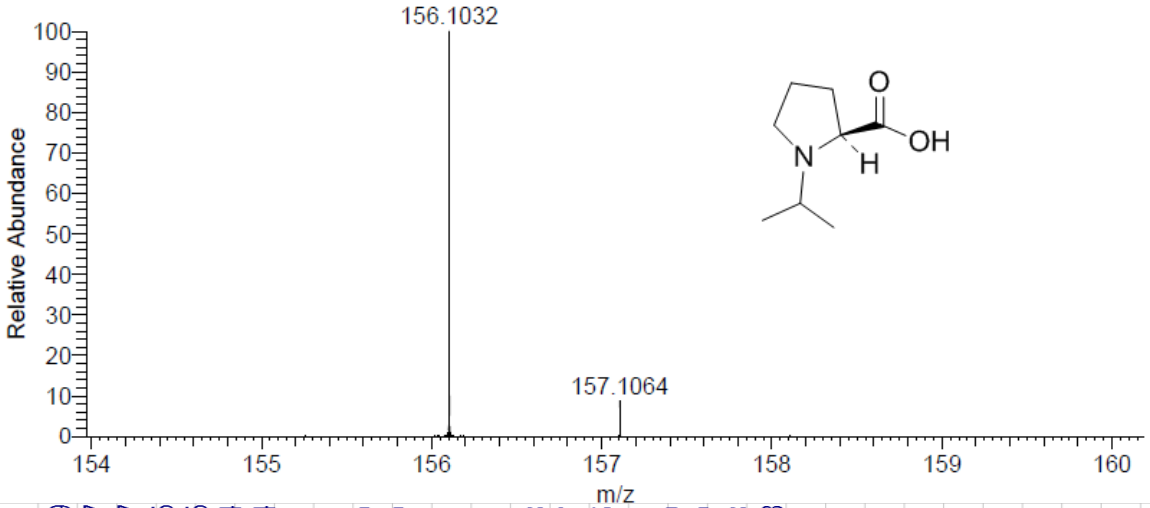
156.1032
157.1064
Relative Abundance
m/z
O
OH
N
H

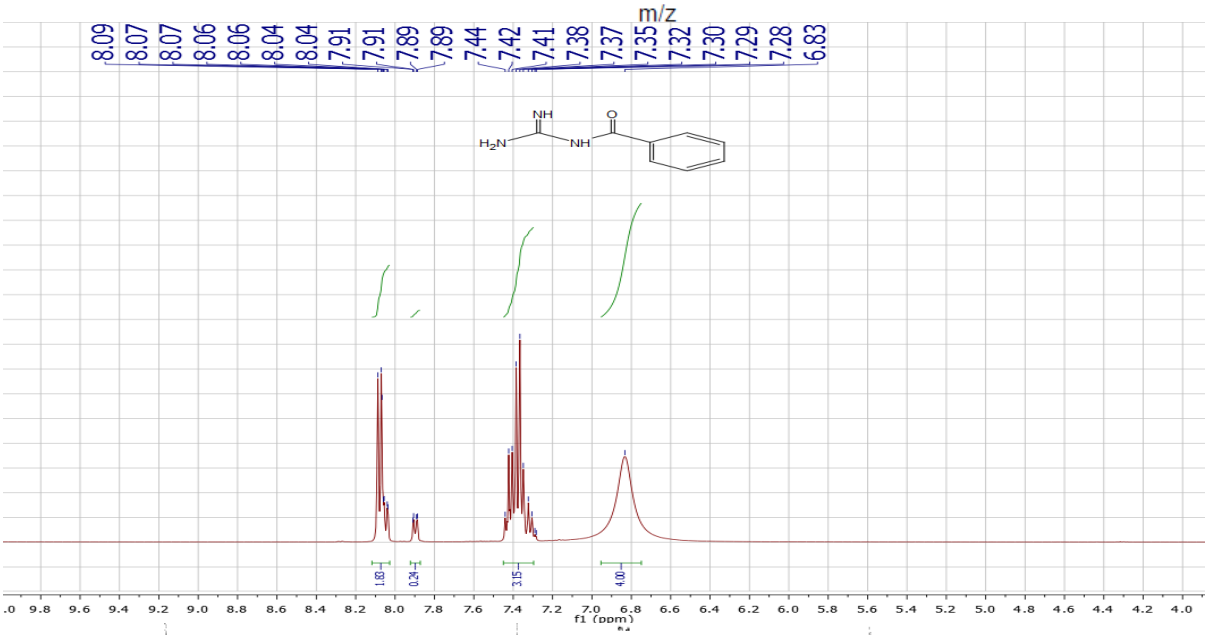
8.09
8.07
8.07
8.06
8.06
8.04
8.04
7.91
7.91
7.89
7.89
7.44
7.42
7.41
7.38
7.37
7.35
7.32
7.30
7.29
7.28
6.83
NH
O
H2N
NH
1.00
0.24
3.15
4.00
f1 (ppm)

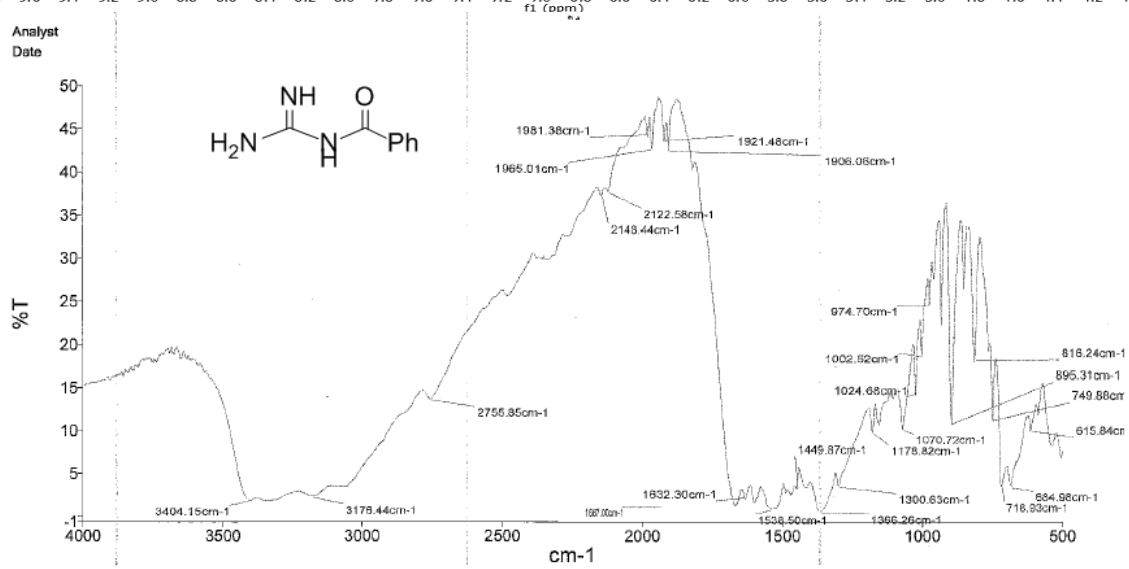
Analyst
Date
NH
O
H2N
N
H
Ph
%T
cm-1
1981.38cm-1
1965.01cm-1
1921.48cm-1
1906.08cm-1
2122.58cm-1
2148.44cm-1
2755.85cm-1
3404.15cm-1
3175.44cm-1
1632.30cm-1
1538.50cm-1
1449.87cm-1
1366.26cm-1
1300.63cm-1
1178.82cm-1
1070.72cm-1
1024.68cm-1
1002.62cm-1
974.70cm-1
816.24cm-1
895.31cm-1
749.88cm
615.84cm
716.33cm-1
684.98cm-1

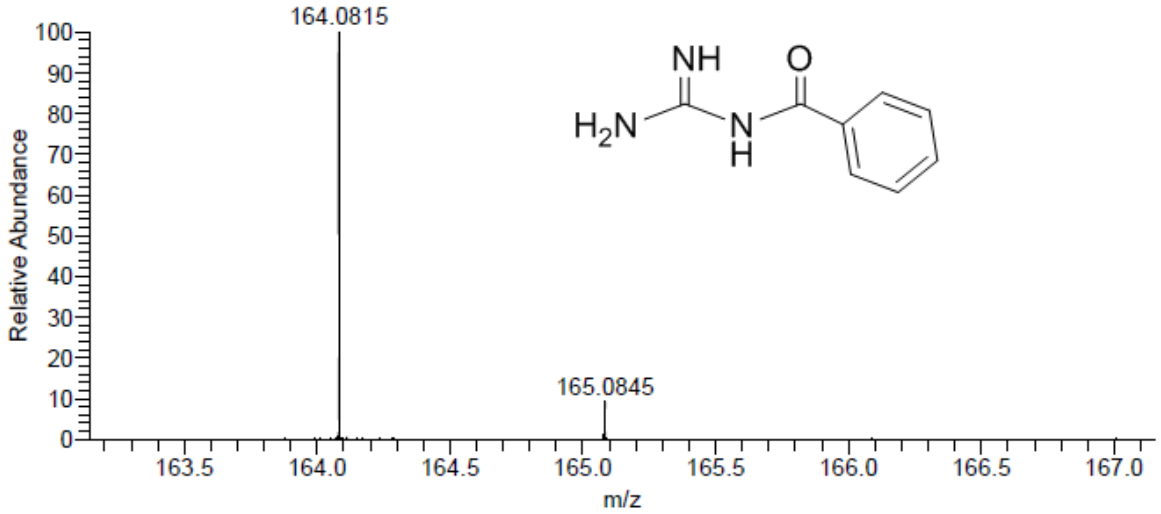
164.0815
165.0845
Relative Abundance
m/z
NH
O
H_2N
N
H

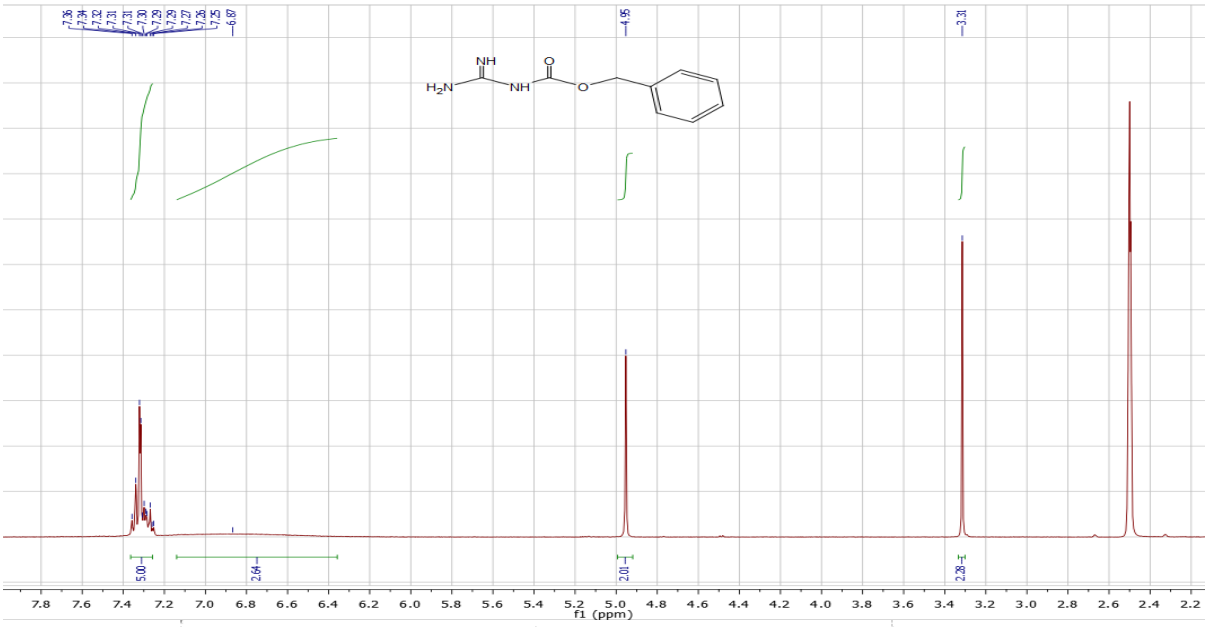
NH
O
H_2N
NH
O
f1 (ppm)

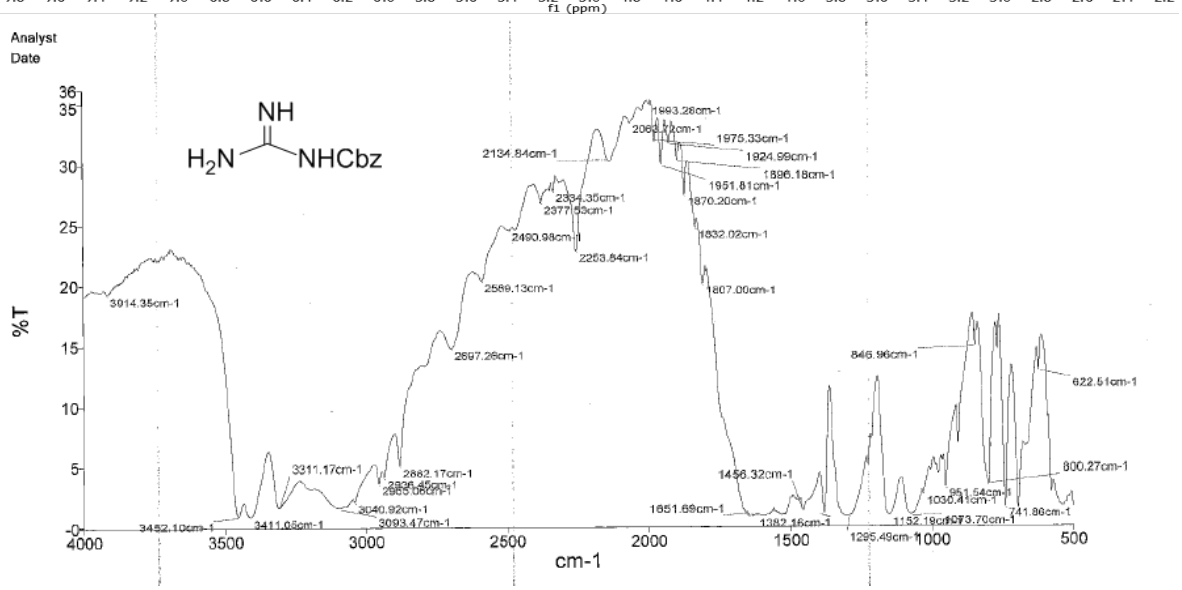
Analyst
Date
NH
H_2N
NHCbz
%T
cm-1
3914.35cm-1
3311.17cm-1
3452.10cm-1
3411.08cm-1
2882.17cm-1
3040.92cm-1
3093.47cm-1
2697.26cm-1
2589.13cm-1
2490.98cm-1
2377.53cm-1
2334.35cm-1
2253.84cm-1
2134.84cm-1
1993.26cm-1
1975.33cm-1
1924.99cm-1
1896.18cm-1
1951.81cm-1
1870.20cm-1
1832.02cm-1
1807.00cm-1
1651.69cm-1
1456.32cm-1
1382.16cm-1
1295.49cm-1
1152.19cm-1
1073.70cm-1
1030.41cm-1
951.54cm-1
846.96cm-1
800.27cm-1
741.86cm-1
622.51cm-1

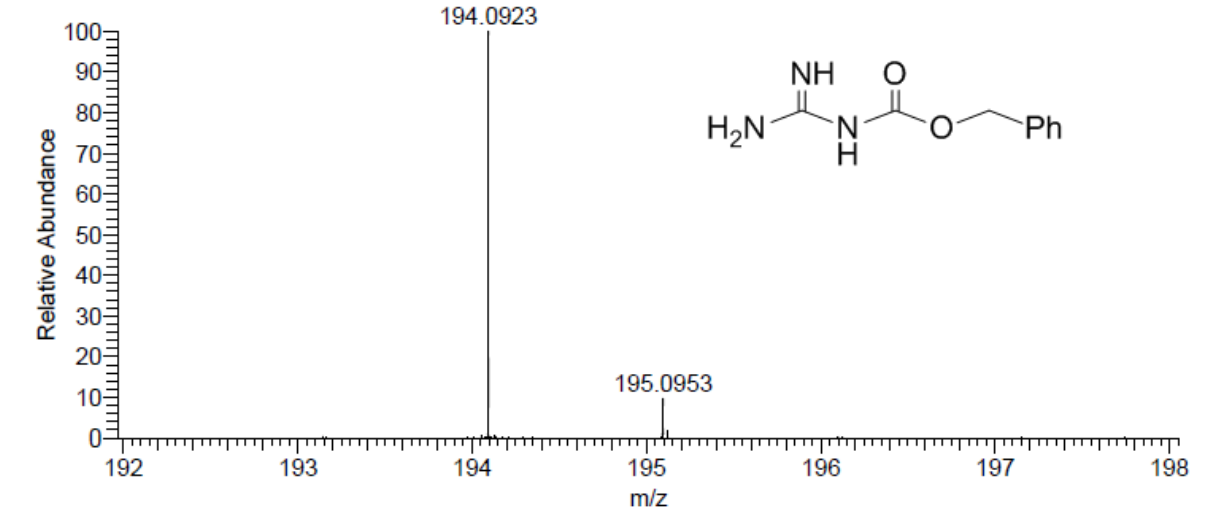
194.0923
195.0953
Relative Abundance
m/z
NH
O
H2N
N
H
O
Ph

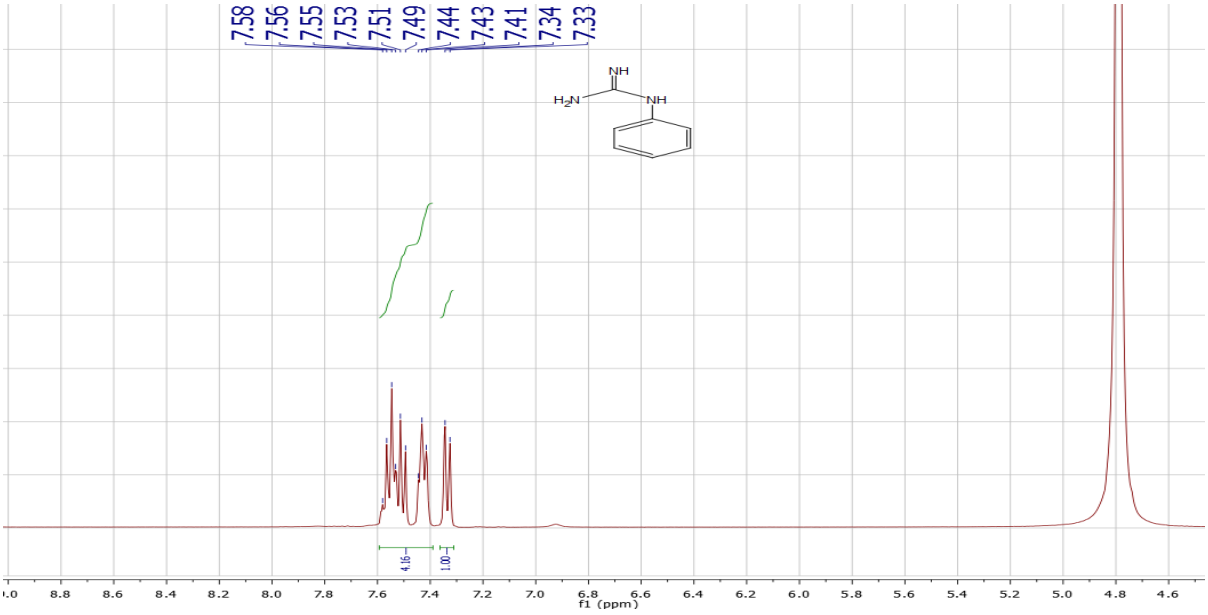
7.58
7.56
7.55
7.53
7.51
7.49
7.44
7.43
7.41
7.34
7.33
NH
H2N
NH
4.16
1.00
f1 (ppm)


NH
H2N
NHPh
%T
cm-1
4000
3500
3000
2500
2000
1500
1000
500
3953.32cm-1
3347.17cm-1
3170.88cm-1
2590.88cm-1
2425.49cm-1
2397.70cm-1
2365.61cm-1
1989.54cm-1
1965.72cm-1
1907.76cm-1
1846.41cm-1
1801.51cm-1
1764.22cm-1
1597.97cm-1
1582.44cm-1
1629.10cm-1
1675.67cm-1
1493.97cm-1
1384.30cm-1
1194.32cm-1
1150.01cm-1
1112.72cm-1
1089.95cm-1
1030.25cm-1
826.23cm-1
744.19cm-1
683.72cm-1
616.01cm-1
589.86cm-1
526.04cm-1
475.62cm-1
420.18cm-1

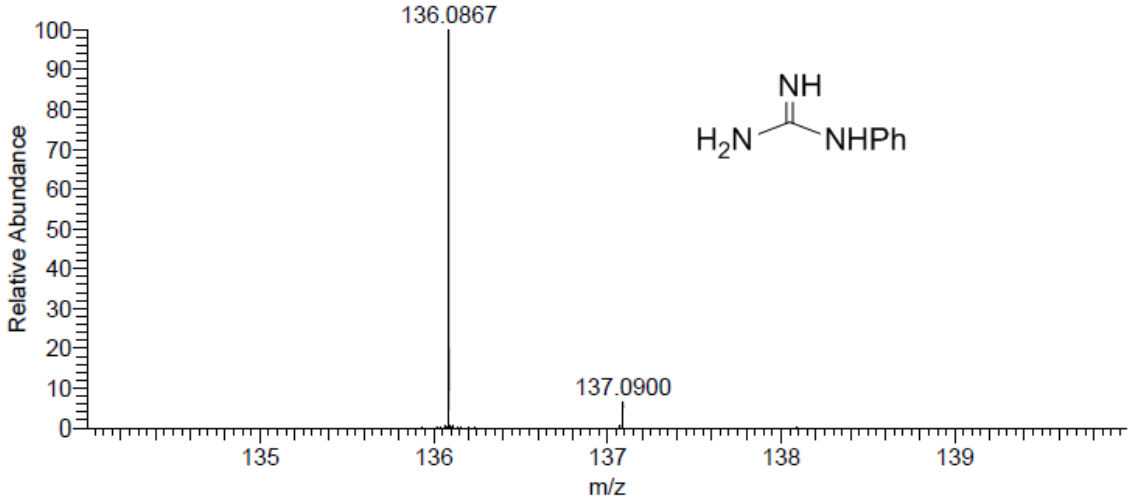
136.0867
137.0900
Relative Abundance
m/z
NH
H2N
NHPh

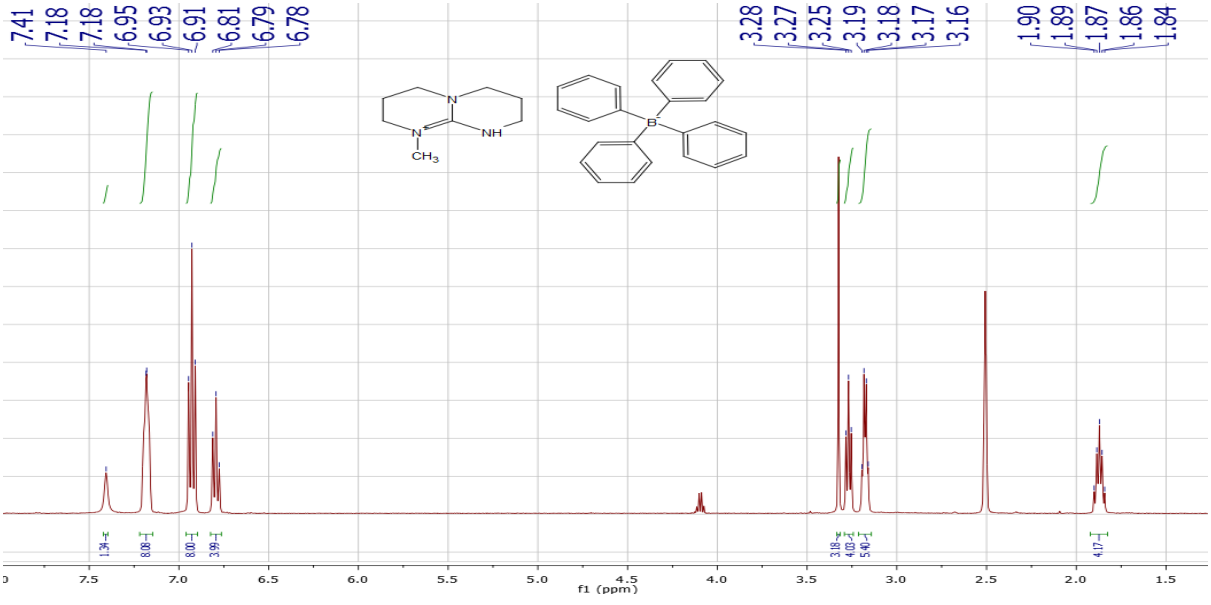
7.41
7.18
7.18
6.95
6.93
6.91
6.81
6.79
6.78
3.28
3.27
3.25
3.19
3.18
3.17
3.16
1.90
1.89
1.87
1.86
1.84
N
NH
CH3
B
f1 (ppm)

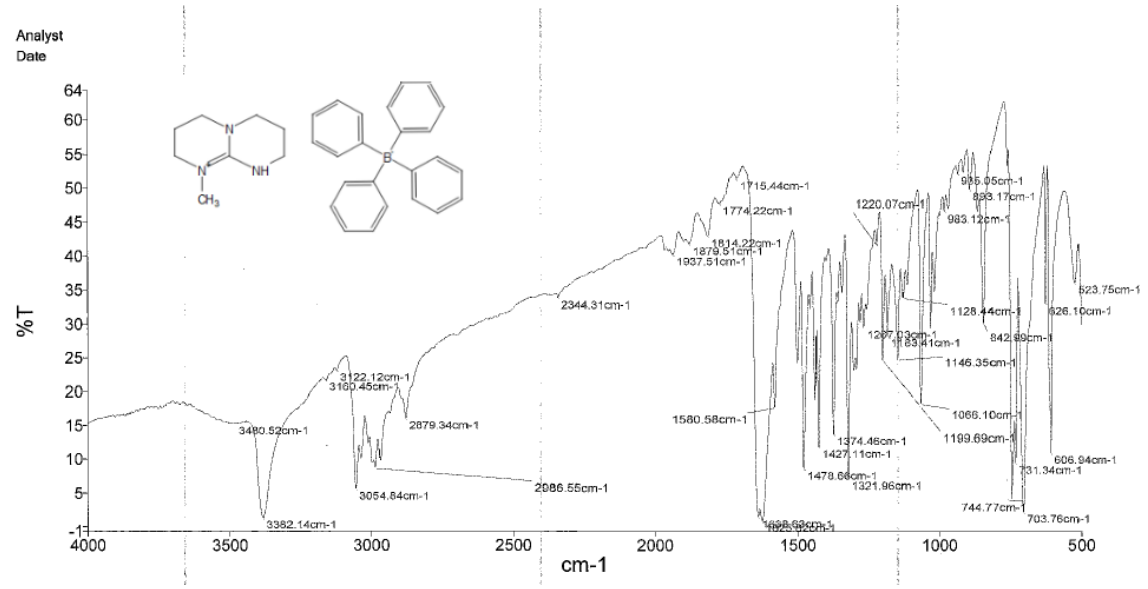
Analyst
Date
%T
cm-1
3480.52cm-1
3382.14cm-1
3122.12cm-1
3160.45cm-1
2879.34cm-1
3054.84cm-1
2086.55cm-1
2344.31cm-1
1715.44cm-1
1774.22cm-1
1814.22cm-1
1879.51cm-1
1937.51cm-1
1580.58cm-1
1220.07cm-1
1374.46cm-1
1427.11cm-1
1478.66cm-1
1321.96cm-1
1207.93cm-1
1183.41cm-1
1146.35cm-1
1066.10cm-1
1199.69cm-1
1128.44cm-1
935.05cm-1
893.17cm-1
983.12cm-1
842.89cm-1
744.77cm-1
703.76cm-1
731.34cm-1
606.94cm-1
626.10cm-1
523.75cm-1

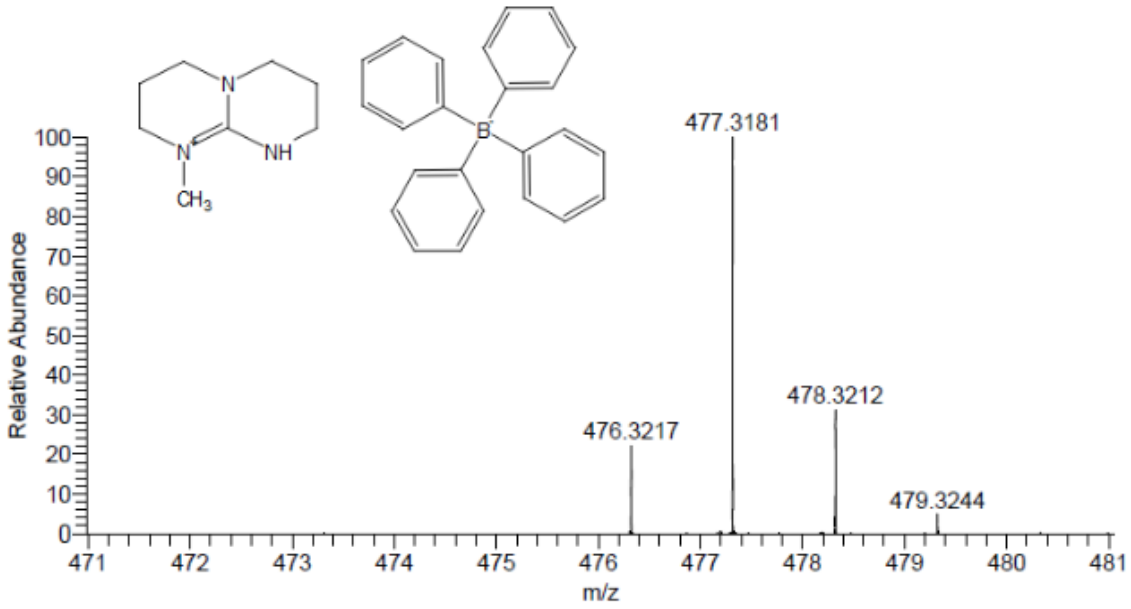
Relative Abundance
m/z
477.3181
478.3212
476.3217
479.3244

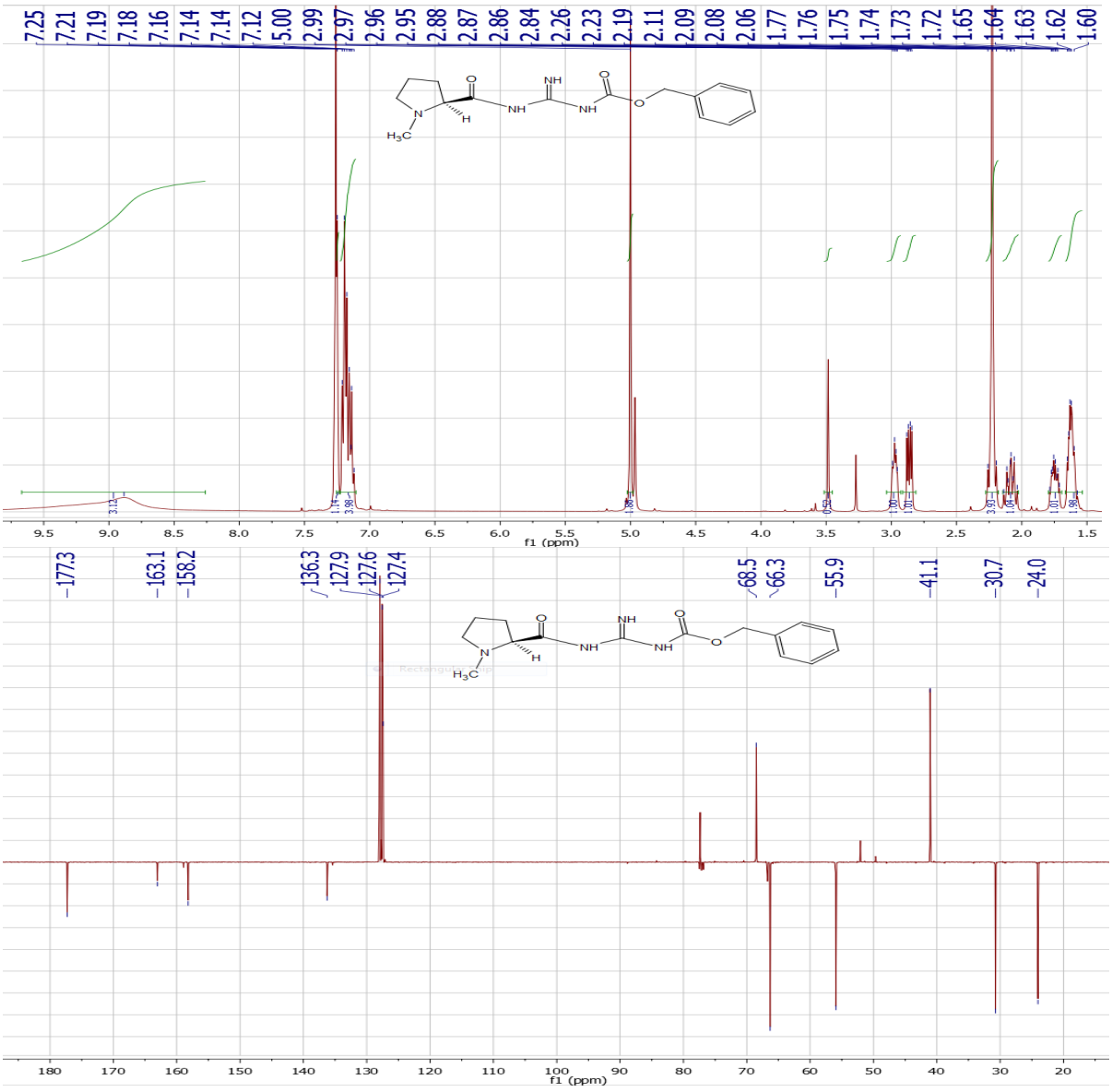
7.25
7.21
7.19
7.18
7.16
7.14
7.14
7.12
5.00
2.99
2.97
2.96
2.95
2.88
2.87
2.86
2.84
2.26
2.23
2.19
2.11
2.09
2.08
2.06
1.77
1.76
1.75
1.74
1.73
1.72
1.65
1.64
1.63
1.62
1.60
f1 (ppm)
177.3
163.1
158.2
136.3
127.9
127.6
127.4
68.5
66.3
55.9
41.1
30.7
24.0
f1 (ppm)

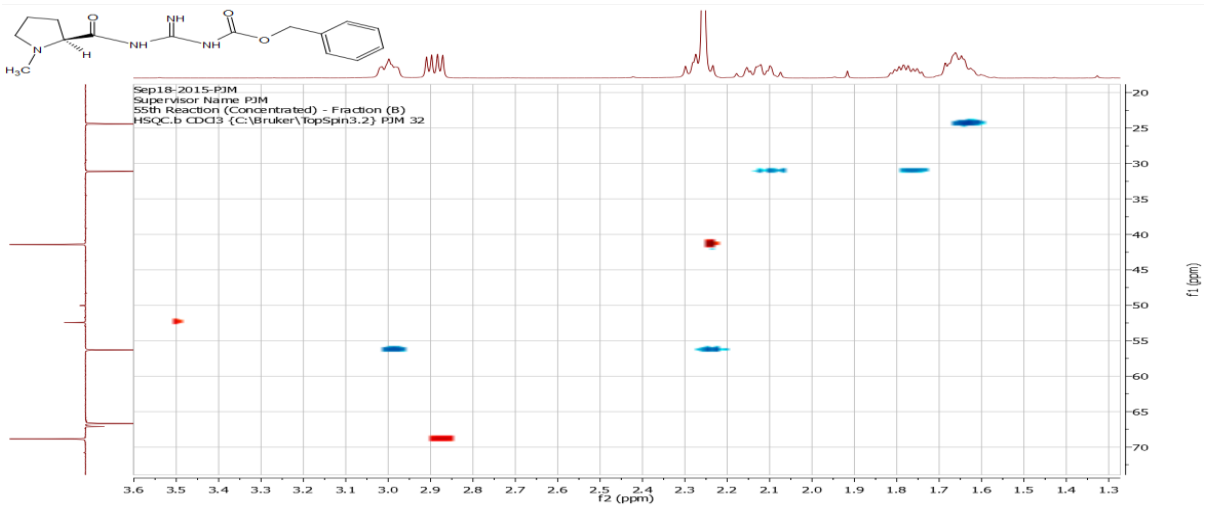
Sep18-2015-PJM
Supervisor Name PJM
55th Reaction (Concentrated) - Fraction (B)
HSQC.b CDCl3 {C:\Bruker\TopSpin3.2} PJM 32
f2 (ppm)
f1 (ppm)

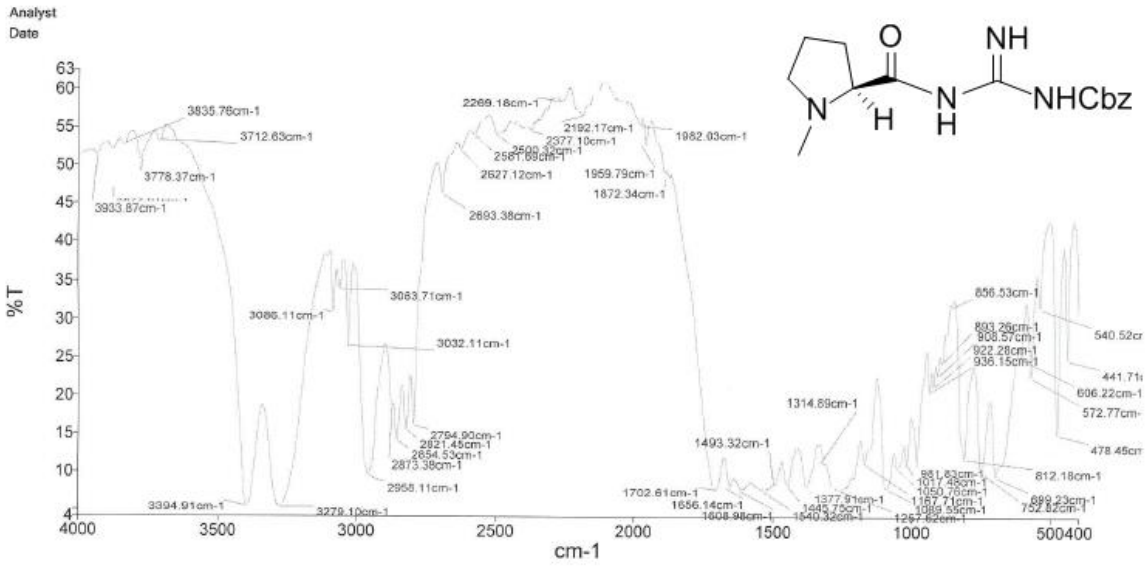
Analyst
Date
%T
cm-1
NHCbz

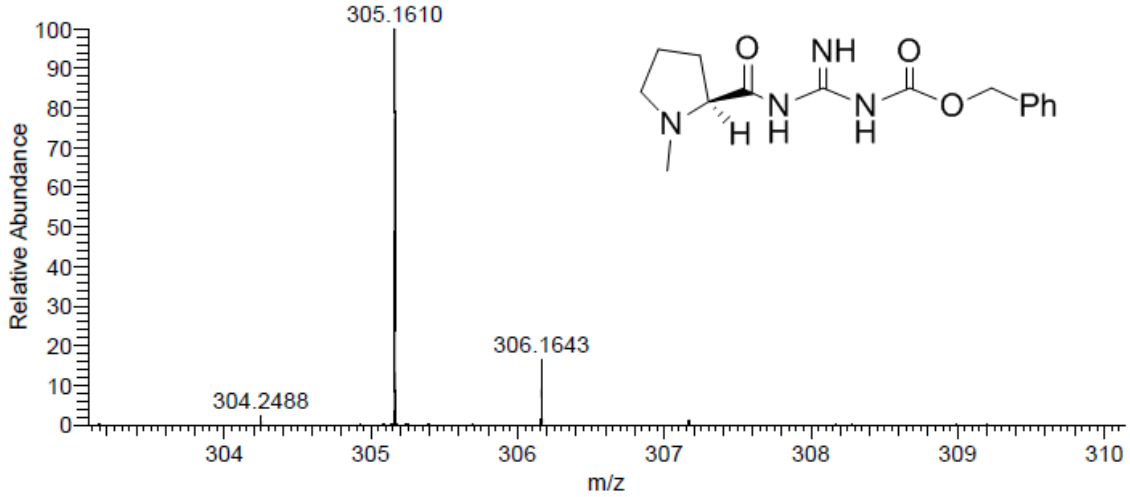
305.1610
306.1643
304.2488
Relative Abundance
m/z
Ph


3889.9
3506.5
2067.7
2055.2
2048.2
2035.8
1301.6
1297.3
1291.3
1286.9
O
NH
NH
NH
O
O
N
H
1.55
10.12
2.00
1.94
0.96
0.93
0.99
1.00
3.00
f1 (ppm)
177.9
163.6
158.5
136.8
136.7
129.5
128.6
128.4
128.1
128.0
127.8
67.0
66.9
59.7
54.2
31.0
24.2
f1 (ppm)

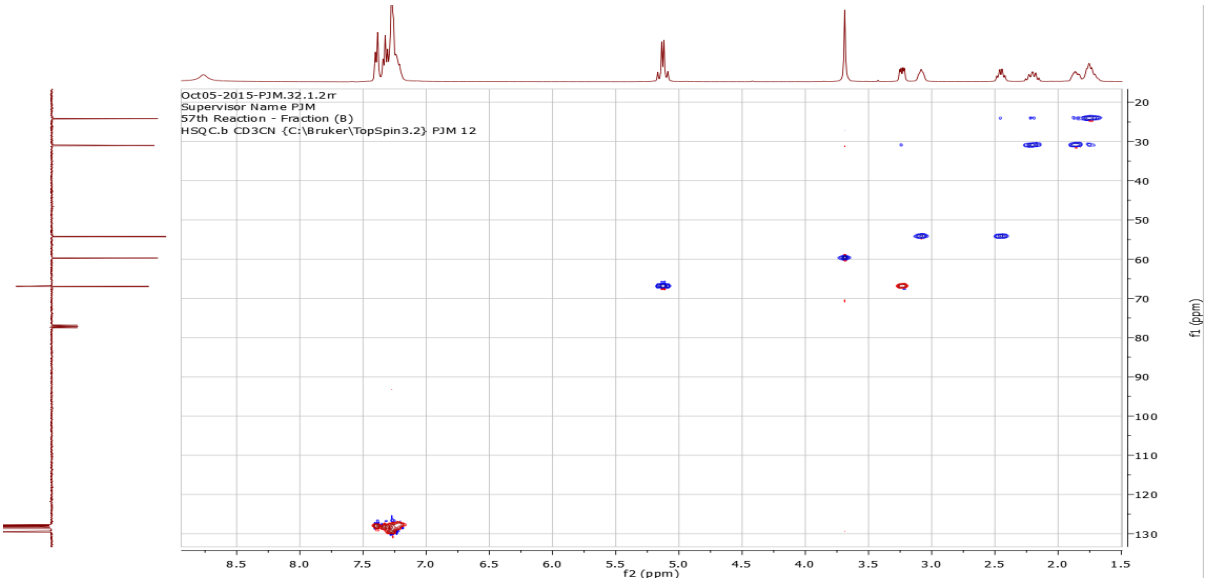
Oct05-2015-PJM.32.1.2rr
Supervisor Name PJM
57h Reaction - Fraction (B)
HSQC.b CD3CN {C:\Bruker\TopSpin3.2} PJM 12
f2 (ppm)
f1 (ppm)

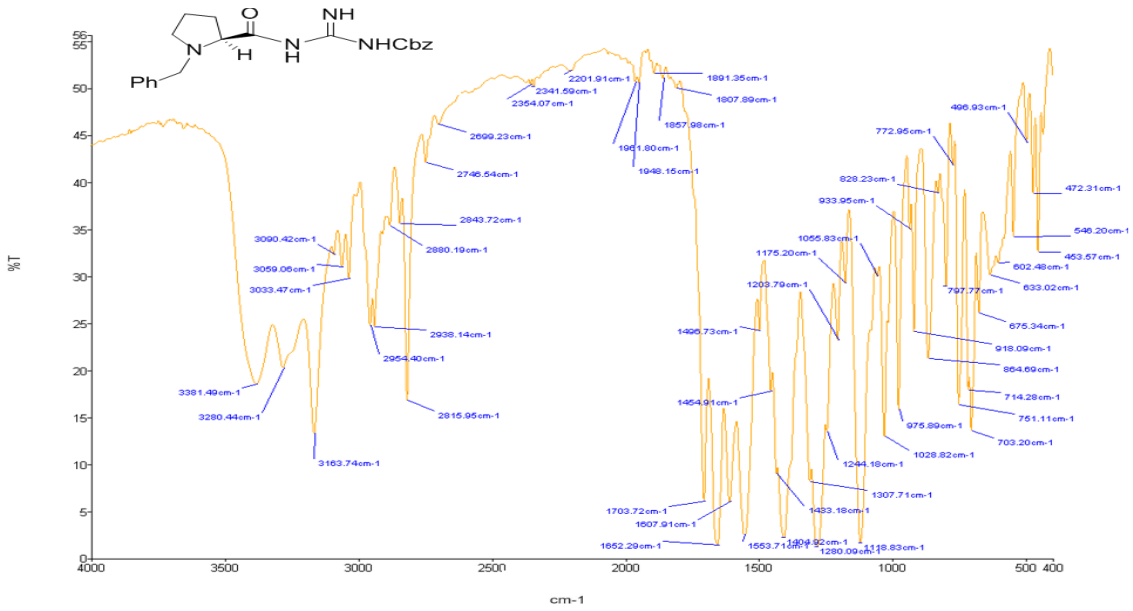
NHCbz
Ph
%T
cm-1

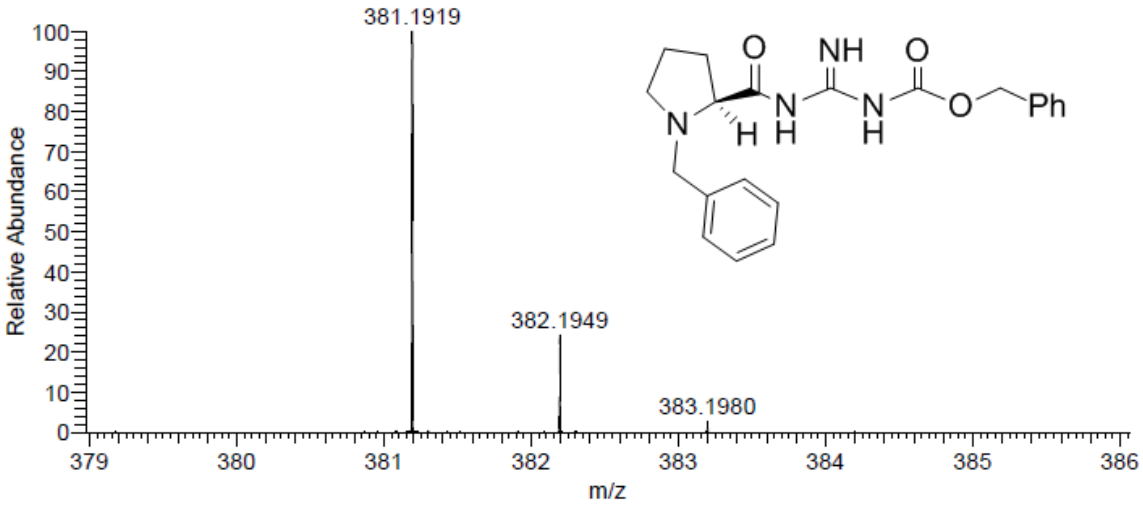
381.1919
382.1949
383.1980
Relative Abundance
m/z
Ph

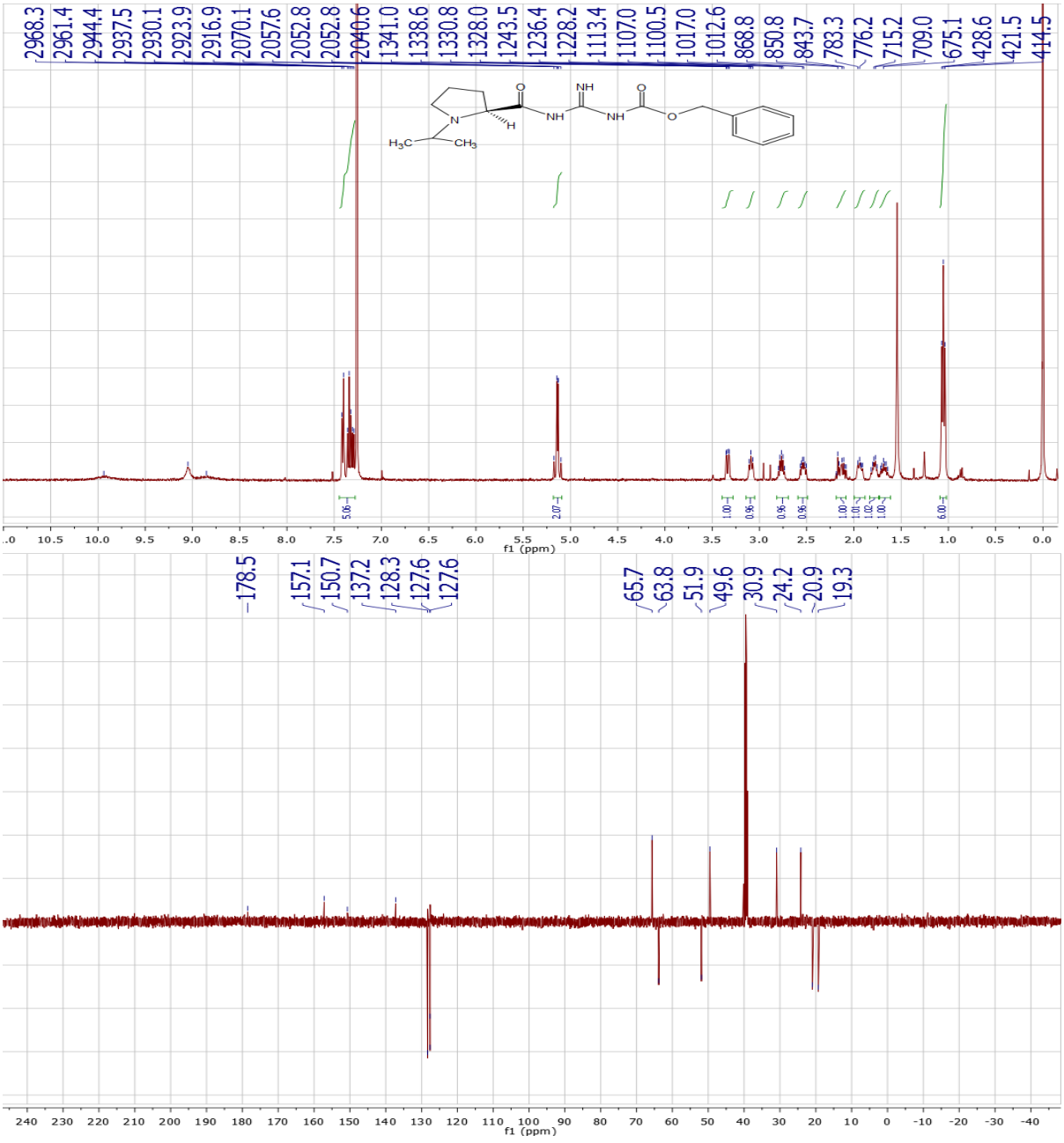
2968.3
2961.4
2944.4
2937.5
2930.1
2923.9
2916.9
2070.1
2057.6
2052.8
2052.8
2040.6
1341.0
1338.6
1330.8
1328.0
1243.5
1236.4
1228.2
1113.4
1107.0
1100.5
1017.0
1012.6
868.8
850.8
843.7
783.3
776.2
715.2
709.0
675.1
428.6
421.5
414.5
f1 (ppm)
178.5
157.1
150.7
137.2
128.3
127.6
127.6
65.7
63.8
51.9
49.6
30.9
24.2
20.9
19.3
f1 (ppm)

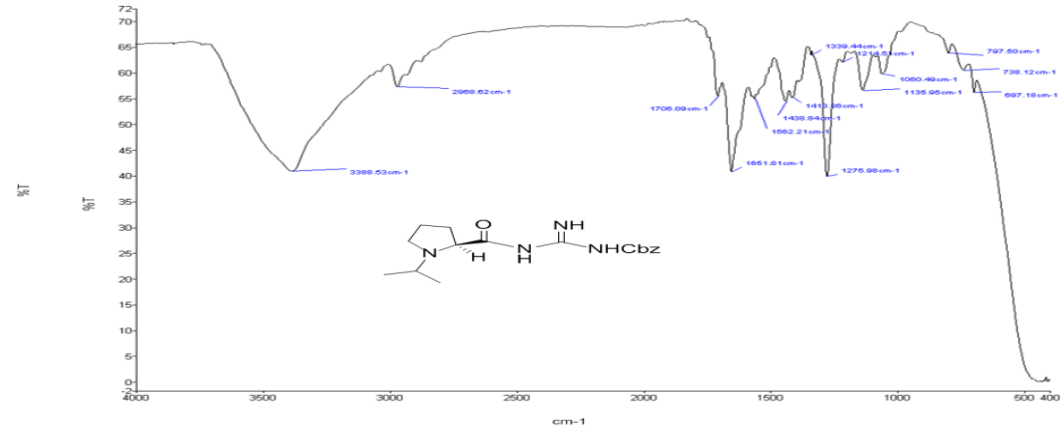
%T
cm-1
3388.53cm-1
2968.62cm-1
1706.09cm-1
1651.81cm-1
1562.21cm-1
1439.84cm-1
1413.36cm-1
1339.44cm-1
1275.98cm-1
1135.95cm-1
1060.49cm-1
797.50cm-1
738.12cm-1
697.19cm-1
NH
NHCbz

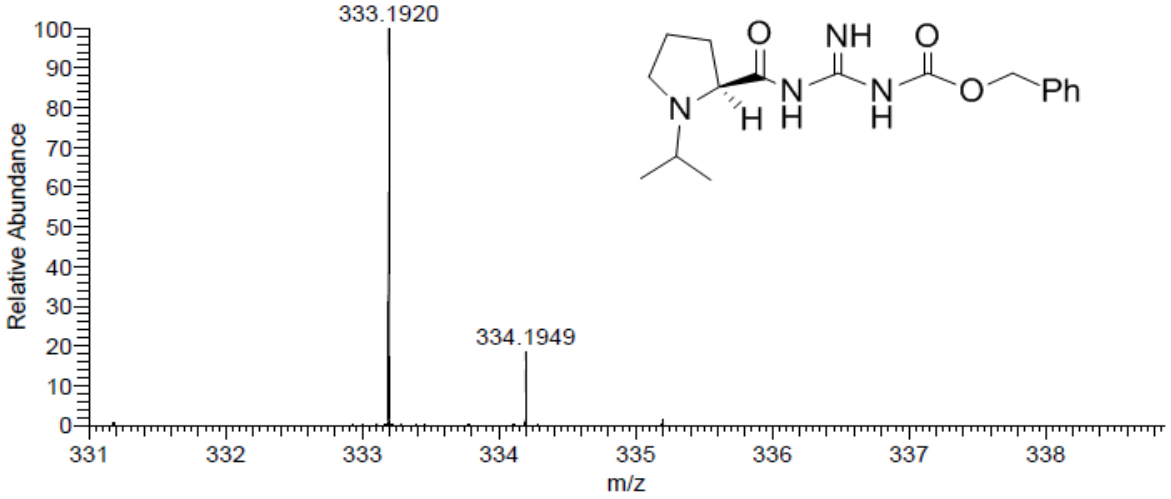
333.1920
334.1949
Relative Abundance
m/z
O
NH
O
N
H
N
H
N
H
O
Ph

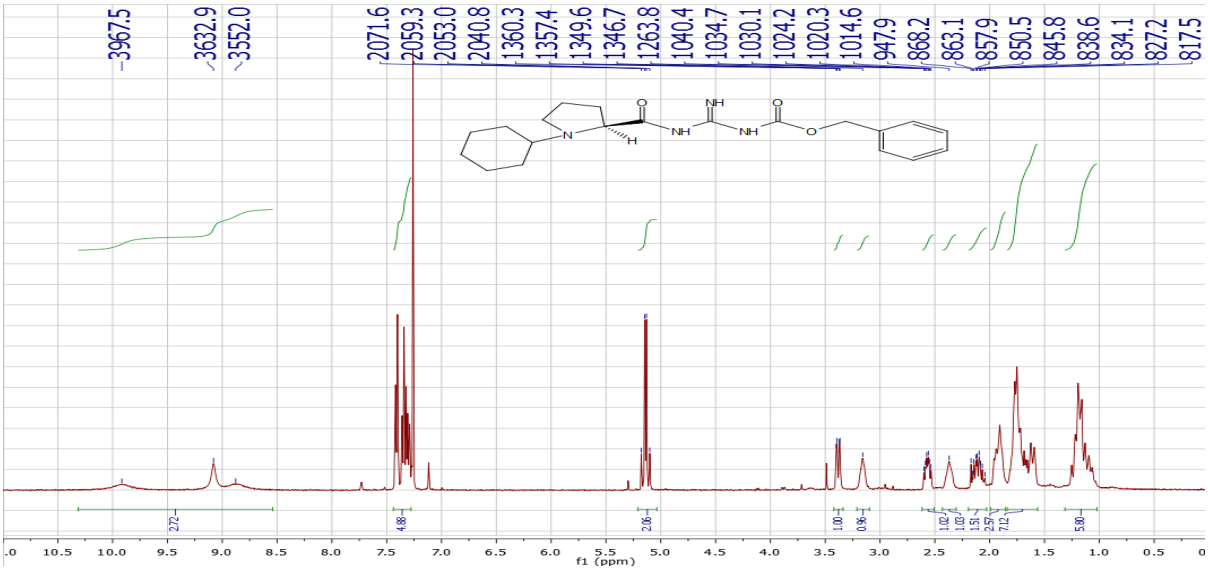
3967.5
3632.9
3552.0
2071.6
2059.3
2053.0
2040.8
1360.3
1357.4
1349.6
1346.7
1263.8
1040.4
1034.7
1030.1
1024.2
1020.3
1014.6
947.9
868.2
863.1
857.9
850.5
845.8
838.6
834.1
827.2
817.5
f1 (ppm)

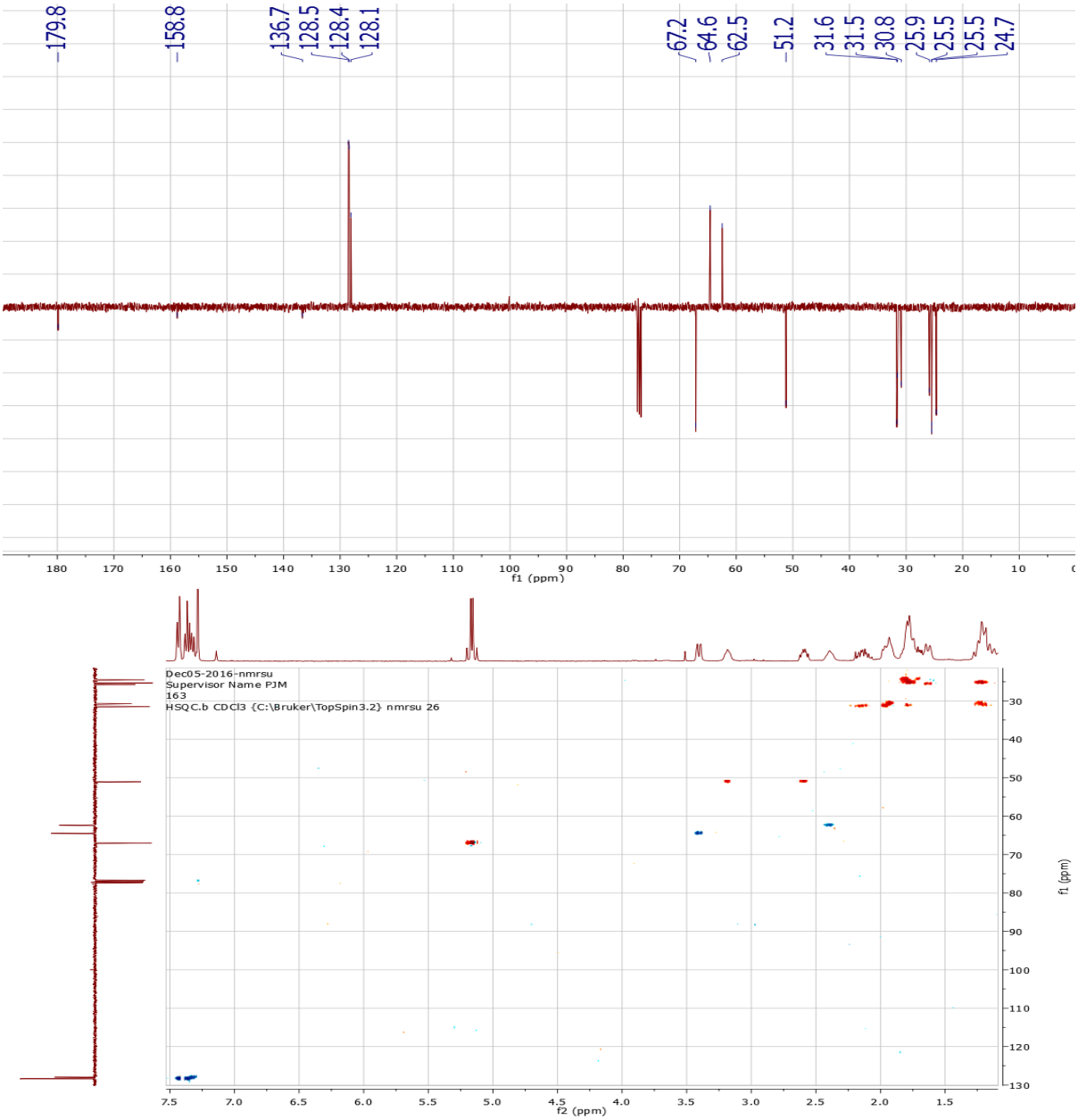
179.8
158.8
136.7
128.5
128.4
128.1
67.2
64.6
62.5
51.2
31.6
31.5
30.8
25.9
25.5
25.5
24.7
f1 (ppm)
Dec05-2016-nmrsu
Supervisor Name PJM
163
HSQC.b CDCl3 {C:\Bruker\TopSpin3.2} nmrsu 26
f2 (ppm)
f1 (ppm)

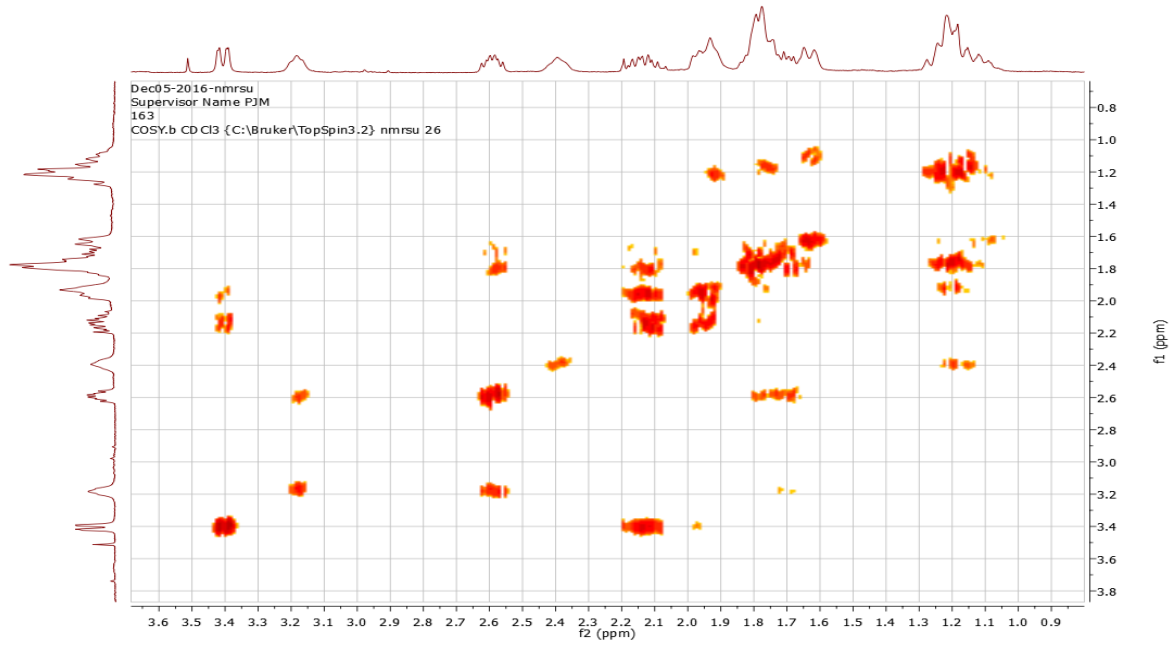
Dec05-2016-nmrsu
Supervisor Name PJM
163
COSY.b CDCl3 {C:\Bruker\TopSpin3.2} nmrsu 26
f2 (ppm)
f1 (ppm)

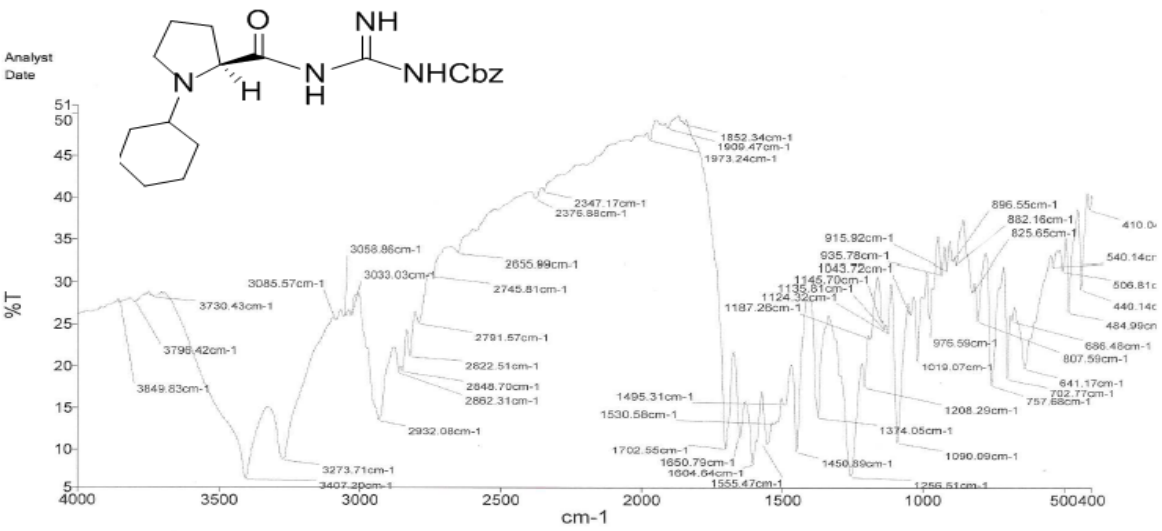
Analyst
Date
O
NH
N
H
N
H
NHCbz
%T
cm-1
3730.43cm-1
3796.42cm-1
3849.83cm-1
3085.57cm-1
3058.86cm-1
3033.03cm-1
2655.89cm-1
2745.81cm-1
2791.57cm-1
2822.51cm-1
2848.70cm-1
2862.31cm-1
2932.08cm-1
3273.71cm-1
3407.2pcm-1
2347.17cm-1
2376.88cm-1
1852.34cm-1
1908.47cm-1
1973.24cm-1
1495.31cm-1
1530.58cm-1
1702.55cm-1
1650.79cm-1
1604.64cm-1
1555.47cm-1
1187.28cm-1
1124.32cm-1
1135.81cm-1
1145.70cm-1
1043.72cm-1
935.78cm-1
915.92cm-1
896.55cm-1
882.16cm-1
825.65cm-1
976.59cm-1
1019.07cm-1
1208.29cm-1
1374.05cm-1
1450.89cm-1
1090.09cm-1
1256.51cm-1
686.48cm-1
807.59cm-1
641.17cm-1
702.77cm-1
757.68cm-1

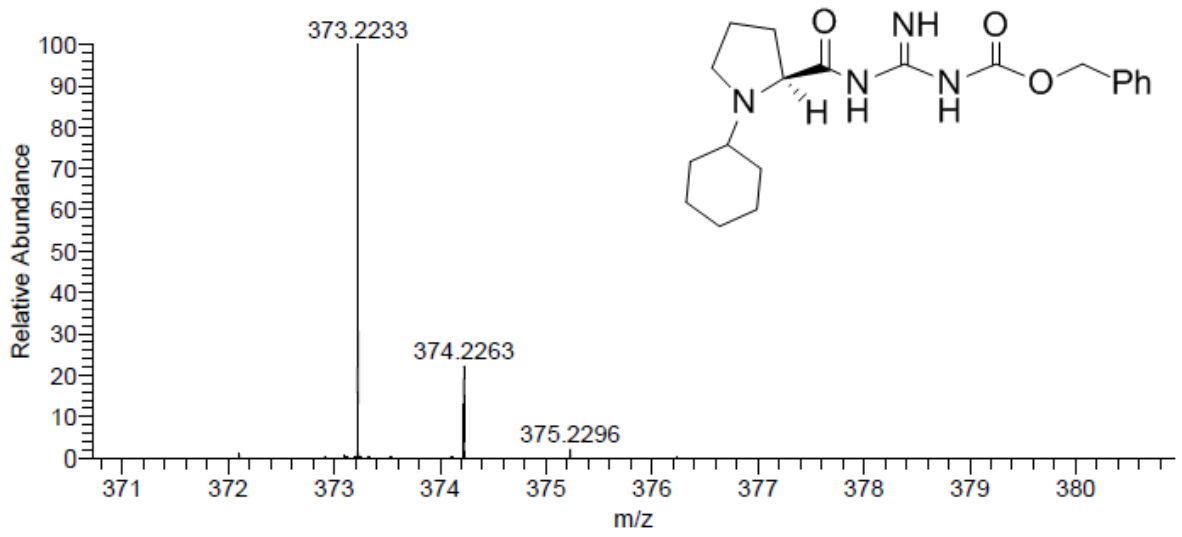
373.2233
374.2263
375.2296
Relative Abundance
m/z
O
NH
O
N
N
N
H
H
H
O
Ph

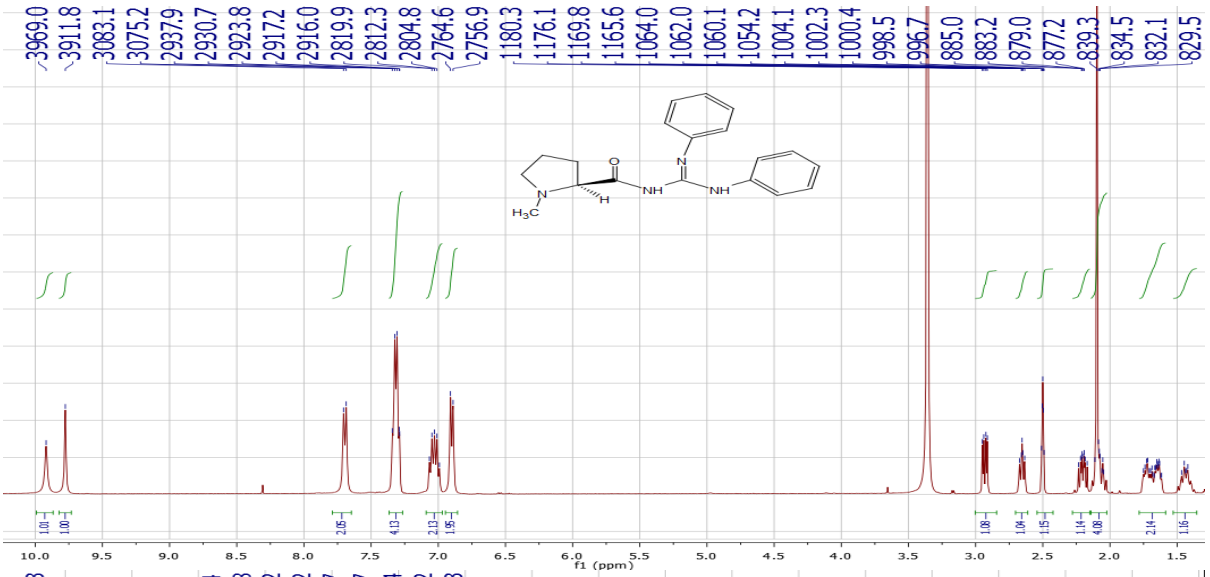
3969.0
3911.8
3083.1
3075.2
2937.9
2930.7
2923.8
2917.2
2916.0
2819.9
2812.3
2804.8
2764.6
2756.9
1180.3
1176.1
1169.8
1165.6
1064.0
1062.0
1060.1
1054.2
1004.1
1002.3
1000.4
998.5
996.7
885.0
883.2
879.0
877.2
839.3
834.5
832.1
829.5
f1 (ppm)

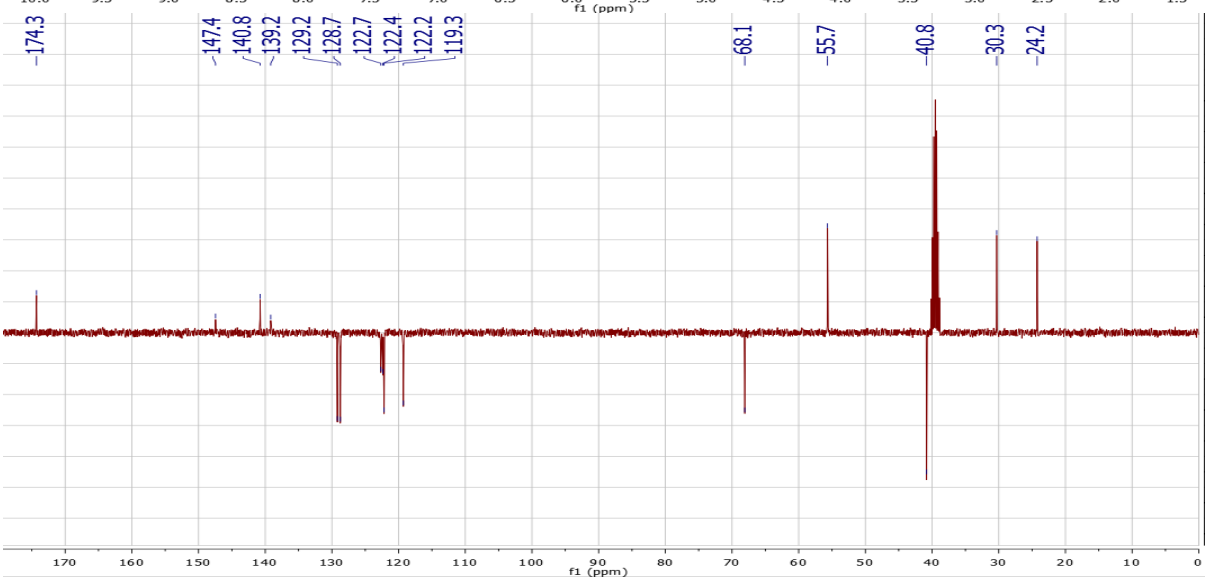
174.3
147.4
140.8
139.2
129.2
128.7
122.7
122.4
122.2
119.3
68.1
55.7
40.8
30.3
24.2
f1 (ppm)

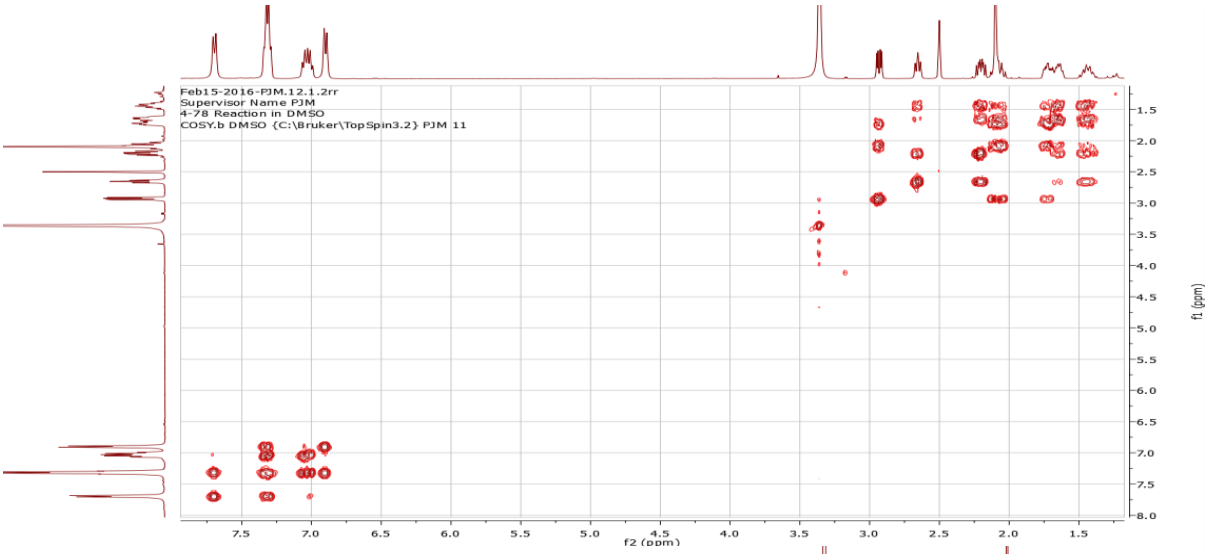
Feb15-2016-PJM.12.1.2rr
Supervisor Name PJM
4-78 Reaction in DMSO
COSY.b DMSO {C:\Bruker\TopSpin3.2} PJM 11
f2 (ppm)
f1 (ppm)

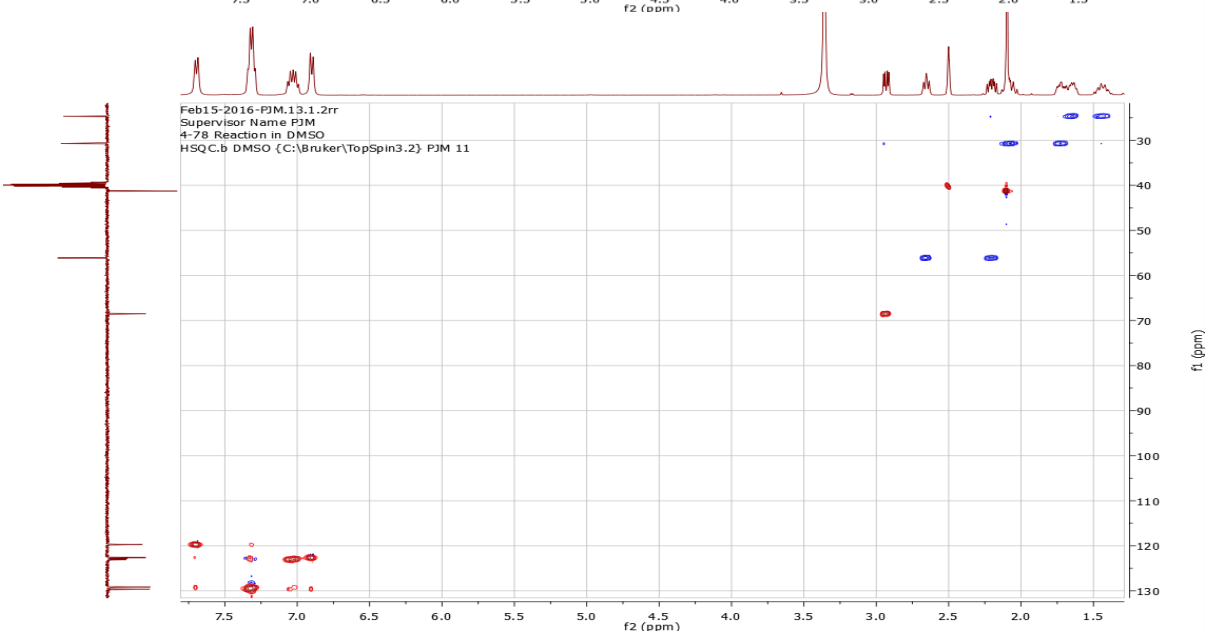
Feb15-2016-PJM.13.1.2rr
Supervisor Name PJM
4-78 Reaction in DMSO
HSQC.b DMSO {C:\Bruker\TopSpin3.2} PJM 11
f2 (ppm)
f1 (ppm)

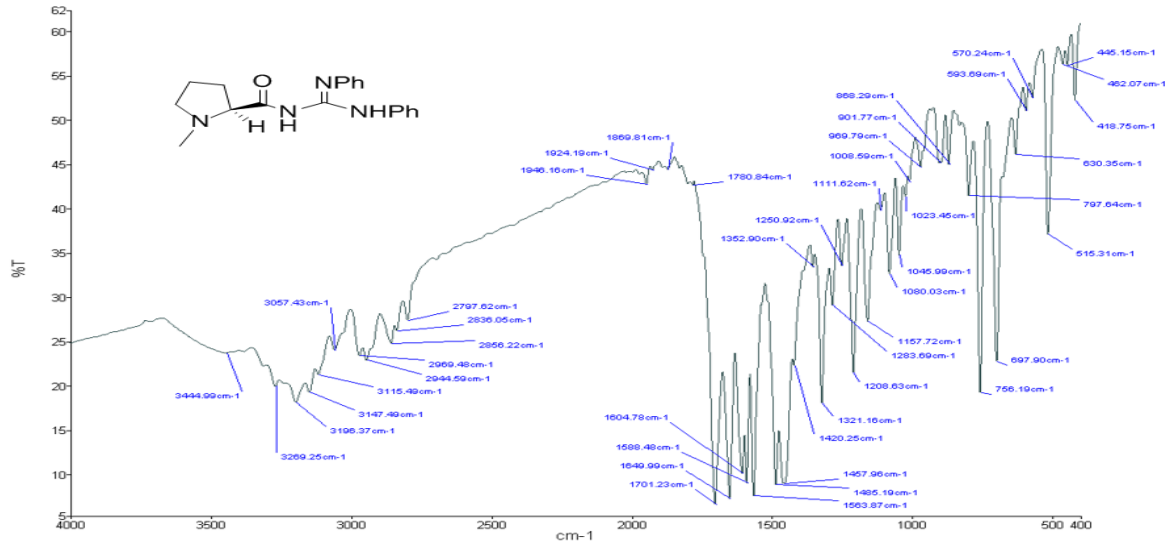
%T
cm-1
3444.99cm-1
3269.25cm-1
3198.37cm-1
3147.49cm-1
3115.49cm-1
2969.48cm-1
2944.59cm-1
2856.22cm-1
2836.05cm-1
2797.62cm-1
3057.43cm-1
1946.16cm-1
1924.19cm-1
1869.81cm-1
1780.84cm-1
1701.23cm-1
1649.99cm-1
1588.48cm-1
1604.78cm-1
1563.87cm-1
1485.19cm-1
1457.96cm-1
1420.25cm-1
1321.16cm-1
1208.63cm-1
1283.69cm-1
1157.72cm-1
1080.03cm-1
1045.99cm-1
1023.45cm-1
1111.62cm-1
1008.59cm-1
969.79cm-1
901.77cm-1
868.29cm-1
1352.90cm-1
1250.92cm-1
756.19cm-1
697.90cm-1
797.64cm-1
630.35cm-1
515.31cm-1
418.75cm-1
462.07cm-1
445.15cm-1
593.69cm-1
570.24cm-1
O
NPh
N
H
N
H
NHPh

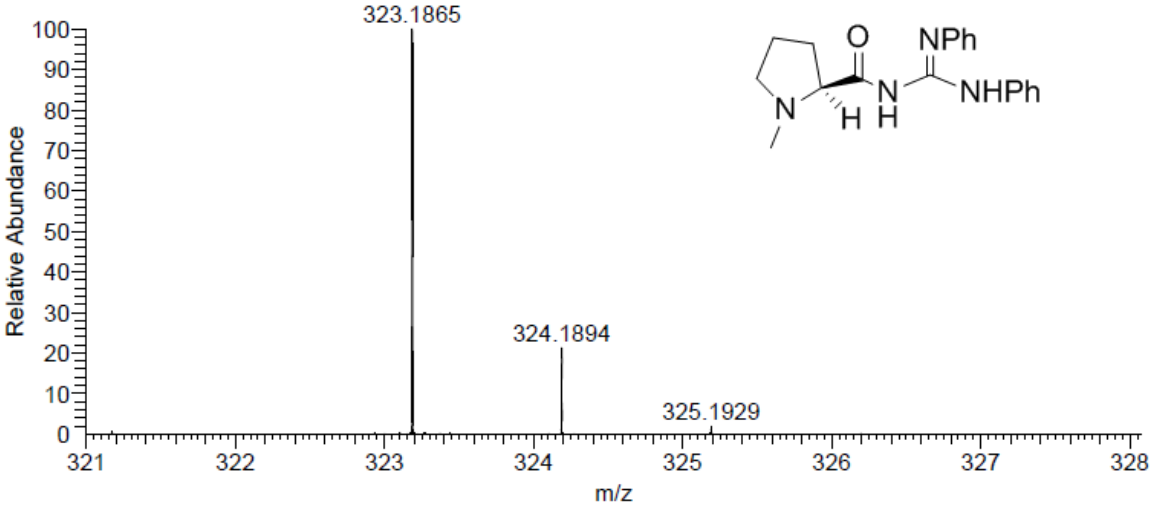
Relative Abundance
m/z
323.1865
324.1894
325.1929
O
NPh
N
H
N
H
NHPh

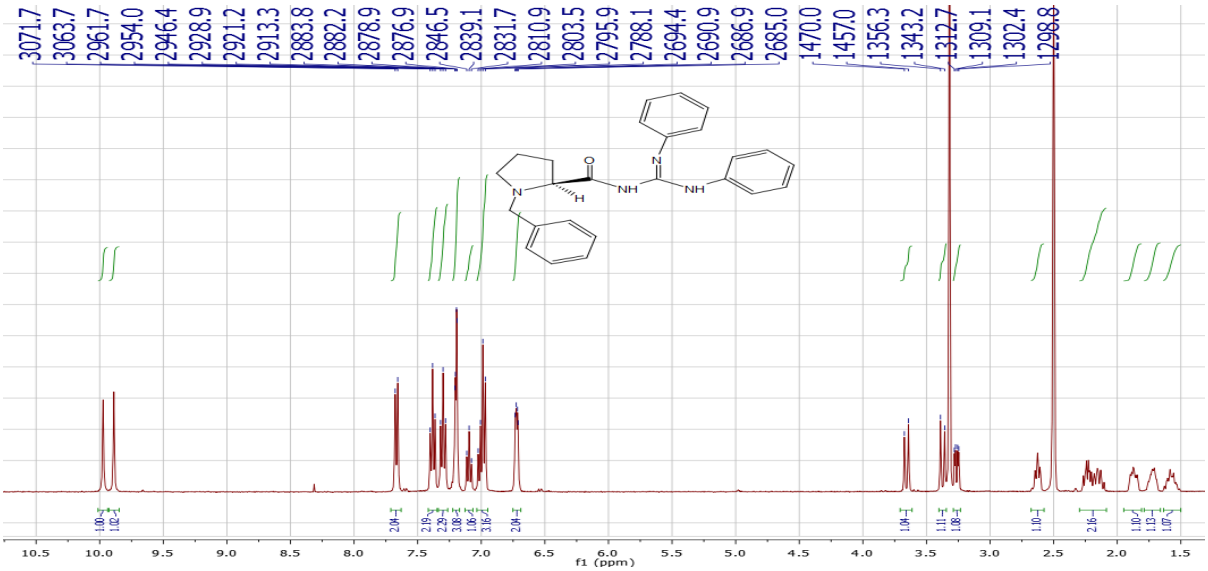
3071.7
3063.7
2961.7
2954.0
2946.4
2928.9
2921.2
2913.3
2883.8
2882.2
2878.9
2876.9
2846.5
2839.1
2831.7
2810.9
2803.5
2795.9
2788.1
2694.4
2690.9
2686.9
2685.0
1470.0
1457.0
1356.3
1343.2
1312.7
1309.1
1302.4
1298.8
O
NH
NH
N
H
N
f1 (ppm)

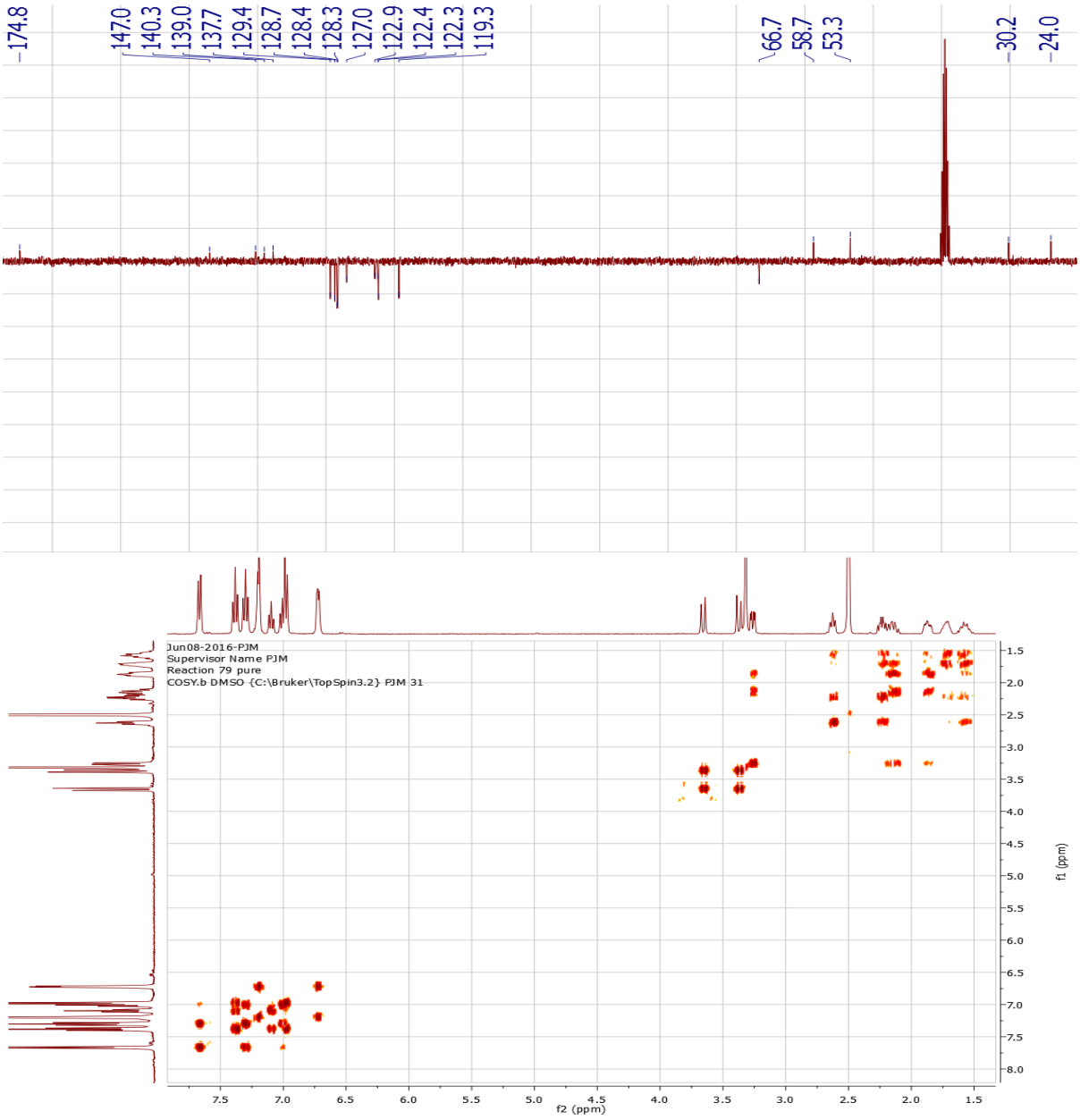
174.8
147.0
140.3
139.0
137.7
129.4
128.7
128.4
128.3
127.0
122.9
122.4
122.3
119.3
66.7
58.7
53.3
30.2
24.0
Jun08-2016-PJM
Supervisor Name PJM
Reaction 79 pure
COSY.b DMSO {C:\Bruker\TopSpin3.2} PJM 31
f2 (ppm)
f1 (ppm)

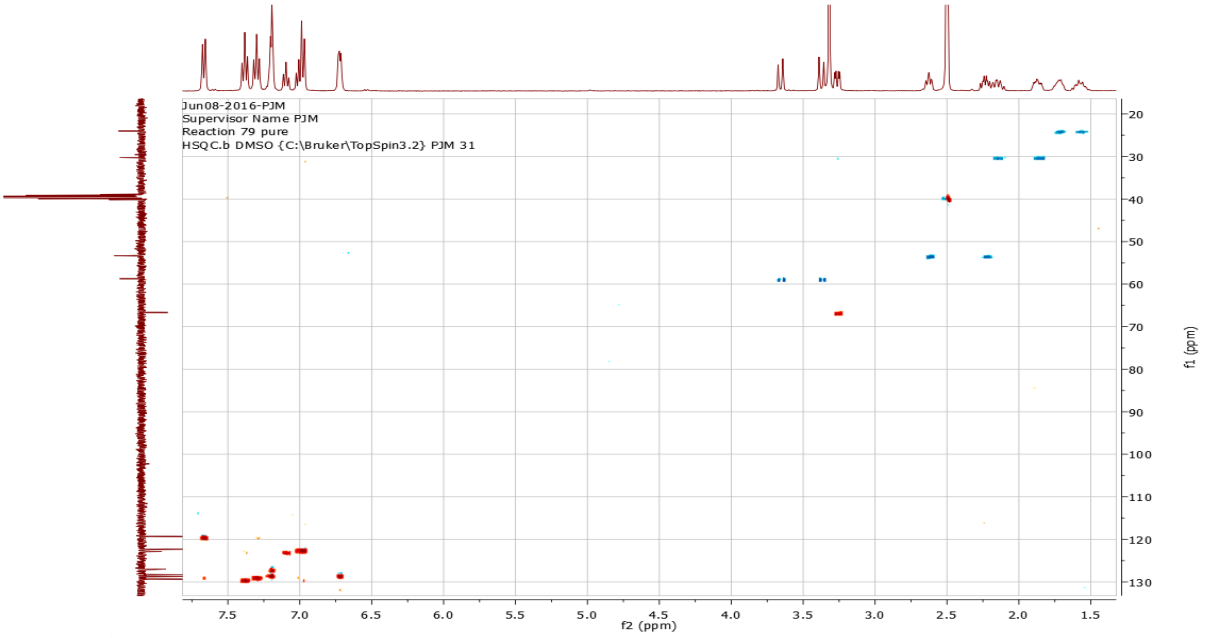
Jun08-2016-PJM
Supervisor Name PJM
Reaction 79 pure
HSQC.b DMSO {C:\Bruker\TopSpin3.2} PJM 31
f2 (ppm)
f1 (ppm)


NPh
NHPh
Ph
%T
cm-1

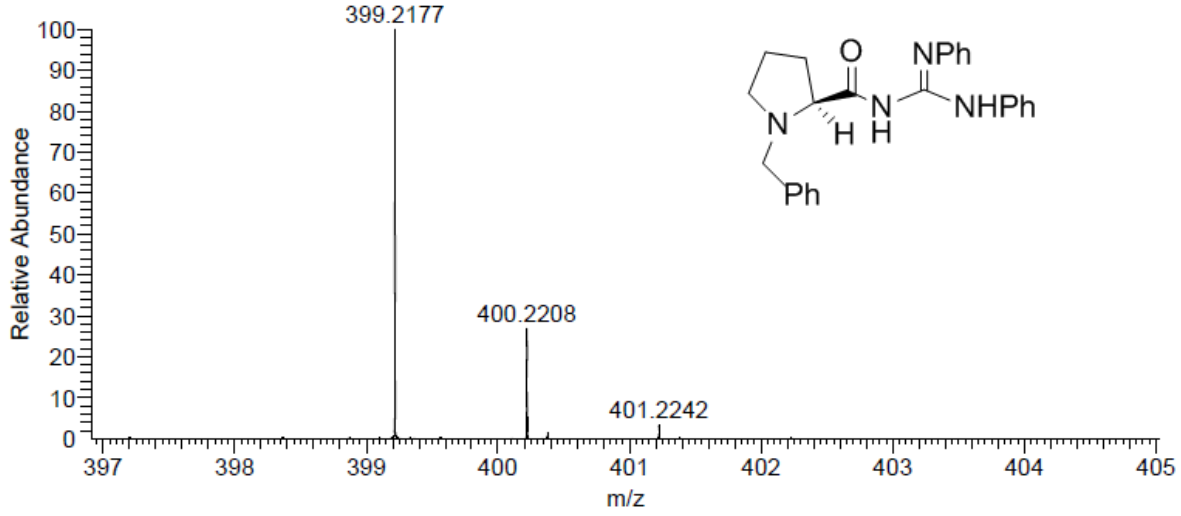
399.2177
400.2208
401.2242
Relative Abundance
m/z
NPh
NHPh
Ph

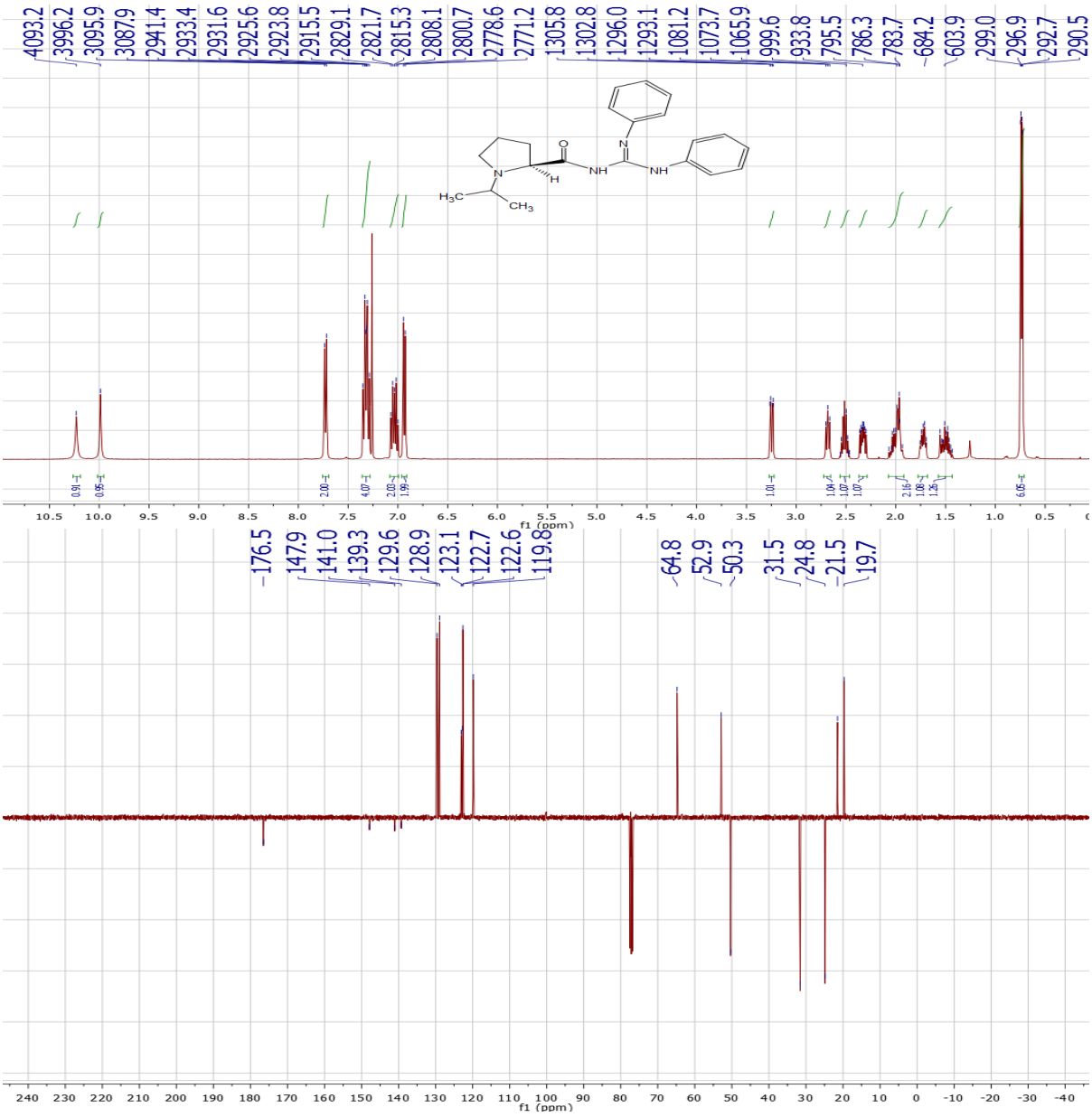
4093.2
3996.2
3095.9
3087.9
2941.4
2933.4
2931.6
2925.6
2923.8
2915.5
2829.1
2821.7
2815.3
2808.1
2800.7
2778.6
2771.2
1305.8
1302.8
1296.0
1293.1
1081.2
1073.7
1065.9
999.6
933.8
795.5
786.3
783.7
684.2
603.9
299.0
296.9
292.7
290.5
O
N
NH
NH
N
H
H3C
CH3
f1 (ppm)

176.5
147.9
141.0
139.3
129.6
128.9
123.1
122.7
122.6
119.8
64.8
52.9
50.3
31.5
24.8
21.5
19.7
f1 (ppm)

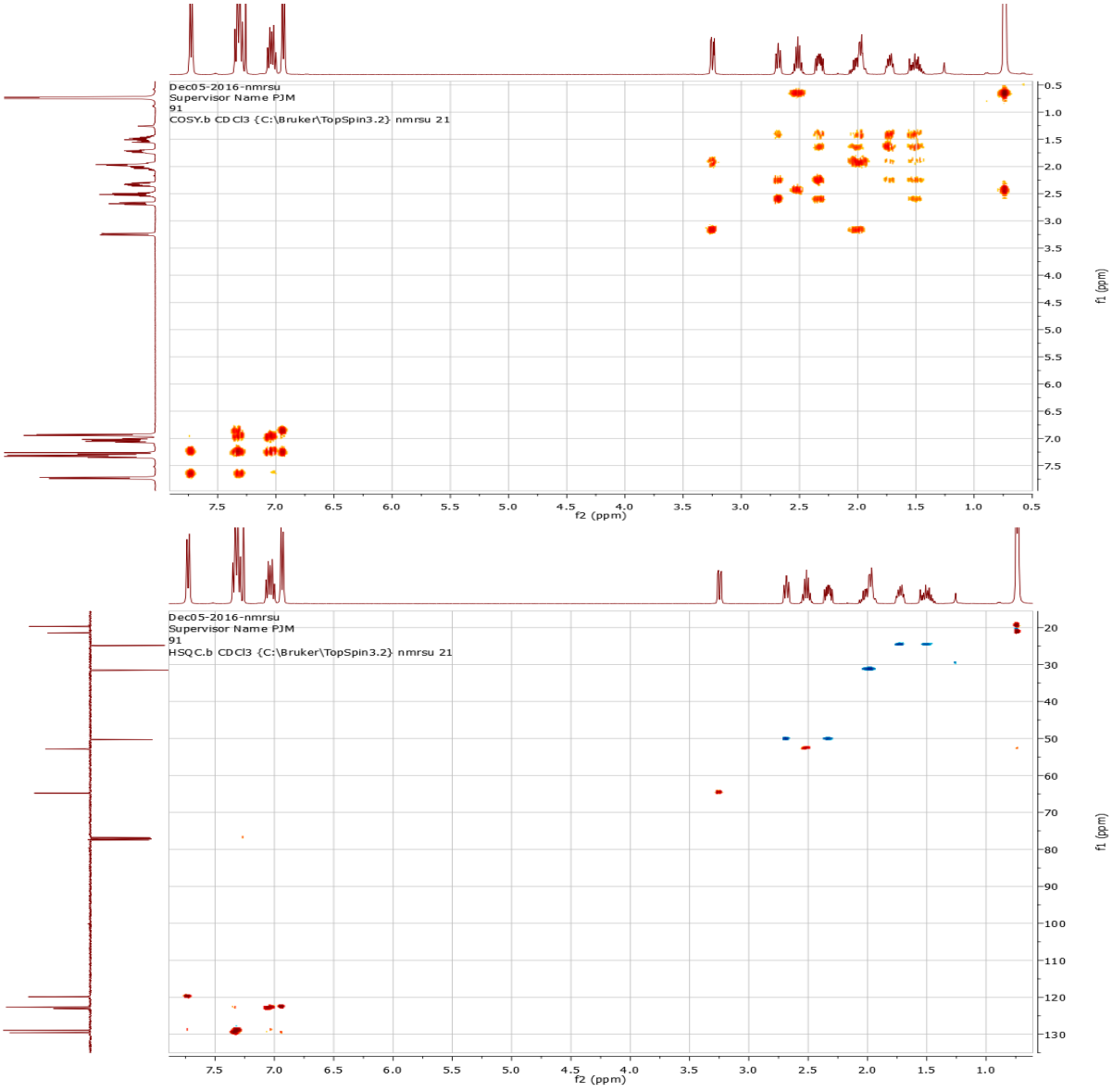
Dec05-2016-nmrsu
Supervisor Name PJM
91
COSY.b CDCl3 {C:\Bruker\TopSpin3.2} nmrsu 21
f2 (ppm)
f1 (ppm)
Dec05-2016-nmrsu
Supervisor Name PJM
91
HSQC.b CDCl3 {C:\Bruker\TopSpin3.2} nmrsu 21
f2 (ppm)
f1 (ppm)

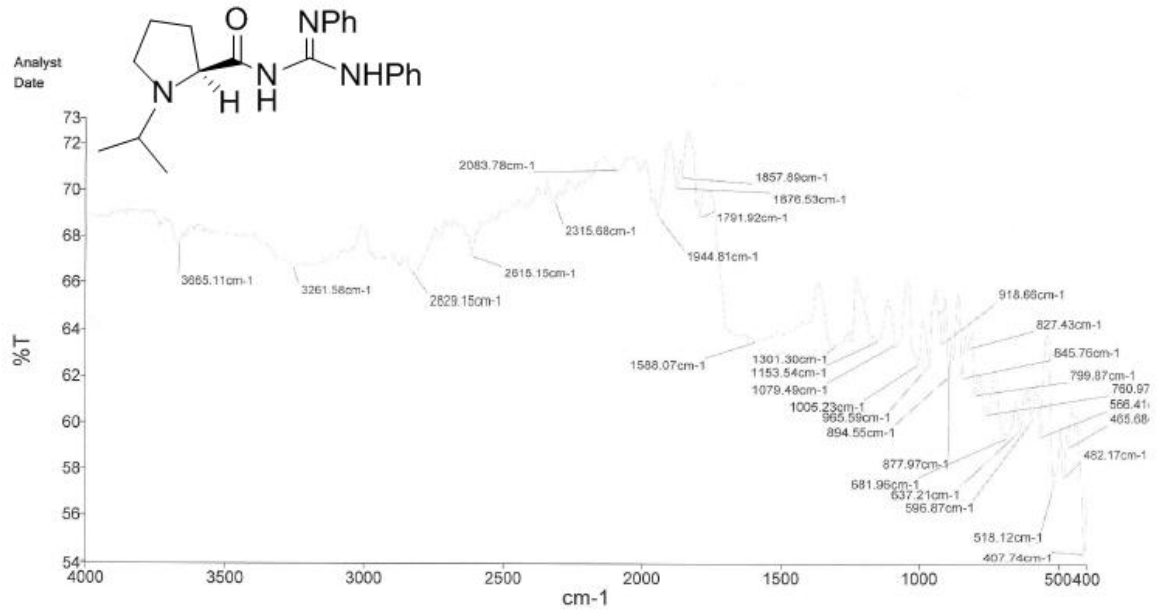
Analyst
Date
O
NPh
N
NHPh
H
N
%T
cm-1
2083.78cm-1
1857.89cm-1
1876.53cm-1
1791.92cm-1
2315.68cm-1
1944.81cm-1
3865.11cm-1
3261.58cm-1
2829.15cm-1
2615.15cm-1
1588.07cm-1
1301.30cm-1
1153.54cm-1
1079.49cm-1
1005.23cm-1
965.59cm-1
894.55cm-1
918.66cm-1
827.43cm-1
845.76cm-1
799.87cm-1
760.97
566.41
465.68
482.17cm-1
877.97cm-1
681.96cm-1
637.21cm-1
596.87cm-1
518.12cm-1
407.74cm-1

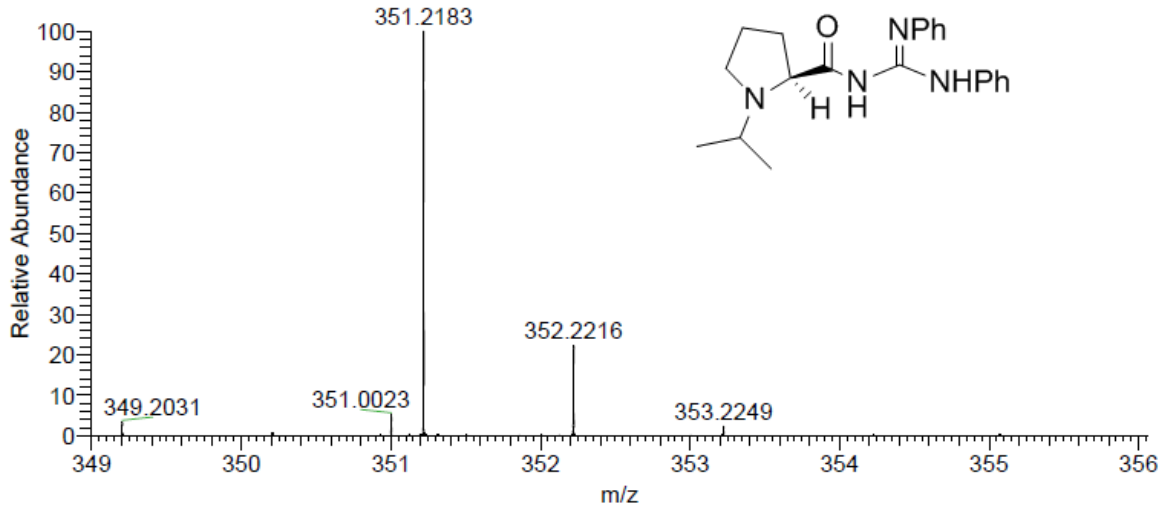
Relative Abundance
m/z
351.2183
352.2216
349.2031
351.0023
353.2249
O
NPh
N
NHPh
H
N

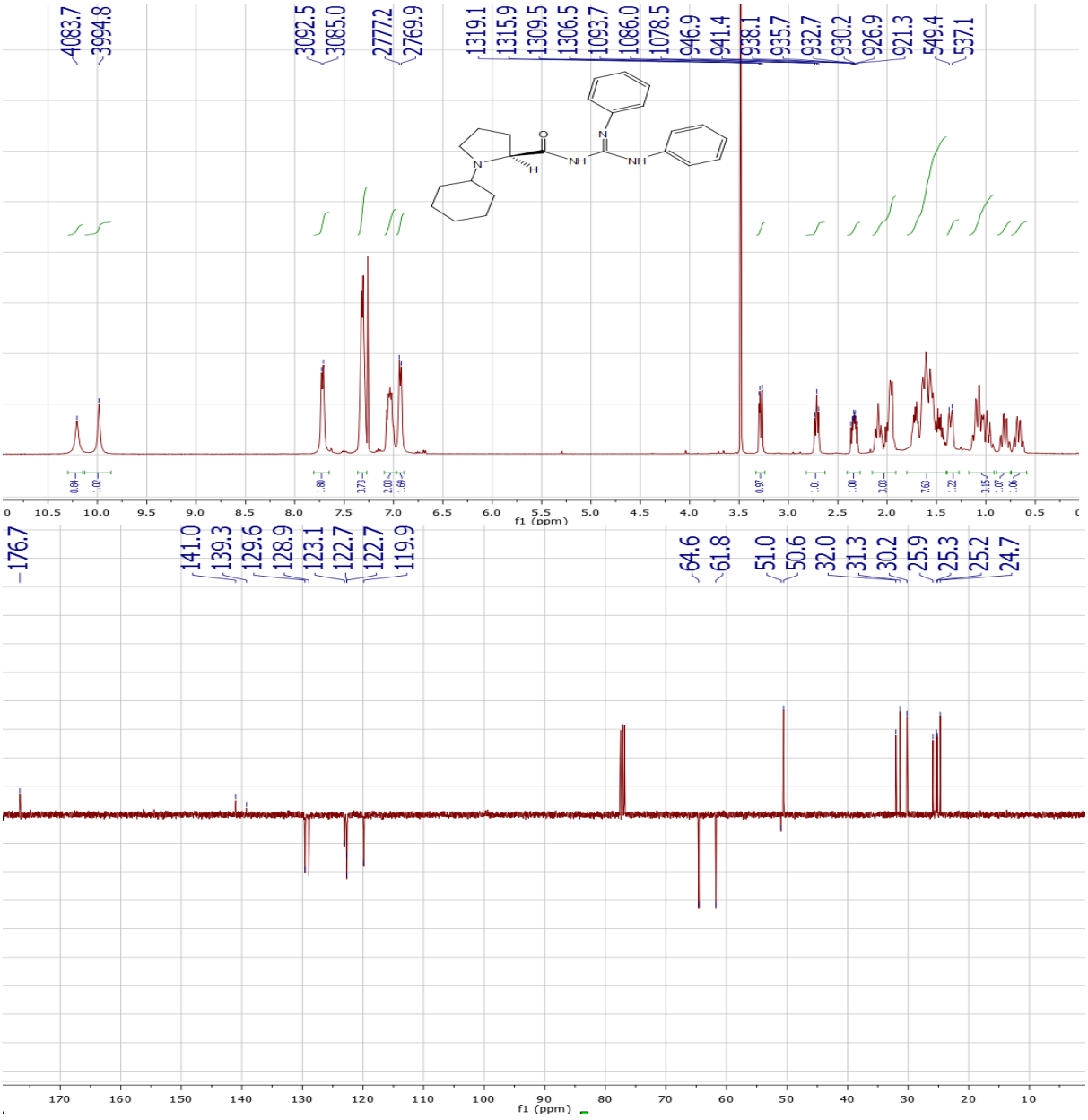
4083.7
3994.8
3092.5
3085.0
2777.2
2769.9
1319.1
1315.9
1309.5
1306.5
1093.7
1086.0
1078.5
946.9
941.4
938.1
935.7
932.7
930.2
926.9
921.3
549.4
537.1
O
N
H
NH
NH
N
f1 (ppm)
176.7
141.0
139.3
129.6
128.9
123.1
122.7
122.7
119.9
64.6
61.8
51.0
50.6
32.0
31.3
30.2
25.9
25.3
25.2
24.7
f1 (ppm)

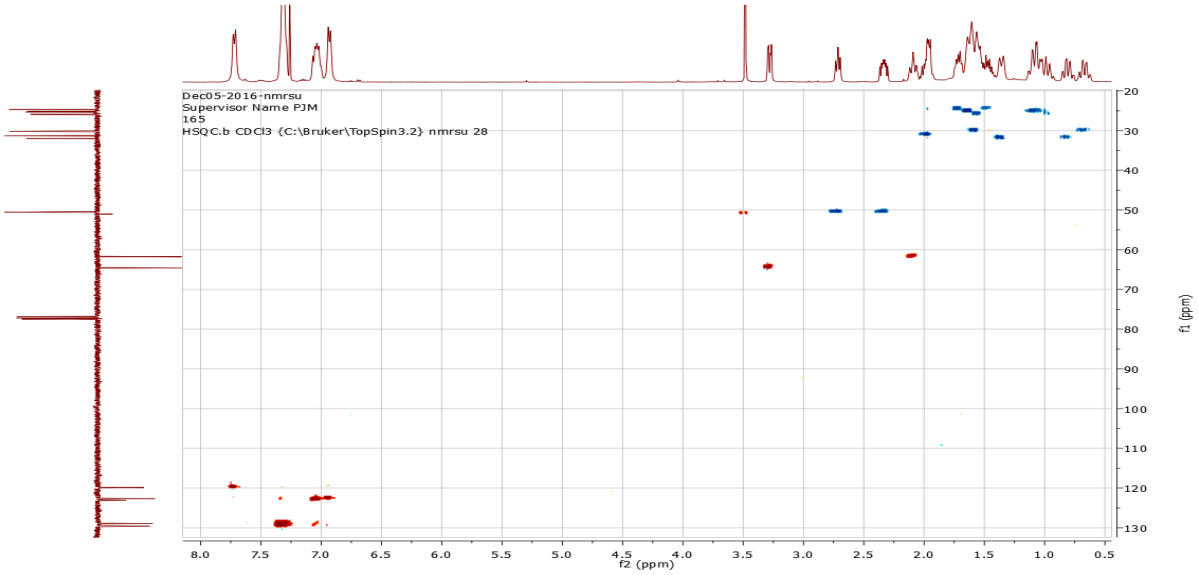
Dec05-2016-nmrsu
Supervisor Name PJM
165
HSQC.b CDCl3 {C:\Bruker\TopSpin3.2} nmrsu 28
f2 (ppm)
f1 (ppm)

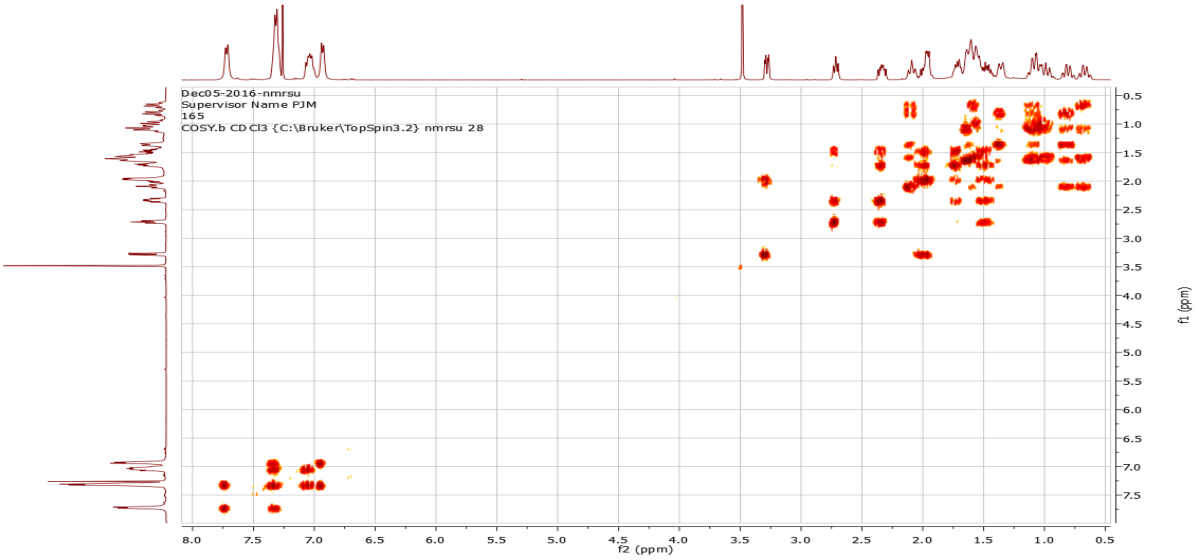
Dec05-2016-nmrsu
Supervisor Name PJM
165
COSY.b CDCl3 {C:\Bruker\TopSpin3.2} nmrsu 28
f2 (ppm)
f1 (ppm)

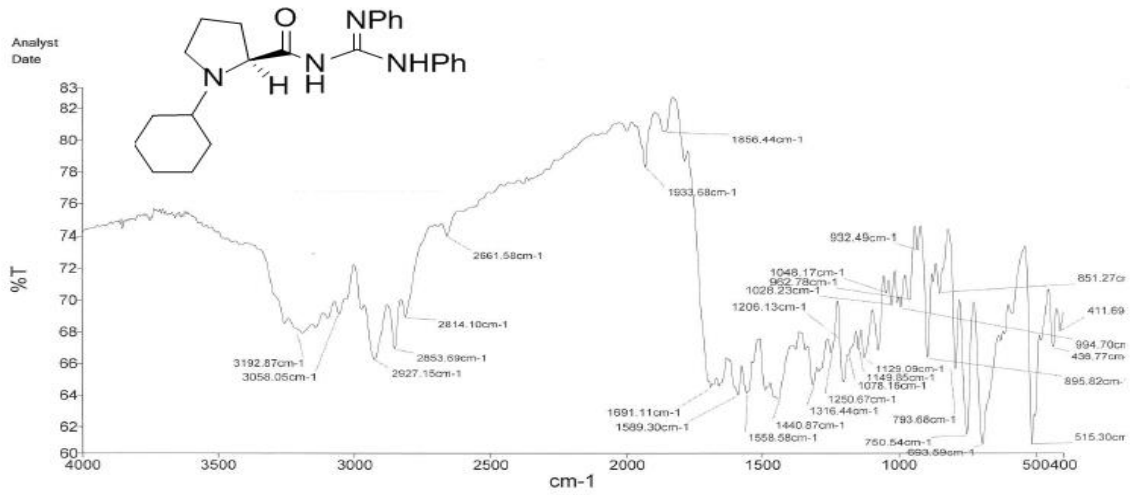
Analyst
Date
O
NPh
N
NHPh
H
N
H
%T
cm-1
1856.44cm-1
1933.68cm-1
2661.58cm-1
2814.10cm-1
2853.69cm-1
2927.15cm-1
3192.87cm-1
3058.05cm-1
932.49cm-1
1048.17cm-1
962.78cm-1
1028.23cm-1
1206.13cm-1
851.27cm-1
411.69
994.70cm-1
439.77cm-1
1129.09cm-1
1149.85cm-1
1078.18cm-1
895.82cm-1
1250.67cm-1
1316.44cm-1
793.68cm-1
1691.11cm-1
1589.30cm-1
1440.87cm-1
1558.58cm-1
750.54cm-1
693.59cm-1
515.30cm-1

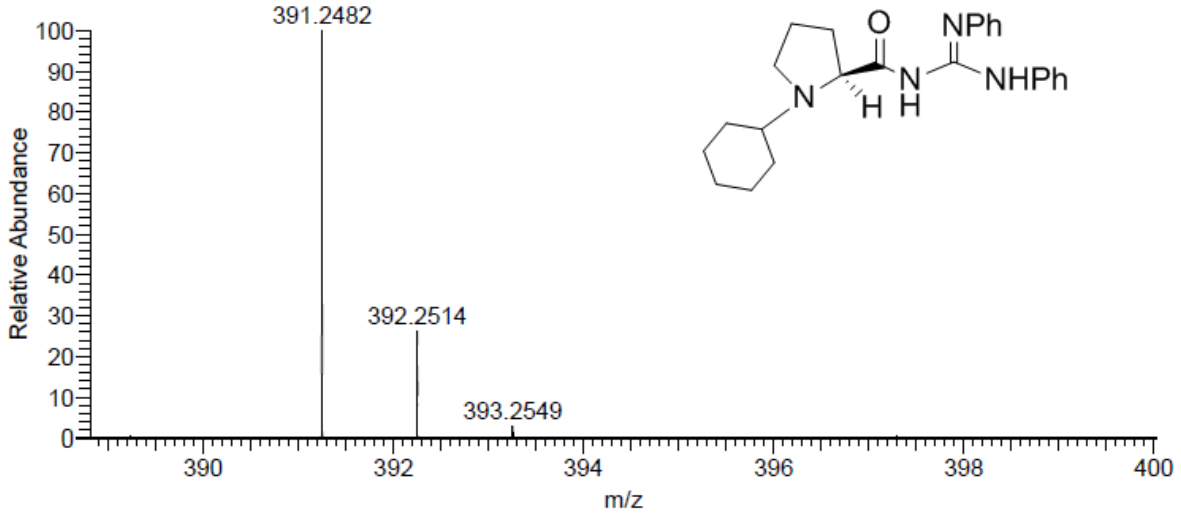
391.2482
392.2514
393.2549
Relative Abundance
m/z
O
NPh
N
NHPh
H
N

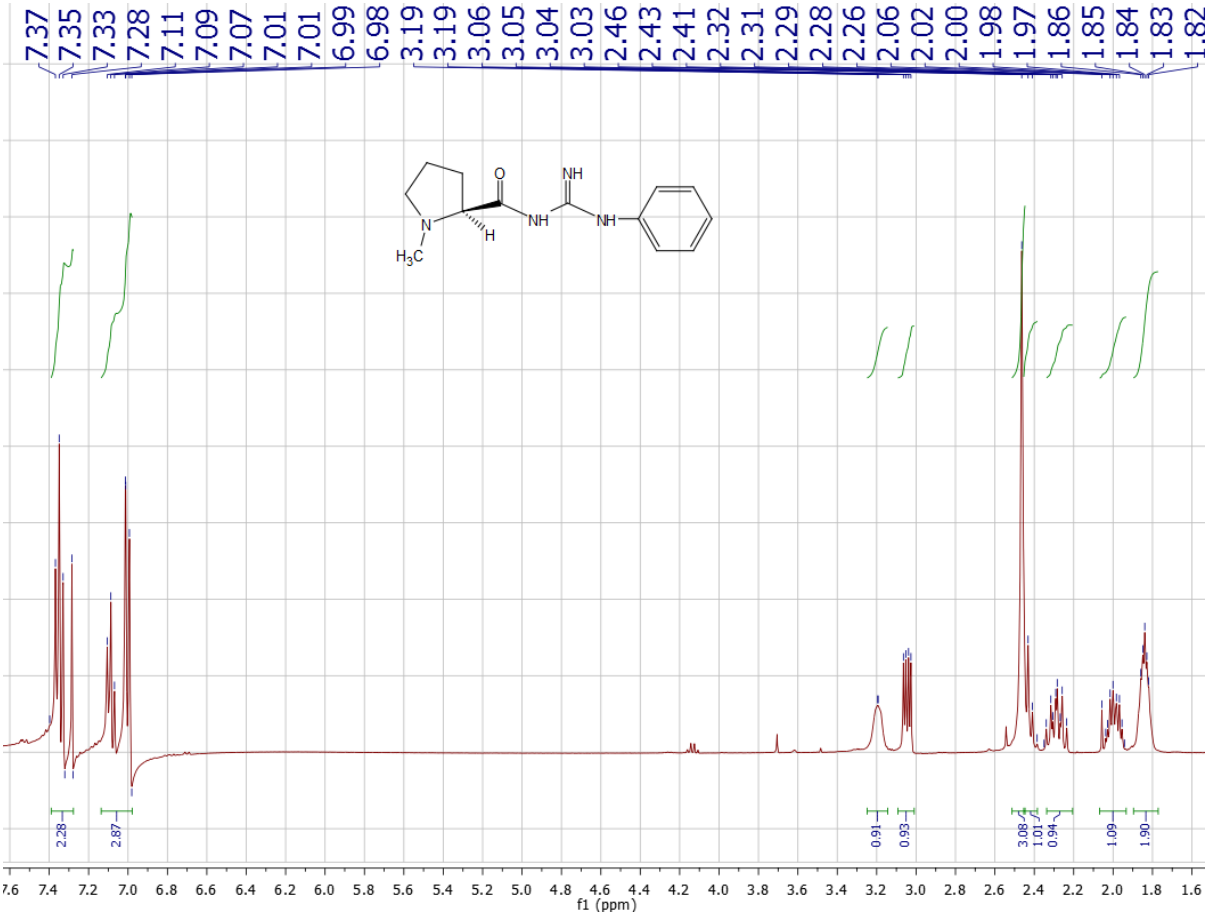
7.37
7.35
7.33
7.28
7.11
7.09
7.07
7.01
7.01
6.99
6.98
3.19
3.19
3.06
3.05
3.04
3.03
2.46
2.43
2.41
2.32
2.31
2.29
2.28
2.26
2.06
2.02
2.00
1.98
1.97
1.86
1.85
1.84
1.83
1.82
O
NH
N
NH
NH
H
H3C
2.28
2.87
0.91
0.93
3.08
1.01
0.94
1.09
1.90
f1 (ppm)

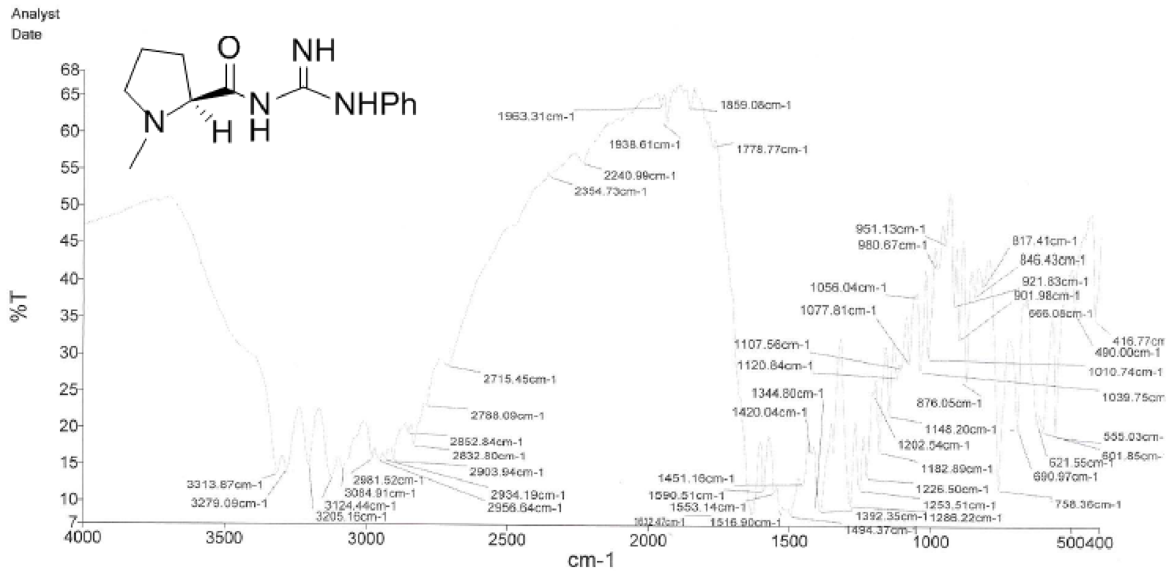
Analyst
Date
O
NH
N
H
NHPh
N
H
%T
cm-1
4000
3500
3000
2500
2000
1500
1000
500400
68
65
60
55
50
45
40
35
30
25
20
15
10
7
1963.31cm-1
1859.08cm-1
1938.61cm-1
1778.77cm-1
2240.99cm-1
2354.73cm-1
951.13cm-1
980.67cm-1
817.41cm-1
846.43cm-1
1056.04cm-1
921.83cm-1
901.98cm-1
1077.81cm-1
666.08cm-1
416.77cm
490.00cm-1
1107.56cm-1
1120.84cm-1
1010.74cm-1
2715.45cm-1
1039.75cm
1344.80cm-1
876.05cm-1
1420.04cm-1
2788.09cm-1
1148.20cm-1
555.03cm-
2852.84cm-1
1202.54cm-1
601.85cm-
2832.80cm-1
621.55cm-1
2903.94cm-1
1182.89cm-1
690.97cm-1
1451.16cm-1
3313.87cm-1
2981.52cm-1
1226.50cm-1
3084.91cm-1
1590.51cm-1
2934.19cm-1
3279.09cm-1
3124.44cm-1
2956.64cm-1
1553.14cm-1
1253.51cm-1
758.36cm-1
3205.16cm-1
1516.90cm-1
1392.35cm-1
1286.22cm-1
1494.37cm-1

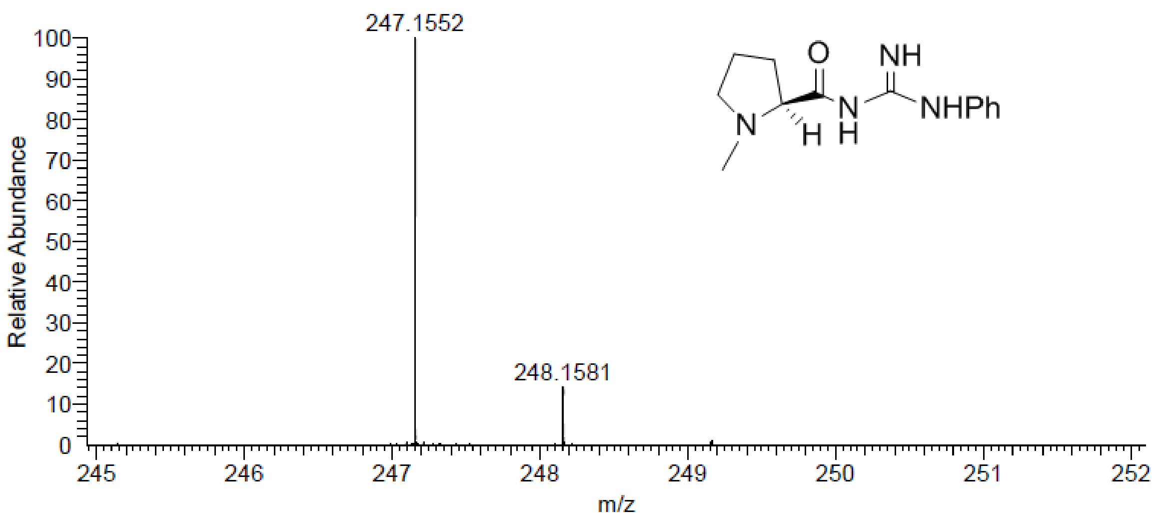
247.1552
248.1581
Relative Abundance
m/z
100
90
80
70
60
50
40
30
20
10
0
245
246
247
248
249
250
251
252
O
NH
N
H
NHPh
N
H

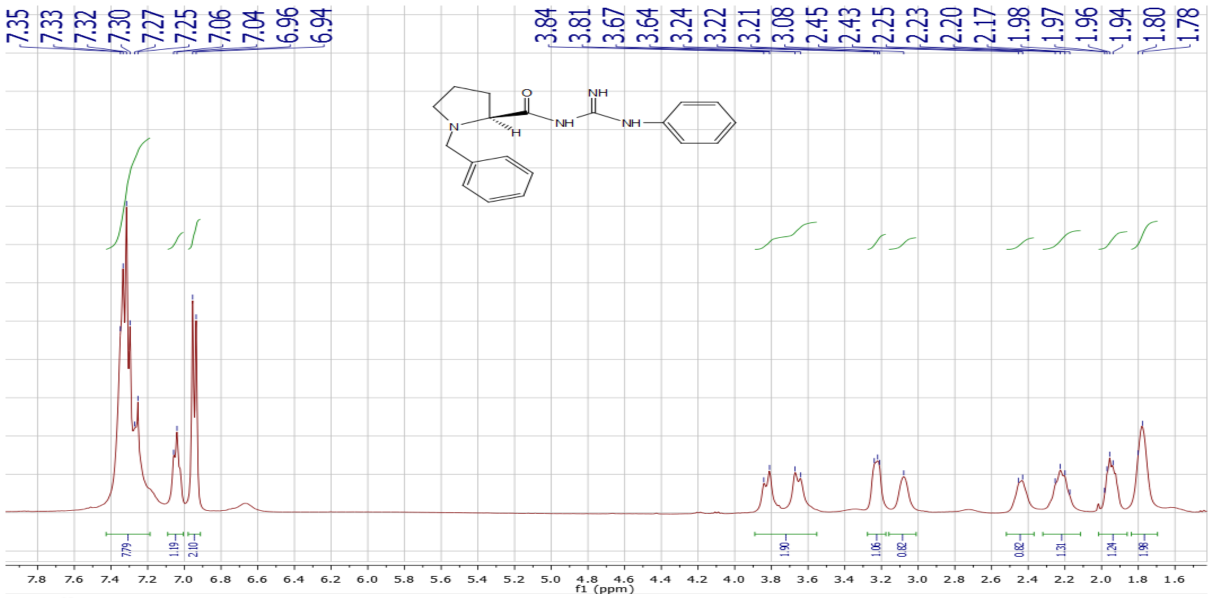
7.35
7.33
7.32
7.30
7.27
7.25
7.06
7.04
6.96
6.94
3.84
3.81
3.67
3.64
3.24
3.22
3.21
3.08
2.45
2.43
2.25
2.23
2.20
2.17
1.98
1.97
1.96
1.94
1.80
1.78
N
O
NH
NH
NH
H
7.79
1.19
2.10
1.90
1.06
0.82
0.82
1.31
1.24
1.98
f1 (ppm)

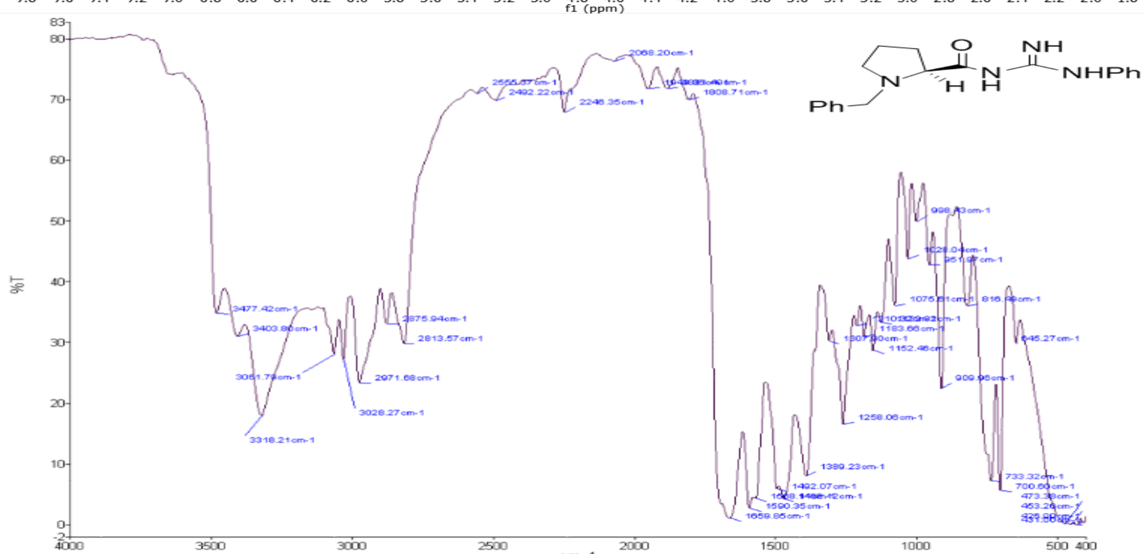
%T
cm-1
O
NH
N
H
H
N
NHPh
Ph
3477.42cm-1
3403.80cm-1
3318.21cm-1
2971.68cm-1
3028.27cm-1
2875.94cm-1
2813.57cm-1
2492.22cm-1
2246.35cm-1
2068.20cm-1
1808.71cm-1
1659.85cm-1
1590.35cm-1
1492.07cm-1
1389.23cm-1
1258.06cm-1
1152.46cm-1
1183.66cm-1
1076.81cm-1
998.43cm-1
909.96cm-1
816.49cm-1
733.32cm-1
700.60cm-1
645.27cm-1
473.39cm-1
453.26cm-1

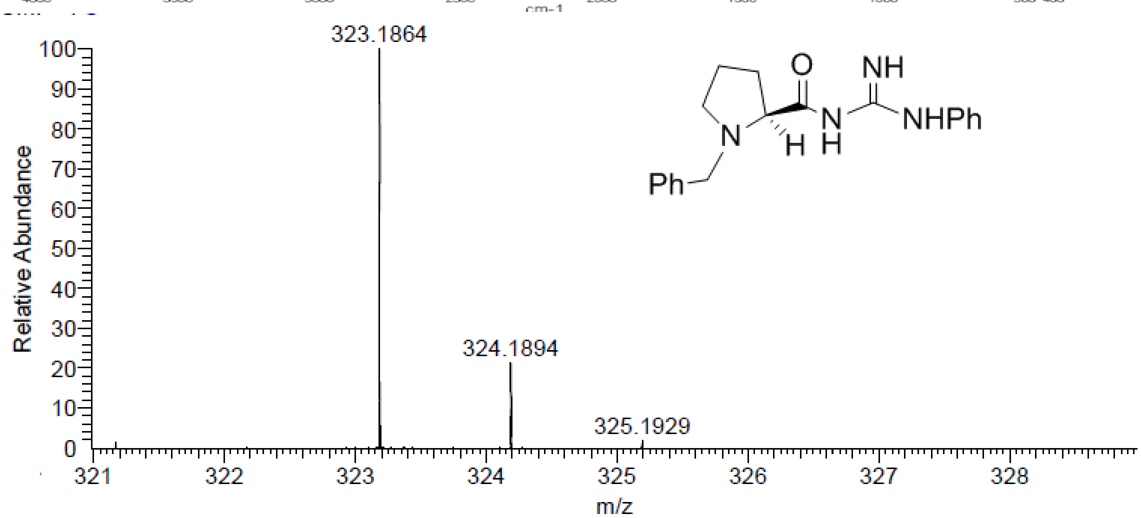
323.1864
324.1894
325.1929
Relative Abundance
m/z
O
NH
N
H
H
N
NHPh
Ph

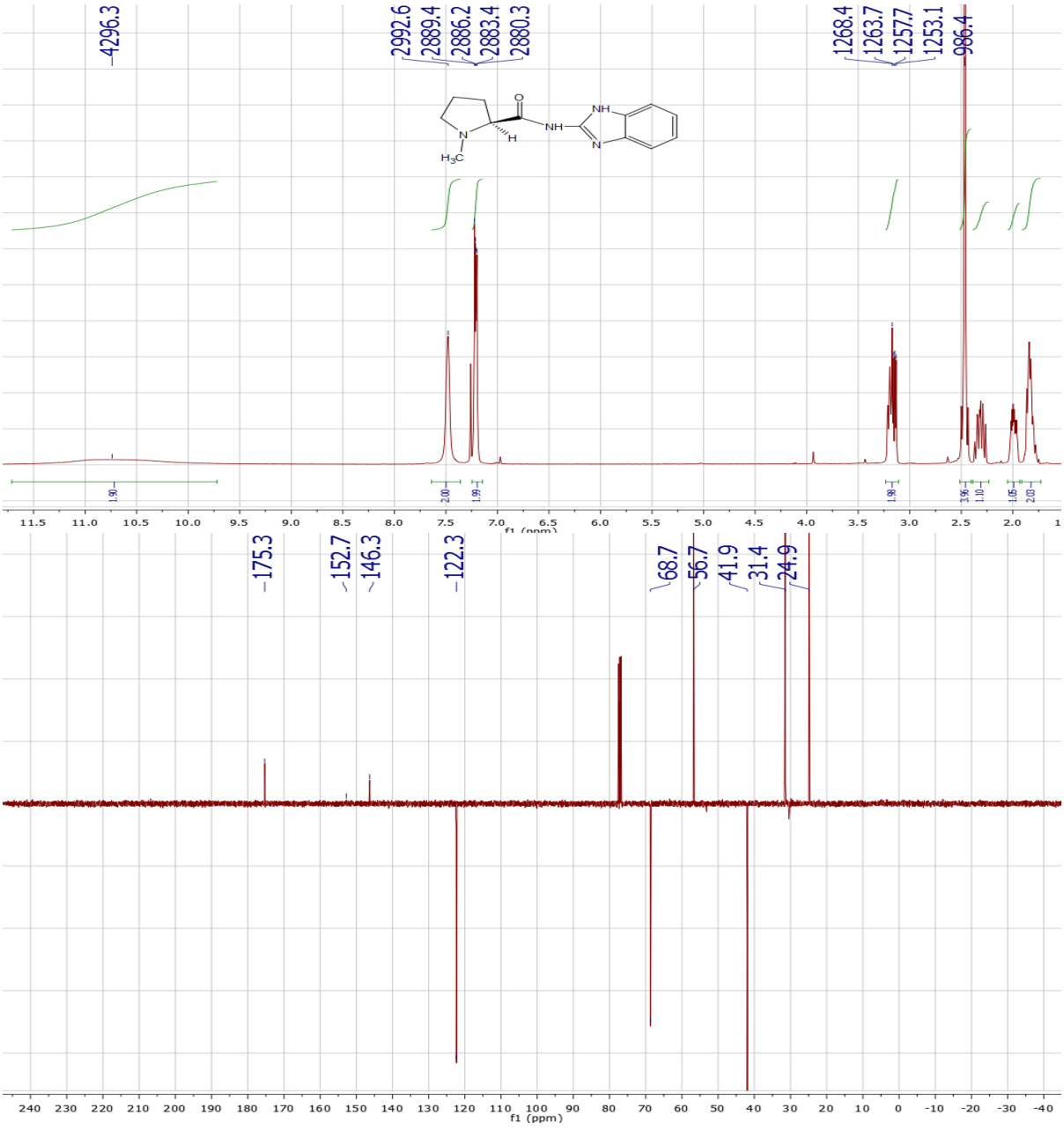
4296.3
2992.6
2889.4
2886.2
2883.4
2880.3
1268.4
1263.7
1257.7
1253.1
986.4
O
NH
NH
N
H
N
H3C
11.5 11.0 10.5 10.0 9.5 9.0 8.5 8.0 7.5 7.0 6.5 6.0 5.5 5.0 4.5 4.0 3.5 3.0 2.5 2.0 1
f1 (ppm)
175.3
152.7
146.3
122.3
68.7
56.7
41.9
31.4
24.9
240 230 220 210 200 190 180 170 160 150 140 130 120 110 100 90 80 70 60 50 40 30 20 10 0 -10 -20 -30 -40
f1 (ppm)

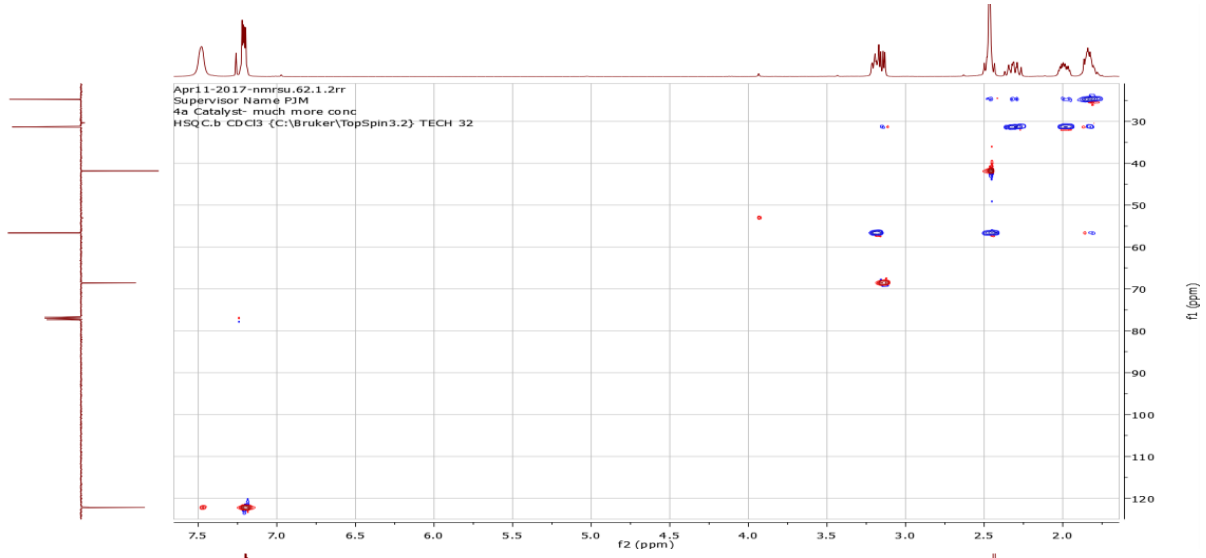
Apr11-2017-nmrsu.62.1.2rr
Supervisor Name PJM
4a Catalyst- much more conc
HSQC.b CDCl3 {C:\Bruker\TopSpin3.2} TECH 32
f2 (ppm)
f1 (ppm)

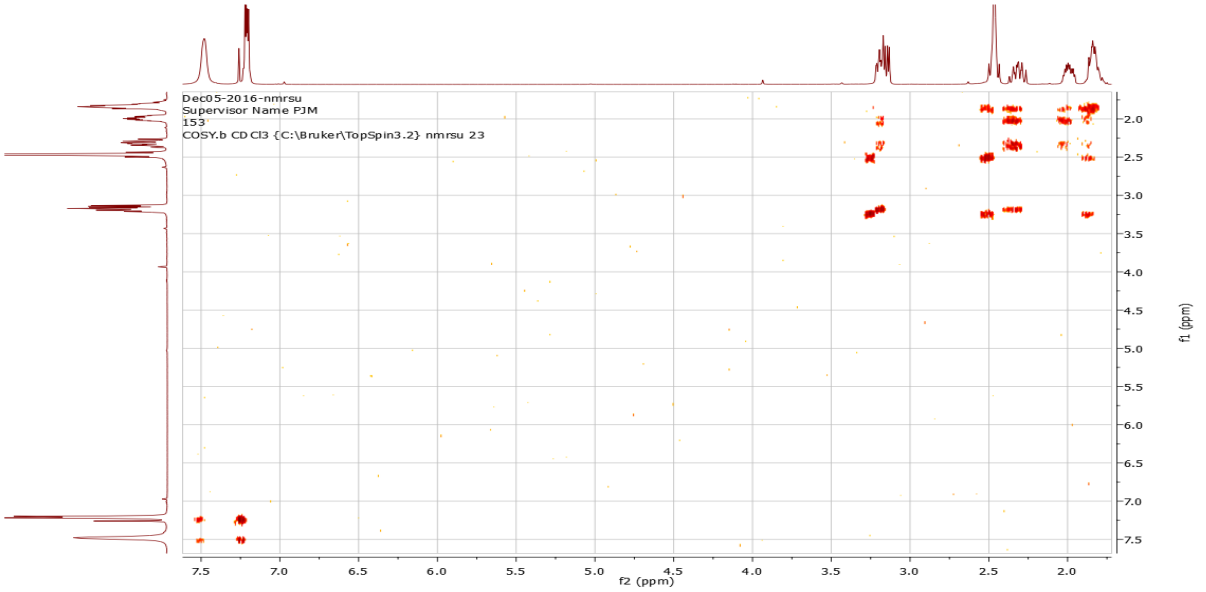
Dec05-2016-nmrsu
Supervisor Name PJM
153
COSY.b CDCl3 {C:\Bruker\TopSpin3.2} nmrsu 23
f2 (ppm)
f1 (ppm)

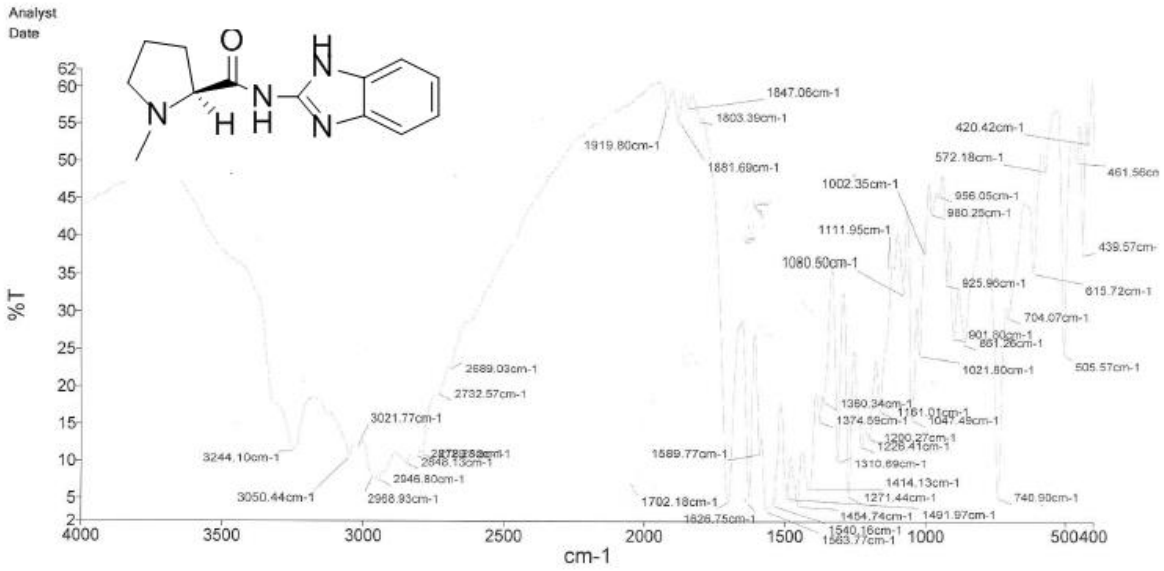
Analyst
Date
%T
cm-1
3244.10cm-1
3050.44cm-1
3021.77cm-1
2968.93cm-1
2946.80cm-1
2889.03cm-1
2732.57cm-1
1919.80cm-1
1881.69cm-1
1847.06cm-1
1803.39cm-1
1589.77cm-1
1702.18cm-1
1826.75cm-1
1540.16cm-1
1002.35cm-1
1111.95cm-1
1080.50cm-1
956.05cm-1
980.25cm-1
925.96cm-1
1021.80cm-1
420.42cm-1
572.18cm-1
461.56cm-1
439.57cm-1
615.72cm-1
704.07cm-1
505.57cm-1
740.99cm-1

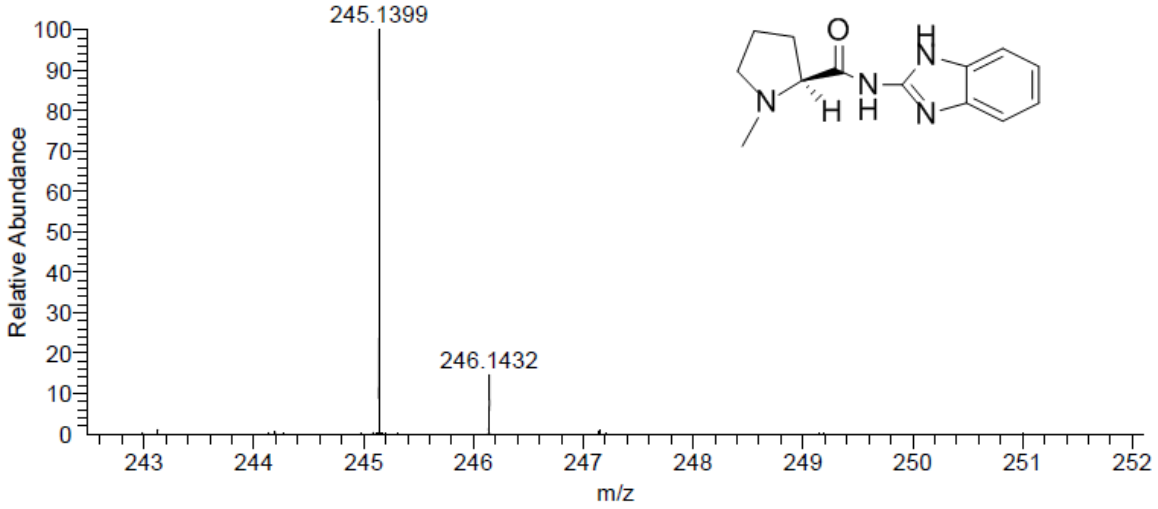
245.1399
246.1432
Relative Abundance
m/z
100
90
80
70
60
50
40
30
20
10
0
243
244
245
246
247
248
249
250
251
252
O
N
H
N
N
H
N

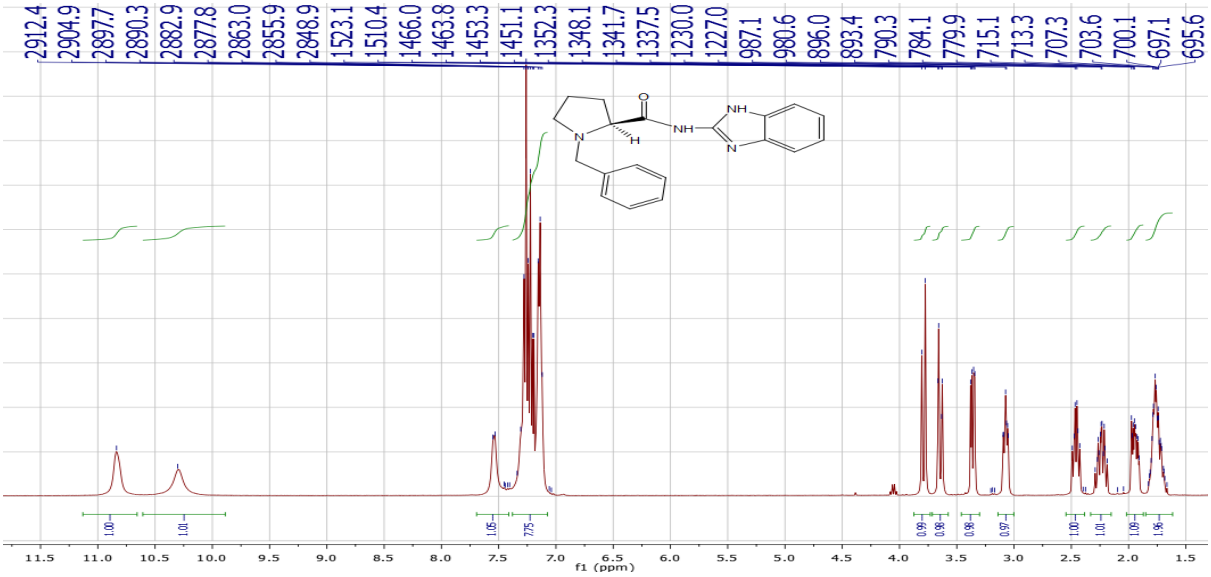
2912.4
2904.9
2897.7
2890.3
2882.9
2877.8
2863.0
2855.9
2848.9
1523.1
1510.4
1466.0
1463.8
1453.3
1451.1
1352.3
1348.1
1341.7
1337.5
1230.0
1227.0
987.1
980.6
896.0
893.4
790.3
784.1
779.9
715.1
713.3
707.3
703.6
700.1
697.1
695.6
O
NH
NH
N
N
H
f1 (ppm)

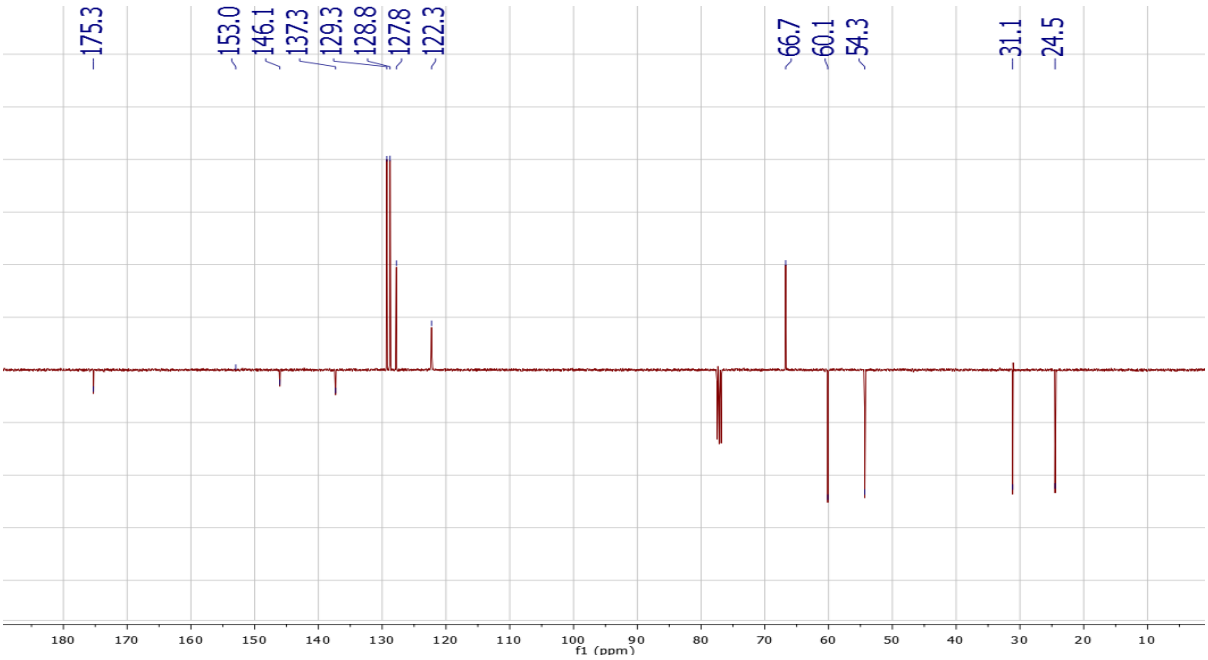
175.3
153.0
146.1
137.3
129.3
128.8
127.8
122.3
66.7
60.1
54.3
31.1
24.5
f1 (ppm)

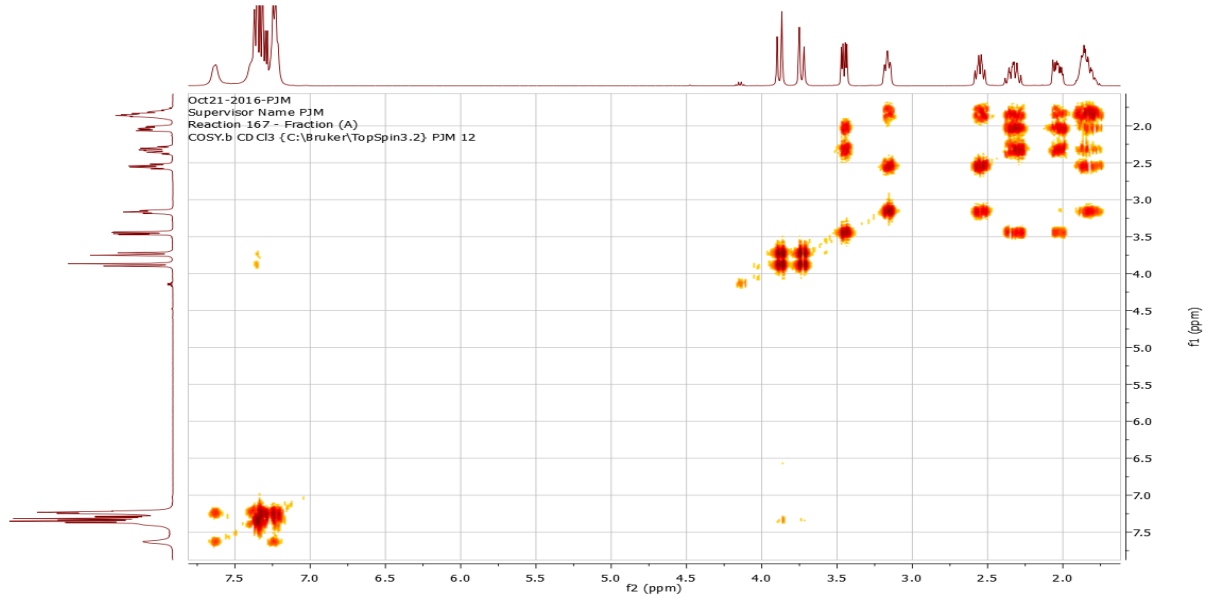
Oct21-2016-PJM
Supervisor Name PJM
Reaction 167 - Fraction (A)
COSY.b CD Cl3 {C:\Bruker\TopSpin3.2} PJM 12
f2 (ppm)
f1 (ppm)

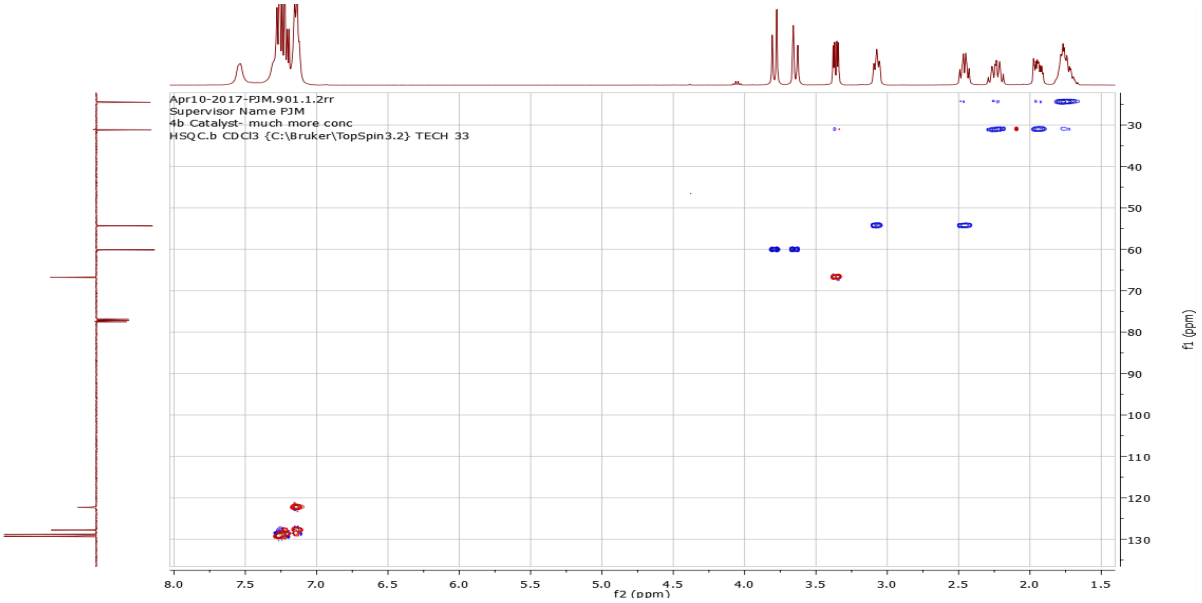
Apr10-2017-PJM.901.1.2rr
Supervisor Name PJM
4b Catalyst- much more conc
HSQC.b CDCl3 {C:\Bruker\TopSpin3.2} TECH 33
f2 (ppm)
f1 (ppm)

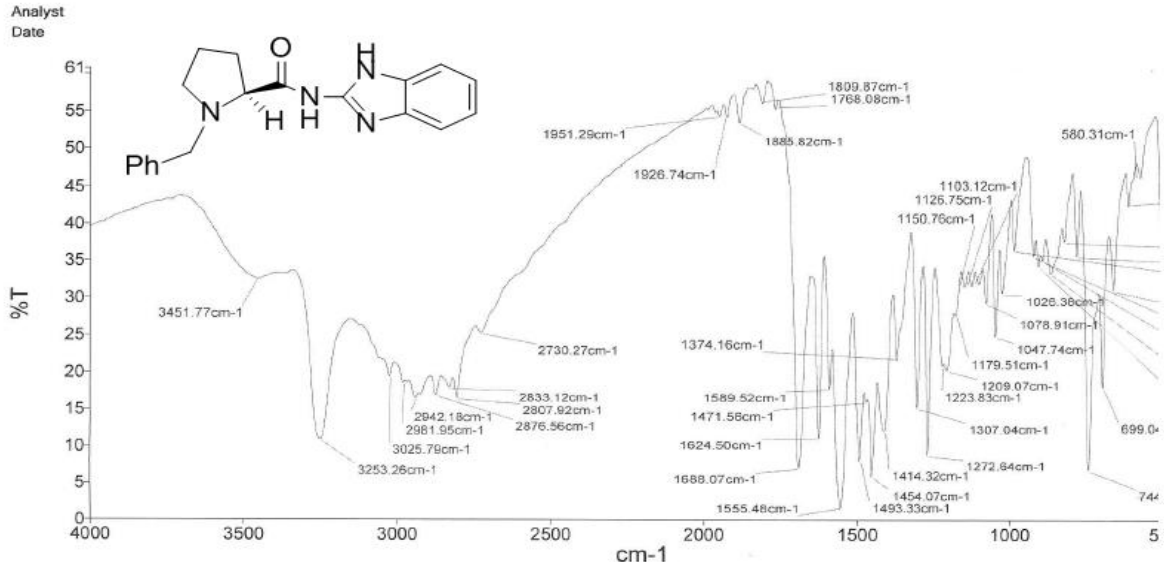
Analyst
Date
Ph
%T
cm-1
3451.77cm-1
3253.26cm-1
3025.79cm-1
2981.95cm-1
2942.18cm-1
2876.56cm-1
2807.92cm-1
2833.12cm-1
2730.27cm-1
1951.29cm-1
1926.74cm-1
1885.82cm-1
1809.87cm-1
1768.08cm-1
1688.07cm-1
1624.50cm-1
1589.52cm-1
1555.48cm-1
1493.33cm-1
1471.58cm-1
1454.07cm-1
1414.32cm-1
1374.16cm-1
1307.04cm-1
1272.64cm-1
1223.83cm-1
1209.07cm-1
1179.51cm-1
1150.76cm-1
1126.75cm-1
1103.12cm-1
1078.91cm-1
1047.74cm-1
1026.38cm-1
580.31cm-1

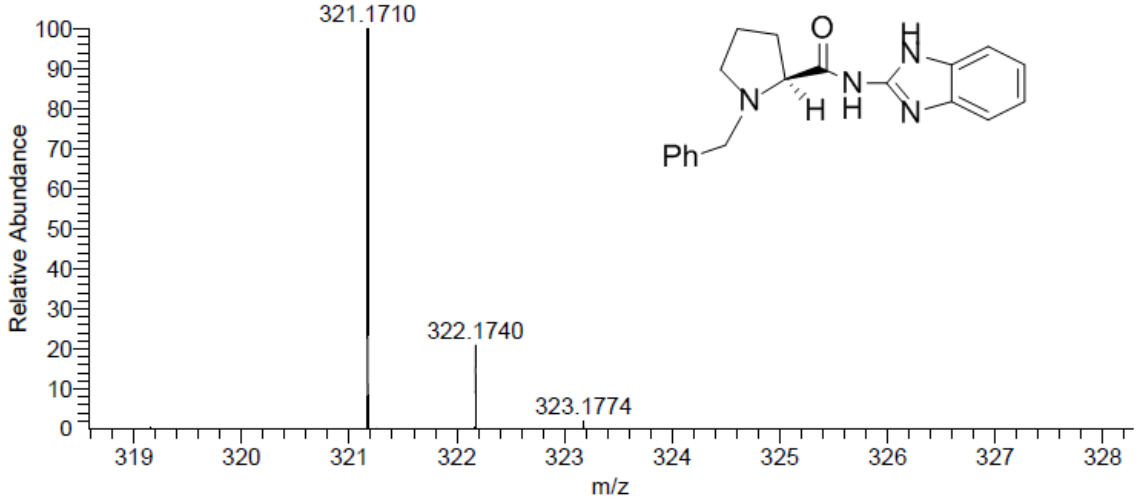
Relative Abundance
m/z
321.1710
322.1740
323.1774
Ph


7.50
7.23
7.23
7.22
7.21
3.51
3.51
3.49
3.48
3.22
3.20
2.88
2.87
2.85
2.63
2.62
2.62
2.61
2.60
2.59
2.58
2.19
2.18
2.18
2.16
2.16
2.07
1.85
1.83
1.83
1.77
1.13
1.13
1.12
1.11
O
NH
N
H
NH
N
H3C
CH3
f1 (ppm)
176.7
153.1
146.1
122.3
64.2
53.4
50.9
31.7
24.9
21.5
20.1
f1 (ppm)

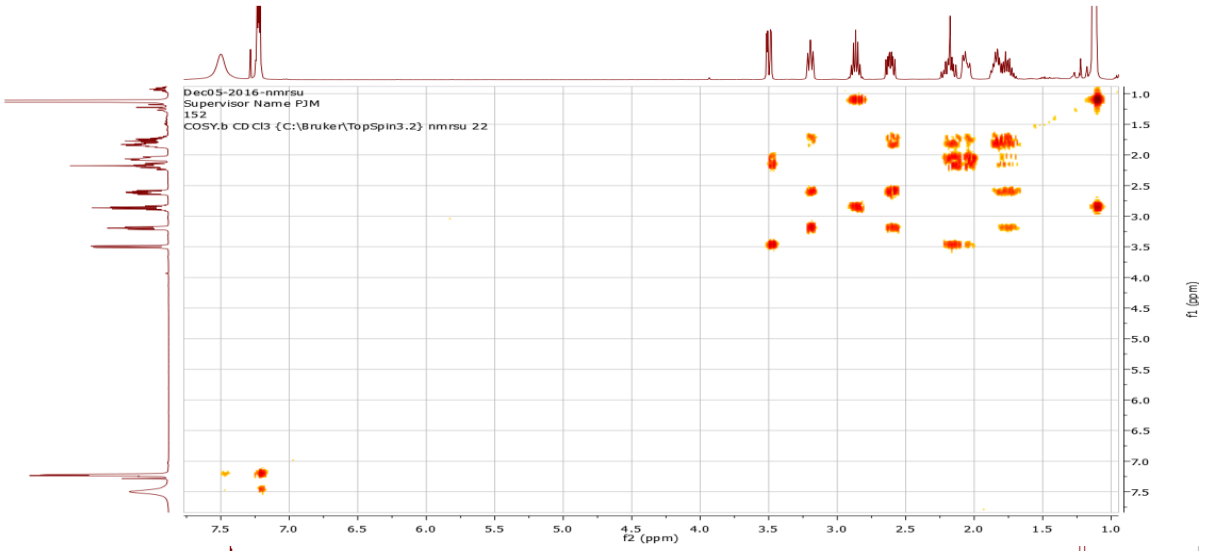
Dec05-2016-nmrsu
Supervisor Name PJM
152
COSY.b CDCl3 {C:\Bruker\TopSpin3.2} nmrsu 22
f2 (ppm)
f1 (ppm)

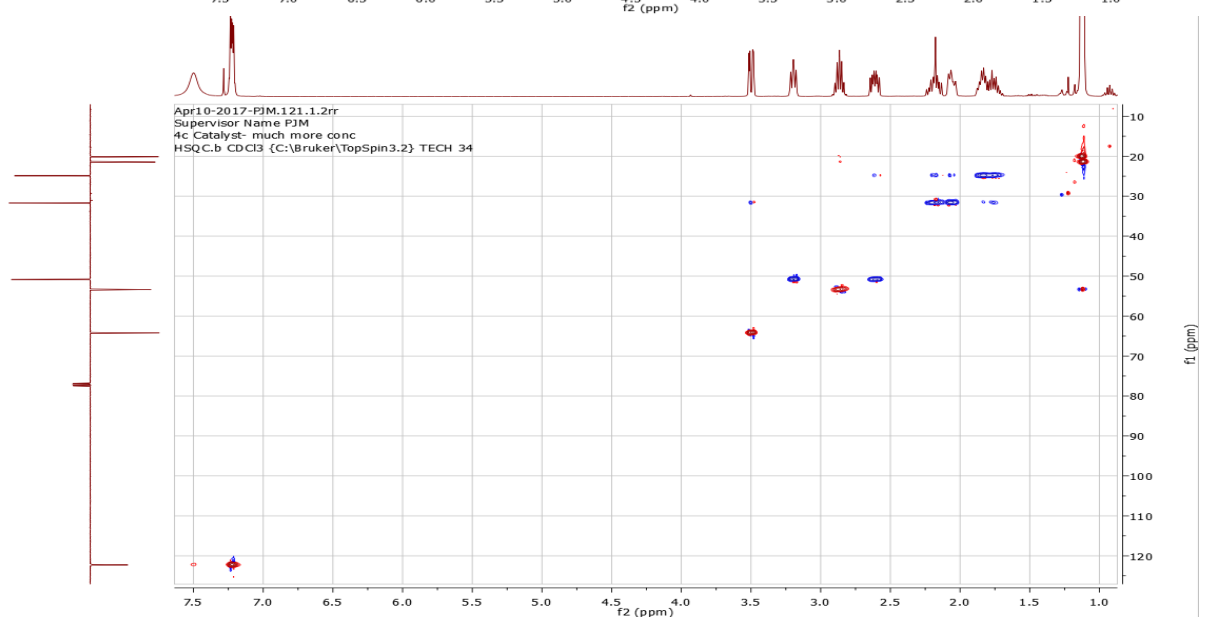
Apr10-2017-PJM.121.1.2rr
Supervisor Name PJM
4c Catalyst- much more conc
HSQC.b CDCl3 {C:\Bruker\TopSpin3.2} TECH 34
f2 (ppm)
f1 (ppm)

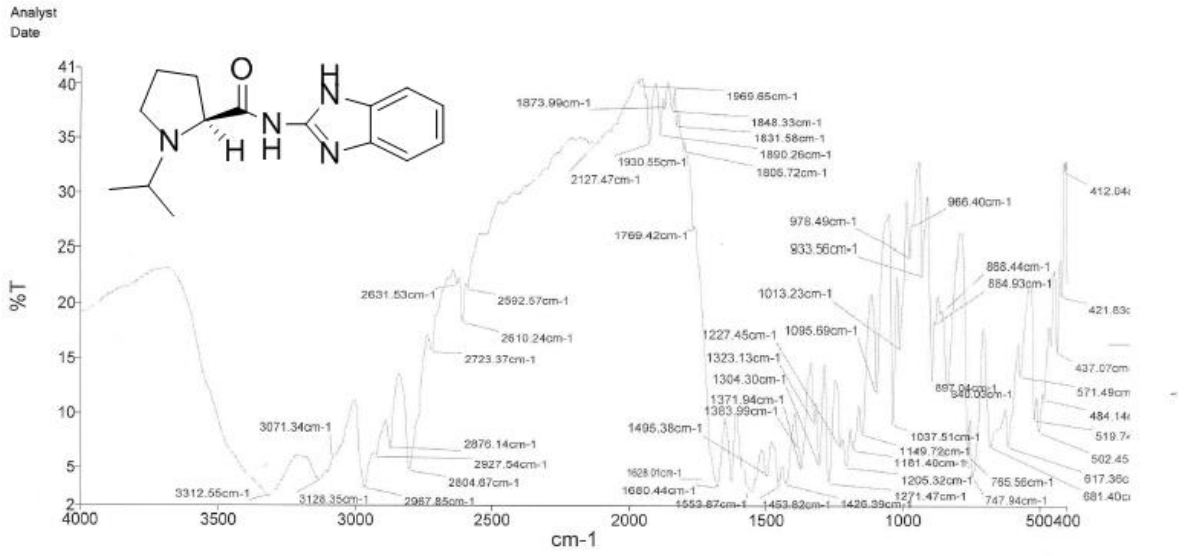
Analyst
Date
%T
cm-1
4000
3500
3000
2500
2000
1500
1000
500400
3312.55cm-1
3128.35cm-1
3071.34cm-1
2987.85cm-1
2927.54cm-1
2876.14cm-1
2804.67cm-1
2723.37cm-1
2631.53cm-1
2592.57cm-1
2610.24cm-1
1873.99cm-1
1969.65cm-1
1848.33cm-1
1831.58cm-1
1890.26cm-1
1806.72cm-1
1930.55cm-1
2127.47cm-1
1769.42cm-1
1680.44cm-1
1628.01cm-1
1553.67cm-1
1495.38cm-1
1453.82cm-1
1426.39cm-1
1383.99cm-1
1371.94cm-1
1304.30cm-1
1323.13cm-1
1227.45cm-1
1205.32cm-1
1271.47cm-1
1095.69cm-1
1013.23cm-1
978.49cm-1
966.40cm-1
933.56cm-1
888.44cm-1
884.93cm-1
1037.51cm-1
1149.72cm-1
1181.40cm-1
755.56cm-1
747.94cm-1

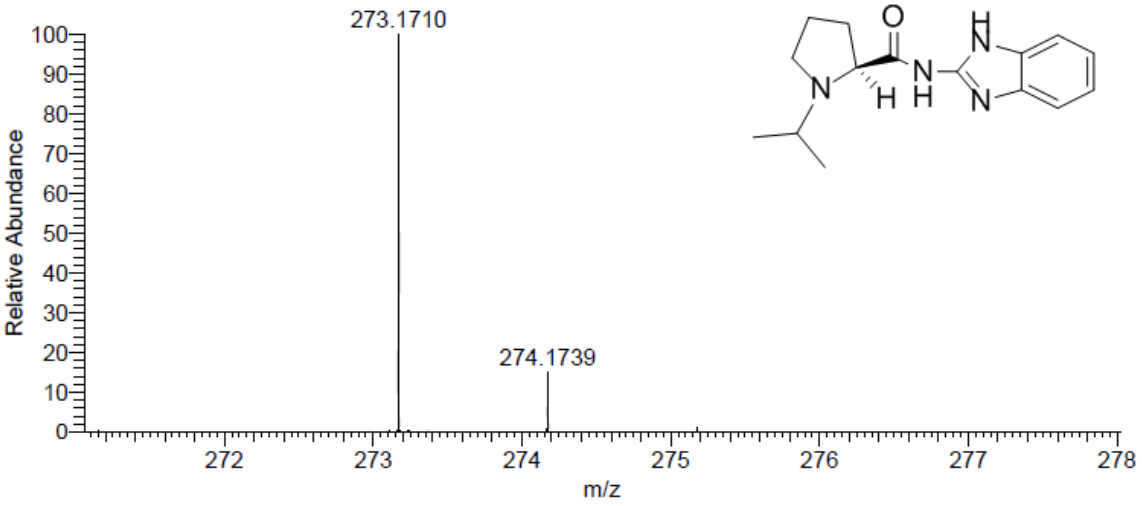
Relative Abundance
m/z
273.1710
274.1739
100
90
80
70
60
50
40
30
20
10
0
272
273
274
275
276
277
278

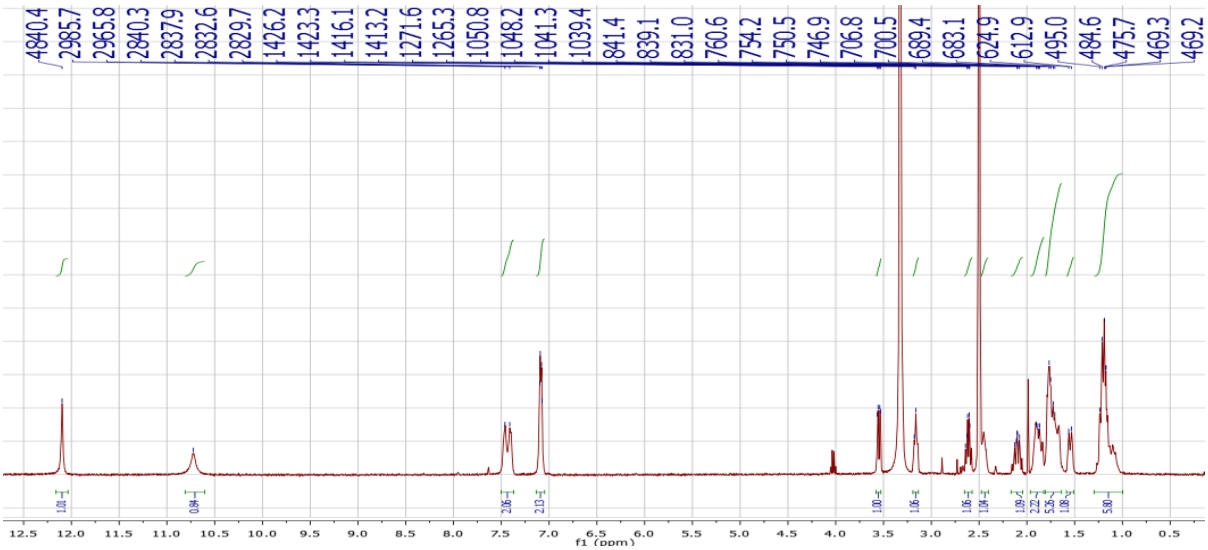
4840.4
2985.7
2965.8
2940.3
2837.9
2832.6
2829.7
1426.2
1423.3
1416.1
1413.2
1271.6
1265.3
1050.8
1048.2
1041.3
1039.4
841.4
839.1
831.0
760.6
754.2
750.5
746.9
706.8
700.5
689.4
683.1
624.9
612.9
495.0
484.6
475.7
469.3
469.2
f1 (ppm)

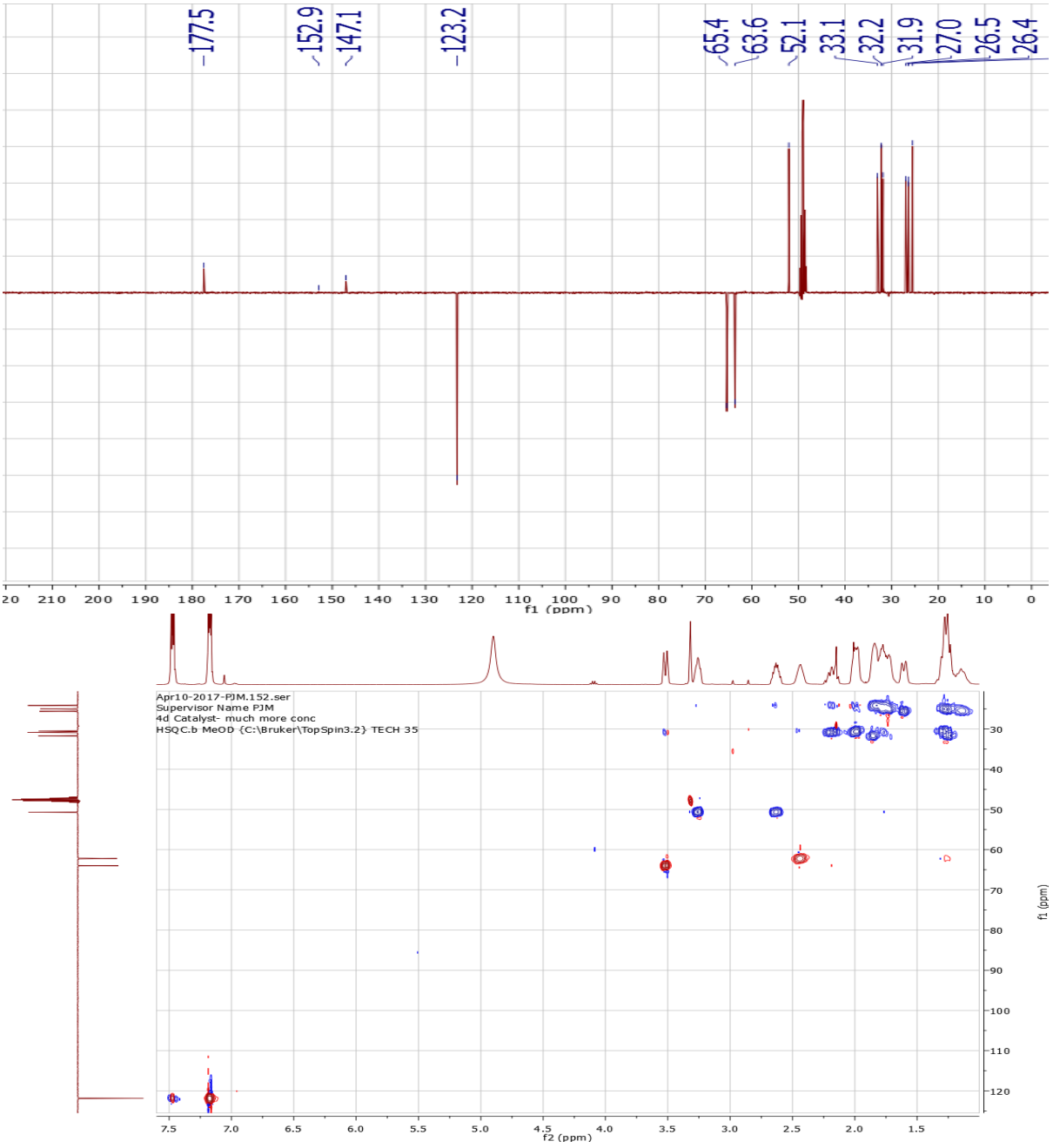
177.5
152.9
147.1
123.2
65.4
63.6
52.1
33.1
32.2
31.9
27.0
26.5
26.4
f1 (ppm)
Apr10-2017-PJM.152.ser
Supervisor Name PJM
4d Catalyst- much more conc
HSQC.b MeOD {C:\Bruker\TopSpin3.2} TECH 35
f2 (ppm)
f1 (ppm)

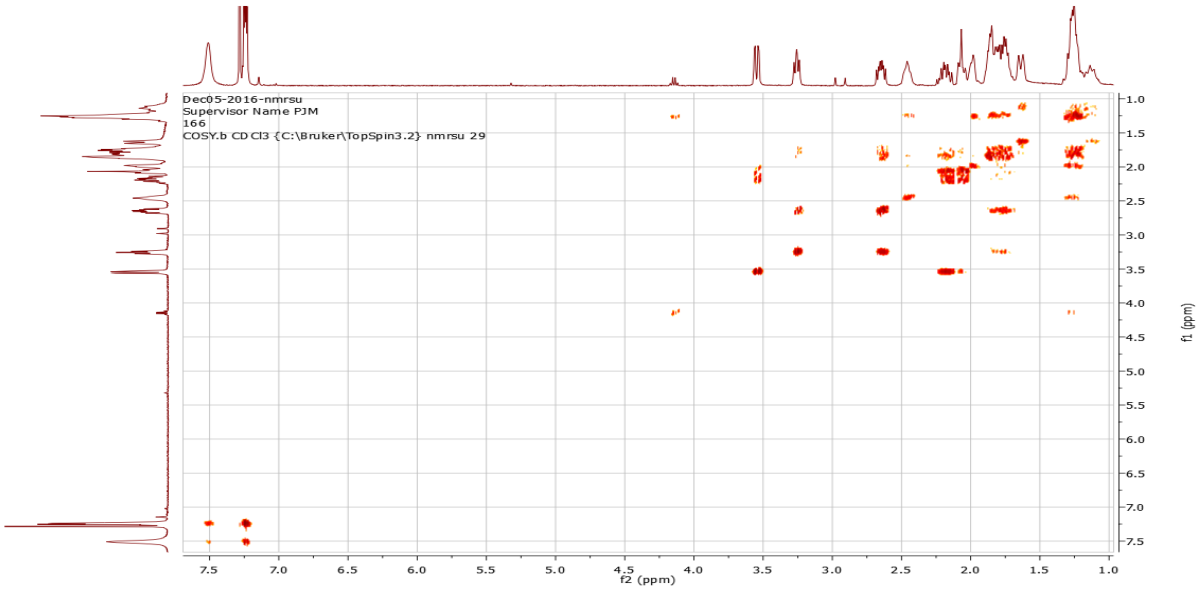
Dec05-2016-nmrsu
Supervisor Name PJM
166
COSY.b CDCl3 {C:\Bruker\TopSpin3.2} nmrsu 29
f2 (ppm)
f1 (ppm)

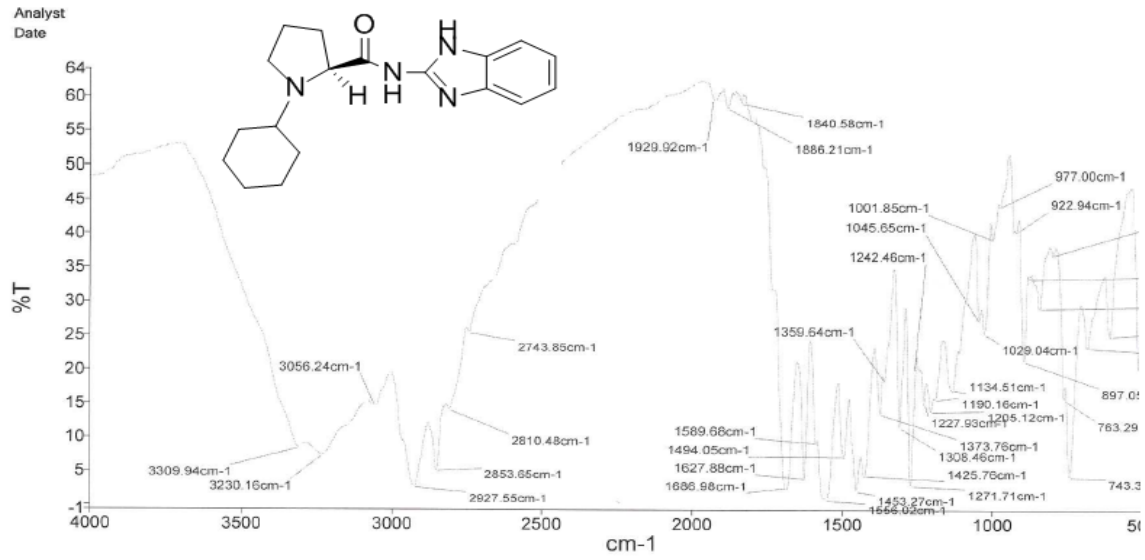
Analyst
Date
%T
cm-1
3309.94cm-1
3230.16cm-1
3056.24cm-1
2927.55cm-1
2853.65cm-1
2810.48cm-1
2743.85cm-1
1929.92cm-1
1840.58cm-1
1886.21cm-1
1686.98cm-1
1627.88cm-1
1589.68cm-1
1494.05cm-1
1453.27cm-1
1425.76cm-1
1373.76cm-1
1359.64cm-1
1308.46cm-1
1271.71cm-1
1242.46cm-1
1227.93cm-1
1205.12cm-1
1190.16cm-1
1134.51cm-1
1045.65cm-1
1029.04cm-1
1001.85cm-1
977.00cm-1
922.94cm-1

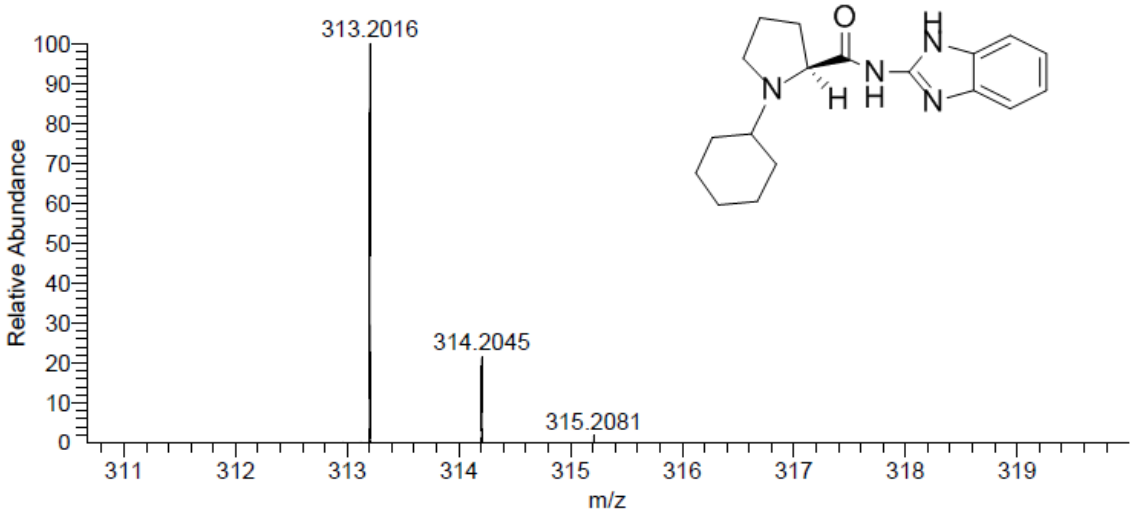
313.2016
314.2045
315.2081
Relative Abundance
m/z

1- HPLC of reaction β-nitrostyrene 52 and diethyl malonate 53

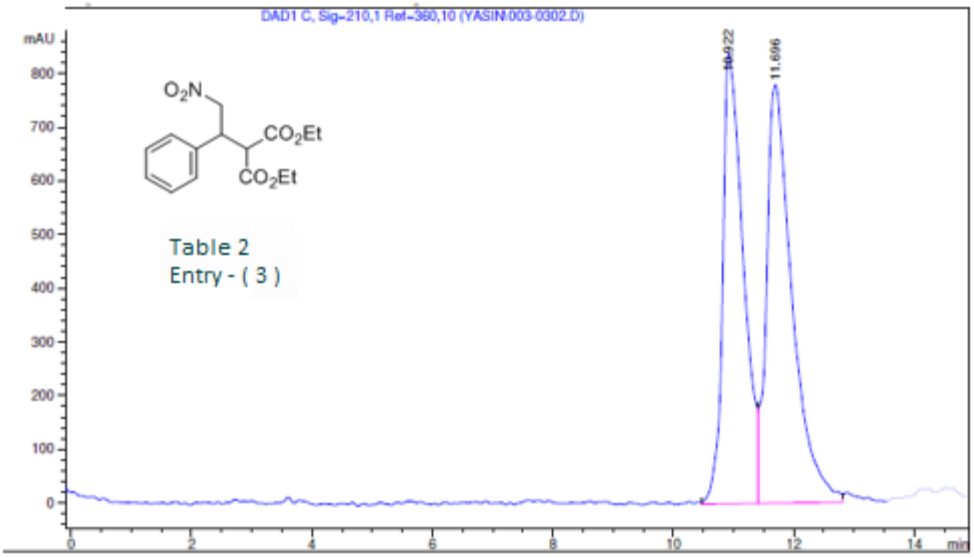

Peak #	RetTime [min]	Type	Width [min]	Area [mAU*s]	Height [mAU]	Area %
1	10.922	VV	0.3656	1.99712e4	839.47815	46.3512
2	11.696	VV	0.4339	2.31155e4	779.54199	53.6488
Totals :				4.30867e4	1619.02014	

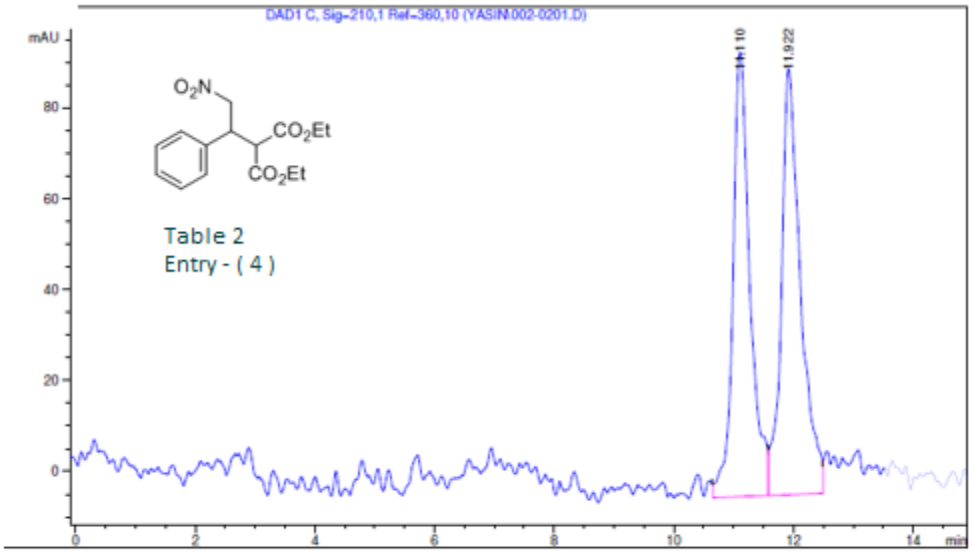

Peak #	RetTime [min]	Type	Width [min]	Area [mAU*s]	Height [mAU]	Area %
1	11.110	VV	0.2955	1942.66663	97.88555	48.1672
2	11.922	VV	0.3078	2090.50757	93.88264	51.8328

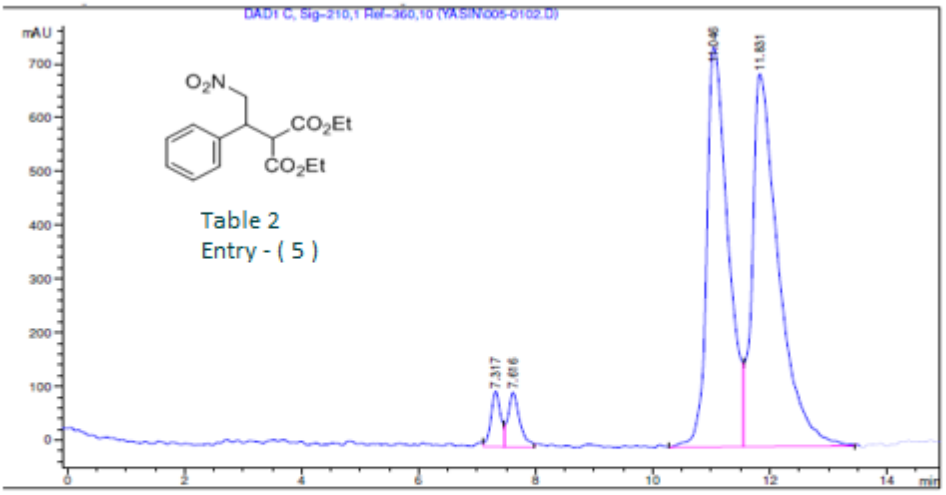

Peak #	RetTime [min]	Type	Width [min]	Area [mAU*s]	Height [mAU]	Area %
1	7.317	VV	0.1707	1195.40112	103.51807	2.7686
2	7.616	VV	0.1984	1413.62244	101.57545	3.2740
3	11.046	VV	0.3752	1.88110e4	743.55243	43.5663
4	11.831	VB	0.4383	2.17578e4	693.00214	50.3911
Totals :				4.31777e4	1641.64809	

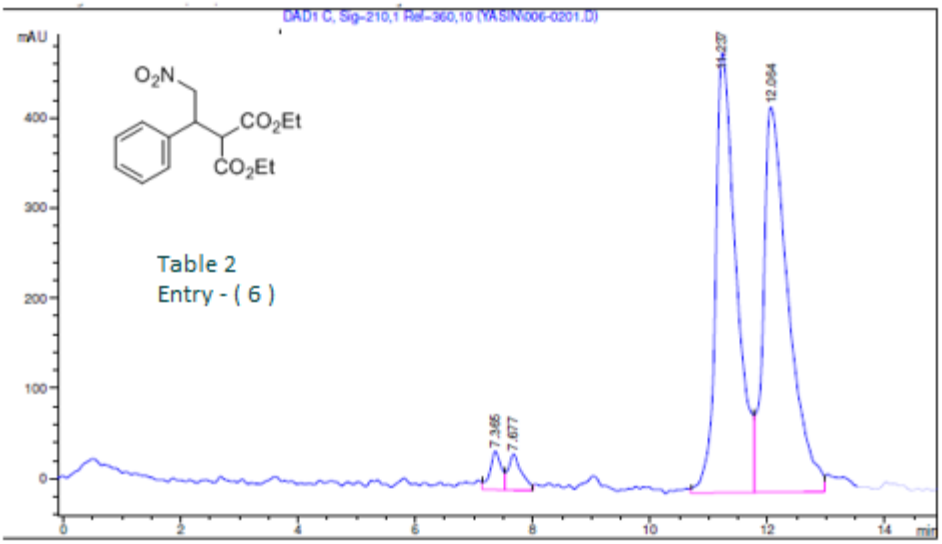

Peak #	RetTime [min]	Type	Width [min]	Area [mAU*s]	Height [mAU]	Area %
1	7.365	VV	0.1867	565.58008	42.66311	2.1919
2	7.677	VV	0.2126	618.98743	39.98927	2.3989
3	11.237	VV	0.3572	1.19345e4	488.20691	46.2518
4	12.064	VV	0.4343	1.26843e4	427.35684	49.1574
Totals :				2.58034e4	998.21613	

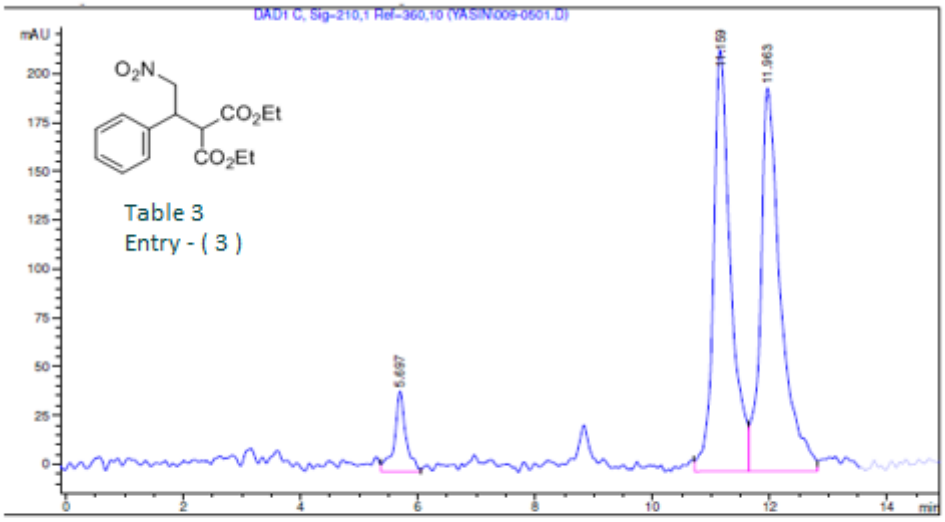

Peak #	RetTime [min]	Type	Width [min]	Area [mAU*s]	Height [mAU]	Area %
1	5.697	VV	0.1895	556.16534	41.18879	5.7755
2	11.159	VV	0.2930	4385.53516	215.91087	45.5417
3	11.963	VV	0.3466	4688.00342	196.29034	48.6827
Totals :				9629.70392	453.39001	

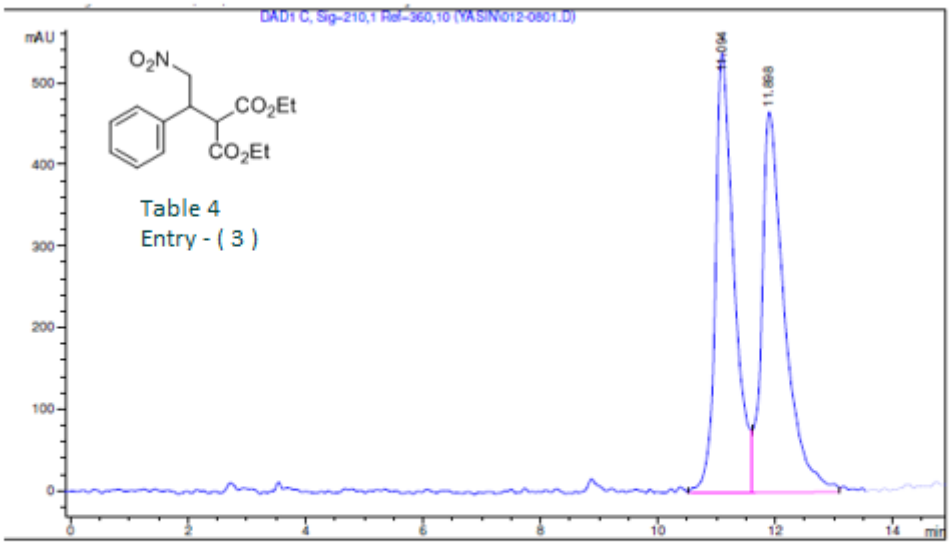

Peak #	RetTime [min]	Type	Width [min]	Area [mAU*s]	Height [mAU]	Area %
1	11.094	VV	0.3141	1.19227e4	538.91772	48.6135
2	11.898	VV	0.3791	1.26028e4	466.64035	51.3865
Totals :				2.45255e4	1005.55807	

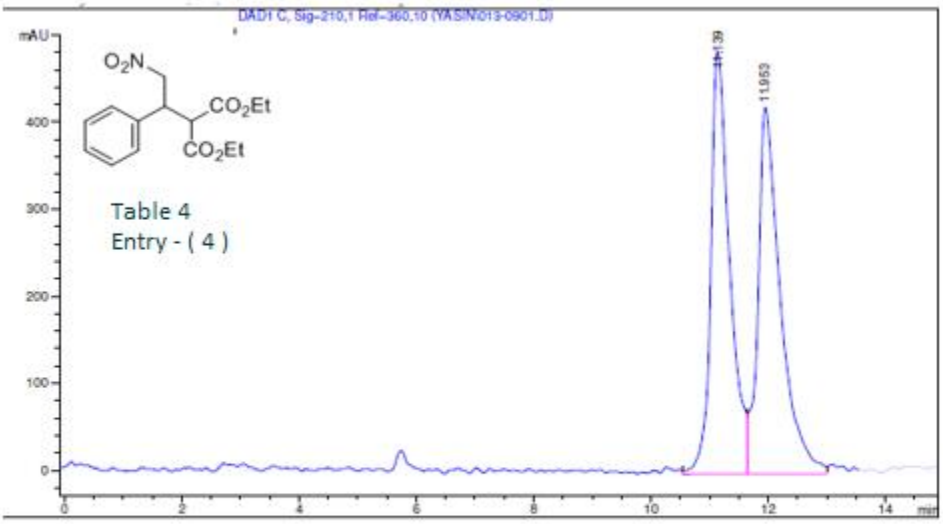

Peak #	RetTime [min]	Type	Width [min]	Area [mAU*s]	Height [mAU]	Area %
1	11.139	VV	0.3251	1.08776e4	485.96387	49.3409
2	11.953	VV	0.3696	1.11682e4	420.88135	50.6591
Totals :				2.20459e4	906.84521	

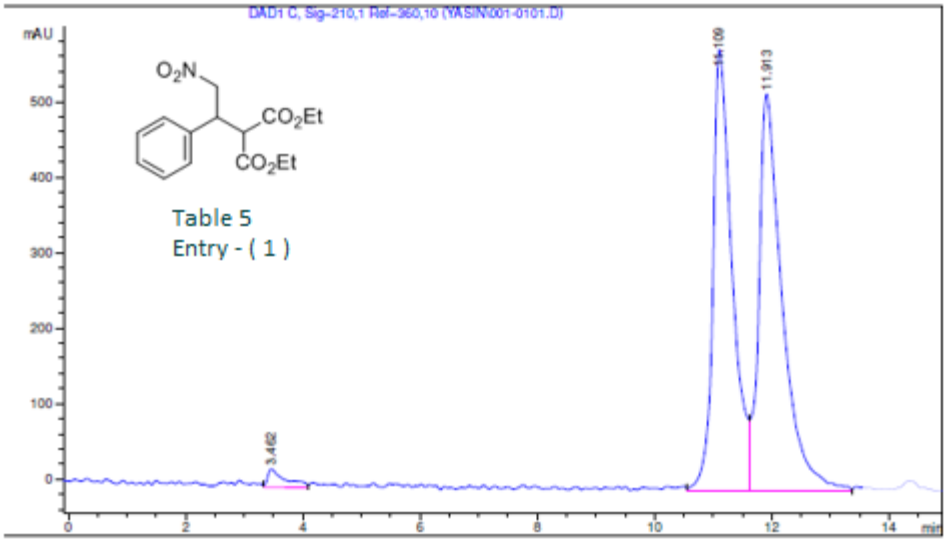

Peak #	RetTime [min]	Type	Width [min]	Area [mAU*s]	Height [mAU]	Area %
1	3.462	VV	0.2880	514.44360	24.19685	1.8118
2	11.109	VV	0.3288	1.32706e4	584.77081	46.7385
3	11.913	VV	0.3802	1.46083e4	525.72522	51.4497
Totals :				2.83934e4	1134.69288	

2- **HPLC of reaction β-nitrostyrene 52 and 2-hydroxy-1,4-napthoquinone 93**

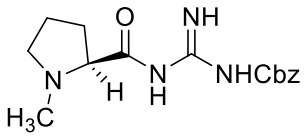

Result File : C:\HPLC1\Aileen\ChiralPakIA\YM65_2016__01_05_011.rst
Sequence File : C:\HPLC1\Aileen\ChiralPakIA\5Jan15_1.seq

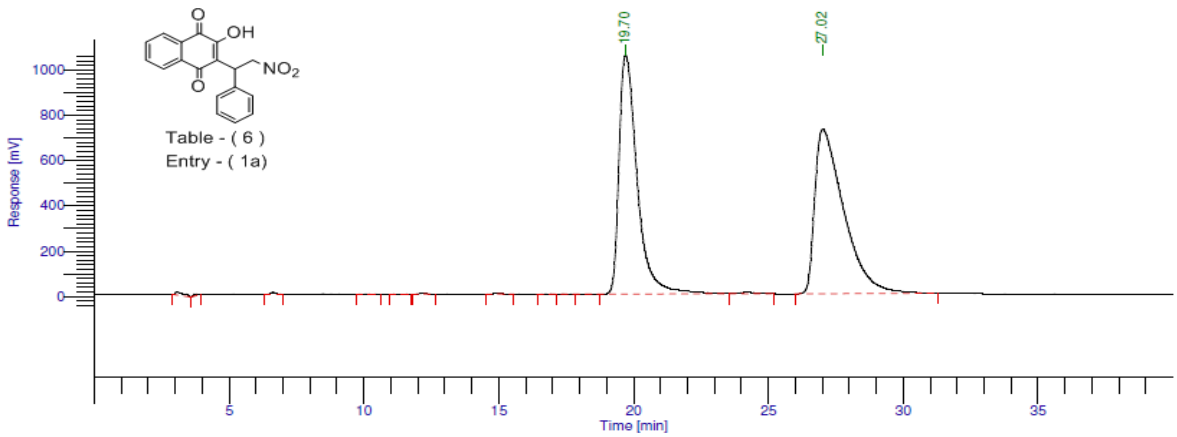

Peak #	Component Name	Time [min]	Area [uV*sec]	Height [uV]	Area [%]	BL	Adjusted Amount
10		19.702	49338866.84	1.05e+06	47.69	VV	49.3389
12		27.016	54124836.24	725956.36	52.31	BB	54.1248
			1.03e+08	1.78e+06	100.00		103.4637

Column: Chiralpak IA, 250 x 4.6 mm
Mobile Phase: 90% Hexane, 8% Ethanol, 2% Dichloromethane, 0.1% TFA
1ml/min, 254nm

Result File : C:\HPLC1\Aileen\ChiralPakIA\YM53_2_2015__08_12_011.rst
Sequence File : C:\HPLC1\Aileen\ChiralPakIA\12Aug15_1.seq

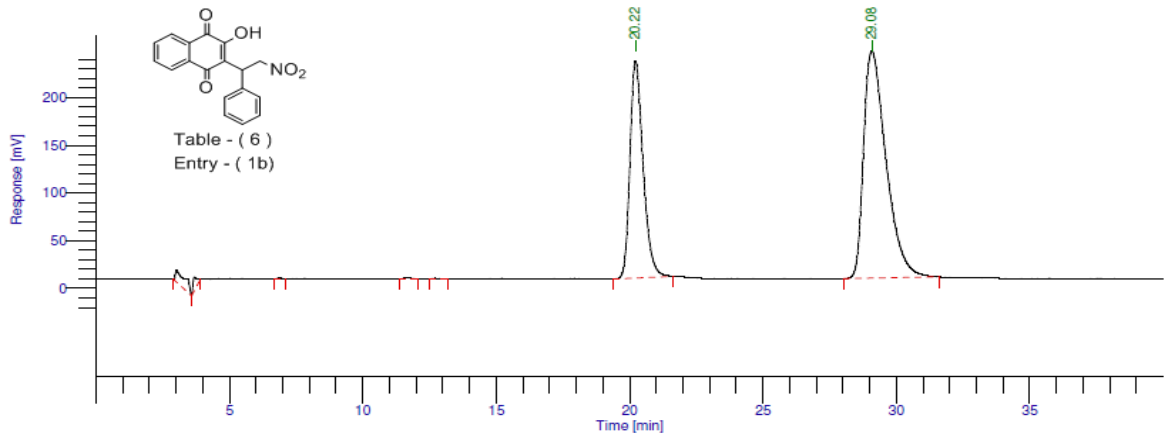

Peak #	Component Name	Time [min]	Area [uV*sec]	Height [uV]	Area [%]	BL	Adjusted Amount
6		20.221	7804981.77	227421.51	35.86	BB	7.8050
7		29.078	13962283.33	238494.83	64.14	BB	13.9623
			21767265.10	465916.35	100.00		21.7673

Column: Chiralpak IA, 250 x 4.6 mm
Mobile Phase: 90% Hexane, 8% Ethanol, 2% Dichloromethane, 0.1% TFA
1ml/min, 254nm

Result File : C:\HPLC1\Aileen\ChiralPakIA\YM54_2_2015__08_12_012.rst
Sequence File : C:\HPLC1\Aileen\ChiralPakIA\12Aug15_1.seq

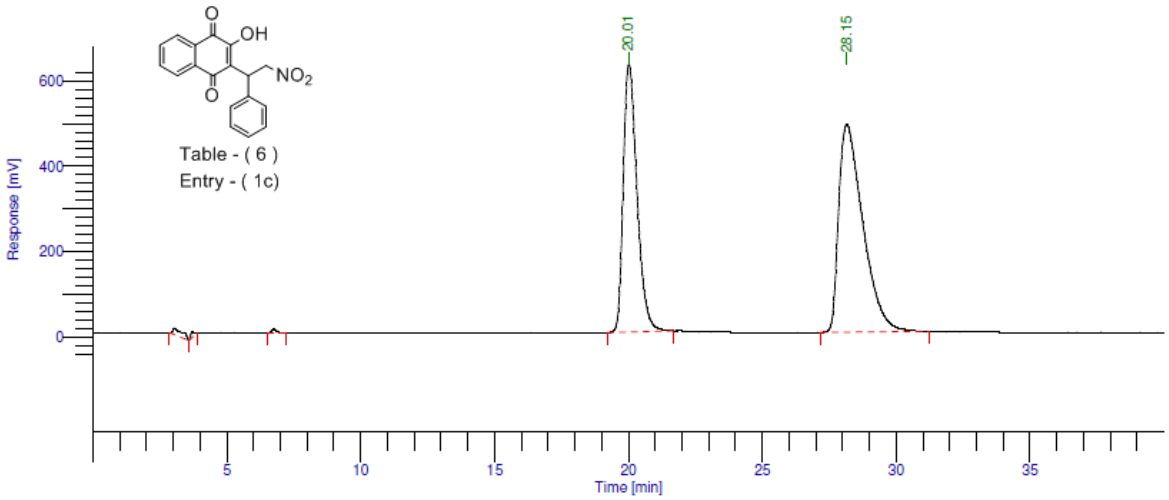

Peak #	Component Name	Time [min]	Area [uV*sec]	Height [uV]	Area [%]	BL	Adjusted Amount
4		20.014	22380874.03	627820.69	42.23	BB	22.3809
5		28.154	30619673.61	487045.14	57.77	BB	30.6197
			53000547.65	1.11e+06	100.00		53.0005

Column: Chiralpak IA, 250 x 4.6 mm
Mobile Phase: 90% Hexane, 8% Ethanol, 2% Dichloromethane, 0.1% TFA
1ml/min, 254nm

Result File : C:\HPLC1\Aileen\ChiralPakIA\YM58_2016__01_05_004.rst
Sequence File : C:\HPLC1\Aileen\ChiralPakIA\5Jan15_1.seq

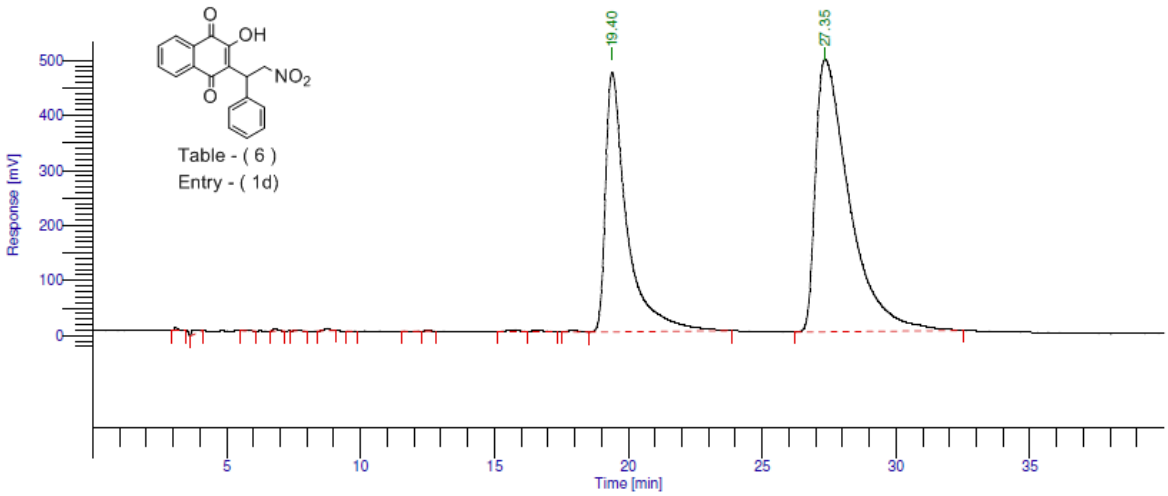

Peak #	Component Name	Time [min]	Area [uV*sec]	Height [uV]	Area [%]	BL	Adjusted Amount
13		19.399	26034480.03	471169.84	37.39	BB	26.0345
14		27.355	43587426.47	494859.86	62.61	BB	43.5874
			69621906.50	966029.71	100.00		69.6219

Column: Chiralpak IA, 250 x 4.6 mm
Mobile Phase: 90% Hexane, 8% Ethanol, 2% Dichloromethane, 0.1% TFA
1ml/min, 254nm

Injection Details

Injection Name:	**YM-59**	*Run Time (min):*	**40.00**
Vial Number:	**BA4**	*Injection Volume:*	**20.00**
Injection Type:	**Unknown**	*Channel:*	**UV_VIS_1**
Calibration Level:		*Wavelength:*	**254.0**
Instrument Method:	**Chiralpak AS-H**	*Bandwidth:*	**n.a.**
Processing Method:	**Caffiene16**	*Dilution Factor:*	**1.0000**
Injection Date/Time:	**28/Feb/17 19:25**	*Sample Weight:*	**1.0000**

Chromatogram

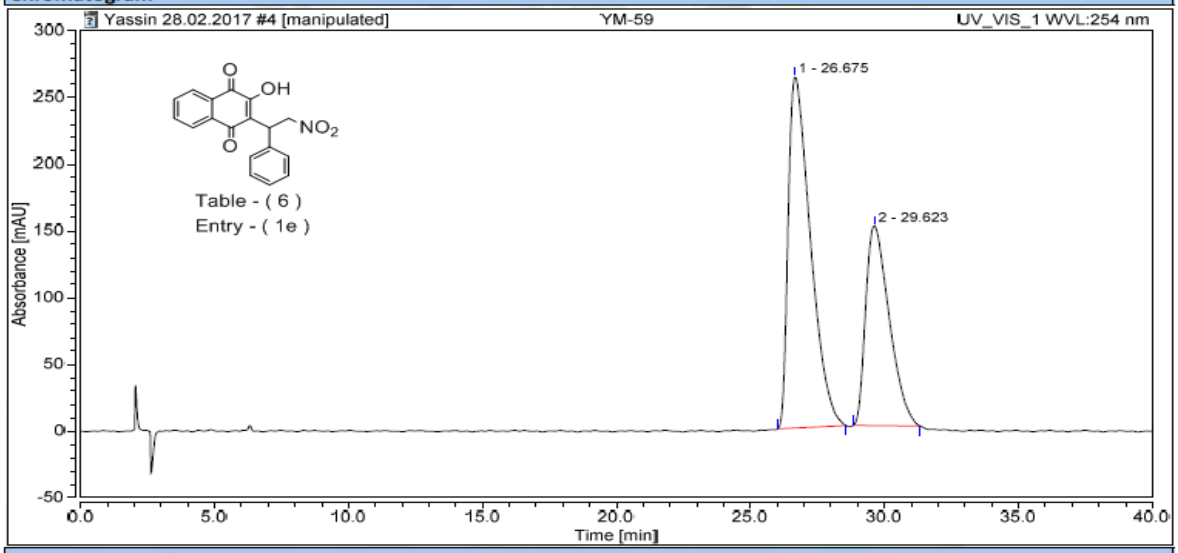

Integration Results

No.	Peak Name	Retention Time min	Area mAU*min	Height mAU	Relative Area %	Relative Height %	Amount
n.a.	Caffeine	n.a.	n.a.	n.a.	n.a.	n.a.	n.a.
1		26.675	252.966	263.382	62.39	63.75	n.a.
2		29.623	152.487	149.753	37.61	36.25	n.a.
Total:			**405.453**	**413.135**	**100.00**	**100.00**	

Injection Details			
Injection Name:	**YM-162**	*Run Time (min):*	**40.00**
Vial Number:	**BE8**	*Injection Volume:*	**20.00**
Injection Type:	**Unknown**	*Channel:*	**UV_VIS_1**
Calibration Level:		*Wavelength:*	**254.0**
Instrument Method:	**Chiralpak AS-H**	*Bandwidth:*	**n.a.**
Processing Method:	**Caffiene16**	*Dilution Factor:*	**1.0000**
Injection Date/Time:	**01/Mar/17 20:43**	*Sample Weight:*	**1.0000**

Chromatogram

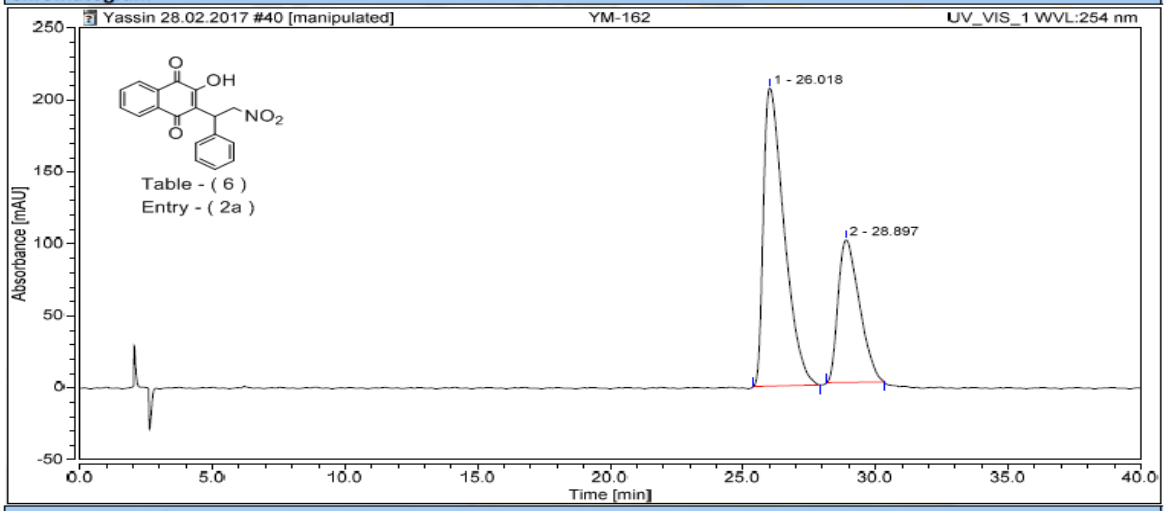

Integration Results

No.	Peak Name	Retention Time min	Area mAU*min	Height mAU	Relative Area %	Relative Height %	Amount
n.a.	Caffeine	n.a.	n.a.	n.a.	n.a.	n.a.	n.a.
1		26.018	187.711	207.390	66.97	67.65	n.a.
2		28.897	92.567	99.190	33.03	32.35	n.a.
Total:			**280.278**	**306.580**	**100.00**	**100.00**	

Injection Details			
Injection Name:	**YM-158**	*Run Time (min):*	**40.00**
Vial Number:	**BE4**	*Injection Volume:*	**20.00**
Injection Type:	**Unknown**	*Channel:*	**UV_VIS_1**
Calibration Level:		*Wavelength:*	**254.0**
Instrument Method:	**Chiralpak AS-H**	*Bandwidth:*	**n.a.**
Processing Method:	**Caffiene16**	*Dilution Factor:*	**1.0000**
Injection Date/Time:	**01/Mar/17 17:54**	*Sample Weight:*	**1.0000**

Chromatogram

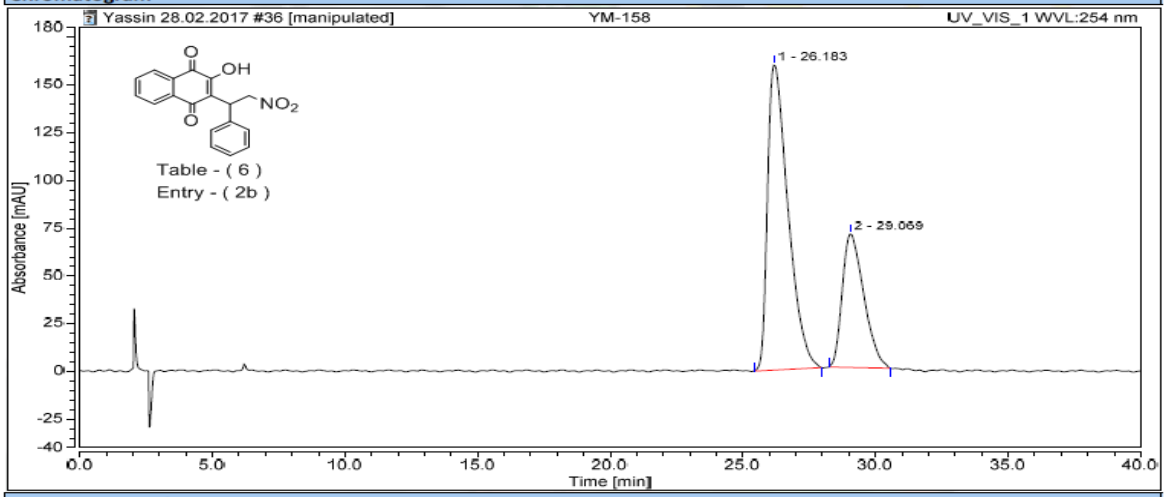

Integration Results

No.	Peak Name	Retention Time min	Area mAU*min	Height mAU	Relative Area %	Relative Height %	Amount
n.a.	Caffeine	n.a.	n.a.	n.a.	n.a.	n.a.	n.a.
1		26.183	143.072	160.214	68.49	69.60	n.a.
2		29.069	65.829	69.975	31.51	30.40	n.a.
Total:			**208.901**	**230.190**	**100.00**	**100.00**	

Injection Details

Injection Name:	**YM-157-THF**	*Run Time (min):*	**40.00**
Vial Number:	**BA3**	*Injection Volume:*	**20.00**
Injection Type:	**Unknown**	*Channel:*	**UV_VIS_1**
Calibration Level:		*Wavelength:*	**254.0**
Instrument Method:	**Chiralpak AS-H**	*Bandwidth:*	**n.a.**
Processing Method:	**Caffiene16**	*Dilution Factor:*	**1.0000**
Injection Date/Time:	**24/Mar/17 13:37**	*Sample Weight:*	**1.0000**

Chromatogram

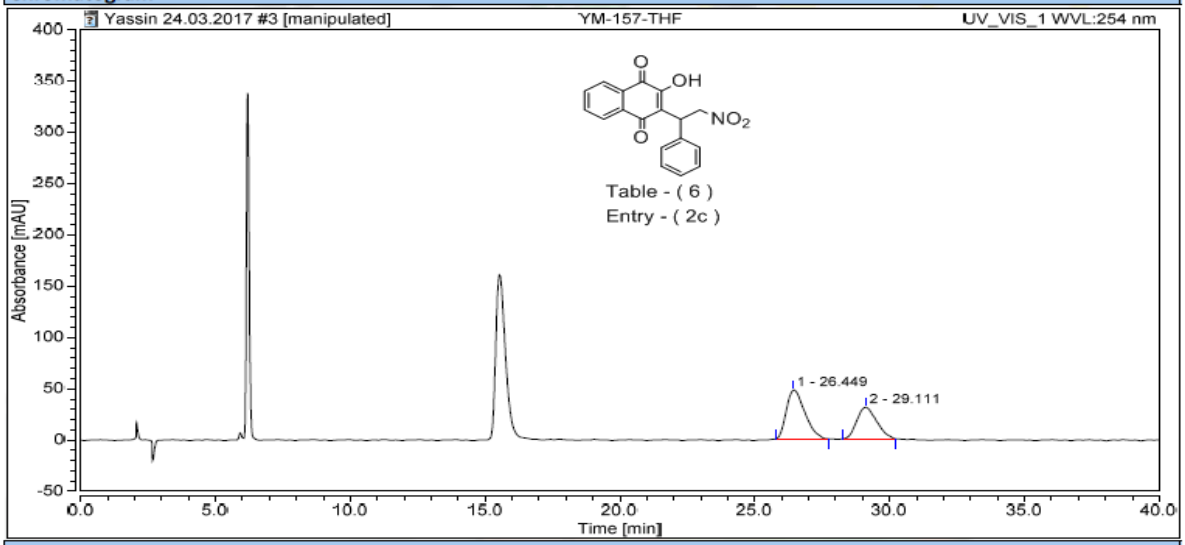

Integration Results

No.	Peak Name	Retention Time min	Area mAU*min	Height mAU	Relative Area %	Relative Height %	Amount
n.a.	Caffeine	n.a.	n.a.	n.a.	n.a.	n.a.	n.a.
1		26.449	37.532	47.607	58.77	60.59	n.a.
2		29.111	26.333	30.962	41.23	39.41	n.a.
Total:			**63.865**	**78.570**	**100.00**	**100.00**	

Injection Details

Injection Name:	**YM-157-Toluene**	*Run Time (min):*	**40.00**
Vial Number:	**BA4**	*Injection Volume:*	**20.00**
Injection Type:	**Unknown**	*Channel:*	**UV_VIS_1**
Calibration Level:		*Wavelength:*	**254.0**
Instrument Method:	**Chiralpak AS-H**	*Bandwidth:*	**n.a.**
Processing Method:	**Caffiene16**	*Dilution Factor:*	**1.0000**
Injection Date/Time:	**24/Mar/17 14:19**	*Sample Weight:*	**1.0000**

Chromatogram

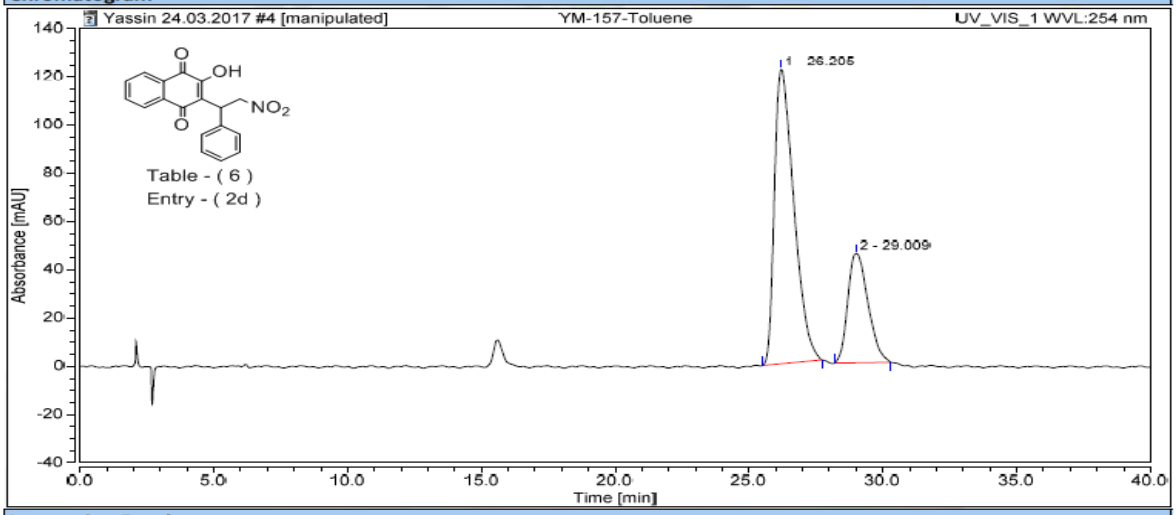

Integration Results

No.	Peak Name	Retention Time min	Area mAU*min	Height mAU	Relative Area %	Relative Height %	Amount
n.a.	Caffeine	n.a.	n.a.	n.a.	n.a.	n.a.	n.a.
1		26.205	102.769	122.096	72.14	72.88	n.a.
2		29.009	39.680	45.432	27.86	27.12	n.a.
Total:			**142.449**	**167.528**	**100.00**	**100.00**	

Injection Details

Injection Name:	**YM-157-EtOAc**	*Run Time (min):*	**40.00**
Vial Number:	**BA5**	*Injection Volume:*	**20.00**
Injection Type:	**Unknown**	*Channel:*	**UV_VIS_1**
Calibration Level:		*Wavelength:*	**254.0**
Instrument Method:	**Chiralpak AS-H**	*Bandwidth:*	**n.a.**
Processing Method:	**Caffiene16**	*Dilution Factor:*	**1.0000**
Injection Date/Time:	**24/Mar/17 15:01**	*Sample Weight:*	**1.0000**

Chromatogram

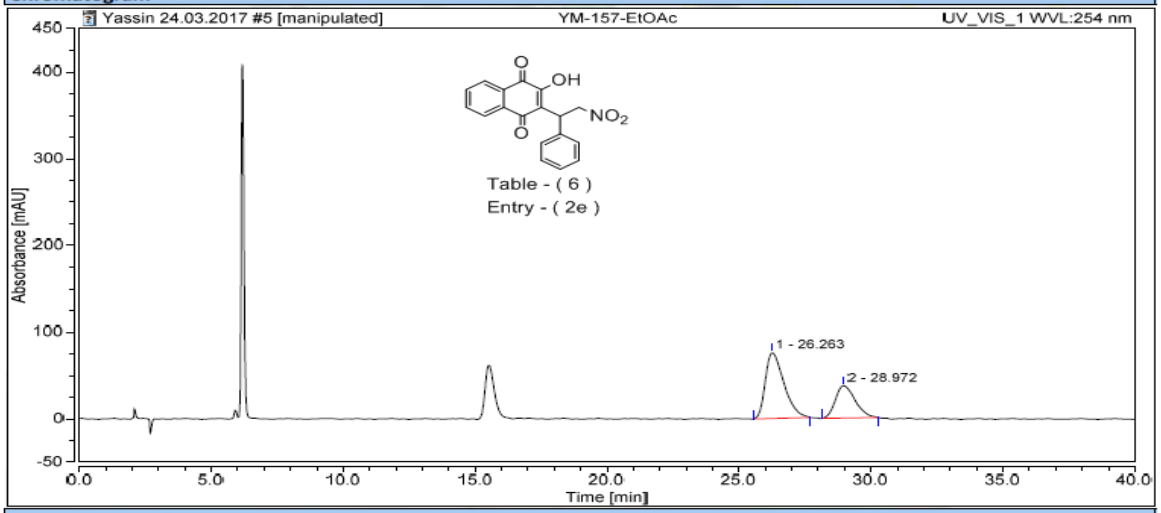

Integration Results

No.	Peak Name	Retention Time min	Area mAU*min	Height mAU	Relative Area %	Relative Height %	Amount
n.a.	Caffeine	n.a.	n.a.	n.a.	n.a.	n.a.	n.a.
1		26.263	61.939	75.849	65.68	67.03	n.a.
2		28.972	32.371	37.315	34.32	32.97	n.a.
Total:			**94.310**	**113.164**	**100.00**	**100.00**	

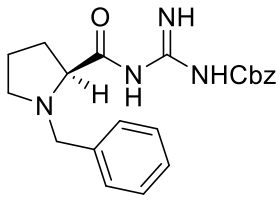

Result File : C:\HPLC1\Aileen\ChiralPakIA\YM64_2016__01_05_010.rst
Sequence File : C:\HPLC1\Aileen\ChiralPakIA\5Jan15_1.seq

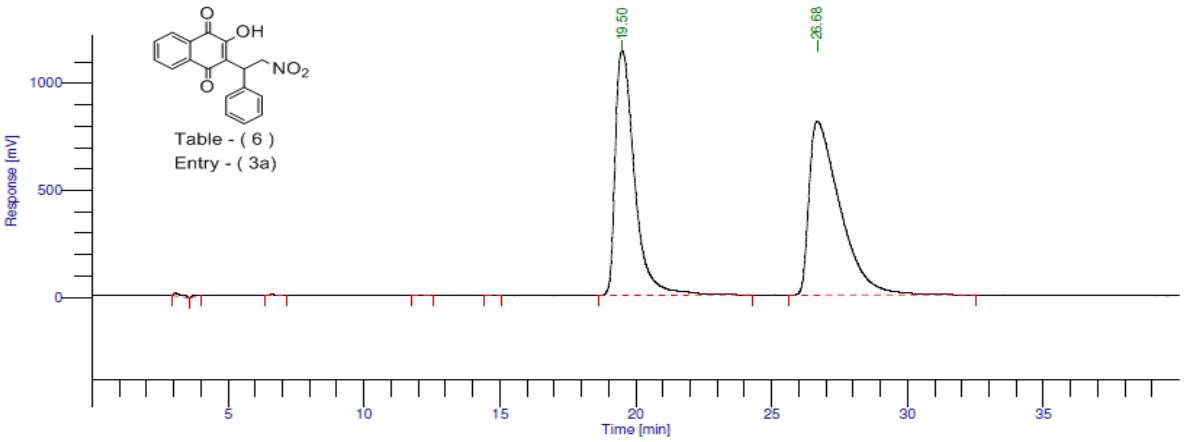

Peak #	Component Name	Time [min]	Area [uV*sec]	Height [uV]	Area [%]	BL	Adjusted Amount
6		19.497	56323489.49	1.14e+06	46.68	BB	56.3235
7		26.679	64343888.07	811720.81	53.32	BB	64.3439
			1.21e+08	1.95e+06	100.00		120.6674

Column: Chiralpak IA, 250 x 4.6 mm
Mobile Phase: 90% Hexane, 8% Ethanol, 2% Dichloromethane, 0.1% TFA
1ml/min, 254nm

Result File : C:\HPLC1\Aileen\ChiralPakIA\YM61_2016__01_05_007.rst
Sequence File : C:\HPLC1\Aileen\ChiralPakIA\5Jan15_1.seq

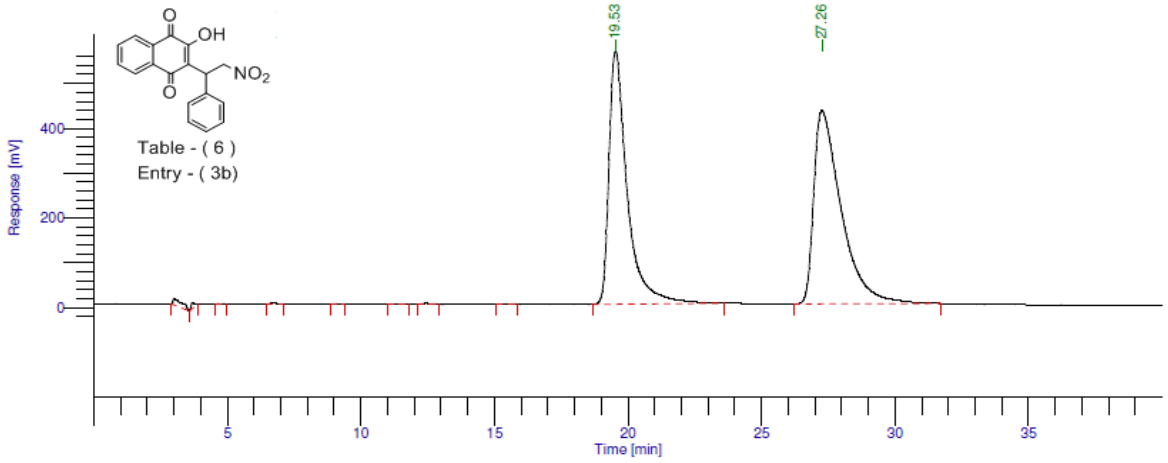

Peak #	Component Name	Time [min]	Area [uV*sec]	Height [uV]	Area [%]	BL	Adjusted Amount
9		19.531	26763471.37	565092.49	46.47	BB	26.7635
10		27.264	30834327.29	430784.38	53.53	BB	30.8343
			57597798.66	995876.87	100.00		57.5978

Column: Chiralpak IA, 250 x 4.6 mm
Mobile Phase: 90% Hexane, 8% Ethanol, 2% Dichloromethane, 0.1% TFA
1ml/min, 254nm

Result File : C:\HPLC1\Aileen\ChiralPakIA\YM62_2016__01_05_008.rst
Sequence File : C:\HPLC1\Aileen\ChiralPakIA\5Jan15_1.seq

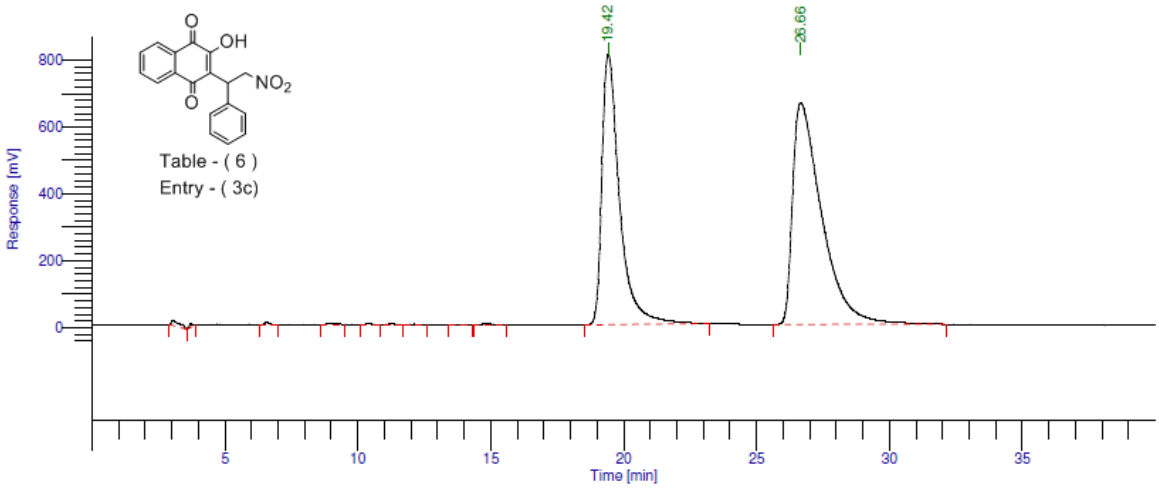

Peak #	Component Name	Time [min]	Area [uV*sec]	Height [uV]	Area [%]	BL	Adjusted Amount
10		19.420	37328223.85	808629.72	42.55	BB	37.3282
11		26.661	50391303.99	663211.43	57.45	BB	50.3913
			87719527.84	1.47e+06	100.00		87.7195

Column: Chiralpak IA, 250 x 4.6 mm
Mobile Phase: 90% Hexane, 8% Ethanol, 2% Dichloromethane, 0.1% TFA
1ml/min, 254nm

Result File : C:\HPLC1\Aileen\ChiralPakIA\YM60_2016__01_05_006.rst
Sequence File : C:\HPLC1\Aileen\ChiralPakIA\5Jan15_1.seq

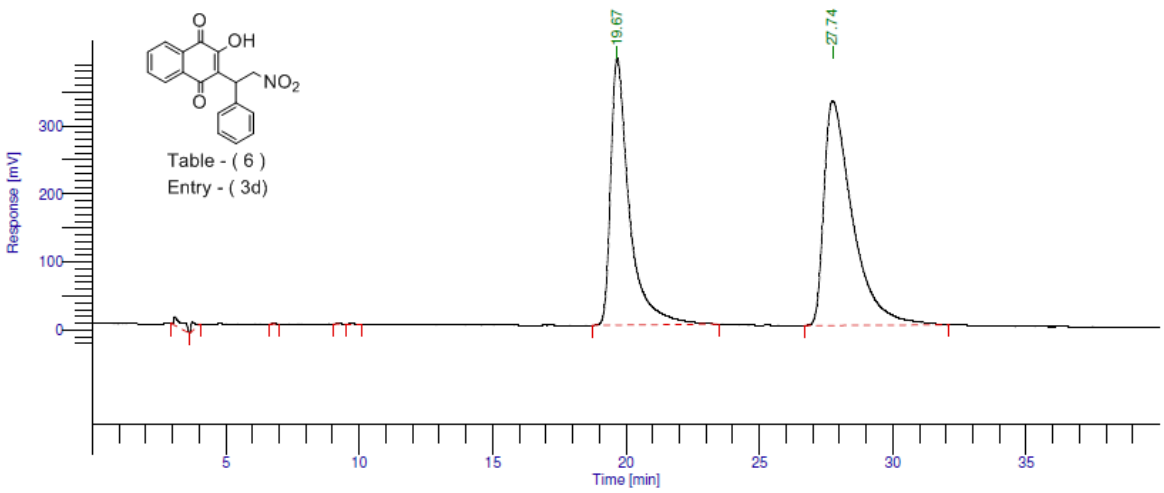

Peak #	Component Name	Time [min]	Area [uV*sec]	Height [uV]	Area [%]	BL	Adjusted Amount
6		19.667	19035528.49	392608.23	43.63	BB	19.0355
7		27.739	24598744.83	330605.37	56.37	BB	24.5987
			43634273.32	723213.60	100.00		43.6343

Column: Chiralpak IA, 250 x 4.6 mm
Mobile Phase: 90% Hexane, 8% Ethanol, 2% Dichloromethane, 0.1% TFA
1ml/min, 254nm

Result File : C:\HPLC1\Aileen\ChiralPakIA\YM63_2016__01_05_009.rst
Sequence File : C:\HPLC1\Aileen\ChiralPakIA\5Jan15_1.seq

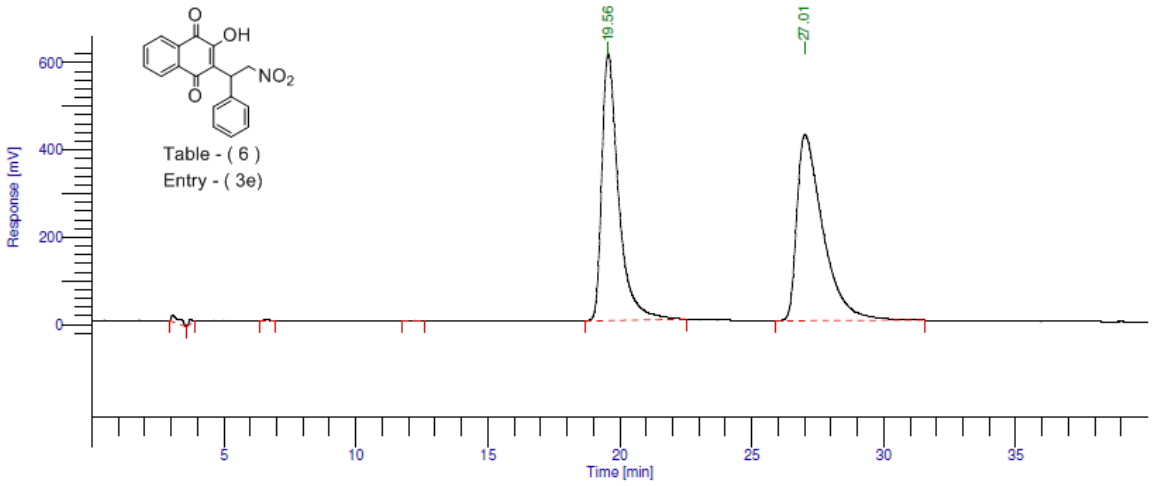

Peak #	Component Name	Time [min]	Area [uV*sec]	Height [uV]	Area [%]	BL	Adjusted Amount
5		19.558	26964946.49	612012.15	47.95	BB	26.9649
6		27.009	29275674.95	426636.44	52.05	BB	29.2757
			56240621.44	1.04e+06	100.00		56.2406

Column: Chiralpak IA, 250 x 4.6 mm
Mobile Phase: 90% Hexane, 8% Ethanol, 2% Dichloromethane, 0.1% TFA
1ml/min, 254nm

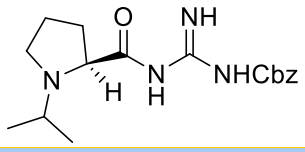

Injection Details

Injection Name:	**YM-96**	*Run Time (min):*	**40.00**
Vial Number:	**BD6**	*Injection Volume:*	**20.00**
Injection Type:	**Unknown**	*Channel:*	**UV_VIS_1**
Calibration Level:		*Wavelength:*	**254.0**
Instrument Method:	**Chiralpak AS-H**	*Bandwidth:*	**n.a.**
Processing Method:	**Caffiene16**	*Dilution Factor:*	**1.0000**
Injection Date/Time:	**01/Mar/17 13:41**	*Sample Weight:*	**1.0000**

Chromatogram

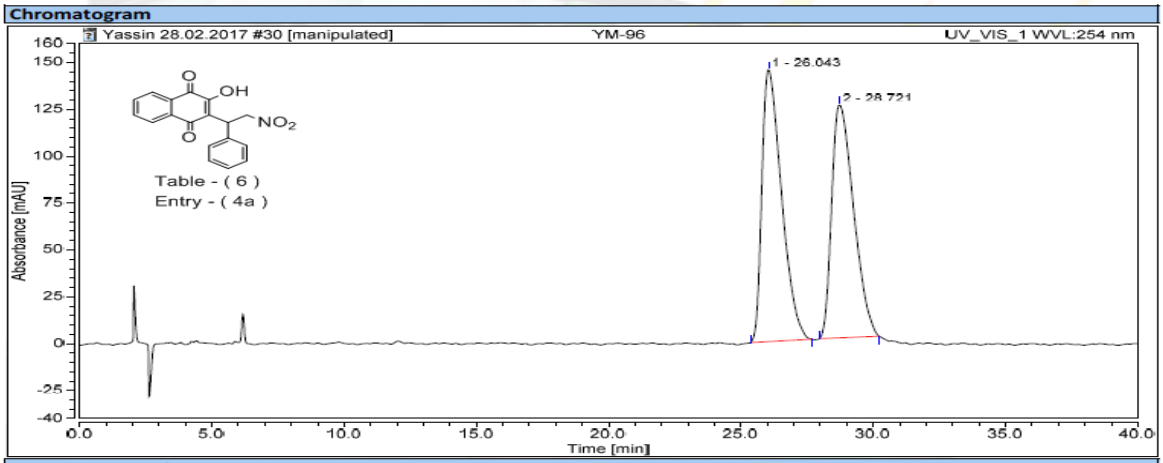

Integration Results

No.	Peak Name	Retention Time min	Area mAU*min	Height mAU	Relative Area %	Relative Height %	Amount
n.a.	Caffeine	n.a.	n.a.	n.a.	n.a.	n.a.	n.a.
1		26.043	124.807	145.166	51.14	53.85	n.a.
2		28.721	119.266	124.422	48.86	46.15	n.a.
Total:			**244.073**	**269.588**	**100.00**	**100.00**	

Result File : C:\HPLC1\Aileen\ChiralPakIA\AMOD\YM95_2016__07_14_017.rst
Sequence File : C:\HPLC1\Aileen\ChiralPakIA\AMOD\12July16_2.seq

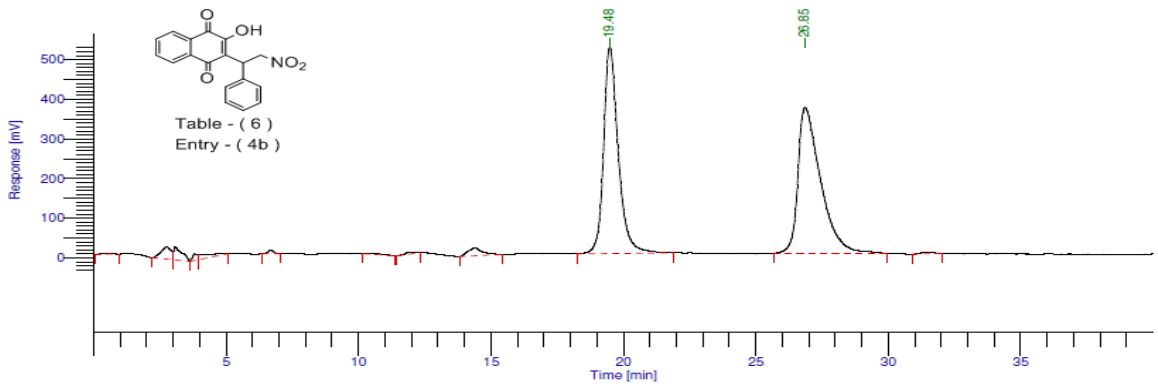

Peak #	Component Name	Time [min]	Area [uV*sec]	Height [uV]	Area [%]	BL	Adjusted Amount
10		19.483	19977653.89	520412.01	47.80	BB	19.9777
11		26.852	21813322.59	367675.13	52.20	BB	21.8133
			41790976.48	888087.14	100.00		41.7910

Column: Chiralpak IA, 250 x 4.6 mm
Mobile Phase: 90% Hexane, 8% Ethanol, 2% Dichloromethane, 0.1% TFA
1ml/min, 254nm

Result File : C:\HPLC1\Aileen\ChiralPakIA\AMOD\YM97_2016__07_14_002.rst
Sequence File : C:\HPLC1\Aileen\ChiralPakIA\AMOD\14July16_1.seq

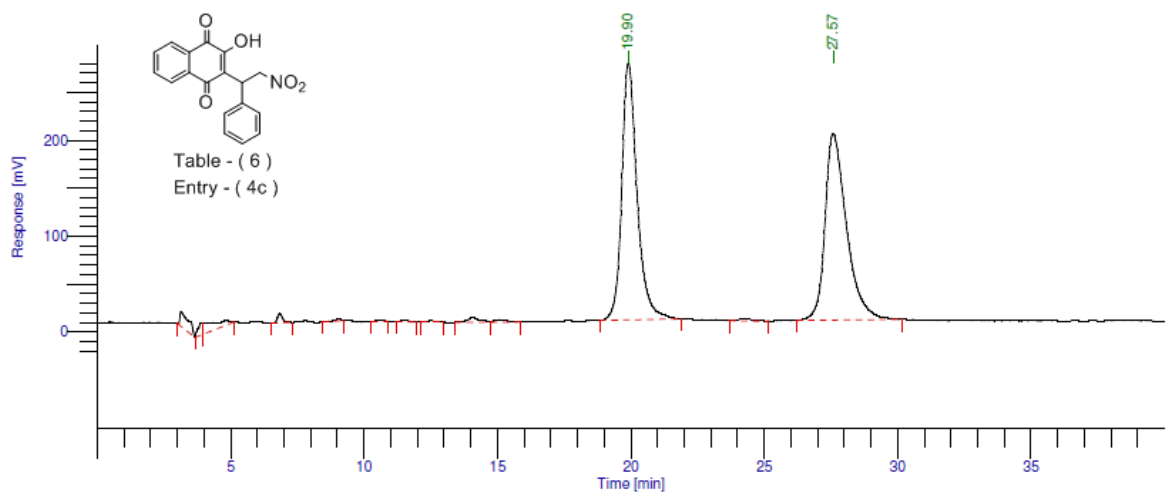

Peak #	Component Name	Time [min]	Area [uV*sec]	Height [uV]	Area [%]	BL	Adjusted Amount
11		19.903	10729837.75	268376.20	49.62	BB	10.7298
13		27.575	10893043.86	194530.46	50.38	BB	10.8930
			21622881.61	462906.66	100.00		21.6229

Column: Chiralpak IA, 250 x 4.6 mm
Mobile Phase: 90% Hexane, 8% Ethanol, 2% Dichloromethane, 0.1% TFA
1ml/min, 254nm

Result File : C:\HPLC1\Aileen\ChiralPakIA\AMOD\YM98_2016__07_13_004.rst
Sequence File : C:\HPLC1\Aileen\ChiralPakIA\AMOD\12July16_2.seq

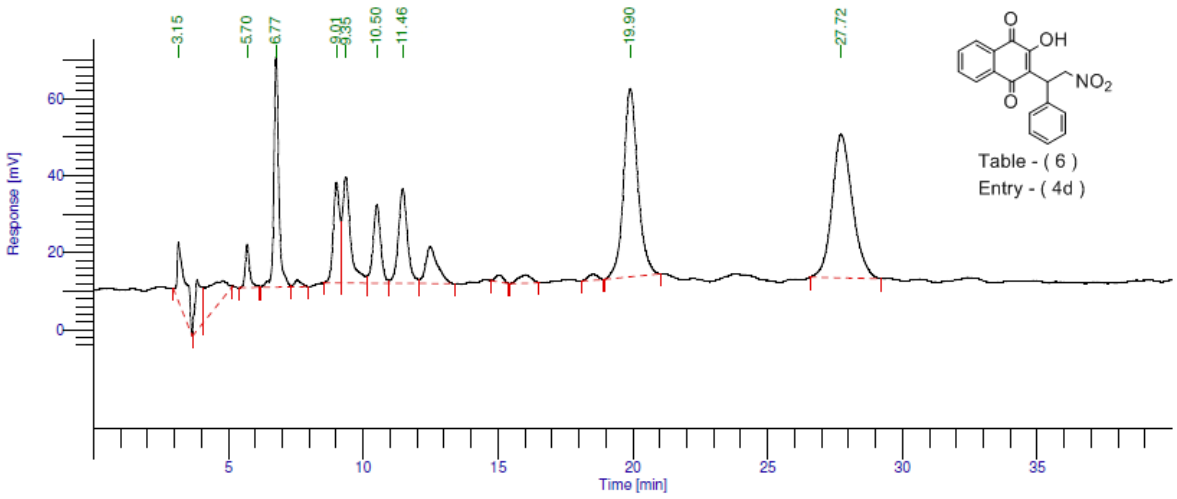

Table - (6)
Entry - (4d)

Peak #	Component Name	Time [min]	Area [uV*sec]	Height [uV]	Area [%]	BL	Adjusted Amount
15		19.897	1795552.57	48848.66	47.92	BB	1.7956
16		27.724	1951602.88	37252.12	52.08	BB	1.9516
			3747155.44	86100.78	100.00		3.7472

Column: Chiralpak IA, 250 x 4.6 mm
Mobile Phase: 90% Hexane, 8% Ethanol, 2% Dichloromethane, 0.1% TFA
1ml/min, 254nm

Result File : C:\HPLC1\Aileen\ChiralPakIA\AMOD\YM99_2016__07_13_005.rst
Sequence File : C:\HPLC1\Aileen\ChiralPakIA\AMOD\12July16_2.seq

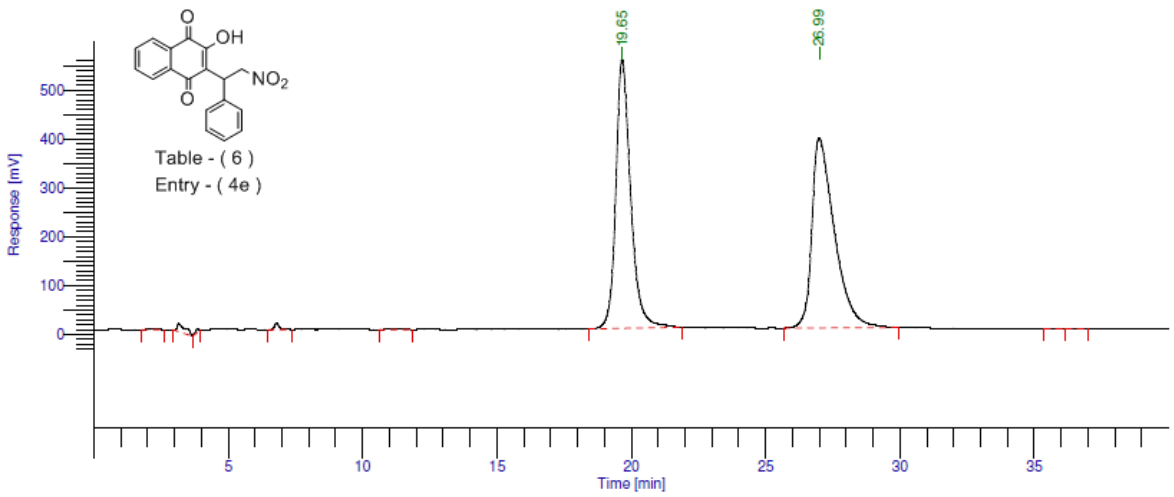

Peak #	Component Name	Time [min]	Area [uV*sec]	Height [uV]	Area [%]	BL	Adjusted Amount
6		19.654	21088720.93	551010.68	48.26	BB	21.0887
7		26.989	22608768.81	388115.76	51.74	BB	22.6088
			43697489.73	939126.43	100.00		43.6975

Column: Chiralpak IA, 250 x 4.6 mm
Mobile Phase: 90% Hexane, 8% Ethanol, 2% Dichloromethane, 0.1% TFA
1ml/min, 254nm

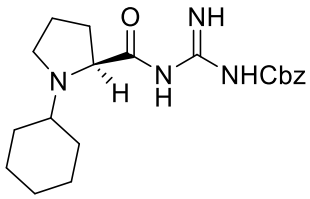

Injection Details

Injection Name:	**YM-169**	*Run Time (min):*	**40.00**
Vial Number:	**RA2**	*Injection Volume:*	**20.00**
Injection Type:	**Unknown**	*Channel:*	**UV_VIS_1**
Calibration Level:		*Wavelength:*	**254.0**
Instrument Method:	**Chiralpak AS-H**	*Bandwidth:*	**n.a.**
Processing Method:	**Caffiene16**	*Dilution Factor:*	**1.0000**
Injection Date/Time:	**01/Mar/17 22:07**	*Sample Weight:*	**1.0000**

Chromatogram

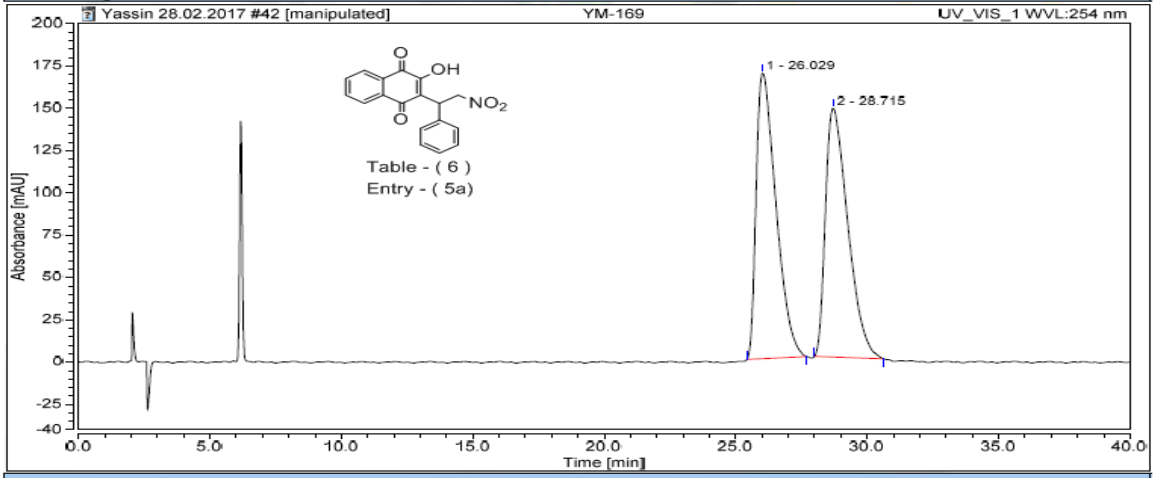

Integration Results

No.	Peak Name	Retention Time min	Area mAU*min	Height mAU	Relative Area %	Relative Height %	Amount
n.a.	Caffeine	n.a.	n.a.	n.a.	n.a.	n.a.	n.a.
1		26.029	147.115	168.966	50.36	53.46	n.a.
2		28.715	145.013	147.100	49.64	46.54	n.a.
Total:			**292.128**	**316.065**	**100.00**	**100.00**	

Injection Details

Injection Name:	**YM-168**	*Run Time (min):*	**40.00**
Vial Number:	**RA1**	*Injection Volume:*	**20.00**
Injection Type:	**Unknown**	*Channel:*	**UV_VIS_1**
Calibration Level:		*Wavelength:*	**254.0**
Instrument Method:	**Chiralpak AS-H**	*Bandwidth:*	**n.a.**
Processing Method:	**Caffiene16**	*Dilution Factor:*	**1.0000**
Injection Date/Time:	**01/Mar/17 21:25**	*Sample Weight:*	**1.0000**

Chromatogram

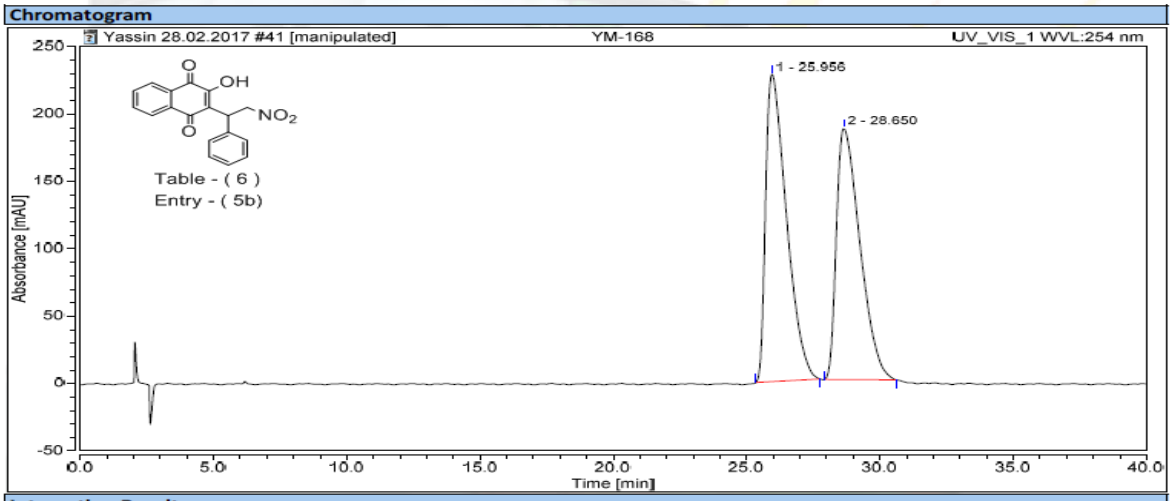

Integration Results

No.	Peak Name	Retention Time min	Area mAU*min	Height mAU	Relative Area %	Relative Height %	Amount
n.a.	Caffeine	n.a.	n.a.	n.a.	n.a.	n.a.	n.a.
1		25.956	206.508	228.105	52.02	55.02	n.a.
2		28.650	190.466	186.476	47.98	44.98	n.a.
Total:			**396.974**	**414.581**	**100.00**	**100.00**	

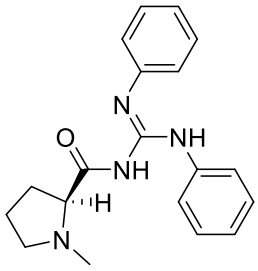

Result File : C:\HPLC1\Aileen\ChiralPakIA\AMOD\YM81_2016__07_13_008.rst
Sequence File : C:\HPLC1\Aileen\ChiralPakIA\AMOD\12July16_2.seq

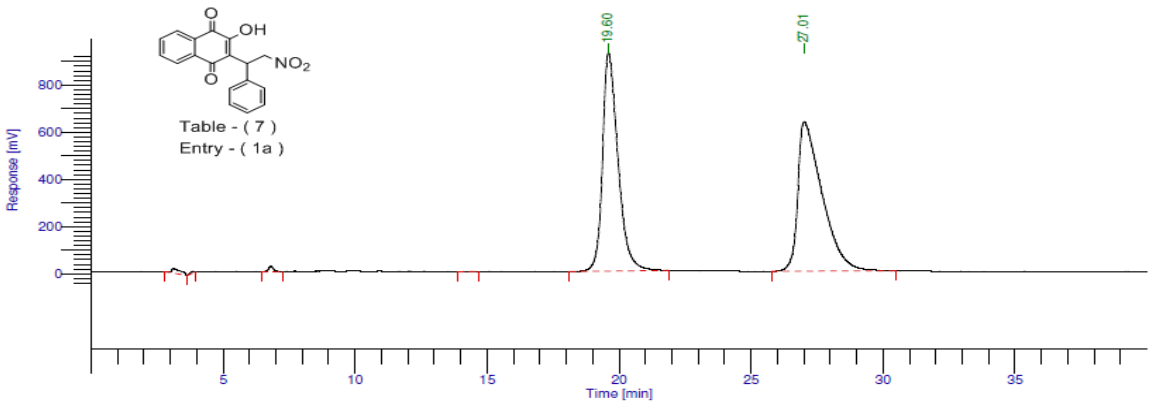

Peak #	Component Name	Time [min]	Area [uV*sec]	Height [uV]	Area [%]	BL	Adjusted Amount
5		19.595	37638502.91	924727.83	48.17	BB	37.6385
6		27.011	40499885.95	633248.55	51.83	BB	40.4999
			78138388.86	1.56e+06	100.00		78.1384

Column: Chiralpak IA, 250 x 4.6 mm
Mobile Phase: 90% Hexane, 8% Ethanol, 2% Dichloromethane, 0.1% TFA
1ml/min, 254nm

Result File : C:\HPLC1\Aileen\ChiralPakIA\AMOD\YM80_2016__07_14_004.rst
Sequence File : C:\HPLC1\Aileen\ChiralPakIA\AMOD\14July16_1.seq

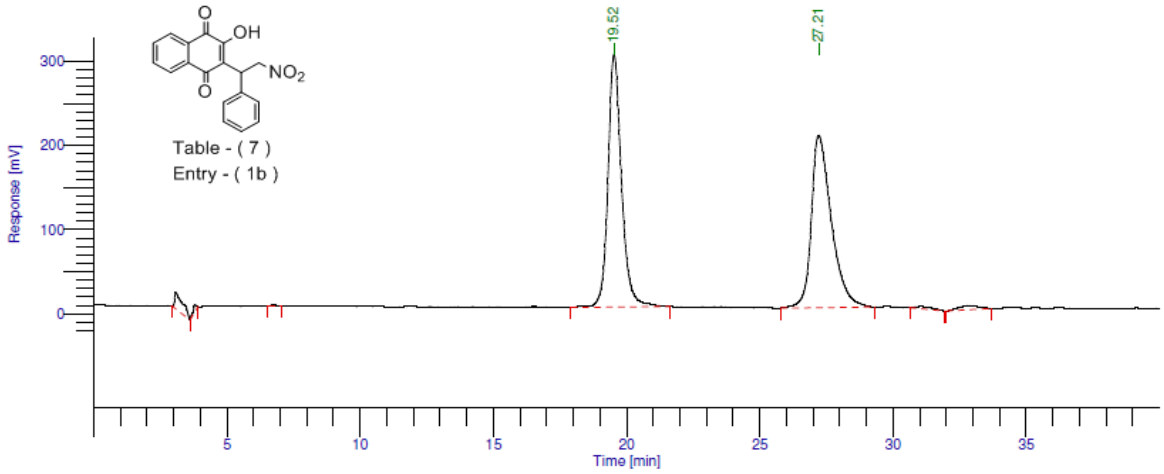

Peak #	Component Name	Time [min]	Area [uV*sec]	Height [uV]	Area [%]	BL	Adjusted Amount
4		19.522	10601458.03	300365.73	49.65	BB	10.6015
5		27.209	10753027.93	205415.11	50.35	BB	10.7530
			21354485.95	505780.84	100.00		21.3545

Column: Chiralpak IA, 250 x 4.6 mm
Mobile Phase: 90% Hexane, 8% Ethanol, 2% Dichloromethane, 0.1% TFA
1ml/min, 254nm

Result File : C:\HPLC1\Aileen\ChiralPakIA\AMOD\YM82_2016__07_13_009.rst
Sequence File : C:\HPLC1\Aileen\ChiralPakIA\AMOD\12July16_2.seq

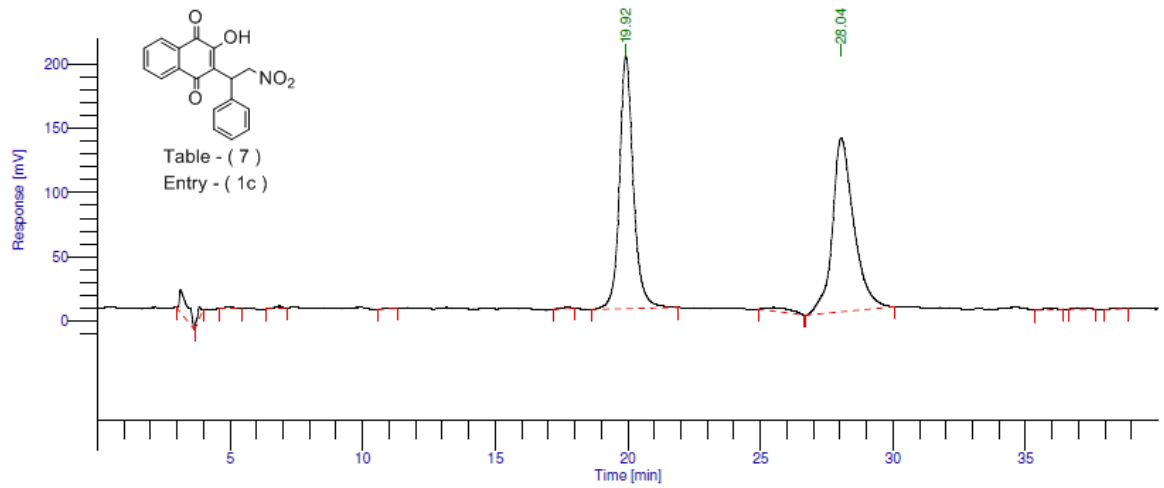

Peak #	Component Name	Time [min]	Area [uV*sec]	Height [uV]	Area [%]	BL	Adjustec Amount
7		19.921	7163704.24	196785.50	48.54	BB	7.1637
9		28.040	7594697.43	135230.28	51.46	BB	7.5947
			14758401.67	332015.79	100.00		14.7584

Column: Chiralpak IA, 250 x 4.6 mm
Mobile Phase: 90% Hexane, 8% Ethanol, 2% Dichloromethane, 0.1% TFA
1ml/min, 254nm

Result File : C:\HPLC1\Aileen\ChiralPakIA\AMOD\YM83_2016__07_13_010.rst
Sequence File : C:\HPLC1\Aileen\ChiralPakIA\AMOD\12July16_2.seq

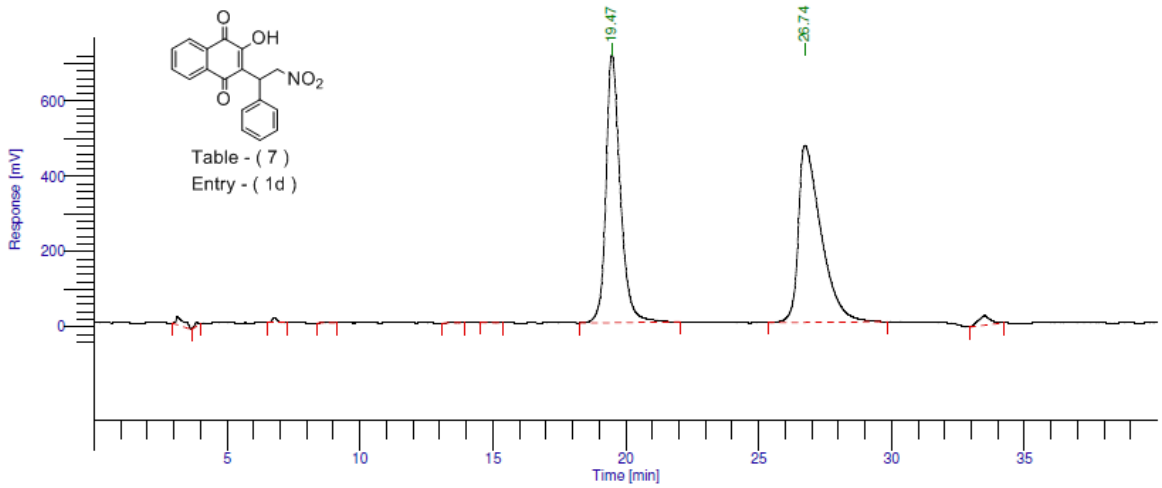

Peak #	Component Name	Time [min]	Area [uV*sec]	Height [uV]	Area [%]	BL	Adjusted Amount
7		19.474	26539943.89	711599.43	48.71	BB	26.5399
8		26.744	27950204.12	470514.53	51.29	BB	27.9502
			54490148.00	1.18e+06	100.00		54.4901

Column: Chiralpak IA, 250 x 4.6 mm
Mobile Phase: 90% Hexane, 8% Ethanol, 2% Dichloromethane, 0.1% TFA
1ml/min, 254nm

Result File : C:\HPLC1\Aileen\ChiralPakIA\AMOD\YM84_2016__07_13_011.rst
Sequence File : C:\HPLC1\Aileen\ChiralPakIA\AMOD\12July16_2.seq

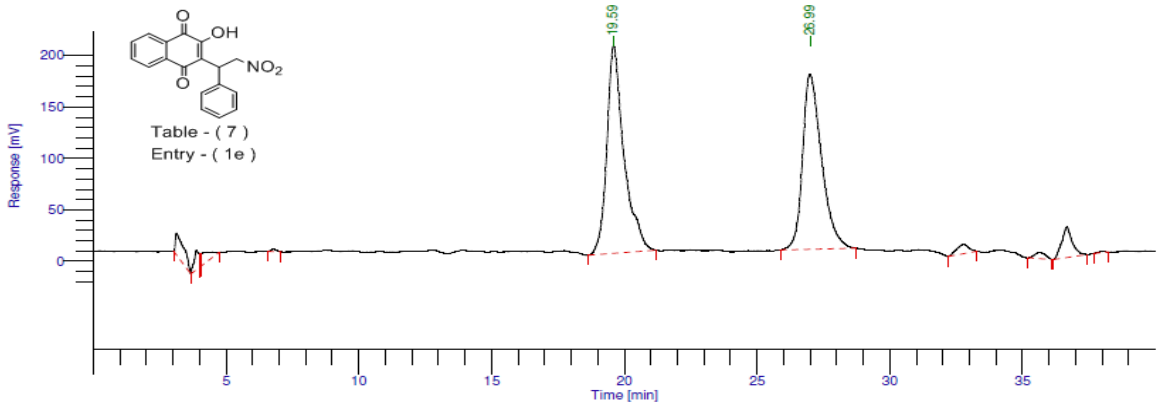

Peak #	Component Name	Time [min]	Area [uV*sec]	Height [uV]	Area [%]	BL	Adjusted Amount
5		19.592	9050987.32	201827.24	51.64	BB	9.0510
6		26.988	8475061.81	170067.85	48.36	BB	8.4751
			17526049.13	371895.09	100.00		17.5260

Column: Chiralpak IA, 250 x 4.6 mm
Mobile Phase: 90% Hexane, 8% Ethanol, 2% Dichloromethane, 0.1% TFA
1ml/min, 254nm

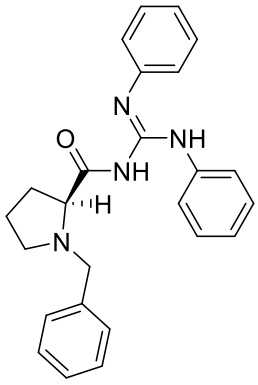

Result File : C:\HPLC1\Aileen\ChiralPakIA\AMOD\YM87_2016__07_13_013.rst
Sequence File : C:\HPLC1\Aileen\ChiralPakIA\AMOD\12July16_2.seq

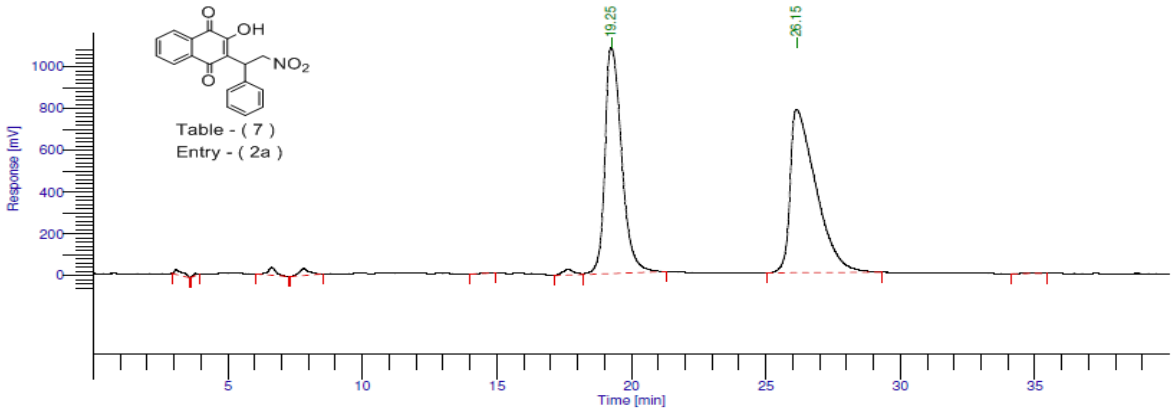

Peak #	Component Name	Time [min]	Area [uV*sec]	Height [uV]	Area [%]	BL	Adjusted Amount
7		19.252	46832882.14	1.08e+06	47.23	VB	46.8329
8		26.147	52321587.63	782628.03	52.77	BB	52.3216
			99154469.77	1.87e+06	100.00		99.1545

Column: Chiralpak IA, 250 x 4.6 mm
Mobile Phase: 90% Hexane, 8% Ethanol, 2% Dichloromethane, 0.1% TFA
1ml/min, 254nm

Result File : C:\HPLC1\Aileen\ChiralPakIA\AMOD\YM86_2016__07_14_005.rst
Sequence File : C:\HPLC1\Aileen\ChiralPakIA\AMOD\14July16_1.seq

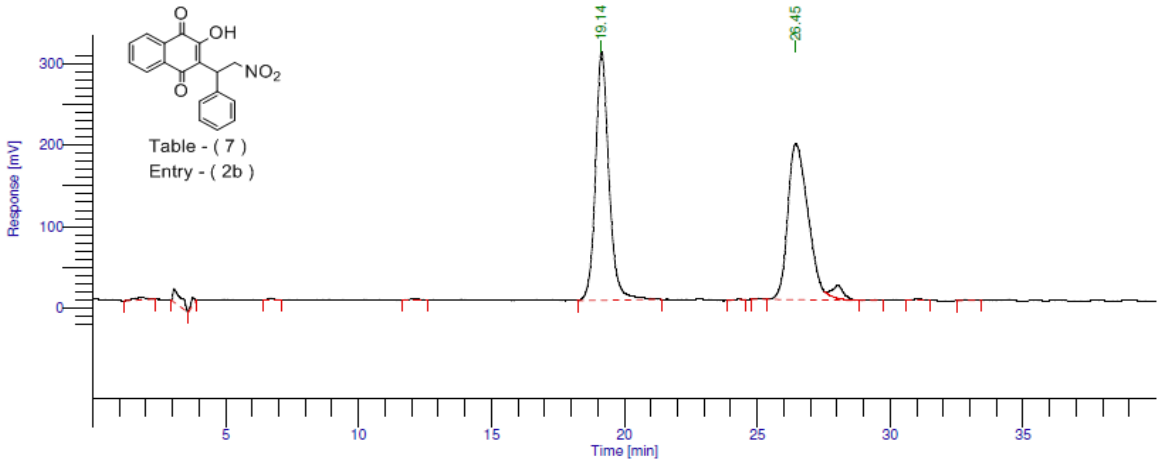

Peak #	Component Name	Time [min]	Area [uV*sec]	Height [uV]	Area [%]	BL	Adjusted Amount
6		19.140	10748920.61	304868.84	51.21	BB	10.7489
9		26.449	10239238.91	191164.30	48.79	VE	10.2392
			20988159.52	496033.14	100.00		20.9882

Column: Chiralpak IA, 250 x 4.6 mm
Mobile Phase: 90% Hexane, 8% Ethanol, 2% Dichloromethane, 0.1% TFA
1ml/min, 254nm

Result File : C:\HPLC1\Aileen\ChiralPakIA\AMOD\YM88_2016__07_13_014.rst
Sequence File : C:\HPLC1\Aileen\ChiralPakIA\AMOD\12July16_2.seq

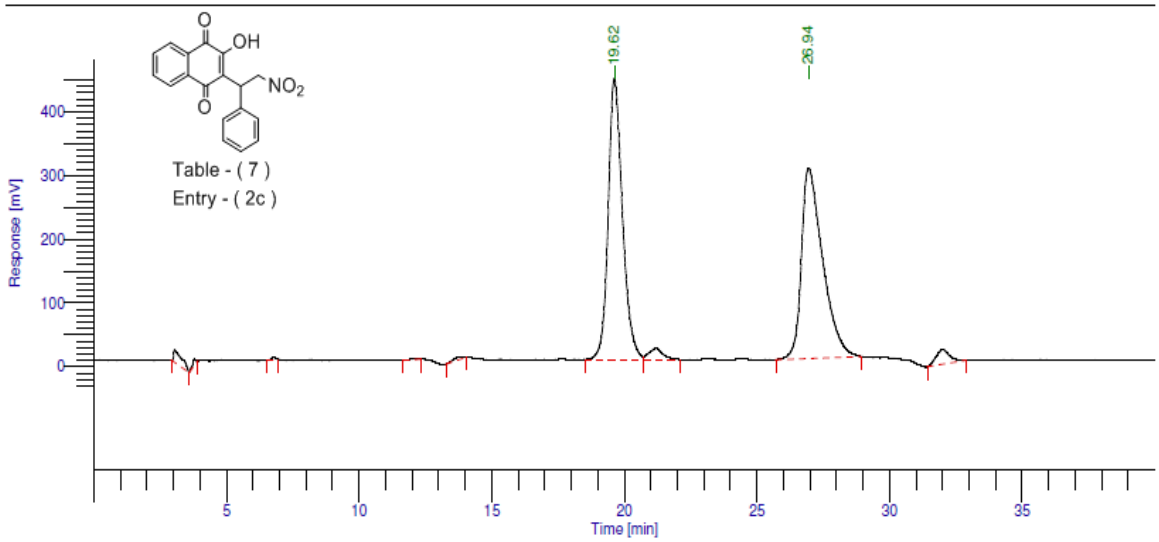

Peak #	Component Name	Time [min]	Area [uV*sec]	Height [uV]	Area [%]	BL	Adjusted Amount
6		19.622	16479489.01	441408.93	49.77	BV	16.4795
8		26.945	16628953.28	298764.09	50.23	BB	16.6290
			33108442.29	740173.02	100.00		33.1084

Column: Chiralpak IA, 250 x 4.6 mm
Mobile Phase: 90% Hexane, 8% Ethanol, 2% Dichloromethane, 0.1% TFA
1ml/min, 254nm

Result File : C:\HPLC1\Aileen\ChiralPakIA\AMOD\YM89_2016__07_14_015.rst
Sequence File : C:\HPLC1\Aileen\ChiralPakIA\AMOD\12July16_2.seq

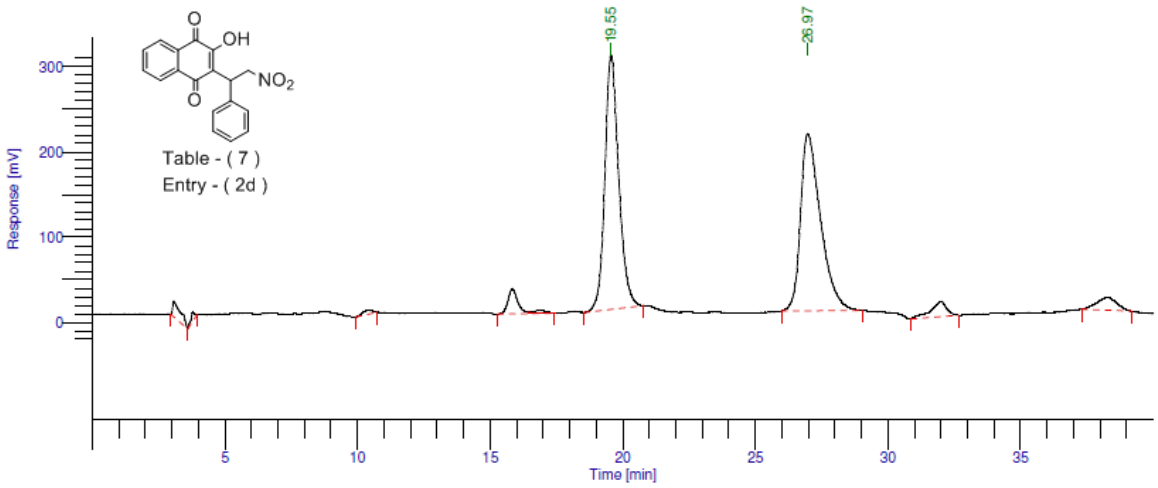

Peak #	Component Name	Time [min]	Area [uV*sec]	Height [uV]	Area [%]	BL	Adjusted Amount
6		19.555	10825661.46	298912.20	49.71	BB	10.8257
7		26.972	10954152.79	207692.90	50.29	BB	10.9542
			21779814.25	506605.10	100.00		21.7798

Column: Chiralpak IA, 250 x 4.6 mm
Mobile Phase: 90% Hexane, 8% Ethanol, 2% Dichloromethane, 0.1% TFA
1ml/min, 254nm

Result File : C:\HPLC1\Aileen\ChiralPakIA\AMOD\YM90_2016__07_14_016.rst
Sequence File : C:\HPLC1\Aileen\ChiralPakIA\AMOD\12July16_2.seq

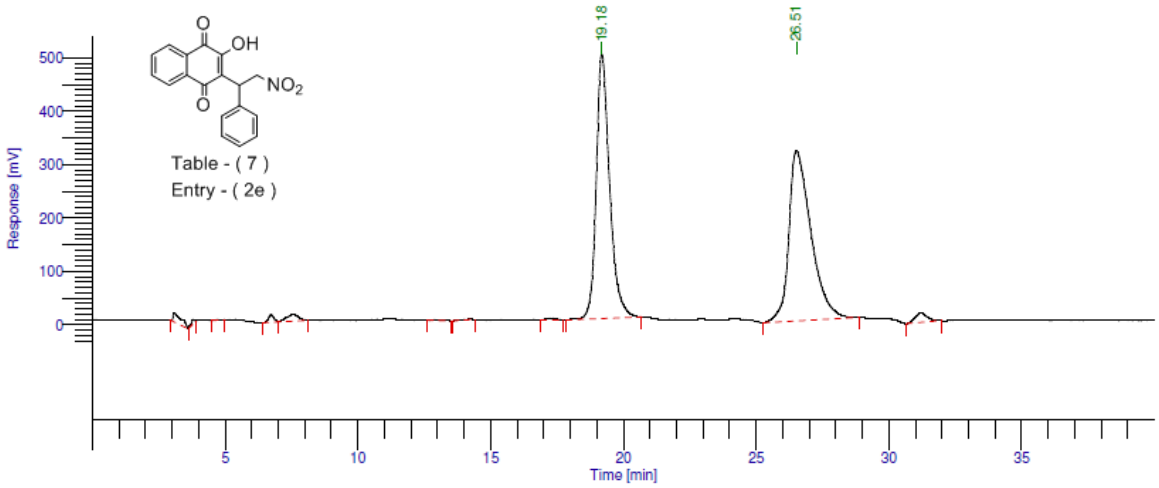

Peak #	Component Name	Time [min]	Area [uV*sec]	Height [uV]	Area [%]	BL	Adjusted Amount
9		19.184	17401082.16	495729.47	48.60	BB	17.4011
10		26.514	18403733.58	318617.63	51.40	BB	18.4037
			35804815.73	814347.09	100.00		35.8048

Column: Chiralpak IA, 250 x 4.6 mm
Mobile Phase: 90% Hexane, 8% Ethanol, 2% Dichloromethane, 0.1% TFA
1ml/min, 254nm

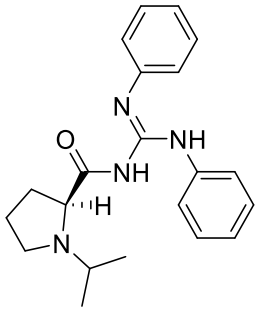

Injection Details

Injection Name:	**YM-139**	*Run Time (min):*	**40.00**
Vial Number:	**BE3**	*Injection Volume:*	**20.00**
Injection Type:	**Unknown**	*Channel:*	**UV_VIS_1**
Calibration Level:		*Wavelength:*	**254.0**
Instrument Method:	**Chiralpak AS-H**	*Bandwidth:*	**n.a.**
Processing Method:	**Caffiene16**	*Dilution Factor:*	**1.0000**
Injection Date/Time:	**01/Mar/17 17:12**	*Sample Weight:*	**1.0000**

Chromatogram

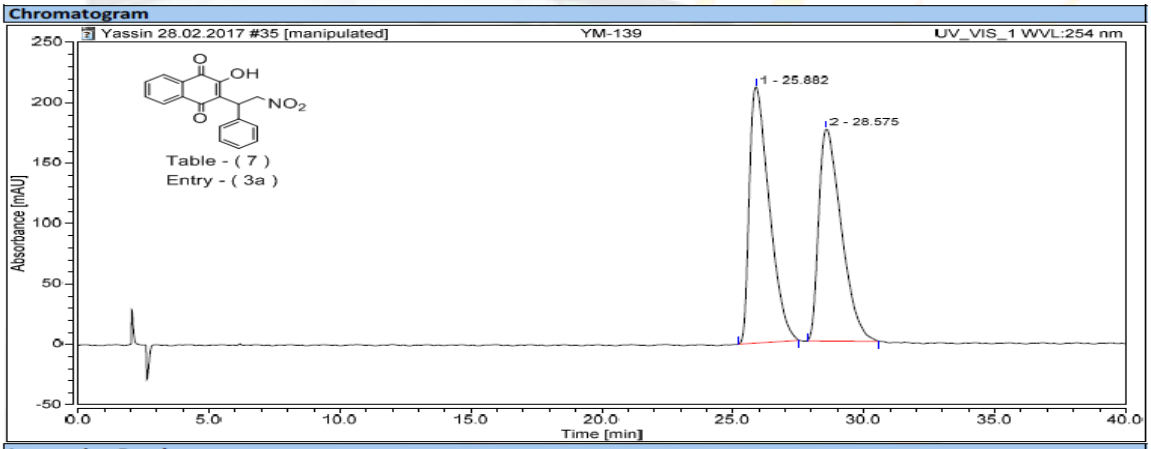

Integration Results

No.	Peak Name	Retention Time min	Area mAU*min	Height mAU	Relative Area %	Relative Height %	Amount
n.a.	Caffeine	n.a.	n.a.	n.a.	n.a.	n.a.	n.a.
1		25.882	187.239	212.049	51.58	54.71	n.a.
2		28.575	175.750	175.544	48.42	45.29	n.a.
Total:			**362.989**	**387.593**	**100.00**	**100.00**	

Injection Details

Injection Name:	**YM-138**	*Run Time (min):*	**40.00**
Vial Number:	**BE2**	*Injection Volume:*	**20.00**
Injection Type:	**Unknown**	*Channel:*	**UV_VIS_1**
Calibration Level:		*Wavelength:*	**254.0**
Instrument Method:	**Chiralpak AS-H**	*Bandwidth:*	**n.a.**
Processing Method:	**Caffiene16**	*Dilution Factor:*	**1.0000**
Injection Date/Time:	**01/Mar/17 16:30**	*Sample Weight:*	**1.0000**

Chromatogram

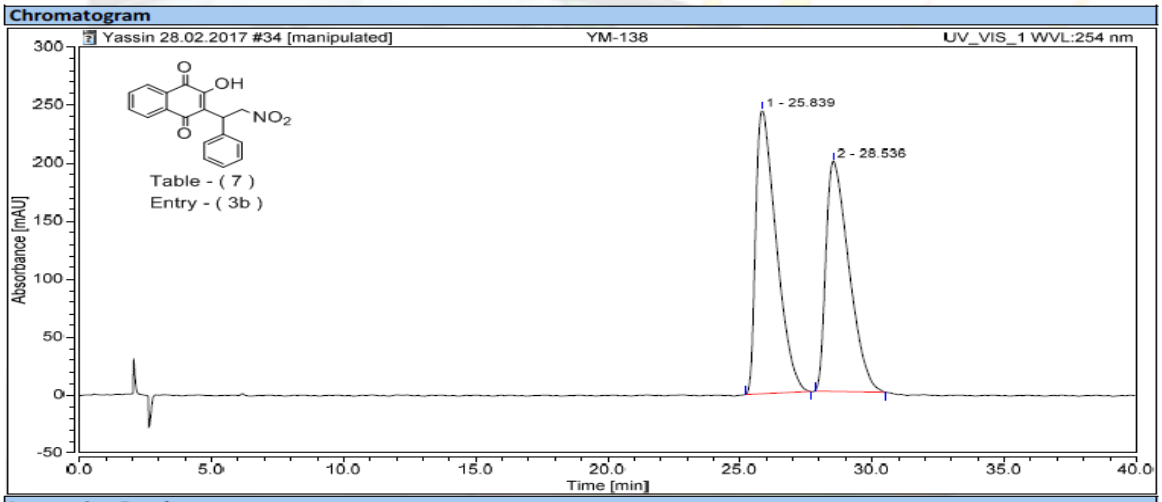

Integration Results

No.	Peak Name	Retention Time min	Area mAU*min	Height mAU	Relative Area %	Relative Height %	Amount
n.a.	Caffeine	n.a.	n.a.	n.a.	n.a.	n.a.	n.a.
1		25.839	220.298	244.564	52.27	55.16	n.a.
2		28.536	201.132	198.775	47.73	44.84	n.a.
Total:			**421.429**	**443.339**	**100.00**	**100.00**	

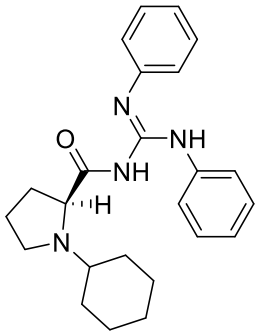

Injection Details

Injection Name:	**YM-179**	*Run Time (min):*	**40.00**
Vial Number:	**RB4**	*Injection Volume:*	**20.00**
Injection Type:	**Unknown**	*Channel:*	**UV_VIS_1**
Calibration Level:		*Wavelength:*	**254.0**
Instrument Method:	**Chiralpak AS-H**	*Bandwidth:*	**n.a.**
Processing Method:	**Caffiene16**	*Dilution Factor:*	**1.0000**
Injection Date/Time:	**02/Mar/17 05:09**	*Sample Weight:*	**1.0000**

Chromatogram

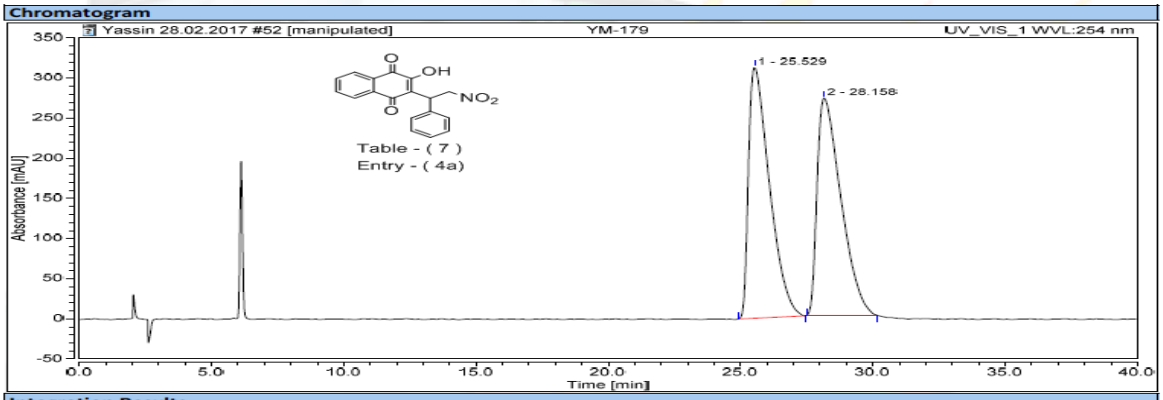

Integration Results

No.	Peak Name	Retention Time min	Area mAU*min	Height mAU	Relative Area %	Relative Height %	Amount
n.a.	Caffeine	n.a.	n.a.	n.a.	n.a.	n.a.	n.a.
1		25.529	287.148	312.814	50.40	53.59	n.a.
2		28.158	282.602	270.938	49.60	46.41	n.a.
Total:			**569.750**	**583.751**	**100.00**	**100.00**	

Injection Details

Injection Name:	**YM-178**	*Run Time (min):*	**40.00**
Vial Number:	**RB3**	*Injection Volume:*	**20.00**
Injection Type:	**Unknown**	*Channel:*	**UV_VIS_1**
Calibration Level:		*Wavelength:*	**254.0**
Instrument Method:	**Chiralpak AS-H**	*Bandwidth:*	**n.a.**
Processing Method:	**Caffiene16**	*Dilution Factor:*	**1.0000**
Injection Date/Time:	**02/Mar/17 04:27**	*Sample Weight:*	**1.0000**

Chromatogram

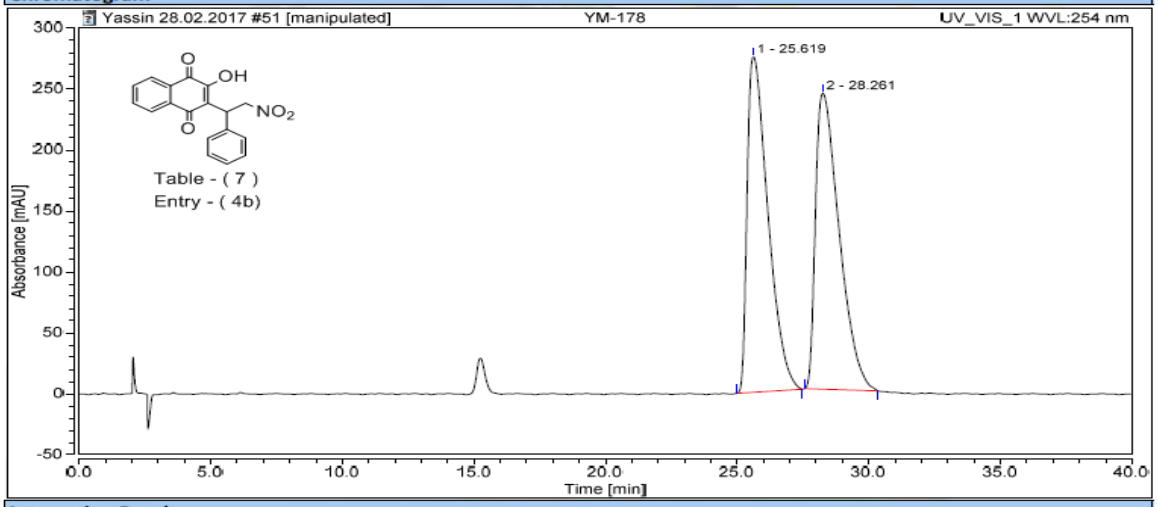

Integration Results

No.	Peak Name	Retention Time min	Area mAU*min	Height mAU	Relative Area %	Relative Height %	Amount
n.a.	Caffeine	n.a.	n.a.	n.a.	n.a.	n.a.	n.a.
1		25.619	251.748	275.629	49.84	53.16	n.a.
2		28.261	253.356	242.883	50.16	46.84	n.a.
Total:			**505.104**	**518.512**	**100.00**	**100.00**	

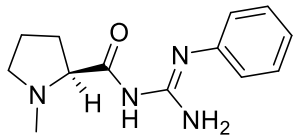

Result File : C:\HPLC1\Aileen\ChiralPakIA\YM67_2016__01_05_013.rst
Sequence File : C:\HPLC1\Aileen\ChiralPakIA\5Jan15_1.seq

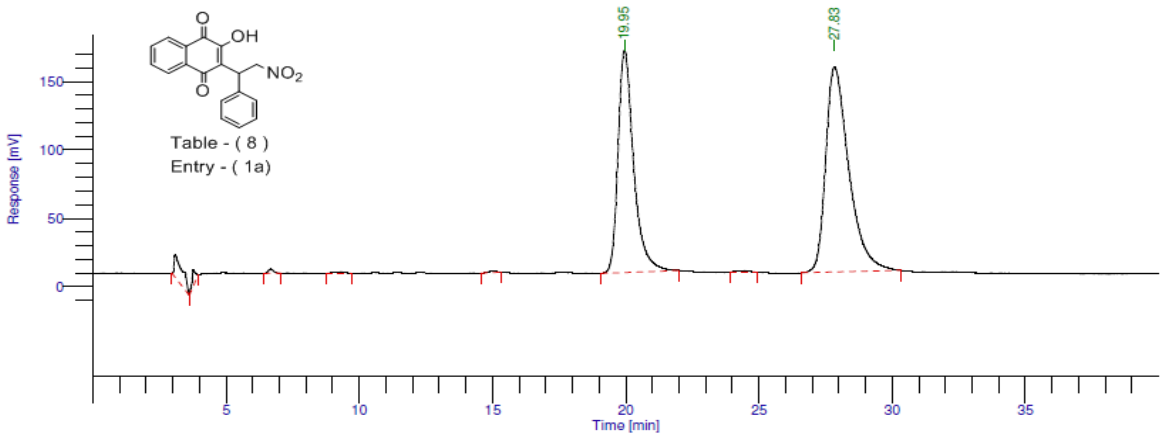

Peak #	Component Name	Time [min]	Area [uV*sec]	Height [uV]	Area [%]	BL	Adjusted Amount
6		19.952	6622897.23	162609.78	42.24	BB	6.6229
8		27.829	9057279.07	149920.19	57.76	BB	9.0573
			15680176.30	312529.97	100.00		15.6802

Column: Chiralpak IA, 250 x 4.6 mm
Mobile Phase: 90% Hexane, 8% Ethanol, 2% Dichloromethane, 0.1% TFA
1ml/min, 254nm

Injection Details

Injection Name:	**YM-69**	*Run Time (min):*	**40.00**
Vial Number:	**BB4**	*Injection Volume:*	**20.00**
Injection Type:	**Unknown**	*Channel:*	**UV_VIS_1**
Calibration Level:		*Wavelength:*	**254.0**
Instrument Method:	**Chiralpak AS-H**	*Bandwidth:*	**n.a.**
Processing Method:	**Caffiene16**	*Dilution Factor:*	**1.0000**
Injection Date/Time:	**01/Mar/17 01:02**	*Sample Weight:*	**1.0000**

Chromatogram

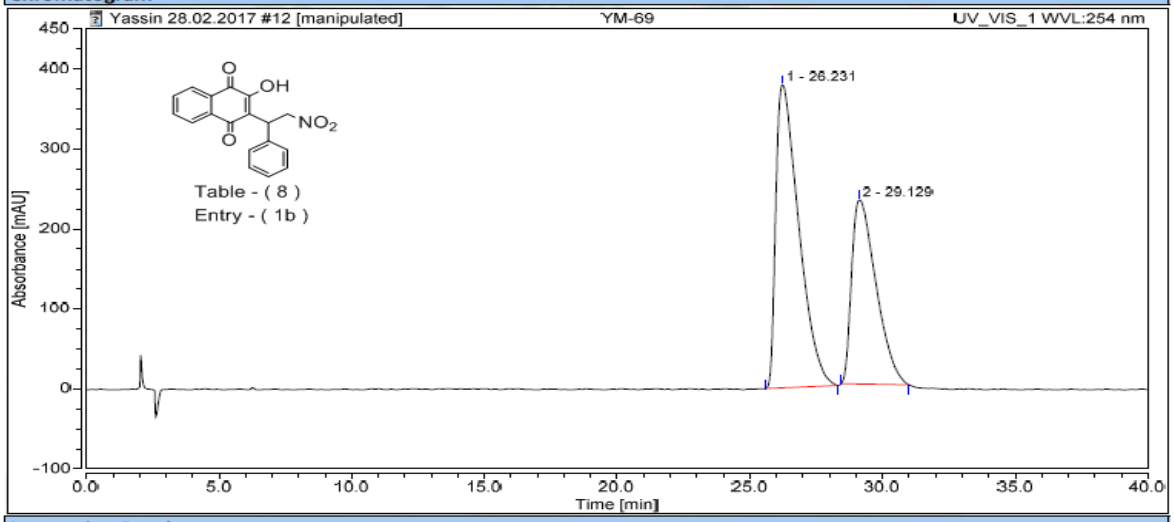

Integration Results

No.	Peak Name	Retention Time min	Area mAU*min	Height mAU	Relative Area %	Relative Height %	Amount
n.a.	Caffeine	n.a.	n.a.	n.a.	n.a.	n.a.	n.a.
1		26.231	379.701	379.287	60.72	62.23	n.a.
2		29.129	245.596	230.213	39.28	37.77	n.a.
Total:			**625.296**	**609.500**	**100.00**	**100.00**	

Result File : C:\HPLC1\Aileen\ChiralPakIA\YM71_2016__01_06_017.rst
Sequence File : C:\HPLC1\Aileen\ChiralPakIA\5Jan15_1.seq

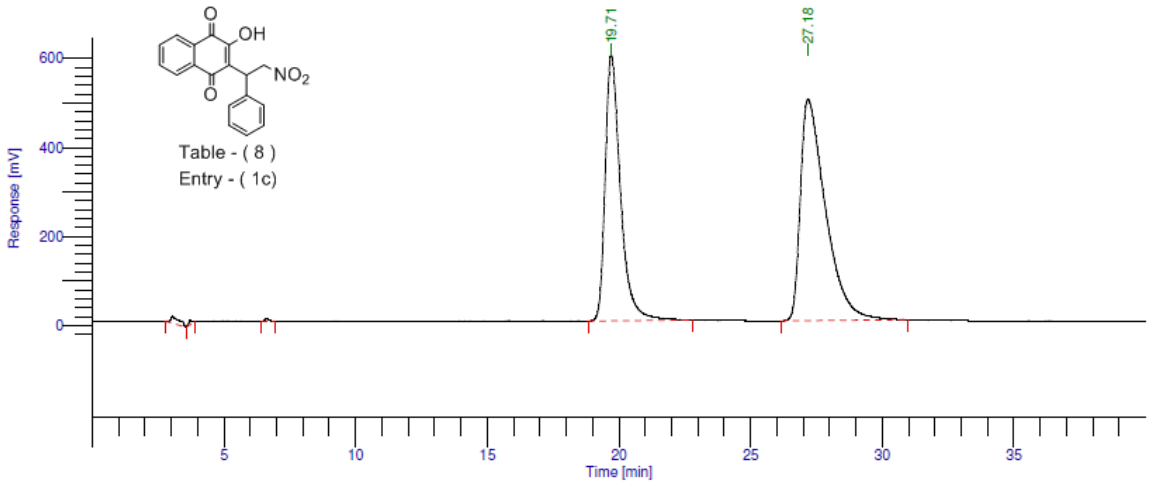

Peak #	Component Name	Time [min]	Area [uV*sec]	Height [uV]	Area [%]	BL	Adjusted Amount
4		19.707	24068604.21	596317.87	42.20	BB	24.0686
5		27.183	32962305.92	497302.84	57.80	BB	32.9623
			57030910.14	1.09e+06	100.00		57.0309

Column: Chiralpak IA, 250 x 4.6 mm
Mobile Phase: 90% Hexane, 8% Ethanol, 2% Dichloromethane, 0.1% TFA
1ml/min, 254nm

Result File : C:\HPLC1\Aileen\ChiralPakIA\YM70_2016__01_06_016.rst
Sequence File : C:\HPLC1\Aileen\ChiralPakIA\5Jan15_1.seq

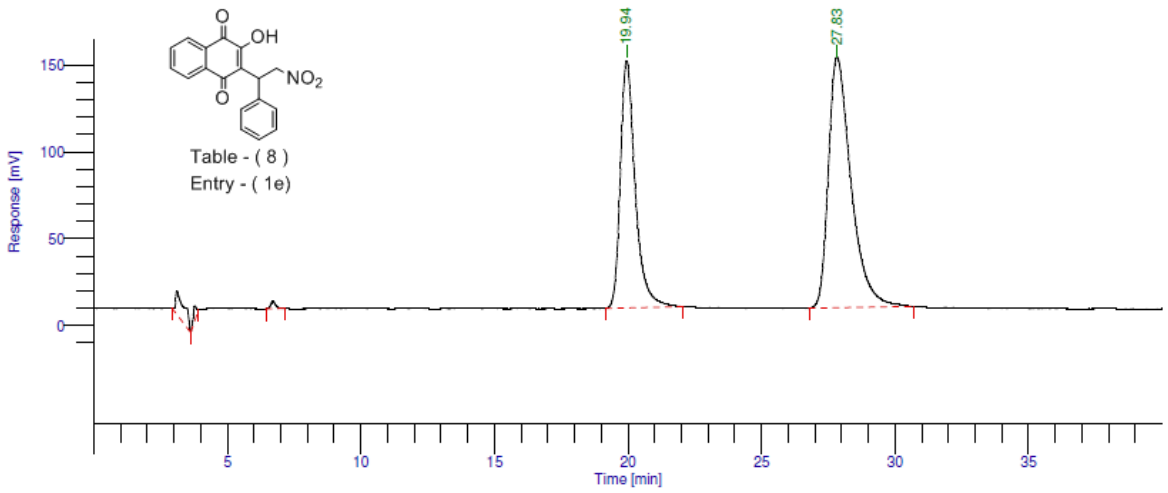

Peak #	Component Name	Time [min]	Area [uV*sec]	Height [uV]	Area [%]	BL	Adjusted Amount
4		19.944	5524531.17	142412.61	39.38	BB	5.5245
5		27.826	8504328.17	144446.44	60.62	BB	8.5043
			14028859.34	286859.04	100.00		14.0289

Column: Chiralpak IA, 250 x 4.6 mm
Mobile Phase: 90% Hexane, 8% Ethanol, 2% Dichloromethane, 0.1% TFA
1ml/min, 254nm

Injection Details

Injection Name:	**YM-72**	*Run Time (min):*	**40.00**
Vial Number:	**BA1**	*Injection Volume:*	**20.00**
Injection Type:	**Unknown**	*Channel:*	**UV_VIS_1**
Calibration Level:		*Wavelength:*	**254.0**
Instrument Method:	**Chiralpak AS-H**	*Bandwidth:*	**n.a.**
Processing Method:	**Caffiene16**	*Dilution Factor:*	**1.0000**
Injection Date/Time:	**24/Mar/17 12:12**	*Sample Weight:*	**1.0000**

Chromatogram

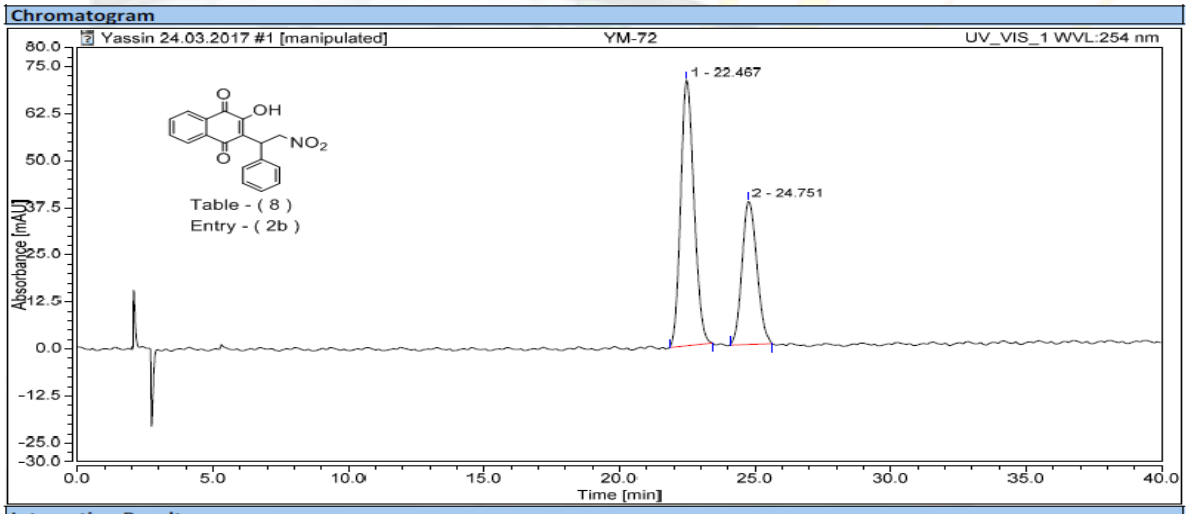

Integration Results

No.	Peak Name	Retention Time min	Area mAU*min	Height mAU	Relative Area %	Relative Height %	Amount
n.a.	Caffeine	n.a.	n.a.	n.a.	n.a.	n.a.	n.a.
1		22.467	40.323	70.537	62.53	64.90	n.a.
2		24.751	24.163	38.154	37.47	35.10	n.a.
Total:			**64.486**	**108.691**	**100.00**	**100.00**	

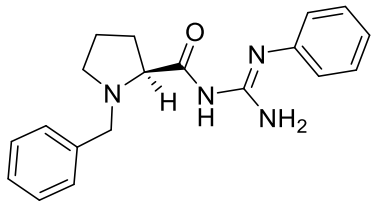

Result File : C:\HPLC1\Aileen\ChiralPakIA\AMOD\YM73dil_2016__03_07_002.rst
Sequence File : C:\HPLC1\Aileen\ChiralPakIA\AMOD\7March16_1.seq

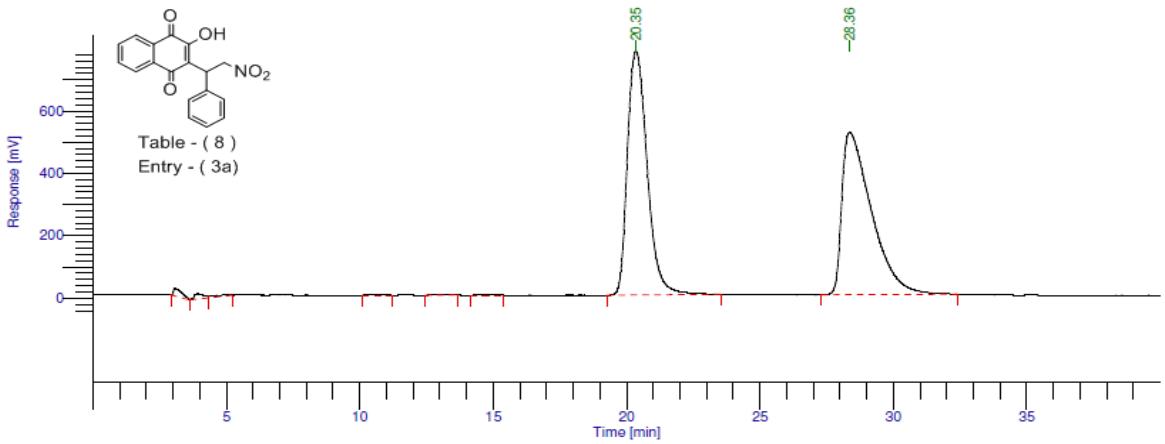

Peak #	Component Name	Time [min]	Area [uV*sec]	Height [uV]	Area [%]	BL	Adjusted Amount
7		20.351	40308828.16	782049.91	50.10	BB	40.3088
8		28.361	40146594.82	520460.76	49.90	BB	40.1466
			80455422.98	1.30e+06	100.00		80.4554

Column: Chiralpak IA, 250 x 4.6 mm
Mobile Phase: 90% Hexane, 8% Ethanol, 2% Dichloromethane, 0.1% TFA
1ml/min, 254nm

Result File : C:\HPLC1\Aileen\ChiralPakIA\AMOD\YM74dilrep_2016__03_07_009.rst
Sequence File : C:\HPLC1\Aileen\ChiralPakIA\AMOD\7March16_1.seq

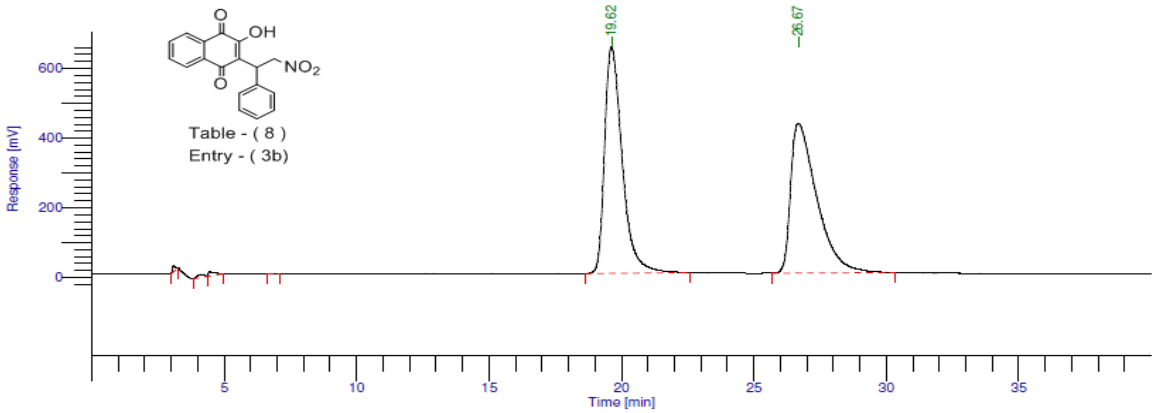

Peak #	Component Name	Time [min]	Area [uV*sec]	Height [uV]	Area [%]	BL	Adjusted Amount
5		19.621	29996656.31	651036.88	50.48	BB	29.9967
6		26.675	29429723.63	430601.19	49.52	BB	29.4297
			59426379.94	1.08e+06	100.00		59.4264

Column: Chiralpak IA, 250 x 4.6 mm
Mobile Phase: 90% Hexane, 8% Ethanol, 2% Dichloromethane, 0.1% TFA
1ml/min, 254nm

Injection Details			
Injection Name:	**YM-76**	*Run Time (min):*	**40.00**
Vial Number:	**BC1**	*Injection Volume:*	**20.00**
Injection Type:	**Unknown**	*Channel:*	**UV_VIS_1**
Calibration Level:		*Wavelength:*	**254.0**
Instrument Method:	**Chiralpak AS-H**	*Bandwidth:*	**n.a.**
Processing Method:	**Caffiene16**	*Dilution Factor:*	**1.0000**
Injection Date/Time:	**01/Mar/17 04:33**	*Sample Weight:*	**1.0000**

Chromatogram

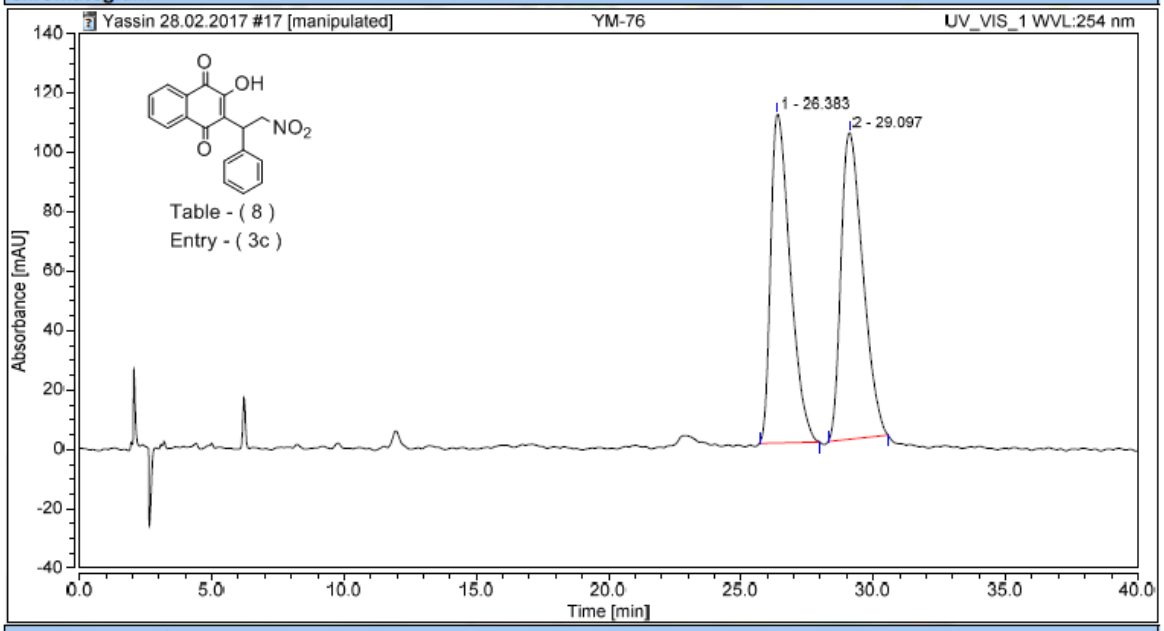

Integration Results

No.	Peak Name	Retention Time min	Area mAU*min	Height mAU	Relative Area %	Relative Height %	Amount
n.a.	Caffeine	n.a.	n.a.	n.a.	n.a.	n.a.	n.a.
1		26.383	94.881	110.993	48.94	51.75	n.a.
2		29.097	98.979	103.492	51.06	48.25	n.a.
Total:			**193.860**	**214.485**	**100.00**	**100.00**	

Result File : C:\HPLC1\Aileen\ChiralPakIA\AMOD\YM77dil_2016__03_07_005.rst
Sequence File : C:\HPLC1\Aileen\ChiralPakIA\AMOD\7March16_1.seq

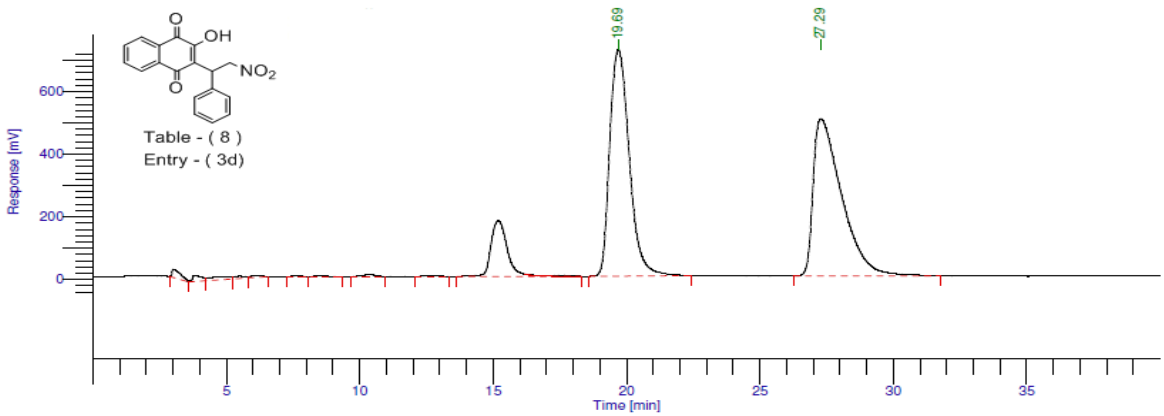

Peak #	Component Name	Time [min]	Area [uV*sec]	Height [uV]	Area [%]	BL	Adjusted Amount
10		15.190	7597153.73	177971.47	9.31	BE	7.5972
12		19.685	36695850.87	724166.22	44.96	BB	36.6959
13		27.286	37333852.42	502639.71	45.74	BB	37.3339
			81626857.01	1.40e+06	100.00		81.6269

Column: Chiralpak IA, 250 x 4.6 mm
Mobile Phase: 90% Hexane, 8% Ethanol, 2% Dichloromethane, 0.1% TFA
1ml/min, 254nm

Injection Details

Injection Name:	**YM-75**	*Run Time (min):*	**40.00**
Vial Number:	**BB8**	*Injection Volume:*	**20.00**
Injection Type:	**Unknown**	*Channel:*	**UV_VIS_1**
Calibration Level:		*Wavelength:*	**254.0**
Instrument Method:	**Chiralpak AS-H**	*Bandwidth:*	**n.a.**
Processing Method:	**Caffiene16**	*Dilution Factor:*	**1.0000**
Injection Date/Time:	**01/Mar/17 03:51**	*Sample Weight:*	**1.0000**

Chromatogram

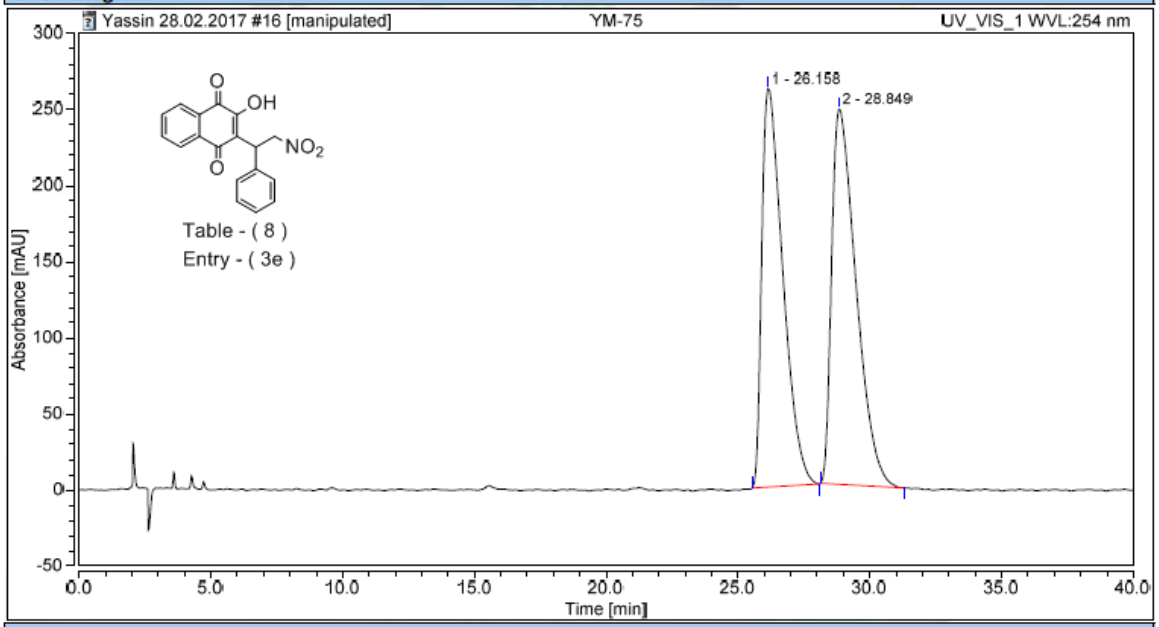

Integration Results

No.	Peak Name	Retention Time min	Area mAU*min	Height mAU	Relative Area %	Relative Height %	Amount
n.a.	Caffeine	n.a.	n.a.	n.a.	n.a.	n.a.	n.a.
1		26.158	242.382	262.173	47.82	51.51	n.a.
2		28.849	264.469	246.818	52.18	48.49	n.a.
Total:			**506.851**	**508.991**	**100.00**	**100.00**	

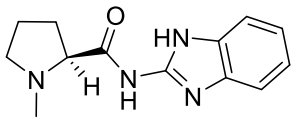

Injection Details

Injection Name:	**YM-175**	*Run Time (min):*	**40.00**
Vial Number:	**RA8**	*Injection Volume:*	**20.00**
Injection Type:	**Unknown**	*Channel:*	**UV_VIS_1**
Calibration Level:		*Wavelength:*	**254.0**
Instrument Method:	**Chiralpak AS-H**	*Bandwidth:*	**n.a.**
Processing Method:	**Caffiene16**	*Dilution Factor:*	**1.0000**
Injection Date/Time:	**02/Mar/17 02:20**	*Sample Weight:*	**1.0000**

Chromatogram

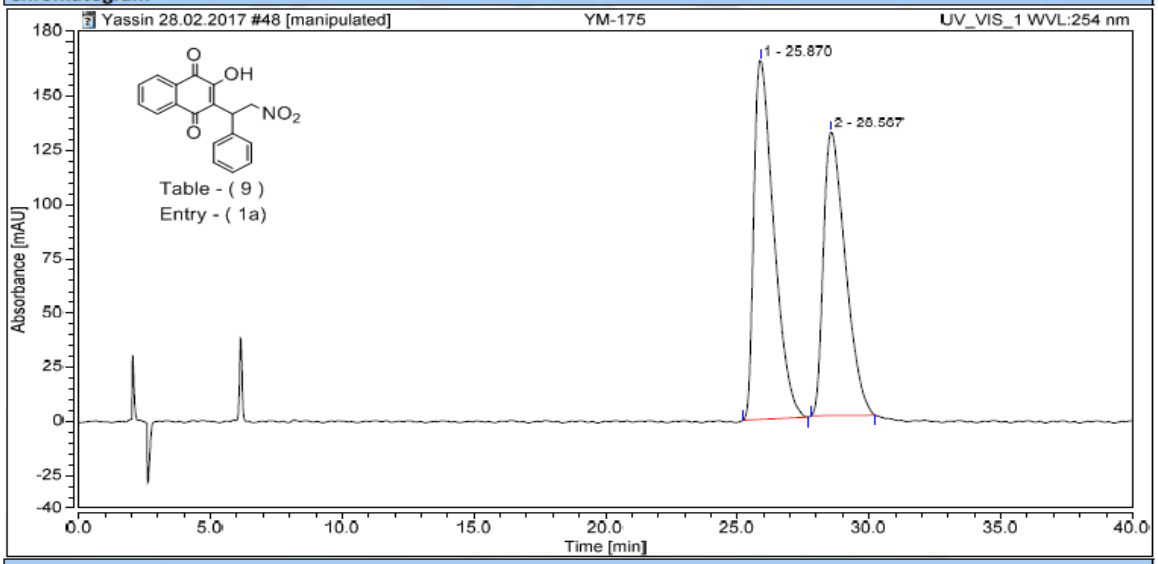

Integration Results

No.	Peak Name	Retention Time min	Area mAU*min	Height mAU	Relative Area %	Relative Height %	Amount
n.a.	Caffeine	n.a.	n.a.	n.a.	n.a.	n.a.	n.a.
1		25.870	145.229	165.877	53.49	55.89	n.a.
2		28.567	126.281	130.928	46.51	44.11	n.a.
Total:			**271.510**	**296.804**	**100.00**	**100.00**	

Injection Details

Injection Name:	**YM-174**	*Run Time (min):*	**40.00**
Vial Number:	**RA7**	*Injection Volume:*	**20.00**
Injection Type:	**Unknown**	*Channel:*	**UV_VIS_1**
Calibration Level:		*Wavelength:*	**254.0**
Instrument Method:	**Chiralpak AS-H**	*Bandwidth:*	**n.a.**
Processing Method:	**Caffiene16**	*Dilution Factor:*	**1.0000**
Injection Date/Time:	**02/Mar/17 01:38**	*Sample Weight:*	**1.0000**

Chromatogram

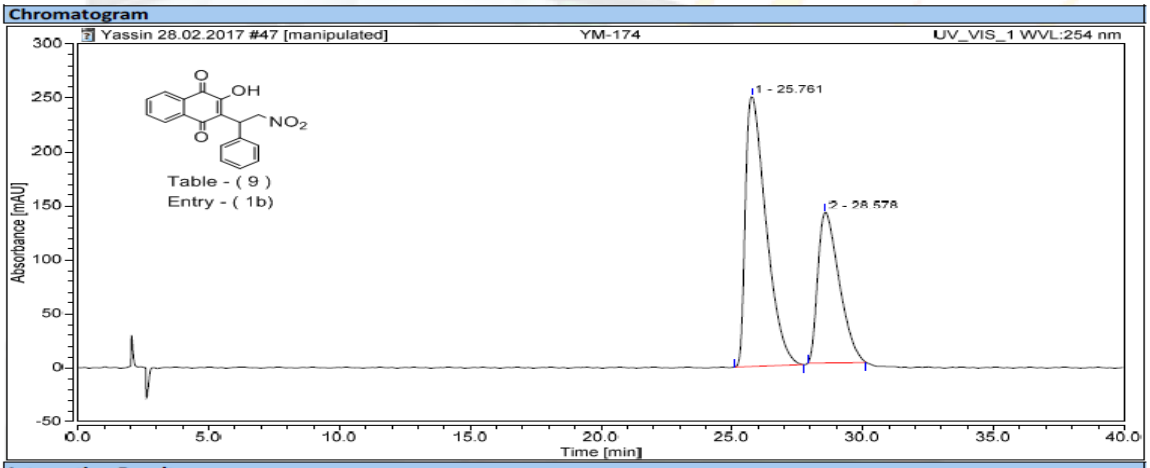

Integration Results

No.	Peak Name	Retention Time min	Area mAU*min	Height mAU	Relative Area %	Relative Height %	Amount
n.a.	Caffeine	n.a.	n.a.	n.a.	n.a.	n.a.	n.a.
1		25.761	229.725	250.398	63.40	64.17	n.a.
2		28.578	132.603	139.797	36.60	35.83	n.a.
Total:			**362.328**	**390.195**	**100.00**	**100.00**	

Injection Details

Injection Name:	**YM-153**	*Run Time (min):*	**40.00**
Vial Number:	**BA2**	*Injection Volume:*	**20.00**
Injection Type:	**Unknown**	*Channel:*	**UV_VIS_1**
Calibration Level:		*Wavelength:*	**254.0**
Instrument Method:	**Chiralpak AS-H**	*Bandwidth:*	**n.a.**
Processing Method:	**Caffiene16**	*Dilution Factor:*	**1.0000**
Injection Date/Time:	**24/Mar/17 12:54**	*Sample Weight:*	**1.0000**

Chromatogram

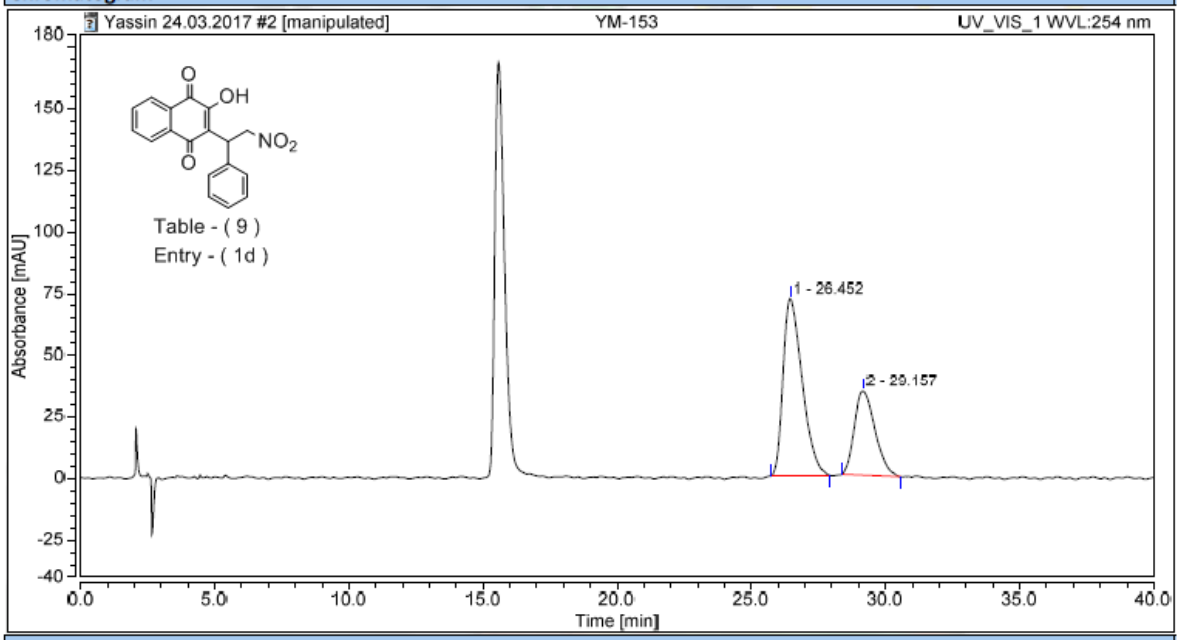

Integration Results

No.	Peak Name	Retention Time min	Area mAU*min	Height mAU	Relative Area %	Relative Height %	Amount
n.a.	Caffeine	n.a.	n.a.	n.a.	n.a.	n.a.	n.a.
1		26.452	59.507	72.137	66.09	67.82	n.a.
2		29.157	30.532	34.232	33.91	32.18	n.a.
Total:			**90.039**	**106.369**	**100.00**	**100.00**	

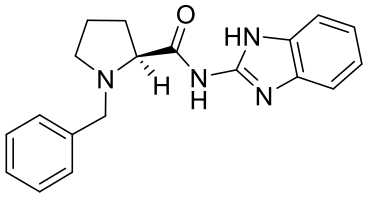

Injection Details

Injection Name:	**YM-183**	*Run Time (min):*	**40.00**
Vial Number:	**RB8**	*Injection Volume:*	**20.00**
Injection Type:	**Unknown**	*Channel:*	**UV_VIS_1**
Calibration Level:		*Wavelength:*	**254.0**
Instrument Method:	**Chiralpak AS-H**	*Bandwidth:*	**n.a.**
Processing Method:	**Caffiene16**	*Dilution Factor:*	**1.0000**
Injection Date/Time:	**02/Mar/17 07:58**	*Sample Weight:*	**1.0000**

Chromatogram

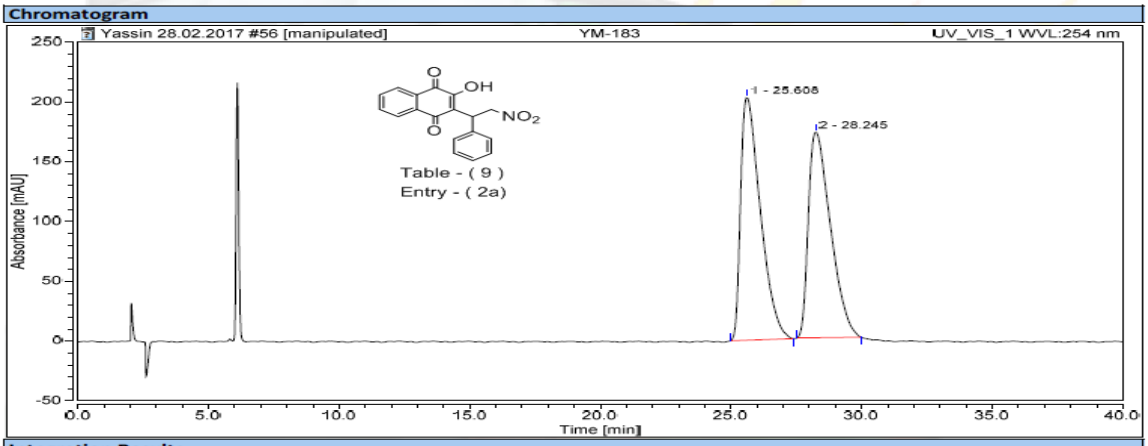

Integration Results

No.	Peak Name	Retention Time min	Area mAU*min	Height mAU	Relative Area %	Relative Height %	Amount
n.a.	Caffeine	n.a.	n.a.	n.a.	n.a.	n.a.	n.a.
1		25.608	178.302	203.331	51.36	54.12	n.a.
2		28.245	168.826	172.360	48.64	45.88	n.a.
Total:			**347.128**	**375.691**	**100.00**	**100.00**	

Injection Details

Injection Name:	**YM-182**	*Run Time (min):*	**40.00**
Vial Number:	**RB7**	*Injection Volume:*	**20.00**
Injection Type:	**Unknown**	*Channel:*	**UV_VIS_1**
Calibration Level:		*Wavelength:*	**254.0**
Instrument Method:	**Chiralpak AS-H**	*Bandwidth:*	**n.a.**
Processing Method:	**Caffiene16**	*Dilution Factor:*	**1.0000**
Injection Date/Time:	**02/Mar/17 07:16**	*Sample Weight:*	**1.0000**

Chromatogram

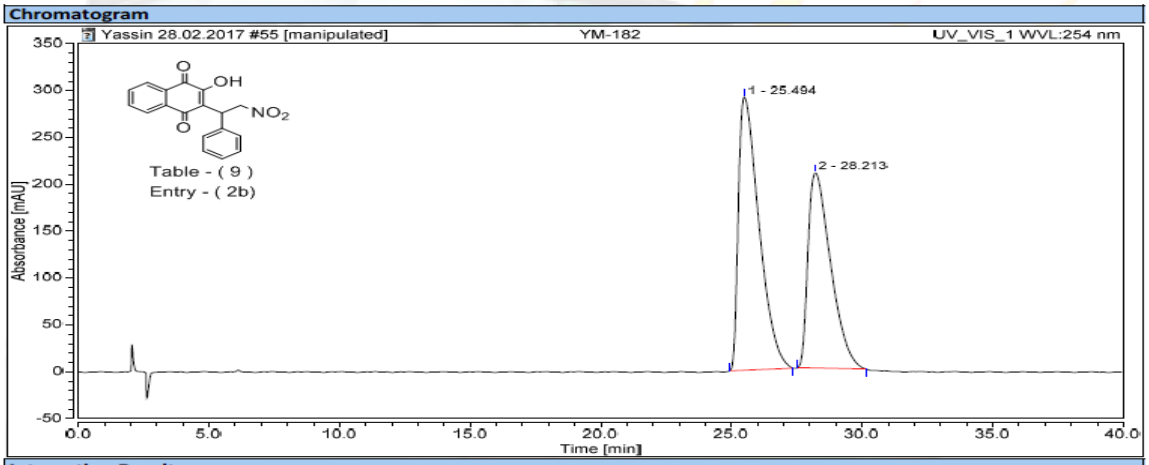

Integration Results

No.	Peak Name	Retention Time min	Area mAU*min	Height mAU	Relative Area %	Relative Height %	Amount
n.a.	Caffeine	n.a.	n.a.	n.a.	n.a.	n.a.	n.a.
1		25.494	266.142	291.341	56.00	58.33	n.a.
2		28.213	209.122	208.151	44.00	41.67	n.a.
Total:			**475.264**	**499.493**	**100.00**	**100.00**	

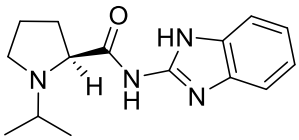

Injection Details

Injection Name:	**YM-161**	*Run Time (min):*	**40.00**
Vial Number:	**BE7**	*Injection Volume:*	**20.00**
Injection Type:	**Unknown**	*Channel:*	**UV_VIS_1**
Calibration Level:		*Wavelength:*	**254.0**
Instrument Method:	**Chiralpak AS-H**	*Bandwidth:*	**n.a.**
Processing Method:	**Caffiene16**	*Dilution Factor:*	**1.0000**
Injection Date/Time:	**01/Mar/17 20:01**	*Sample Weight:*	**1.0000**

Chromatogram

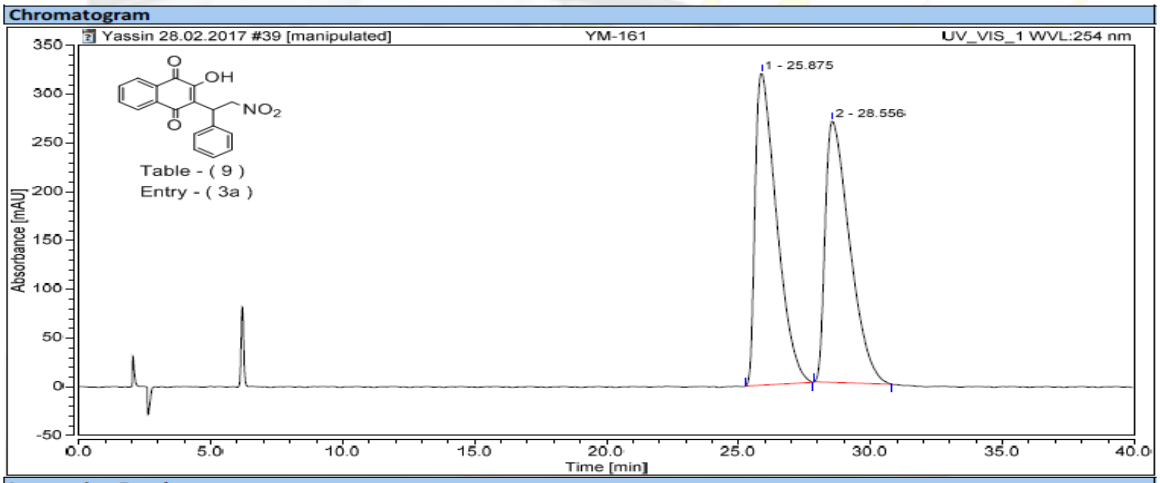

Integration Results

No.	Peak Name	Retention Time min	Area mAU*min	Height mAU	Relative Area %	Relative Height %	Amount
n.a.	Caffeine	n.a.	n.a.	n.a.	n.a.	n.a.	n.a.
1		25.875	302.228	320.158	51.13	54.40	n.a.
2		28.556	288.903	268.325	48.87	45.60	n.a.
Total:			**591.131**	**588.483**	**100.00**	**100.00**	

Injection Details

Injection Name:	**YM-160**	*Run Time (min):*	**40.00**
Vial Number:	**BE6**	*Injection Volume:*	**20.00**
Injection Type:	**Unknown**	*Channel:*	**UV_VIS_1**
Calibration Level:		*Wavelength:*	**254.0**
Instrument Method:	**Chiralpak AS-H**	*Bandwidth:*	**n.a.**
Processing Method:	**Caffiene16**	*Dilution Factor:*	**1.0000**
Injection Date/Time:	**01/Mar/17 19:19**	*Sample Weight:*	**1.0000**

Chromatogram

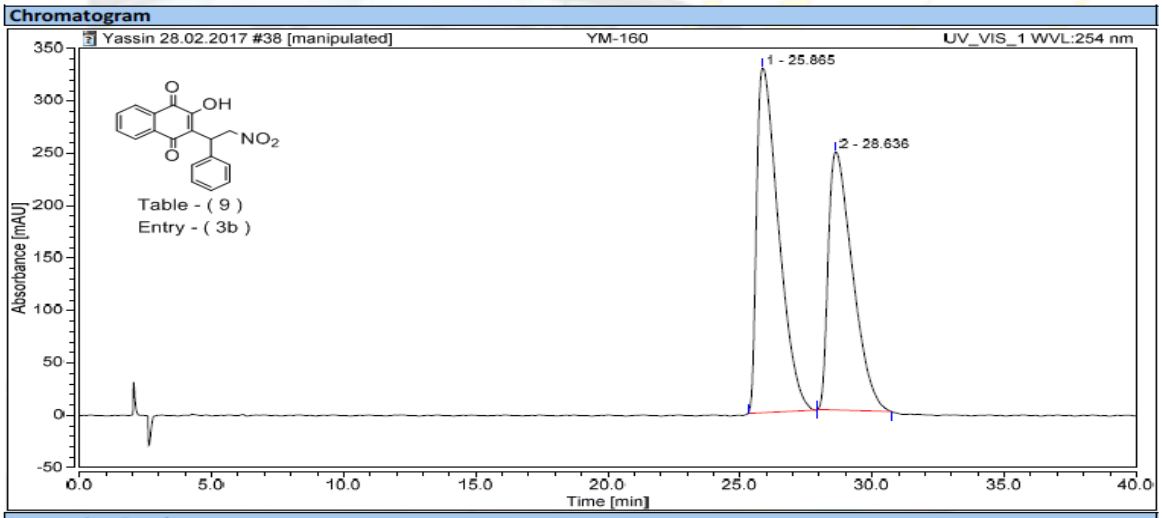

Integration Results

No.	Peak Name	Retention Time min	Area mAU*min	Height mAU	Relative Area %	Relative Height %	Amount
n.a.	Caffeine	n.a.	n.a.	n.a.	n.a.	n.a.	n.a.
1		25.865	316.338	329.251	54.67	57.18	n.a.
2		28.636	262.321	246.567	45.33	42.82	n.a.
Total:			**578.658**	**575.819**	**100.00**	**100.00**	

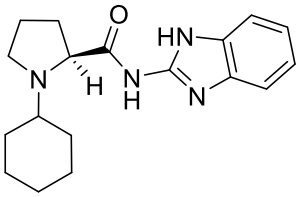

Injection Details

Injection Name:	**YM-181**	*Run Time (min):*	**40.00**
Vial Number:	**RB6**	*Injection Volume:*	**20.00**
Injection Type:	**Unknown**	*Channel:*	**UV_VIS_1**
Calibration Level:		*Wavelength:*	**254.0**
Instrument Method:	**Chiralpak AS-H**	*Bandwidth:*	**n.a.**
Processing Method:	**Caffiene16**	*Dilution Factor:*	**1.0000**
Injection Date/Time:	**02/Mar/17 06:33**	*Sample Weight:*	**1.0000**

Chromatogram

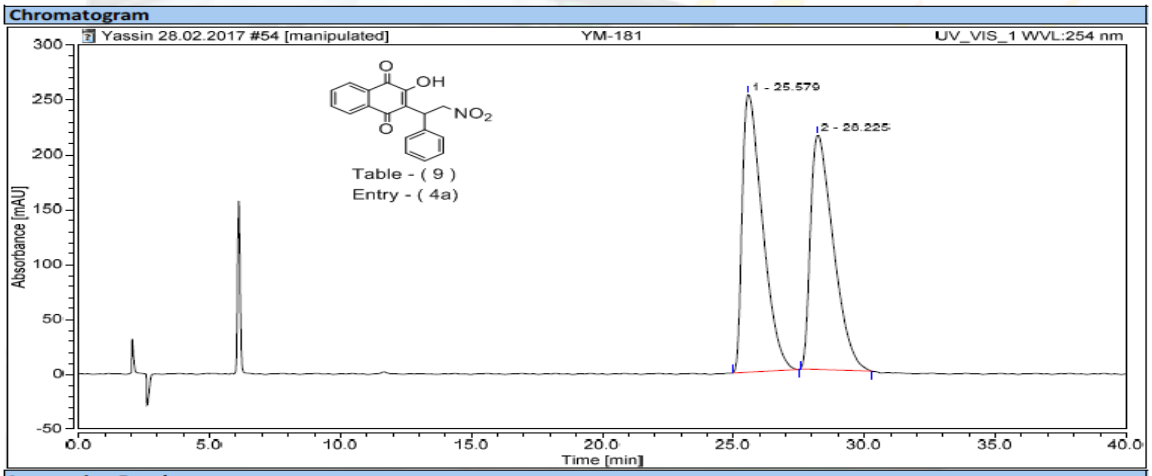

Integration Results

No.	Peak Name	Retention Time min	Area mAU*min	Height mAU	Relative Area %	Relative Height %	Amount
n.a.	Caffeine	n.a.	n.a.	n.a.	n.a.	n.a.	n.a.
1		25.579	227.509	253.374	51.20	54.24	n.a.
2		28.225	216.853	213.741	48.80	45.76	n.a.
Total:			**444.362**	**467.115**	**100.00**	**100.00**	

Injection Details

Injection Name:	**YM-180**	*Run Time (min):*	**40.00**
Vial Number:	**RB5**	*Injection Volume:*	**20.00**
Injection Type:	**Unknown**	*Channel:*	**UV_VIS_1**
Calibration Level:		*Wavelength:*	**254.0**
Instrument Method:	**Chiralpak AS-H**	*Bandwidth:*	**n.a.**
Processing Method:	**Caffiene16**	*Dilution Factor:*	**1.0000**
Injection Date/Time:	**02/Mar/17 05:51**	*Sample Weight:*	**1.0000**

Chromatogram

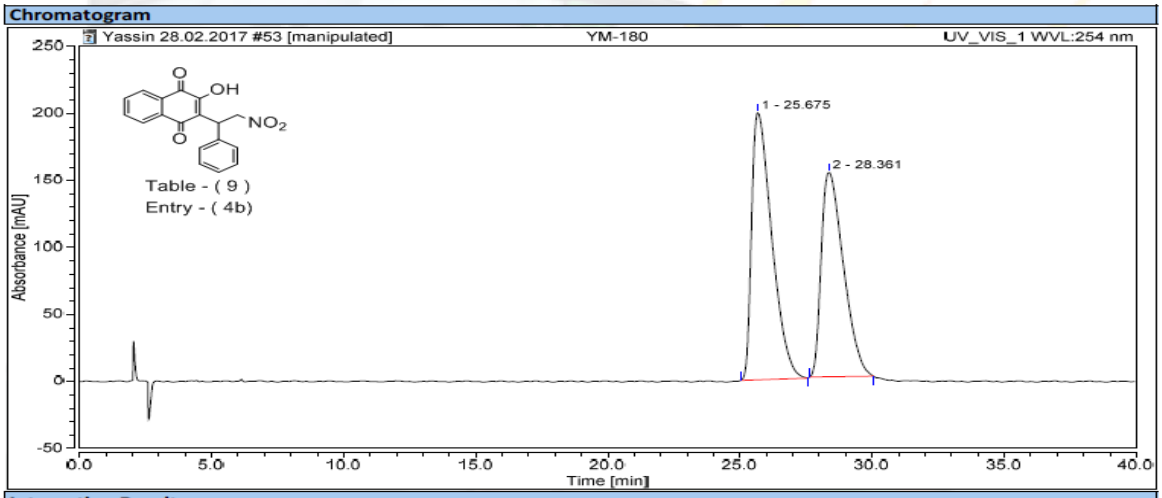

Integration Results

No.	Peak Name	Retention Time min	Area mAU*min	Height mAU	Relative Area %	Relative Height %	Amount
n.a.	Caffeine	n.a.	n.a.	n.a.	n.a.	n.a.	n.a.
1		25.675	176.652	199.374	54.32	56.63	n.a.
2		28.361	148.580	152.684	45.68	43.37	n.a.
Total:			**325.232**	**352.058**	**100.00**	**100.00**	